

11/10 20210

GESP-703

JANUARY 1970

NASA-CR-108893



THERMIONIC SPACECRAFT DESIGN STUDY

**CASE FILE
COPY**

PHASE I REPORT

COVERING THE PERIOD 4 FEBRUARY 1969 TO 4 JANUARY 1970

JANUARY 20, 1970

**PREPARED UNDER CONTRACT JPL 952381
FOR
THERMIONIC REACTOR SYSTEMS PROJECT**

**PROPULSION RESEARCH AND ADVANCED CONCEPTS SECTION
JET PROPULSION LABORATORY
4800 OAK GROVE DRIVE
PASADENA, CALIFORNIA, 91103**



THERMIONIC SPACECRAFT DESIGN STUDY

PHASE I REPORT

COVERING THE PERIOD 4 FEBRUARY 1969 TO 4 JANUARY 1970

JANUARY 20, 1970

PREPARED UNDER CONTRACT JPL 952381
FOR
THERMIONIC REACTOR SYSTEMS PROJECT

THIS WORK WAS PERFORMED FOR THE JET PROPULSION
LABORATORY, CALIFORNIA INSTITUTE OF TECHNOLOGY AS
SPONSORED BY THE NATIONAL AERONAUTICS AND SPACE
ADMINISTRATION UNDER CONTRACT NAS7-100

ISOTOPE POWER SYSTEMS OPERATION

GENERAL  ELECTRIC

SPACE DIVISION

This report contains information prepared by the General Electric Company under JPL subcontract. Its content is not necessarily endorsed by the Jet Propulsion Laboratory, California Institute of Technology, or the National Aeronautics and Space Administration.

ABSTRACT

This topical report presents the work from the first phase of a design study of nuclear-electric propelled unmanned spacecraft. The electric power source is in-core thermionic reactors based on either the flashlight or externally fueled diode concept. The study guidelines and approach are defined, and the characteristics of the candidate launch vehicles, thruster subsystem, and the payload and communications subsystem are presented. These areas are common to all candidate thermionic reactors.

The definition of two spacecraft/power plant configurations are presented which deliver 270 kWe power to the power conditioning units. This definition, presented for both the flashlight and externally fueled reactors includes the key items of spacecraft arrangement and a detailed weight breakdown. Power conditioning, heat rejection subsystem, shielding and spacecraft structure are detailed. The results show about a 20 lb/kWe weight advantage for the spacecraft based on the externally fueled reactor. This is primarily due to a 120 vdc power output from the externally fueled reactor, as compared to a 15 vdc power output from the flashlight reactor.

The computer code employed in the spacecraft weight optimization is discussed, and some preliminary discussion of key mission operations is presented.

TABLE OF CONTENTS

Section		Page
1	SUMMARY	1-1
	1.1 Performance Comparison	1-1
	1.2 Externally Fueled Reactor Based Spacecraft	1-4
	1.2.1 Reference Design Layout	1-4
	1.2.2 Weight and Power Summary	1-7
	1.2.3 Key Characteristics	1-13
	1.3 Flashlight Powerplant/Spacecraft	1-19
	1.3.1 Reference Design Layout-Flashlight Reactor Spacecraft	1-19
	1.3.2 Weight and Power Summary	1-24
	1.3.3 Key Characteristics	1-32
	1.4 Common Parameters	1-40
2	INTRODUCTION	2-1
3	STUDY GUIDELINES	3-1
	3.1 System Requirements	3-1
	3.2 Subsystem Definition	3-4
	3.2.1 Reactor Definition	3-4
	3.2.2 Thrusters	3-24
	3.2.3 Science Payload and Communication Subsystem	3-25
	3.2.4 Thermal Control Subsystem	3-35
4	LAUNCH VEHICLE	4-1
	4.1 Physical Constraints on Shroud Size	4-1
	4.2 Required Launch Vehicle Modifications	4-2
	4.3 Flight Fairing Weight and Payload Penalty	4-2
	4.4 Alternate Launch Vehicle	4-5
5	POWERPLANT BASELINE CONCEPT	5-1
	5.1 Design Summary	5-1
	5.1.1 Primary Radiator	5-1
	5.1.2 Power Conditioning Radiator	5-3
	5.1.3 Primary Loop System	5-8
	5.1.4 Low Voltage Cable	5-9
	5.1.5 Payload	5-9
	5.1.6 Thrusters	5-9
	5.1.7 Weight Summary of the Baseline Concept System	5-9

TABLE OF CONTENTS (Continued)

Section		Page
5.2	Spacecraft Structural Requirements	5-16
5.2.1	Launch Environment	5-17
5.2.2	Configuration Selection	5-19
5.2.3	Structural Analysis Summary	5-24
5.2.4	Structure Definition	5-29
5.2.5	Structural Analysis	5-32
5.2.6	Structural Dynamic Analysis	5-38
5.2.7	Application of Results to Spacecraft Using Externally Fueled Reactors	5-46
5.3	Coolant Activation	5-52
5.3.1	Geometrical Model	5-53
5.3.2	Analytical Models	5-55
5.3.3	Results	5-63
5.3.4	Discussion of the Results	5-72
6	SHIELD ANALYSIS	6-1
7	BASELINE ELECTRICAL SYSTEM DESIGN	7-1
7.1	Requirements/Characteristics	7-1
7.1.1	Base-Line Load Requirements	7-1
7.1.2	Base-Line Mission Requirements	7-4
7.1.3	Reactor Characteristics	7-4
7.1.4	Electric System Requirements	7-5
7.2	Baseline Electrical Power System Design	7-6
7.2.1	Flashlight Reactor Electrical Power System Baseline Design	7-6
7.2.2	Externally Fueled Thermionic Reactor Power System Design	7-46
8	SPACECRAFT DESIGN DEFINITION	
8.1	Externally Fueled Powerplant/Spacecraft	8-1
8.1.1	Powerplant Subsystem Group	8-9
8.1.2	Thruster Subsystem Group	8-23
8.1.3	Propellant System	8-25
8.1.4	Spacecraft Payload Components	8-26
8.1.5	Launch Components	8-26
8.2	Flashlight Powerplant/Spacecraft	8-26
8.2.1	Powerplant Subsystem Group	8-35
8.2.2	Thruster Subsystem Group	8-47
8.2.3	Propellant System	8-51
8.2.4	Spacecraft Components	8-57

TABLE OF CONTENTS (Continued)

Section		Page
	8.2.5 Launch Components	8-51
8.3	Weight Reduction Concepts	8-51
	8.3.1 Phase I Results	8-52
	8.3.2 Phase II Program Plan	8-53
9	WEIGHT TRADEOFF COMPUTER CODE	9-1
	9.1 Code Description	9-1
	9.1.1 Reactor Models	9-11
	9.1.2 Shield Model	9-15
	9.1.3 Heat Exchanger Model	9-21
	9.1.4 Power Conditioning Models	9-26
	9.1.5 Main Radiator Model	9-31
	9.1.6 Coolant Loop Models	9-40
	9.1.7 Low Voltage Cable	9-47
	9.1.8 Power Conditioning Radiator Model	9-52
	9.1.9 Auxiliary Radiator Model	9-56
	9.1.10 Payload Model	9-57
	9.1.11 Thruster System Model	9-59
	9.1.12 Structure Model	9-61
	9.1.13 Cesium System Model	9-63
	9.1.14 EM Pump Model	9-66
	9.2 Code Utilization	9-68
	9.2.1 Flashlight Reactor System Investigations	9-69
	9.2.2 Externally Fueled Reactor System	9-79
10	MISSION OPERATIONS	10-1
	10.1 Operations Analysis	10-1
	10.1.1 Definition of Major Events	10-1
	10.1.2 Power Plant Startup	10-5
	10.2 Nuclear Safety Evaluation	10-11
	10.2.1 Purpose and Scope	10-11
	10.2.2 Acceptance Testing	10-13
	10.2.3 Preliminary Fault Tree Analysis	10-15
	10.2.4 Possible Hazardous Operations and Potential Nuclear Accidents	10-19
11	CONCLUSIONS	11-1
12	RECOMMENDATIONS	12-1
13	REFERENCES	13-1
	APPENDICES	

LIST OF ILLUSTRATIONS

Figure		Page
1-1	Externally Fueled Diode 240 kWe (Net) Thermionic Spacecraft	1-5
1-2	Main Radiator Cross-Sectional View, Externally Fueled Reactor/ Spacecraft	1-8
1-3	Power Conditioning Radiator Cross-Sectional View, Externally Fueled Reactor/Spacecraft	1-9
1-4	Payload Bay Cross-Sectional View, Externally Fueled Reactor/Spacecraft	1-10
1-5	Shield Subsystem-Externally Fueled Reactor/Spacecraft	1-15
1-6	Heat Rejection System Externally Fueled Reactor/Spacecraft	1-17
1-7	Heat Rejection System Externally Fueled Reactor/Spacecraft	1-18
1-8	Low Voltage Cable Externally Fueled Reactor/Spacecraft	1-20
1-9	240 kWe (net) Thermionic Spacecraft ("Flashlight" Thermionic Reactor)	1-21
1-10	Equipment Bay Cross-Sectional View, Flashlight Reactor/ Spacecraft	1-25
1-11	Power Conditioning Radiator Cross-Sectional View, Flashlight Reactor/Spacecraft	1-26
1-12	Main Radiator Cross-Sectional View, Flashlight Reactor/ Spacecraft	1-27
1-13	Payload Bay Cross-Sectional View, Flashlight Reactor/ Spacecraft	1-28
1-14	Shield Subsystem - Flashlight Reactor/Spacecraft	1-33
1-15	Heat Rejection System - Flashlight Reactor/Spacecraft	1-35
1-16	Heat Rejection System - Flashlight Reactor/Spacecraft	1-36
1-17	Low Voltage Cable-Flashlight Reactor/Spacecraft	1-39
3-1	Externally Fueled Diode Reactor Concept	3-5
3-2	Flashlight Reactor Concept	3-5
3-3	Pancake Reactor Concept	3-6
3-4	Typical Reactor Geometry - Externally Fueled Diode Reactor	3-8
3-5	Variation in Pancake Reactor Power and Efficiency with Coolant Outlet Temperature	3-21
3-6	Thruster System Design Layout	3-29
3-7	Electrical Power Distribution (Communications and Science Payload Subsystem)	3-35
4-1	Flight Fairing Weight and Payload Penalty (Titan III C/7)	4-3
4-2	Effect of Shroud Retention on Payload Capability (Titan III C/7)	4-4

LIST OF ILLUSTRATIONS (Continued)

Figure		Page
5-1	Meteoroid Armor Bumper Relationship	5-3
5-2	Power Conditioning Radiator Panel	5-4
5-3	Baseline Concept-Cylindrical Radiator Configuration	5-11
5-4	Baseline Concept Triform Radiator Configuration	5-12
5-5	Baseline Concept-Cruciform Radiator Configuration	5-13
5-6	Baseline Concept Flat Panel Radiator Configuration	5-14
5-7	Example-Flat Plate Radiator Shield Geometry	5-16
5-8	Baseline Concept-Cylinder-Conical Radiator Spacecraft Weight Distributions	5-20
5-9	Baseline Concept-Triform Radiator Spacecraft Weight Distributions	5-21
5-10	Load/Boundary Conditions for Cylindrical-Conical Radiator Spacecraft Design	5-22
5-11	Load/Boundary Conditions for Triform Radiator Spacecraft Design.	5-23
5-12	Structural System Weight Summary, Cylindrical Conical Radiator	5-30
5-13	Structural System Weight Summary Triform Radiation	5-31
5-14	Stiffened Panel Geometry	5-36
5-15	Baseline Concept Dynamic Models	5-39
5-16	Conical Configuration Dynamic Properties	5-40
5-17	Triform Configuration Dynamic Properties	5-40
5-18	Baseline Concept Upright Conical Mode Shapes	5-44
5-19	Baseline Concept - Inverted Conical Mode Shapes	5-44
5-20	Baseline Concept Triform Mode Shapes	5-45
5-21	Baseline Concept-Inverted Triform Mode Shapes	5-45
5-22	Externally Fueled Reactor/Spacecraft Loading Distribution . . .	5-48
5-23	Power Conditioning Radiator Structure-Externally Fueled Concept	5-51
5-24	Stringer-Panel Configuration of Power Conditioning Radiator - Externally Fueled Concept	5-51
5-25	Single Loop and Two-Loop Power Plant Concepts	5-52
5-26	Vehicle Geometry Baseline Concept Power Plant - Flashlight Design	5-53
5-27	Vehicle Geometry Baseline Concept Power Plant - External Fuel Design	5-54
5-28	Flashlight Reactor Regions and Coolant Flow	5-54
5-29	Externally Fueled Reactor Regions and Assumed Coolant Flow. .	5-55
5-30	Primary Coolant Radiator Geometry - Flashlight Reactor . . .	5-56
5-31	Primary Coolant Radiator Geometry - Externally Fueled Reactor	5-56

LIST OF ILLUSTRATIONS (Continued)

Figure		Page
5-32	Reactor Power as a Function of Mission Time	5-69
5-33	Integrated Gamma Dose History - Single Loop System	5-72
6-1	Flashlight Reactor/Shield Mock-Up	6-2
6-2	Mission Profile	6-3
6-3	Gamma Dose Rate vs Time	6-4
6-4	Neutron Flux vs Time (Neutron Energies > 1 Mev)	6-4
6-5	Neutron and Gamma Heating Rates vs Depth in Shield	6-5
6-6	Neutron Flux and Gamma Dose Rate vs Depth in Shield (Neutron Energies > 1 Mev)	6-5
7-1	Baseline Flashlight Reactor Powered Spacecraft Electric Network	7-11
7-2	Basic Converter Module, Schematic	7-12
7-3	Typical Thermionic Reactor I-V Characteristics	7-14
7-4	Transistor Conduction and Switching Loss	7-20
7-5	Comparison of Transistor Losses with Frequency	7-20
7-6	Typical Circuit Screen Circuit Interrupter	7-33
7-7	Alternative Screen Supply Interruption Techniques	7-35
7-8	Component Geometry Main Power Converters Flashlight Reactor System	7-36
7-9	Reactor Power Regulation Arrangement Nominal 3kWe Module Flashlight Reactor System	7-36
7-10	DC-EM Pump Power Conditioning Parallel-Commutated SCR Converter	7-40
7-11	Low Voltage Cable System Weights	7-44
7-12	Detailed Weight Optimization, Sodium-Stainless Steel Low Voltage Cable System	7-44
7-13	Detailed Weight Optimization, Aluminum High Voltage Cable System	7-45
7-14	Detailed Weight Optimization, Aluminum Medium Voltage Cable System	7-47
7-15	Externally Fueled Reactor Electrical Power System	7-50
7-16	Main Power Conditioner Externally Fueled Thermionic Reactor System	7-51
7-17	Parametric Characteristics Main Power Conditioner Externally Fueled Reactor	7-52
7-18	Commutating Pulse	7-56
7-19	Component Geometry, Externally Fueled Reactor Main Power Conditioner	7-59

LIST OF ILLUSTRATIONS (Continued)

Figure		Page
8-1	Externally Fueled Reactor Schematic	8-10
8-2	Cross Section of Main Radiator Tube-Fin Arrangement	8-13
8-3	Coolant Header Arrangement for Externally- Fueled Reactor	8-14
8-4	Main Radiator Feed Line Network	8-15
8-5	Schematic Diagram of a DC Powered EM Pump	8-17
8-6	Hotel Power Distribution System for Externally Fueled Reactor Spacecraft	8-20
8-7	Schematic Representation of Auxiliary Loop	8-21
8-8	Schematic of Reactor Loop	8-37
8-9	Cross Section of Main Radiator Coolant Channel - Fin Section	8-40
8-10	Schematic of Main Radiator Loop	8-41
8-11	Hotel Load Power Distribution	8-43
8-12	Schematic of Auxiliary Cooling Loop	8-44
8-13	High Voltage Power Distribution	8-49
9-1	Simplified Logic Diagram for Computer Program	9-2
9-2	Calculation Sequence of Computer Program	9-7
9-3	Externally-Fueled Reactor Spacecraft	9-27
9-4	Offset Fin and Tube Configuration used in Main Radiator Design	9-32
9-5	Main Radiator Weight	9-34
9-6	Main Radiator Area	9-34
9-7	Weight Ratio of Area Limited Radiators	9-36
9-8	Main Radiator Pressure Drop	9-38
9-9	Pressure Drop Ratio in Area Limited Radiator	9-38
9-10	Flashlight Reactor System - Weight of Coolant in Radiator	9-40
9-11	Sketch of PC Radiator Panel Model	9-53
9-12	Flight Fairing Weight and Payload Penalty (Titan IIC/7)	9-63
9-13	Schematic of Cesium System in Equipment Bay Between Flashlight Reactor and Shield	9-64
9-14	EM Pump Weight	9-67
9-15	Flashlight Reactor	9-72
9-16	Flashlight Reactor System - Effect of Reactor Coolant Outlet Temperature	9-73
9-17	Flight Reactor System - Change in Output Power Level	9-75

LIST OF ILLUSTRATIONS (Continued)

Figure		Page
9-18	Flashlight Reactor System - Parameter Variation Effect	9-76
9-19	Flashlight Reactor - Parameter Variation Effect	9-77
9-20	Flashlight Reactor - Influence of Power Conditioning Temperature and P. C. Radiator Temperature	9-78
9-21	Externally Fueled Reactor - Effect of Reactor Output Voltage	9-81
9-22	Externally Fueled Reactor - Influence of Reactor Output Power	9-83
9-23	Externally Fueled Reactor - Variation of System Parameters	9-85
9-24	Externally Fueled Reactor - Influence of Power Conditioning Temperature and PC Radiator Temperature . . .	9-85
9-25	Externally Fueled Reactor - Effect of Reactor Outlet Coolant Temperature	9-86
10-1	Typical Mission (Reactor-Thermionic Jupiter)	10-3
10-2	Model for Thermionic Spacecraft Radiator Startup Study	10-7
10-3	Radiator Temperature on Sun Side	10-8
10-4	Radiator Temperature on Shade Side	10-9
10-5	Radiator Average Temperature vs Beta Angle	10-10
10-6	Radiator Average Temperature vs Beta Angle	10-10
10-7	Shade Time vs Beta Angle	10-11
10-8	Proposal Mission Profile and Accident Groups for Unmanned Nuclear Powered Spacecraft for Planetary Exploration	10-16
10-9	Iterations Necessary to Define Optimum Mission/Power Plant Combinations	10-17

LIST OF TABLES

Table		Page
1-1	Spacecraft Performance Comparison	1-3
1-2	Weight Summary 240 kWe (Net) Thermionic Spacecraft (Externally Fueled Reactor)	1-11
1-3	Electric Power Summary 240 kWe (Net) Thermionic Spacecraft (Externally Fueled Reactor)	1-14
1-4	Weight Summary 240 kWe (Net) Thermionic Spacecraft (Flashlight Reactor)	1-29
1-5	Electric Power Summary 240 kWe (Net) Thermionic Spacecraft (Flashlight Reactor)	1-31
3-1	Externally Fueled Diode Reactor Characteristics - 300 kWe EOM	3-11
3-2	Externally Fueled Diode Reactor Characteristics - 276 kWe EOM	3-13
3-3	Mesh Structure - Externally Fueled Diode Reactor	3-14
3-4	Externally Fueled Diode Reactor Composition By Regions	3-14
3-5	Performance of 300 kWe Flashlight Reactor Designs	3-17
3-6	Relative Power Distribution for Flashlight Reactor Alternate Design No. 1	3-19
3-7	Reactor Material Designation for Flashlight Reactor Alternate Reactor No. 1	3-20
3-8	Pancake Reactor Dimensions and Thermal Power Level for A 300 kW Thermionic Reactor	3-23
3-9	Pancake Reactor Characteristics When Operated at 10 Percent Power	3-23
3-10	Guidelines for Thruster Subsystem Design	3-25
3-11	Ion Engine Power Supply Requirements	3-26
3-12	Thruster Subsystem Weights	3-27
3-13	Science Payload and Data Handling Equipment Summary	3-31
3-14	Communications Subsystem Characteristics	3-34
4-1	Maximum Payload Capability With Shroud Ejection at 280 Seconds	4-4
4-2	Maximum Earth Orbital Altitude for a 30,000 Pound Payload With Shroud Jettison at 280 Seconds	4-5
4-3	Maximum Payload Capability at 630 Nautical Mile With Shroud Ejection After Achieving Earth Orbit	4-5
4-4	Comparison of Payload Capability (Pounds) for Titan and Saturn Launch Vehicles	4-6

LIST OF TABLES (Continued)

Table		Page
5-1	Primary Radiator Characteristics (Baseline Concept Power Plant, Single Loop)	5-4
5-2	Weight Summary, Baseline Concept Powerplant Systems	5-10
5-3	Summary of Structural Analysis	5-25
5-4	Mass Data for Lumped Mass Model	5-42
5-5	Thermionic Spacecraft Structural Dynamics	5-43
5-6	Structural Margins of Power Conditioning Radiator During Titan III C/7 Launch	5-49
5-7	Power Conditioning Radiator Structure Weight Summary - Externally Fueled Concept	5-50
5-8	Neutron Energy Groups and Activation Cross Sections - Flashlight Reactor	5-60
5-9	Neutron Energy and Activation Cross Sections - Externally Fueled Reactor	5-60
5-10	Photon Production Characteristics	5-62
5-11	Flux-to-Dose Conversion Factors	5-62
5-12	Energy Group and Reactor Region Contributions to the Coolant Activation Density - Flashlight Reactor	5-64
5-13	Energy Group and Reactor Region Contributions to the Coolant Activation Density - Flashlight Reactor	5-64
5-14	Energy Group and Reactor Region Contributions to the Coolant Activation Density - Externally Fueled Reactor	5-65
5-15	Energy Group and Reactor Region Contributions to the Coolant Activation Density - Externally Fueled Reactor	5-65
5-16	Flashlight Reactor Residence Times	5-66
5-17	Externally Fueled Reactor Residence Times	5-66
5-18	Reactor Region Contributions to the Coolant Activation Density - Flashlite Reactor	5-67
5-19	Reactor Region Contributions to the Coolant Activation Density - Externally Field Reactor	5-67
5-20	Coolant Photon Source Strengths Flashlite Reactor	5-68
5-21	Coolant Photon Source Segments Externally Fueled Reactor	5-68
5-22	Integrated Gamma Doses Due to Activated Coolant - Flashlight Reactor	5-70
5-23	Integrated Gamma Doses Due to Activated Coolant - Externally Fueled Reactor	5-71

LIST OF TABLES (Continued)

Table		Page
7-1	Baseline Spacecraft Electrical Load Requirements	7-2
7-2	Thruster Power Requirements	7-3
7-3	Flashlight Reactor Electrical Characteristics	7-5
7-4	Electric System Weight Summary Flashlight Reactor System	7-7
7-5	Flashlight Reactor System Main Converter Weight Breakdown	7-8
7-6	Flashlight Baseline System Power Balance	7-9
7-7	Characteristics of Candidate Power Transistors	7-18
7-8	Auxiliary Power Conditioning Characteristics	7-41
7-9	Selected Power Cable Characteristics	7-43
7-10	Externally Fueled Reactor Power Condition Power Loss	7-48
7-11	Externally Fueled Reactor Main Power Conditioner Weight	7-49
8-1	Characteristics of a 300 kWe Externally Fueled Reactor Power-Plant/Spacecraft	8-3
8-2	Weight Summary 240 kWe (Net) Thermionic Spacecraft (Externally Fueled Reactor)	8-5
8-3	Electric Power Summary 240 kWe (Net) Thermionic Spacecraft (Externally Fueled Reactor)	8-7
8-4	Characteristics of a 300 kWe Flashlite Reactor Powerplant/Spacecraft System	8-29
8-5	Weight Summary 240 kWe (Net) Thermionic Spacecraft (Flashlight Reactor)	8-31
8-6	Electric Power Summary 240 kWe (Net) Thermionic Spacecraft (Flashlite Reactor)	8-33
9-1	Flashlight Reactor System - Comparison of Low Voltage Cable Compositions	9-71
9-2	Flashlight Reactor System - Comparison of Results For Varying Reactor Coolant Outlet Temperature	9-74
10-1	Reactor-Thermionic Power System Prelaunch Testing	10-14

1 SUMMARY

1. SUMMARY

Characteristics of the reference designs for both the externally fueled and flashlight reactor based spacecraft are summarized in this section.

Preliminary design analysis to determine spacecraft component arrangement and configuration was conducted. The resultant spacecraft design is referred to as the baseline concept, with guidance from the weight optimization computer code studies, has resulted in a refined design layout derived from the computer code. This final spacecraft configuration is the reference design.

Reference spacecraft design layouts, and weight and power distribution summaries, are presented for each of the two powerplant concepts. For this study, the externally fueled reactor and flashlite reactor concepts are required to provide 240 kWe to the thrust system. Comparison of the two powerplant concepts and their effect on the total spacecraft are presented below. Each of the reference designs were developed under the common guidelines that all of the powerplant components except the reactor are current technology.

1.1 PERFORMANCE COMPARISON

Using terminology recommended by the NASA-OART electric propulsion systems analysis task group*, the spacecraft initial mass, m_o , is defined as:

$$m_o = m_{ps} + m_p + m_t + m_n$$

where the masses are

m_{ps} = low thrust propulsion system

m_p = propellant

*Electric Propulsion Mission Analysis Terminology and Nomenclature NASA SP-120, 1969.

m_t = tankage

m_n = net spacecraft (guidance, thermal control, attitude control, telecommunications, structure, science, etc.) - includes the science payload, m_L

The propulsion system is further broken down:

$$m_{ps} = m_w + m_{ts}$$

where these masses are

m_w = power subsystem

m_{ts} = thrust subsystem

Similarly, net propulsion power is defined as

$$P_{NP} = P_{TN} + P_{TPC}$$

where the component powers are

P_{TH} = ion engine grid power

P_{TPC} = other ion engine power

Gross reactor power is that reactor output power required to supply net propulsion power, P_{NP} , to the thruster subsystem. Gross propulsion power is given by:

$$P_e = P_{NP} / \eta_{MPC}$$

where η_{MPC} is the main power conditioning efficiency. Specific weight of the propulsion system, α , is defined by

$$\alpha = \frac{m_{ps}}{P_e}$$

From the detailed weight and power breakdown, presented in Tables 1-2 and 1-3 for the externally fueled reactor and in Tables 1-4 and 1-5 for the flashlight reactor, spacecraft performance is summarized in Table 1-1.

TABLE 1-1. SPACECRAFT PERFORMANCE COMPARISON

Reactor Concept	Externally Fueled Reactor Spacecraft	Flashlight Reactor Spacecraft
$M_{eo} \sim$ pounds Liftoff mass	31495 (14330)*	37605 (17100)
$M_o \sim$ pounds Initial mass	30420 (13810)	36325 (16500)
$M_{ps} \sim$ pounds Low thrust propulsion system	13210 (6000)	19330 (8790)
$M_w \sim$ pounds Power subsystem	9045 (4106)	12170 (5525)
$M_{ts} \sim$ pounds Thrust subsystem	4165 (1891)	7160 (3250)
$M_p \sim$ pounds Propellant	14500 (6580)	14500 (6580)
$M_t \sim$ pounds Tankage	460 (209)	245 (111)
$M_n \sim$ pounds Net spacecraft	2235 (1015)	2235 (1015)
$M_e \sim$ pounds Science payload	2265 (~1000)	2265 (~1000)
$P_G \sim$ kWe Reactor gross power	274	318
$P_e \sim$ kWe Effective Power Input to PC Units	262	273.1
$P_{NP} \sim$ kWe Net Propulsion Power	240	240
$P_{TH} \sim$ kWe Ion Engine Grid Power	223	223
$P_{TPC} \sim$ kWe Other Ion Engine Power	17	17
$\alpha \sim$ pounds/kWe Specific Weight	50.4	71.1

*Number in parenthesis is weight in Kg.

Propulsion system specific weight, α , for the externally fueled reactor/spacecraft is 50.4 pounds/kWe, and propulsion system specific weight of the flashlight reactor is 71.1 pounds/kWe. These specific weights are based on propulsion system power input of 262 kWe for the externally fueled reactor/spacecraft and 273.1 kWe for the flashlight reactor/spacecraft.

1.2 EXTERNALLY FUELED REACTOR BASED SPACECRAFT

The reference spacecraft utilizing the externally fueled reactor concept is based on the following assumptions:

- a. Reactor coolant outlet temperature of 1350° F
- b. Single heat rejection loop between reactor and main radiator
- c. Main radiator in a position directly behind the forward Hg propellant tank and in front of the power conditioning radiator
- d. Aluminum as electrical cable material.

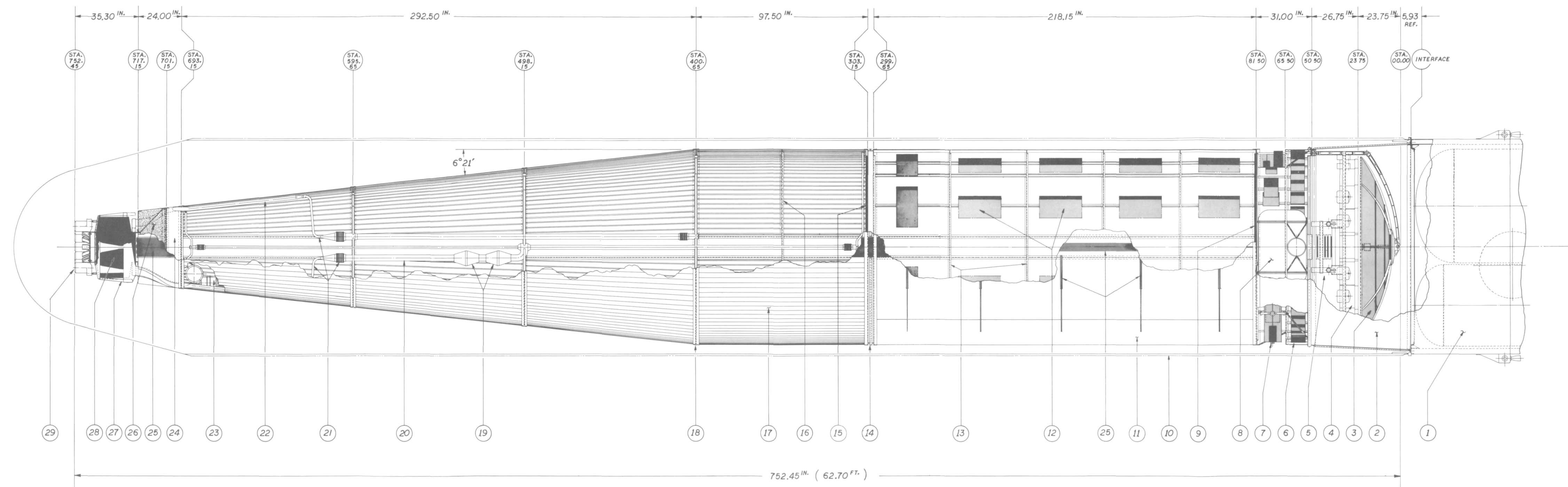
Further details are presented in Subsection 8.1.

1.2.1 REFERENCE DESIGN LAYOUT

Figure 1-1 shows a design layout of the spacecraft powered by the externally fueled reactor. The reference spacecraft is approximately 62.7 feet long and 9.2 feet in diameter. The conically shaped forward end of the spacecraft includes the reactor at the apex and 75 percent of the main radiator. Half-angle of the conical portion is 6.6 degrees. The remainder of the vehicle from this point rearward is essentially a cylinder.

Figure 2-1 provides an overall arrangement of the major spacecraft components. The reactor is located at the apex of the conical section to provide maximum separation distance from the payload at the opposite end of the spacecraft and to assure minimum required shield volume. The shield consists of a LiH block of neutron shielding followed by the forward tank of mercury (Hg) propellant which acts as a gamma shield.

ITEM	DESCRIPTION
1	LAUNCH VEHICLE (TITAN III C 7)
2	PAYLOAD ADAPTER
3	COMMUNICATION ANTENNA
4	THRUSTER PLATFORM (37 MERCURY ION ENGINES)
5	TVC SYSTEM
6	SPECIAL THRUSTER CONDITIONING UNITS
7	PAYLOAD EQUIPMENT BAY
8	MERCURY PROPELLANT TANKS
9	THERMAL BULKHEAD AFT.
10	FLIGHT FAIRING
11	POWER CONDITIONING RADIATOR (MAIN AND HOTEL PC)
12	POWER CONDITIONING UNITS (MOUNTING ENVELOPE)
13	INTERNAL STIFFENING RINGS
14	AUXILIARY RADIATOR (MOUNTED TO TRANSITION RING)
15	THERMAL BULKHEAD FORWARD
16	INTERNAL STIFFENING RINGS (PRIMARY RADIATOR)
17	PRIMARY RADIATOR
18	MATING RING TYP
19	EM PUMPS
20	PRIMARY RADIATOR RETURN DUCT
21	DIFFERENTIAL EXPANSION COMPENSATION
22	PRIMARY RADIATOR FEED DUCT
23	ACCUMULATORS
24	MERCURY PROPELLANT TANKS (GAMMA SHIELD)
25	LOW VOLTAGE CABLES
26	NEUTRON SHIELD
27	HEADERS
28	REACTOR
29	ACTUATORS (12)



FAIRCHILD-HILLER (EXTERNALLY-FUELED DIODE)
240 KW_e(NET) THERMIONIC SPACECRAFT

Figure 1-1. Externally Fueled Diode 240 kW_e (Net) Thermionic Spacecraft

Located directly behind the propellant tank is the main radiator, which dissipates waste heat from the reactor by means of a single loop NaK-78 coolant. A very short section of auxiliary radiator, which dissipates heat generated in the EM pumps and the neutron shield, separates the main radiator from the power conditioning radiator. Individual power conditioning modules are placed uniformly on the eight-sided power conditioning radiator. Low voltage cables extend longitudinally from the reactor exit along the surfaces of the shield and main radiator to the power conditioning radiator. At five axial locations on the radiator, these cables run circumferentially to the 38 individual modules. Thirty-seven of these modules are required for the 37 ion engines, of which 31 are operational and 6 are spares. The remaining PC module provides for the necessary hotel load power conditioning.

The rear section of the spacecraft includes the Hg propellant not required for gamma shielding, the payload bay, and the thruster bay that houses 37 mercury ion engines. A communication antenna which extends radially for operation are shown in the stowed position behind the thrusters for launch.

Cross-sectional views through the main radiator, power conditioning radiator, and payload sections of the externally fueled reactor/spacecraft are presented in Figures 1-2, 1-3, and 1-4, respectively. Location of the cross-sections is indicated on the reference design layout in Figure 1-1.

1.2.2 WEIGHT AND POWER SUMMARY

The weight summary for the reference designs of the spacecraft utilizing the externally fueled reactor concept is presented in Table 1-2. In order to provide 240 kWe of power to the ion engine system, a gross reactor power output of 274 kWe is required. Total spacecraft weight at launch is 31,485 pounds. Disposable launch vehicle adapter and payload shroud weights, which are jettisoned, result in an Earth orbit spacecraft weight of 30,410 pounds.

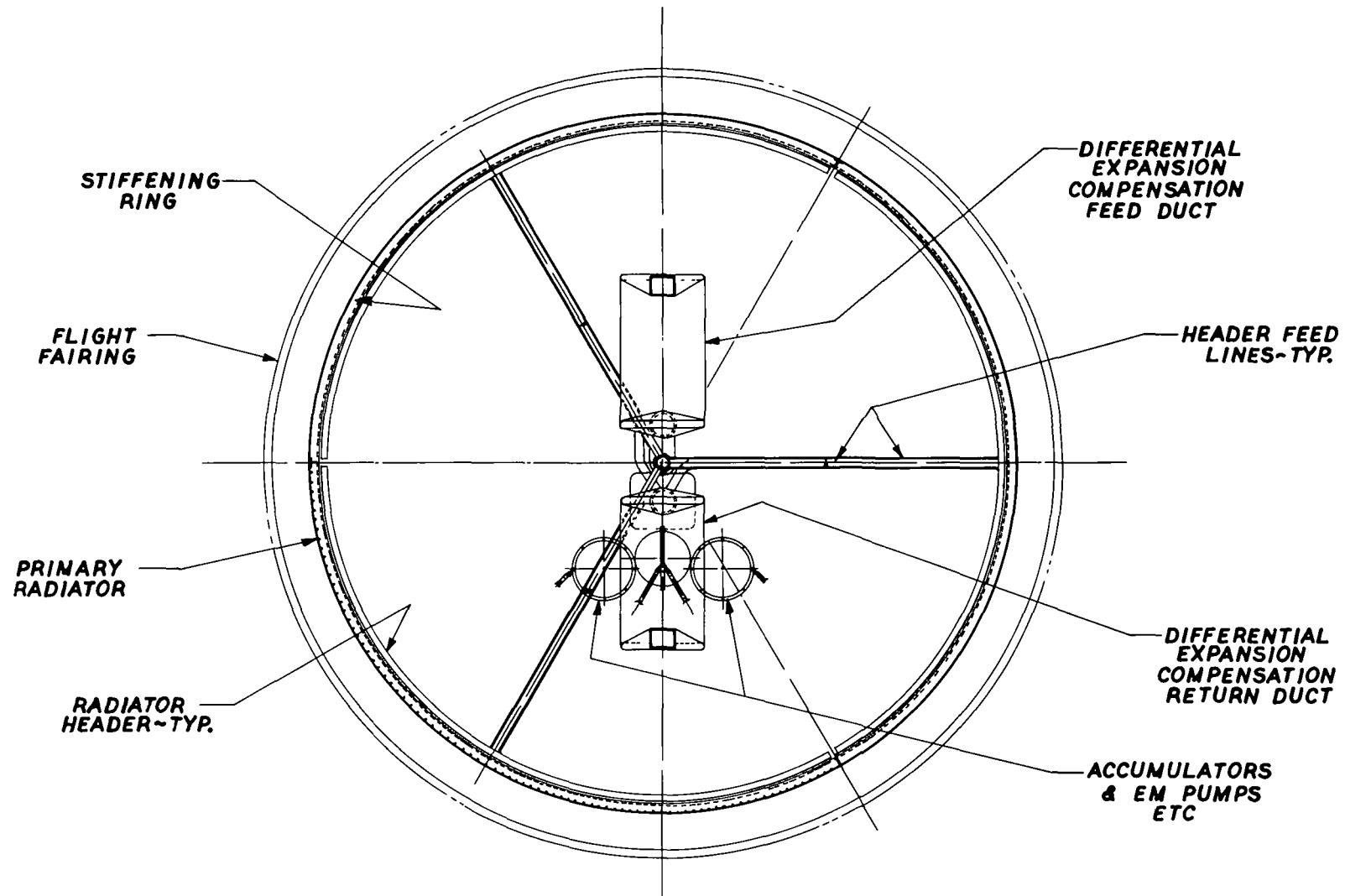


Figure 1-2. Main Radiator Cross-Sectional View, Externally Fueled Reactor/Spacecraft

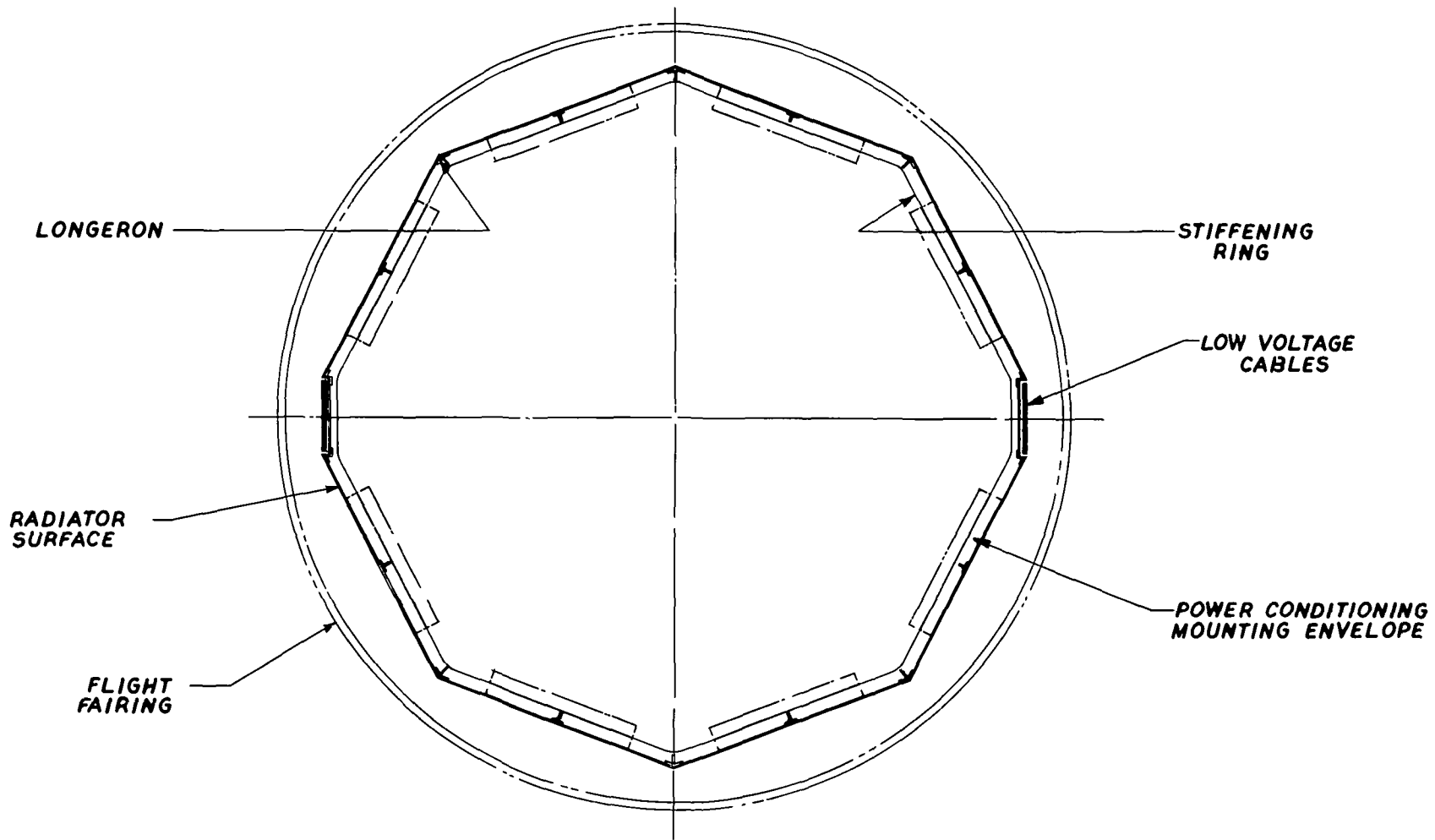


Figure 1-3. Power Conditioning Radiator Cross-Sectional View, Externally Fueled Reactor/Spacecraft

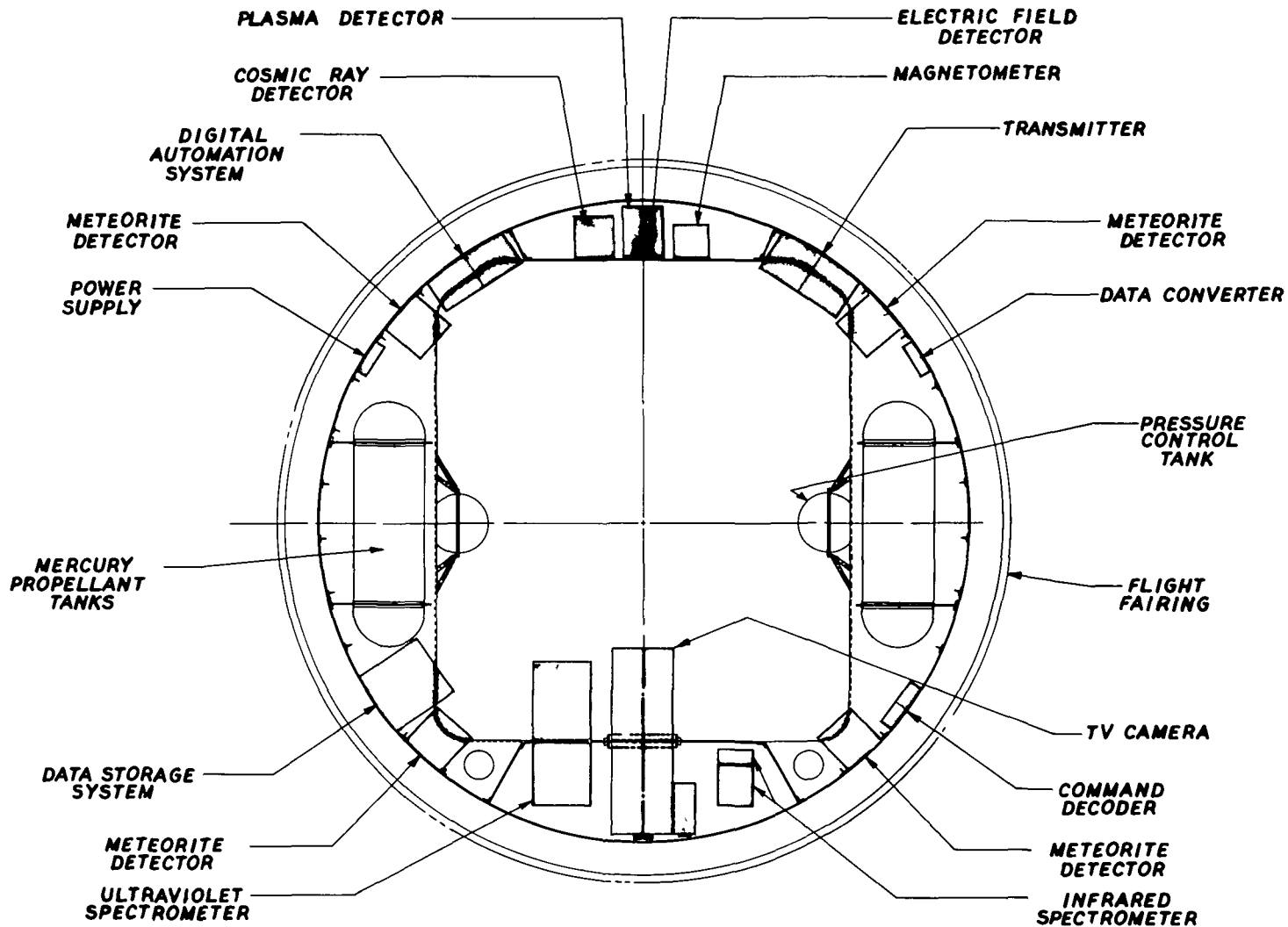


Figure 1-4. Payload Bay Cross-Sectional View, Externally Fueled Reactor/Spacecraft

TABLE 1-2. WEIGHT SUMMARY 240 kWe (NET) THERMIONIC SPACECRAFT
(EXTERNALLY FUELED REACTOR)

Component	Weight-Pounds				
Propulsion System					13,210
Power Plant Subsystem				9045	
Reactor Subsystem			4380		
Reactor (Dry)		4150			
Actuator		230			
Primary Heat Rejection			2550		
Ducts		250			
EM Pumps (2)		100			
Accumulators		140			
Main Radiator		1335			
Coolant		650			
Insulation		75			
Shield			950		
Neutron		765			
Permanent Gamma		185			
Electric and Controls			155		
Hotel Load		105			
Power Conditioning	45				
Radiator	20				
Distribution Cables	40				
Power Plant, Control		50			
Auxiliary Coolant Loop			100		
Ducts		35			
EM Pumps (2)		20			
Accumulators		10			
Radiators		10			
Coolant		25			
Structure			860		
Reactor Support		40			
Neutron Shield (external)		70			
Power Conditioning Radiator		360			
Area Blocked by LV Cables	65				
Mating/Stiffening Rings	85				
Longerons	210				
Transition Ring		55			
Main Radiator		335			
Mating/Stiffening Rings	170				
Longerons	165				
Miscellaneous			50		
Thruster Subsystem				4165	
Ion Engine Subsystems			1235		
Ion Engine Units		585			
TVC Unit		550			
Miscellaneous		100			
Power Conditioning Electronics			1660		
HV Power Supply		1390			
Special Ion Engine PC		270			
Power Conditioning Radiators			830		
HV Power Supply		745			
Special Ion Engine PC		85			
High Voltage Power Cables			15		
3100 Volt Cables		10			
Insulation		5			
Low Voltage Power Cables			385		
Main Bus		195			
Payload and Thruster Bus		30			
Electrical Insulation		80			
Thermal Insulation		80			
Structure			40		
Special PC Bay		40			
Propellant System					14,975
Propellant				14,500	
Tanks and Distribution				460	
Structure				15	
Net Spacecraft					2235
Guidance and Control				50	
Communications				60	
Science				2065	
Radiator				25	
Structure				35	
Gross spacecraft in Earth Orbit					30,420
Launch Vehicle Adapter					250
Launch Shroud Payload Weight Penalty					825
Launch Vehicle Payload Requirement					31,495

Weight of each of the three major spacecraft systems are:

- a. Propulsion system 13,210 pounds
- b. Propellant system 14,975 pounds
- c. Payload system 2,235 pounds

For this study, the propellant and payload systems have been defined by the study guidelines. Therefore, this design effort is devoted to configuring a weight optimum propulsion system. Summary of the key characteristics of each subsystem that comprise the propulsion system are discussed below.

Electric power utilization for the externally fueled reactor concept is summarized in Table 1-3. Net power to the ion engine system is 240 kWe, of which 223 kWe are required for the 3100 volt screen supply operation of the ion engines, and 17 kWe are required for other special ion engine power conditioning. A total of 274 kWe of gross reactor output power is required.

For purposes of mission analyses, 262 kWe are delivered to the main power conditioning, which operates at an effective efficiency of 91.6 percent, including high voltage cable losses, to deliver 240 kWe to the 31 operating ion engines.

1.2.3 KEY CHARACTERISTICS

A summary of design characteristics of the shield, heat rejection and power conditioning subsystems are discussed in this section for the externally fueled reactor spacecraft reference design.

1.2.3.1 Reactor-Shield Subsystem

Shielding is provided to insure that the power conditioning and payload components meet the radiation criteria established by the design guidelines. These are that integrated neutron radiation shall not exceed 10^{12} nvt > 1 Mev and that the integrated gamma radiation shall not exceed 10^7 rads. Neutron radiation is attenuated primarily by a lithium hydride shield, located immediately behind the externally fueled reactor.

TABLE 1-3 ELECTRIC POWER SUMMARY 240 kWe (NET)
THERMIONIC SPACECRAFT (EXTERNALLY FUELED REACTOR)

Component	Power	kWe	
Reactor Output			274
Low Voltage cable loss		5.87	
Hotel load section		4.031	
Cable losses	.055		
PC losses	.5246		
Reactor pump input	2.745		
Auxiliary pump input	.0064		
Reactor controls input	.20		
Cesium heater input	.50		
Payload and Thruster section		19.1	
Cable losses	0.1		
Special Ion Engine PC input	17.0		
Payload input	1.0		
Spacecraft control input	0.5		
Powerplant control	0.5		
High Voltage PC Input		245	
PC losses	22.5		
Cable losses	0.5		
Thruster Engine Input	223		
Net Power to Thruster*			240
*The net power is the sum of the ion engine grid power input, after power conditioning, and the other special ion engine power.			

Additional attenuation is provided by the tank of mercury propellant located behind the shield. However, the primary purpose of mercury propellant in the forward section is to act as the primary gamma shield. Location of the neutron shield and forward propellant tank is shown in Figure 1-5.

The lithium hydride shield is 16 inches thick with an average diameter of 41.8 inches. Total weight of the neutron shield is 765 pounds, of which 575 pounds is lithium hydride.

Approximately 4500 pounds of mercury propellant is contained in the tank located directly behind the shield. The conically shaped tank is 6 inches thick with an average diameter of 44.4 inches.

REACTOR AND SHIELD SUBSYSTEM WEIGHTS
 EXTERNALLY FUELED REACTOR SPACECRAFT

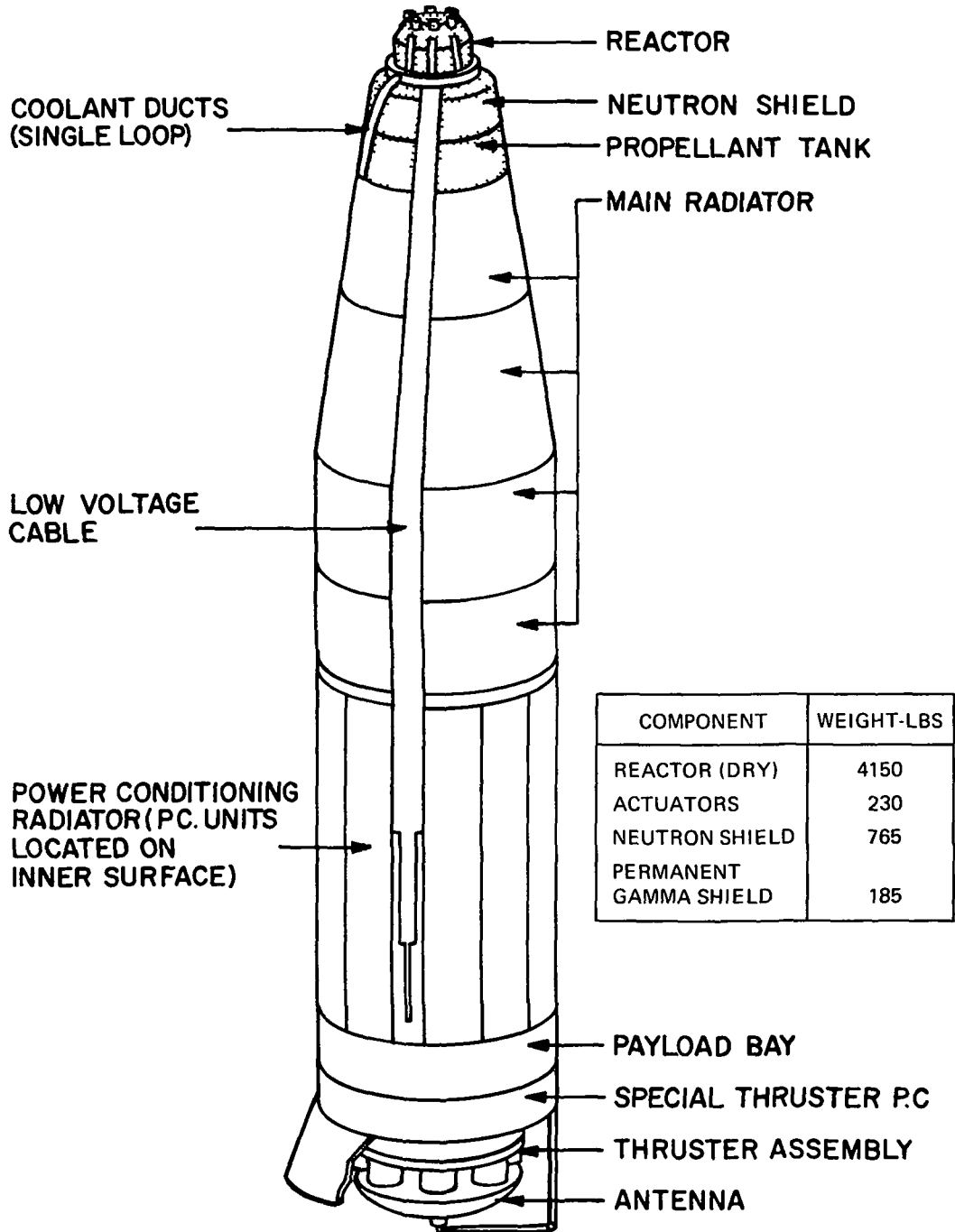


Figure 1-5. Shield Subsystem-Externally Fueled Reactor/Spacecraft

Plugs of tungsten weighing 185 pounds back up the propellant shield where auxiliary coolant lines pass through the propellant tank.

1.2.3.2 Heat Rejection Subsystem

Heat rejection from the spacecraft is accomplished by the primary, auxiliary, power conditioning, payload and thruster PC radiators. The primary and auxiliary radiators as shown in Figures 1-6 and 1-7 are part of an active cooling network; whereas, the power conditioning, payload and thruster radiators transfer heat from temperature sensitive components to space by passive means. In both the primary and auxiliary active loops, NaK-78 is used as the coolant fluid. The payload and thruster subsystem have essentially been defined by the design guidelines.

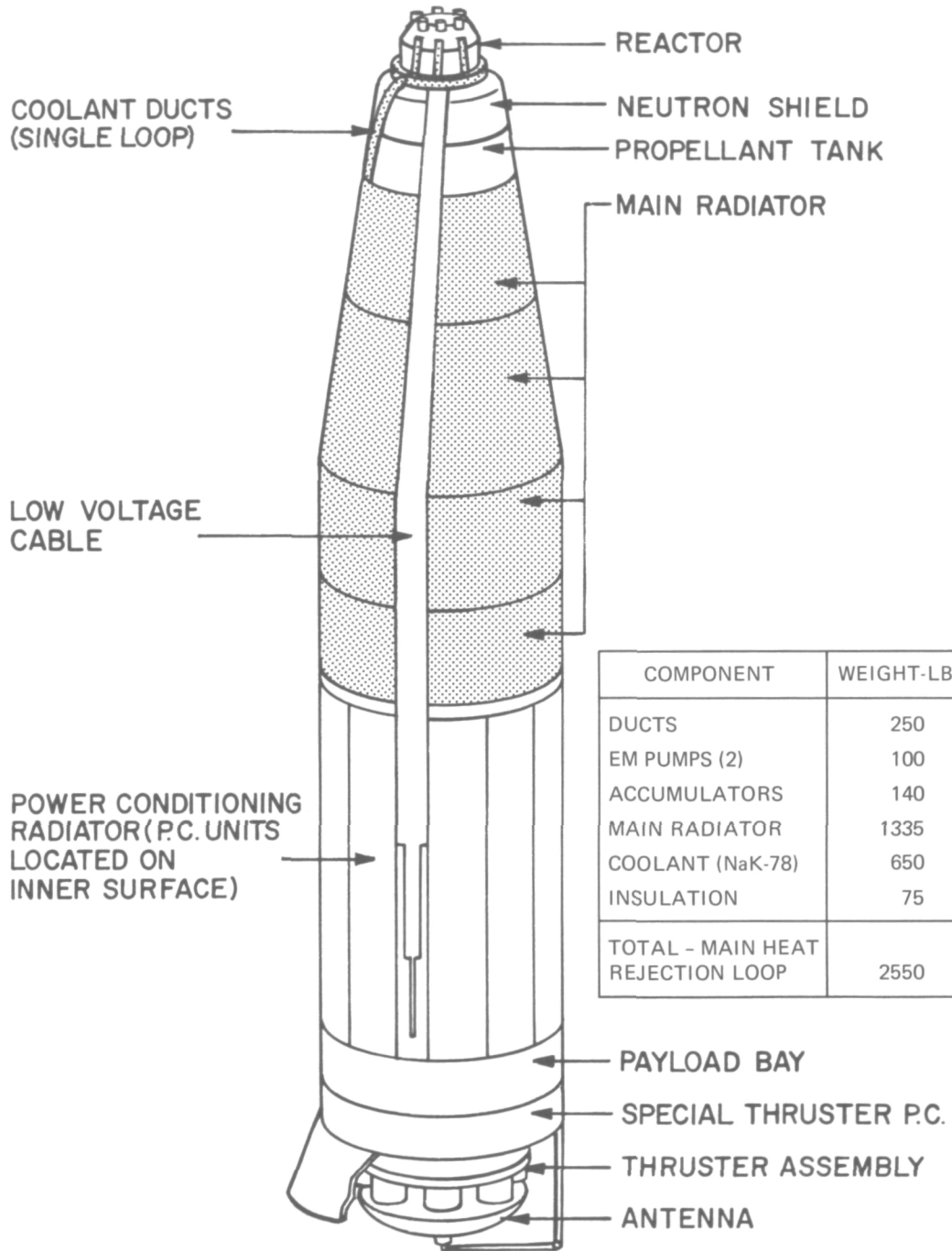
The function of the primary heat rejection system is to actively transfer heat from the reactor to space. The main radiator is located in the forward section of the spacecraft because the high reactor output voltage, about 120 volts, permits the aft location of the power conditioning radiator without excessive I^2R losses. The forward location of the main radiator also minimizes coolant and piping weight, and the weight penalty associated with NaK-78 coolant pumping.

The relative location of the main heat rejection system is shown in Figure 1-6. The main radiator consists of four bays of equal length, three of which form the conical surface of the spacecraft while the fourth occupies the forward section of the cylindrical spacecraft area. Each of the bays is divided into three 120° panels. Dry weight of the copper/stainless steel radiator, which is 660 square feet in area, and associated headers is 1335 pounds. In addition to the required piping and two EM pumps (one working and one redundant), bellows in the input and return radiator feed lines take up extension motion among the individual bays of the main radiator.

1.2.3.3 Power Conditioning

Low voltage cables transport 120 volts of reactor electrical power output to the 37 high voltage supply power conditioning units, the special payload and thruster power

PRIMARY HEAT REJECTION SYSTEM WEIGHTS
EXTERNALLY FUELED REACTOR SPACECRAFT



COMPONENT	WEIGHT-LBS
DUCTS	250
EM PUMPS (2)	100
ACCUMULATORS	140
MAIN RADIATOR	1335
COOLANT (NaK-78)	650
INSULATION	75
TOTAL - MAIN HEAT REJECTION LOOP	2550

Figure 1-6. Heat Rejection System Externally Fueled Reactor/Spacecraft

AUXILIARY COOLANT LOOP AND SPECIAL ELECTRIC AND CONTROLS
 SUBSYSTEM WEIGHTS
 EXTERNALLY FUELED REACTOR SPACECRAFT

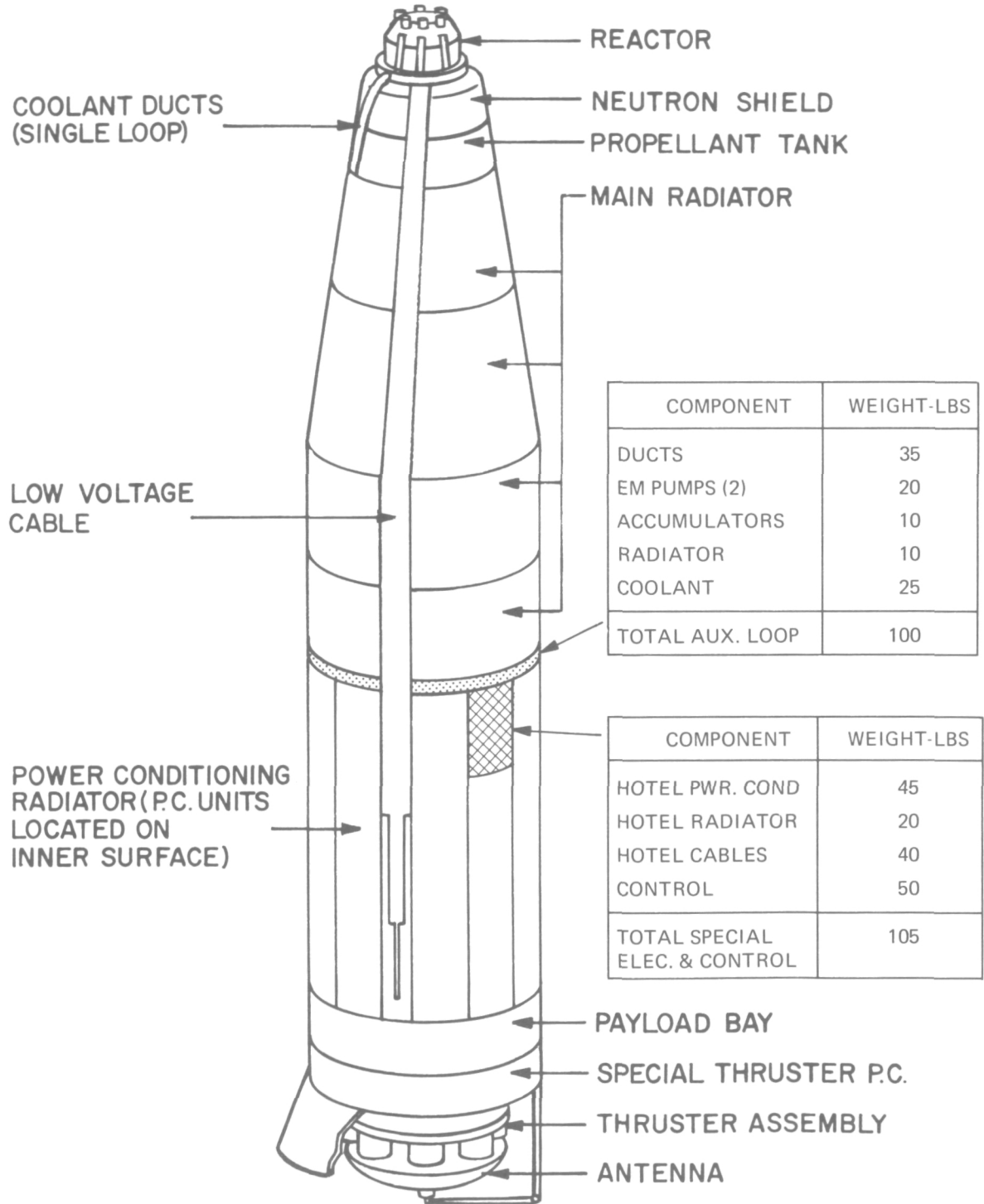


Figure 1-7. Auxiliary Heat Rejection System Externally Fueled Reactor/Spacecraft

conditioning modules and hotel load low voltage power module. Path of the low voltage cables is shown in Figure 1-8. Each of the 37 main power conditioning modules supplies 3100 volts to each ion engine. The hotel power conditioning distributes low voltage power to operate the power plant as well as the electronic components which monitor and control the actuator drives of the reactor and the pumps of the active heat rejection loops in the power plant.

Located directly behind the auxiliary radiator is the passive power conditioning radiator, also shown on Figure 1-8. The 38 power conditioning modules are placed uniformly over the aluminum radiator in which 380 square feet are required to dissipate waste heat to space. This radiator, based on a 0.115 inch panel thickness, weighs 745 pounds.

1.3 FLASHLIGHT REACTOR/SPACECRAFT

The reference flashlight power plant and spacecraft design is based on the following assumptions:

- a. Reactor coolant outlet temperature of 1350^oF
- b. Two heat rejection loops in series between reactor and main radiator
- c. Power conditioning radiator located directly behind the shield and in front of the main radiator
- d. Aluminum as the low voltage cable material.

1.3.1 REFERENCE DESIGN LAYOUT-FLASHLIGHT REACTOR SPACECRAFT

Figure 1-9 presents the design layout of the spacecraft powered by the flashlight reactor. The reference design spacecraft is a long, narrow vehicle, approximately 84 feet long and 9.2 feet in diameter. The conical front end section is 25.6 feet long with a 7.4 degree half angle while the rear of the vehicle is essentially a cylindrical section. The reactor is located at the apex of the conical section to provide maximum separation distance from the payload, which is at the rear of the cylindrical section, and to assure minimum required shadow shield volume. The neutron shield is located

MAJOR ELECTRIC SUBSYSTEM WEIGHTS
 EXTERNALLY FUELED REACTOR SPACECRAFT

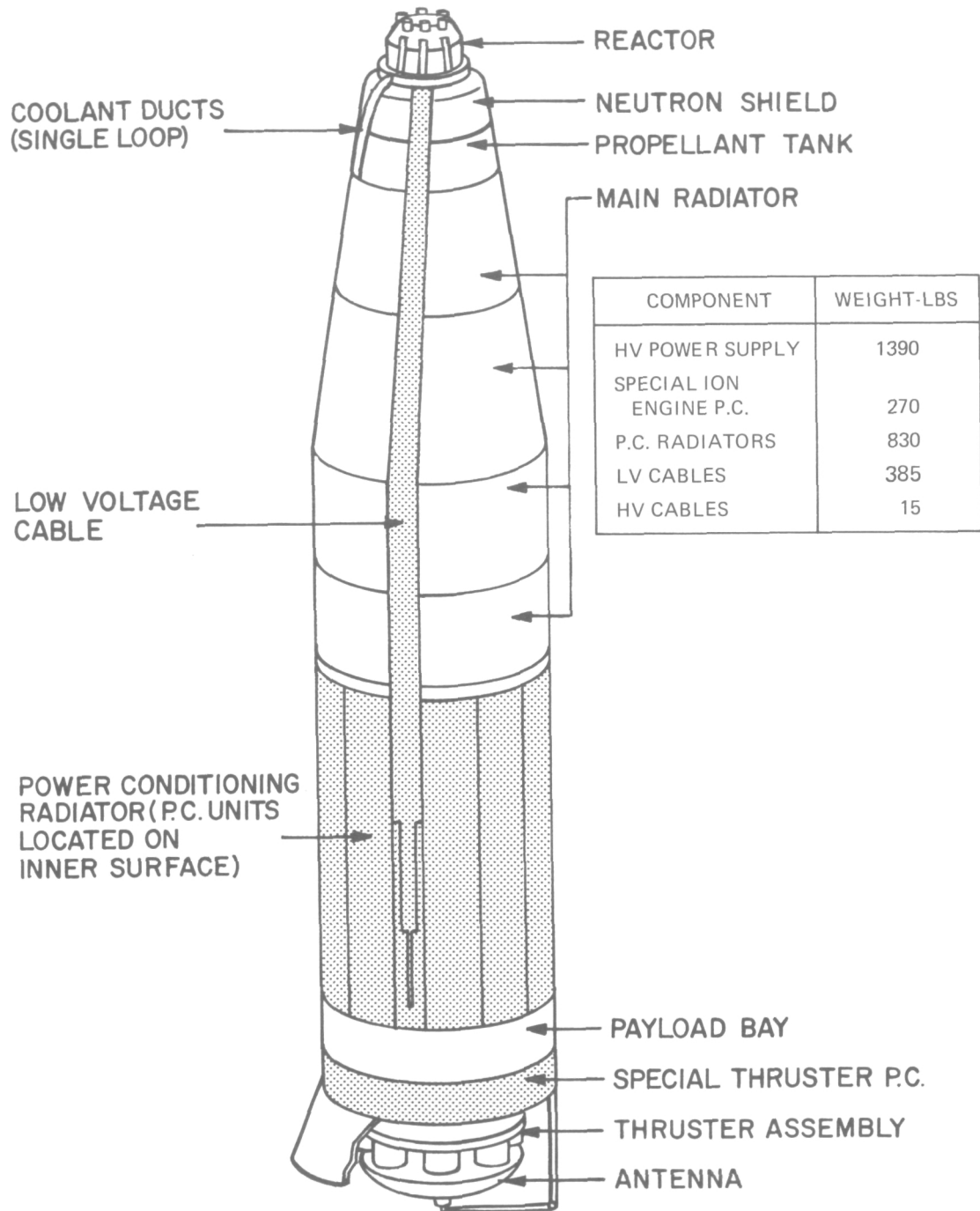
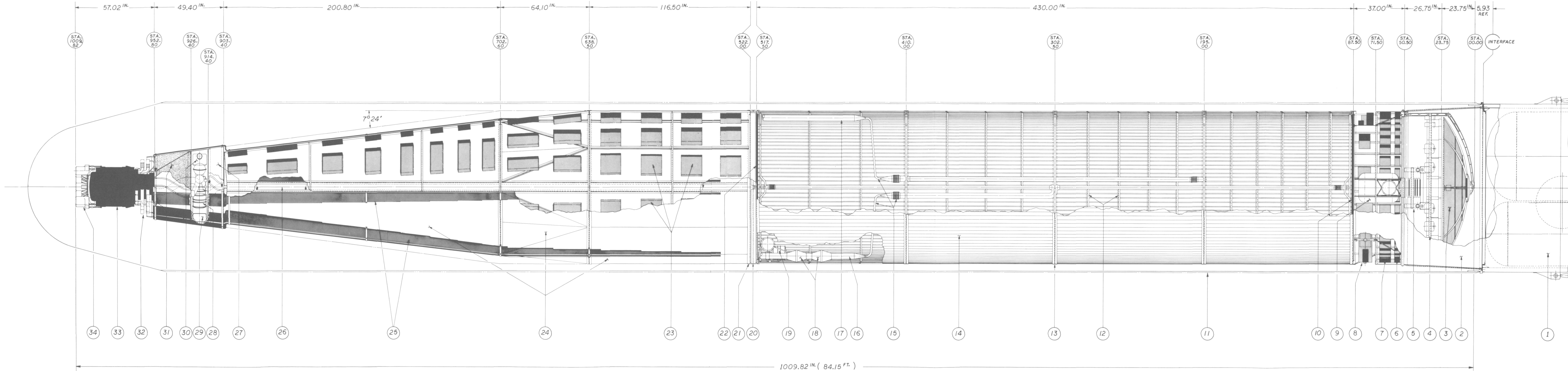


Figure 1-8. Low Voltage Cable Externally Fueled Reactor/Spacecraft

ITEM	DESCRIPTION
1	LAUNCH VEHICLE (TITAN III C-7)
2	PAYLOAD ADAPTER
3	COMMUNICATIONS ANTENNA
4	THRUSTER PLATFORM (37 MERCURY ION ENGINES)
5	TVC SYSTEM
6	THRUSTER ISOLATION UNITS
7	SPECIAL THRUSTER POWER CONDITIONING UNITS
8	PAYLOAD EQUIPMENT BAY
9	MERCURY PROPELLANT TANKS
10	AFT THERMAL RADIATION SHIELD
11	FLIGHT FAIRING
12	STIFFENING RING (TYP)
13	MATING RING (TYP)
14	PRIMARY RADIATOR
15	DIFFERENTIAL EXPANSION COMPENSATION
16	RETURN DUCT
17	FEED DUCT
18	EM PUMPS - RADIATOR LOOP (2)
19	ACCUMULATORS - RADIATOR LOOP (1)
20	AUXILIARY RADIATOR
21	TRANSITION RING
22	FWD THERMAL RADIATION SHIELD
23	POWER CONDITIONING MOUNTING ENVELOPE (TYP)
24	POWER CONDITIONING RADIATOR (MAIN AND HOTEL PC)
25	LOW VOLTAGE CABLES
26	PRIMARY RADIATOR DUCT
27	MERCURY PROPELLANT (GAMMA SHIELDING)
28	ACCUMULATORS - REACTOR LOOP (1)
29	HEAT EXCHANGER
30	EM PUMPS - REACTOR LOOP (2)
31	NEUTRON SHIELD
32	REACTOR EQUIPMENT BAY
33	REACTOR
34	ACTUATORS (12)



240 KWe (NET) THERMIONIC SPACECRAFT
 ("FLASHLITE" THERMIONIC REACTOR)

Figure 1-9. 240 kWe (net) Thermionic Spacecraft Thermionic Reactor - Flashlight

as close as possible to the reactor, again to provide minimum shield volume and weight, with a portion of the mercury propellant located in a tank behind the neutron shield to act as gamma shielding

The power conditioning modules and power conditioning radiator section are located directly behind the shield and propellant tank to minimize the length and, hence, the power losses in the low voltage cable. This is required due to the low voltage, 14 to 16 volts, characteristic of the flashlight reactor. Individual PC modules are distributed uniformly on the surface of the PC radiator, one module per pair of reactor fuel elements and low voltage cables. The cables are strung along the outer surface of the shield and PC radiator surface so that they can radiate their I^2R power losses directly to space.

The PC radiator occupies most the conical surface of the spacecraft plus 9.7 feet of the cylindrical section. A very short section auxiliary radiator surface, together with internal insulation rings, acts as a thermal buffer between the low temperature PC radiator and the high temperature main radiator, which covers most of the cylindrical section surface.

The reactor waste heat is transported to the main radiator in two stages. The first loop pipes the NaK-78 reactor coolant, outside the shield to a heat exchanger placed between the neutron shield and the gamma shield (forward propellant tank). A second NaK-78 loop carries the heat along the outer surface of the PC radiator to the main radiator. This nominal 1300°F duct is insulated from the 175°F power conditioning radiator by combined nickel/aluminum multifoil insulation.

Two series coolant loops are required because of unacceptable coolant activation due to the beryllium or beryllium oxide reflectors used in the flashlight reactor. This differs from the externally fueled reactor because of its heavy metal reflectors, which reduce coolant activation to the point where a single loop is acceptable. Comparing Tables 1-2 and 1-4, it is seen that the externally fueled reactor weighs about 1,000 pounds more than the flashlight reactor. This is more than offset by a 2,300 pound

reduction in the primary heat rejection system for the externally fueled reactor, relative to the flashlight reactor

The payload section, thruster power conditioning section, and ion thruster engines are located in sequence at the rear of the vehicle. A single disk communication antenna is shown in the launch position behind the thruster engines on Figure 1-9. After launch, it would be extended radially, beyond the vehicle diameter and forward of the thruster engines.

Cross-sectional views through the heat exchanger bay, power conditioning radiator, main radiator, and payload sections of the flashlight reactor/spacecraft are presented in Figure 1-10, 1-11, 1-12, and 1-13, respectively.

1.3.2 WEIGHT AND POWER SUMMARY

The weight summary for the reference design spacecraft utilizing the flashlight reactor concept is presented in Table 1-4. In order to provide 240 kWe of power to the thruster system, a gross reactor power output of 316 kWe is required. Total spacecraft weight at launch is 37,605 pounds. Disposable launch vehicle adapter and payload shroud weights result in an Earth orbit spacecraft weight of 36,325 pounds.

Weight of each of the three major spacecraft systems are:

a	Propulsion system	19,330 pounds
b	Propellant system	14,760 pounds
c	Payload system	2235 pounds

For this study, the propellant and payload systems have been defined by the study guidelines. Therefore, this design effort is devoted to configuring a weight optimum propulsion system. Summary of the key characteristics of each subsystem that comprise the propulsion system are discussed in Paragraph 1.3.3.

Electric power utilization for the flashlight reactor concept is summarized in Table 1-5. Net power to the propulsion system is 240 kWe of which 223 kWe are required.

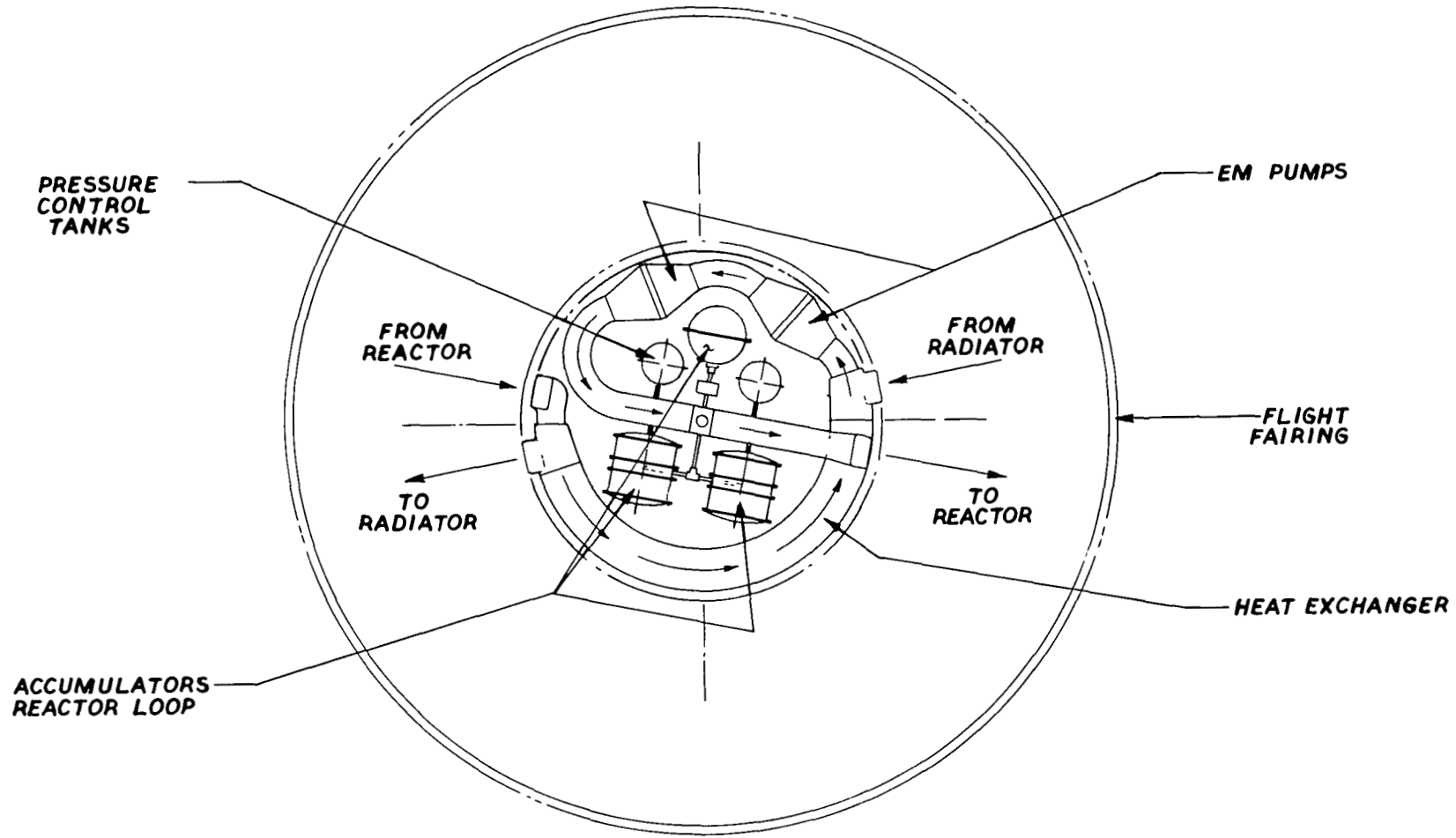


Figure 1-10 Equipment Bay Cross-Sectional View, Flashlight Reactor/Spacecraft

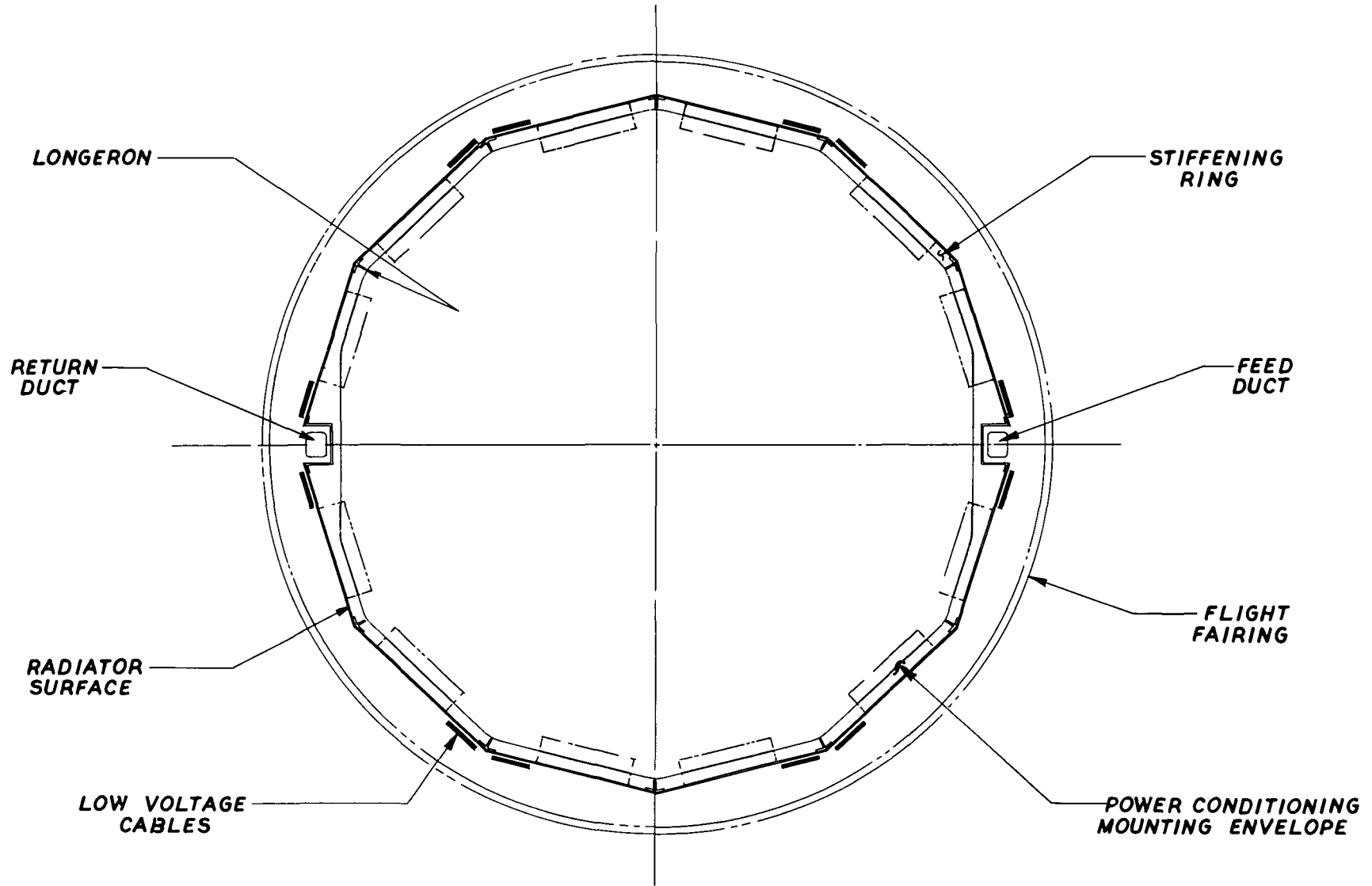


Figure 1-11. Power Conditioning Radiator Cross-Sectional View, Flashlight Reactor/Spacecraft

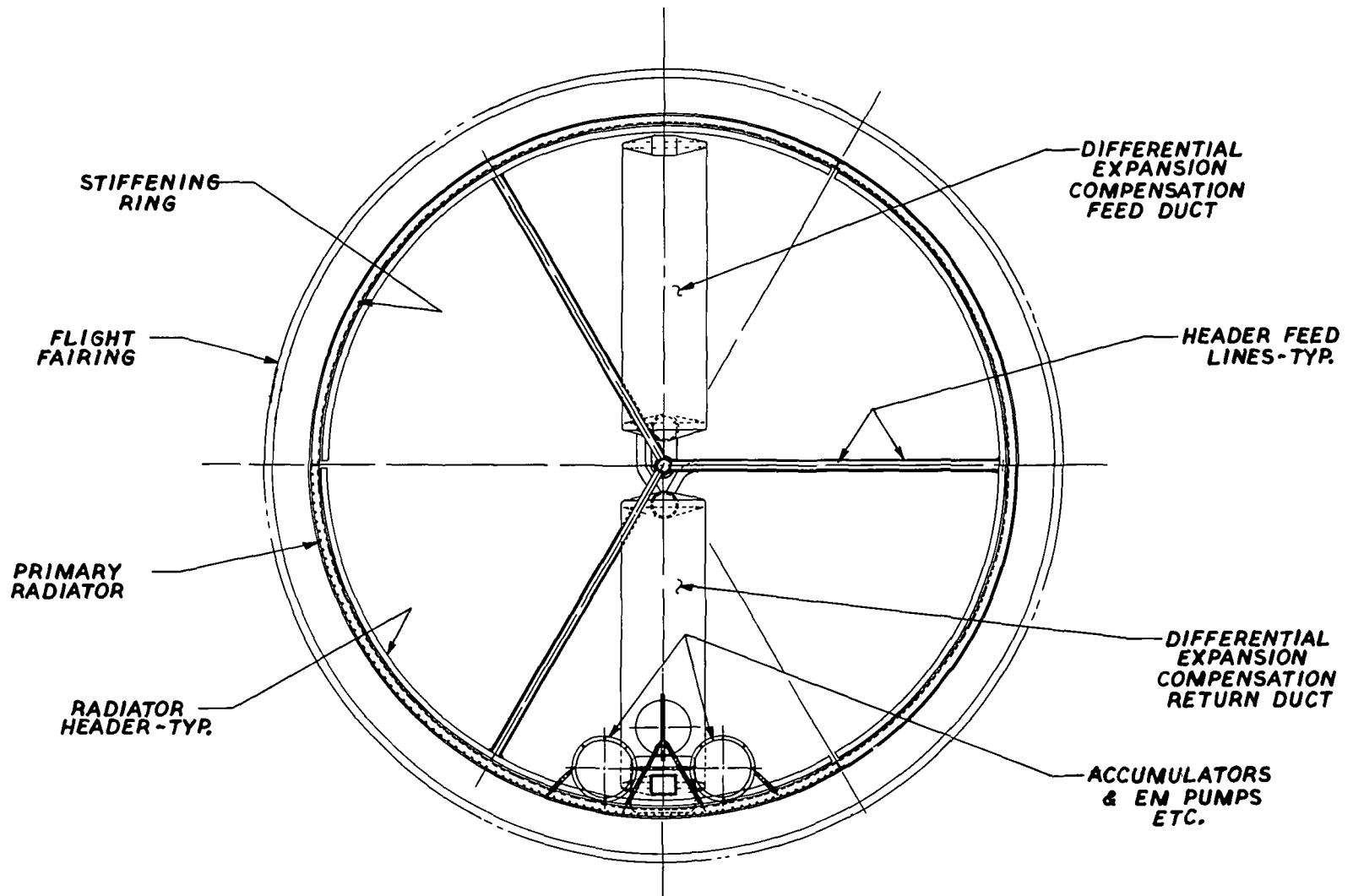


Figure 1-12. Main Radiator Cross-Sectional View,
Flashlight Reactor/Spacecraft

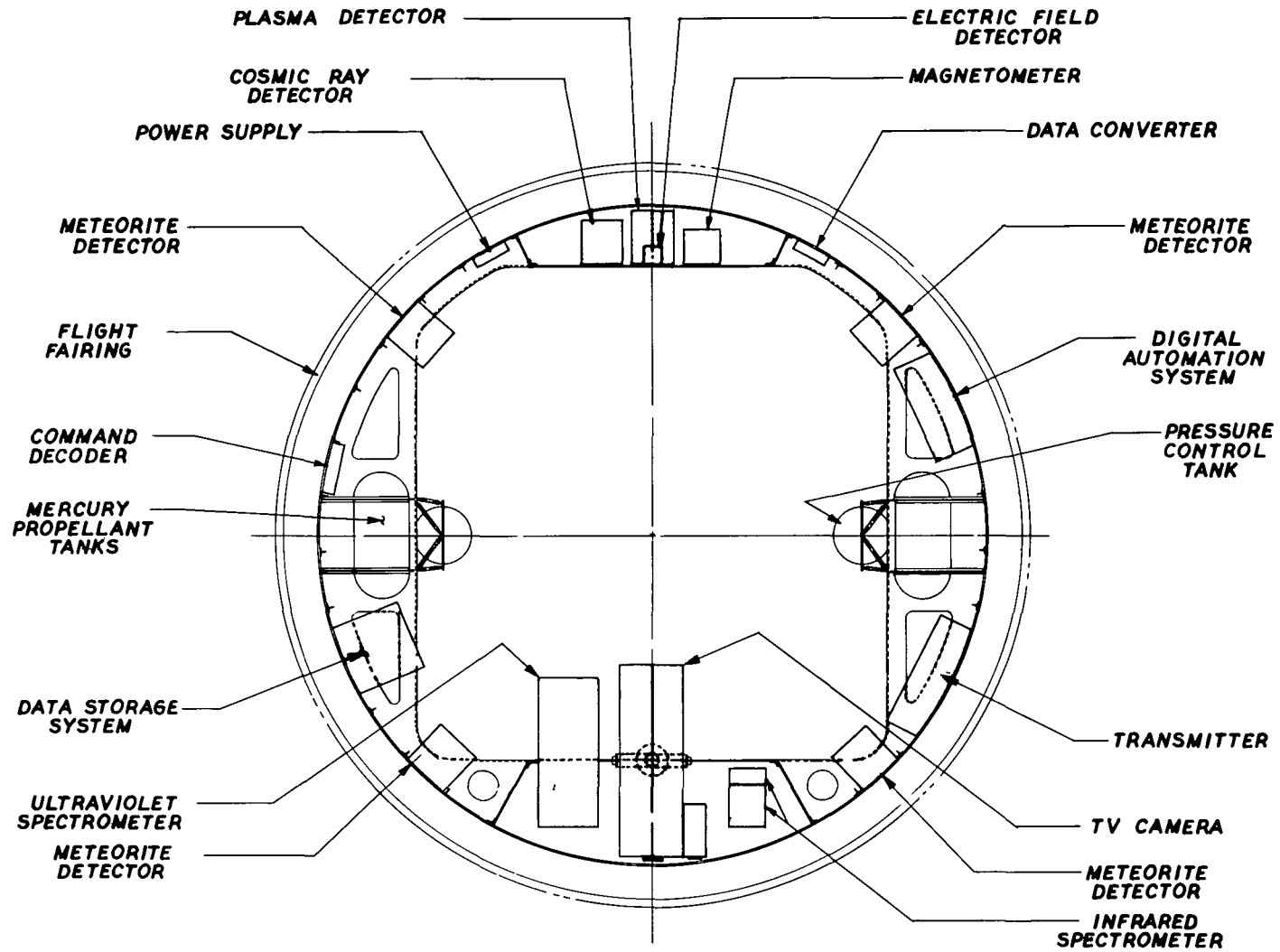


Figure 1-13. Payload Bay Cross-Sectional View,
Flashlight Reactor/Spacecraft

TABLE 1-4. WEIGHT SUMMARY 240 kWe (NET) THERMIONIC SPACECRAFT
(FLASHLIGHT REACTOR)

Component	Weight - Pounds				
Propulsion System					19,330
Power Plant Subsystem Group				12,170	
Reactor Subsystem			3300		
Reactor (Dry)		3060			
Actuators		230			
CS Radiator		10			
Primary Heat Rejection			4840		
Reactor Loop		645			
Ducts	140				
EM Pumps (2)	100				
Accumulators	60				
Coolant	280				
Insulation	65				
Radiator Loop		4195			
Heat Exchanger (Dry)	180				
Ducts	440				
EM Pumps (2)	90				
Accumulators	100				
Main Radiator	2190				
Coolant	985				
Insulation	210				
Shield			1875		
Neutron		1610			
Permanent Gamma		265			
Electric and Controls			340		
Hotel Load		290			
Power Conditioning	185				
Radiator	60				
Distribution Cables	45				
Power Plant Control		50			
Auxiliary Coolant Loop			110		
Ducts		35			
EM Pumps (2)		20			
Accumulators		10			
Radiator		20			
Coolant		25			
Structure			1655		
Reactor Support		60			
Neutron Shield (External)		50			
Power Conditioning Radiator		405			
Area Blocked by LV Cables	225				
Main Coolant Duct	25				
Mating/Stiffening Rings	35				
Longerons	120				
Transition Ring		65			
Main Radiator		1075			
Mating/Stiffening Rings	425				
Longerons	650				
Miscellaneous			50		
Thruster Subsystem Group				7160	
Ion Engine Subsystem			1235		
Ion Engine Units		585			
TVC Unit		550			
Miscellaneous		100			
Power Conditioning Electronics			3220		
HV Power Supply		2640			
Special Ion Engine PC		270			
Thruster Isolation		310			
Power Conditioning Radiators			890		
HV Power Supply		770			
Special Ion Engine Units		70			
Thruster Isolation		50			
High Voltage Power Cables			70		
3100 Volt Cables		25			
250 Volt Cables		35			
Insulation		10			
Low Voltage Power Cables			1680		
Main Bus		1620			
Insulation		60			
Structure			65		
Special P. C. Bay		65			
Propellant System					14,760
Propellant				14,500	
Tanks and Distribution				245	
Structure				15	
Net Spacecraft					2235
Guidance and Control				50	
Communications				60	
Science				2065	
Radiator				25	
Structure				35	
GROSS SPACECRAFT IN EARTH ORBIT					36,325
LAUNCH VEHICLE ADAPTER					250
LAUNCH SHROUD PAYLOAD WEIGHT					
PENALTY (84.3 FT. LONG, 4400 POUNDS SHROUD)					1030
LAUNCH VEHICLE PAYLOAD REQUIREMENT					37,605

TABLE 1-5. ELECTRIC POWER SUMMARY 240 kWe (NET)
THERMIONIC SPACECRAFT (FLASHLIGHT REACTOR)

	POWER - kWe					
Reactor Output						318
Losses and Distribution						
Low voltage cable loss					20.5	
Main P. C. input					297.5	
P. C. loss				35.32		
Main P. C. output				262.18		
3100 volt output			224.53			
Cable losses		0.28				
Thruster interrupter		1.25				
Thruster engine input		223				
250 volt output			37.65			
Payload and ion engine section		19.3				
Cable losses	0.3					
Thruster P. C. input	17.0					
Payload input	1.0					
Spacecraft control input	0.5					
Powerplant control input	0.5					
Hotel load section		18.35				
Cable losses	0.19					
P. C. losses	2.71					
Reactor pump input	8.06					
Radiator pump input	6.5					
Shield pump input	0.16					
Auxiliary pump input	0.03					
Reactor controls input	0.2					
Cesium heater input	0.5					
Net Power to Ion Engines*						240

*The net power to the thrusters is the sum of the ion engine grid power input (223 kWe), after power conditioning, and the special ion engine power requirements (17 kWe).

for the 3100 volt screen supply operation of the ion engines, and 17 kWe are required for other special thruster power conditioning. A total of 316 kWe of reactor output power is required to meet the net 240 kWe requirement

For purposes of mission analysis, 273.1 kWe (P_e) are delivered to the main power conditioning, to deliver 240 kWe to the 31 operating ion engines. This power conditioning operates at an effective efficiency of 85.8 percent, including subsequent high voltage cable and necessary thruster isolation losses

1.3.3 KEY CHARACTERISTICS

A summary of the key characteristics of the reference design spacecraft that utilizes the flashlight reactor is presented in this section. The shield, heat rejection, and power conditioning subsystems are discussed

1.3.3.1 Reactor-Shield Subsystem

Neutron and gamma shielding for the flashlight reactor is shown in Figure 1-14 and is accomplished in the same manner as that described for the externally fueled reactor (Paragraph 1.2.3.1). In the spacecraft powered by the flashlight reactor there is, however, an equipment bay between the lithium hydride neutron shield and the forward tank of mercury propellant, which functions as a gamma shield. The can of lithium hydride is configured as a section of a cone, with a mean diameter of 48 inches and thickness of 26 inches. Total weight of the neutron shield is 1610 pounds

Adequate gamma shielding is provided by 10,800 pounds of mercury propellant in the forward section. The conically shaped propellant tank is 9 inches deep with a mean diameter of 56 inches

The increased gamma and neutron shielding requirement for the flashlight reactor, compared to the externally fueled reactor, is due primarily to the shorter distance between the flashlight reactor and the radiation sensitive power conditioning units

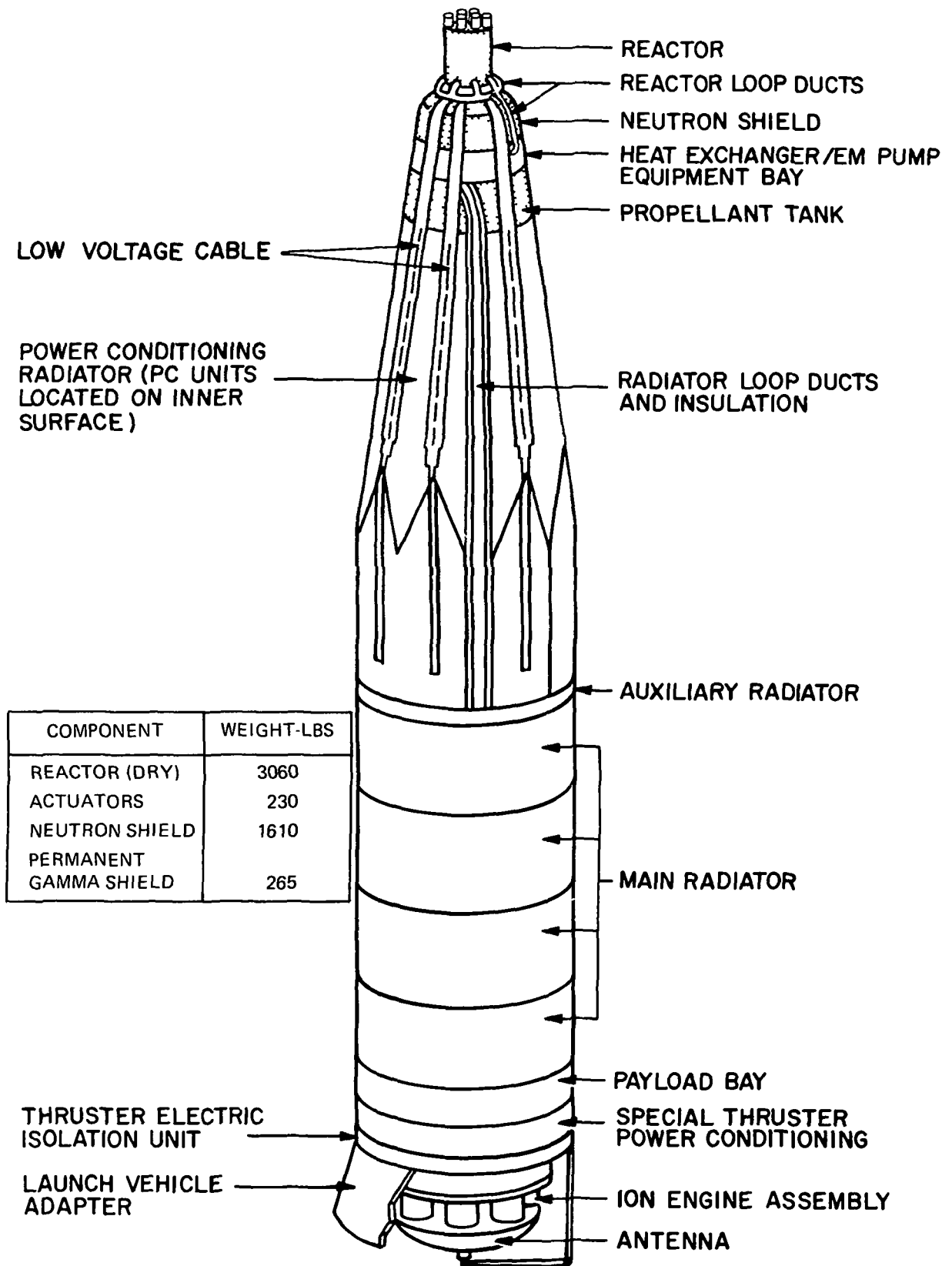


Figure 1-14. Shield Subsystem - Flashlight Reactor/Spacecraft

**PRIMARY HEAT REJECTION SYSTEM WEIGHTS
FLASHLIGHT REACTOR SPACECRAFT**

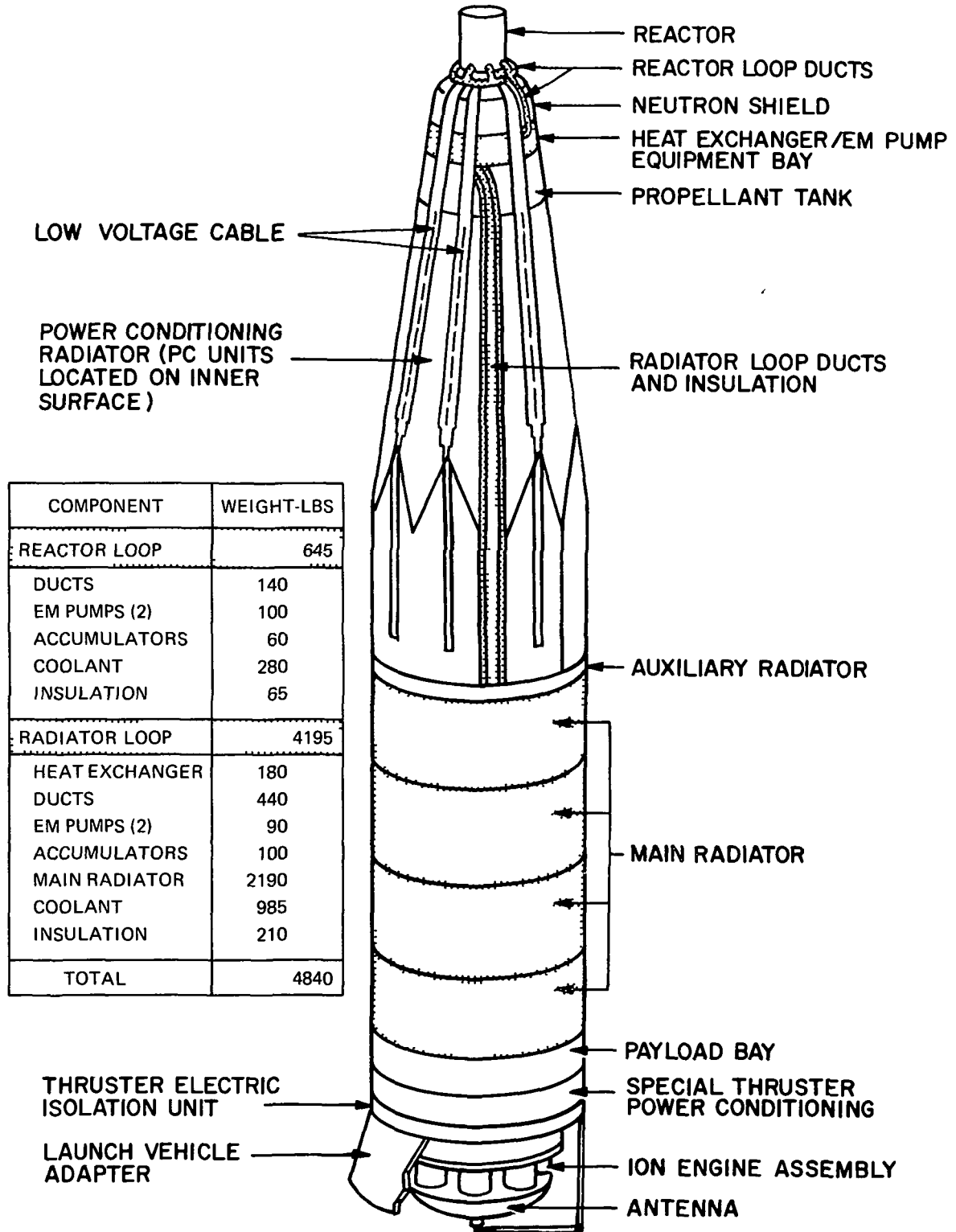


Figure 1-15. Heat Rejection System - Flashlight Reactor/Spacecraft

**AUXILIARY COOLANT LOOP AND SPECIAL ELECTRIC AND CONTROLS
SUBSYSTEM WEIGHTS FLASHLIGHT REACTOR SPACECRAFT**

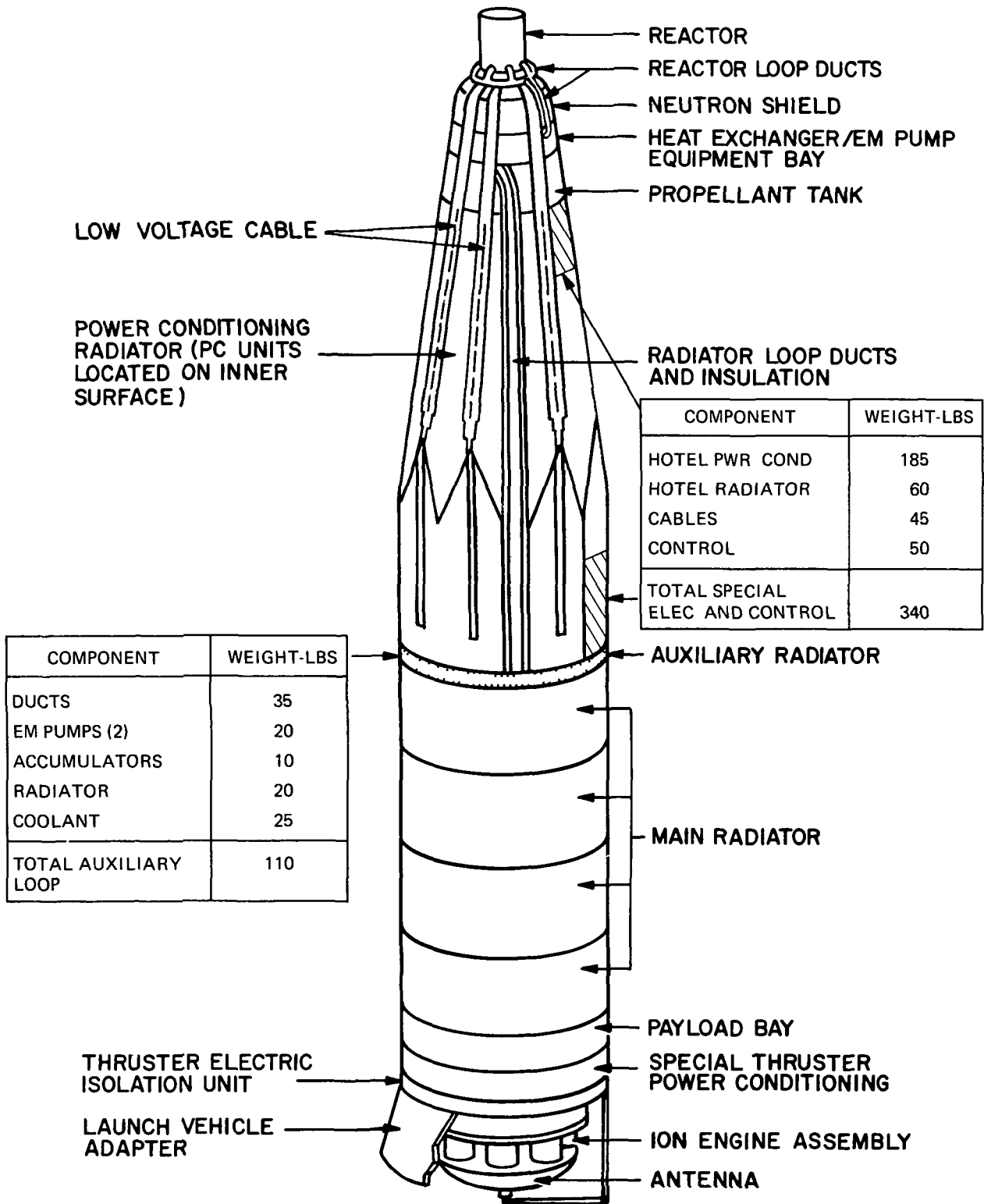


Figure 1-16. Auxiliary Heat Rejection System - Flashlight Reactor/Spacecraft

- Heat exchanger diameter 4.6 inches
- Shell Wall Thickness 0.10 inches
- Tube diameter 0.2 inches
- Number of tubes 433
- Tube wall thickness 0.02 inches
- Tube side pressure drop 1.67 psi
- Cold side pressure drop 4.37 psi

Weight of the dry heat exchanger is 180 pounds

The main radiator has a total area of 945 square feet divided into 4 axial bays with three panels per bay. Each panel covers one-third of a cylindrical lateral surface (120° of arc) and is 9.8 feet wide and approximately 9 feet in axial length. Sixty-five coolant tubes, which run the length of each panel, are joined by solid fin sections of copper-stainless steel construction. The total weight of all panels plus their headers is 2190 pounds. Total weight of the primary heat rejection system is 4840 pounds.

The auxiliary cooling loop, Figure 1-16, provides a thermal heat rejection mechanism for those system components which have temperature limitations lower than the temperatures in the main heat rejection system and higher than the electronic components in the spacecraft. These intermediate components are the electrical and magnetic sections of the EM pumps, and the neutron shield. Self cooling EM pumps force the NaK-78 coolant through cooling passages in the reactor EM pump electrical section, then through cooling passages in the frontal regions of the neutron shield, and is passed through the auxiliary radiator. The cooled flow is then circulated through the cooling passages of the radiator loop EM pump and returned to the auxiliary pump to complete the circuit. Accumulators control the expansion and pressure level of the coolant as in the main heat rejection loops.

The auxiliary radiator is a narrow band, containing a single cooling channel, attached to the 65 pound transition ring between the low temperature PC radiator and the high temperature main radiator. The radiating surface is ten square feet in area and only

4.5 inches wide Its weight is approximately 20 pounds. Total weight of the auxiliary loop is 110 pounds.

1.3.3.3 Power Conditioning

The power conditioning radiator rejects the heat generated in the high voltage supply and the hotel load power conditioners. The portion of the radiator, 35 square feet, corresponding to the hotel load power conditioning waste heat generation, weighs 60 pounds. The remaining radiator area, 558 square feet, is attributable to the main power conditioning. The weight of this portion is 770 pounds, based on 0.10 inch thick aluminum radiator panels.

The radiator heat loads from the special ion engine PC modules and the thruster isolation units located at the base (rear) of the spacecraft, are 1.7 and 1.25 kW, respectively. The corresponding radiator areas and weights are 36 square feet and 70 pounds for the PC modules, and 26 square feet and 50 pounds for the isolation units.

A low voltage cable assembly is a two component arrangement in series: a copper cable extending from the reactor fuel element extension to the front rim of the neutron shield, and an aluminum bus bar to a power conditioning module. A low voltage cable assembly is attached to each of the 216 reactor fuel elements. Path of the low voltage cable along the spacecraft and the power conditioning equipment is shown in Figure 1-17. Because of the low voltage (14 to 16 volts) transported by the cable and resultant high I^2R power losses, the power conditioning radiator with attached modules was located at the forward end of the spacecraft. One hundred and eight power conditioning modules, constituting the high ion engine screen grid (3100 volts) and medium hotel load (250 volts) power supply, are distributed on the inner surface of the power conditioning radiator panels. The integrated high/medium voltage supply power conditioning modules weigh 2640 pounds

The high voltage cable subsystem consists of the 3100 volt lines between the main power conditioning modules and the ion engines and the 250 volt lines between the main power conditioning modules and the hotel load, special payload, and thruster power conditioning modules.

MAJOR ELECTRIC SUBSYSTEM WEIGHTS
FLASHLIGHT REACTOR SPACECRAFT

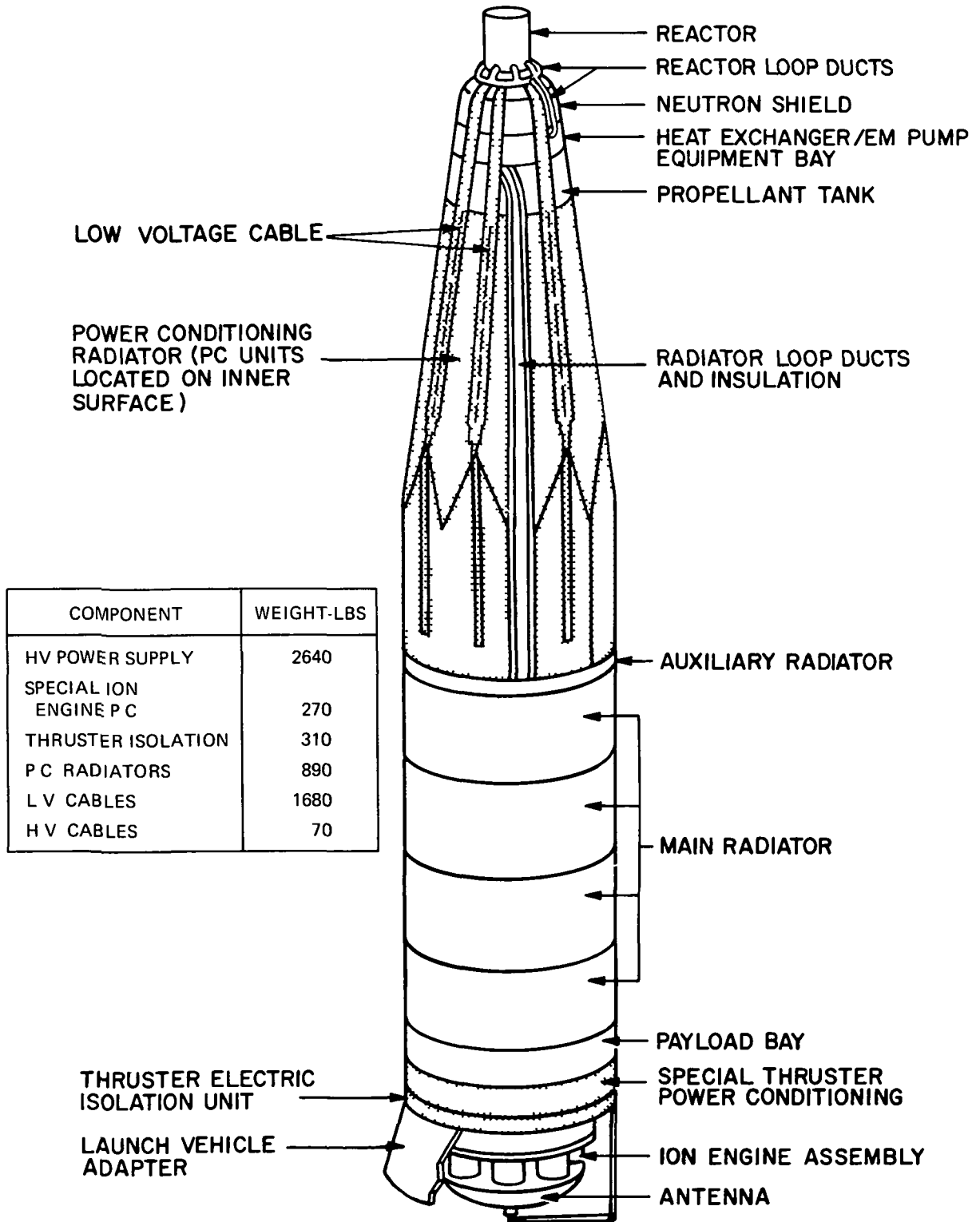


Figure 1-17. Low Voltage Cable-Flashlight Reactor/Spacecraft

The 3100 volt cabling consists of four separate wires forming two complete circuits. The extra circuit provides greatly increased reliability with negligible penalty. The cable starts at the rear end of one side panel of the PC radiator, runs forward the entire length of that panel, then returns down the length of an adjacent panel. This procedure, picking up the output power of all the main PC units, occurs across the six side panels of the PC radiator. The cable then traverses the axial length of main radiator and payload sections to reach the ion engines.

The 250 volt line to the payload and thruster PC modules is of similar 4 strand construction and follows the same path. The level of 250 volts was selected from the moderately high voltage line because of the rather low I^2R power losses and its convenience in designing hotel load power conditioning equipment compared to the low voltage (14 to 16 volts) cable. Difficulty of power handling and of power conditioning component selection precluded use of 3100 volts for these lines.

The power plant electric system consists of the hotel power conditioning units, and their radiators, plus the cabling to the pumps and equipment using the power. The special power conditioning modules convert a 250 volt input power to the voltages required for the EM pumps and the reactor controls. Total hotel power conditioning weight is 185 pounds.

1.4 COMMON PARAMETERS

To aid in the design of the thermionic spacecraft and the comparison of the two propulsion systems, whose characteristics have been summarized in Subsections 2.1 and 2.2, a group of mission and component parameters which are common to both reactor concepts has been established. The following basic study ground rules define the mission objectives and remain constant throughout the study:

- Mission Definition - 600 day, unmanned Jupiter orbiter mission.
- Launch Vehicle Interface - Spacecraft initial mass in earth orbit of 30,000 pounds to be placed in 750 nautical mile circular orbit by Titan III C/7.
- Payload - 2205 pounds based on Navigator studies and the Mariner program.

- Thruster - 37 mercury ion engines (including 6 spares), weighing 1233 pounds, based on current technology.
- Reactor Lifetime - Full power reactor operating time is 10,000 hours.
- Propellant - 14,500 pounds of mercury propellant is required to accomplish mission.
- Radiation Limits - The integrated neutron flux shall not exceed 10^{12} nvt for neutron energy levels > 1 Mev; the integrated gamma dose shall not exceed 10^7 rads.
- Maximum power conditioning temperature of 200°F
- NaK-78 coolant in all active coolant loops
- Stainless steel coolant containment material
- Copper-stainless steel material for active radiators

Furthermore, common characteristics identified in this study for the externally fueled reactor concept and the flashlight reactor power plants are listed below:

- Sink Temperature - approximate mean sink temperature for entire mission is 300°R.
- Aluminum material for passive radiators
- Active shield cooling mode
- No parallel cooling loops
- One working and one redundant pump in each cooling loop
- Maximum shield temperature of 1000°F
- Reactor controls power requirement of 0.2 kWe
- Cesium reservoir power requirement of 0.5 kWe.

2. INTRODUCTION

2. INTRODUCTION

A design study program of thermionic reactor power systems for nuclear electric propelled, unmanned spacecraft was initiated by the General Electric Company on February 4, 1969 for the Jet Propulsion Laboratory under Contract Number JPL 952381. The purpose of this program is to provide designs of selected thermionic reactor power systems integrated with nuclear electric unmanned spacecrafts over the range of 70 to 500 kWe unconditioned power. The key design objective is a weight of 10,000 pounds, including reactor, shielding, structure, radiators, power conditioning, and thruster subsystems at a 300 kWe unconditioned power level. Spacecraft propulsion will be provided by mercury electron bombardment ion thruster engines.

The design study is performed in two consecutive phases:

- a. Phase I - Design of unmanned spacecraft and power plant configurations, including power plants with emphasis on state-of-art technology. Key ground rules include:
 1. 300 kWe unconditioned power
 2. NaK-78 coolant
 3. 1350°F reactor outlet temperature
 4. Copper-stainless steel conduction fin radiators
 5. 200°F maximum electronic component temperature limits
 6. 10,000 pounds power plant weight (design objective)
 7. 10,000 to 15,000 full power hours.

- b. Phase II - Emphasis on weight reduction techniques and the investigation of the effect of key parameters on power performance:
 1. Power level: 70 to 500 kWe
 2. Coolant: substitution of lithium for NaK-78

3. Radiator type: the use of beryllium/stainless steel or vapor fin radiators
4. Extended life: 20,000 full power hours

In the first phase of this study, two spacecraft designs were completed. These designs are based on the externally fueled diode thermionic reactor, utilizing reactor data supplied by the Republic Aviation Division of the Fairchild-Hiller Corporation, and a flashlight thermionic reactor, utilizing reactor data supplied by Nuclear Systems Programs of the General Electric Company. These two spacecraft designs are based upon the results of a spacecraft weight optimization computer code which was developed during the Phase I of the study. The scope of the designs presented include detailed spacecraft layouts, and detailed weight summaries, including a discussion of the major causes for weight differences between the two spacecraft based on different reactor designs.

This report also presents the study design guidelines, including the definition of the reactors, the payload and ion engines. Launch vehicle capabilities are discussed, and structural requirements are defined. A discussion of coolant activation, shield analysis and electric power processing design precedes the detailed design definition of the two spacecraft.

Some preliminary results in the Mission Operations area are presented, including power plant startup, pre-launch operations, and aerospace nuclear safety.

3. STUDY GUIDELINES

3. STUDY GUIDELINES

Program guidelines have been identified for the design study of a thermionic reactor powered spacecraft. System requirements and subsystem definition that comprise the established guidelines are presented in the following sections.

3.1 SYSTEM REQUIREMENTS

System requirements that have been defined for this study are summarized below:

- a. Reference powerplant shall provide 10,000 to 15,000 effective full power hours at a nominal 300 kWe gross reactor unconditioned electric power output.
- b. The spacecraft system shall be designed for launch by the Titan III C/7, and shall be compatible with the launch environment of this vehicle.
- c. The reference point for the launch vehicle/spacecraft interface shall be 30,000 pounds delivered into a 750 nautical mile circular orbit.
- d. The reference mission is a Jupiter planetary orbiter. Starting from the 750 nautical mile circular orbit, the 30,000 pound spacecraft will spiral away from earth (~50 days) and begin the trip to Jupiter. The following times and power levels are applicable

Mission Mode	Power Level (kWe)	Time (days)
Initial Thrust	300	210
Coast	30	120
Final Thrust	300	270
Jupiter Orbit	30	(one orbit, 17 days minimum)

- e. The meteoroid model will be compatible with the following models:

1. Penetration Model

$$t = 0.5 m^{0.352} \rho_m^{1/6} v^{0.875}$$

where

t = armor thickness, cm

ρ_m = meteoroid density, gm/cm³

m = meteoroid mass, gm

v = meteoroid velocity, km/sec

2. Meteoroid Flux

$$\Phi = \alpha m^{-\beta}$$

where

Φ = cumulative meteoroid flux, number particles/m² sec

α = empirical coefficient

β = empirical exponent

m = meteoroid mass, gm

3. Probability of Penetration

The non-puncture probability is,

$$P_{(0)} = e^{-\Phi AT}$$

where

$P_{(0)}$ = non-puncture probability

Φ = cumulative meteoroid flux, number particles/m² sec

A = projected vulnerable area of the spacecraft (radiator), m²

T = exposure time, seconds

The baseline data listed below is used in conjunction with the previous models to calculate an equivalent near earth meteoroid protection requirement:

$$\bar{\rho}_m = 0.5 \text{ g/cm}^3$$

$$\bar{v} = 20 \text{ km/sec}$$

$$\alpha = 6.62 (10)^{-15}$$

$$\beta = 1.34$$

$$P_{(O)} = 0.95$$

$$T = 7.2 (10)^7 \text{ sec [20,000 hr]}$$

Then, an effective thickness, t_{eff} , for the Jupiter orbiter may be calculated from

$$t_{\text{eff}} = 0.432 t \text{ (Jupiter)}$$

The radiator models used in this study have been developed from the SPARTAN III computer code (Reference 1) results and are based on the preceding near earth meteoroid protection requirement.

f. The reference design shall be based on:

1. NaK-78 coolant at 1350° F reactor outlet temperature
2. Electromagnetic pumps
3. Payload, power conditioning, and communications shielded to 10^{12} NVT > 1 mev, and 10^7 rad γ . Credit should be taken for attenuation from nonshielding materials.
4. 14,500 pounds of mercury propellant
5. A stainless-steel tube, copper fin, nondeployable radiator.

g. Power Conditioning

1. The power conditioning concepts identified in the reactor design studies will be evaluated and power conditioning systems will be defined which meet system requirements. Power conditioning module temperature is not to exceed 200° F.

2. Reactor control concepts will be those specified by the reactor contractors. The externally fueled reactor is controlled by maintaining constant voltage; whereas, the flashlight reactor is controlled by maintaining constant emitter temperature.

h. Payload and Communications

1. The total payload and communications system will be assumed to weigh 2200 pounds.
 2. The total power requirement for this system is assumed to be one kWe. Electrical component temperature limit is 200° F.
- i. Since reliability of individual components is unknown at this time, a reliability goal will not be established for the spacecraft. Emphasis will be placed on suitable configuration, light weight, careful design, and good engineering judgement.

3.2 SUBSYSTEM DEFINITION

Characteristics of the externally fueled and flashlight reactor concepts have been provided by the reactor contractors. Also, characteristics of the thruster, science payload, communications, and thermal control subsystems have been identified; these systems are common to each of the thermionic reactor spacecraft concepts.

3.2.1 REACTOR DEFINITION

This study was initially directed toward the evaluation of the impact of three reactor types on the spacecraft configuration and weight. Under study by three separate contractors, these reactors are:

- a. Externally fueled diode/Fairchild Hiller
- b. Flashlight/General Electric
- c. Pancake/Gulf General Atomic

These different reactor configurations are illustrated in Figures 3-1, 3-2, and 3-3, respectively.

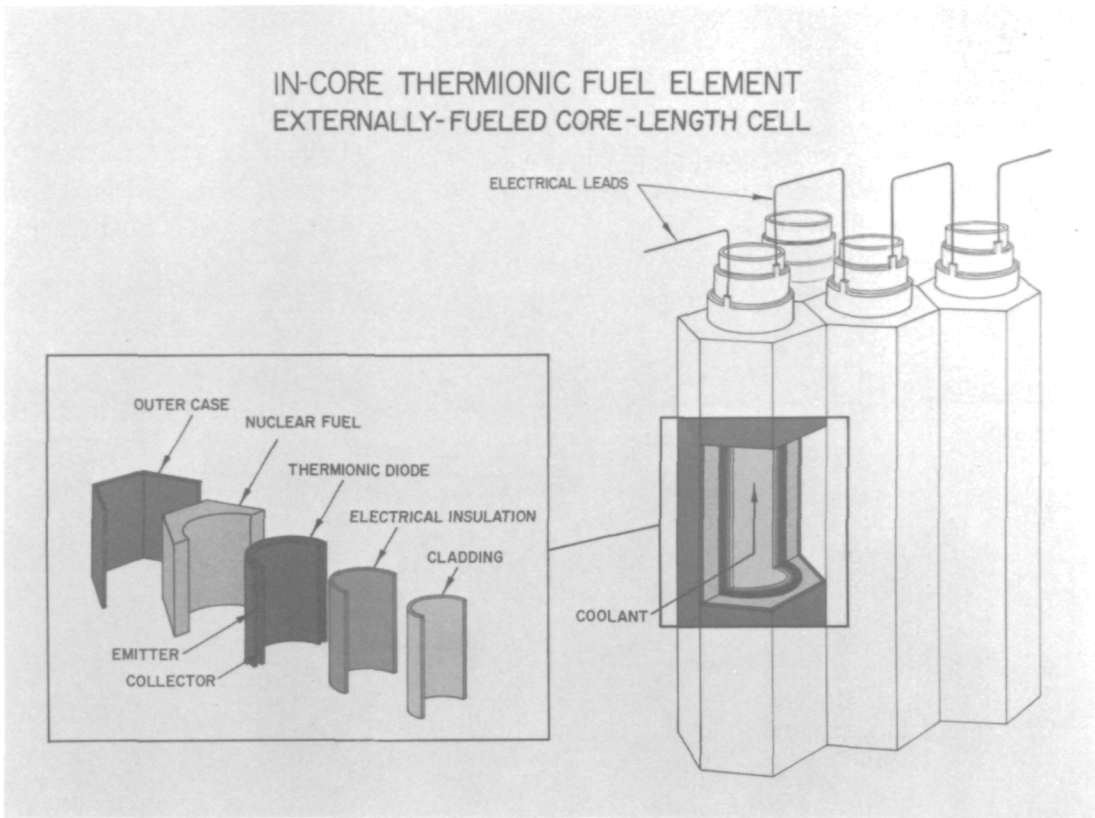


Figure 3-1. Externally Fueled Diode Reactor Concept

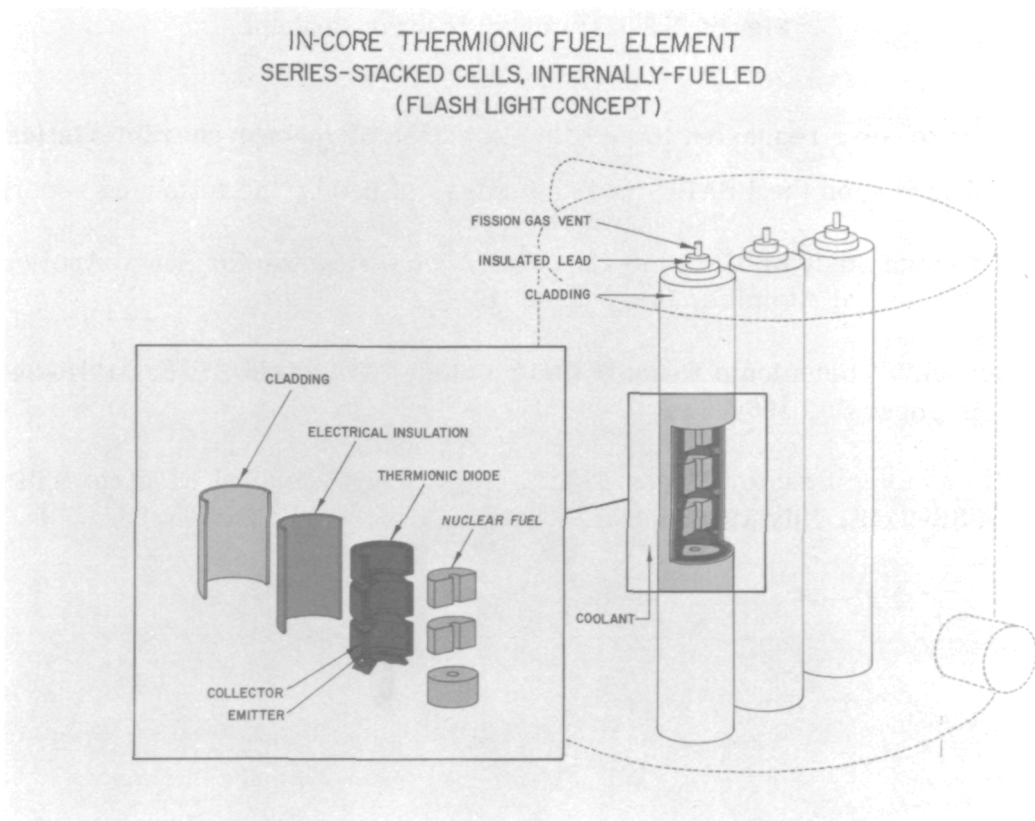


Figure 3-2. Flashlight Reactor Concept

IN-CORE THERMIONIC FUEL ELEMENT
SERIES CELL INTERNALLY-FUELED
(PANCAKE CONCEPT)

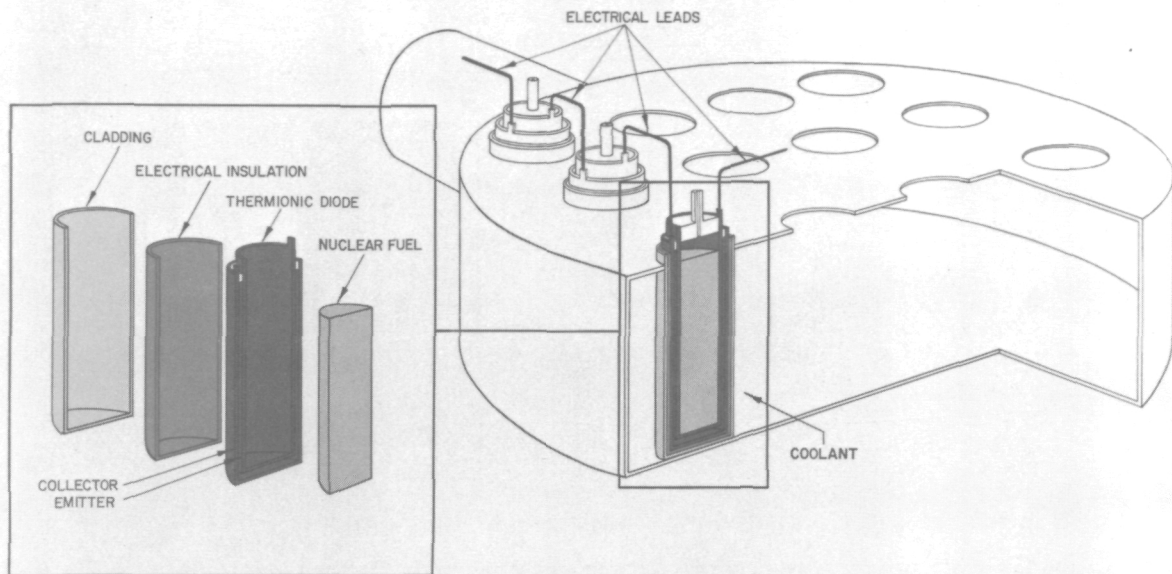


Figure 3-3. Pancake Reactor Concept

The contractors were requested to provide definition of reactor characteristics for this study, based upon the USAEC funded studies defined by the following reports:

- a. A Design Study of The Unit-Cell Thermionic Reactor for Space Application, Gulf General Atomics, Inc., GA-8917
- b. 300-ekW Thermionic Reactor Design Study, Fairchild Hiller, FHR-3428-2 September 30, 1968.
- c. Thermionic Reactor Power Plant Design Study, General Electric NTPO, GESR-2115, July 1968.

The additional reactor information was requested. The data presented below was supplied.

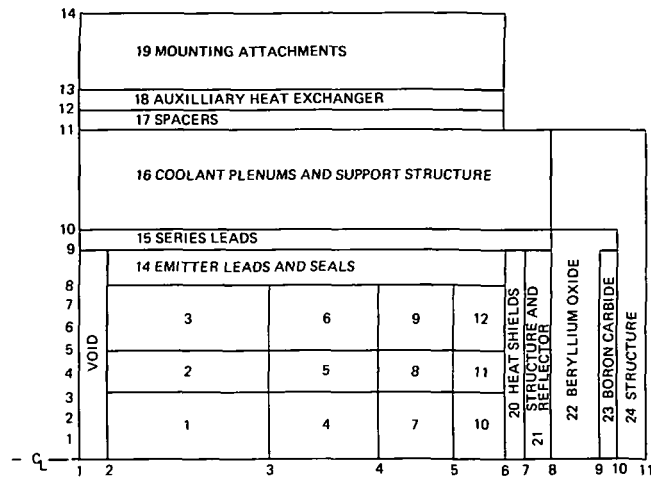
3.2.1.1 Externally Fueled Diode Reactor

The basic element of the Fairchild Hiller thermionic reactor is the converter module. Each module consists of a fuel element which surrounds a cylindrical emitter. Co-axial with and inside the emitter is the cylindrical collector separated from the emitter by a 10 mil gap. Inside the collector is the liquid metal coolant. The module configuration is different from other designs in that the fuel is external to the emitter. This geometry allows the maximum fuel volume fraction in the core.

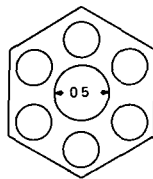
Two alternative fuel element configurations were considered. These are illustrated in Figure 3-4. One of the alternatives utilizes an hexagonal "revolver" body, in which the central emitter hole is surrounded by six fuel chamber holes loaded with bulk UO_2 fuel. The other alternative examined is an annular cylindrical cermet fuel element, containing 93 percent enriched U-235, with the UO_2 not exceeding 60 volume percent of the fuel.

The externally fueled reactor consists of 624 fueled converter modules, configured in an essentially cylindrical reactor core. The diodes are arranged in a triangular lattice with a uniform center-to-center distance of 1.33 inches. The cylindrical modules are separated by 0.060 inch vacuum gaps.

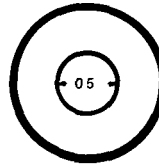
The maximum emitter temperature in the reactor is 3270°F (1800°C) and the cesium reservoirs operate at 675°F. The NaK coolant nominal flow rate is 234 gpm, corresponding to an average velocity of 6.5 ft/sec and a core pressure drop of 0.53 psi. The collector temperature varies from 1096°F to 1404°F.



FUEL EMITTER GEOMETRY



HEXAGONAL REVOLVER



CYLINDRICAL CERMET

Figure 3-4. Typical Reactor Geometry - Externally Fueled Diode Reactor

Radial power flattening is achieved by arranging the 624 diodes in four concentric rings and varying the emitter diameters from 0.50 inch for those diodes in the outer ring to about 0.71 inch in the innermost ring. The outer diameter of all diodes in the core, however, is constant. Thus, the further a diode is from the center of the core, the higher is its fuel volume fraction. With the above dimensions, the fuel volume fraction of a diode in the innermost ring is 75 percent of that of one in the outer ring. Axial flattening is achieved by varying the UO_2 fraction in the fuel from 50 percent at the midplane to 60 percent at each end. This flattening produces, over the whole core, a variation in the maximum emitter temperature of less than $15^\circ F$. The emitter power density varies from 8.53 to 8.64 watts/cm².

Around the periphery of the core are heat shields, radial reflector, control drums, and structure. Axially there are the emitter leads, series leads, coolant plenums, and support structure.

The 624 converters in the core are arranged electrically into 156 series-connected groups, each consisting of four converters in parallel, one from each ring. The reactor is designed for an unconditioned power output of 332 kW at beginning-of-life. Assuming 10 percent converter failures (20 percent power degradation), this yields an end-of-mission conditioned power of 240 kW at the electric thrusters.

The baseline reactor design produces 300 kWe gross at the end of mission. As discussed in Section 8, only about 274 kWe gross are required to provide the 240 kWe required by the thrusters. The reactor characteristics for both the 300 kWe gross, and for the 274 kWe gross are presented on Tables 3-1 and 3-2, respectively. The data on these tables are taken from the computer printout sheets supplied by Fairchild-Hiller for this study.

Representative reactor geometry is presented on Figure 3-4, for which the corresponding dimensions are presented on Table 3-3. The material composition for each region is summarized on Table 3-4.

3.2.1.2 Flashlight Reactor Characteristics

The flashlight reactor utilizes a twelve of diodes stacked in series to form a Thermionic Fuel Element (TFE). A total of 216 TFE's are grouped together to form the active core of the nominal, 300 kWe gross flashlight reactor, as illustrated in Figure 3-2.

Details of the reactor electrical characteristics and the constant emitter temperature reactor control are presented in Reference 1. The TFE units are series connected in pairs, with the center connection grounded. Each TFE pair requires an individual power converter so that the electrical operation of each TFE can be adjusted

TABLE 3-1. EXTERNALLY FUELED DIODE REACTOR
CHARACTERISTICS - 300 kWe EOM

T _O = 2073 K T _R = 630 K Core Height = 10 in. Reactor Height = 20 in. Output Power = 300 kw (EOM) = 360 kw (BOM)							
Coolant Outlet Temperature (F)	Coolant Temperature Rise (F)	Reactor Terminal Voltage (volt)	Thermal Power (kw)	Reactor Diameter (in)	Reactor Weight (lb)	Coolant Flow Rate (gpm)	Core Pressure Drop (psi)
1100.	50.	59.74	3937.	33.33	4002.	3285.	73.54
1100.	50.	83.01	2921.	32.23	3727.	2352.	55.83
1100.	50.	100.39	2535.	32.81	3872.	1997.	33.59
1100.	50.	122.12	2312.	34.89	4406.	1793.	14.12
1100.	100.	60.03	3927.	33.38	4014.	1638.	19.12
1100.	100.	83.71	2918.	32.34	3755.	1175.	14.30
1100.	100.	103.72	2559.	33.12	3950.	1010.	8.26
1100.	100.	123.76	2331.	35.28	4510.	905.	3.40
1100.	200.	60.76	3884.	33.49	4044.	810.	4.81
1100.	200.	84.42	2904.	32.69	3841.	585.	3.39
1100.	200.	104.13	2569.	33.73	4105.	508.	1.84
1100.	200.	124.54	2372.	36.33	4794.	462.	0.69
1100.	400.	65.52	3723.	33.95	4162.	386.	1.02
1100.	400.	92.76	2906.	34.32	4257.	293.	0.54
1100.	400.	109.41	2627.	36.28	4780.	261.	0.24
1100.	400.	130.48	2629.	41.43	6264.	261.	0.06
1200.	50.	59.77	3944.	33.24	3979.	3292.	76.04
1200.	50.	82.70	2922.	32.00	3671.	2353.	60.35
1200.	50.	100.68	2539.	32.41	3773.	2001.	38.49
1200.	50.	120.16	2280.	34.06	4190.	1764.	17.69
1200.	100.	59.03	3949.	33.25	3981.	1648.	20.18
1200.	100.	82.81	2926.	32.02	3677.	1178.	16.04
1200.	100.	101.05	2544.	32.48	3789.	1003.	10.10
1200.	100.	121.41	2288.	34.18	4221.	885.	4.57
1200.	200.	59.39	3954.	33.30	3996.	826.	5.31
1200.	200.	82.34	2928.	32.13	3702.	590.	4.17
1200.	200.	101.95	2545.	32.67	3837.	502.	2.55
1200.	200.	120.89	2302.	34.57	4321.	446.	1.10
1200.	400.	61.89	3896.	33.52	4051.	406.	1.29
1200.	400.	85.73	2917.	32.74	3854.	294.	0.91
1200.	400.	102.12	2567.	33.73	4105.	254.	0.50
1200.	400.	125.23	2384.	36.46	4830.	233.	0.18
1200.	600.	66.37	3731.	34.01	4177.	258.	0.47
1200.	600.	90.14	2880.	34.29	4249.	193.	0.25
1200.	600.	109.91	2630.	36.49	4837.	174.	0.10
1200.	600.	132.50	2707.	42.69	6650.	180.	0.02
1350.	50.	61.36	3799.	33.26	3986.	3159.	69.63
1350.	50.	84.99	2868.	32.31	3748.	2303.	52.07
1350.	50.	101.22	2512.	32.65	3832.	1977.	34.71
1350.	50.	122.33	2284.	34.37	4271.	1767.	16.09
1350.	100.	61.39	3830.	33.25	3983.	1593.	18.88
1350.	100.	83.46	2876.	32.21	3723.	1155.	14.49
1350.	100.	101.47	2518.	32.56	3809.	991.	9.62
1350.	100.	121.65	2278.	34.21	4228.	881.	4.49
1350.	200.	60.37	3885.	33.23	3978.	810.	5.24
1350.	200.	82.86	2901.	32.08	3692.	584.	4.15
1350.	200.	101.71	2531.	32.44	3779.	499.	2.73
1350.	200.	121.02	2278.	34.03	4183.	441.	1.28
1350.	400.	59.03	3954.	33.27	3989.	413.	1.44
1350.	400.	82.07	2933.	32.06	3687.	296.	1.16
1350.	400.	100.58	2543.	32.48	3789.	251.	0.74
1350.	400.	121.11	2298.	34.25	4239.	223.	0.33
1350.	600.	60.29	3946.	33.43	4029.	275.	0.64
1350.	600.	85.56	2952.	32.49	3791.	199.	0.47
1350.	600.	102.73	2573.	33.20	3971.	169.	0.28
1350.	600.	123.43	2360.	35.53	4578.	153.	0.11
1500.	50.	66.49	3556.	33.69	4094.	2935.	52.79
1500.	50.	89.75	2787.	33.53	4053.	2229.	32.81
1500.	50.	106.59	2519.	34.18	4221.	1983.	21.31
1500.	50.	125.75	2347.	36.46	4830.	1825.	9.16
1500.	100.	65.79	3595.	33.60	4073.	1485.	14.73
1500.	100.	88.99	2798.	33.28	3990.	1120.	9.54
1500.	100.	105.31	2513.	33.85	4136.	989.	6.27
1500.	100.	124.18	2330.	36.00	4703.	905.	2.74
1500.	200.	64.29	3673.	33.45	4033.	761.	4.34
1500.	200.	86.75	2822.	32.84	3879.	566.	3.03
1500.	200.	103.60	2512.	33.31	3997.	495.	2.01
1500.	200.	122.94	2307.	35.23	4497.	447.	0.90
1500.	400.	60.84	3823.	33.29	3993.	398.	1.34
1500.	400.	83.60	2881.	32.29	3742.	290.	1.03
1500.	400.	101.26	2526.	32.64	3830.	249.	0.69
1500.	400.	121.60	2291.	34.33	4260.	222.	0.32
1500.	600.	60.48	3938.	33.31	3997.	274.	0.66
1500.	600.	84.11	2942.	32.16	3710.	198.	0.53
1500.	600.	101.46	2558.	32.53	3802.	168.	0.34
1500.	600.	121.57	2309.	34.23	4233.	149.	0.16
1500.	800.	60.22	3975.	33.41	4024.	208.	0.38
1500.	800.	84.33	2967.	32.34	3755.	150.	0.29
1500.	800.	101.66	2583.	32.92	3900.	128.	0.18
1500.	800.	123.40	2357.	35.02	4441.	115.	0.07
1600.	50.	70.60	3398.	34.42	4283.	2790.	38.11
1600.	50.	93.88	2766.	35.18	4485.	2210.	19.27
1600.	50.	110.86	2569.	36.23	4767.	2029.	12.00
1600.	50.	129.63	2476.	39.48	5685.	1944.	4.53
1600.	100.	70.11	3433.	34.24	4236.	1411.	10.92
1600.	100.	93.02	2767.	34.74	4368.	1105.	5.85
1600.	100.	108.71	2546.	35.64	4605.	1004.	3.72
1600.	100.	127.87	2435.	38.62	5435.	953.	1.45
1600.	200.	68.25	3512.	33.93	4156.	724.	3.38
1600.	200.	90.74	2778.	33.97	4167.	556.	2.02
1600.	200.	108.13	2532.	34.73	4363.	499.	1.30
1600.	200.	127.44	2381.	37.23	5042.	464.	0.54
1600.	400.	64.18	3672.	33.50	4045.	381.	1.15
1600.	400.	87.37	2832.	32.94	3903.	284.	0.80
1600.	400.	103.92	2521.	33.40	4021.	248.	0.53
1600.	400.	123.03	2319.	35.36	4532.	225.	0.24
1600.	600.	61.42	3829.	33.34	4006.	266.	0.61
1600.	600.	85.82	2910.	32.45	3782.	195.	0.47
1600.	600.	103.36	2558.	32.84	3878.	168.	0.31
1600.	600.	121.29	2308.	34.47	4297.	149.	0.14
1600.	800.	61.17	3955.	33.39	4019.	207.	0.38
1600.	800.	84.00	2961.	32.27	3737.	149.	0.30
1600.	800.	100.14	2572.	32.63	3826.	127.	0.20
1600.	800.	121.25	2336.	34.43	4285.	114.	0.09

**TABLE 3-2. EXTERNALLY FUELED DIODE REACTOR
CHARACTERISTICS - 276 kWe EOM**

$T_o = 2073 \text{ K}$ $T_R = 630 \text{ K}$ Core Height = 10 m Reactor Height = 20 m Output Power = 332 kw (BOM) = 276 kw (BOM)							
Coolant Outlet Temperature (F)	Coolant Temperature Rise (F)	Reactor Terminal Voltage (volt)	Thermal Power (kw)	Reactor Diameter (in)	Reactor Weight (lb)	Coolant Flow Rate (gpm)	Core Pressure Drop (psi)
1350	250	110 12	2209	31 94	3657	345	1 62
1350	250	121 31	2105	32 96	3909	326	1 03
1350	250	131 62	2053	34 37	4269	316	0 61
1350	250	142 99	2048	36 22	4764	315	0 35
1350	250	152 92	2088	38 46	5389	323	0 19
1350	350	107 85	2213	31 99	3669	247	0 85
1350	350	120 77	2114	33 06	3934	234	0 53
1350	350	132 85	2066	34 51	4307	228	0 32
1350	350	144 22	2064	36 39	4810	227	0 18
1350	350	152 96	2101	38 60	5431	232	0 10
1350	450	111 31	2236	32 28	3740	194	0 49
1350	450	122 40	2141	33 43	4028	185	0 30
1350	450	132 40	2088	34 91	4412	179	0 18
1350	450	146 24	2105	36 99	4974	181	0 10
1350	450	153 59	2144	39 23	5612	185	0 05

TABLE 3-3. MESH STRUCTURE -
EXTERNALLY FUELED DIODE REACTOR

Region	Radial, cm	Region	Axial, cm
1	.8873	1	1.5875
2	1.7747	2	3.1750
3	15.7735	3	4.7625
4	22.2364	4	6.3500
5	27.2050	5	7.9375
6	31.3969	6	9.5250
7	32.9170	7	11.1125
8	34.3670	8	12.7000
9	37.6470	9	15.545
10	38.3070	10	16.561
11	40.3370	11	23.546
		12	24.613
		13	25.908
		14	30.988

TABLE 3-4. EXTERNALLY FUELED
DIODE REACTOR COMPOSITION BY REGIONS

Region	Number Density (Barn-CM) ⁻¹			
	UO ₂ *	W	Nb	Na
1	.005436	.019108	.012387	.000433
2	.005980	.017710	.012387	.000433
3	.006523	.016311	.012387	.000433
4	.005835	.019715	.010822	.000433
5	.006418	.018214	.010822	.000433
6	.007002	.016713	.010822	.000433
7	.006487	.020680	.008292	.000433
8	.007136	.019010	.008292	.000433
9	.007784	.017340	.008292	.000433
10	.007248	.021750	.005405	.000433
11	.007973	.019885	.005405	.000433
12	.008698	.018019	.005405	.000433

* Uranium Taken as 93% U-235, 7% U-238

TABLE 3-4. EXTERNALLY FUELED DIODE
REACTOR COMPOSITION BY REGIONS (CONTINUED)

Extracore Regions		
Region	Component	Number Density (Barn-CM) ⁻¹
13	Void	---
14	W	.005849
	Nb	.02973
	Al ₂ O ₃	.000814
	Re	.001995
15	Nb	.01622
	Mo	.03438
16	Na	.009885
	Fe	.02016
	Ni	.01220
	Al ₂ O ₃	.000485
	Nb	.01102
17	Al ₂ O ₃	.001157
	Nb	.008867
18	Na	.008789
	Nb	.005949
19	Fe	.03702
	Nb	.00637
	Al ₂ O ₃	.00653
20	W	.01419
	Nb	.01598
21	Nb	.05549
22	BeO	.07251
23	B ₄ C	.0290
24	Nb	.05549
25	Void	---

for optimum conditions. The outputs of the 108 converters are subsequently connected in parallel to provide common electrical outputs to the loads.

The flashlight reactor data employed in this study is summarized in Table 3-5. The first column lists the parameters for the reference 300 kWe design reported in Reference 1 (GESR-2115). The basic TFE for this reference design uses an unbonded trilayer, where the interface between the insulator and the collectors of each diode is a slip fit. The remainder of the data of Table 3-5 presents the flashlight reactor characteristics under the assumption of a bonded trilayer. These data were employed in the Phase I effort reported here. The Phase II effort will assess the effect of the unbonded design on the spacecraft performance.

The various alternate designs presented in Table 3-5 provide the capability to assess the impact of various reactor operating points on the spacecraft performance. Reactor parameters varied include coolant temperature rise, coolant exit temperature, coolant pressure drop inside the reactor and their effect on reactor weight and dimensions. These data were employed to develop a model for use in the spacecraft weight optimization computer code, as discussed in Section 9.

Past studies have shown that a nominal 1-inch TFE is close to the optimum diameter for this power range. No attempt was made to vary TFE diameter for these studies. The basic core arrangement was not changed for any of the alternate designs.

Studies indicate that a fixed electric output from a fixed number of diodes leads to an optimum emitter temperature distribution. If the emitters are run too hot, the maximum efficiency point is passed. If the emitters are run too cool, the current density increases forcing increased losses on the electrical system. The value of 1950°K selected for the reference design is very near optimal for the 300 kWe configuration, 216 TFE units, each with 12 diodes. Recent improvements in analyses indicate that it is in fact possible to achieve a somewhat lower emitter temperature distributions

TABLE 3-5. PERFORMANCE OF 300 kWe
FLASHLIGHT REACTOR DESIGNS

Alternate Parameter	Base Design AEC Study	Alt No 1 1000°K (1350°F) Outlet		Alt No 2 868°K (1100°F) Outlet		Alt No 3 1145°K (1600°F) Outlet		Alt No 4 200°K Core ΔT		Alt No 5 6.8 psi Reactor Δp	
TFE	Unbonded	Fully Bonded		Fully Bonded		Fully Bonded		Fully Bonded		Fully Bonded	
TFE Diameter, in	1.02	1.02		1.02		1.02		1.02		1.02	
Number of TFE	217	217		217		217		217		217	
Number of Cells/TFE	12	12		12		12		12		12	
Core Structure	SS	SS		SS		SS		SS		SS	
Coolant	NaK-44	NaK-78		NaK-78		NaK-78		NaK-78		NaK-78	
Inlet Temp, °K	800 (980°F)	906	(1170°F)	768	(920°F)	945	(1420°F)	806	(990°F)	906	(1170°F)
Outlet Temp, °K	900 (1160°F)	1006	(1350°F)	868	(1100°F)	1045	(1600°F)	1006	(1350°F)	1006	(1350°F)
Reactor, Δp, psi	3.1	4.5	3.7	4.5		4.5		4.5		6.8	
Max Emitter Temp, °K	1950	1915	1950	1955		1955		1955		1915	
Electric Power, kWe	330	330	330	330		330		330		330	
Voltage Output Power, v	14.3	12.7	15.7	12.6		12.0		12.5		12.7	
Current (TFE pairs), amp	23100	26000	21000	26300		27600		26400		26000	
Thermal Power, kW	2840	2900	2470	2980		2960		2980		2900	
Coolant Heat, kW min	2510	2570	2140	2650		2630		2650		2570	
EOM	----	2600	2170	2680		2660		2680		2600	
Reactor Weight, lb	2970	2960		2960		2960		3040		3000	
Overall Length, in	35.5	35.5		35.5		35.5		35.5		35.5	
Overall Diameter, in	28.8	28.8		28.8		28.8		28.0		28.4	
Flow Rate (EOM Cond) lbs/sec		64.9	54.1	66.7		66.4		33.4		64.9	
10% POWER (est)											
Max Emitter Temp, °K		~1600									
Voltage Output Power, v		12.5									
Current (TFE pairs), amp		3000									
Thermal Power, kW		590									
Coolant Heat Load, kW		552									

(see Alternate No. 1; there is approximately 100°K gained by going from unbonded to bonded TFE's). The design alternates shown in the table were thus selected on the basis of the minimum emitter temperature distribution to provide 330 kWe (BOM) at the reactor terminals. A second column is shown for Alternate No. 1 since the optimal emitter temperature distribution is slightly higher than the minimum. However, there is a common basis for comparison of Alternate No. 1(a) and the other alternates.

Note Alternate No. 3. At temperatures above 1000°K, it is clear that stainless steel (SS) or other iron/nickel base metals cannot provide the necessary strength for structural and containment use. This means the use of Columbium in the liquid metal system, including its use in the TFE sheath, which considerably complicates the testing program. Thermal vacuum tests will be required. The data shown depend on the use of stainless steel (more generally, iron/nickel alloys) even up to the 1145°K (1600°F) limit specified. Since this is not feasible, systems involving these temperatures should be reevaluated at some future date.

The highest temperature proposed (1145°K) is above the normal boiling point of NaK, and just below that of Na. This increases the concern about high temperature strength of structural materials since additional over-pressure is needed to prevent bulk boiling. This effect on reactor design has been ignored.

Voltage and current are quoted on the basis of TFE pairs. Thermal powers include all sources of heating within the reactor which must be removed by the coolant or by electron cooling. The coolant heat load is, thus, just the thermal power minus the electric power. The optimum cesium reservoir temperature is 610°K.

Reactor weight includes the weight of all components within the reactor vessel, the external reflector, control drive actuators, and the cesium reservoir area. Reactor length does not include the one foot needed above the reactor vessel for the cesium reservoir area. Reactor diameter is specified for the reactor control in its normal operating (in) position.

Table 3-6 gives the relative fission power distribution for Alternate No. 1.

Table 3-7 gives the material designation for cylindricized and homogenized core regions for Alternate design No. 1.

TABLE 3-6. RELATIVE POWER DISTRIBUTION FOR FLASHLIGHT REACTOR ALTERNATE DESIGN NO. 1

Axial Zone	Radial Zone					
	1(7TFE)	2(30TFE)	3(48TFE)	4(72TFE)	5(36TFE)	6(24TFE)
6	1.092	1.071	1.026	0.936	0.872	0.880
5	1.085	1.065	1.021	0.932	0.886	0.901
4	1.102	1.095	1.054	0.965	0.923	0.936
3	1.103	1.102	1.082	0.994	0.950	0.965
2	1.103	1.102	1.100	1.001	0.950	0.967
1	1.102	1.102	1.099	1.001	0.948	0.967

3.2.1.3 Pancake Reactor

The pancake reactor has been deleted from the scope of the study at the request of the Jet Propulsion Laboratory, primarily because:

1. This reactor concept is not now under active development by any government agency.
2. The externally fueled diode reactor can provide output voltages up to 130 to 140 volts, in the same range as that of the pancake reactor.

TABLE 3-7. REACTOR MATERIAL DESIGNATION FOR FLASHLIGHT REACTOR
ALTERNATE REACTOR NO. 1

Region	Geometry			Composition - Percent									
	OD (in.)	ID (in.)	Length (in.)	SS	Coolant	Be	BeO	UO ₂	W	Al ₂ O ₃	Nb	Cermavar	Cu
Core	17.3	0	16.0	15.1	13.1	0	0	31.4	8.4	7.4	6.2	6.9	0
Internal Reflector	20.6	17.7	28.0	8.4	24.8	0	66.8	0	0	0	0	0	0
Axial Reflector	17.7	0	10.5 (6/4.5)	4.9	11.2	76.4	0	0	0	1.5	0	1.7	3.2
Pressure Vessel	22.2	20.6	34.0	41.1	58.9	0	0	0	0	0	0	0	0
External Reflector	28.8	22.2	28.0	0	0	100.0	0	0	0	0	0	0	0
Lower Axial Plenum	21.6	0	~3.0	0	100.0	0	0	0	0	0	0	0	0
Upper Axial Plenum	21.6	0	3.0	0	95.1	0	0	0	0	0	1.0	1.1	2.1

The evaluation of the externally fueled diode reactor in this study, together with the lower voltage (14 to 16 volts) flashlite reactor, provides the necessary assessment of the impact of reactor output voltage on spacecraft configuration and performance. However, since the pancake reactor may become of greater importance in the future, the data provided by Gulf General Atomic are included.

The pancake reactor, as illustrated on Figure 3-5 configures many single diodes in a cylindrical, pancake array. Several of these pancakes are stacked vertically to form the active core. Electric connections are made between each of the diodes, across the top of each pancake, and the separate pancakes are then series connected to provide an output of 140 volts at 300 kWe gross, at the reactor terminals. Waste heat removal is accomplished by directing the liquid metal coolant flow, in ribbon ducts about each diode, running across each pancake layer.

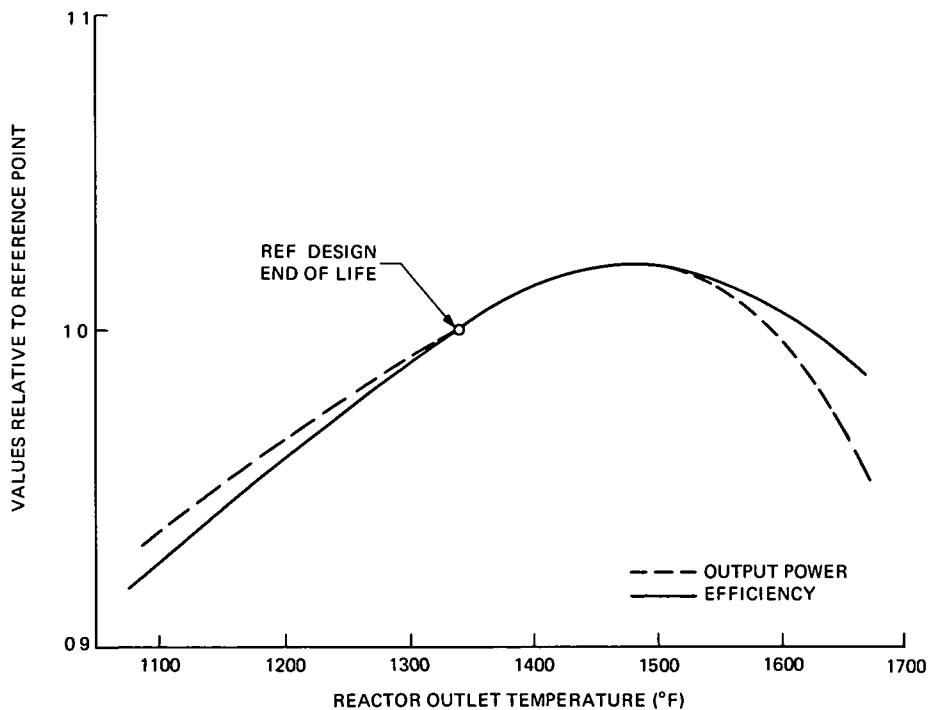


Figure 3-5. Variation in Pancake Reactor Power and Efficiency with Coolant Outlet Temperature

Estimates of reactor size and primary coolant heat load were obtained by using the data of Figure 3-5. The reactor power levels and primary coolant heat loads in Table 3-8 are obtained directly from the efficiency values in Figure 3-5. The mass and diameter of the reactors were calculated from the increment in thermionic cells required to deliver 300 kWe at the required conditions. The data in Table 3-9 were calculated for a reactor control scheme which maintains constant voltage output from the reactor.

There are several operating temperature limits in the reference reactor design which must be considered in evaluating the effect of changing the coolant outlet temperature. These comments are made relative to the AEC study reported in Reference 2.

The maximum operating temperature for the cell closure braze is 800°C. Any reactor with a coolant outlet temperature greater than 700°C (1290°F) will have to contain all-welded cells. The insulator seal is qualified to 1200°C. In the reference design, this seal operates at 1105°C. An increase of 135°C in coolant temperature would increase the insulator seal temperature to 1200°C. Therefore, an upper limit of 835°C (1535°F) is imposed upon the coolant outlet temperature.

The reliability analysis, which was used to establish the required number of ribbon ducts in the design, applied to a coolant temperature of 700°C. It was shown that an upper duct height of 0.15 inch would permit cell operation after the failure of a ribbon duct. If the final closure of the thermionic diode were welded, this same duct size would permit cell operation after duct failure only if the coolant is held to 790°C (1454°F) or below. If the maximum coolant temperature is greater than 1450°F, more ribbon ducts would be required in order that the thermionic fuel elements survive loss of coolant in the duct nearest the insulator seal. Reactor material designation, and reactor neutron flux and its energy distribution are defined in Reference 2 (GA-8918).

TABLE 3-8. PANCAKE REACTOR DIMENSIONS AND THERMAL POWER LEVEL FOR A 300 kW THERMIONIC REACTOR (EOM)

Primary Coolant Outlet Temperature (°F)	Reactor Power Level (kW)	Primary Coolant Heat Load (kW)	Reactor Diameter (inches)	Reactor Mass (lbs)
1100	3240	2940	27.4	3200
1200	2921	2621	27.1	3140
1300	2836	2536	26.8	3100
1400	2459	2159	25.6	2880
1500	2336	2036	25.2	2810
1600	2671	2371	26.8	3090

All reactors deliver 2140 amperes at 140 volts; reactor length is unchanged from the 30.8 inches for the reference design.

TABLE 3-9. PANCAKE REACTOR CHARACTERISTICS WHEN OPERATED AT 10 PERCENT POWER

Primary Coolant Outlet Temperature (°F)	Reactor Thermal Power (kW)	Primary Coolant Heat Load (kW)
1100	888	858
1200	857	827
1300	831	801
1400	721	791
1500	685	655
1600	783	753

All reactors deliver 214 amperes at 140 volts.

The primary coolant temperature rise and pressure drop affect the reactor size and operating characteristics principally through the coolant volume fraction or spacing between elements to allow for coolant flow in the ribbon ducts. The coolant temperature rise has a small additional effect on the electrical power density and efficiency which can be estimated from the results given above. In the reference design, however, the spacing cannot be reduced because of the requirement for clearance between electrical leads in the stem region of the fuel elements.

The primary coolant temperature rise and pressure drop can be traded with each other with the fixed coolant duct configuration. The coolant velocity is inversely proportional to the temperature rise, while the pressure drop is approximately proportional to the square of the coolant velocity in the ribbon ducts. The exact formula for this pressure drop is given in Reference 2 (GA-8917, CRD).

The restriction on pitch spacing of the fuel elements and hence on the space for coolant flow is for the lead and stem design shown in Section 3 of GA-8917. If a more compact design could be developed without excessive electrical losses, the pitch spacing could be reduced to reduce the size of the reactor. Influence coefficients for such a change are given in GA-8917.

3.2.2 THRUSTERS

Spacecraft propulsion will be provided by 31 equal size electron bombardment ion thruster engines. Mercury was chosen over other propellants because of the relatively well developed technology of mercury systems. Information concerning the weight, volume, and position requirements of the thruster subsystem has been specified by JPL. The general guidelines used to design the thrust subsystem are given in Table 3-10.

TABLE 3-10. GUIDELINES FOR THRUSTER SUBSYSTEM DESIGN

Power to the thrusters	240 kWe
True specific impulse	5000 sec
Thruster redundancy	20 percent
Attitude control	Electric propulsion
Maximum envelope diameter	10 feet
Thrust duration	10,000 hrs
Number of thrusters (includes 6 spares)	37

Six spare thrusters will bring the total to 37 units. Considering switching and power conditioning requirements, this number of spares provides one spare thruster for each group of five operating thrusters. Switching, logic, and spare Power Conditioning Control (PCC) units can also be grouped in this way to reduce the number of possible thruster - PCC combinations. Thrust vector control will be provided by a three axis attitude control system (two axis translation, one axis gimbal). Thruster power supply requirements and subsystem weights are given in Tables 3-11 and 3-12, respectively. The thruster system design layout, which was contributed by JPL, is presented in Figure 3-6.

3.2.3 SCIENCE PAYLOAD AND COMMUNICATION SUBSYSTEM

The general size, power requirements and key capabilities of representative Science and Communications subsystems have been defined for a Jupiter orbiter mission. The major guidelines used in the selection of these systems are:

- The total electric power available to the science payload and communications subsystems is one kWe.
- The total weight allocated to the science payload and communication subsystems (including thermal control radiators for these subsystems) is one metric ton.

TABLE 3-11. ION ENGINE POWER SUPPLY REQUIREMENTS

Supply Number	Supply Name	Type	Output ⁽¹⁾	NOMINAL RATING					MAX RATING			Control Range, A
				Volts	Amps	Watts	Reg. %	Peak Ripple	Volts	Amps	Amps Limit ⁽²⁾	
1	Screen	DC	V	3100	2 32	7200	1 0(V)	5	3200	2 32	2 60	2 0 - 2 4
2	Accelerator	DC	F	2000	02	40	1 0(V)	5 @ 0 2 A	2100	0 20 ⁽³⁾	0 21	---
3	Discharge	DC	V	35	8 3	290	1 0(V)	2	150 @ 50 mA	9 @ 37V	10	7 5 - 9 0
4	Mag - Man	DC	F	15	7	11	1.0(I)	5	20	1 0	1 0	---
5	Cath Htr ⁽⁴⁾	AC	F	10	4 0	40	5.0	5	11	4 4	4 1	---
6	Cath Keeper	DC	F	10	0 5	5	1 0(I)	5	150 @ 50 mA	1 0 @ 20 V	1 0	---
7	Main Vapor	AC	V	0 6	1 0	1	Loop	5	8 ⁽⁵⁾	2 0	2 2	0 5 - 1 5
8	Cath Vapor	AC	V	0.3	0 5	1	Loop	5	8 ⁽⁵⁾	1 0	1 1	0 2 - 0 8
9	Neut Cath Htr	AC	F	10	2 0	20	5 0	5	11	2 2	2 2	---
10	Neut Vapor	AC	V	0.3	0 5	1	Loop	5	8 ⁽⁵⁾	1 0	1 1	0 2 - 0 8
11	Neut Keeper	DC	F	10	0 5	5	1 0(I)	5	150 @ 50 mA	1 0 @ 20 V	1 0	---

(1) V = Variable, F = Fixed

(2) Current limit or overload trip level

(3) Current at this level for less than
5 min at low repetition rate(4) Needed only during startup or until
discharge reaches 3A

(5) Startup only

TABLE 3-12. THRUSTER SUBSYSTEM WEIGHTS

Component	Weight (lbs.)
Thrusters (37)	585
Thrust Vector Control System	550
Miscellaneous (wiring, adapters, etc.)	100
TOTAL	1235

3.2.3.1 Science Payload Subsystem

A variety of experiments have been identified to provide answers to the basic scientific questions of interest in a Jupiter mission. A brief description of the science payload equipment is given below. Individual payload subsystem characteristics are summarized in Table 3-13. Total subsystem weight is 185 pounds and will require 87 watts of spacecraft power (all science operating).

3.2.3.1.1 Television System - In order to meet scientific objectives, particularly in terms of both high spatial resolution and large area coverage, a two-camera, slow scan vidicon television system with optics having 10:1 focal length ratio is assumed. Both cameras are identical except for lenses and shutters. The cameras are electromagnetically deflected and focused to obtain the spot size required for high resolution operation.

3.2.3.1.2 Infrared Spectrometer System - This equipment will acquire data concerning Jupiter surface composition, gas temperature, albedo, surface temperature, and atmospheric photochemistry. The infrared spectrometer telescope-monochromator weighs approximately 19 pounds. The gas system, consisting of two pressure vessels, weighs approximately 12 pounds and is also mounted on the scan platform. The power required by the infrared spectrometer is:

1. 4 watts of 2.4-kHz square wave for the electronics during orbit
2. 2 watts of 400 Hz square wave for the motor during orbit.

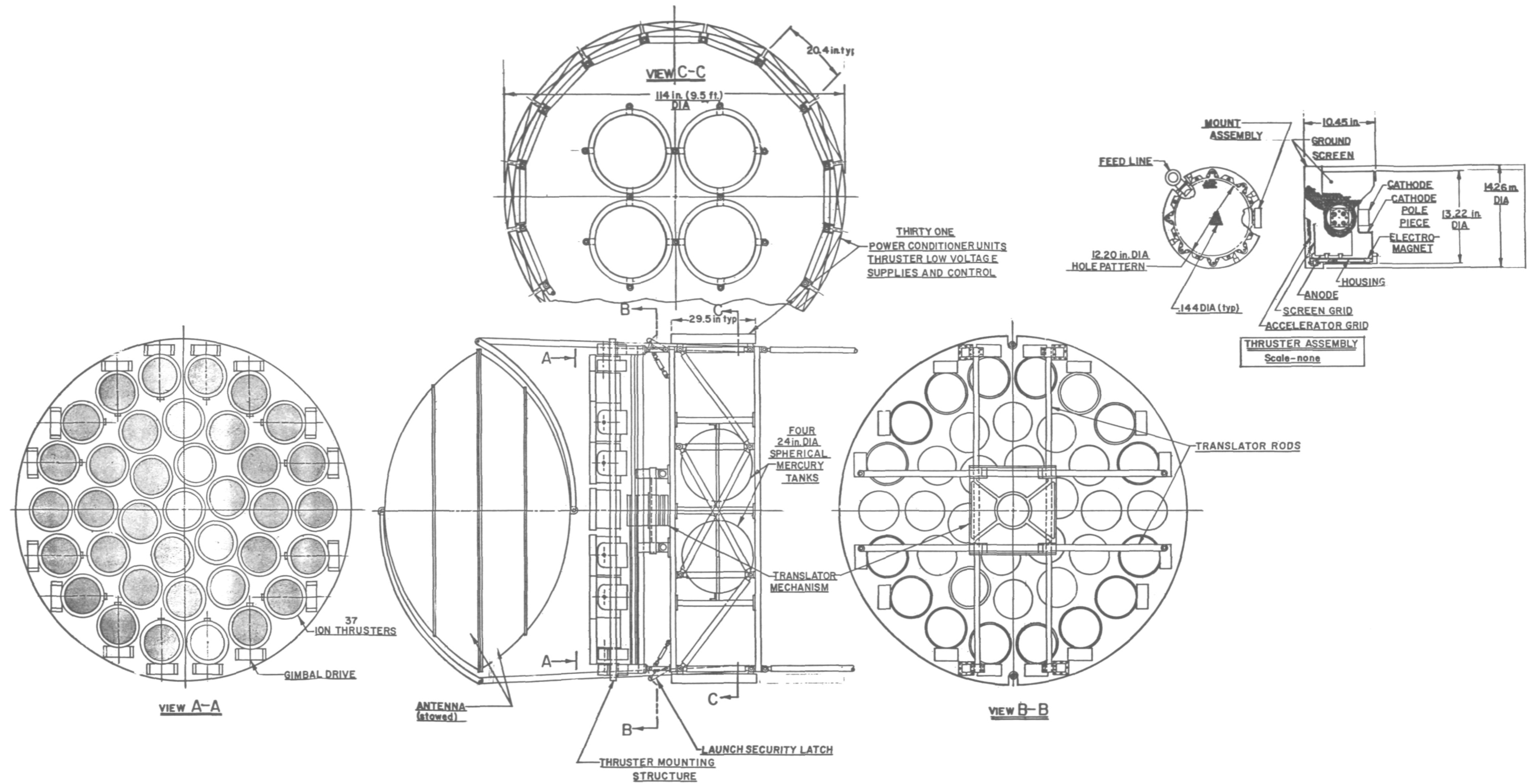


Figure 3-6. Thruster System Design Layout

TABLE 3-13. SCIENCE PAYLOAD AND DATA HANDLING EQUIPMENT SUMMARY

COMPONENT	QUANTITY	UNIT CHARACTERISTICS					
		WEIGHT LBS.	DIMENSIONS INCHES	POWER (WATTS)	VOLTS	BIT RATE (SEC ⁻¹)	
						CRUISE	SPECIAL EVENT
PAYLOAD							
TV System							
Camera A (50 mm focal length)	1	7	9 x 5 x 4	---			
Camera B (508 mm focal length)	1	28.5	32 x 10 x 10	---			
Logic and Data Control	1	3	6 x 14 x 1.5	---			
Camera Drivers	1	4	6 x 14 x 1.5	---			
Data Converter	1	3	6 x 14 x 1.5	---			
Power Supply	1	4	6 x 7 x 2	32	28 VDC	---	1.5 x 10 ⁶ /picture
Infrared Spectrometer System	1	31 ^(a)	6 x 10 x 8 ^(b)	6	28 VDC	---	---
Ultraviolet Spectrometer	1	30	20 x 10 x 6 ^(b)	12	28 VDC	---	---
Infrared Radiometer	1	5	6 x 6 x 6 ^(b)	3	28 VDC		
Micrometeoroid	4	5	8 x 8 x 9	0.5	28 VDC	3	60
Interplanetary Fields							
Plasma	1	9.5	7 x 7 x 6	4.0	28 VDC	10	150
Cosmic Ray	1	5.0	9 x 7 x 6	2.0	28 VDC	10	40
Magnetometer	1	7.5	6 x 6 x 6	2.5	28 VDC	3	3
Electric	1	1.5	3 x 3 x 4	0.5	28 VDC	3	3
DATA HANDLING							
Digital Automation System	1	13.0	10 x 7 x 17	19.0	28 VDC	NA	NA
Data Storage System	1	10.0	12 x 12 x 12 ^(b)	3.0	28 VDC	NA	NA
Command Decoder	1	3.0	9 x 6 x 2	1.0	28 VDC	256 Commands	
TOTALS	20	185.0	---	87.0	---	---	1.5 x 10⁶

(a) includes gas system
(b) estimated.

3.2.3.1.3 Ultraviolet Spectrometer - The scientific objective of this experiment will be to detect the presence of certain atoms, ions and molecules in the upper atmosphere of Jupiter. The total weight of the ultraviolet spectrometer is 30 pounds and requires 12 watts of spacecraft power. The dimensions are estimated to be 20 by 10 by 6 inches.

3.2.3.1.4 Infrared Radiometer - The scientific objective of this experiment will be to determine the temperature of the Jovian atmosphere. The total weight of the instrument is five pounds and its size is estimated at 20 by 10 by 6 inches. Three watts of power will be required.

3.2.3.1.5 Micrometeoroid Sensors - The meteoroid environment experiment will investigate the momentum, energy and spatial distribution of meteoroids in the interplanetary region, as well as probable changes in this distribution in the asteroid belts and near Jupiter. It is planned to incorporate four sensors on the spacecraft, located 90 degrees apart in the payload bay in order to minimize the dependence of this experiment on spacecraft orientation during the interplanetary propulsion mode. Each unit is eight by eight by nine inches, weighs about five pounds and requires two watts of electric power.

3.2.3.1.6 Interplanetary Fields - Table 3-13 has listed the approximate weight, size and power requirements of the experiments required to investigate various aspects of interplanetary and Jovian fields. However, the ability to conduct such measurements from an electrically propelled spacecraft remains to be established. Such measurements will be complicated by either the inherent magnetic field setup by the operating electric power plant, or by the use of electric propulsion, or both.

3.2.3.1.7 Data Automation Subsystem - The data automation subsystem will control and sequence the science instruments, accept and convert the raw data, code and format the data into frames, provide temporary (buffer) storage, and route the data to either the flight telemetry subsystem or the data storage subsystem for direct or delayed

transmission to earth. This subsystem will include both the logic portion and the power converter, and will occupy a volume of 1190 cubic inches. It will weigh approximately 13 pounds and will consume 19 watts of power.

3.2.3.1.8 Data Storage Subsystem - This subsystem will provide buffering between the high rate at which data is acquired by the TV and other scientific instruments and the lower rate at which these data can be returned to earth (about 10^4 bits/sec). It is estimated that a storage subsystem with a capacity of 2×10^8 bits of data would weigh ten pounds, and occupy about one cubic foot of space. Total power requirements will be about three watts. Since a typical TV picture requires about 1.5×10^6 bits of storage, a system of this size will store about 100 pictures and have adequate capacity for simultaneous storage of raw data from the other science experiments.

3.2.3.1.9 Command Decoder - This system is required to provide on-board time sequenced event control in the spacecraft in time periods where this cannot be accomplished by the ground station, and to initiate particular events in the scientific payload or spacecraft operation upon command from the ground station. The representative unit selected for this function will provide for 256 discrete commands, will weigh three pounds and will require one watt of power. Further study is required to define the total command requirements and their distribution between the science payload and other spacecraft or power plant operations.

3.2.3.2 Communications Subsystems

The total science payload power requirement has been identified as 87 watts(e). Allowing for a possible 100 percent growth in payload power requirements, the remaining power available to the communications subsystem is approximately 800 watts (based on the one kWe limitation).

A low gain omnidirectional receiving antenna, a high gain transmitting antenna, and a transmitter comprise the communications subsystem. Characteristics of these components are summarized in Table 3-14.

TABLE 3-14. COMMUNICATIONS SUBSYSTEM CHARACTERISTICS

Low Gain Antenna (Receiving)	
Diameter	6 inches
Weight (including cable)	2.5 pounds
Deployment, lbs.	Negligible
High Gain Antenna (Transmitting)	
Diameter	9.0 feet
Weight, (including cable)	31.0 pounds
Deployment	8.0 pounds
Power Input	800 watts(e)
Power Transmitted	200 watts(e)
Bit Rate	10^4 bits/sec
Transmitter	
Weight	20.0 pounds
Geometry, inches	6 x 6 x 20

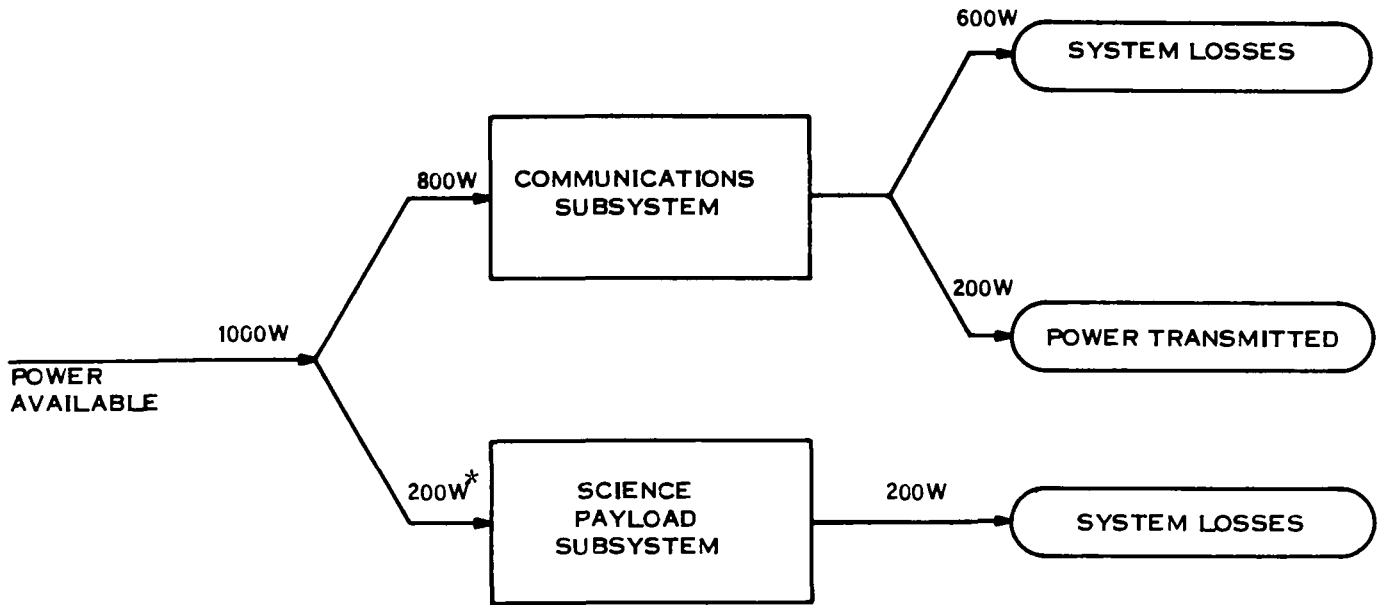
The high gain antenna is nine feet in diameter, and paraboloid in shape. Its weight is estimated to be 31 pounds, including cabling. The deployment and pointing system is estimated to be eight pounds. The low gain antenna is approximately six inches in diameter by two inches in depth, and weighs about two and one-half pounds.

Power input to the communications subsystem will be 800 watts(e). Operating at an overall efficiency of 25 percent the power transmitted will be 200 watts, permitting a data rate of about 10^4 bits/second from Jupiter orbit. This estimate is based on a 120 foot diameter earth-based receiver antenna and the nine foot spacecraft transmitting antenna discussed above. It is estimated that the transmitter will weigh about 20 pounds and occupy a volume of 400 cubic inches. These requirements are based upon a 28 volt DC ($\pm 5\%$) power input. Some weight could be saved if the spacecraft could supply 2000 Hz to 3000 Hz power directly to the transmitter.

3.2.4 THERMAL CONTROL SUBSYSTEM

With 1000 watts(e) supplied to the communications and payload subsystems, approximately 800 watts(t) must be rejected by thermal radiation (Figure 3-7). To dissipate this quantity of heat, a 17 pound passive radiator with 16.6 ft² of surface area will be required. These estimates were based on the following assumptions:

1. 175°F maximum radiator surface temperature
2. A surface emissivity of 0.85 on a 60-mil thick aluminum radiator structure
3. 70 percent fin efficiency
4. Ten percent allowance on weight for fittings and structure.



* NOMINAL, BUT ASSUMES - 100% INCREASE IN POWER TO ALLOW FOR PAYLOAD GROWTH

Figure 3-7. Electrical Power Distribution
(Communications and Science Payload Subsystem)

4. LAUNCH VEHICLE

4. LAUNCH VEHICLE

The Titan IIIC/7 launch vehicle is defined as the reference booster for placing the spacecraft into a 750 nautical mile (design objective) circular earth orbit. This vehicle is similar to the Titan IIIF except that it uses a standard transtage. It is a nonmanrated vehicle and employs the stretched Stage I tanks and seven segment, 120 inch diameter solids characteristic of the Titan IIIM. The overall length of the vehicle to the payload separation plane is approximately 117 feet.

4.1 PHYSICAL CONSTRAINTS ON SHROUD SIZE

The height of the 50-ton bridge crane above the launch vehicle is one identified constraint on the aerodynamic shroud (hence payload) overall length. At the Eastern Test Range (ETR) Titan vehicles are launched from Launch Complex 40 or 41. With the Titan vehicle in place on the Mobile Service Tower, the clearance between the bridge crane and the Titan IIIC/7 payload interface is only 75 feet while for the Titan IIIC, this clearance is 88 feet. The decrease in available clearance is due to: a 5.5 foot increase in the length of the first stage, and a 7.5 foot increase in launch stand height. The launch vehicle contractor suggests the possibility of using ETR Launch Pad 37B, which has been used for S-IB launches. There would be virtually no height limitations.

On the launch pad, a universal environmental shelter is used to provide temperature and humidity control, and RF protection. It also acts as a clean room for the transtage and payload envelope. At the present time, the limit of this facility is 55 feet, which means that this is the maximum payload-plus-transtage length which can be accommodated. Longer lengths will require construction revisions to the shelter.

4.2 REQUIRED LAUNCH VEHICLE MODIFICATIONS

For a payload that requires a 35 foot fairing length, the launch probability on an arrival basis is 99 percent with a worst quarter probability of 95 percent. As fairing length increases to 60 feet, the arrival launch probability decreases to 75 percent with a worst quarter probability of 45 percent. To maintain this launch probability for payload fairing lengths of 60 to 80 feet, the vehicle guidance steering must be modified. Moreover, for payload fairing lengths of greater than 80 feet, modification of guidance steering and strengthening of the transtage control module skirt is required. Weight penalty for skirt revision is estimated to be 60 pounds.

4.3 FLIGHT FAIRING WEIGHT AND PAYLOAD PENALTY

During a "nominal" launch of the Titan III F vehicle, the flight fairing is normally jettisoned at 280 seconds, which is just after completion of the Stage I burn. In order to prevent freezing of the liquid metal coolant during launch, it may be desirable to retain the flight fairing as a radiation barrier until after reactor startup in earth orbit. However, this procedure imposes a severe payload weight penalty which depends on the shroud length (weight) and the terminal orbit altitude.

Figure 4-1 shows the flight fairing weight and the payload penalty as a function of shroud length, assuming shroud jettison at 280 seconds into the mission. If the shroud is retained past Earth orbital insertion, then the payload weight penalty will be equal to the shroud weight. It should be noted that as the terminal orbital altitude increases, the payload penalty decreases for normal shroud ejection since a larger portion of the ΔV is added after shroud ejection. The curves are based on the data supplied by the Martin Marietta Corporation.

The effect of shroud retention on payload capability is shown in Figure 4-2. The upper lines define the Titan III C/7 payload capability for a 28.5 degree orbital inclination mission with shroud jettison occurring at 280 seconds into the mission. The lower curves show the effect of retaining the shroud through achievement of final Earth orbit.

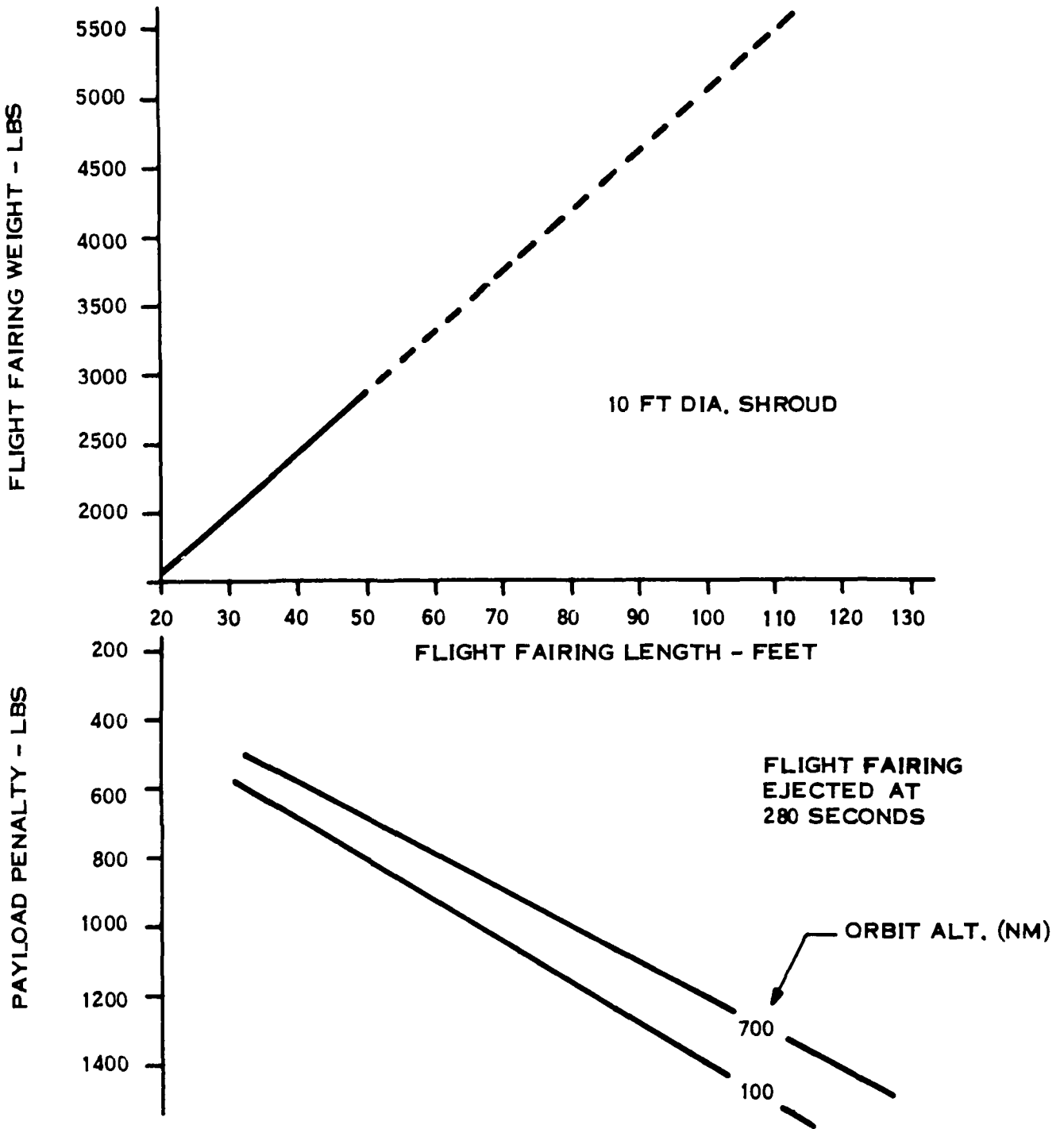


Figure 4-1. Flight Fairing Weight and Payload Penalty (Titan III C/7)

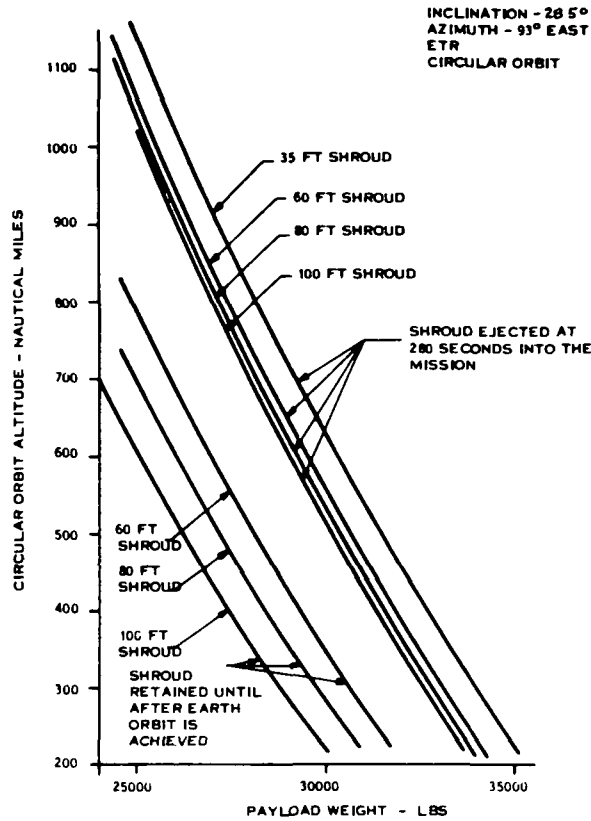


Figure 4-2. Effect of Shroud Retention on Payload Capability (Titan III C/7)

Under nominal conditions, and with a 35-foot shroud, the vehicle can deliver 30,000 pounds into a 630 nm circular orbit. Employing longer shrouds, with jettison at 280 seconds, reduces the payload capability (initial mass in Earth orbit) as shown in Table 4-1.

TABLE 4-1. MAXIMUM PAYLOAD CAPABILITY WITH SHROUD EJECTION AT 280 SECONDS

Shroud Length (feet)	Shroud Penalty (pounds)	Maximum Payload Weight (pounds)
60	808	29,191
80	1021	28,978
100	1234	28,765

Alternatively, injecting 30,000 pounds of payload into circular orbit will decrease the maximum possible orbit altitude as shown in Table 4-2.

TABLE 4-2. MAXIMUM EARTH ORBITAL ALTITUDE FOR A
30,000 POUND PAYLOAD WITH SHROUD JETTISON
AT 280 SECONDS

Shroud Length (feet)	Maximum Orbit Altitude (nm)
60	555
80	530
100	512

If the shroud is jettisoned after achieving Earth orbit (630 nm), the payload capability will be reduced as shown in Table 4-3.

TABLE 4-3. MAXIMUM PAYLOAD CAPABILITY AT 630 NAUTICAL MILE
WITH SHROUD EJECTION AFTER ACHIEVING EARTH ORBIT

Shroud Length (feet)	Shroud Penalty (pounds)	Maximum Payload Weight (pounds)
60	3300	26,700
80	4200	25,800
100	5000	25,000

4.4 ALTERNATE LAUNCH VEHICLE

To provide flexibility in the selection of a launch vehicle, alternates to the Titan IIC/7 have been examined. A moderate increase in payload capability or initial Earth orbit altitude is offered by other members of the Titan family, such as Titan IID/Centaur and Titan IID/7/Centaur. The Titan IID/Centaur is similar to the Titan IIC except

that the transtage has been replaced by the Centaur upper stage. The Titan III D/7/Centaur utilizes the stretched Stage I tanks and seven segment, 120 inch diameter solid rocket motors. These launch vehicles would experience even greater physical constraints than those outlined in Subsection 4.1. Consequently, launch from ETR Pad 37B, which has been used for S-IB launches, and major redesign of the universal environmental shelter would be required if a Titan launch vehicle is used.

Substantial increase in payload capability can be realized from the intermediate class of Saturn launch vehicles. For this study, the SIC/SII and SIC/SIVB configurations have been considered. Launch pad modifications would not be required if a Saturn family launch vehicle were employed.

Payload capability of the previously discussed launch vehicles are compared in Table 4-4 for circular orbit altitude of 500, 630 and 750 nautical miles. For this configuration, the payload capability of the Titan launch vehicles is based on nominal conditions and the use of a 35 foot shroud, which is jettisoned at 280 seconds into the mission. Similarly, shroud weight penalty associated with the longer thermionic spacecraft is not included in the payload capability presented for the Saturn vehicles.

TABLE 4-4. COMPARISON OF PAYLOAD CAPABILITY (POUNDS)
FOR TITAN AND SATURN LAUNCH VEHICLES

Launch Vehicle \ Orbit Altitude (nm)	500	630	750
Titan III F	31,400	30,000	28,700
Titan III D/Centaur	32,000	30,700	29,500
Titan III D/7/Centaur	41,000	39,300	38,000
SIC/SII	54,000	-	-
SIC/SIVB	120,000	106,000	103,000

A 750 nautical mile circular Earth orbit altitude represents the design objective of this study, and a 630 nautical mile altitude is the maximum altitude to which the Titan IIIF can lift 30,000 pounds. At present, the SIC/SII is not programmed to lift payloads to the higher orbit altitudes.

5. POWERPLANT BASELINE CONCEPT

5. POWERPLANT BASELINE CONCEPT

A design summary of the baseline concept is presented in the following section. The structural requirements, radiator configuration analysis and coolant activation analysis that resulted in the baseline concept are also discussed.

5.1 DESIGN SUMMARY

Powerplant calculations were performed to define preliminary estimates of component weights and weight distributions. These baseline concept estimates are required for evaluation of spacecraft structural requirements, one loop versus two loop studies, and radiator configuration studies. The design is based on the following assumptions:

- a. A bonded wet cell trilayer diode reactor (13% reactor efficiency, 2010 kW reactor heat rejection) (At the direction of JPL).
- b. An allowable power conditioning and payload electronics temperature level of 200°F; a corresponding radiator temperature of 175°F.
- c. A power conditioning efficiency of 88 percent.
- d. An effective meteoroid flux based on an averaged environment for a Jupiter mission. The resultant radiator armor reduction factor is 0.435, relative to Earth orbit missions.
- e. A sink temperature is 300°R (approximate average for the entire mission).
- f. Payload and communications subsystem weights are assumed to be 2200 pounds.
- g. A copper-stainless steel conduction radiator.

5.1.1 PRIMARY RADIATOR

The main heat rejection loop is required to reject 2010 kW of energy utilizing a conduction fin stainless steel radiator with copper clad fins (Cu-SS) and NaK-78 coolant. The radiator is divided into two panels per bay; panel flow tubes are oriented

parallel to the axis of the vehicle. An iron titanate coating is assumed to provide the radiator with an 0.9 emissivity.

The Cu-SS radiator data of Reference 1 (796 square feet optimized area limited case) was used as the basis for the radiator calculations. Based on 2010 kW of heat rejection, a radiator area requirement of 681 square feet was calculated with a corresponding radiator weight of 2860 pounds. This weight, however, was further reduced by a consideration of the following:

- a. Reduced armor thickness due to the change in vulnerable radiator area.
- b. Reduced armor thickness due to the Volkoff correction for the Jupiter mission average meteoroid flux.
- c. Reduced bumpered armor thickness which is a function of the required armor thickness.

The required radiator armor thickness is proportional to the vulnerable area and is given by the following relationship:

$$t_k = A^{0.249}$$

At 796 ft², the required armor thickness is 0.163 inches. At 681 ft², the armor thickness is:

$$t_k = 0.163 (681/796)^{0.249} = 0.157 \text{ inches}$$

Applying the Volkoff armor thickness correction factor yields the minimum required armor thickness:

$$t_a = 0.435 \times 0.157 = 0.069 \text{ inches}$$

The relationship between bumpered armor thickness and required armor thickness is shown in Figure 5-1 (Reference 1). Assuming a fin thickness of 0.045 inches (which

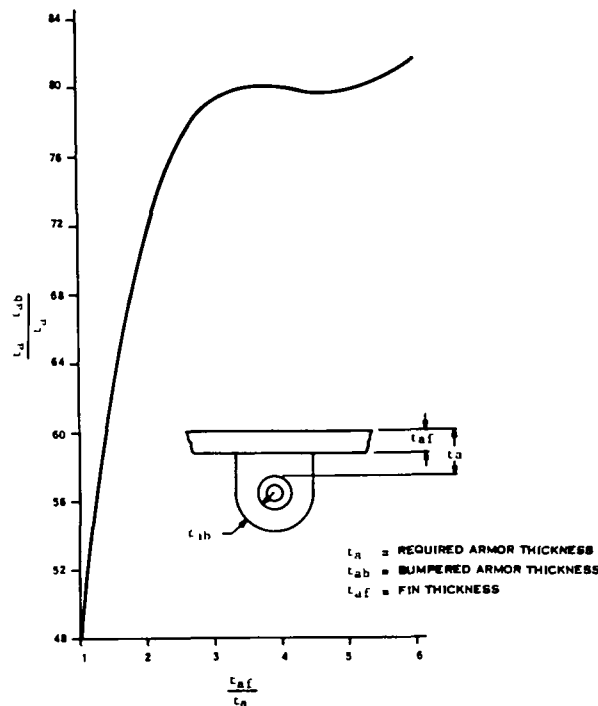


Figure 5-1. Meteoroid Armor Bumper Relationship

is the optimized value reported in Reference 3 for similar radiator conditions), the fin thickness to required armor thickness ratio is $0.045/0.069 = 0.65$, which is outside the range of Figure 5-1. Therefore, assuming a conservative ordinate value of 0.8, the bumpered armor thickness is found to be 0.0138 inches. Rounding off, this is assumed to be 0.015 inches, yielding a corresponding total radiator weight of 1860 pounds. Table 5-1 summarizes the major characteristics of the primary radiator.

5.1.2 POWER CONDITIONING RADIATOR

The Power Conditioning (PC) radiator consists of an array of square panels with a PC unit attached to each panel. Each panel dissipates the heat from a single PC module. In Figure 5-2, the PC module is attached to the central shaded section on the panel back side. Preliminary definition of the modules indicates that they will be approximately one foot square ($S = 1$). Limiting the module to this area is

TABLE 5-1. PRIMARY RADIATOR CHARACTERISTICS
(Baseline Concept Power Plant, Single Loop)

Heat Rejection, kW	2010
Radiator Weight, lb	1860
Radiator Area, ft ²	681
Inlet Temperature, °F	1350
Fluid ΔT in Radiator, °F	180
Number of Panels	6
Panel Width, ft.	10
Number of Tubes per Panel	60
Tube, ID, inches	0.250
Tube Length, ft	11.1
Fin Thickness, inches	0.045
Required Armor Thickness, inches	0.069
Bumpered Armor Thickness, inches	0.015
Fin Length, inches	0.820
Coolant Flow Rate, lb/sec	51.2
Radiator ΔP , psi	6.52

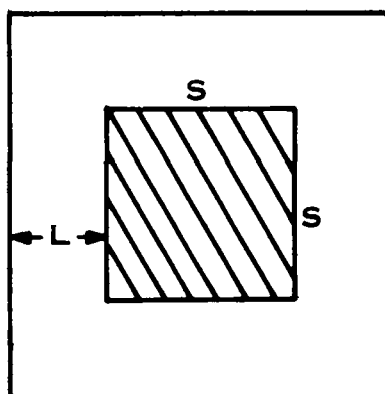


Figure 5-2. Power Conditioning Radiator Panel

pessimistic from a heat rejection viewpoint because this limits the quantity of radiator area which operates at the maximum allowable temperature; however, dispersing the module components over the entire radiator area incurs weight penalties in additional electrical wiring. Since trade-off calculations were not performed for this point of departure design, the concentrated module arrangement shown in Figure 5.2 was assumed. The heat rejection penalties associated with this arrangement were offset somewhat by assuming one-dimensional heat conduction in the fin area.

The point of departure power conditioning radiator calculations were based on the following conditions and assumptions:

- a. A maximum allowable radiator temperature of 175°F (635°R)
- b. An average sink temperature of -160°F (300°R)
- c. One hundred and twenty PC modules, approximately 110 of which are for low voltage power conditioning, and 10 for other special purposes.
- d. A radiator fin thickness of 0.15 inches.
- e. A radiator surface emissivity of 0.88.

Radiator fin efficiency calculations were based on the 35.2 kW heat rejection reported in Reference 1. The fin efficiency (η_f) for unidirectional heat conduction in a fin is

$$\eta_f = \tanh (m L) / mL$$

where L is the fin length. The overall surface effectiveness is given by

$$\eta_o = 1 - (1 - \eta_f) (A_f/A)$$

The ratio of fin area to total radiator area, for S equal to one foot, is given by

$$A_f/A = 1 - \left(\frac{1}{1 + 2L} \right)^2$$

From thermal considerations, the required radiator area is given by:

$$A = q / \eta_o \xi \sigma (T_R^4 - T_S^4)$$

Assuming 120 modules (at 1 square foot each) the total base area ($A - A_F$) is constant at 120 square feet, and the total radiator area requirement must satisfy the following geometric relationship:

$$A = 120 / (1 - A_F / A)$$

The calculational procedure is one of trial and error. Various values were assumed for the fin length (L) until the area determined by thermal requirements matched the area determined by geometrical considerations.

The radiator heat flux is:

$$\frac{q}{A} = \xi (\sigma T_R^4 - \sigma T_S^4) = h_r (T_R - T_S)$$

where h_r is assumed to be an equivalent heat transfer coefficient.

Evaluating h_r for the temperatures and surface emissivity of interest yields:

$$h_r = \frac{.88 (278.5 - 13.9)}{(635 - 300)} = 0.7 \frac{\text{BTU}}{\text{hr-ft}^2 \text{ } ^\circ\text{F}}$$

Then,

$$m = \sqrt{\frac{2 (0.7)}{100 \frac{0.15}{12}}} = 1.06$$

Assume $L = .59$ feet, then

$$mL = 1.06 (0.59) = 0.626$$

and

$$\eta_F = \frac{\tanh .626}{0.626} = 0.886$$

The fin area fraction is

$$\frac{A_F}{A} = 1 - \left(\frac{1}{1+2(.59)} \right)^2 = 0.789$$

and the surface effectiveness is

$$\eta_o = 1 - .789 (1 - 0.886) = 0.91$$

The radiator area required for heat rejection is found to be

$$A = \frac{35.2 (3413)}{0.91 (.88) (278.5-13.9)} = 568 \text{ square feet}$$

and the area needed to satisfy the geometric constraint is

$$A = \frac{120}{1 - .789} = 568 \text{ square feet}$$

Thus, the required area equalization has been achieved with a fin length of 0.59 feet.

Subsequent to the power conditioning radiator calculations, the efficiency of the power conditioning modules was lowered from 90 percent to 88 percent which is more representative of PC performance at low voltage reactor output. Rather than maintain the one square foot area per module assumption and take the large penalty in additional radiator fin area and weight, it was assumed that the module area was increased sufficiently to achieve a fin efficiency and fin area fraction as computed above. Thus, the required total radiator area becomes:

$$A = 1.2 (568) = 680 \text{ square feet}$$

The total power conditioning radiator weight is 1540 pounds.

The performance of low temperature radiators are influenced greatly by sink temperature conditions. The 300°R sink temperature assumed for the PC radiator analyses is an approximate average for the entire flight, but 50 to 70 days will be spent in the spiral-out escape from earth orbit where the sink temperature averages

455°R. The equations presented above were used to show that the PC radiator effective fin efficiency would decrease to 0.83 and the maximum operating temperature would increase to 212°F for the near earth sink temperature environment. If it is imperative to maintain a 175°F maximum PC radiator temperature in orbit, then the system power level must be maintained below 77 percent of full power.

The heat rejection rate for the payload, high voltage leads and thruster PC totals approximately 3.2 kW. By ratio, the heat rejection area (at 175°F) is 52 square feet and the radiator weights total 114 pounds.

5.1.3 PRIMARY LOOP SYSTEM

The weight of the primary loop system is dependent on the axial length of the power conditioning radiator which is located between the reactor-shield assembly and the main radiator. The change in vehicle axial length and the various radiator axial lengths were estimated in the following manner.

The total radiator area required aft of the shield is 1445 square feet, which is 330 square feet greater than the design in Reference 3. In order to maintain a small shield half angle, the added area is assumed to be added in the form of right circular cylinder, placed at the aft end of the vehicle. The length of the cylindrical addition is 11.4 feet, resulting in an overall vehicle length of 78.5 feet, and an overall shroud length of 81.5 feet.

The increase in primary loop piping length is approximately 35 percent due to the change in PC radiator dimensions. With the added length, the optimum pipe diameter will decrease, however, the net change in piping weight will increase. This increase is estimated to be +25 percent, and since the piping accounted for 1000 pounds of the total primary loop weight in the original design, a 250 pound increase was assumed for the point of departure primary loop system. The primary loop weight is therefore 2090 pounds.

5.1.4 LOW VOLTAGE CABLE

The average length of the low voltage cable has been increased by approximately 30 percent over the original design, increasing the cable weight to 890 pounds.

5.1.5 PAYLOAD

Revised estimates for the payload component weights indicate that the minimum scientific package will weigh about 185 pounds, the communications set will weigh 60 pounds, and 17 pounds will be needed for thermal control. The total minimum payload package weight is 262 pounds. However, in accordance with the design guidelines, the total payload weight, including communications subsystems is assumed to remain at 2200 pounds.

5.1.6 THRUSTERS

The total weight for the thruster subassembly has been stipulated at 1235 pounds. This subassembly includes 37 thrusters, thruster vector control system, and miscellaneous hardware.

5.1.7 WEIGHT SUMMARY OF THE BASELINE CONCEPT SYSTEM

Initial power plant calculations were based on the assumption of cylindrical or conical shaped radiators. A summary of the weights for this system is given in Table 5-2. Additional calculations were made to determine spacecraft weight distributions assuming triform, cruciform, and flat panel radiator configurations. A summary of the weights for these systems are also given in Table 5-2. The weight distributions and component sizes are illustrated in Figures 5-3 through 5-6. Since these designs will be used, in part, to determine launch load structural requirements, no launch support structure weights are specifically included.

For similar temperature, and heat rejection rates, cylindrical and flat panel radiators have equal areas, but the triform and cruciform radiators require greater

TABLE 5-2. WEIGHT SUMMARY, BASELINE CONCEPT POWERPLANT SYSTEMS
(ALL WEIGHTS IN POUNDS)

	Cylindrical Configuration	Triform Configuration	Cruciform Configuration	Flat Panel Configuration
Propulsion System - Subsystem	10621	10720	11035	10995
Reactor	3100	3100	3100	3100
Neutron Shield	1500	1310	1415	1240
Gamma Shield	600	520	560	500
Radiator - Primary	1861	1860	2200	1575
- Auxiliary	90	90	110	75
Coolant Loop - Primary	2090	2350	2215	2830
- Auxiliary	60	70	65	75
Power Cables - Low Voltage	890	980	930	1140
- High Voltage	280	290	290	310
Miscellaneous	150	150	150	150
Thruster Subsystem	6763	6043	6238	5923
Ion Engines	1233	1233	1233	1233
Propellant Tanks	810	810	810	810
Radiator - Power Cond.	1540	900	1095	780
Power Conditioning - High Volt.	2800	2800	2800	2800
- Spec. Duty	300	300	300	300
Payload Subsystem	2314	2270	2285	2260
Payload (Science, Communication)	2200	2200	2200	2200
Radiator - Payload	114	70	85	60
Total Spacecraft	19618	19033	19558	19178
Propellant	14500	14500	14500	14500
Initial Mass Mass in Earth Orbit	34118	33533	34058	33678

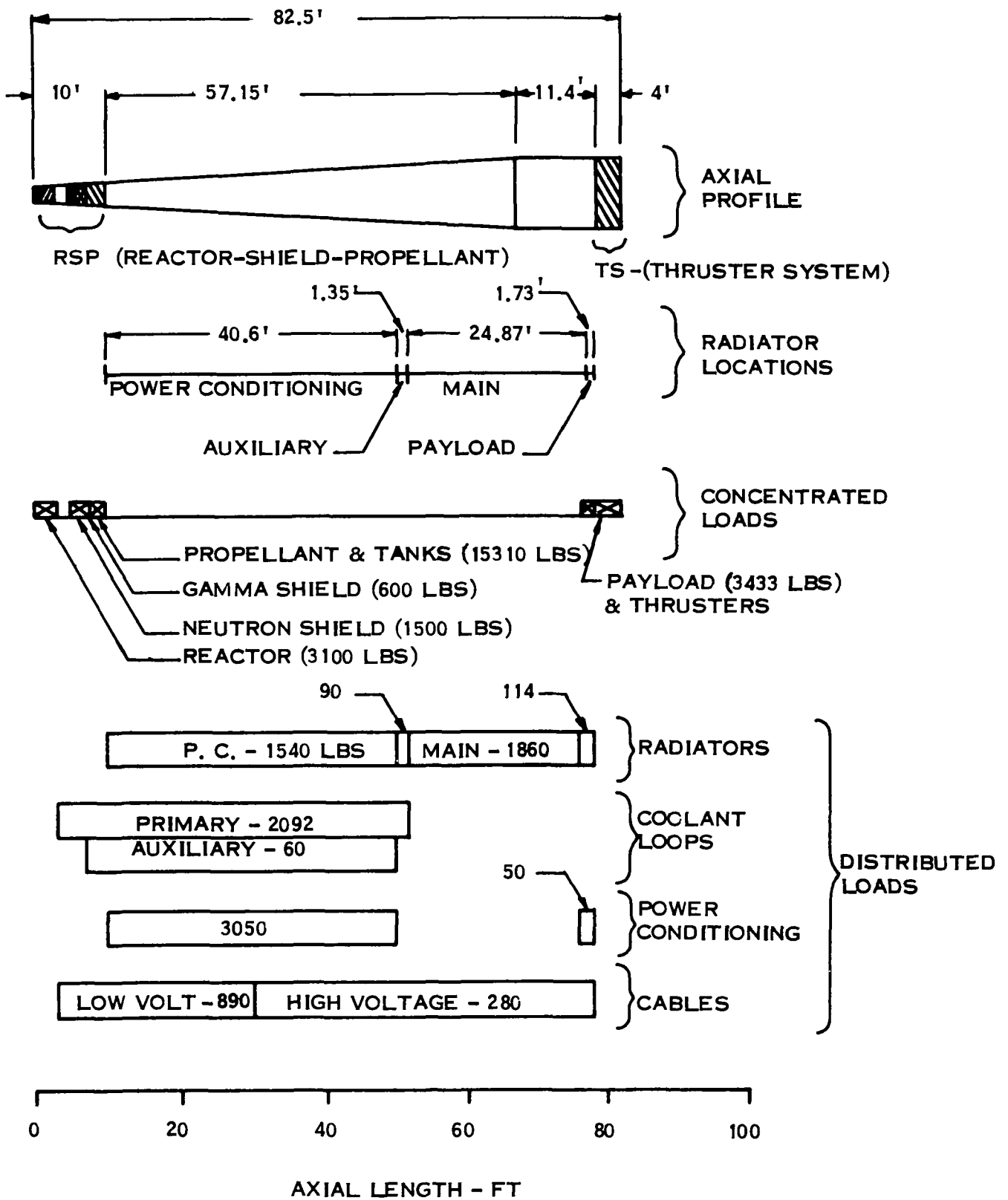


Figure 5-3. Baseline Concept-Cylindrical Radiator Configuration

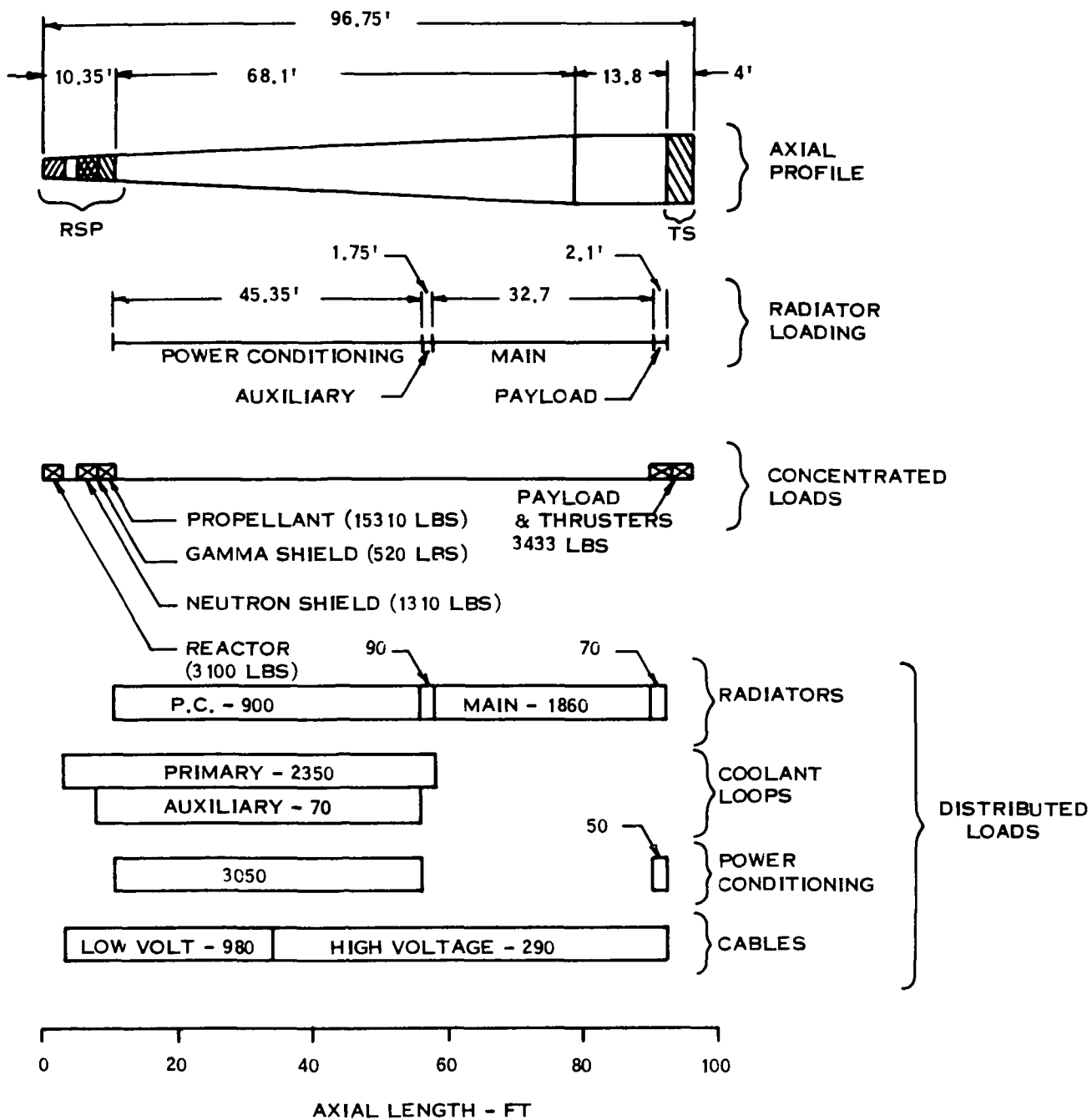


Figure 5-4. Baseline Concept Triform Radiator Configuration

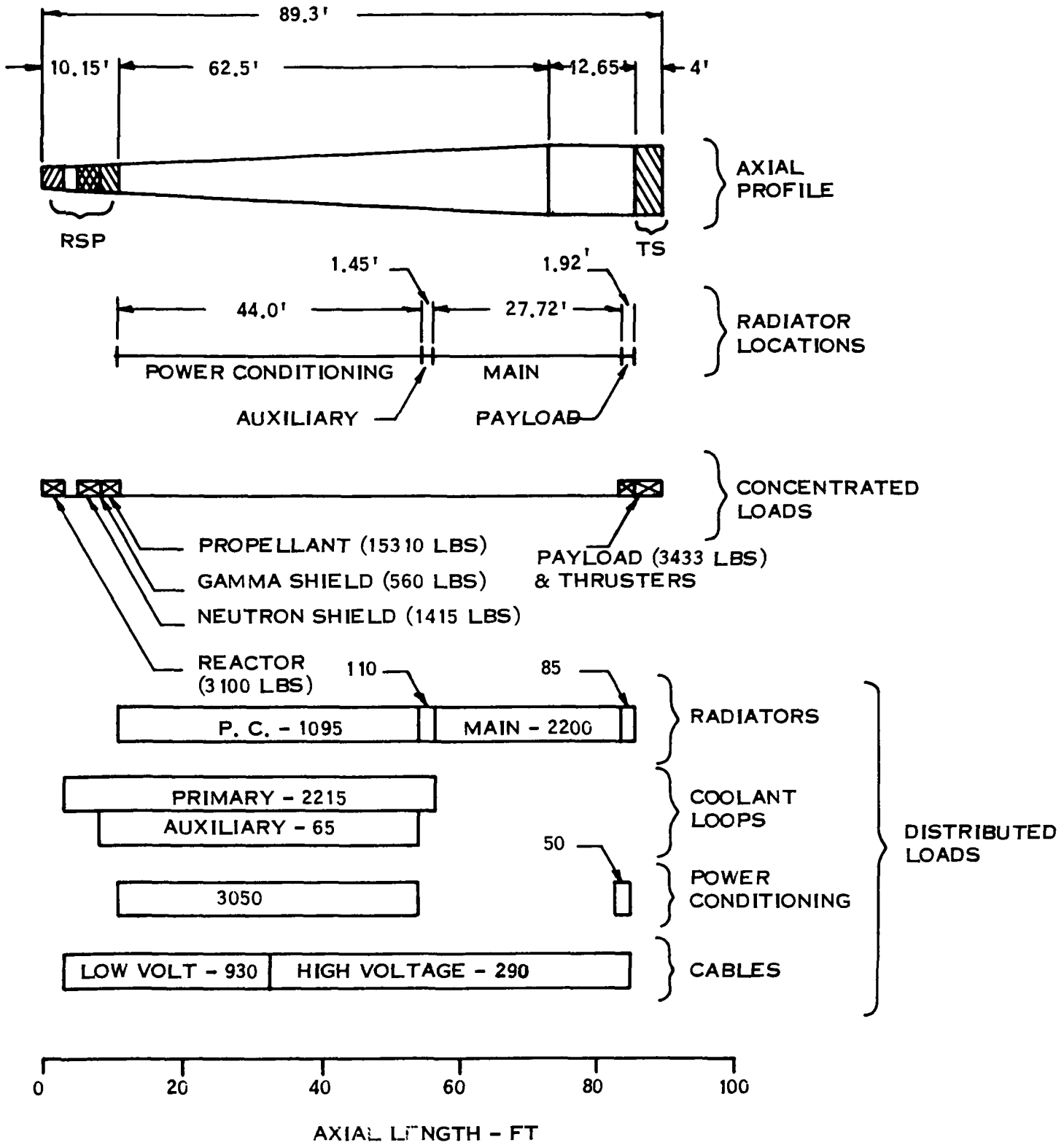


Figure 5-5. Baseline Concept-Cruciform Radiator Configuration

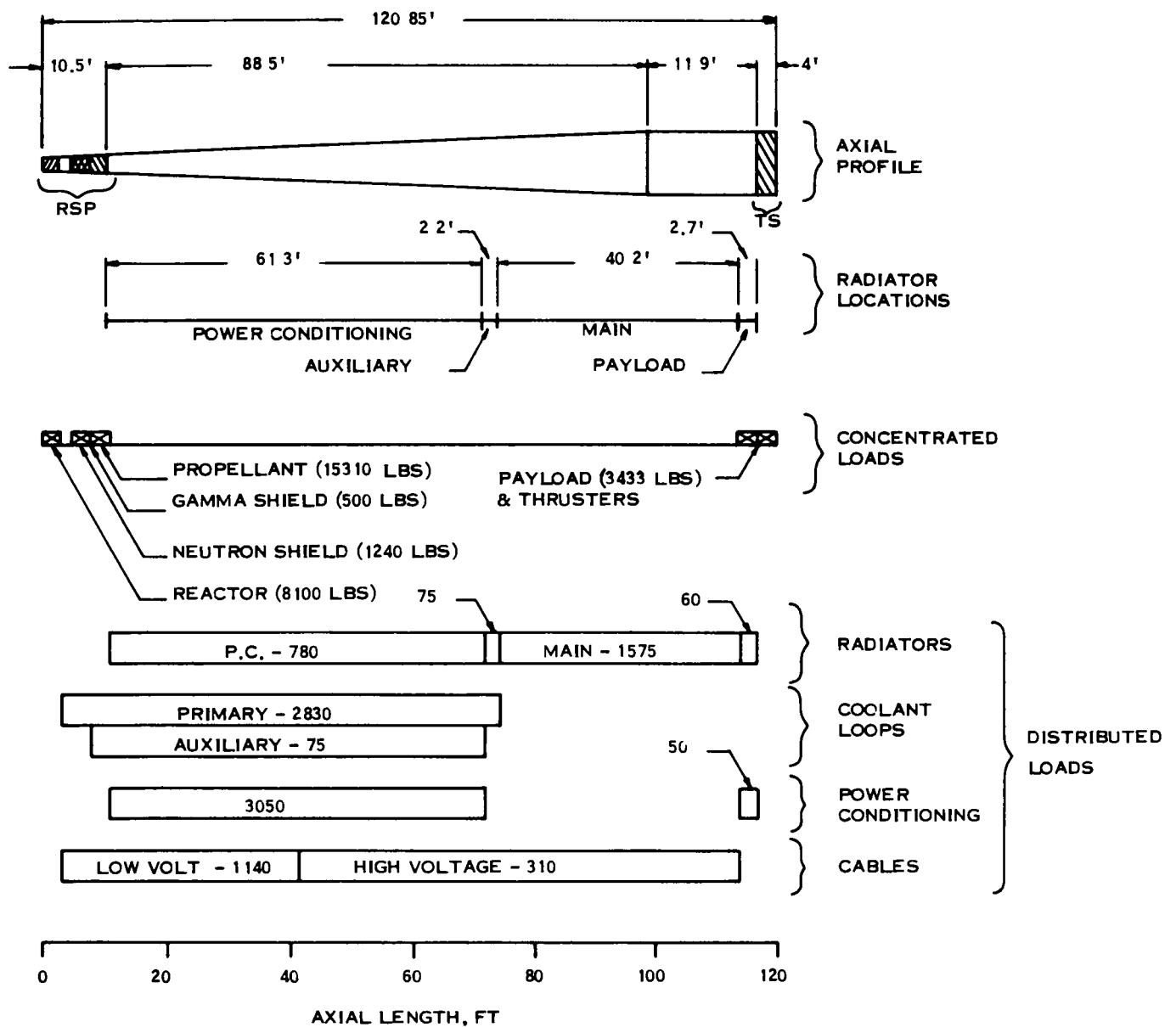


Figure 5-6. Baseline Concept Flat Panel Radiator Configuration

area because of lower effective view factors. The difference in geometry also results in different radiator lengths for the same radiator area and diameter envelope. The difference in lengths can be seen from the following ratios:

$\frac{\text{Triform length}}{\text{Cylindrical length}}$	1.21
$\frac{\text{Cruciform length}}{\text{Cylindrical length}}$	1.11
$\frac{\text{Flat Panel length}}{\text{Cylindrical length}}$	1.57

These ratios were used to estimate total vehicle lengths, radiator lengths, and changes in piping lengths and weights, for the various radiator shapes.

As shown in Table 5-2, shield weights vary slightly as a function of radiator shape. The reason for this change is best described by an example corresponding to the flat panel radiator configuration. The shield must protect the payload and thruster assemblies which are positioned around the backface of the vehicle. The minimum diameter conical shield is therefore a function of relative placement of the reactor, shield and payload. However, the shield must also shadow the radiators to prevent radiation scattering back to the payload. The shape of this portion of the shield will be a slab having the same width as the cylindrical shield and a height sufficient to protect the radiator thickness. Figure 5-7 compares the cross sectional shape of the two shield components - the circular shield for payload thruster protection and the slab shield for radiator protection.

The elliptical dashed outline illustrates the probable shape of the combined shield. This elliptical shape encompasses the areas of both the circular and slab shields, this geometry being required to prevent neutron or gamma radiation from being scattered into the payload or power conditioning areas behind the shield. Without the elliptical shape, radiation could be scattered out of the circular shield before it is attenuated to the desired level, and for example, be further scattered from the slab shield into the payload area.

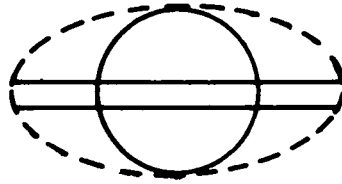


Figure 5-7. Example-Flat Plate Radiator Shield Geometry

Shield volumes, normalized to the shield volume for the cylindrical vehicle configuration, were determined to be:

Triform/Cylindrical	0.87
Cruciform/Cylindrical	0.94
Flat Panel/Cylindrical	0.83

The neutron and permanent gamma shield weights listed in Table 5-2 were computed directly from the above ratios.

5.2 SPACECRAFT STRUCTURAL REQUIREMENTS

The conical and triform radiator configurations for the baseline concept have been evaluated in terms of the additional structure required to survive the launch environments imposed by the Titan III C/7 launch vehicle. This evaluation was accomplished as a function of the spacecraft orientation on the launch vehicle, upright or inverted, and the utilization of the launch vehicle shroud as launch support structure. The preferred system is identified as the conical radiator, configured in the upright position on the launch vehicle. This configuration provides the minimum Initial Mass in Earth Orbit (IMEO), and therefore required the minimum structural addition necessary to survive launch, relative to a spacecraft nominally optimized for thermal performance.

The results of this analysis was employed in the weight optimization computer code discussed in Section 9. Particular structural requirements for the two spacecraft to be defined will be separately evaluated.

5.2.1 LAUNCH ENVIRONMENT

5.2.1.1 Titan III C/7 Launch Environment

Discussions with Martin Denver, Titan III Structural Dynamics Loads group, indicated that the Stage I burnout event, including the transient oscillation "Pogo" condition just prior to burnout, results in the most severe upper vehicle-spacecraft loadings. The Stage II burnout event was, in their experience, a less severe loading condition. However, they have no existing payloads of comparable size and flexibility. Both the conical radiator and the triform radiator spacecraft will be required to survive the Stage I burnout loads. However, in order to permit early separation of the supporting truss that is required for the triform radiator spacecraft, it will be required to survive the less severe Stage II burnout loads without a separate supporting truss. This approach permits the truss to be jettisoned at the time of shroud separation, normally accomplished just prior to Stage II burnout, at 280 seconds after launch. The truss weight penalty, in terms of IMEO, is then proportional to that of the shroud. The quasi-steady state load environments are therefore defined as:

- | | |
|---|----------------------------------|
| ● Cylindrical-conical vehicle (Stage I burnout) | 3g lateral
6g longitudinal |
| ● Triform vehicle - unsupported
(Stage II burnout) | 0.67g lateral
4g longitudinal |
| - with launch support truss
(Stage I burnout) | 3g lateral
6g longitudinal |

When informed that the spacecraft first lateral mode would be below the desired 6 cps, Martin Denver indicated that this may present some problems; but the launch vehicle could be designed around them. This problem was also present on the MOL

program, where the Titan IIIM was designed to accommodate 3 cps. The principal problem is that a low spacecraft natural frequency would couple the spacecraft directly with the booster during launch and ascent. This dynamic coupling manifests itself in two ways: first, it creates problems with the autopilot stability, which would be most critical during Stage "0" flight; and second, although the gravity loads given would not be increased, the dynamic effects would be experienced more often during flight rather than in the normal case where the maximum response is seen as a transient at the time of Stage I burnout.

5.2.1.2 Shroud Attachment

The use of a "snubbing" technique to transmit 5000 pound loads laterally from the payload structure to the shroud is possible for a 60 by 10 ft. diameter shroud configuration. This load would be taken 60 feet from the interface adapter, and is dumped into the shroud to limit the deflection of payload structure. A major consideration in this approach is that the launch probability (WTR) is reduced when based on the worst quarter winds or annual winds. The airload on the shroud is the major portion of the load encountered during boost phase. This airload can be altered by placarding, in which careful assessment of the environment, especially wind velocity up to 40,000 feet is made. This approach limits the days in which launching can be achieved.

5.2.1.3 Wind Placarding

Martin has performed a wind placarding study for 90 and 105 foot payload fairing configurations. The basic ground rules for each configuration were as follows:

90 foot fairing on a Titan IIIC/7

- 850,000 pound ultimate P_{EQ} transtage
- 3500 pound payload
- Mach 1.4

- $q_{\alpha} = 4000$ PSF-degree
- $q = 800$ PSF

105 foot fairing on a Titan III C/7

- 1,080,000 pound ultimate P_{EQ} adapter skirt
- 3500 pound payload plus Agena
- Mach 1.4
- $q_{\alpha} = 4000$ PSF-degree
- $q = 800$ PSF

Results of Martin study show that for each configuration, the percent of maximum design wind velocity that may be flown is approximately 53 percent. From this, the probability of launch from WTR is 72 percent for the worst quarter winds or 87 percent for annual winds.

5.2.2 CONFIGURATION SELECTION

Two basic vehicle configurations were investigated. One vehicle is a three section cylinder-conical assembly, 990.6 inches long. Details of the design and the loading diagram are shown in Figure 5-8. The second vehicle is a three section triform, 1155 inches long. Details of this configuration and a loading diagram are shown in Figure 5-9.

Five load/boundary conditions were analyzed for the cylinder-conical vehicle. The conditions are summarized below and are schematically shown in Figure 5-10. The combined dynamic launch environment is 3 g's lateral superimposed on 6 g's axial.

C1 - Upright unsupported, propellant loading divided between upper section, and base

C2 - Upright with two supports to the shroud, propellant loading divided between upper section and base

C3 - Inverted with two supports to the shroud, propellant loading in base

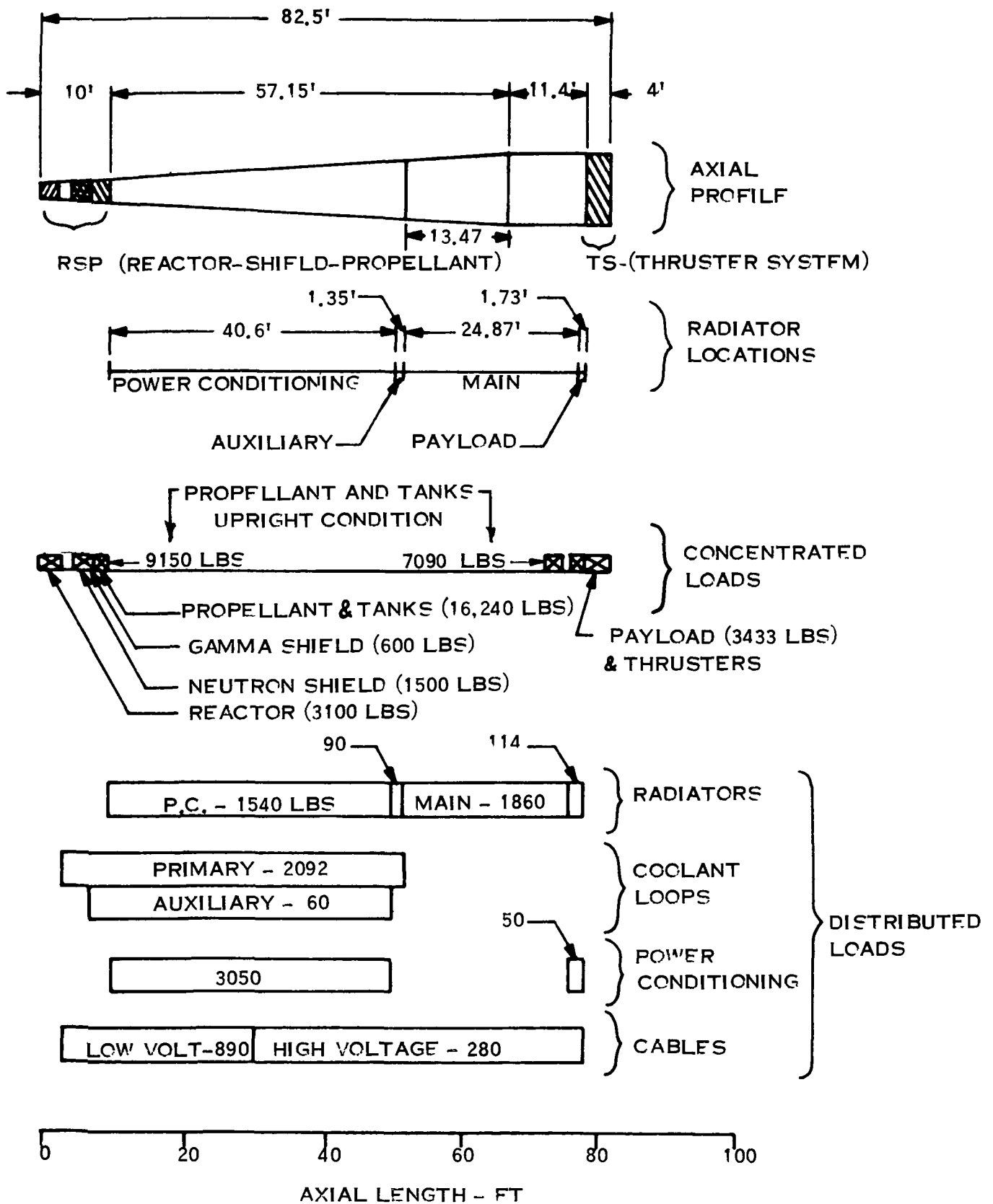


Figure 5-8. Baseline Concept-Cylinder-Conical Radiator Spacecraft Weight Distributions

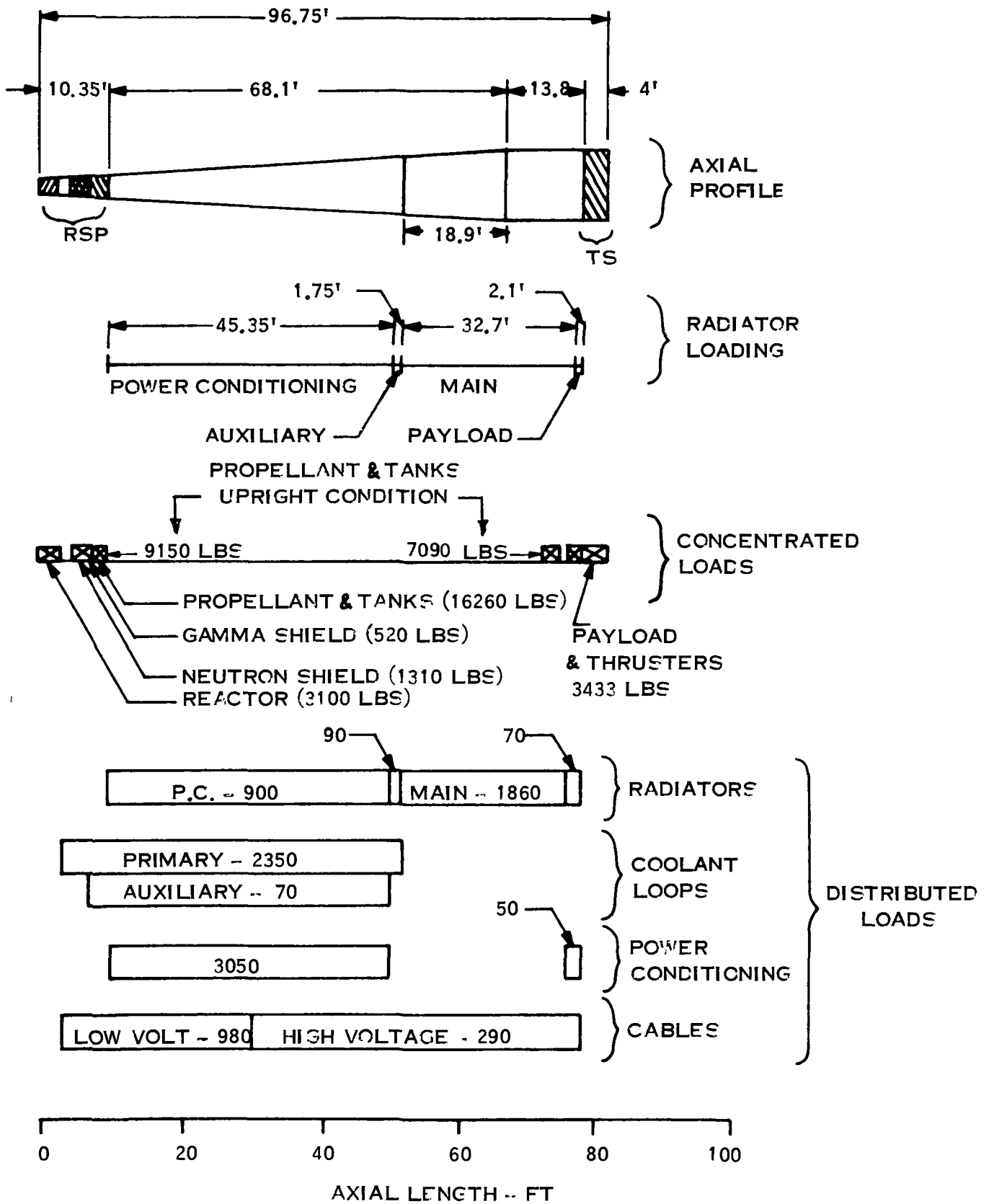
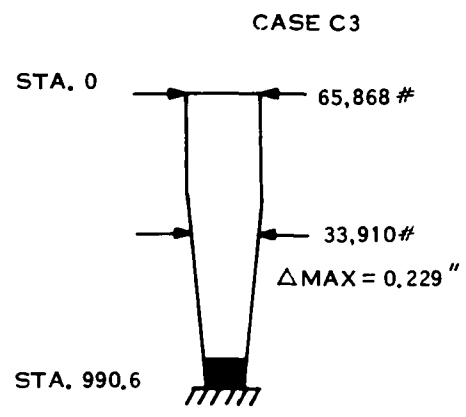
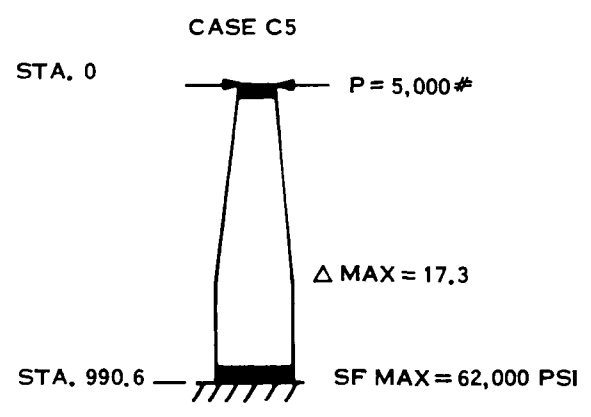
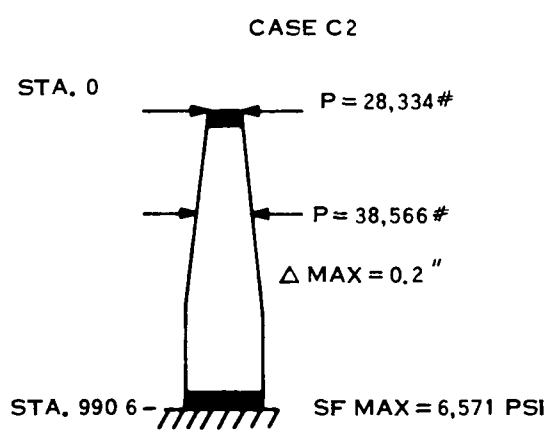
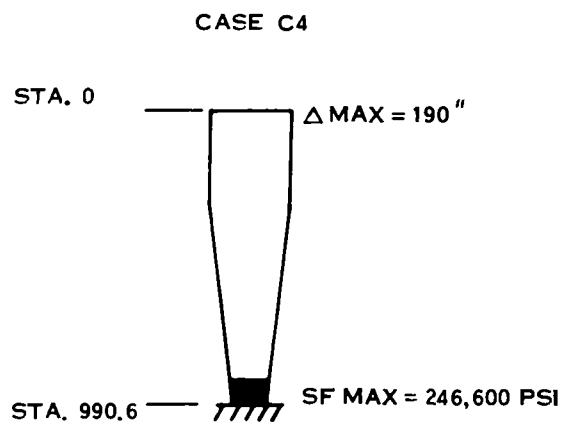
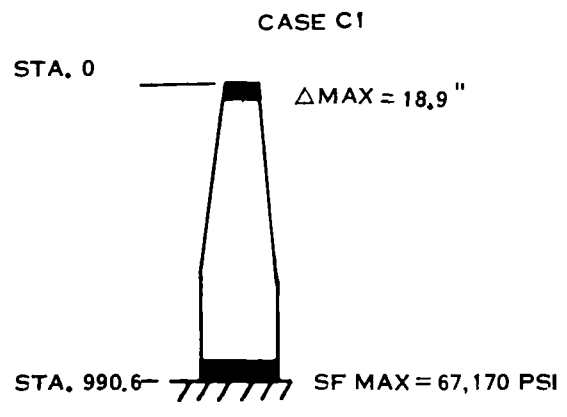
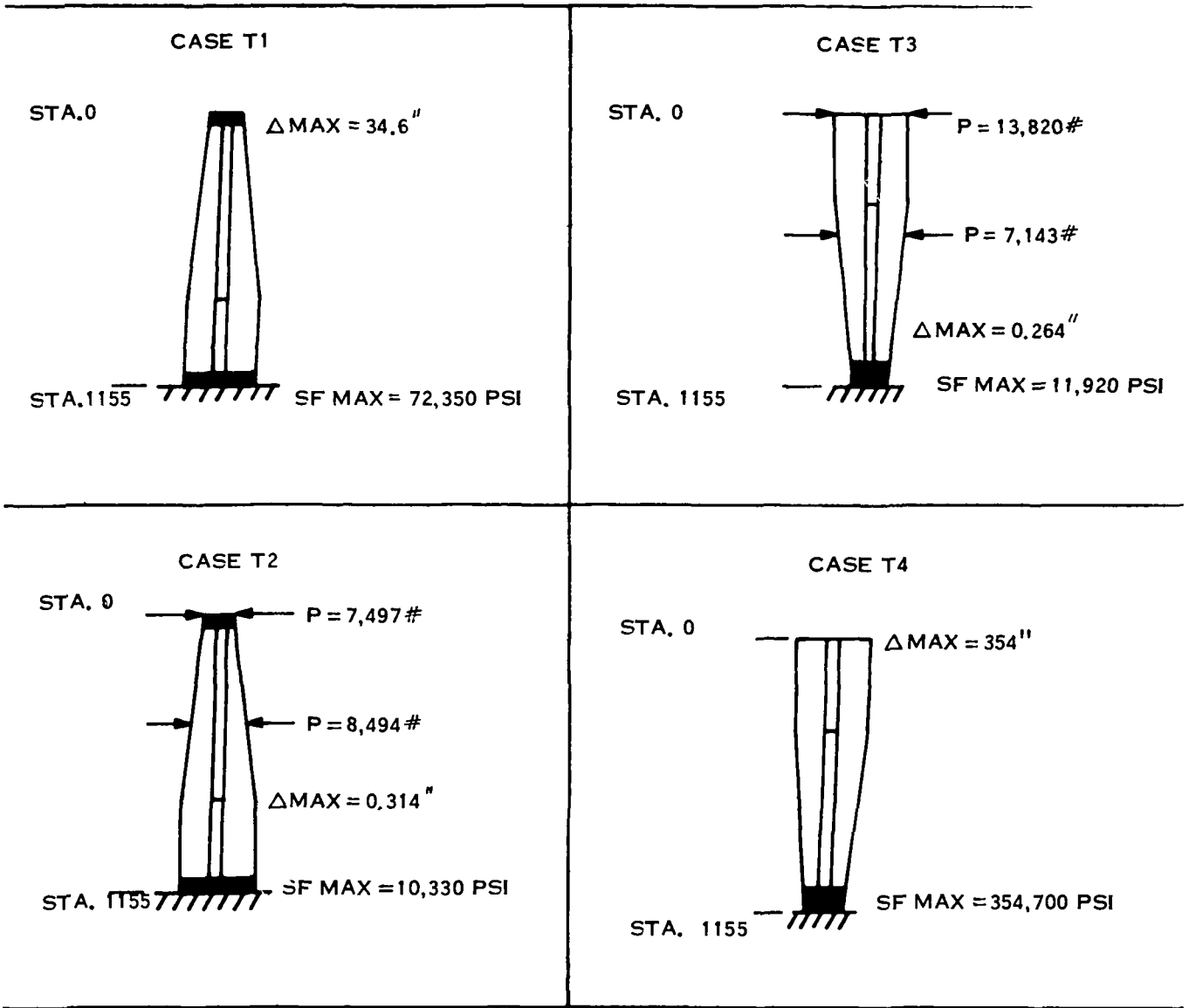


Figure 5-9. Baseline Concept-Triform Radiator Spacecraft Weight Distributions



LATERAL LOAD 3 G
 AXIAL LOAD 6 G

Figure 5-10. Load/Boundary Conditions for Cylindrical-Conical Radiator Spacecraft Design



LATERAL LOAD 0.67 G
 AXIAL LOAD 4.0 G

Figure 5-11 Load/Boundary Conditions for Triform Radiator Spacecraft Design

C4 - Inverted unsupported, propellant loading in base

C5 - Upright with maximum allowable reaction to shroud (5,000 pounds), propellant loading divided between upper section and base.

Four load/boundary conditions were analyzed using the triform vehicle. The conditions are stated below and illustrated in Figure 5-11. The combined dynamic launch environment employed is 0.67 g's lateral superimposed on 4 g's axial. This load environment occurs after second stage burnout. An auxiliary truss used to support the triform will accommodate the launch loads of 3 g's lateral and 6 g's axial. An analysis was also performed to determine the support truss weight and payload effects.

T1 - Upright unsupported, propellant loading divided between upper section and base

T2 - Upright with two supports to the shroud, propellant loading divided between upper section and base

T3 - Inverted with two supports to the shroud, propellant loading in base

T4 - Inverted unsupported, with propellant loading in base.

The propellant and tank weights shown on Figures 5-8 and 5-9 reflect an early selection of 15,000 pounds of propellant plus an assumed eight percent tank fraction (because of the unusual shield configuration of the tank, a truncated cone structure) for a total weight of 16,240 pounds. Current values are 14,500 pounds of mercury propellant, with a probable four percent allowance for structure, feed lines, valves, etc. However, this small difference does not effect the results of this structural analysis.

The data of Figures 5-10 and 5-11 also present maximum stresses, deflections and loads imposed on the shroud, where applicable, for the various cases investigated. The definition of these parameters are discussed below.

5.2.3 STRUCTURAL ANALYSIS SUMMARY

The results of the structural analysis are summarized on Table 5-3 for the five conical and four triform configurations investigated. Maximum stresses, maximum

TABLE 5-3. SUMMARY OF STRUCTURAL ANALYSIS

Load/Boundary Conditions	Case	Max Stress (psi)	Max Deflection (in)	Max Lateral Load (lbs)	Total Space-Craft Structure Wt at Launch (lbs)	Fundamental Frequency (cps)	Remarks
3 0 g's Lateral 6 0 g's Axial Conical -	C1	67,170	18 9	---	4944	1 17	This is the preferred configuration which meets the environmental requirements at the minimum structural weight with few design modifications
	C2	6,571	0 2	38,566	4944 plus fairing increment	1 36	A major redesign and additional weight would be required in the launch vehicle (LV) shroud to react the lateral loads
	C3	7,691	0 229	65,868	Same as 2	1 10	Same as 2 Also the LV shroud loads are higher and a larger adapter would be required for attachment to the launch vehicle
	C4	246,600	190 0	---	4944 plus conical LV adapter	0 56	The stresses and deflections are excessive Additional structure is required to bring the levels into an acceptable range A larger adapter is also required
	C5	62,000	17 3	5,000	4944 plus fairing increment	1 34	This configuration also meets the environmental requirements A special adapter is necessary to limit the LV shroud lateral load to a 5000 lb maximum
0 67 g's Lateral 4 0 g's Axial Triform -	T1	72,350	34 6	---	8689	0 49	The configuration, the best identified for the triform, will fly with an auxiliary truss during the launch environment The total weight is greater than the cone
	T2	10,330	0 314	8,494	8689 plus fairing increment	0 92	Same as 1 Also the LV shroud would require major redesign and additional weight to react the high lateral loads
	T3	11,920	0 264	13,820	Same as 2	0 99	Same as 2 Also the LV shroud loads are higher and a larger spacecraft-launch vehicle adapter would be required
	T4	354,700	354 0	---	8689 plus LV Adapter	0 19	The stresses and deflections are excessive Additional structure is required to bring the levels into an acceptable range A larger LV adapter is also required

deflections, maximum axial loads (where applicable), fundamental frequency and the total weight of the spacecraft structure required at launch are presented. The weight numbers shown are the total structure required to survive launch including those spacecraft components such as radiator which have been assumed to serve as structure. The definition of this effective spacecraft structure is presented in Paragraph 5.2.4.

The preferred configuration is the conical radiator spacecraft mounted in the upright configuration on the launch vehicle, Case C1, Figure 5-10. It meets all launch requirements with only minor modifications to the baseline spacecraft presented on Figure 5-8. These are the addition of longerons to stiffen the aluminum radiator section, some additional tube wall thickness in the copper/stainless steel radiator section, and circumferential rings throughout to prevent compressive buckling instability. The net weight increase for this additional structure is 1299 pounds, as defined in Paragraph 5.2.4. This configuration is selected because it provides the following advantages:

- a. Minimum spacecraft IMEO
- b. Acceptable stresses and deflections
- c. No required redesign of the standard Titan III shroud to provide lateral support

The upright conical, supported by the shroud (Case C2) is eliminated because, although no estimates were made, the weight increase associated with redesigning the shroud is certain to be greater than the integral structure concept selected, reducing the useful IMEO. The inverted conical, supported by the shroud is rejected for the same reasons. The shroud weight penalty would be even greater than for Case C2 since the inverted launch orientation does not efficiently utilize the available conical radiator as structure. Case C4, the unsupported, inverted conical arrangement also does not efficiently utilize the available radiator as structure, and weight of additional

structure necessary to provide acceptable stresses and deflections would probably exceed the weight of the Cu/SS radiator, about 2000 pounds. The case where one tie point is provided to the shroud might be acceptable since no shroud redesign is required because the axial load has been limited to 5000 psi, the maximum load that can be reacted to the shroud without major redesign. A spring system would be needed to limit the input loads to the 5000 pound level. Addition of this support has the effect of decreasing the overall deflection by 1.6 inches and the maximum stress by 5170 psi while increasing the frequency by 0.19 cps. These changes from the unsupported Case C1 condition are too small to warrant the additional weight and complexity of the required spring system.

Configuration T1 (Figure 5-11) is the most attractive of the triform radiator configurations. The triform configurations required an auxiliary truss system to prevent the inherent compressive buckling instability of the section. During Stage I launch environment, the auxiliary truss would require a great number of attachments to the triform structure in order to prevent buckling. Releasing these attachments can cause design problems during separation. The estimated minimum weight increase associated with the multiple attachment supporting truss is 4928 pounds.

The supporting truss is assumed to be jettisoned along with the shroud during the Titan IIC/7 Stage II burn (280 seconds after launch). The basic triform radiator structure is designed to survive Stage 2 burnout loads (0.67 g lateral and 4 g axial) and therefore the lower, subsequent transtage loads. The IMEO penalty associated with the 4928 pounds truss is therefore only about 1250 pounds. This, coupled with additional stiffening of the aluminum and Cu/SS radiator section of the triform results in a minimum net structural weight penalty of about 2580 pounds, ideally about twice the net structural weight penalty for the conical structure. However, many structural attachments between the truss and the triform radiator structure are required to prevent buckling failure prior to truss (and shroud) separation. Although not assessed, the weight penalty associated with stiffening the basic triform radiator structure, in

order to minimize the number of truss-to-radiator attachment points, represents a permanent weight increase, an increase in the IMEO which must be carried throughout the Jupiter orbiter mission. The primary reasons for rejecting the triform radiator configuration are:

- a. Higher IMEO, and/or
- b. Complex truss attachment and separation
- c. No potential to eliminate the standard Titan III shroud.

As in the case of the conical configuration, inversion of the triform configurations resulted higher stresses, higher shroud reactions and lower fundamental frequencies than the corresponding upright conditions. In addition, a larger adapter attachment between the spacecraft and the launch vehicle would be required. For these reasons the inverted conditions are considered undesirable.

The addition of shroud supports to the unsupported spacecraft reduced the deflections considerably, but tended to produce fairing loads which could not be accepted without a major redesign of the shroud. Hence, the unsupported (by the shroud) or the single, limited capability, fairing tie for the upright configuration is the most desirable condition for both the conical and triform configurations.

Although several of the configuration/boundary condition cases investigated meet the thermal structural and envelope requirements, none meet the current Titan launch vehicle autopilot minimum frequency requirement of three Hertz. To meet this frequency requirement, the spacecraft stiffness would have to be increased by a factor of 6.6 or the shroud by a factor of eleven with provisions for one support into the existing spacecraft. Probably the simplest, and certainly the minimum weight approach is to modify the autopilot to accept payload frequencies in the range of one Hertz.

5.2.4 STRUCTURE DEFINITION

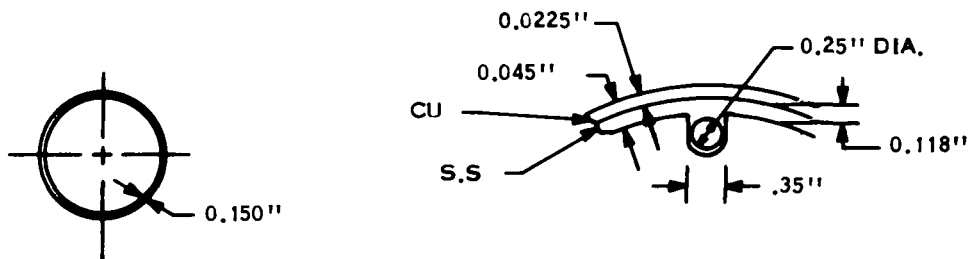
The portion of the baseline thermionic spacecraft designs which can be readily utilized as structure are the radiators, the aluminum passive power conditioning radiator and the active, copper-stainless steel tube and fin primary radiators. The weight and geometry of these components is summarized on Figures 5-12 and 5-13 for the conical and triform radiator spacecraft, respectively, under the following assumptions:

- a. The spacecraft is at ambient temperature when launched
- b. The aluminum radiator structure is characterized by the 2024-T3 alloy which has an ultimate tensile strength of 65,000 psi, and a compressive yield strength of 40,000 psi
- c. The stainless steel radiator structure is characterized by the 301 alloy, half-hard, which has an ultimate tensile strength of 150,000 psi, and a compressive yield strength of 58,000 psi
- d. The copper structure in the Cu/SS' radiator is expressed as an equivalent thickness of stainless steel for stress analysis purposes.

Although the main radiator terminates at the start of the payload equipment bay, at least an equivalent structure will be required to transmit the accumulated loads from this point to the launch vehicle (upright launch) or the launch vehicle shroud (inverted launch). Therefore, the cross sectional characteristics, and the associated weight per unit length of the main radiator are assumed to extend aft through both the payload bay and the ion engine thruster bay, located immediately behind (Figures 5-8 and 5-9). The weight of the payload and special thruster power conditioning radiators is to be included in the structural weight of these two spacecraft bays.

A preliminary assessment of the baseline structure indicated that it would require some stiffening and/or additional support structure. This requirement would be most severe for the triform, and less for the cylindrical conical radiator. Therefore, the

Spacecraft Component	Available Structure Weight, lbs. (Baseline Design)	Assigned Structure Weight, lbs. (As Analyzed)	Required ^(a) Additional Structure Weight, lbs.	Total ^(a) Structure Weight, lbs.
Low Voltage Power Conditioning Radiator	1540	1644	150 ^(c)	1694
Auxiliary Radiator	90	206		
Primary Radiator	1860	2266	18 ^(d)	3250
Payload Bay	(b)	300		
Thruster Bay	(b)	360		
Total	3490	4876		4944 ^(e)
Net Structural Weight Penalty IMEO = 4944 - 3490 - 155 ^(e) = 1299				



ALUMINUM RADIATOR

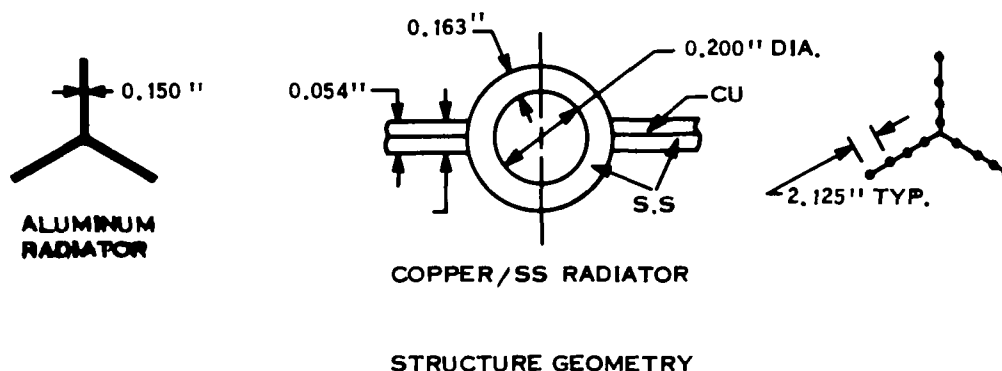
COPPER/SS RADIATOR
(180 TUBES - NOMINAL)

STRUCTURE GEOMETRY

- (a) Preferred (minimum weight) configuration; upright conical
- (b) Except for local radiators, concentrated loads of payload and thruster subsystem components assumed as no structural value.
- (c) Circumferential rings.
- (d) Circumferential rings (300 lbs), less 282 lbs weight reduction from tapered bumper on radiator tubes.
- (e) Includes estimated 155 lbs required for radiators in payload and thruster subsystem bay.

Figure 5-12. Structural System Weight Summary, Cylindrical Conical Radiator

Spacecraft Component	Available Structure Weight, lbs. (Baseline Design)	Assigned Structure Weight, lbs. (As Analyzed)	Required ^(a) Additional Structure Weight, lbs.	Total ^(a) Structure Weight lbs.
Low Voltage Power Conditioning Radiator	900	900	336 ^(c)	1236
Auxiliary Radiator	90	112	none ^(c)	112
Primary Radiator	1860	2234	none ^(c)	2234
Payload Bay	(b)	139	none ^(c)	139
Thruster Bay	(b)	264	none ^(c)	264
Launch Support Truss	-	-	4928 ^(d)	4928
Total	2850	3649		8913^(e)
Net Structural Weight Penalty at Launch = $8913 - 2850 - 155^{(e)} = 5908$ lbs. Net Structural Weight Penalty, IMEO = $3649 + 336 - 155^{(e)} - 1250^{(d)} = 2580$ lbs.				



- (a) Best (minimum weight) triform configuration; upright and unsupported.
- (b) Except for local radiators, concentrated loads of payload and thruster subsystem components assumed as no structural value.
- (c) Required additional structure to survive Titan IIIC/7 stage 2 burnout loads.
- (d) Required to survive initial launch loads; jettisoned with shroud just prior to stage 2 burnout, IMEO penalty is 1250 lbs.
- (e) Includes estimated 155 lbs required for radiators in payload and thruster subsystem bays.

Figure 5-13. Structural System Weight Summary
Triform Radiation

following changes were made in the baseline structure prior to initiation of detailed analyses:

- a. Ninety aluminum "hat shaped" 0.04 square inch (effective) longerons were added to the aluminum power conditioning radiator in the conical configuration, i. e. , one-half of the number of tubes in the copper-stainless steel radiator.
- b. The area and therefore moment of inertia of the copper-stainless steel radiator was increased by the addition of 0.1 inch of stainless steel to the armor of each of the 180 tubes. Although this additional structure could be placed elsewhere, the selected location provides additional, although unnecessary, meteoroid protection.
- c. The thickness of the stainless steel tubes in the triform radiator was similarly increased.

The effect of these changes on the spacecraft structural weight are also shown on Figures 5-12 and 5-13. The results of the analyses performed support these preliminary weight adjustments in that still additional structure is required to survive launch, primarily in the form of stiffening rings to reduce the buckling loads on the conical radiator and, in the form of separate truss work for the triform radiator. These additional weights are also illustrated on Figures 5-12 and 5-13. The details of this analyses, presented below, also indicate that about one half of the 0.1 inch added to the bumper thickness on the conical radiator can be removed, so long as this is accomplished by tapering this thickness from 0.1 inch at the base of the spacecraft, to zero at the top of the Cu/SS radiator. This effect is included in the total spacecraft structural weight at launch presented on Figures 5-12 and 5-13.

5.2.5 STRUCTURAL ANALYSIS

5.2.5.1 Computer Programmed Analysis

Two computer programs were written to determine the physical properties of the cylinder-conical and the triform spacecraft configurations. The physical shapes and member sizes used in computation were as per the thermionic designs shown in Figures 5-12 and 5-13.

Program "Cone" determined the properties of the cylinder-conical configuration including the area, inertia, torsional and shear constants. An integration method was used to determine the varying properties along specified vehicle stations. The second program "Triform" determined similar properties for the triform configuration.

Due to the number of conditions to be analyzed, combined with the complexity of the loads and redundant boundary restraints, the analysis was completed using the General Electric "MASS" computer program. Both spacecrafts were modeled for the program using 27 nodal points, each with six degrees of freedom. The physical properties, as determined by the "Cone" and "Triform" computer, were used at the respective nodal points.

The concentrated and distributed loads shown in Figures 5-8 and 5-9 were applied to the spacecraft models. A quasi-static steady state load magnification of 3 g's lateral superimposed on 6 g's axial were used for the cylinder-conical model analysis. Load magnification factors of 0.67 g's lateral and 4 g's axial were used for the triform model analysis. The loads used for the triform model are equivalent to the second stage burnout environment. The triform is basically unstable relative to compressive buckling, and the analysis assumed an auxiliary support truss would be used to accommodate the launch load environment prior to Stage 2 burnout. Since the loads distribution is proportional to the magnification factor, their magnitude can be modified for other load environments, if required.

Nine load/boundary conditions, as shown in Figures 5-10 and 5-11 were analyzed. Selected results in terms of stresses, displacements, loads and physical properties were plotted versus station number and are included in Appendix A.

5.2.5.2 Compressive Buckling Analysis

A compressive buckling analysis was performed to determine the stability of the preferred cylinder-conical and triform configurations, Cases C1 and T1. The

cylinder-conical configuration was found to be stable, requiring only stiffening rings about the circumference at average intervals of 24 inches. The triform configuration was found to be critical in buckling. Considerable stiffening in the form of attached members to reduce the panel widths or an auxiliary truss is required. The analysis performed on these sections is presented below.

5.2.5.2.1 Instability Analysis of Cone-Cylinder Configuration C1 - The configuration of cone and longerons in question will remain stable up to a certain length after which circular frames or supporting rings must be used to maintain stability. The maximum axial load per longeron is 11,754 pounds; the effective area of longeron with skin is 0.252 square inches and the inertia of longeron with skin is 0.0043 inches. Therefore, the maximum axial stress per longeron is 46,642 psi.

The column equation (Reference 4) used to find the required spacing of circular frames is:

$$F_C = \frac{C\pi^2 E}{(L/P)^2}$$

which yields a required spacing of 15 inches, assuming an end restraint factor of 2.0 for C. Hence, supporting rings are required.

The moment and EI versus station curves presented in Appendix A show that the moment varies more rapidly than the inertia thus allowing an increase in frame spacing, and a tapering of the tube wall thickness along the length of the radiator. An average spacing of 24 inches will be used and, therefore, 30 frames will be required.

The frame size is calculated using the following frame stiffness equation (Reference 4):

$$(EI) = MD^2/16000 (L)$$

The required frame inertia at the base of the spacecraft is found to be 0.071 inch⁴. This inertia requirement is met by a tube frame 1.5 inch square with a 0.049 inch wall.

The required frame size at the top of the spacecraft is a 0.625 inch square tube frame with a 0.028 inch wall, which meets an inertia requirement of 0.004 inch⁴. Therefore, the average frame area required is 0.165 square inches, and the additional weight per frame is 15 pounds. The total weight for the thirty frames required is 450 pounds. Because smaller, wider spaced frames may be used in the aluminum section, it is estimated that the weight allocation will be 150 pounds in the aluminum radiator and 300 pounds in the Cu/SS radiator.

5.2.5.2.2 Buckling and Lateral Instability Analysis of Triform T1 Configuration -

As previously noted, the triform structure is required to be self-supporting at, and after, Stage 2 burnout, where the worst loading conditions are 0.67 g lateral and 4 g axial. Prior to this condition, the 3 g lateral and 6 g axial loads are taken up by a separate truss (See Paragraph 5.2.5.3), which is jettisoned along with the shroud just prior to Stage 2 burnout. The following analysis is directed toward the structural requirements necessary for the triform configuration to survive the Stage 2 burnout loads.

a. Aluminum Section - The maximum column loading at the base of this section is a moment of 7.732×10^6 inch-pounds and a load of 9.162×10^4 pounds. Combining the moment and axial load to find the total column load on one flange (one third) of the triform:

$$P_{\text{axial}} = \frac{M_0}{48} + \frac{P}{3}$$

$$P_{\text{axial}} = 1.9158 \times 10^5 \text{ pounds}$$

where the factor 48 is the distance in inches from the center to the outer edge of one flange of the triform. The axial stress, based on the local area, is therefore 31,930 psi.

One flange of the 0.15 inch thick aluminum section triform has a b/t of 300 (48/0.15), for which the buckling stress is much lower than the axial stress of

31,930 psi. Therefore, the flanges of the triform will have to be stiffened to prevent them from buckling.

For an efficient section (Reference 4), referring to Figure 5-14 values of b_w/b_s equal to 0.3 and t_w/t_s equal to 1.0 are required. Assuming a working stress of σ_c at 25,000 psi, and using the equation:

$$\sigma_c = \frac{K_s \pi^2 E}{12 (1-\nu^2)} \left(\frac{t_s^2}{b_s} \right)$$

with a K_s value of 4.0, corresponding to the selected values of b_w/b_s and t_w/t_s , nine stiffeners of 1.7 by 0.16 inches are required for each aluminum panel. This increases the total panel area by 38 percent and reduces the axial stress to 22,875 psi. This compares favorably with the assumed stress of 25,000 psi and the stiffened, aluminum radiator section will be stable.

b. Cu/SS Section - Following the same procedure, at the nominal five foot wide base of the active radiator, for the geometry of Figure 5-13, a moment of 15.82×10^6 inch-pounds, and a load of 1.48×10^5 pounds, the axial stress is found to be 41,000 psi. The allowable stress for the existing structure (K_s of 5 (Reference 4) is found to be 86,862 psi.

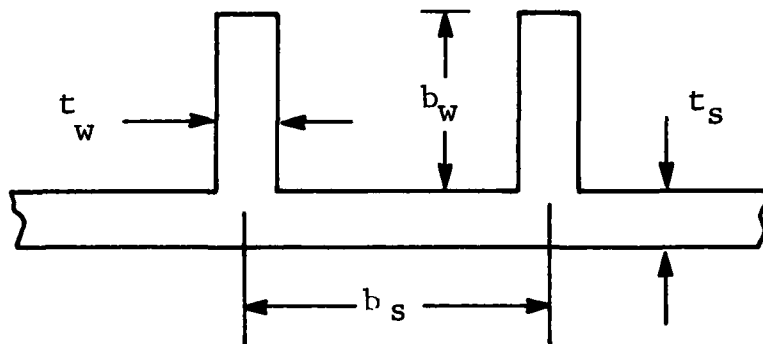


Figure 5-14. Stiffened Panel Geometry

Since the compression yield for 301 SS - half hard is only 58,000 psi, it becomes the allowable. However, the actual stress of 41,000 psi is lower than the compressive yield stress, and therefore, the steel section is stable without reinforcement.

Under the reduced load conditions of 0.67 g lateral and 4 g axial, the weights of the triform, Case I, after second stage burnout are:

- a. Weight of copper/stainless steel section - 2749 pounds
- b. Weight of aluminum section - 900 pounds
- c. Weight of aluminum section, with reinforcement - 1236 pounds.

Hence, after jetisoning the supporting truss required at launch to reduce the load levels, the triform structure will weigh 3985 pounds.

5.2.5.3 Launch Support Truss - Triform

The truss required to withstand the more severe Stage 1 burnout launch loads will now be examined. These conditions are 3 g lateral and 6 g axial.

5.2.5.3.1 Aluminum Section - Ratioing the moment and axial loads at the base of the aluminum section up to the increased launch loads, the moment increases to 34.62×10^6 inch-pounds and the load increases to 13.74×10^4 pounds. The load on one flange of the triform becomes 7.67×10^5 pounds. The maximum F_{cy} for the reinforced aluminum triform is 25,000 psi. Therefore, the load which can be carried by the reinforced area is:

$$F_{AL} = 25,000 (8.375) = 209,375 \text{ pounds}$$

Hence, the load which must be carried by the truss is:

$$F_{\text{truss}} = P_{\text{axial}} - F_{AL} = 557,625 \text{ pounds}$$

Now, assuming the truss to be made of 17-7 PH stainless steel, 1/2 hard, with an allowable F_{cy} of 147,000 psi, the truss area required is 3.8 square inches.

5.2.5.3.2 Steel Section - Proceeding in the same manner, the area increase at the base of the spacecraft is found to be 5.2 square inches.

The total weight of the truss required for the triform, under launch load conditions, is computed at 4928 pounds. This represents a minimum weight, which requires many truss-to-triform attachment points along the length of the spacecraft (at least every two feet). Weight required for connection of the truss work to the spacecraft has not been calculated, but it could be as much as 10 to 15 percent of the truss weight.

5.2.6 STRUCTURAL DYNAMIC ANALYSIS

The two baseline thermionic spacecraft configurations (conical and triform) discussed in the first section of this report were analyzed. The nine cases discussed there and three additional cases are analyzed and results tabulated herein.

A basic minimum vibrational characteristic of 3 cps on frequency is desirable to insure against interactions between the current launch vehicle control system (e.g., Titan IIM) and the spacecraft.

The structural dynamic analysis was carried out by applying methods of linear algebra, along with the dynamical equations of motion, to lumped-parameter-models of the two basic thermionic spacecraft configurations. Each configuration corresponds to varying boundary conditions as shown in Figures 5-10 and 5-11.

5.2.6.1 Lumped Mass Model

Both the conical and the triform configurations use the same basic lumped mass model. Figure 5-15 shows the basic dynamic model used. The cantilevered system is shown fixed free with none, 1 and 2 ties into the shroud. The mass to be lumped at the various mass points consists of various concentrated loads such as propellant, reactor, thrusters, and various distributed loads such as structure and radiators.

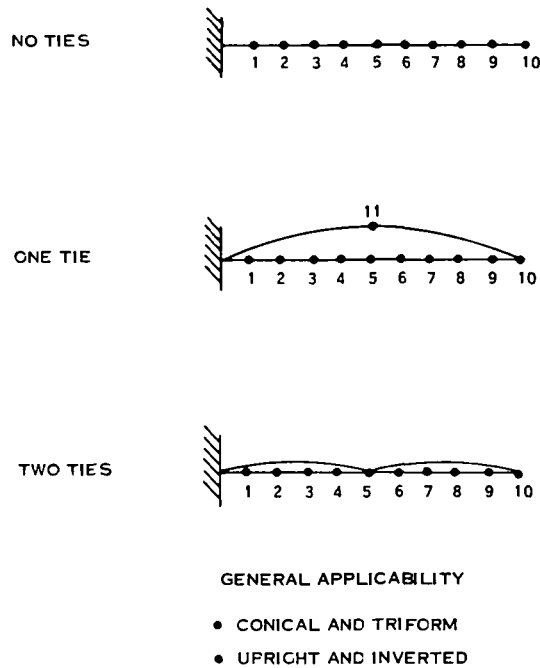


Figure 5-15. Baseline Concept Dynamic Models

The mass was lumped as shown in Table 5-4. Point zero is taken as the base of the structure. In this configuration, 9150 pounds of propellant and tank were located at the apex near the reactor to provide additional shielding for the reactor. The remaining 7090 pounds of mercury and tank was located at the base. In the inverted launch position, with the reactor (and apex) located at the interface, the 9150 pounds of propellant and tank was also moved to the apex to increase the natural frequency, and reduce the load.

Figures 5-16 and 5-17 show the area and inertia distributions used in determining the spacecraft stiffness. The material used in the structure is stainless steel, copper, and aluminum. Length between mass points was 100 inches and 115 inches for the conical and triform configurations, respectively.

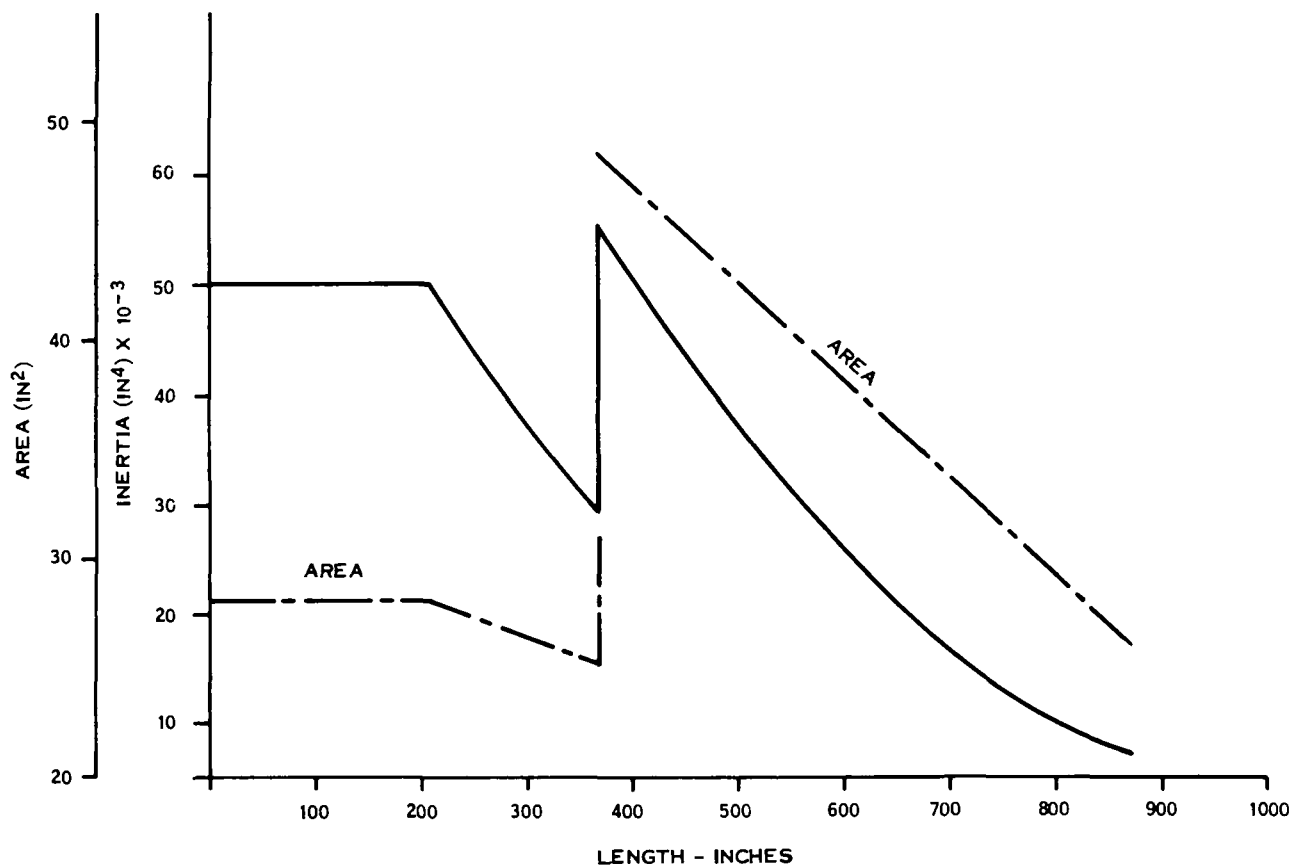


Figure 5-16. Conical Configuration Dynamic Properties

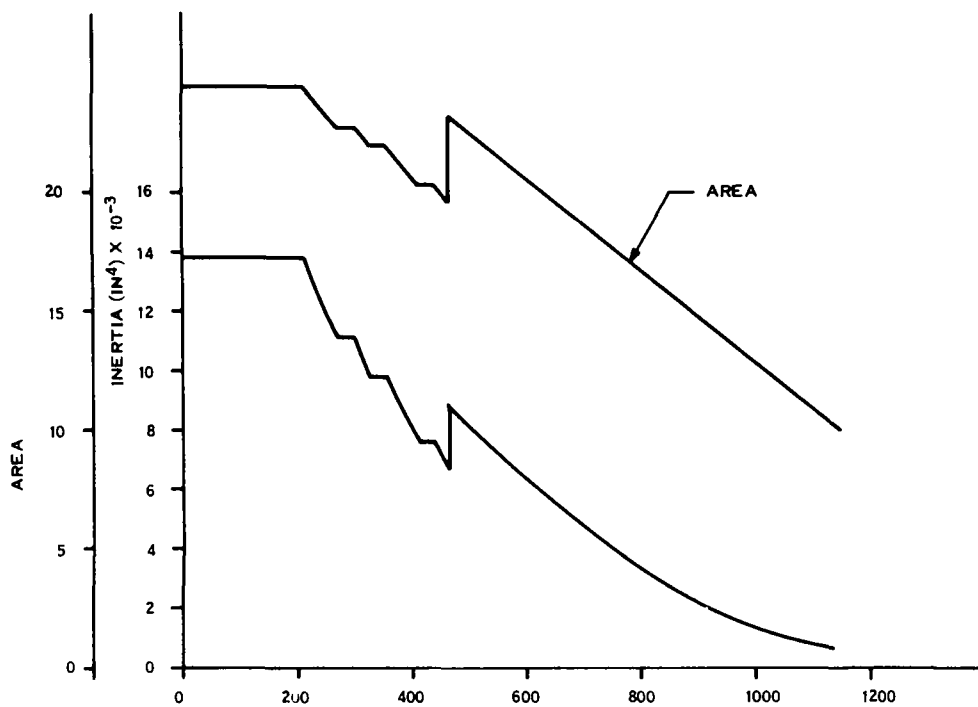


Figure 5-17. Triform Configuration Dynamic Properties

5.2.6.2 Normal Mode Shapes and Natural Frequencies

The two configurations were examined in the upright and inverted positions for cases of zero, 1 and 2 ties into the shroud. The frequencies of vibration as well as the mode shapes of these cases were obtained. Frequency results are presented in Table 5-5 for the lowest three modes. The triform configuration is immediately seen to be very bad dynamically in view of the current 3 cps requirement for prevention of interaction with the launch vehicle control system. The conical configuration is also poor, but better than the triform configuration. For both configurations, the upright position is far better than the inverted. Mode shapes corresponding to the lowest natural frequency of each of the 12 cases are shown in Figures 5-18 through 5-21. These figures show the effect of the ties to the shroud. While two ties are not appreciably better than one tie from a frequency viewpoint, it does significantly reduce displacements.

As a check on the validity of the model used in the analysis, a single degree of freedom frequency computation was made on the upright conical configuration with no shroud ties. This computation yielded 1.27 Hz, which compares with 1.17 Hz obtained from the 10 point 30 degree of freedom model. Thus, a high level of confidence may be associated with the lowest frequency results.

5.2.6.3 Shroud Stiffness Requirements

An approximate calculation was made to determine how much stiffness must be added to the shroud to bring the lowest frequency of the spacecraft shroud system up to 3 cps (MOL Program Requirements). The computation was made for the case of two shroud ties, and for the upright conical configuration.

Since the system is basically a beam, the lowest frequency may be considered proportional to the square root stiffness to mass ratio

$$f_1 \sim \sqrt{EI/\mu}$$

TABLE 5-4. MASS DATA FOR LUMPED MASS MODEL

Upright Conical Configuration

<u>Mass Point</u>	<u>Weight (lb)</u>	<u>Bending Inertia (lb-in²) x 10⁻⁴</u>
0	7776	142
1	5033	264
2	1635	264
3	1610	232
4	1577	101
5	1825	81
6	1780	65
7	1790	52
8	1740	40
9	12588	31
10	3215	9.5
	Shroud	
0	2000	4550
11	4000	9040
10	2000	4550

TABLE 5-5. THERMIONIC SPACECRAFT STRUCTURAL DYNAMICS

Configuration	Frequencies (cps)		
	1st	2nd	3rd
Upright Cone No Ties	1.17	6.47	11.86
1 Tie	1.32	6.55	11.31
2 Ties	1.36	6.79	11.32
Inverted Cone No Ties	.56	4.73	8.77
1 Tie	1.06	4.92	7.22
2 Ties	1.10	5.45	8.43
Upright Triform No Ties	.49	2.98	5.82
1 Tie	.89	3.51	6.41
2 Ties	.92	5.10	6.93
Inverted Triform No Ties	.19	2.02	4.85
1 Tie	.98	2.51	5.04
2 Ties	.99	3.71	5.36

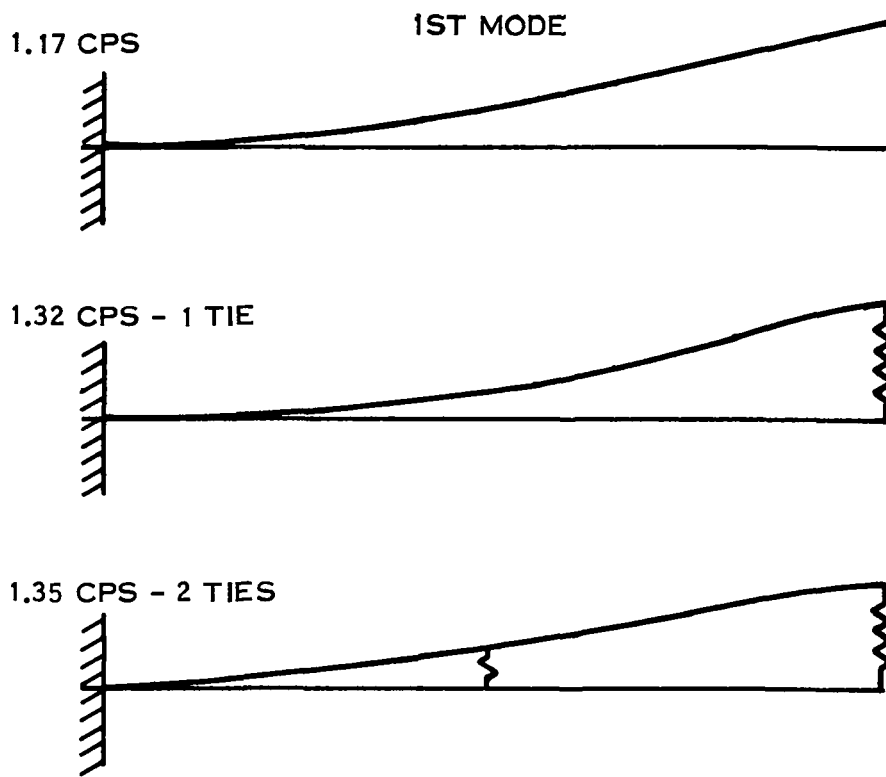


Figure 5-18. Baseline Concept Upright Conical Mode Shapes

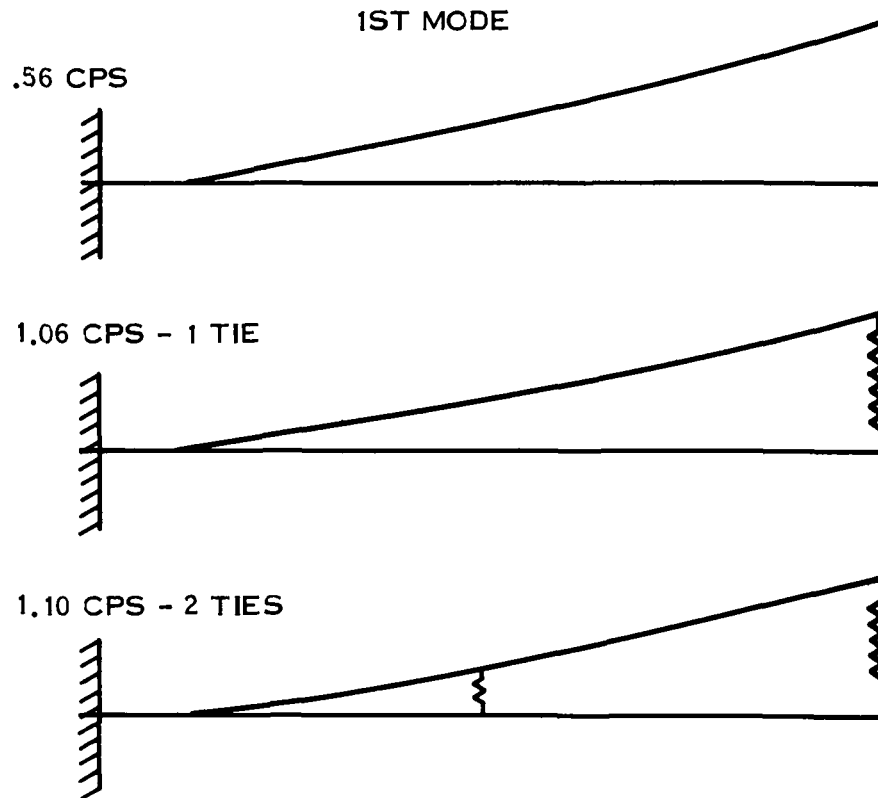


Figure 5-19. Baseline Concept - Inverted Conical Mode Shapes

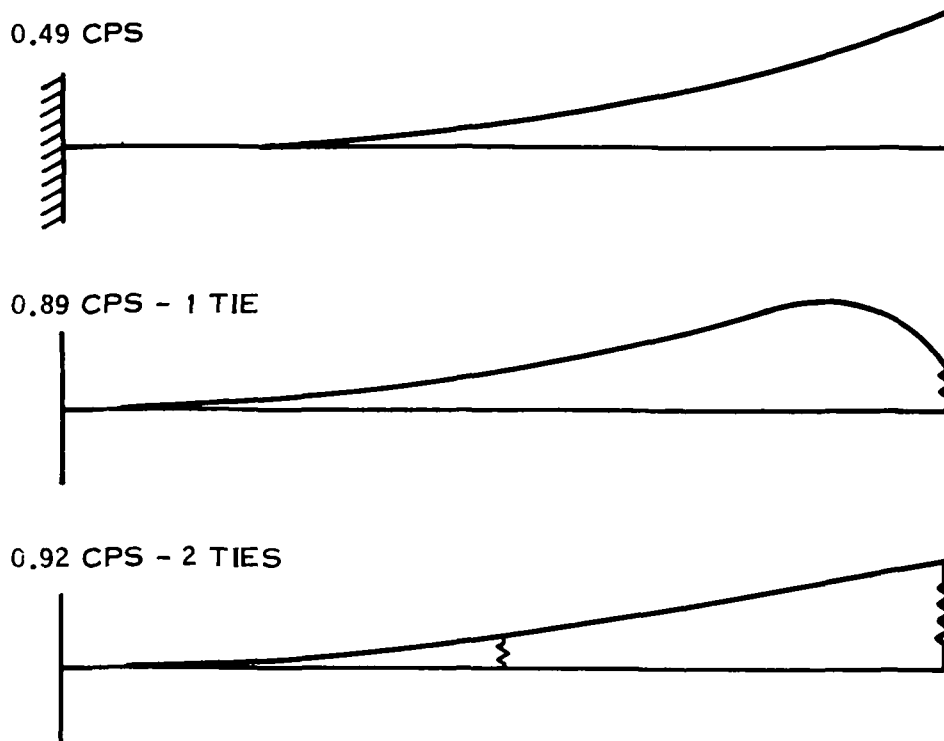


Figure 5-20. Baseline Concept Triform Mode Shapes

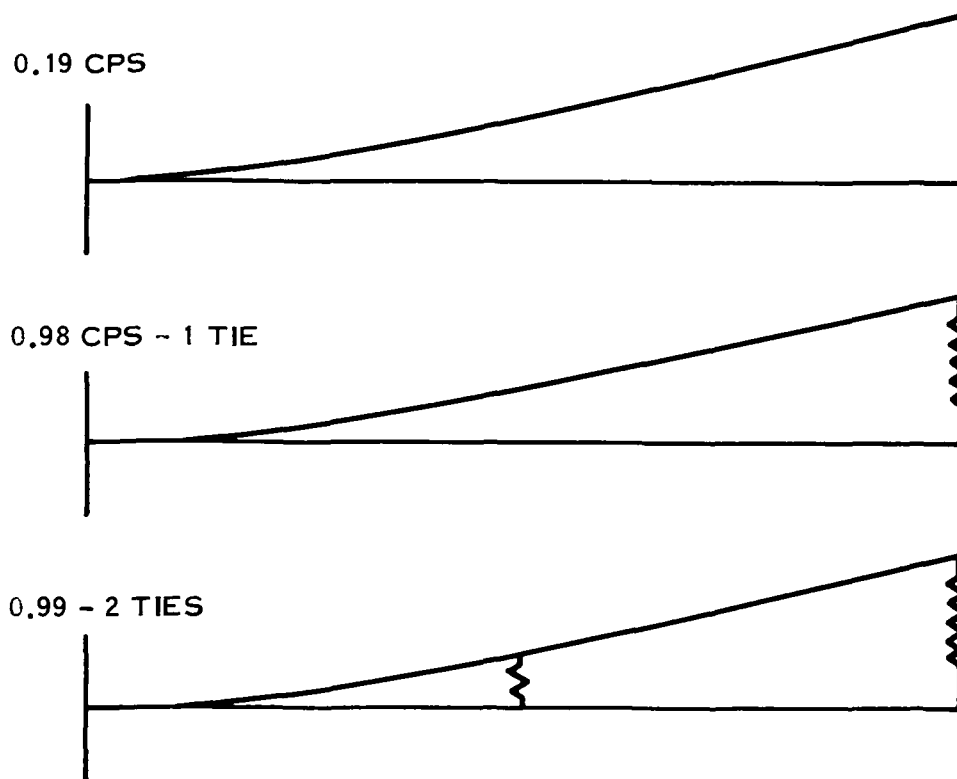


Figure 5-21. Baseline Concept - Inverted Triform Mode Shapes

where μ denotes mass per unit length, and the EI here is to be considered an equivalent stiffness. The shroud is essentially an additional spring in parallel with the spacecraft and hence its stiffness is additive. The frequency obtained for this case was 1.36 cps. The additional shroud mass required, in comparison to the unstiffened system weight is found from the equation

$$\frac{f_{\text{desired}}}{f_{\text{current}}} = \sqrt{\frac{(EI)_{s/c} + (EI)_{\text{new shrd}}}{(EI)_{s/c} + (EI)_{\text{shrd}}}} = \frac{3.00}{1.36}$$

or

$$\frac{(EI)_{\text{new shrd}}}{(EI)_{\text{shrd}}} = 11.0$$

as the amount of stiffening required in the shroud to give a minimum natural frequency of 3 cps.

Using this factor of 11 and considering the shroud as a simple monocoque cone whose original weight is about 8000 pounds, the required shroud would weigh around 88,000 pounds. Using the 0.24 pounds of payload per pound of shroud weight penalty (Reference 15) for a 700 nautical mile circular orbit, this shroud increase results in a 21,120 pound payload reduction. Therefore, a redesign of the autopilot to accommodate payload frequencies in the one cps range will be required.

5.2.7 APPLICATION OF RESULTS TO SPACECRAFT USING EXTERNALLY FUELED REACTORS

The major impact on the arrangement of spacecraft using the externally fueled diode reactors is that the higher voltages permit the location of the aluminum power conditioning radiator at the base of the spacecraft, immediately above the thrusters. The primary and auxiliary radiators would be located immediately aft of the shield. This arrangement is desirable in that it eliminates the need to locate the low temperature power conditioning radiator between adjacent higher temperature components. However,

this change in arrangement will have a minor effect on the overall load distribution, relative to that employed for the flashlight reactor spacecraft. Therefore, the stress distributions are expected to be similar. The percent net structural weight penalty, and natural frequencies are therefore not expected to change appreciably. However, the distribution of the launch support structure will change.

The aluminum power conditioning radiator, if located at the base, will be required to survive higher stresses, and more stiffening structure will be required. Structural requirements for the power conditioning radiator to withstand loads imposed by the launch environment are presented in the remaining paragraphs of Section 5.2.7. Conversely, the relocated Cu/SS primary radiator will see lower stresses, and less stiffening will be required. The total structural requirements should be the same as identified for the flashlight reactor spacecraft evaluated.

5.2.7.1 Design Analysis

A structural design analysis has been performed on the proposed aluminum radiator of the spacecraft using the externally fueled reactor concept. The analysis was performed to determine the stringer and frame geometry and associated weight penalty necessary to withstand the loads imposed by the Titan IIIC/7 launch vehicle. The type of analysis, aluminum material properties and launch environment definition are similar to those defined in the preceding paragraphs of Subsection 5.2 for spacecraft powered by flashlight reactors.

The radiator is a twelve sided, 2024-T3 aluminum cylinder, 18 feet in length and 110 inches in diameter. The original panel thickness as determined by the heat rejection load of the power conditioning equipment was 0.105 inches. For loading distribution and other required dimensions refer to Figure 5-22.

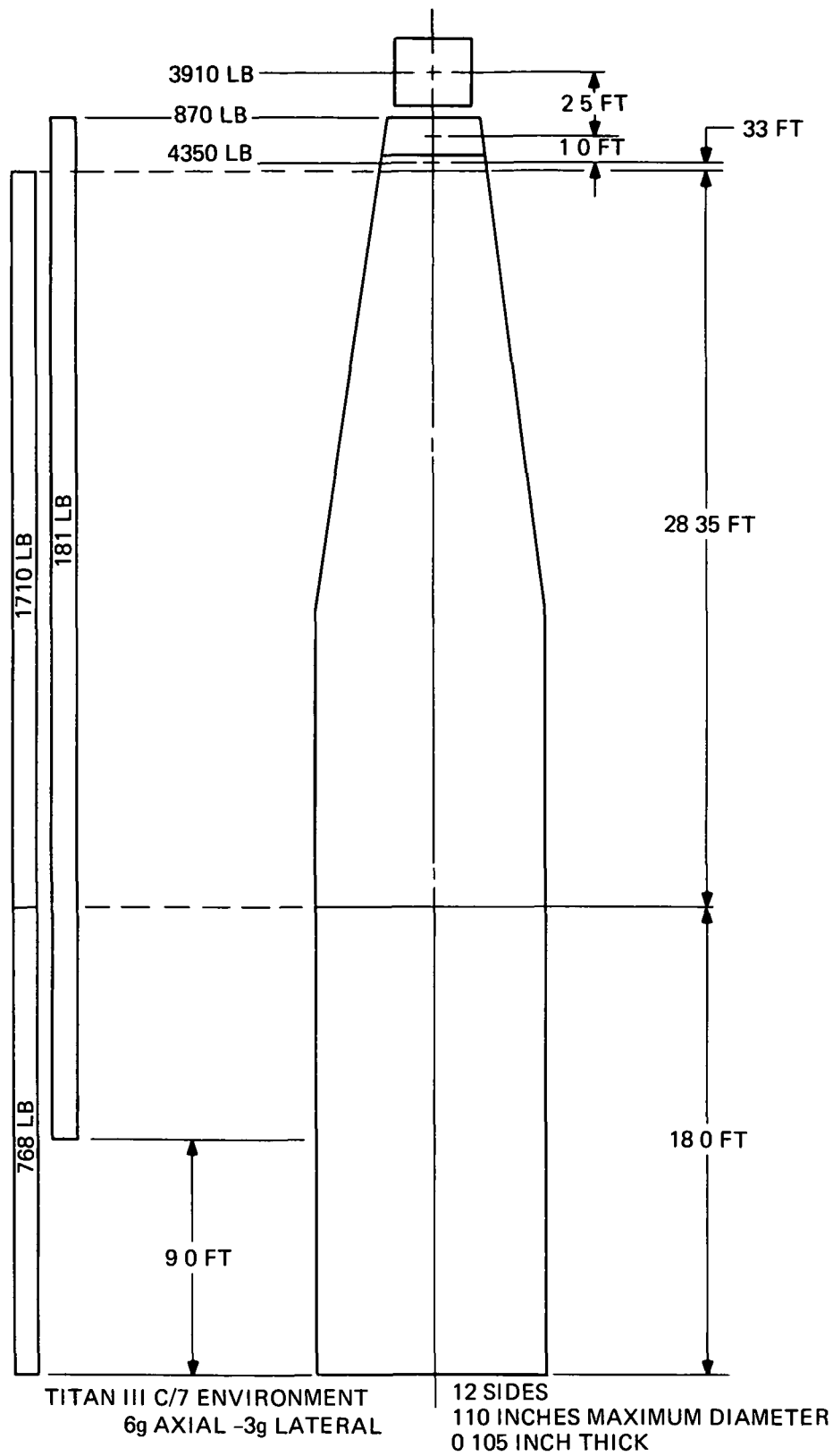


Figure 5-22. Externally Fueled Reactor/Spacecraft Loading Distribution

The radiator described herein was analyzed to determine its as-re-received structural capability, and then to determine the specific structural geometry required to insure the structural integrity under the given environment. To perform this analysis, the radiator was assumed to be cylindrical in shape rather than multisided, and that loading occurred while the radiator was at ambient temperature. The analysis assumed that no buckling is permitted, including local, panel, and general instability type of buckling modes. It is also assumed that the g loadings are not cumulative. The bending moment used in the analysis was an average of the applied moment at Station 0 and Station 18 feet and equals 14.6×10^6 inch-pounds. The axial load used in the analysis was approximately 70,000 pounds.

5.2.7.2 Design Results

The structural margins are identified in Table 5-6 for the unreinforced PC radiator. Shear buckling was briefly examined and found to result in large margins, and is, therefore, not presented. Also, stringer and frame web crippling was checked and found to be non-critical.

TABLE 5-6. STRUCTURAL MARGINS OF POWER CONDITIONING RADIATOR DURING TITAN III C/7 LAUNCH

Load	Structural Margin
<u>Bending</u> (3g lateral load)	
Stinger Buckling	0.152
Sheet Buckling	0.152
<u>Axial Compression</u> (6g axial load)	
Stinger Buckling	6.88
Sheet Buckling	7.63
<u>General Instability</u>	2.91

To achieve structural integrity of the power conditioning radiator during the launch phase of the mission, twenty-four longitudinal stringers and six circumferential frames were required. In addition, radiator panel thickness was increased 0.025 inches to 0.13 inches. A section of the required structure is shown in Figure 5-23. Weight summary of these structural additions is given in Table 5-7.

It is recommended that the flat panels be joined along their axial length to insure shear continuity. It is further recommended that the stringers be placed over the panel joints and in the center of the panels. This arrangement coincides with the 15 degree circumferential spacing of the stringers as shown in Figure 5-24.

**TABLE 5-7. POWER CONDITIONING RADIATOR STRUCTURE
WEIGHT SUMMARY - EXTERNALLY FUELED CONCEPT**

Structure	Weight (pounds)
Additional Panel Thickness = 0.025 inches	187
Stringers -24 "T" Sections (1.75x1.125x0.156 inches)	217
Frames - 6 "Z" Sections (2 x 2 x 0.094 inches)	75
Attachments	24
Total Structure Weight	503

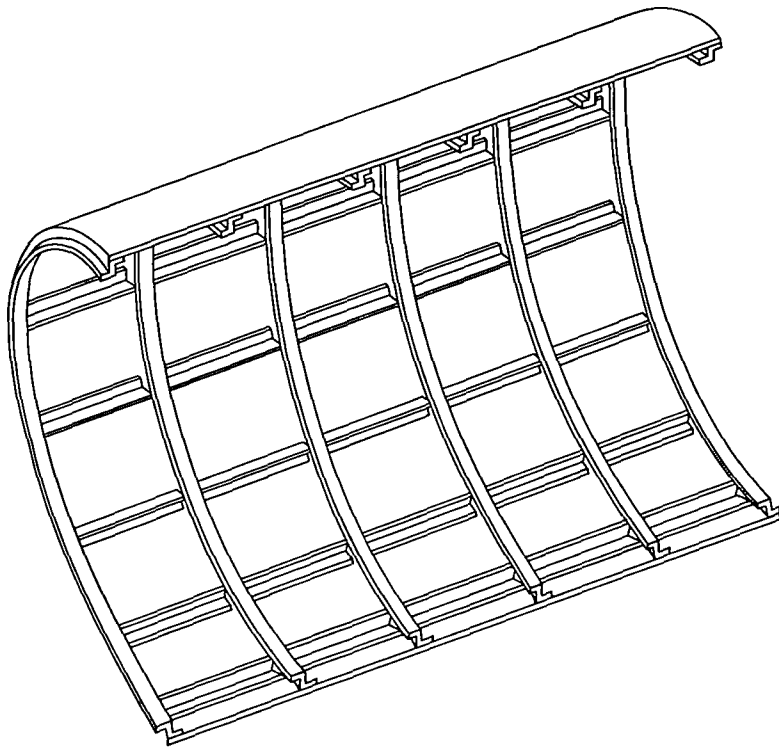


Figure 5-23. Power Conditioning Radiator Structure - Externally Fueled Concept

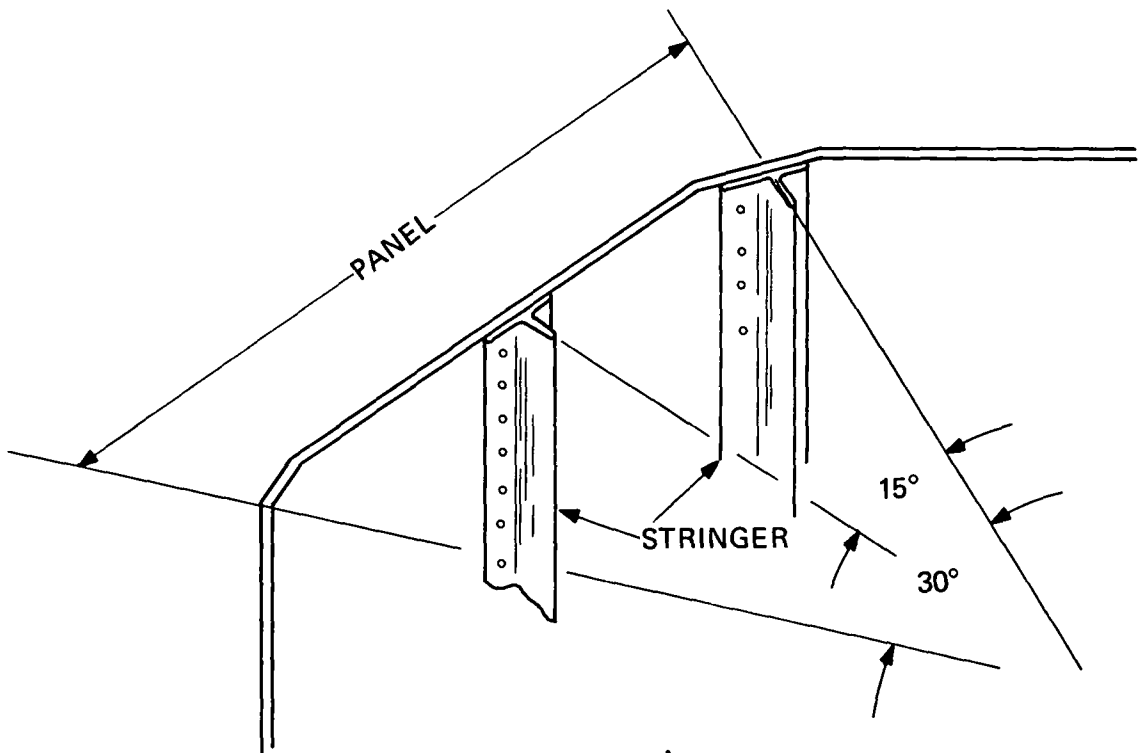


Figure 5-24. Stringer-Panel Configuration of Power Conditioning Radiator-Externally Fueled Concept

5.3 COOLANT ACTIVATION

Activated NaK-78 coolant is a major source of gamma radiation, particularly at collection points such as radiator header and feed line locations. In a single loop heat rejection system, the activated nuclei are distributed over large areas outside of the primary shields, and this source of gamma radiation, combined with contributions from the reactor and mercury propellant (secondary gamma source), determine the amount of local shielding required for power conditioning and payload electronic equipment. If radiation levels are excessive, a two-loop system must be used to confine the activated coolant within the reactor shield assembly. This is accomplished by locating the heat exchanger within the shield, preferably in a low neutron flux region to avoid excessive activation of the secondary loop. However, a weight penalty is incurred due to the addition of an intermediate heat exchanger, an additional pump(s), and a lower radiator inlet temperature. Figure 5-25 illustrates the two power plant concepts.

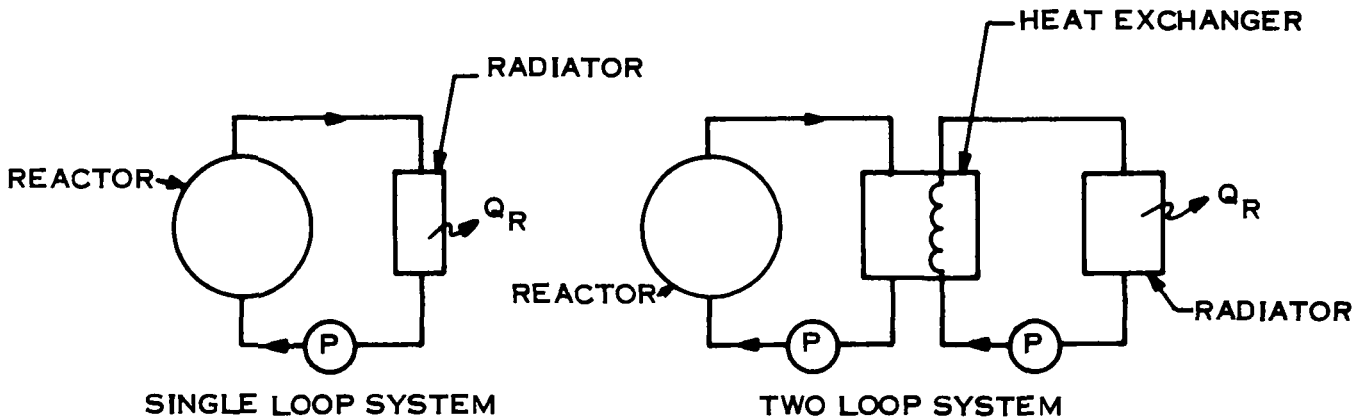


Figure 5-25. Single Loop and Two-Loop Power Plant Concepts

The use of a two-in series, or a single loop heat rejection system for the thermionic reactor requires that consideration be given to the resulting distribution of activated coolant throughout regions adjacent to radiation sensitive components. In order to estimate the magnitude of the problem, a geometrical and analytical model is identified which considers:

- a. The flashlight and the externally fueled reactors
- b. A single loop primary heat rejection system including feed lines, headers and radiators
- c. NaK-78 coolant

5.3.1 GEOMETRICAL MODEL

An outline of the principle components under consideration and their relative locations are shown in Figures 5-26 and 5-27. The various reactor regions and the coolant flow path through these regions are shown in Figures 5-28 and 5-29. In the coolant activation analysis, it is assumed that the only significant activation occurs within these

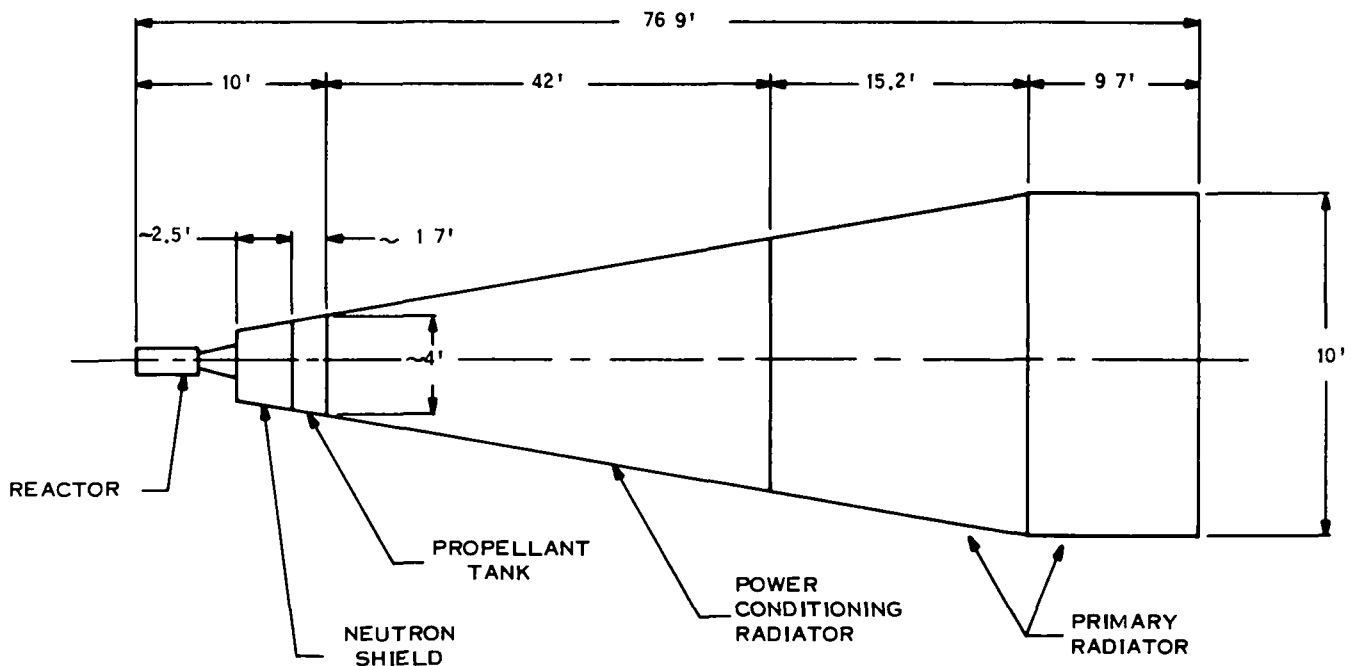


Figure 5-26. Vehicle Geometry Baseline Concept Power Plant - Flashlight Design

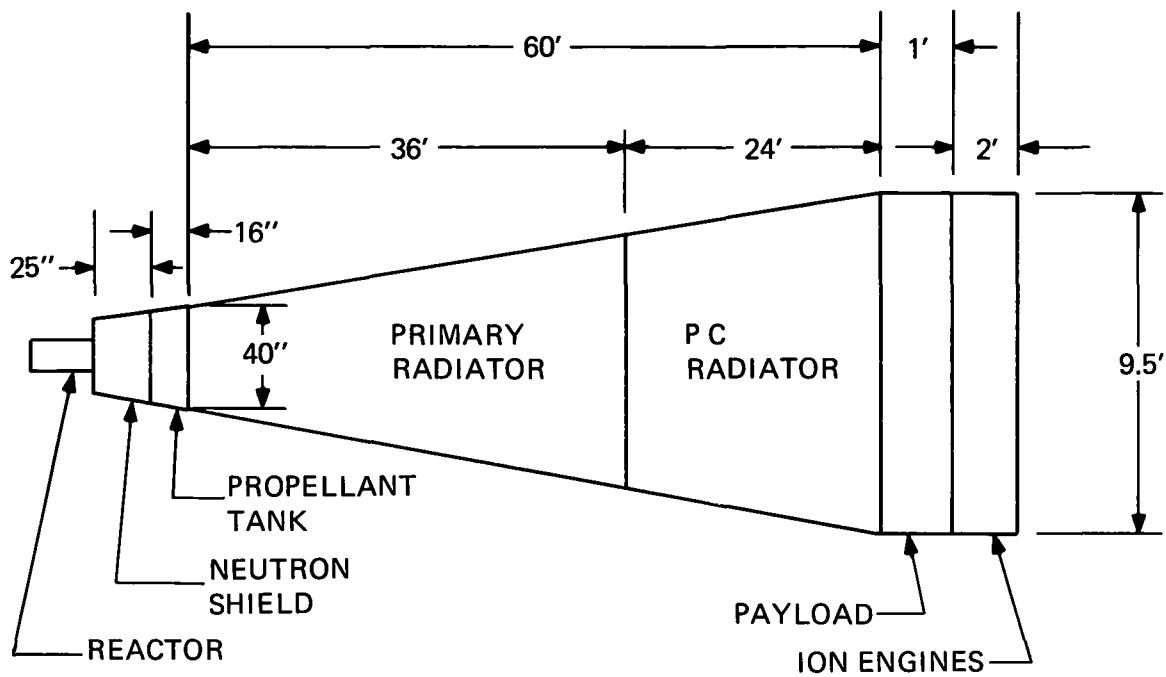


Figure 5-27. Vehicle Geometry Baseline Concept Power Plant - External Fuel Design

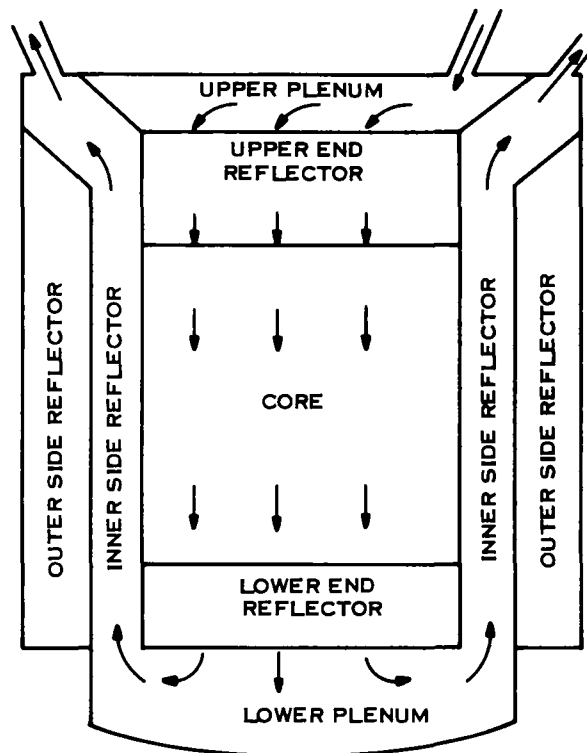


Figure 5-28. Flashlight Reactor Regions and Coolant Flow

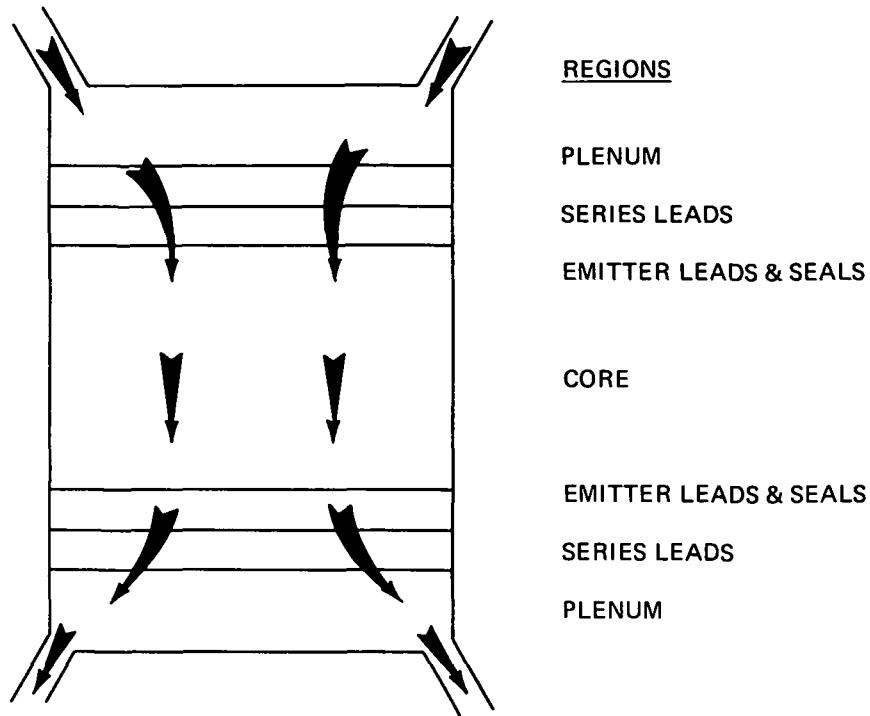


Figure 5-29. Externally Fueled Reactor Regions and Assumed Coolant Flow

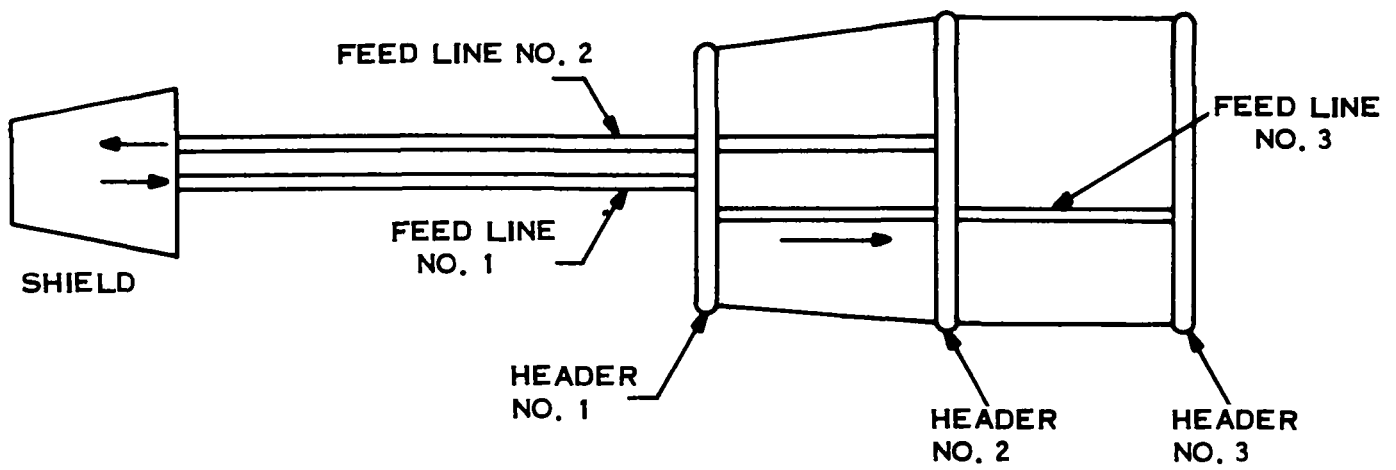
regions. The primary radiators for the two reactor types are shown in Figures 5-30 and 5-31.

5.3.2 ANALYTICAL MODELS

5.3.2.1 Coolant Activation Analytical Model

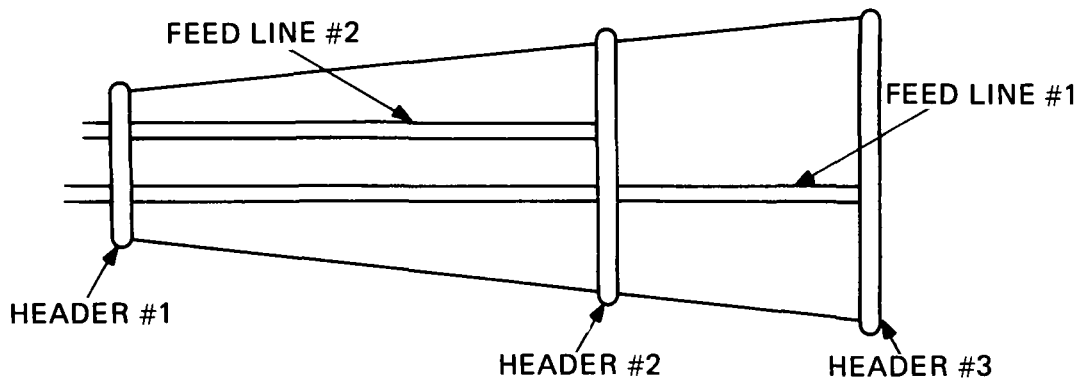
The density of activated coolant nuclei at any given point in time and space depends upon the following factors:

- a. Coolant activation cross section
- b. Activated nuclei decay constants
- c. Neutron fluxes
- d. Coolant distribution and flow rate throughout the system.



COMPONENT	INSIDE DIAMETER (IN.)
FEED LINE NO. 1	7.25
NO. 2	7.25
NO. 3	5.13
HEADER NO. 1	2.95
NO. 2	4.18
NO. 3	2.95

Figure 5-30. Primary Coolant Radiator Geometry - Flashlight Reactor



COMPONENT	INSIDE DIAMETER (IN.)
FEED LINE NO. 1	5.13
NO. 2	7.25
HEADER NO. 1	2.95
NO. 2	4.18
NO. 3	2.95

Figure 5-31. Primary Coolant Radiator Geometry - Externally Fueled Reactor

If the attention is fixed upon a given small volume element, the instantaneous rates of production and loss of activated nuclei within the volume element are defined as follows:

$$\text{Production rate} = dV \int_0^{E_0} \Sigma_a(E) \phi(E, \vec{r}) dE$$

$$\text{Loss rate} = \lambda A dV$$

where

dV = element of volume

$\Sigma_a(E)$ = activation cross section for neutrons of energy E

$\phi(E, \vec{r})dE$ = flux of neutrons with energies in the range dE about E at the point r

λ = activated nuclei decay constant

A = density of activated nuclei

E_0 = maximum neutron energy.

The time rate of change of the density of activated nuclei can then be written:

$$\frac{dA}{dt} = \int_0^{E_0} \Sigma_a(E) \phi(E, \vec{r})dE - \lambda A \quad (1)$$

Since the coolant is in motion, the neutron flux seen by the coolant volume element is a function of time. Hence, the position coordinate, r , can be written as a function of time. The time dependence of r will depend upon the volume element of coolant considered, since in general different elements will follow different paths. This fact would require solution of Equation (1) for all possible paths and then averaging the results to obtain the average density of activated nuclei. The assumptions discussed below were made in order to simplify the calculation.

It is assumed that the reactor/heat rejection system could be broken up into several regions, and that within each region the neutron flux, as a function of position, could be related with its space averaged value. The residence time in a given region is taken as the ratio of the coolant volume to the coolant volumetric flow rate in that region.

Equation (1) can now be rewritten, for example, for region "j", as:

$$\frac{da_j}{dt} = \int_0^{E_0} \Sigma_a(E) \phi_j(E) dE - \lambda A_j \quad (2)$$

The integration over energy in Equation 2 is recast into a summation over the multi-group neutron fluxes which are calculated with a two-dimensional transport computer program. The final form of Equation 1 then becomes:

$$\frac{dA_j}{dt} = \sum_{g=1}^G \Sigma_g \phi_{gj} - \lambda A_j \quad (3)$$

where

Σ_g = the g^{th} group averaged activation cross section

ϕ_{gj} = the g^{th} group neutron flux averaged over region j

Integration of Equation (3) gives:

$$A_j = \frac{1}{\lambda} \sum_{g=1}^G \Sigma_g \phi_{gj} + C_j e^{-\lambda t} \quad (4)$$

The constants of integration, C_j , are determined by the requirement that A_j at the exit of region j is equal to A_{j+1} at the entrance to region j + 1.

In the steady state case, i. e. , after several half lives of the activated nuclei, the density of activated nuclei at the exit from the reactor is:

$$A = \frac{1}{\lambda T} \sum_{j=1}^{J-1} \Delta t_j \left[\sum_{g=1}^G \Sigma_g \phi_{gj} \right] \quad (5)$$

where

T = time for one complete cycle of the coolant

J = total number of regions

Δ_{tj} = average time spent by coolant in region j.

Equation (5) also reflects the assumption that the neutron fluxes outside the reactor are small enough to be ignored. Hence, the summation over j does not include the activation in the radiator and radiator feed lines and headers.

In order to apply Equation (5) to a given problem, the neutron fluxes must be defined, as well as the activation cross sections of all nuclear species included in the coolant, and the decay constants of any activated nuclear species.

The NaK-78 coolant contains two nuclear species which become activated when exposed to a neutron flux. They are Na^{23} and K^{41} which, upon neutron capture, become Na^{24} and K^{42} . Their respective decay constants are $1.3 \times 10^{-5} \text{ sec}^{-1}$ and $1.55 \times 10^{-5} \text{ sec}^{-1}$.

The group average activation cross sections used for these nuclides are given in Tables 5-8 and 5-9.

5.3.2.2 Coolant Activation Dose Rate Model

The basic approach is based on the fact that the interaction cross sections of the emitted photons with the coolant, and with the containing structure, are relatively

TABLE 5-8. NEUTRON ENERGY GROUPS AND ACTIVATION CROSS SECTIONS - FLASHLIGHT REACTOR

Group	Group Energy Bounds (ev)	Sodium Activation Cross Section (barns)	Potassium Activation Cross Section (barns)
1	1.4×10^6 to 10.5×10^6	10^{-4}	10^{-3}
2	0.4×10^6 to 1.4×10^6	2×10^{-4}	2×10^{-3}
3	1×10^5 to 4×10^5	10^{-3}	10^{-2}
4	0.1×10^5 to 1×10^5	2×10^{-3}	2×10^{-2}
5	0.215 to 10^4	0.04	0.4
6	0.001 to 0.215	0.53	1.3

TABLE 5-9. NEUTRON ENERGY AND ACTIVATION CROSS SECTIONS - EXTERNALLY FUELED REACTOR

Group	Group Energy Bounds (ev)	Sodium Activation Cross Section (barns)	Potassium Activation Cross Section (barns)
1	4×10^6 to ∞	5×10^{-5}	5×10^{-4}
2	2.5×10^6 to 4×10^6	2×10^{-4}	2×10^{-3}
3	1.4×10^6 to 2.5×10^6	2×10^{-4}	2×10^{-3}
4	0.8×10^6 to 1.4×10^6	2×10^{-4}	2×10^{-3}
5	4×10^5 to 8×10^5	3×10^{-4}	3×10^{-3}
6	2×10^5 to 4×10^5	6×10^{-4}	6×10^{-3}
7	1×10^5 to 2×10^5	1.2×10^{-3}	1.2×10^{-2}
8	0.465×10^5 to 1×10^5	1.6×10^{-3}	1.6×10^{-2}
9	2.15×10^4 to 4.65×10^4	2.6×10^{-3}	2.6×10^{-2}
10	1×10^4 to 2.15×10^4	1×10^{-3}	1×10^{-2}
11	465 to 1×10^4	3×10^{-2}	3×10^{-1}
12	0.215 to 465	8.5×10^{-3}	8.5×10^{-2}
13	Thermal	0.53	1.3

small. The photons are emitted with energies of 1.37, 1.52 and 2.76 Mev. These photons have mean free paths in the coolant of approximately ten inches, and in the coolant containing structure, of approximately two inches. Hence, in these materials, there will be very little photon scattering and pure absorption will be negligible. The scattering will reduce the energy of the scattered photons, and hence their contribution to the total dose will be reduced. Ignoring photon scattering will act to slightly overestimate the dose rate. However, it is assumed that the coolant and containing structure are transparent to the photons.

The half lives of the activated sodium and potassium are 15 and 12.4 hours, respectively; whereas, the residence time in the radiator region is about one minute. The density of activated nuclei will not change appreciably during the residence time in the radiator region, and it is assumed that the activated coolant density was constant in this region.

With these considerations, the equation for the photon flux at a given point, due to photons of energy E, emitted by the i^{th} type of nuclear species within the volume element dV, can be written as:

$$d\phi(E) = \frac{SdV}{4\pi r^2} \quad (6)$$

where

S = emission of photons of energy E, per unit time, per unit volume

r = separation distance between the element dV and the point at which the flux is to be calculated.

The source strength, S, is simply the product of the appropriate decay constant and the density of activated nuclei in the radiator region, which is given by Equation (5). Hence,

$$d\phi(E) = \frac{\lambda AdV}{4\pi r^2} \quad (7)$$

The total flux is obtained by integrating Equation (7) over that region of space containing activated coolant. The integration is performed by a computer program for the geometries describing the coolant distribution in feed lines, headers and conical radiators, as shown in Figures 5-30 and 5-31. This model calculates the flux at a given point due to photons that are emitted in directions that will bring them to the point of interest. However, photons emitted in other directions could be subsequently scattered to the point of interest. These scattered photons are not accounted for.

The photon energies and their numbers per decay for Na²⁴ and K⁴² are given in Table 5-10.

TABLE 5-10. PHOTON PRODUCTION CHARACTERISTICS

Nuclide	Photon Energy (Mev)	No. of Photons/Decay
Na ²⁴	1.37	1.0
Na ²⁴	2.76	1.0
K ⁴²	1.52	0.2

The flux-to-dose conversion factors used are summarized in Table 5-11 (Reference 2).

TABLE 5-11. FLUX-TO-DOSE CONVERSION FACTORS

Photon Energy	Conversion Factor (r/hr per photon/cm ² -sec)
1.37	2.38 x 10 ⁻⁶
1.52	2.56 x 10 ⁻⁶
2.76	3.92 x 10 ⁻⁶

5.3.3 RESULTS

The reactor region and neutron energy dependence of the coolant activation, the quantity A_{gj} is displayed in Tables 5-12 through 5-15. The numbers refer to the full power reactor operating points. The quantity A_{gj} is defined as:

$$A_{gj} = \Delta t_j \sum_g \phi_{gj}$$

where

Δt_j = coolant residence time in reactor region j

\sum_g = activation cross section for energy group g

ϕ_{gj} = neutron flux in energy group g in reactor region j.

Thus, A_{gj} is the total number of activating interactions per unit volume due to neutrons in energy group g during transit through region j.

The energy groups and group cross sections are given in Tables 5-8 and 5-9. The calculated residence times are given in Table 5-16 for the flashlight reactor. The externally fueled reactor residence times were assumed to be comparable to those in the flashlight reactor and the estimates are given in Table 5-17.

A measure of the total contribution of each region to the density of activated nuclei is given in Tables 5-18 and 5-19, where the quantity A_j is listed for each region. This is defined now as,

$$A_j = \sum_{g=1}^{g=G} A_{gj}$$

The reactor regions are shown in Figures 5-28 and 5-29.

TABLE 5-12. ENERGY GROUP AND REACTOR REGION CONTRIBUTIONS
TO THE COOLANT ACTIVATION DENSITY - FLASHLIGHT REACTOR

A _g (Sodium)								
Energy Group	Group Energy Bounds (ev)	Upper Plenum	Upper End Reflector	Core	Lower End Reflector	Energy Group	Lower Plenum	Inner Side Reflector
1	1.4×10^6 to 10.5×10^6	3.3×10^5	2.4×10^5	4.3×10^6	2.2×10^5	1	9.7×10^5	1.5×10^6
2	0.4×10^6 to 1.4×10^6	1.6×10^6	1.0×10^6	1.6×10^7	9.0×10^5	2	4.9×10^6	6.3×10^6
3	1.0×10^5 to 4.0×10^5	8.1×10^6	6.7×10^6	8.4×10^7	6.0×10^6	3	2.4×10^7	4.5×10^7
4	0.1×10^5 to 1.0×10^5	4.9×10^7	2.0×10^7	1.1×10^8	1.8×10^7	4	1.5×10^8	1.4×10^8
5	0.215 to 10^4	2.6×10^9	3.4×10^8	4.3×10^8	3.0×10^8	5	7.8×10^9	2.7×10^9
6	0.001 to 0.215	8.6×10^9	4.4×10^7	3.1×10^6	3.9×10^7	6	2.6×10^{10}	3.8×10^8

TABLE 5-13. ENERGY GROUP AND REACTOR REGION CONTRIBUTIONS TO
THE COOLANT ACTIVATION DENSITY - FLASHLIGHT REACTOR

A _g (Potassium)								
Energy Group	Group Energy Bounds (ev)	Upper Plenum	Upper End Reflector	Core	Lower End Reflector	Energy Group	Lower Plenum	Inner Side Reflector
1	1.4×10^6 to 10.5×10^6	4.4×10^5	3.3×10^5	5.9×10^6	3.0×10^5	1	1.3×10^6	2.0×10^6
2	0.4×10^6 to 1.4×10^6	2.2×10^6	1.4×10^6	2.3×10^7	1.2×10^6	2	6.7×10^6	8.8×10^6
3	1.0×10^5 to 4.0×10^5	1.1×10^7	9.0×10^6	1.1×10^8	8.0×10^6	3	3.3×10^7	6.1×10^7
4	0.1×10^5 to 1.0×10^5	6.6×10^7	2.8×10^7	1.4×10^8	2.5×10^7	4	2.0×10^8	2.0×10^8
5	0.215 to 10^4	3.6×10^9	4.6×10^8	5.6×10^8	4.1×10^8	5	1.1×10^{10}	3.8×10^9
6	0.001 to 0.215	2.9×10^9	1.5×10^7	1.0×10^6	1.3×10^7	6	8.6×10^9	1.3×10^8

TABLE 5-14. ENERGY GROUP AND REACTOR REGION CONTRIBUTIONS TO THE COOLANT ACTIVATION DENSITY - EXTERNALLY FUELED REACTOR

Energy Group	Group Energy Bounds (EV)	A_{gj} (Sodium)			
		Plenums	Series Leads	Emitter Leads Seals	Core
1	4×10^6 to	1.24×10^5	8.55×10^4	3.16×10^4	1.54×10^5
2	2.5×10^6 to 4×10^6	1.07×10^6	6.83×10^4	2.63×10^5	1.31×10^6
3	1.4×10^6 to 2.5×10^6	2.08×10^6	1.27×10^5	4.38×10^5	2.27×10^6
4	0.8×10^6 to 1.4×10^6	4.16×10^6	2.29×10^5	7.11×10^5	3.03×10^6
5	4×10^5 to 8×10^5	1.64×10^7	8.08×10^6	2.34×10^6	7.93×10^6
6	2×10^5 to 4×10^5	3.9×10^7	2.05×10^6	5.26×10^6	1.89×10^7
7	1×10^5 to 2×10^5	7.02×10^7	3.52×10^6	8.77×10^6	3.03×10^7
8	0.465×10^5 to 1×10^5	5.91×10^7	2.73×10^6	6.42×10^6	2.02×10^7
9	2.15×10^4 to 4.65×10^4	4.35×10^6	1.9×10^5	4.18×10^5	1.21×10^6
10	1×10^4 to 2.15×10^4	7.8×10^6	3.17×10^6	5.36×10^6	1.26×10^6
11	465 to 1×10^4	1.33×10^8	5.13×10^6	6.13×10^6	9.82×10^6
12	0.215 to 465	5.52×10^5	1.34×10^4	6.62×10^3	1.28×10^3
13	Thermal	4.49×10^3	2.47×10^2	7.74×10^1	1.14×10^1

TABLE 5-15. ENERGY GROUP AND REACTOR REGION CONTRIBUTIONS TO THE COOLANT ACTIVATION DENSITY - EXTERNALLY FUELED REACTOR

Energy Group	Group Energy Bounds (EV)	A_{gj} (Potassium)			
		Plenums	Series Leads	Emitter Leads and Seals	Core
1	4×10^6 to	1.68×10^5	1.16×10^5	4.3×10^4	2.1×10^5
2	2.5×10^6 to 4×10^6	1.46×10^6	9.3×10^4	3.58×10^5	1.78×10^6
3	1.4×10^6 to 2.5×10^6	2.83×10^6	1.73×10^5	5.96×10^5	3.1×10^6
4	0.8×10^6 to 1.4×10^6	5.67×10^6	3.11×10^5	9.68×10^5	4.12×10^6
5	4×10^5 to 8×10^5	2.23×10^7	1.1×10^6	3.19×10^6	1.08×10^7
6	2×10^5 to 4×10^5	5.3×10^7	2.79×10^6	7.14×10^6	2.57×10^7
7	1×10^5 to 2×10^5	9.56×10^7	4.8×10^6	1.19×10^7	4.12×10^7
8	0.465×10^5 to 1×10^5	8.04×10^7	3.72×10^6	8.72×10^6	2.75×10^7
9	2.15×10^4 to 4.65×10^4	5.91×10^7	2.59×10^6	5.7×10^6	1.64×10^7
10	1×10^4 to 2.15×10^4	1.06×10^7	4.32×10^5	7.3×10^5	1.72×10^6
11	465 to 1×10^4	1.81×10^8	6.98×10^6	8.35×10^6	1.34×10^7
12	0.215 to 465	7.51×10^5	1.82×10^4	9.0×10^3	1.74×10^3
13	Thermal	1.5×10^3	8.2×10^1	2.58×10^1	3.8

TABLE 5-16. FLASHLIGHT REACTOR RESIDENCE TIMES

Region	Residence Time (Seconds)
Upper Plenum	0.4
Upper End Reflector	0.09
Core	0.31
Lower End Reflector	0.08
Lower Plenum	1.2
Inner Side Reflector	0.8

TABLE 5-17. EXTERNALLY FUELED REACTOR RESIDENCE TIMES

Region	Residence Time (Seconds)
Plenums	1.6
Series Leads	0.06
Emitter Leads and Seals	0.12
Core	0.31

The photon emission rate per unit volume of NaK-78 coolant is given by the product of the decay constant, the density of activated nuclei and the number of photons per decay. In the case of sodium, each decay gives rise to two photons with energies of 1.37 and 2.76 Mev. In the case of potassium, 20 percent of the decays give rise to a single photon of energy 1.52 Mev. The emission rate density for each photon is:

$$S = n\lambda A$$

TABLE 5-18. REACTOR REGION CONTRIBUTIONS TO THE COOLANT ACTIVATION DENSITY-FLASHLITE REACTOR

Reactor Region	A _j	
	Sodium	Potassium
Upper Plenum	1.13 x 10 ¹⁰	6.6 x 10 ⁹
Upper End Reflector	4.1 x 10 ⁸	5.1 x 10 ⁸
Core	6.5 x 10 ⁸	8.4 x 10 ⁸
Lower End Reflector	3.6 x 10 ⁸	4.6 x 10 ⁸
Lower Plenum	3.4 x 10 ¹⁰	2.0 x 10 ¹⁰
Inner Side Reflector	3.3 x 10 ⁹	4.2 x 10 ⁹
Total = $\sum_j A_j$	5.0 x 10 ¹⁰	3.3 x 10 ¹⁰

TABLE 5-19. REACTOR REGION CONTRIBUTIONS TO THE COOLANT ACTIVATION DENSITY-EXTERNALLY FIELD REACTOR

Reactor Region	A _j	
	Sodium	Potassium
Plenums	3.76 x 10 ²	5.12 x 10 ⁸
Series Leads	1.7 x 10 ⁷	2.32 x 10 ⁷
Emitter Leads and Seals	3.5 x 10 ⁷	4.78 x 10 ⁷
Core	1.07 x 10 ⁸	1.46 x 10 ⁸
Total = $\sum_j A_j$	5.35 x 10 ⁸	7.29 x 10 ⁸

where

n = number of photons emitted per decay

λ = decay constant

A = density of activated nuclei

From Equation (5)

$$S = \frac{n}{T} \sum_j A_j \quad (8)$$

Applying Equation (8) to the three photon energies discussed above yields the results given in Tables 5-20 and 5-21.

TABLE 5-20. COOLANT PHOTON SOURCE STRENGTHS
FLASHLIGHT REACTOR

Photon Energy (mev)	Parent Nuclide	Source Strength (Photons/cm ³ -sec)
1.37	Na ²⁴	1.4 x 10 ⁹
1.52	K ⁴²	1.9 x 10 ⁸
2.76	Na ²⁴	1.4 x 10 ⁹

TABLE 5-21. COOLANT PHOTON SOURCE SEGMENTS
EXTERNALLY FUELED REACTOR

Photon Energy (mev)	Parent Nuclide	Source Strength (Photons/cm ³ -sec)
1.37	Na ²⁴	1.57 x 10 ⁷
1.52	K ⁴²	4.27 x 10 ⁶
2.76	Na ²⁴	1.57 x 10 ⁷

These source strengths are then used in Equation (6) which is integrated over the coolant containing regions, i. e., the feedlines, headers and radiator coolant tubes. The photon fluxes so obtained are then converted to dose rates and the total integrated doses for both reactor types are calculated, taking into account the variations in reactor power level during the mission. The reactor power level as a function of mission time is shown in Figure 5-32.

The integrated doses received at several points from each of the radiator components is given in Tables 5-22 and 5-23 for both reactor types. The total integrated doses at each receiver point, due to the presence of activated NaK-78 coolant, are also given. The locations of the receiver points are included in the tables.

The integrated gamma dose, as a function of time for selected receiver points are shown in Figure 5-33. In the case of the flashlight reactor, Receiver Point No. 7, had the smallest calculated integrated dose for that reactor. Receiver Point No. 1 for the externally fueled reactor, had the largest calculated integrated dose for that reactor.

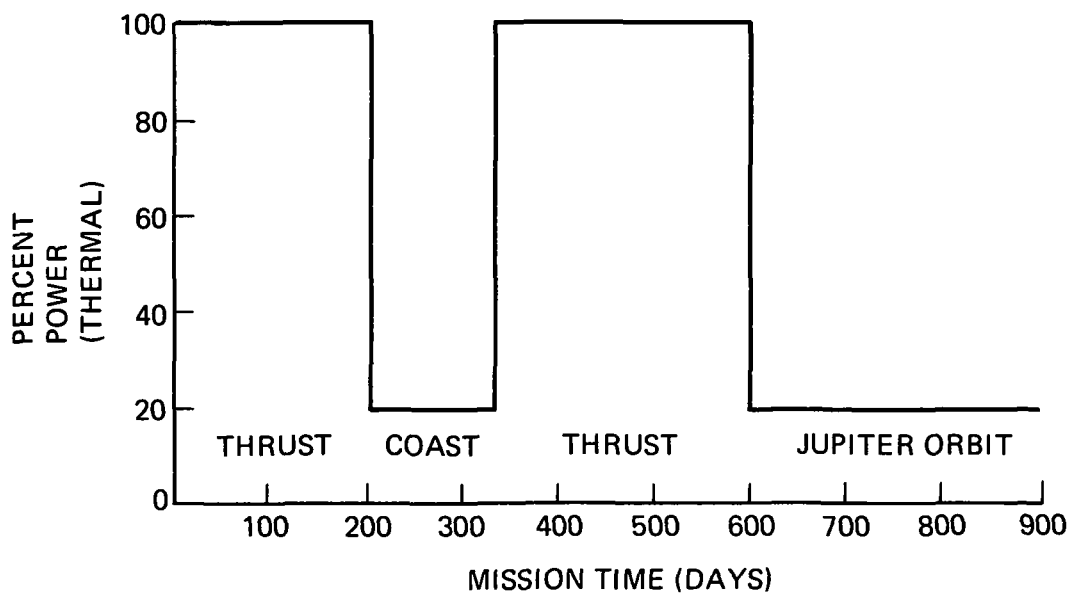


Figure 5-32. Reactor Power as a Function of Mission Time

TABLE 5-22. INTEGRATED GAMMA DOSES DUE TO ACTIVATED COOLANT - FLASHLIGHT REACTOR

Receiver Point Source	Integrated Gamma Dose (Rads x 10 ⁻⁷)						
	1	2	3	4	5	6	7
Radiator	.02	.06	.14	1.08	.86	.92	.79
Header 1	.023	.095	.305	10.1	.0756	.0808	.067
Header 2	.0372	.098	.185	.422	.73	.833	.96
Header 3	.0118	.0241	.0382	.0758	9.7	2.5	1.87
Feedline 1	9.24	9.6	7.69	3.83	.23	.2	—
Feedline 2	9.25	9.74	8.49	7.39	.71	.76	—
Feedline 3	.04	.12	.31	1.7	1.38	2.68	—
Total	18.6	19.7	17.2	24.6	13.7	7.97	3.69

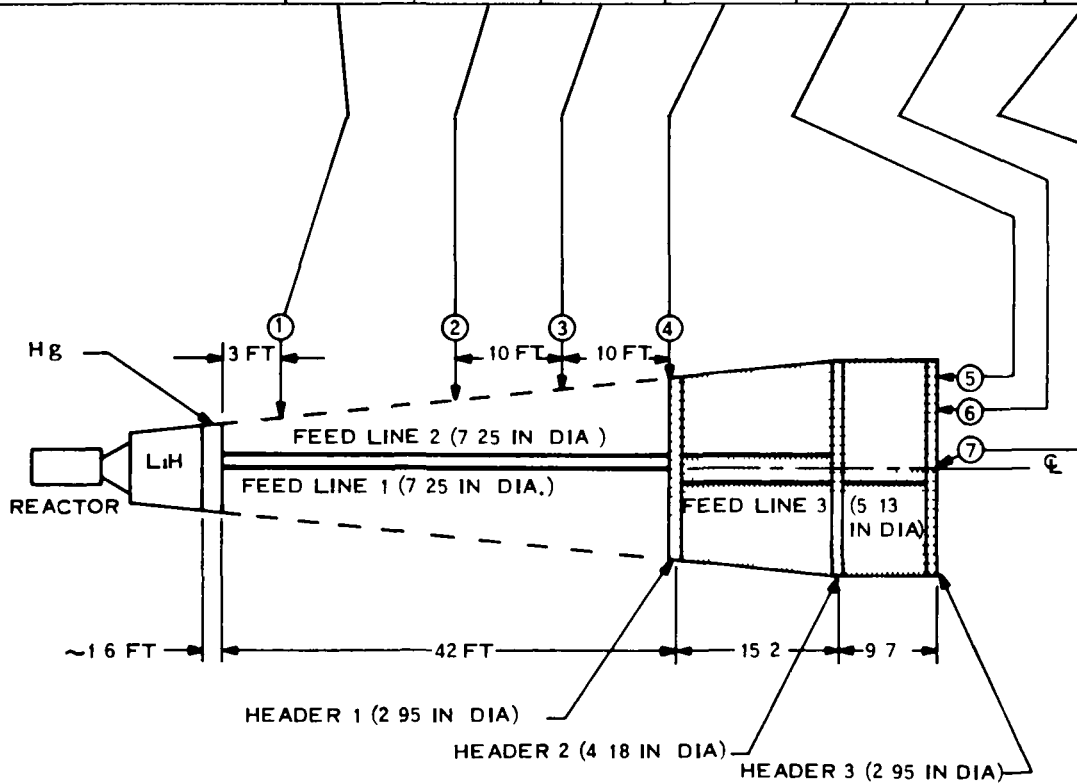
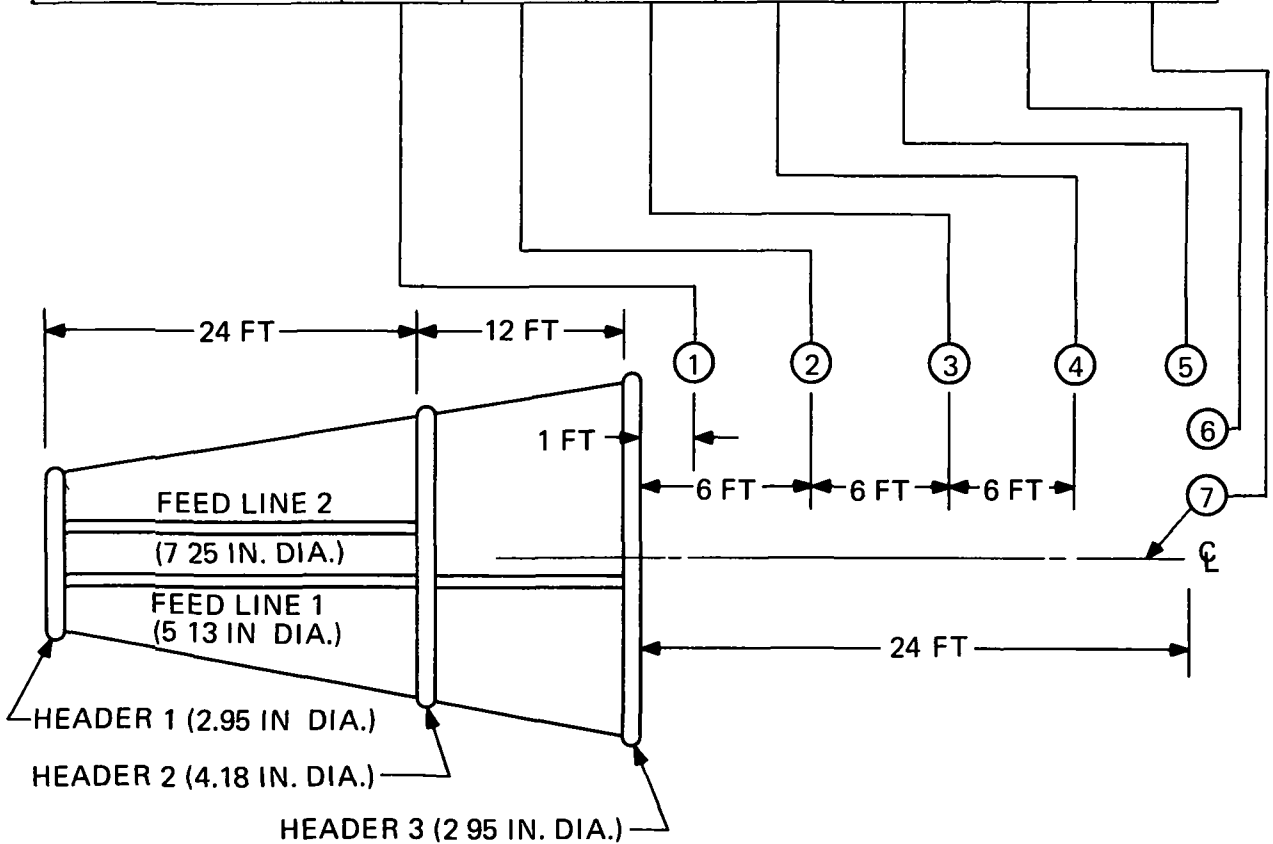


TABLE 5-23. INTEGRATED GAMMA DOSES DUE TO ACTIVATED COOLANT - EXTERNALLY FUELED REACTOR

Receiver Point \ Source	Integrated Gamma Dose (Rads x 10 ⁻⁵)						
	1	2	3	4	5	6	7
Radiator	.542	.189	.0087	.054	.0363	.0367	.0368
Header 1	.0128	.010	.00763	.00605	.00488	.0049	.0049
Header 2	.330	.179	.103	.067	.0465	.0468	.047
Header 3	5.01	.688	.223	.108	.0618	.063	.0633
Feedline 1	2.00	.660	.308	.186	.126	.128	—
Feedline 2	.248	.159	.105	.075	.0561	.0566	—
Total	8.14	1.88	.835	.496	.332	.336	.152



5.3.4 DISCUSSION OF THE RESULTS

The most obvious result is the large difference in dose rates between the two types of reactors considered. Comparing Receiver Points 5 or 6 in the Flashlight reactor case with Receiver Point 1 in the externally fueled reactor case, it is seen that for similar positions relative to the coolant containing regions, the flashlight reactor produces a gamma dose from activated coolant which is roughly 100 times as great as the externally fueled reactor. This difference is almost entirely due to the difference in the neutron spectra of the two reactor types. The flashlight reactor has a softer neutron spectrum and, since the activation cross sections increase rapidly with decreasing neutron energy, the activation rate is correspondingly enhanced.

The calculated magnitudes of the dose rates indicate that the spacecraft incorporating the externally fueled reactor may utilize a single loop primary heat rejection system. The opposite is in the case of the currently configured flashlight reactor, since the integrated doses exceed the assigned limit of 10^7 rads.

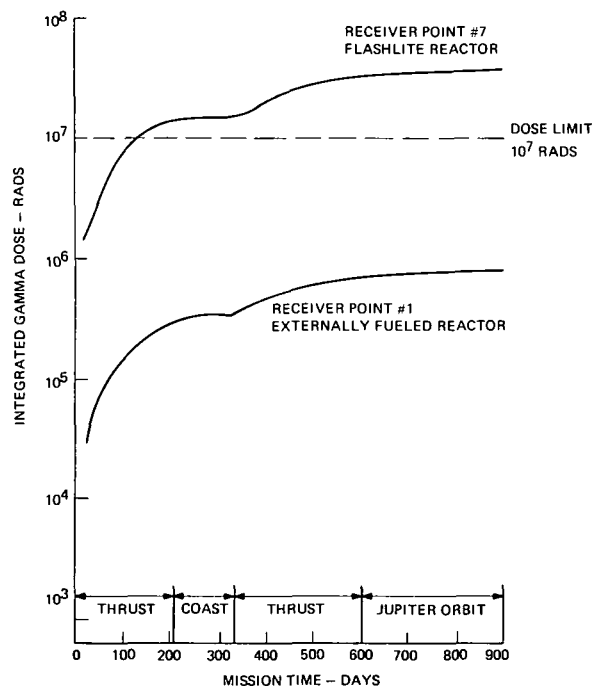


Figure 5-33. Integrated Gamma Dose History - Single Loop System

6. SHIELD ANALYSIS

6 SHIELD ANALYSIS

Preliminary shielding calculations were performed at the Oak Ridge National Laboratory. A one-dimensional spherical geometry mock-up of the Flashlight/Shield assembly formed the basis of the calculations. The neutron shield consisted of LiH containing 3 v/o of stainless steel, and Hg propellant was used as gamma shielding material. The shielding requirements were defined by assigning neutron and gamma dose limits at a point located 3 meters from the backface of the shield. The integrated neutron dose was to be no more than 10^{12} nvt for neutrons with energies greater than 1 Mev. The gamma dose limit was set at 10^7 rads.

The one-dimensional spherical mock-up of the reactor/shield assembly is shown in Figure 6-1. Unlike the usual situation, the gamma shield in this case is composed of a material whose presence is independent of the need for shielding. This permits the location of the gamma shield outside of the neutron shield in the region of the lowest neutron flux, thereby minimizing the secondary gamma sources in the gamma shield. Ordinarily, this location for the gamma shield would be avoided if possible since it tends to increase the total shield weight. The dimensions shown in Figure 6-1 which locate the outer LiH and Hg surfaces were determined by the shielding calculations. All of the other dimensions were fixed input to the problem

Although the use of the Hg propellant as gamma shielding is a welcome weight saving device, it does present some complications. In the first place, it is expended during the mission, thereby becoming a time dependent gamma shield. Secondly, only that fraction of the Hg needed to satisfy the dose limitation is to be placed adjacent to the neutron shield. The remainder of the Hg is to be located at the opposite end of the vehicle. This distribution of the Hg represents a more stable configuration at launch than one in which all of the Hg were located at the shield. Consequently, less spacecraft supporting structure is required.

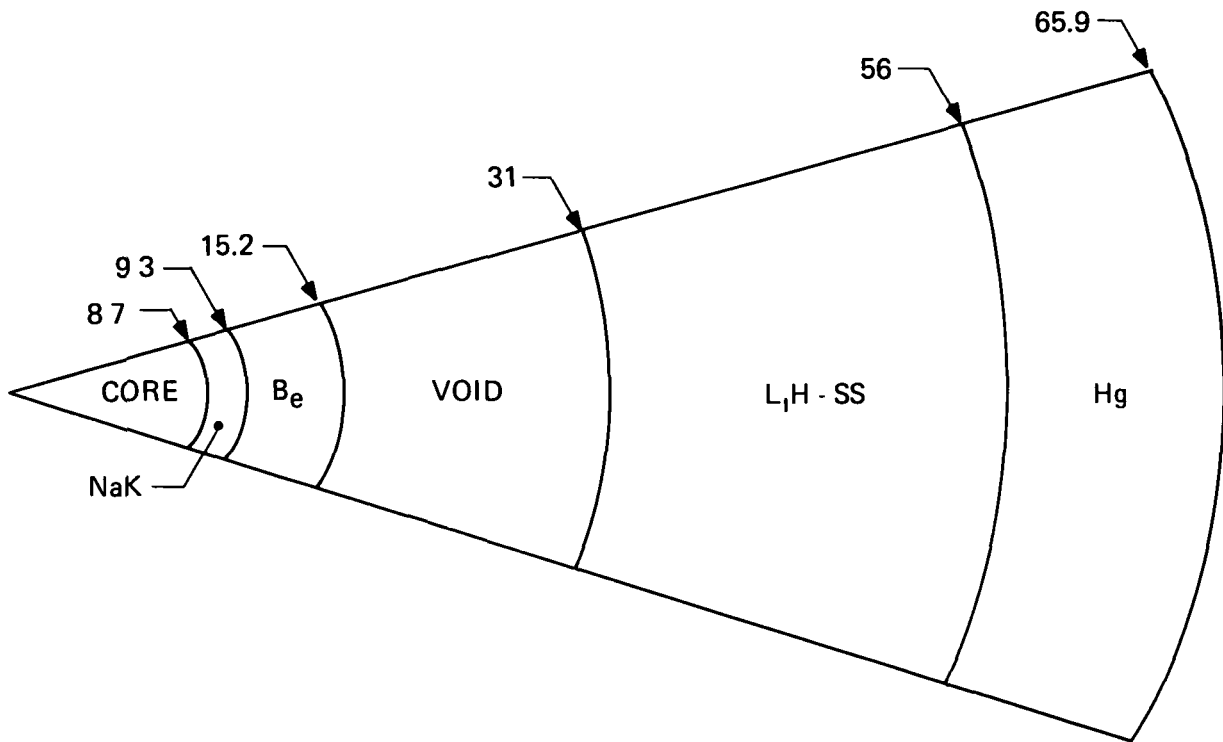


Figure 6-1. Flashlight Reactor/Shield Mock-Up

The time dependence of the Hg shield thickness was determined on the basis of the following conditions. The Hg propellant was to be expended during two thrust periods as indicated in Figure 6-2. In addition, it was to be expended at the same uniform rate during each thrust period. The volume of Hg used for a given gamma shield thickness would be determined by the reactor/gamma shield separation distance and the cone half angle. The separation distance depends in part upon the neutron shield thickness, hence an iterative procedure is required to determine the necessary neutron shield thickness and the time dependence of the gamma shield thickness.

Given the vehicle geometry, cone half angle and total Hg weight assigned as a basis for the shield calculations, it was found that 25 inches of LiH and an initial thickness of Hg of 9.9 inches would be required to satisfy the shielding requirements. The Hg thickness would remain constant until about 45 days into the second thrust period.

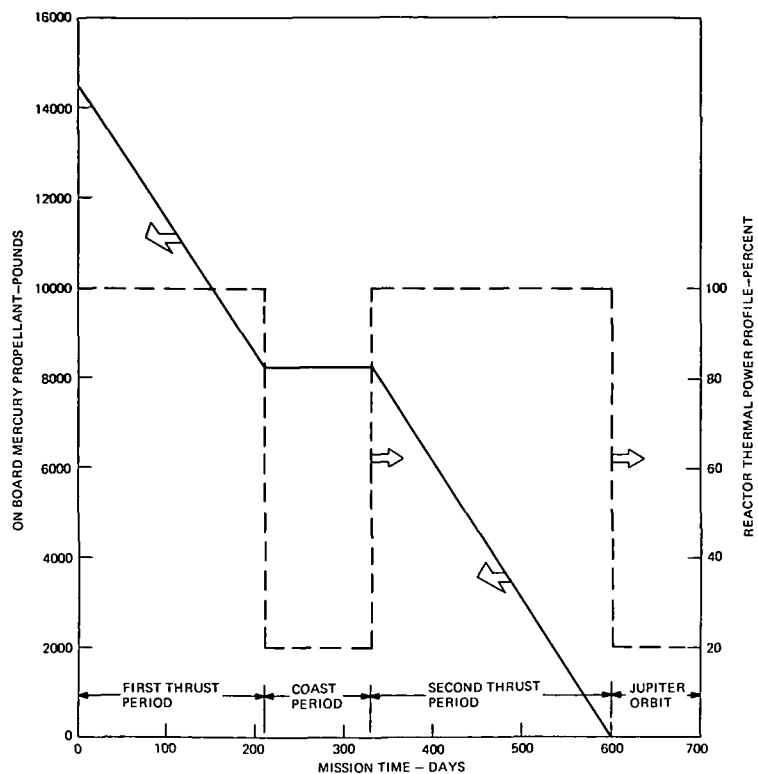


Figure 6-2. Mission Profile

From this point in time to the end of the second thrust period, the Hg thickness would decrease linearly to zero inches.

The gamma dose rate, and the flux of neutrons with energies above 1 Mev at the one meter receiver point, are shown in Figures 6-3 and 6-4 as a function of time. For the conditions of full reactor power and the initial Hg thickness, the neutron and gamma heating rates, the flux of neutrons above 1 Mev and the gamma dose rate as functions of depth in the shield are given in Figures 6-5 and 6-6.

Shielding calculations have yet to be performed for the externally fueled reactor. Hence, the data described above for the flashlight reactor have been used to aid in

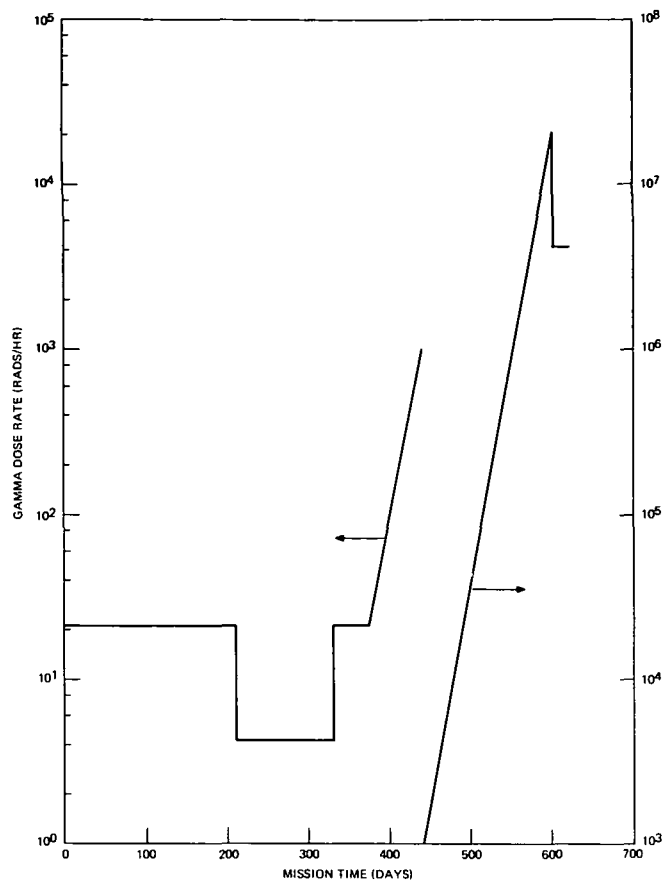


Figure 6-3. Gamma Dose Rate vs Time

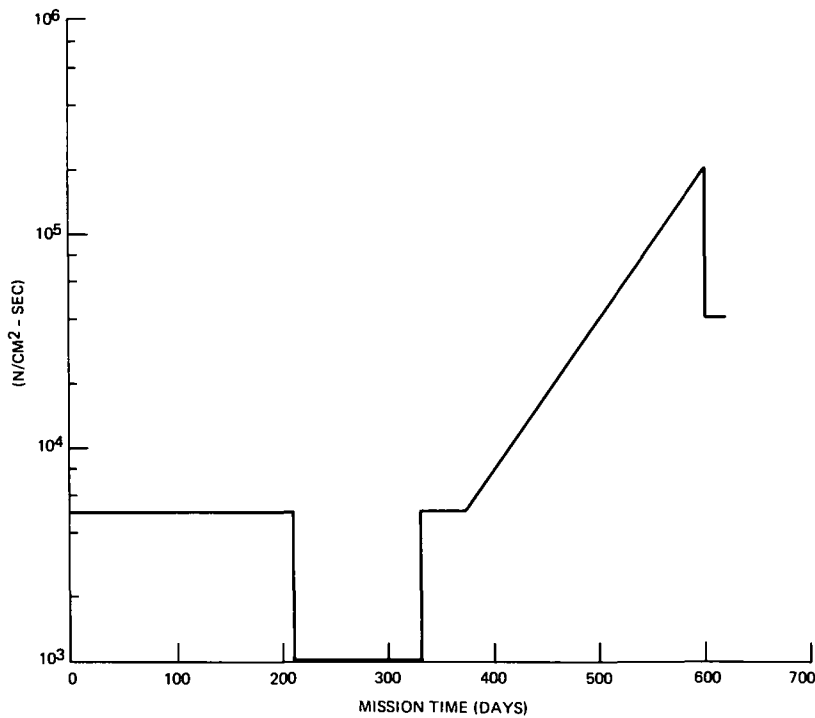


Figure 6-4. Neutron Flux vs Time (Neutron Energies > 1 Mev)

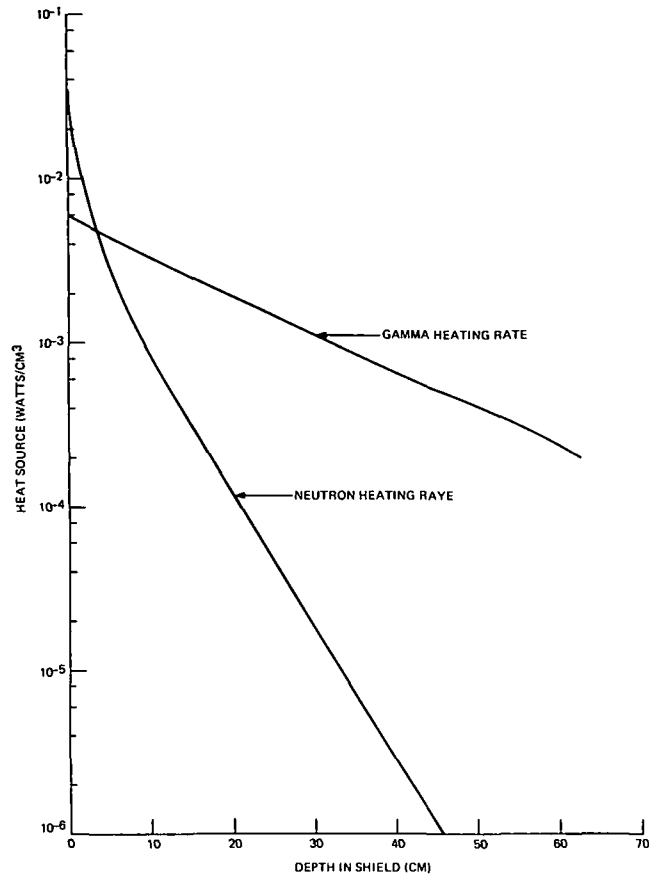


Figure 6-5. Neutron and Gamma Heating Rates vs Depth in Shield

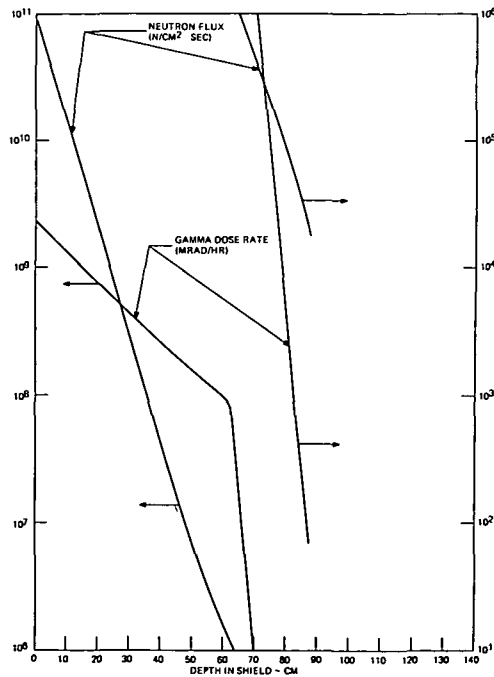


Figure 6-6. Neutron Flux and Gamma Dose Rate vs Depth in Shield (Neutron Energies > 1 Mev)

estimating the externally fueled reactor shielding requirements. The estimates were based upon the assumptions listed below:

- a. Fluxes and dose rates at a point one meter from the Hg tank are the same for both reactor/shield assemblies
- b. Angular fluxes are uniform over the outward directions at the backface of the Hg tank
- c. Scalar fluxes are constant over the backface of the Hg tank
- d. Attenuation of neutrons or photons by LiH or Hg could be adequately treated by fitting simple exponential functions to the curves shown in Figure 6-6.

The second and third assumptions above were used to replace the Hg tank with an equivalent disc, or surface, source located at the backface of the tank. This disk source was then used to derive an expression which describes the variation of the flux or dose rate with distance from the source. The derived expression was:

$$\phi(Z) = \phi(0) \left[1 - \frac{1}{\left(1 + \frac{a^2}{Z^2}\right)^{1/2}} \right]$$

where:

ϕ = flux or dose rate

Z = distance from the disc source along the disc axis

a = disc radius

The quantity $\phi(0)$ was determined by applying the first of the assumptions listed above. The utilization of this approximation for the externally fueled reactor is presented in Section 8.

7. BASELINE ELECTRICAL SYSTEM DESIGN

7. BASELINE ELECTRICAL SYSTEM DESIGN

The electrical power conversion system has been designed for use in each of the thermionic reactor powered spacecraft. The first section describes the electrical network as it appears to the baseline flashlight reactor concept; the following section elaborates on differences in system design as a result of using the externally fueled reactor concept. Furthermore, estimates of size, weight, and efficiency of the electrical system for each of the reactor concepts is presented.

These analyses form the basis for the two spacecraft power conditioning subsystem designs detailed in this report.

7.1 REQUIREMENTS/CHARACTERISTICS

The primary requirements of the electrical system are to convert the electrical power developed by the thermionic reactor power generators to forms suitable for use by the various electrical loads and to distribute the electrical power with proper protection and control.

7.1.1 BASE-LINE LOAD REQUIREMENTS

A tabulation of the baseline spacecraft loads and their electrical requirements is given in Table 7-1. Thruster power requirements are shown in Table 7-2. The main portion of the electrical power is required by the ion thruster screen grids which require about 7.2 kW each at 3100 volts dc. A total of 37 thrusters are on the spacecraft of which 31 are active and 6 are spares.

The ion engines, which represent the principal electrical load of the entire system, are known to arc frequently. The system has been designed that when arcs occur three times within a ten-second period, it becomes necessary to shut down the engine to allow the arc to extinguish, then restart the engine. Since the ion thrusters are a large percentage of the total load, it was necessary to investigate

TABLE 7-1. BASELINE SPACECRAFT ELECTRICAL
LOAD REQUIREMENTS

Item	Function	Power Required - kw
Primary Loop Cooland Pump	Cools Reactor	10 kw flashlight/4 kw ext. fueled
Secondary Loop Cooland Pump	Cools Power Loop	10 kw flashlight/0 kw ext. fueled
Shield Pump	Cools Shield	0.12
Auxiliary Pump*	Cools Pumps, etc.	0.1
Propellant Pump	Pumps Mercury Prop. to Thrusters	0.1
Reactor Controls	Controls Reactivity of Reactor	2.0 (Later reduced to 0.2)
Cesium Heaters	Maintains Temp. of Cesium Vapor	0.5
Thrusters	Propulsion	240
Science and Communications	Payload	1.0
Guidance and Control	Thrust Vector Control of Ion Engines	0.5
Powerplant System Controls	Protection, Switching & Control of Electri- cal System	0.5

* If separate from shield pump

whether the arcing and consequent shutdowns significantly diminish the average load represented by the engines. Analysis shows that even at the extreme arcing rate of 20 per hour the reduction in average load is only about 3.5 percent. Since arcing frequency tends to diminish with time, the reduction in average load by thruster arcing may be neglected.

TABLE 7-2. THRUSTER POWER REQUIREMENTS

Supply Number		Type	Output(1)	NOMINAL RATING					MAX. RATING			Control	Range, A
				Volts	Amps	Watts	Reg. %	Peak Ripple	Volts	Amps	Amps Limit (2)		
1	Screen	DC	V	3100	2.32	7200	1.0(V)	5	3200	2.32	2.60	2.0 - 2.4	
2	Accelerator	DC	F	2000	.02	40	1.0(V)	5 @ 0.2 A	2100	0.20 ⁽³⁾	0.21	---	
3	Discharge	DC	V	35	8.3	290	1.0(V)	2	150 @ 50 mA	9 @ 37V	10	7.5 - 9.0	
4	Mag. - Man	DC	F	15	7	11	1.0(I)	5	20	1.0	1.0	---	
5	Cath. Htr (4)	AC	F	10	4.0	40	5.0	5	11	4.4	4.1	---	
6	Cath. Keeper	DC	F	10	0.5	5	1.0(I)	5	150 @ 50 mA	1.0 @ 20V	1.0	---	
7	Main Vapor.	AC	V	0.6	1.0	1	Loop	5	8 ⁽⁵⁾	2.0	2.2	0.5 - 1.5	
8	Cath. Vapor	AC	V	0.3	0.5	1	Loop	5	8 ⁽⁵⁾	1.0	1.1	0.2 - 0.8	
9	Neut. Cath. Htr.	AC	F	10	2.0	20	5.0	5	11	2.2	2.2	---	
10	Neut. Vapor	AC	V	0.3	0.5	1	Loop	5	8 ⁽⁵⁾	1.0	1.1	0.2 - 0.8	
11	Neut. Keeper	DC	F	10	0.5	5	1.0(I)	5	150 @ 50 mA	1.0 @ 20 V	1.0	---	

(1) V = Variable, F = Fixed

(2) Current limit or overload trip level.

(3) Current at this level for less than 5 min. at low repetition rate.

(4) Needed only during startup or until discharge reaches 3A.

(5) Startup only.

7.1.2 BASE-LINE MISSION REQUIREMENTS

The electrical system must be designed to provide power to the loads under the following conditions during the flight:

- a. Full power operation (300 kW) from beginning of mission to the coast period.
- b. Ten percent power operation (30 kW) during coast; the thrusters are inoperative and only hotel loads and payloads are connected.
- c. Full power operation (300 kW) from the end of the coast period to attainment of orbit around Jupiter.
- d. Ten percent power for at least one orbit of Jupiter.

7.1.3 REACTOR CHARACTERISTICS

7.1.3.1 Flashlight Reactor Characteristics

The reactor power generator is composed of Thermionic Fuel Elements (TFE's) made up of series stacked cells in a configuration resembling batteries in a flashlight. These TFE's are series connected in pairs with the center connection grounded. Each TFE pair requires an individual power converter so that the electrical operation of each TFE can be adjusted for optimum conditions. Outputs of the several converters are subsequently combined in parallel to provide common electrical distribution busses to the loads. The electrical system must be designed to be compatible with the failure of a TFE. This mode of operation requires the system be capable of delivering maximum power from the remaining TFE following the failure of a single TFE in a pair

Details of reactor electrical characteristics as well as the method recommended for reactor control are presented in References 6 and 7. Reactor control is basically a constant current control loop, and is discussed briefly in Paragraph 7.1.4.1, Flashlight Reactor Electrical System Requirements.

The reactor electrical characteristics corresponding to these several operating conditions are presented in Table 7-3.

TABLE 7-3. FLASHLIGHT REACTOR ELECTRICAL CHARACTERISTICS

	BOM	EOM	Coast
Electric Power, (kWe)	300	300	30
Voltage Output, (Volts)	16.8	15.7	12.5
Current, (Amperes)	17,900	19,100	2400
TFE Pairs	108	97*	108
Current/TFE Pair	165.7	196.9	23.8
Emitter Temp., Maximum, °K	1950	1950	1600

*10 percent TFE Pair Loss at EOM

7.1.3.2 Externally Fueled Thermionic Reactor Characteristics

The externally fueled thermionic generator is composed of series-parallel thermionic elements which are similar to those of the flashlight system. Difference of greatest departure is that the reactor fuel surrounds the thermionic diode rather than being internal.

Reactor control is based upon neutron flux and output voltage. The reactor control circuit consists of an inner loop to control neutron density, proportional to heat generation rate, and an outer loop which is slower than inner loop, to produce incremental changes in heat evaluation to maintain constant input voltage.

Output is from a single point at a constant potential of 120 volts direct current, regardless of load. Nominal power capability is 300 kWe (Reference 16).

7.1.4 ELECTRIC SYSTEM REQUIREMENTS

The primary function of the electrical system is that it transforms the generator output for use in the electrical loads. Optimization of transmission cable weight and the corresponding power losses associated with power transmission require that power be transmitted at as high a voltage as practical.

7.1.4.1 Flashlight Reactor Electrical System Requirements

The electrical power conditioning system is to provide control of the amount of power that is extracted from each TFE pair to insure proper electrical and thermal balance within the reactor. The flashlight reactor is divided into six zones for analysis purposes, with different temperature characteristics. Consequently, for the TFE in these zones, the electrical output characteristics are different. Further, the TFE's throughout the reactor may also be electrically different due to construction variations.

On the basis of these requirements and the data of Table 7-3, the power conversion equipment is designed to accommodate input voltages during normal full power operation from a low of 14 volts to a high of 17 volts, and during the coast phase, accommodate an input of 12 volts. Furthermore, since one half of a TFE pair may fail, provisions are included for allowing the conversion equipment to operate from the remaining TFE. For power conditioner design purposes, this is assumed to be one-half voltage condition at EOM under full power.

7.1.4.2 Externally Fueled Thermionic Reactor Electrical System Requirements

The selected basic externally fueled thermionic reactor is a constant 120 volt direct current system. No need for control circuits for the diodes are defined for the power conversion system.

7.2 BASELINE ELECTRICAL POWER SYSTEM DESIGN

7.2.1 FLASHLIGHT REACTOR ELECTRICAL POWER SYSTEM BASELINE DESIGN

The electrical system proposed for the flashlight thermionic reactor is described in Paragraph 7.2.1.1.

The weight of the equipment for the electrical system, including transmission, distribution and interconnecting cables, but not radiators (which are assumed to be the

primary structural mounting member for the electrical equipment), is estimated to be 4864 pounds. Total electrical power losses for the system are estimated to be 52,870 watts, for an overall efficiency of 82.3 percent for the basic 300 kW system. A breakdown of the principal baseline components of weight is given in Tables 7-4 and 7-5. The baseline electrical power balance is given in Table 7-6. Refer to Paragraph 7.2.1.4 for a discussion of the selected components and main power converter configuration.

TABLE 7-4. ELECTRIC SYSTEM WEIGHT SUMMARY FLASHLIGHT REACTOR SYSTEM

Component	Weight, Pounds
Main converters	2690
Auxiliary PC	507
Auxiliary thruster PC	272
Power distribution cables*	935
Screen supply interrupters	310
Total	4714

*See Paragraph 7.2.1.6.1

In order to withstand the 1600°F heat of the reactor and 800°F shield and to minimize weight and power losses, the transmission cables were initially assumed to be sodium contained in stainless steel tubes, 0.7 inch in diameter, at a weight of 917 pounds. Subsequent analysis has shown that the sodium/SS cable to be similar to a combination cable composed of copper and aluminum. Consequently, for that reason and because of the difficulty of constructing and handling the sodium/SS cable, the combination cable is recommended as the design baseline.

TABLE 7-5. FLASHLIGHT REACTOR SYSTEM MAIN
CONVERTER WEIGHT BREAKDOWN

Component	Weight, Pounds
Bypass rectifiers	1.0
Input filter	
Choke	3.0
Capacitor	1.0
Inverter	
Power transformer	4.0
Transistors	1.0
Current transformer	0.25
Contactor	2.0
Base drive circuits	0.5
HV output	
Rectifiers	0.05
Filter inductor	1.5
Filter capacitor	1.5
MV output	
Rectifiers (SCR)	0.2
Filter inductor	0.5
Filter capacitor	0.5
Control circuits	0.5
Total electric parts, (single TFE pair)	17.50
Total electric parts (108 TFE pairs)	1890
Wire, brackets, hardware, heat paths	800
Total Weight Main Converter Flashlight Reactor System	2690

Wiring for high voltage power distribution from the primary power conditioners is composed of aluminum, which weight approximately 7 pounds total. Interconnection wiring, primarily for medium voltage power distribution between the power conditioning area and reactor and engine areas, weighs 13 pounds.

TABLE 7-6. FLASHLIGHT BASELINE SYSTEM POWER BALANCE

<u>LOSSES</u>	<u>WATTS</u>
Main Power Conditioners	
Transistor Conduction Loss (0.55 x 165)	91
Transistor Switching Loss	25
Transistor Base Drive Loss (3v x 165/10)	49
Transformer (3%)	85
Input Filter (1%)	28
Output Rectifiers (HV)	3
Output Filter (HV)	12
Output Rectifiers (MV)	4
Output Filter (MV)	2
Control Circuits	10
Total losses, single TFE pair unit	309
Total main power conditioning losses, 108 units	33,400
Screen supply interrupter	1,250
EM Pump Power Conditioning	3,700
Thruster auxiliary PC*	*
Payload Power Conditioning	100
Reactor, power plant and spacecraft controls	322
Transmission Cables	14,100
Total Losses	(52,872)
<u>LOADS</u>	
Thruster Screen	223,000
Thruster Auxiliary Power	15,500
Payloads, Science	1,000
Guidance	500
System Control	500
Primary EM Pump	10,000
Secondary EM Pump	10,000
Shield Pump	100
Auxiliary Pump	100
Propellant Pump	100
Reactor Control	2,000
Cesium Heater	500
Total Loads	263,300
Total Power Required	316,172
*Losses are included in Ion Engine Efficiency	

7.2.1.1 Flashlight Electrical Power System Description

The basic electrical power system proposed for the spacecraft utilizing the flashlight thermionic reactor is shown in Figure 7-1. In this system, each TFE pair is provided with a power conversion module and each module provides a medium and high output voltage level of 250 volts and 3100 volts, respectively. The outputs of each module are filtered and all modules are connected in parallel to create the two distribution power buses.

The high voltage output bus provides power to all of the screen electrodes of the ion engine thrusters. The 3100-volt level is established by the voltage requirements of the screens.

The 250-volt output provides power to the remaining spacecraft loads including the several power supplies required for each thruster as well as the hotel loads and payloads. The 250-volt potential was selected for auxiliary power distribution being relatively high voltage for cable power loss minimization, but below most corona and arc-over levels regardless of atmospheric pressure and humidity. Electrical insulations, and piece-part components are frequently rated for maximum voltages not to exceed 600 volts at nominal temperatures. To avoid having to use special high voltage components, and considering the higher operating temperature of the spacecraft, 250 volts was confirmed to be the acceptable maximum.

Power to the hotel loads and to the auxiliary thruster power supplies and the payloads is distributed by means of two 250-volt busses; one group of loads near the reactor and one at the thruster/payload area.

7.2.1.2 Main Power Converter Design

Details of the basic TFE power converter modules selected for the flashlight reactor system are shown schematically on Figure 7-2.

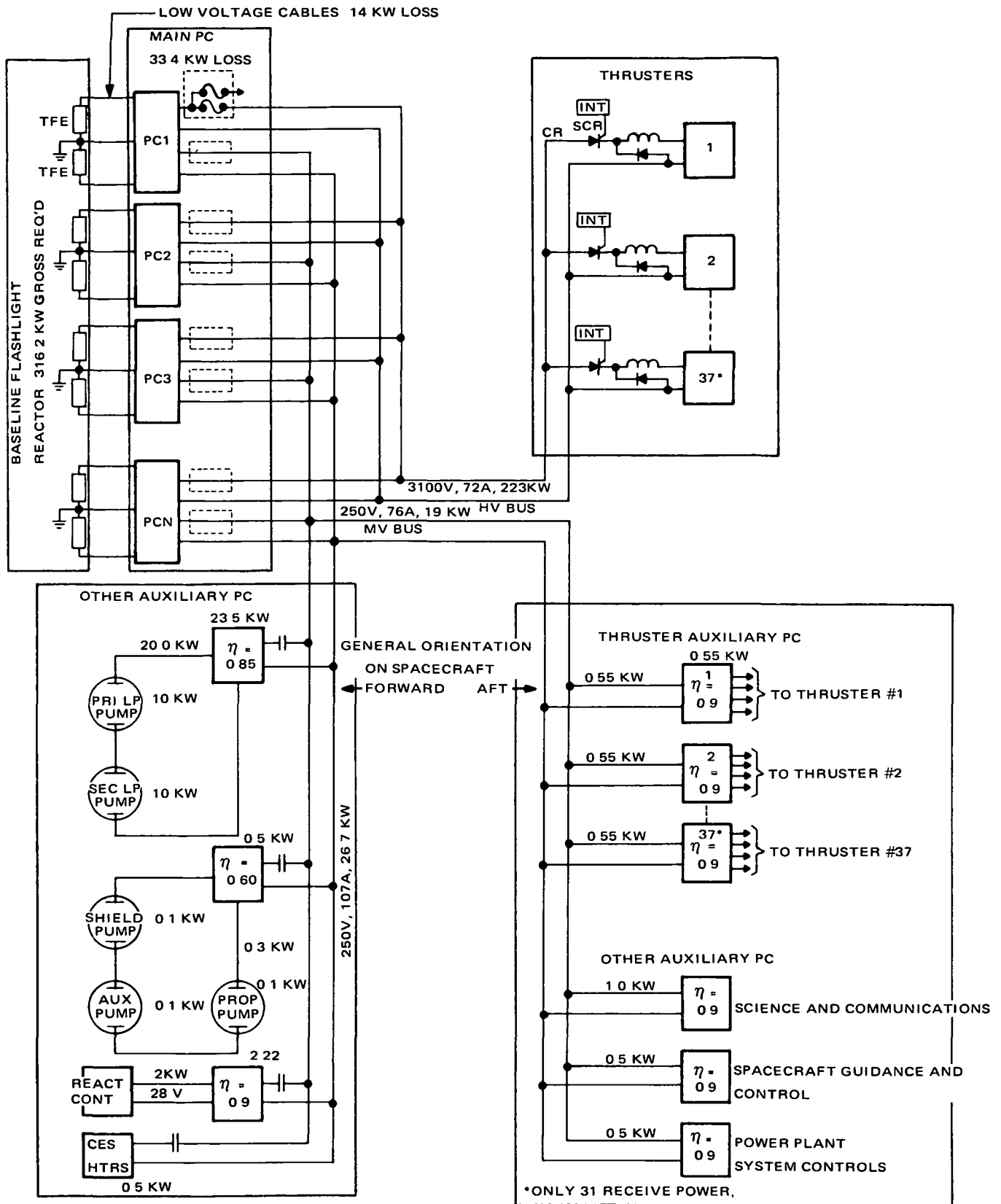


Figure 7-1. Baseline Flashlight Reactor Powered Spacecraft Electric Network

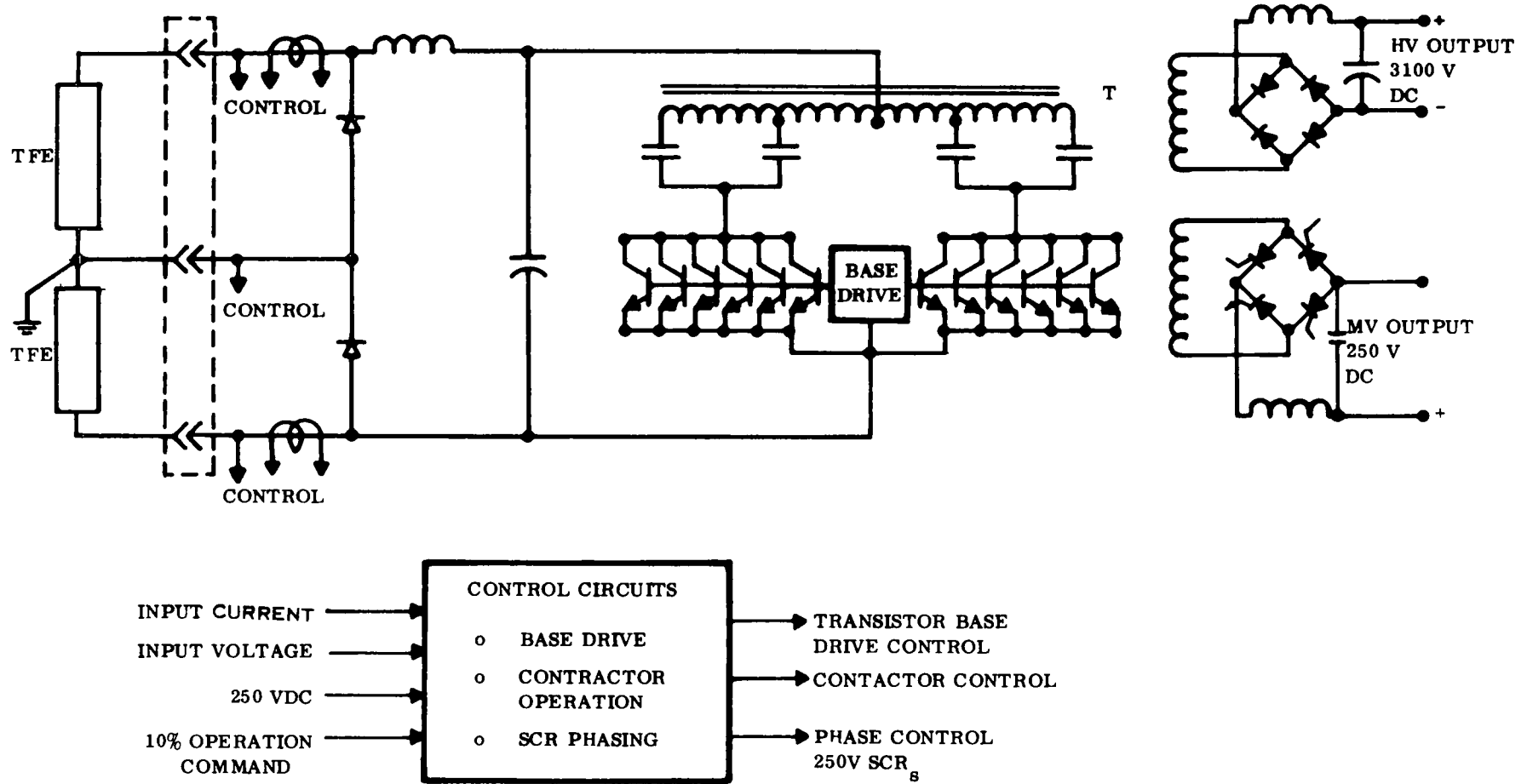


Figure 7-2. Basic Converter Module, Schematic

7.2.1.2.1 Design Approach – Either of two philosophies may be used in sizing the conversion equipment. One is to design the converters for the TFE pairs operating in the several zones of the reactor. This approach results in minimum weight equipment, but may require several different converter sizes. For estimating purposes, equipment weights for this approach can be calculated using average TFE characteristics, recognizing that some equipment may be smaller and lighter than average and some may be larger and heavier. Because of the difference in the electrical characteristics in the six reactor zones, a maximum of six different designs would be required.

The alternate philosophy is to have a single design of power conversion equipment and apply this design to all TFE pair modules. This approach requires that the conversion equipment design be capable of operating with all extremes of TFE characteristics. It must be capable of handling the largest current and the highest voltage of all individual TFE pairs. Considering all TFE modules then, power conversion would be over-designed since the maximum current and maximum voltage do not result coincidentally in any single TFE pair.

Although the latter approach is the preferable one from the standpoint of design commonality, the first approach will be used for equipment sizing for this study, since it results in the optimum design for a weight limited spacecraft. The power conversion equipment will be sized for average TFE current and average TFE voltage. It should be remembered, however, that some converters may be larger and some smaller than average.

From the TFE data for the 300 kWe operating points shown on Table 7-3, it is clear that the TFE pair average current is largest at end of mission, 197 amperes, and average voltage is highest at beginning of mission, 16.8 volts. The end of mission current increase when compared with beginning of mission current primarily is due to the assumed loss of 10 percent of the TFE's, and not necessarily to the reactor characteristic change.

Over the life of the reactor, while delivering full power and excluding failure of one-half of a TFE pair, the average output voltage will range from 15.7 volts to 16.8 volts. In considering the total voltage range for which to design the primary power converters however, it is necessary to consider also the voltage range required by the reactor current regulating control scheme. For this purpose, acknowledging that the primary user of power are the relatively constant ion bombardment engines, assume the spacecraft load can change instantaneously by 10 percent full load, 30 kW. The control system described for the flashlight reactor requires that in the steady state, TFE current be proportional to reactor thermal power so that emitter temperature is controlled following electrical load changes (Reference 6). Transiently, in the first few milliseconds after an electrical load change, diode temperatures remain constant and diode voltage and current approximately follow the isothermal characteristic curves, as shown for example, on Figure 7-3. For large load changes, the corresponding thermionic diode voltage change would be large, but for relatively small load change of concern here, the corresponding instantaneous voltage change is quite small—perhaps

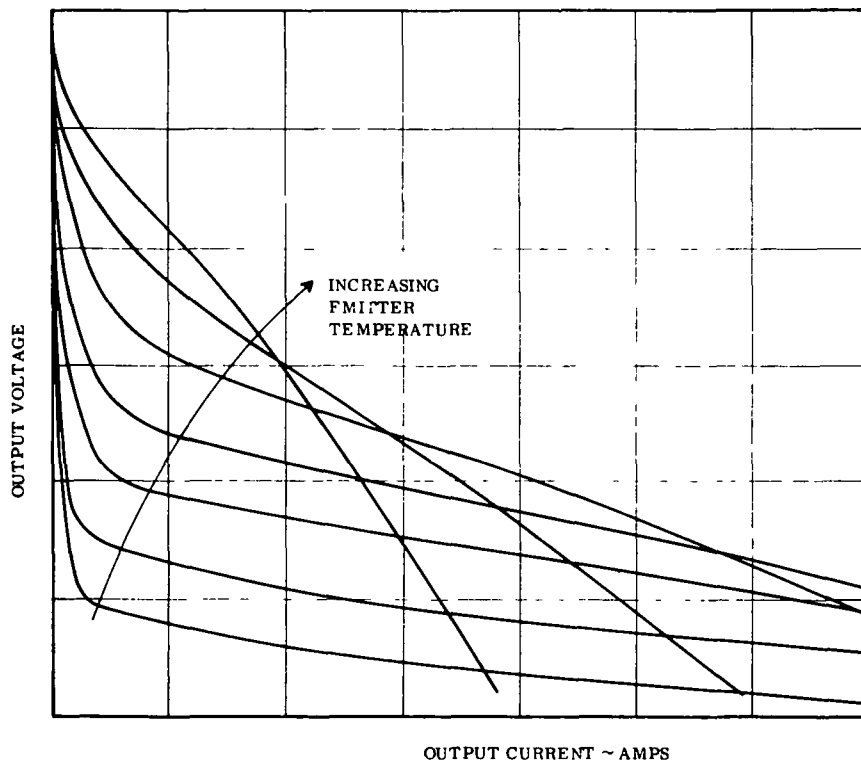


Figure 7-3. Typical Thermionic Reactor I-V Characteristics

0.8 volts which is approximately 5 percent at the operating levels. Assuming that the control system limits the total excursion to this value as a maximum, then the total input voltage range, for which the conversion equipment should be designed, is from about 14 volts to about 18 volts. Additional provisions are required for operation at the failed half input voltage and the coast voltage corresponding to 10 percent power. For this range of input voltages, the output voltage should be held constant. Electrical input characteristics for the primary power conditioners design then are as follows:

Input Voltage

Full power:	14 to 18 VDC
Coast power:	11 VDC (Minimum)
Half TFE failure:	7 to 9 VDC

Input Current

Full power:	196.9 amperes (maximum)
Coast power:	23.8 amperes

Maximum Input Power Rating

$$(18) (196.9) = 3.55 \text{ kW}$$

7.2.1.2.2 Inverter Design — The basic inversion function is performed by a parallel inverter which is the preferred circuit to minimize losses. The inverter is capable of operating in three different modes:

- a. Thrust operation, 100 percent power
- b. One-half voltage operation, corresponding to the failure of one TFE of the pair
- c. Coast mode, 10 percent power

Since the voltage level for normal operation and the failed condition are sufficiently different, provisions are included to select taps on the primary of the main power transformer for these two conditions. During normal operation which is either at 100

percent load during thrust or 10 percent load during coast, the switching devices are connected by means of a contactor to the extreme taps on the power transformer. In the event of failure of one of the TFE's of the pair supplying this converter, the switching devices are transferred to the lower voltage tap. For the 10 percent power operation during coast, the TFE output voltage is sufficiently similar to the regular 100 percent power operation that no transformer tap change is necessary. In this application, where transistors have been selected for the switching devices, the base drive circuits must be designed to recognize the collector current change and reduce the base current accordingly, in order to reduce the unnecessary losses in the base drive circuits during the coast mode.

An alternative to switching the main transistor groups between taps by means of a contactor is to provide a second set of switching devices permanently connected to the one-half voltage transformer taps. Since, however, these switching devices are required to handle the same current levels as the primary transistor groups, the total number of transistors doubles, and base drive circuits must be duplicated. It is lighter and less complex to have one set of transistors and select the proper transformer taps by contactor switching.

7.2.1.2.3 Switching Device Selection — One of the first decisions to be made in considering power conversion equipment for the flashlight reactors system is the type of power switching device to use in the inverter, whether transistor or SCR. Because the voltage output level of the TFE pairs is relatively low, it is important that the losses of the switching devices be low in the interest of efficiency. These losses are primarily composed of conduction losses plus losses during the switch transition times. Typically, transistors are superior when compared to SCR's from the standpoint of conduction losses (saturation voltage drop of 0.8 volt or less for transistors compared to 1 to 1.5 volts for SCR's). Also, transistors have much shorter switching times than SCR's and therefore, can be used at higher frequencies to reduce transformer weight. Thus, the choice is transistors. Furthermore, the selection is confined to

silicon transistors. Germanium transistors, the other possibility, are eliminated from consideration because of low operating temperature tolerance. Hence, the design is based on the use of silicon transistors. To meet the necessary current handling capability, six silicon transistors are switched in parallel to generate alternating current for transformation and subsequent rectification.

Two factors influence the selection of the specific power switching transistors and both affect efficiency. These factors are the switching speed and the conduction drop as a result of the collector-to-emitter saturation voltage.

An examination of the characteristics of several types of silicon power transistors currently available indicates that they can be divided typically into two general categories. The first, typified by the RCA 2N3263 (25 amp, 150 volt), Delco 2N2580 (10 amp, 400 volt), and Westinghouse 1776-1460 (60 amp, 140 volt), exhibit a saturation voltage drop of about 0.75 volts and switching speeds of about 0.5 and 1.0 microseconds (neglecting storage time, which can be compensated for by special circuit techniques).

The second category is defined by a relative newcomer, a Westinghouse low-saturation voltage drop transistor - 0.2 volt at 76 amperes. This device has a switching speed of about 5 microseconds.

Some of the characteristics of these devices are given in Table 7-7. Other high power transistors in addition to those shown in Table 7-7 were considered, such as Solitron 2N4865 and SDT8921 which are 100 ampere units, but which exhibit relatively high saturation voltages at the higher operating currents.

The choice is then between high-speed transistors, which typically have a saturation voltage of 0.75 volts and switching speeds of less than 1 microsecond, and the slower, low-saturation-drop unit with a voltage drop of 0.2 volts and switching speeds of 5 microseconds.

TABLE 7-7. CHARACTERISTICS OF CANDIDATE POWER TRANSISTORS

<u>Type</u>	Max. V_{CEO} (volts)	Max. I_C (amp)	Oper. I_C (amp)	Oper. I_b (amp)	$V_{CE(SAT)}$ (volts)	$V_{BE(SAT)}$ (volts)	tr (μ sec)	tf (μ sec)	Max. T_J $^{\circ}C$	Q_{JC} $^{\circ}C/W$
RCA 2N3263	150	25	15	1.2	0.75 max. @15A	1.6 max.	0.5 max.	0.5 max.	200	1.0
Delco 2N2580	400	10	5	1.0	0.7 typ.	1.5 max.	0.7 typ.	0.6 typ.	150	0.7
<u>W</u> 1776-1440	140	40	20	2.0	0.75	1.5	0.5	0.4	200	0.67
1776-XX40	140	75			est.	est.	max.	typ.		
-XX60										
<u>W</u> 1776-1660	140	60	30	3.0	0.75 est.	1.5 est.	0.5 est.	0.45 max.	200	0.67
<u>W</u> Low Sat V	Up to 120	75A	40	4.0	0.2 max.	1.5 est.	5	5	200	0.7 est.

Both saturation voltage and switching times contribute to transistor losses. Analysis shows that these losses on a per-unit basis are represented by the following expressions:

$$\frac{P_C}{W} = \left[1 - 0.002 T_R f \right] \frac{V_{CE(SAT)}}{E}$$

$$\frac{P_S}{W} = (f) 0.00067 \left[T_R + T_F \right] \left[1 + \frac{V_{CE(SAT)}}{E} \right]$$

In these equations:

P_C = Conduction power loss, watts

P_S = Switching loss, watts

W = Power being converted = (input voltage) X (input current)

T_R = Transistor rise time, microseconds

T_F = Transistor fall time, microseconds

f = Switching frequency, kiloHertz

$V_{CE(SAT)}$ = Transistor collector-emitter saturation voltage, volts

E = Supply voltage

These components of transistor losses have been evaluated by means of a computer program for various values of saturation voltage and transistor switching speed as a function of switching frequency. An input voltage of 16 volts and a power level of 3 kW were assumed. Results are shown in Figure 7-4. Total losses versus frequency for the Westinghouse low saturation drop unit and the typical high speed unit are shown in Figure 7-5. These curves show that at switching speeds below 5.8 kHz the low saturation drop transistor is preferred, because the combined conduction and switching losses are lower than those of the faster transistors. Above 5.8 kHz, switching losses in the 5 microsecond transistor rise rapidly, and the faster transistors are preferred.

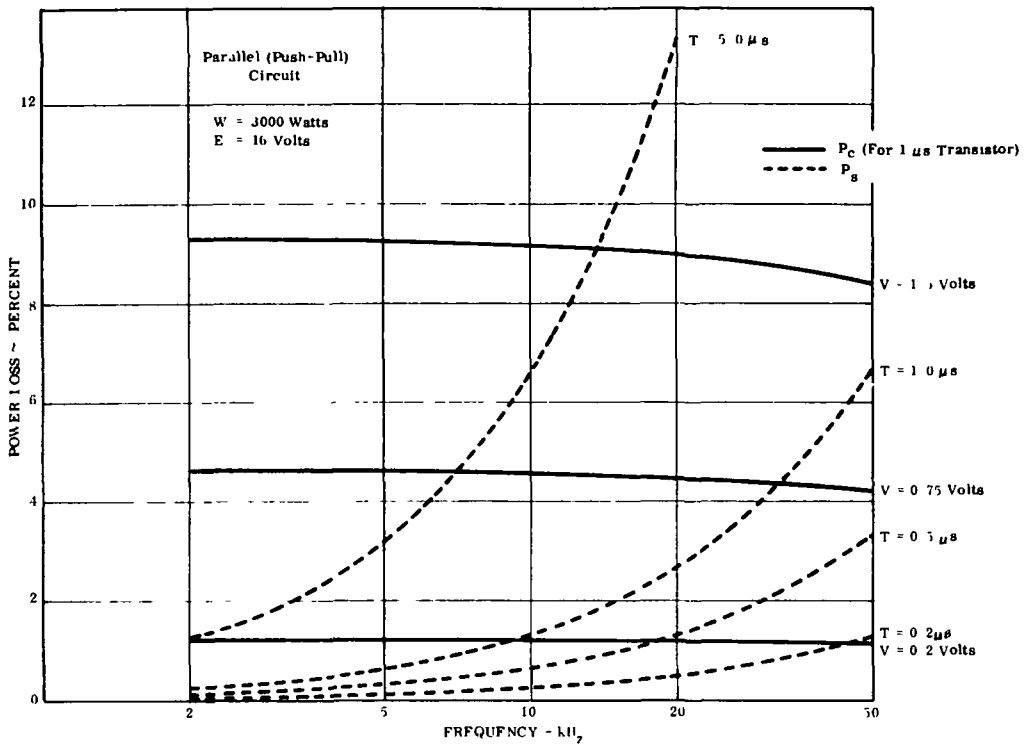


Figure 7-4. Transistor Conduction and Switching Loss

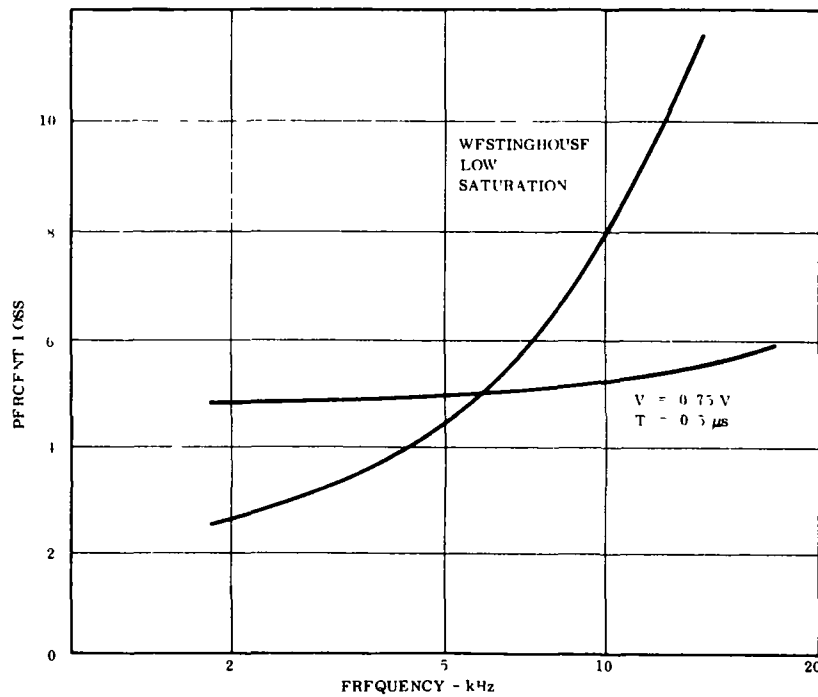


Figure 7-5. Comparison of Transistor Losses with Frequency

7.2.1.2.4 Operating Frequency Selection — Frequency affects transistor losses as well as the size and losses of the inductive elements in the inverter.

Regardless which type of transistor is used, losses rise with frequency, although for high speed transistors the rise is very gradual (See Figures 7-4 and 7-5). Magnetic core losses in the converter power transformer also go up with frequency, but the amount of core material required decreases, and total core loss remains about constant. In general, constant efficiency transformers can be assumed. At very high frequencies of 20 kHz and above, losses in output rectifiers must be considered. Otherwise, other losses can be considered to be independent of frequency.

The increased transistor losses associated with increasing frequency require additional radiator weight. On the other hand, magnetics weight drops with increasing frequency. A brief analysis shows that for an incremental power system weight of 50 pound/kWe, the weight gain penalty is less than 100 pounds total over the frequency range of 2 to 20 kHz. Hence, the selection of a frequency between 2 to 20 kHz may be made without a rigorous weight-efficiency tradeoff. Consequently, the median frequency of 10 kHz is selected for the operating frequency of the transistorized power conditioner for the flashlight reactor.

Gulf General Atomic Inc. designed a low voltage power conditioner for a thermionic reactor and selected 20 kHz for the operating frequency, but showed that a 10 kHz frequency would have improved efficiency (Reference 19).

7.2.1.2.5 Transformer Material Selection — One of the factors which relates to both operating frequency and weight is the type of core material used in the power transformers. One of the candidates is a ferrite. This type of material has the advantages of relatively low density (about 5.3 gm/cm^3 compared to about 8.5 gm/cm^3 for electrical steel) and low core loss at high frequencies, but it has the disadvantages of relatively low saturation flux density and low Curie temperature, (the temperature of

about 180° C at which it loses its magnetic properties) In view of the operating temperature specified for the electronic equipment in this application including the attendant component thermal gradient and the unknown characteristics of ferrite in a nuclear environment, use of this type of material will not be considered. Its evaluation for the thermionic spacecraft application will be left to a more detailed design than this study permits. Therefore, transformer material of electrical steel is selected.

7.2.1.2.6 Inverter Characteristic Summary — For purposes of this study, the power conversion equipment design is based on the following selections:

Switching devices	High Speed silicon transistors (Westinghouse 1776 - 1460)
Operating frequency	10 kHz
Magnetic core material	Electrical steel such as Hymu-80
Module size	Full size for one TFE pair 196.9 amperes, maximum 11-17 volt with provisions for half voltage operation
Reliability provisions	No additional circuit redundancy.

7.2.1.2.7 Component Size Identification — A complicating factor in the use of power transistors in this application is their limited current rating compared to the total current delivered by the source. For example, the rating of the Westinghouse 1776-1460 is 60 amperes, whereas the EOM current of a TFE pair is 196.9 amperes. If the transistors are operated at 30 amperes, both to reduce the saturation collector-emitter voltage drop and to provide normal design margin for reliability (a standard JPL practice) six transistors operating in parallel are required per group. The problems associated with operating many transistors in parallel are at least twofold: proper sharing of current and coordination of turn-off characteristics, especially storage time, so that the transistors in a group all turn off together and one transistor does not carry all of the current during the switching interval.

In 1964, a test was performed by TRW comparing four techniques for balancing paralleled transistors. These methods were:

- a. Direct paralleling
- b. Simple balancing reactor paralleling
- c. Referenced balancing reactor paralleling
- d. Saturating choke seriesed with referenced balancing reactor system.

The lot of transistors was measured for switching times and saturation voltages and worst-case devices were selected for testing. The direct parallel method using no balancing techniques caused the transistors to share current with a ratio of 1.3 to 1; method b caused sharing with a ratio of 1.12 to 1; method c had a sharing ratio of 1.09 to one; and method d was reported to be superior in load sharing but no ratio was given.

The method with the greatest reliability considering series components is method a, direct paralleling, and is selected for use in the flashlight thermionic power conditioner. Transistor selection will be performed forming groups of six transistors with similar electrical characteristics. Since the transistors have been derated in application to carry half-rated current, a current sharing ratio of two to one can be tolerated (neglecting temperature derating). If necessary, a simple series resistor can be introduced in the emitter circuit of the transistors, effecting base drive current as well as collector current sharing.

For purposes of this study, it will be assumed that, by proper control of device characteristics during manufacture, by device selection, and possibly by special circuit techniques, proper operation of up to 10 power transistors in parallel can be achieved at the desired operating frequency without sacrifice of efficiency and with minimal weight increase for additional circuit components.

It should be noted that the saturation voltage drop of a transistor is a function of the transistor collector current. Hence, to within limits, low saturation drop of even ordinary power transistors can be achieved by operating them at low currents. In part, this is the reason for operating the selected transistors at half rated current.

Clearly, there are practical limits to the reduction in saturation voltage, which can be gained by the transistor paralleling technique. For example, if 10 transistors are operating in parallel the addition of one will reduce the current per transistor by about 9 percent and will only reduce the saturation voltage by a similar amount (i. e. , $V_{CE(SAT)10} = 0.44V$, $V_{CE(SAT)11} = 0.40V$). A separate study would be required to determine the optimum balance between saturation voltage and number of transistors.

A decision required in connection with power converter design is the basic size of the converter module. Conversion of all the power of one TFE pair can be performed in a single converter with a single power transformer. On the other hand, the conversion equipment for a single TFE pair can consist of a number of small modules, with their inputs connected in parallel and their outputs in series or parallel. The single converter has the advantage of lowest weight, but has the disadvantage of providing no redundancy. The modular approach has the advantage of a high degree of redundancy but the disadvantage of greater weight.

An estimate of the weight penalty can be made by the following reasoning. The bulk of the weight of a dc-to-dc converter is the power transformer. Let it be assumed that the transformer represents half the total weight, and that the transformer weight varies at the 3/4 power of its electrical rating (Reference 8).

Let W_{10} = weight of transformer for module of 10 modules
 W_1 = weight of transformer for single converter

then

$$\frac{W_1}{W_{10}} = \left(\frac{P_1}{P_{10}} \right)^{3/4} = (10)^{3/4} = 5.63$$

Thus, the weight of a single, full size transformer is 5.6 times that of the transformer in a single module of 1/10 the power rating. Since 10 small transformers are the equivalent of a single large one from a power standpoint, ten small transformers would weigh 10/5.6, or nearly 1.8 times more than a single large unit. Since transformer weight is assumed to represent 1/2 total equipment weight and all other weight is considered to be equivalent in the two cases, the total equipment weight of 10 small modules will be 1.4 times that of a single large converter.

The former analysis does not allow overrating of the small modules to take advantage of redundancy. If the modular equipment were to be designed so that loss of a single module could be tolerated without loss of capacity, each of the 10 modules would have to be designed so that 9 could handle the total power output of the TFE pairs. Hence, each would have to be capable of handling 10/9, or 1.11 of its nominal power; in other words, each should be designed for 11 percent excess capacity. Such excess capacity has not been factored into the computations.

7.2.1.2.8 Redundancy Considerations — Since the flashlight reactor contains 108 TFE pairs, each of which represents a separate power source, it is assumed that no redundancy is required in the conversion equipment. A loss of one power converter channel represents a loss of less than 1 percent in the total power available from the reactor.

If redundancy is desired, however, some of the methods of providing it are as follows:

- a. Use single, full capacity converters for each TFE pair and include additional converters which can be switched in in place of failed units. There would be significant difficulties in providing for fault detection and switching. This does not appear to be a practical approach.

- b. For each TFE pair, provide a redundant full capacity converter so that if one fails the other can take over. This approach doubles the weight of the conversion equipment and appears prohibitive from the weight standpoint.
- c. For each TFE pair, provide N converters in parallel each with sufficient capacity so that one can fail and the others take over the full load without loss of power. This is similar to the second approach, except that more than a single redundant unit would be provided. The penalty for this approach, as noted before, is one of weight: modularized equipment is simply heavier than concentrated equipment of the same rating.
- d. Provide circuit redundancy rather than equipment redundancy; that is, instead of providing complete spare modules or converters, design the necessary conversion equipment conservatively and provide redundant circuits to minimize the probability of failure.

For the flashlight reactor system, the no redundancy approach is selected for the following reasons:

- a. With 108 individual power sources available, failure of any one converter channel represents loss of less than 1 percent of total power.
- b. Study ground rules provide reactors designed to provide BOM power at EOM, even if 10 percent of the TFE units are lost due to failure.
- c. To provide redundancy by additional converters represents a substantial weight penalty for the conversion equipment.

7.2.1.3 Flashlight Power System Integration

7.2.1.3.1 Reactor Integration — The main converter module detailed on Figure 7-2 is connected to the TFE pair through a limiter or fuse, the function of which is to open the circuit between the TFE pair and the converter in case of internal converter faults. The intention is to prevent physical damage within the converter because of high short circuit currents. It is recognized that operation of the fuse open circuits the TFE pair, and may cause overheating and failure of the TFE pairs. The alternative would be to provide some means of short circuiting the TFE's in the case of disconnection of the converter. In this initial study, short circuiting means are not

provided because the condition of open-circuiting by converter failure is considered equivalent to open-circuiting of a TFE because of an internal fault. Consequently, there are no provisions against overheating for either a TFE failure or power conditioning failure. Future study should be performed to determine if a problem could exist.

Diodes across each TFE are included within the converter to provide a path for the current from the surviving TFE, in the event of open circuit failure of the other.

An input filter consisting of a capacitor and reactor is included in the converter design to limit the voltage swings at the input to the converter during those portions of the normal operating cycle when the converter transistors are off and the TFE pairs are unloaded.

At a 10 kHz switching frequency for the converters connected to each TFE pair, it can be assumed that the fluctuations in unfiltered TFE current, represented by converter switching with pulse width modulation, are not detrimental to the thermionic diodes. Diodes have long thermal time constants of several seconds at least, so the rapid switching will not affect instantaneous temperatures.

Filtering is not needed from the standpoint of the diodes. However, instantaneous changes in current between some large value and zero will cause large instantaneous changes in diode output voltages as shown in Figure 7-3, which presents typical I-V characteristics of the diodes. During the intervals when current is zero, diode voltage will go to rather high values. Hence, from the standpoint of protection of the converters, input filtering is required. In addition, the filter circuits provide nearly constant current flow in the low voltage leads from the thermionic reactor during the converter switching cycle, and effectively reduce the low voltage cable power loss.

7.2.1.3.2 Electrical System Control — Current transformers in the converters are included to provide signals representing TFE currents for system control load sharing, reactor control and for telemetry information.

The two output voltage levels are created by separate secondary windings on the same single power transformers. Each output is furnished with its own fuse, or limiter, to protect the converter against physical damage in the event of a load fault or a distribution line fault. The alternatives to this type of protection for these faults require further consideration.

The electric control system performs load sharing control as well as voltage regulation.

During each of the three modes of operation: normal, one-half voltage with one TFE failed, and 10 percent power, the load sharing by the TFE's controlled by pulse width modulation cycling of the individual converters. Control of the inverter conduction cycle relative to the non-conduction time is exercised by regulation circuits which sense the input current. Modifying functions to the control is the location of the TFE in the reactor, and whether the system is operating in the coast phase.

During normal and half voltage operation, when the principal load is the thruster screens and the high voltage output is utilized, voltage regulation is exercised by regulating circuits which sense the high voltage at the load bus and control the reactor operation to maintain this voltage constant. The 250-volt output is separately regulated by phase controlling SCR's as the rectifiers in its output circuit.

During the coast period when 10 percent power is required, the thrusters are de-energized, and there is no load on the 3100-volt bus. Reactor control is maintained by switching regulation to the 250-volt bus.

The third set of control circuits operates the contactor, which switches the main transistor groups from the normal to the 1/2-voltage taps. These control circuits sense voltage unbalance in the TFE pairs and operate the contactors if the voltages become unbalanced because of a fault in one of the TFE's.

7 2.1.3.3 Thruster Integration — The requirement that the power conversion equipment operate from individual TFE pairs so that the operating conditions of the TFE's be controlled individually, requires a system in which the outputs of the individual power converters can be combined electrically at a dC level. Several factors suggest that one of the voltage levels of the combined converter outputs be that required by the ion thruster screens, which in this case is 3100 volts:

- a. Three-quarters of the total reactor capacity is consumed by the thruster screens. Of the total of 300 kilowatts reactor electrical output, 223 kilowatts is required by the 3100 V screens of the 31 operating ion engines.
- b. If another voltage were used for distribution, an additional conversion process would be required to provide screen power. Additional conversion is undesirable because it involves additional weight and additional losses.
- c. A high distribution voltage, such as that required by the screen supplies, tends to minimize conductor size and, hence, conductor weight in the distribution lines.

In order that a common screen supply be feasible, several factors must be considered. If all screens are fed from a common supply, all are interconnected electrically. Hence, it is necessary that such interconnection be compatible with the complete electrical system, including the thruster auxiliary power conditioners. Also, it must be possible to isolate individual thrusters from the common supply in the event that the thrusters fail on momentary arc-over.

To date, operating experience has been confined to the operation of single thrusters with their own power supplies. There is no known case of the operation of several thrusters from a common supply. However, tests of three and more devices from a common supply are planned in the near future at General Electric in Evendale, Ohio

Examination of thruster electrical connections which have been used to date (References 8 through 11) show that one side of the screen supply connects to system ground and the other to the thruster screen. A small resistor is usually inserted in the negative or ground lead to provide a signal representing screen current. The screen current signal in the common supply configuration can be derived satisfactorily either from a resistor in the positive lead or from a current measuring transformer electrically isolated from the screen power supply leads. Individual fault isolation also can be accomplished by including an isolating device, such as a static switch, a relay contact, a fuse or some other circuit interrupting device, in the leads between the common screen supply and the individual thrusters. Transient isolation to decouple the individual thrusters from the common screen supply can be achieved by the use of inductors in the lines between the common screen supply and the individual thrusters. In the event of arcs within the thruster, between the screens and the other electrodes, the inductors would prevent the current from changing abruptly and would absorb the supply voltage until the thrusters could be isolated from the screen supply by means of the individual circuit interrupters.

Thus, it appears feasible to operate all thrusters from the common supply and thus avoid multiple power conversion for the high voltage screen power. This is a major assumption in the design of the electrical system for the flashlight thermionic reactor system, and is the only identified technique to eliminate the additional losses and weight that would be associated with providing thruster isolation via a second power conditioning stage.

7.2.1.3.4 Power Distribution Voltage Selection — The medium voltage power distribution is required to supply power to the remaining thruster loads and the payload and hotel loads. These are in two locations with 60 percent of these total load requirement near the reactor and with the remaining 40 percent near the spacecraft thrusters.

With 19 kWe load located approximately 40 feet from the supply, a reasonably high voltage is necessary for distribution to minimize cable weight and power loss. Since many electrical components and insulations are rated to operate to 600 VDC, allowing 50 percent derating, an optimum potential of 250 volts was selected.

A number of options exist in the manner in which the two output voltage levels, 3100 volts and 250 volts, can be created for the multiplicity of interconnected modules. These are as follows:

- a. High Voltage *Outputs Parallel - Medium Voltage **Outputs Parallel - This concept requires high voltage rectifiers on the output of each module and an individual filter on each output.

One or more modules, designated the master module shall be designed for voltage regulation, with provisions for adjustment of the reactor.

If the high voltage outputs are designed to regulate the reactor characteristics, the medium voltage outputs would also be regulated adequately only if the medium voltage circuits had the same electrical relationships as the high voltage circuits. To insure proper voltage regulation of the medium voltage outputs, regulation must be provided by phase control of the medium voltage output rectifiers; hence, the need for Silicon Controlled Rectifiers (SCR).

- b. High Voltage Outputs Series - Medium Voltage Outputs Parallel - Each high voltage circuit output would be relatively low voltage (3100/108, or about 30 volts), but each would have to carry full output current. Hence, rectifier power losses would be high, and would lower overall efficiency by approximately 4 percent.

Each module could be separately voltage-regulated, with the overall reference voltage level adjusted so that the high voltage is regulated

Only a single high-voltage filter would be required. To make this filter small, the individual inverters could be staggered in phase relationship so that ripple frequency would be high.

If each high voltage output were separately regulated, provisions must be made to allow the medium voltage outputs to share the load properly.

* 3100 volt screen supply
** 250 volt hotel/thruster supply

- c. High Voltage Outputs Series - Medium Voltage Outputs Series - Individual low voltage outputs would be very low and corresponding rectifier losses would be high. This is not a satisfactory approach for that reason.
- d. Separate Converters for High Voltage and Medium Voltage Outputs - High voltage outputs in series or parallel, medium voltage outputs in parallel, each separately regulated. The disadvantage of this approach is that two sets of converters are required, and weight would be high.

Alternate a, the high voltage parallel/medium voltage parallel method, appears superior. It is heavier than the high voltage series/medium voltage parallel method by virtue of requiring individual filters in the high-voltage circuit, but it is about 4 percent more efficient. For weight and efficiency calculations, this is the system which will be assumed. To achieve voltage regulation of the medium voltage circuits, phase-controlled output rectifiers are assumed, although it is recognized that the additional regulating loop thus created may be difficult to construct due to the affect upon system stability. These can be examined in a more detailed study.

7.2.1.3.5 Screen Circuit Control — The high voltage electric system configured for the flashlight thermionic generator is based on the use of a common thruster screen supply with individual static-circuit interrupters for each thruster.

In order that a common screen supply be feasible, several factors must be considered. If all screens are fed from a common supply, all are interconnected electrically. Hence, it is necessary that such interconnection be compatible with the complete electrical system, including the thruster auxiliary power conditioners. Also, it must be possible to isolate individual thrusters from the common supply in the event that the thrusters fail on momentary arc-over.

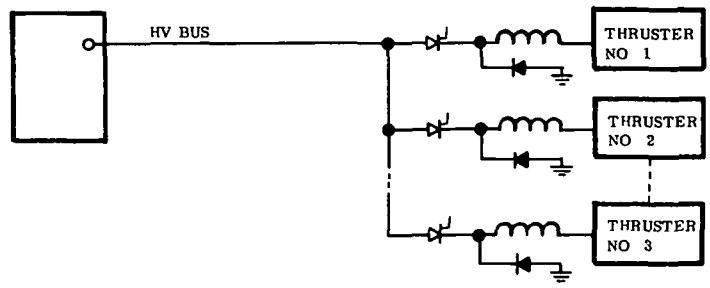
Each individual thruster screen is fed from the common high voltage bus at the thrusters through a series network consisting of a high speed electronic switch (SCR) and a series reactor (L). Simplified schematic diagrams of the common bus connection and the static switch used as the screen circuit interrupter are shown in Figure

thruster conditions to return to normal. After 0.2 seconds, the SCR is switched on again, reestablishing screen voltage and hopefully restoring full thruster operation. If the arc restrikes three times within a ten seconds, the screen supply to that thruster and the inputs to the auxiliary power supplies for that thruster are permanently disconnected. This thruster is considered disabled and one of the six spare thrusters is placed into operation

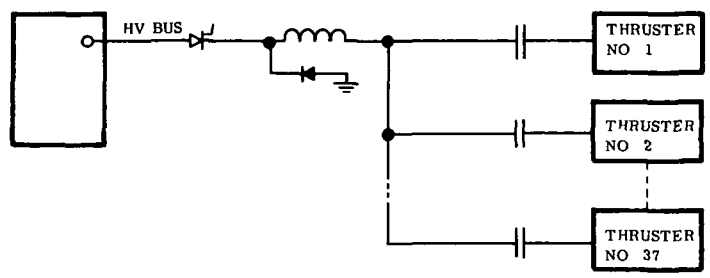
During the spacecraft coast period when the thrusters are not required to operate, power to the thrusters is disconnected by the static switches in the screen supplies and by the contactors in the input circuits to the auxiliary thruster power supplies.

An additional alternative may be considered. The above discussion suggests that each thruster screen circuit be provided with its own circuit interruption device. This suggests that any thruster that arcs, internally, can be isolated individually for the required period in order to allow the arc to clear, without interrupting power to the other thrusters. Another mode of operation is to interrupt power to all thrusters when an arc occurs in any one of them and then to re-apply power after the prescribed delay period, allowing the arc to clear. This somewhat reduces the total average thrust, but also reduces the amount of switching equipment required from 37 pieces to one piece. Of course, some means still must be provided to permit isolating individual thrusters should total thruster failure occur. These alternatives are illustrated in Figure 7-7. This latter arrangement, in effect, treats the entire thruster as a single thruster except that it allows isolation of the individual thrusters when necessary.

Further study may be required to firmly decide between these two approaches. The system which provides separate isolation for each thruster is preferred at this time, because of its greater reliability.



A INDIVIDUAL SCREEN CIRCUIT INTERRUPTION



B COMMON SCREEN CIRCUIT INTERRUPTION

Figure 7-7 Alternative Screen Supply Interruption Techniques

7.2.1.4 Main Converter Mechanical Design

7.2.1.4.1 Geometry — Components of the main power conditioner are to be mounted using a baseplate integral to the radiator. Figure 7-8, layout drawing, and Figure 7-9, isometric drawing, show the components configured within a one square foot area. The suggested layout was designed to accept power at one side and have the outputs on the opposite side, thus simplifying the component construction, testing and integration.

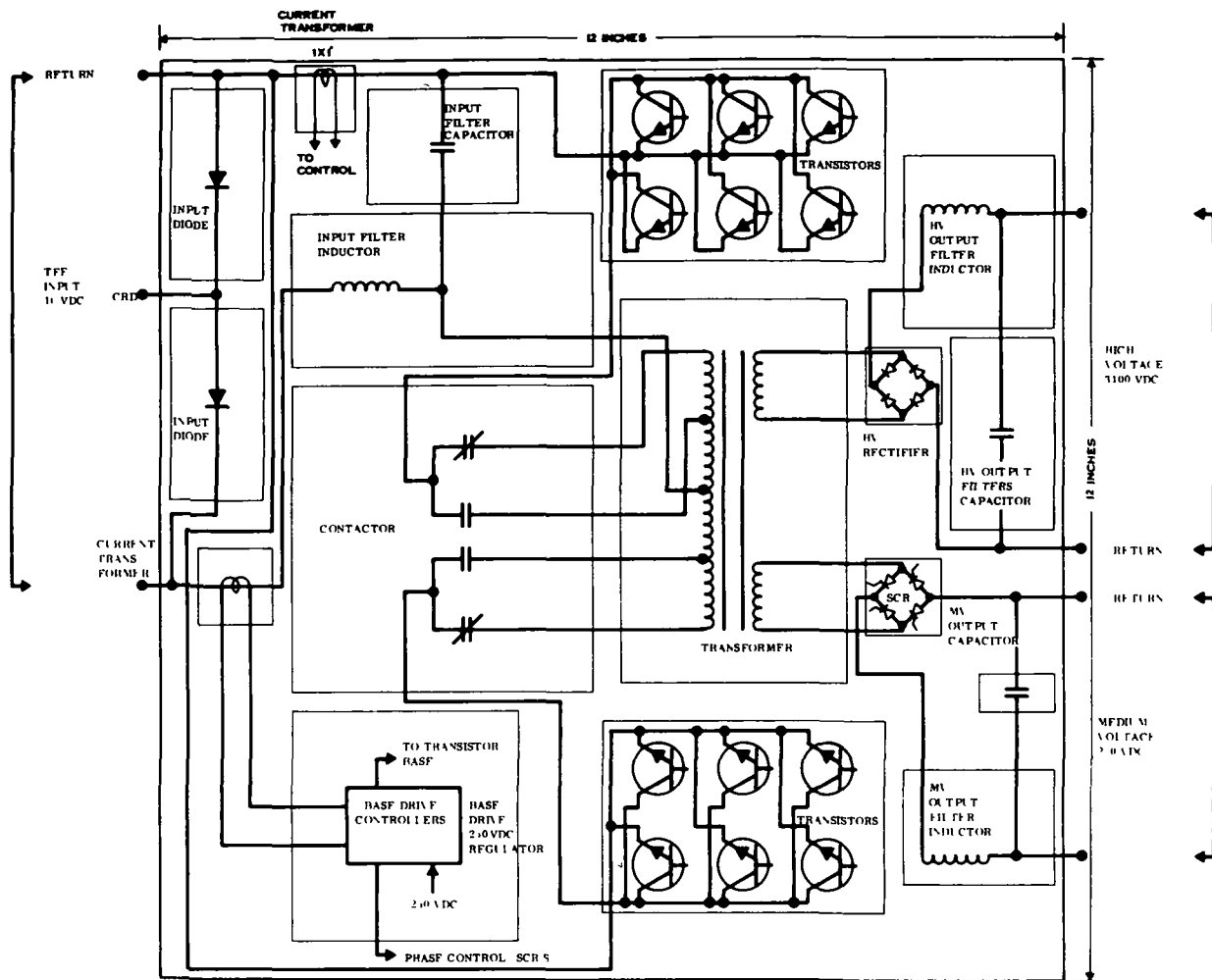


Figure 7-8. Component Geometry Main Power Converters Flashlight Reactor System

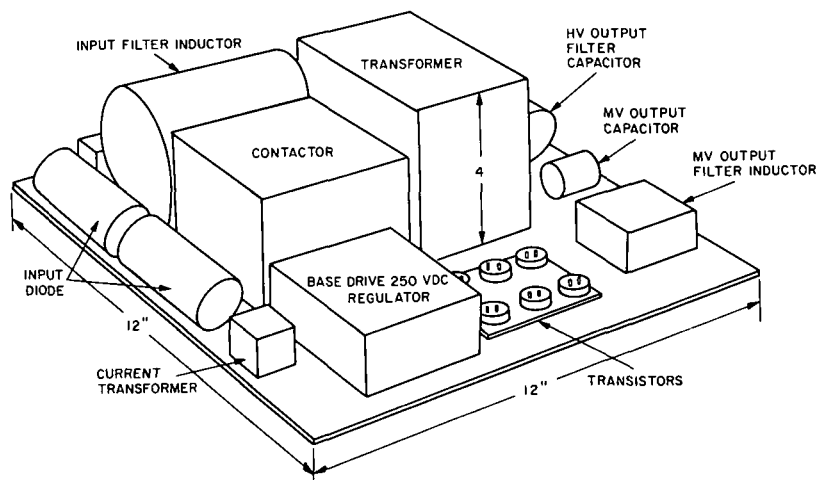


Figure 7-9. Reactor Power Regulation Arrangement Nominal 3kWe Module Flashlight Reactor System

7.2.1.4.2 Component Size — The following components have been selected for use in the main power conditioners. Weights for each device is shown in Table 7-4.

a. Input Filter

Inductor: 2.0 x 4.0 inches diameter
5 h 7 turns, 5 cm length 10 cm diameter
AWG number 4, copper wire

Capacitor: 1.3 x 2.5 x 3.0 inches H
4 - GE-KSR Tantalum Foil
200 μ f, 100V, type 29F3265

b. Bypass Rectifiers: 2.5 x 1.2 inches diameter
200A, 200V
Type GE-1N3264

c. Inverter

Transformer: 5.0 x 3.0 x 4.0 inches H
Electrical steel, Hymu-80
Input: 14 to 18 VDC, 196.9A maximum
Outputs: 3100 VDC, 2.3A
250 VDC, 1.7A
Tapped Primary

Transistors: mounted on two panels bonded to radiator,
Six transistors/heat sink
Transistor type: Westinghouse 1776-1460
0.5 x 0.9 inches diameter
60A, 140V

d. HV Output Rectifiers: Bonded block, 1.0 x 1.0 x 0.5 inches H
12 diodes/block, 3 diodes/branch
Diodes: 3A 800V
Type: GE-A15N
0.15 x 0.2 inches diameter
Axial Lead

e. HV Filter

Inductor: 2.25 x 1.8 x 1.8 inches H
8 cubic inches

- Capacitor: 3.8 x 1.6 inches diamter
Axial
- f. MV Output Rectifiers: 0.4 x 0.3 x 0.6 inches H
3-Silicon controlled rectifiers
Stacked flat pack
SCR: Similar to Type GE-C106
0.4 x 0.3 x 0.2 inches H
- g. MV Filter
- Inductor: 2.0 x 1.5 x 1.0 inches H
- Capacitor: 1.0 x 3.6 in. diam.
Tubular tantalum foil
- h. Contactor: 4.0 x 4.0 x 3.0 inches H
250A, 120VDC, DPDT, latching
- i. Control Circuits: 3.0 x 3.0 x 1.5 inches H
(Base drive, SCR 5 control boards
Phasing) 2 power transistors, similar to 1776-1460
- j. Current transformer: 1.0 x 1.0 x 1.0 inches H
2 toroids and power supply

7.2.1.5 Auxiliary Power Conditioning

7.2.1.5.1 EM Pump Power Conditioning — DC conduction electromagnetic pumps were selected for use with the thermionic reactor system. These pumps require very high current at very low voltage, specifically for the primary pump, 5000 amperes at 0.5 to 1.0 volts. Special additional power conditioning equipment, therefore, is necessary. Using conventional power conversion schemes for very low voltage, efficiencies of less than 50 percent are encountered. With dc-ac-dc conversion, the voltage drop in the output rectifiers approximates or exceeds the output voltage required and hence the efficiency is poor.

In order to obtain the extremely low dc output voltage required at the pumps, standard low-voltage conversion to a higher output voltage is performed and several pumps are

connected in series. Now, with the rectifiers dropping 0.7 volts dc and the output typically 10 volts dc, an efficiency of approximately 85 percent is realizable.

Two power conditions are used in the EM pump system. One feeds the main coolant loop primary and secondary pumps which require 10 kW each. The other feeds the auxiliary pump, the shield pump, and the propellant pump, requiring an estimated 0.1 kW each. Each of the primary and secondary pumps are assumed to be divided into 10 parallel fluid ducts, requiring 0.5 volt for each duct, all connected in series. The conditioner would have an efficiency of 85 percent as previously mentioned.

The remaining EM pumps are single duct machines, which when connected in series require a power conditioner to supply 0.3 kW at 1.5 volts DC. Efficiency for this supply would be approximately 60 percent, but for this relatively low power level the loss would be about 200 watts. Power conditioner circuit for the small EM pumps is a conventional parallel-commutated SCR inverter with a counter-tapped transformer combined with a low voltage rectifier as shown in Figure 7-10.

The characteristics of the power conditioning for the EM pumps are summarized on Table 7-8. A standard 8 pounds/kWe has been applied for weight estimation for the main EM pump power conditioner.

7.2.1.5.2 Other Auxiliary Power Conditioning — Auxiliary power conditioning is required for the following operations:

- a. Reactor Control
- b. Power Plant Control
- c. Special Ion Engine Units
- d. Spacecraft Guidance and Control
- e. Payload Power Conditioning

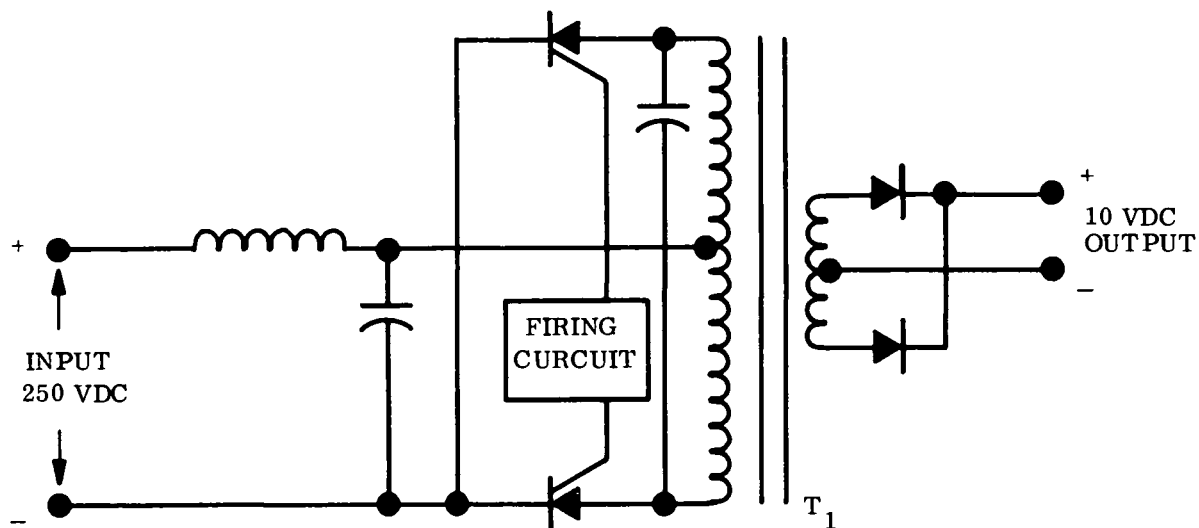


Figure 7-10. DC-EM Pump Power Conditioning Parallel-Commutated SCR Converter

The weight of the power conditioning for all these units, except the special ion engine units, is greater than the 8 pounds/kWe output employed for the main EM pumps because of the smaller size of these special purpose units, as shown in Table 7-8. The weights presented in Table 7-8 for the special ion thruster units are those provided by JPL. The efficiency of these auxiliary units is 90 percent. No losses are shown for the special ion engine units, since this power loss is already factored into the ion thruster efficiency used to calculate the beam power.

7.2.1.6 Electric Cable Design

Three sets of power distribution cables are required for the flashlight reactor electrical system. Low voltage cables conduct power from each TFE pair to the corresponding power conditioning module, and medium voltage cables distribute power

TABLE 7-8. AUXILIARY POWER CONDITIONING CHARACTERISTICS

Component Application	Power Input kWe	Efficiency Percent	Weight Pounds	Power Losses watts (e)
Main EM Pumps	23.5	85	160	3500
Auxiliary EM Pumps	0.50	60	10	200
Reactor Control	2.22	90	15	222
Power Plant Control	0.50	90	10	50
Spacecraft Control	0.50	90	10	50
Special Ion Engine Units	17.0	90	273*	--
Payload Units (included in 2200 pound payload weight)	1.0	90	30	100

*Data supplied by JPL, losses included in engine allocation

from the medium voltage bus in the power conditioning bay to the hotel loads near the reactor and near the thrusters. Screen supply power is distributed via the high voltage cables from the power conditioners to the thrusters.

In selecting the materials and cross-section area of the various cables, a weight optimization was performed. An optimization was made between cable weight and the corresponding inverse electrical losses reflected in the compensating power plant weight.

The following expression relating the cable weight to the power loss was developed:

$$\text{Total Weight} = \frac{\rho (I)^2 (L)^2 (D)}{P} + 0.05 P$$

where ρ = resistivity of the cable material

I = current

L = length

D = density of the cable material

P = power loss

The first term is the cable contribution and the second term is the power plant weight using a plant specific weight of 50 pounds/kWe.

The relation for minimum power loss is obtained by taking the first derivative of the weight equation and solving for minimum power with the derivative equal to zero, which yields:

$$P_{\text{MIN}} = \left(\frac{K}{0.05} \right)^{1/2}$$

where

$$K = (I)^2 (L)^2 D$$

Optimized weight for the cable is then obtained by use of the first term of the weight equation. The corresponding optimized cable cross-section can be calculated once the power loss is known.

Characteristics of the following materials were examined for application to the three cable set requirements:

- a. Copper (Cu)
- b. Aluminum (A1)
- c. Sodium (Na)/SS

- d. Beryllium (Be)
- e. Nickel Clad Silver (NiAg)
- f. Nickel Clad Copper (NiCu)
- g. Sodium Potassium (NaK)

Figure 7-11 shows a comparison of the leading candidate materials for the low, medium and high voltage cables. On the basis of weight/power loss optimization and mechanical integrity at the operating temperatures, the materials summarized on Table 7-9 were initially selected for the cable sets. The detailed optimization results for each of the three cable systems are presented on Figures 7-11 through 7-13.

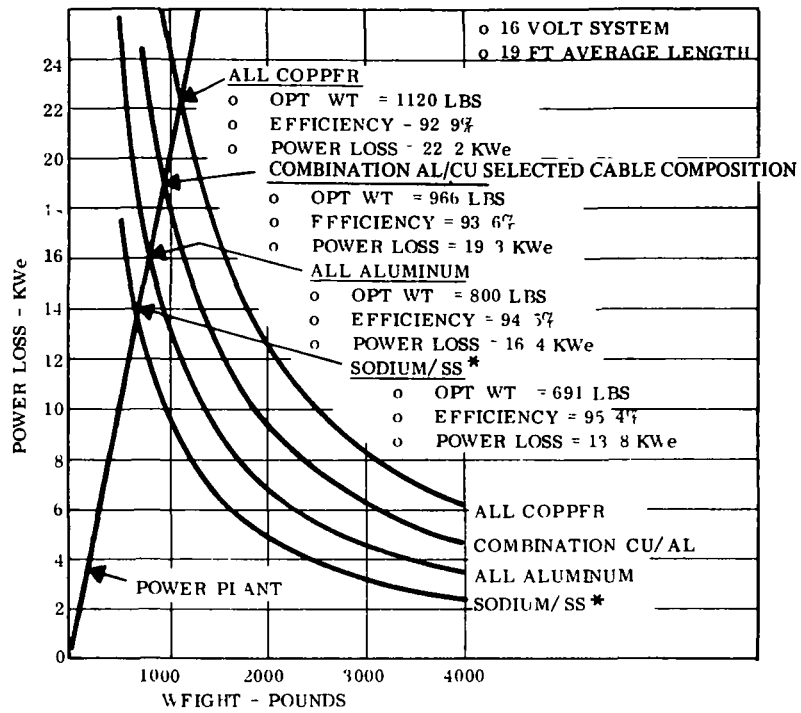
TABLE 7-9. SELECTED POWER CABLE CHARACTERISTICS

Cable Function	Material	Weight	Power (Watts) Loss
Low Voltage	Sodium/Stainless Steel*	(917)*	(13,800)*
Medium Voltage			
Reactor Area	Aluminum	7	140
Thruster Area	Aluminum	5	50
High Voltage	Aluminum	6	120

*See Paragraph 7.2.1.6.1, baseline changed to aluminum/copper

The total weight of all three cable systems is 935 pounds, and the total power loss is approximately 14,100 watts, or 4.67 percent overall, of the 300 kWe system total.

7.2.1.6.1 Low Voltage Cables — Subsequent to the baseline analysis, it was observed that the resistivity used for sodium in the weight/loss calculations was that for solid sodium, whereas because of the reactor/radiator heat most of the cable would be



* SEE PARAGRAPH 7.2.1.6.1 FOR CORRECTION

Figure 7-11. Low Voltage Cable System Weights

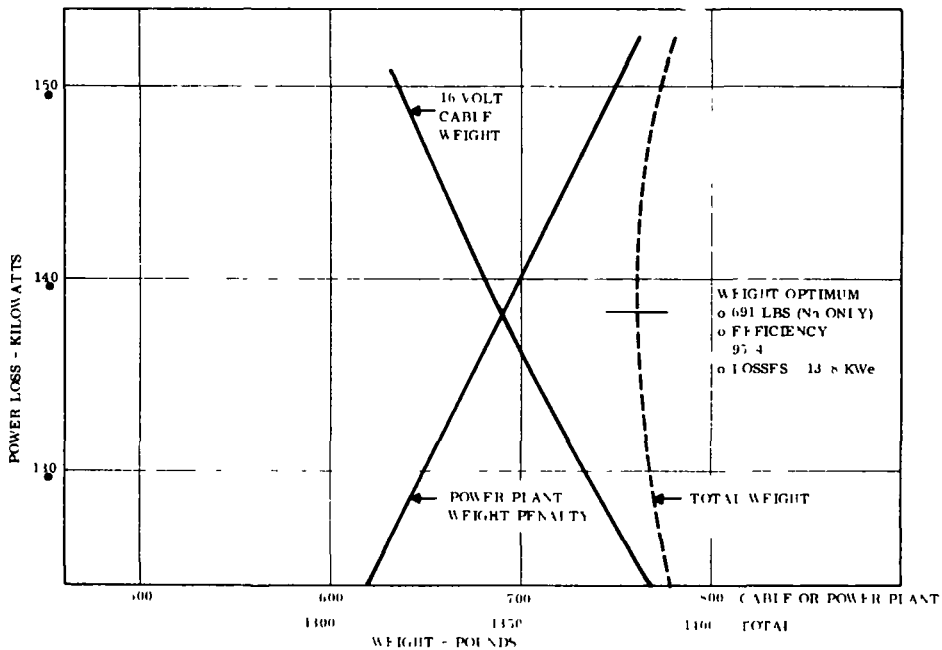


Figure 7-12. Detailed Weight Optimization, Sodium-Stainless Steel Low Voltage Cable System

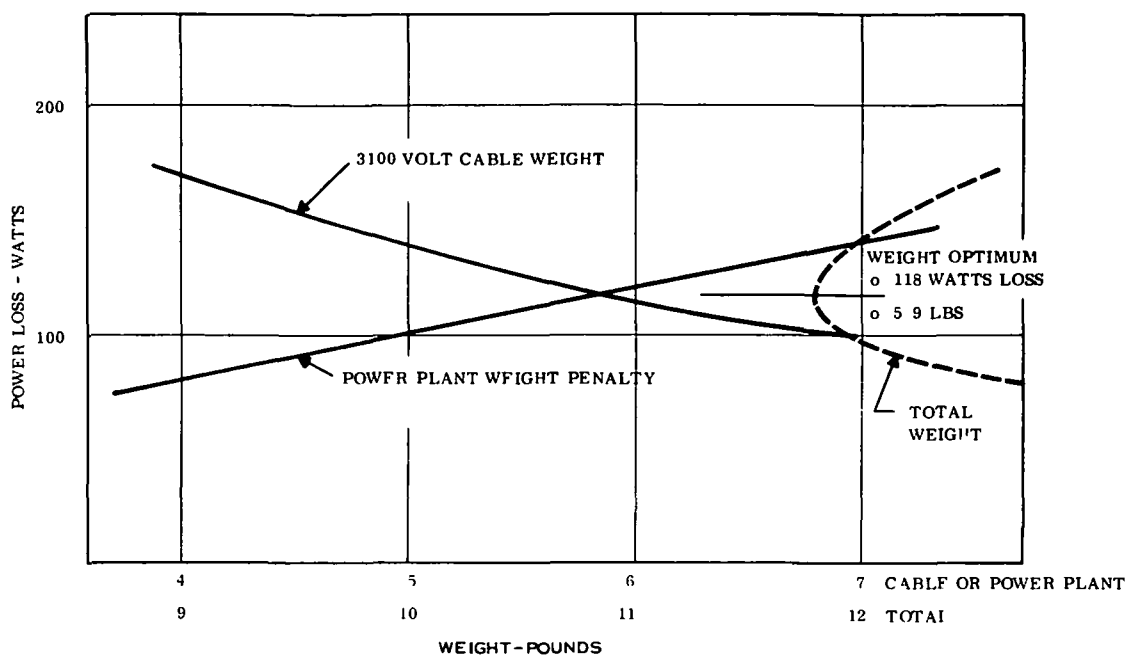


Figure 7-13. Detailed Weight Optimization, Aluminum High Voltage Cable System

liquid with a higher resistivity. Comparison with the combination cable composed of copper/aluminum does not show as great of an advantage to use sodium. The weight and loss are only slightly less for sodium, but because of the manufacturing and handling difficulties, the combination cable is recommended, and the low voltage cable weight and power loss is higher than shows in the Baseline Design tables.

The original analysis with the solid sodium resistivity is as follows: Considering the low generation voltage (16 volts) the quantity of power to be transmitted, and the transportation distance, the selection of the low voltage cable material is more critical than that for the other cables. An optimized system using all copper would weigh 1120 pounds, and would incur a power loss of 22.2 kWe for a transmission efficiency of 93 percent based on the 300 kWe total. An all-aluminum cable, which would not be satisfactory due to its low strength in the high temperature reactor equipment bay,

would weigh 800 pounds, and would have a transmission of 94.5 percent efficient. A cable which does have acceptable strength characteristics and could be used as an alternate is a cable composed of copper in the reactor/shield area combined with an aluminum cable for the lower temperature areas. The combination cable would weigh 970 pounds, with a transmission efficiency of 93.6 percent, of the 300 kW total.

7.2.1.6.2 Medium/High Voltage Cables — Weight optimization shows that aluminum is the preferred, readily available material for the medium and high voltage cable material, but other materials such as copper may be used. The conductor material selection is not critical when the cable weights and power losses are compared with other system contributors. Nor are cross-sectional areas of the conductors critical, within limits.

7.2.2 EXTERNALLY FUELED THERMIONIC REACTOR POWER SYSTEM DESIGN

The electrical power system developed for the Externally Fueled Thermionic Reactor (EFTR) is shown in Figure 7-14.

The following discussion will be concerned with the main power conditioner design. Baseline for the rest of the system is unchanged from the flashlight design insofar as techniques and specific weights are concerned.

Electrical power output from the generator is sufficiently high so as to be an integral part of the medium voltage distribution bus. Power comes from a single output at a potential of 120 volts, and is distributed directly to the auxiliary loads, as well as the main power conditioners without being transformed. The main power conditioners convert the 120 volt input to 3100 volts for the screen electrodes of the ion thrusters. With individual power conditioners for each engine, no separate screen circuit interrupters are necessary. Screen circuit current limiting and thruster turn-off will occur in the affected power conditioner.

Baseline losses and component weight for the EFTR power conditioner are presented in Tables 7-10 and 7-11, respectively.

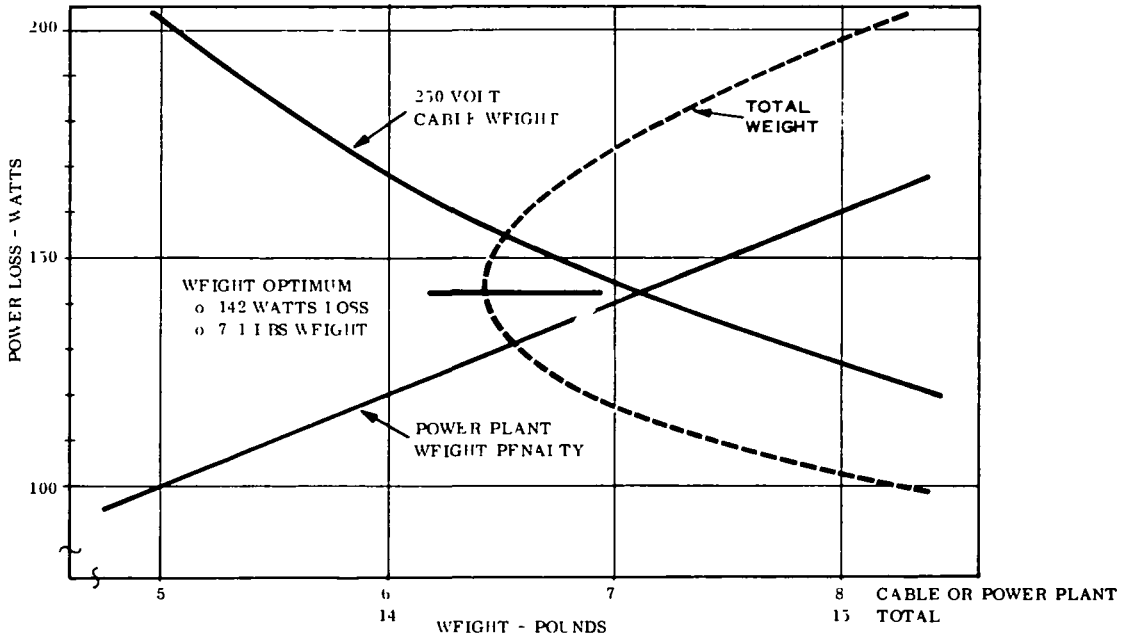


Figure 7-14. Detailed Weight Optimization, Aluminum Medium Voltage Cable System

TABLE 7-10. EXTERNALLY FUELED REACTOR POWER
CONDITIONING POWER LOSS

Component	Loss, Watts
Transformer	216
Main SCR's	464
Auxiliary SCR's	96
Commutating Circuit (inductor/capacitor)	2
Feedback Diodes	8
Rectifier Diodes	7
Output Filter	45
Snubber Circuit (RC Filter)	4
Input Filter	22
Control Circuit	15
Total	879
Efficiency (90 volt Input)	89.1 percent
Specific Weight	5.1 lbs/kWe out 4.5 lbs/kWe in

The electrical schematic of the main power conditioner is shown on Figure 7-15.

Figure 7-17 shows the parametric characteristics of the EFR main power conditioner as a function of input voltage.

7.2.2.1 Design Approach

Electrical system design for the externally fueled reactor system is based upon each ion-thruster being driven by a separate power conditioner. There are 37 thrusters/power conditioner groups on the spacecraft, 6 of which are spares to be used following a failure of one of the initially active engines.

One of the control loops of the reactor senses the reactor output voltage, and regulates incremental changes in heat generation to maintain a constant output voltage. Therefore, under normal conditions, regardless of load, the input potential to the

TABLE 7-11. EXTERNALLY FUELED REACTOR MAIN
POWER CONDITIONER WEIGHT

Component	Weight, lbs.
Transformer	17.20
Main SCR's	1.25
Commutating SCR's	0.10
Commutating Circuit	
Capacitor	1.66
Inductor	0.04
Feedback Diodes	0.12
Rectifier Diodes	0.13
Output Filter	
Capacitor	1.06
Inductor	0.10
Snubber Circuit	
Capacitor	0.04
Resistor	0.04
Input Filter	
Capacitor	1.60
Inductor	1.90
Control Circuit	0.30
Miscellaneous Piece Parts (Wire, Mounting Brackets, Heatsines, etc.)	10.96
Individual Converter Weight	36.50
Total Weight, Main Power Conditioners, Externally Fueled Reactor System	1350.00

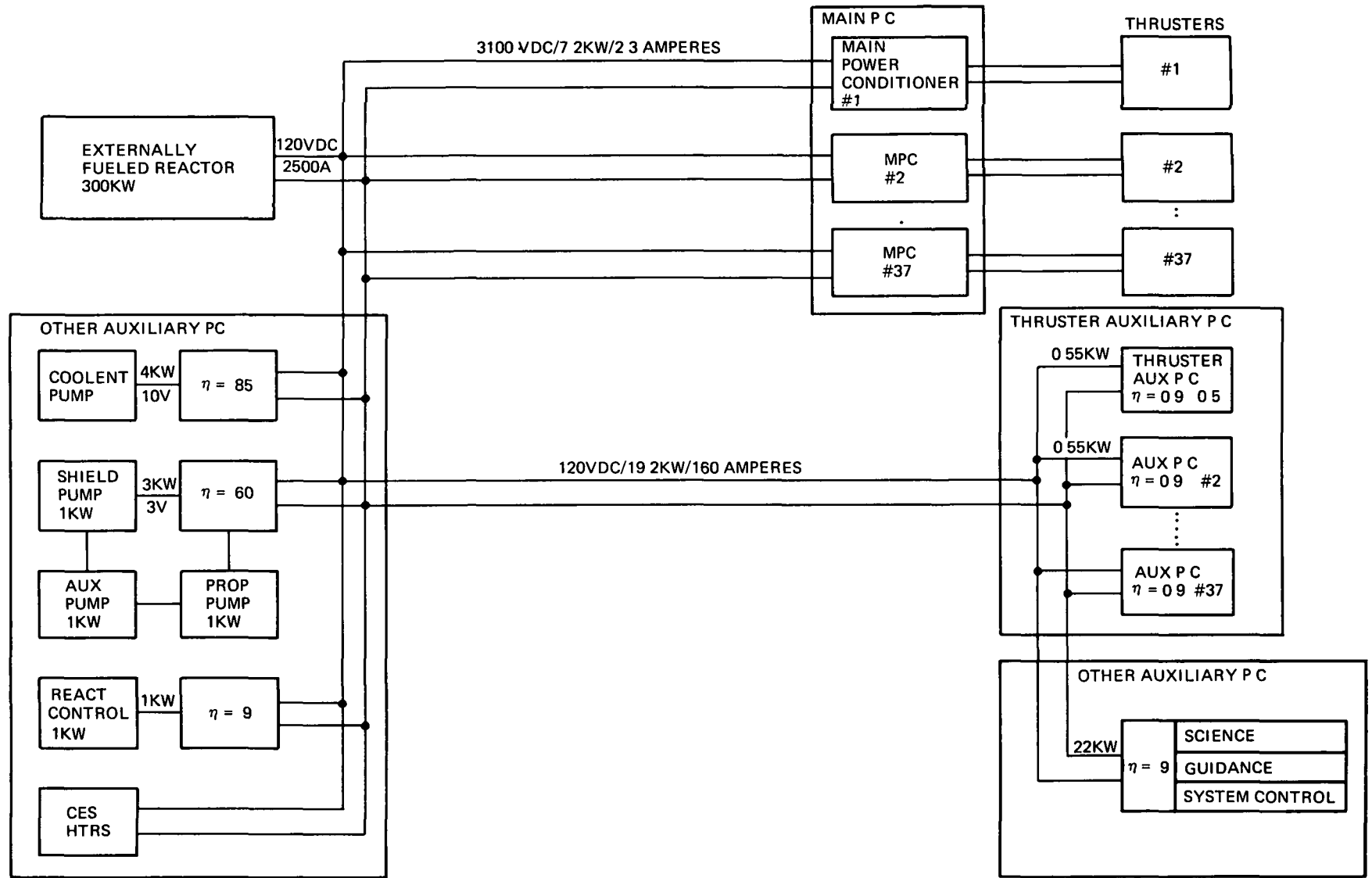


Figure 7-15. Externally Fueled Reactor Electrical Power System

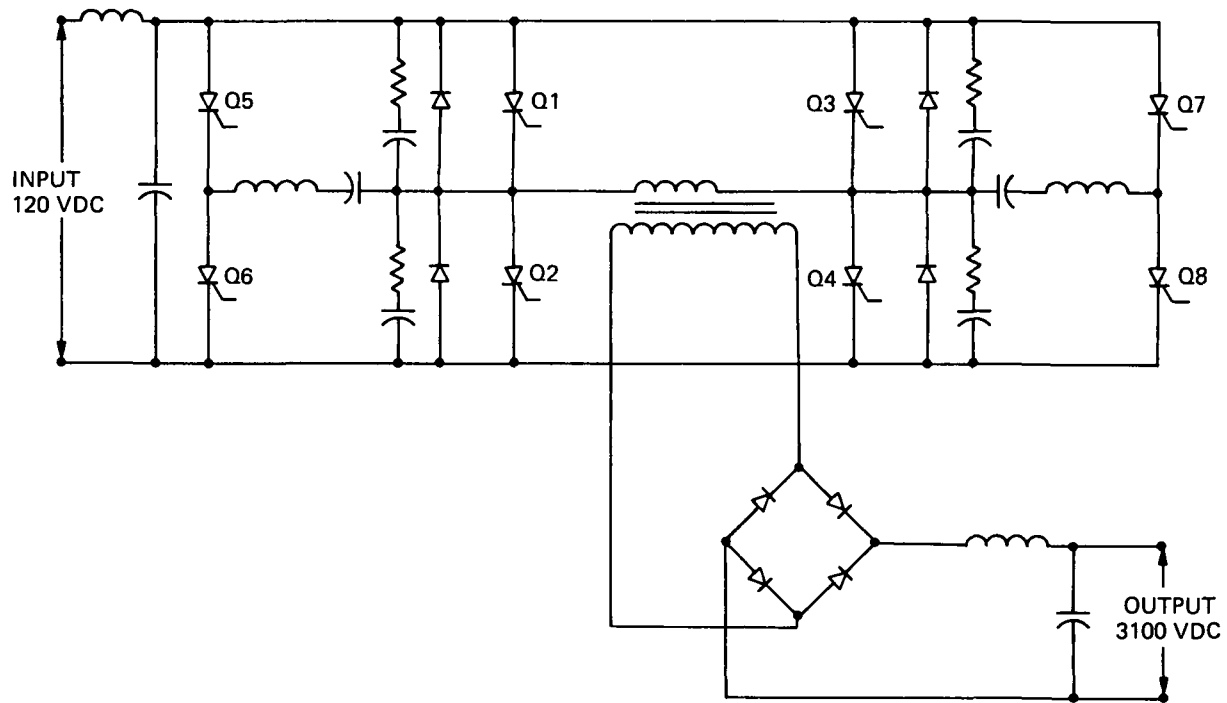


Figure 7-16. Main Power Conditioner Externally Fueled Thermionic Reactor System

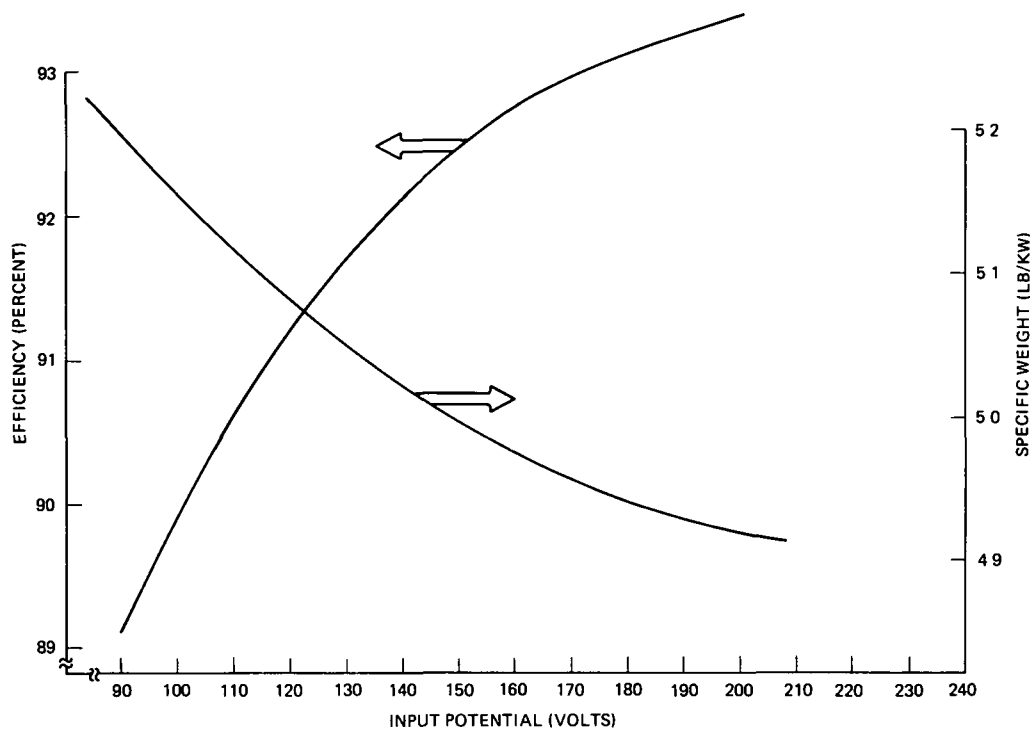


Figure 7-17. Parametric Characteristics Main Power Conditioner Externally Fueled Reactor

power conditioners is 120 volts dc. Allowing for an input voltage to vary over a range due to other than normal reactor operation, the power conditioners are designed to perform with an input voltage of 90 to 130 volts, direct current.

A power conditioner circuit is required which is capable of converting 7.2 kW from the nominal 120 volts input potential to the 3100 volts required by the ion thrusters. This would result in switching 60 amperes in each main power conditioner. Numerous circuits could be used, but considering normal transistor V_{CE} limitations, and silicon controlled rectifier (SCR) commutation problems, the driven bridge circuit appears as the logical preference.

Included in the power conditioners is the capability to current limit the output and to shut down completely for arc extinguishing. During the 10 percent operation phase, which is during coast without engine thrust, the power conditioners will be disabled.

Electrical characteristics for the design of the main power conditioners to be used with the EFR system are as follows:

Input Voltage:	90 to 130 Vdc, 120 Vdc Nominal
Input Current:	60 amperes
Output Voltage:	3100 Vdc, 1% regulation
Current Limited:	125% overload

7.2.2.2 Inverter Design

The basic inversion function for the EFTR main power conditioner was selected to be performed by a bridge circuit, using SCR impulse commutation.

Inverter circuits are typically arranged in either a parallel (push-pull) or bridge configuration with transistors or Silicon Controlled Rectifiers (SCR) switching elements. A bridge circuit has an advantage of operation up to twice the input voltage level limit of a parallel circuit due to the inherent auto-transformer action of the parallel circuit upon the switching device. With a 120 volt input potential, the effect upon transistors in a parallel circuit is to exceed the V_{CE} level of most high current devices. SCR's used in a parallel circuit have commutation difficulty in the presence of pulse width modulation and variable load. Consequently the bridge circuit was selected.

7.2.2.2.1 Switching Device Selection — The two leading switching elements for consideration are the transistor and Silicon Controlled Rectifier (SCR). In arriving at the decision as to the type of device to be used, the characteristics of the device must be compared with the requirements of the power conditioner.

SCR have been used primarily to switch high currents at high voltage. The ability to perform in this manner without series-parallel schemes is the primary advantage relative to the power transistor. With a system requirement to switch 60 amperes at a potential of 120 volts, SCR were selected for use in the bridge circuit.

It should be emphasized that parallel operation of transistors is not necessarily objectionable, but is performed where dictated by system characteristics. (i.e.: in the flashlight reactor system with a low input voltage but high switching current).

Selected switching device was a General Electric type C185 silicon controlled rectifier with a repetitive peak off-state voltage capability of up to 600 volts, and a current capacity of 235 amperes rms. Parallel RC snubber circuit for di/dt control requires a 20 ohm resistor in series with 0.02 microfarad capacitor.

Switching speed of the SCR dictated an operating frequency of 2kHz.

A bridge transistor inverter circuit also appears acceptable and should be analyzed for comparison to the SCR circuit. With the high switching currents, however, using the SCR circuit avoids the necessity of paralleling transistors and performing load division (Reference 17).

7.2.2.2.2 Inverter Circuit Design — Efficient inverter circuits using SCR's can only be achieved by selecting the proper method of commutating — the means of transferring from one SCR to another. Design was based upon an SCR bridge circuit developed by W. McMurray, RDC, General Electric Company whereby the commutating impulse is initiated by gating auxiliary controlled rectifiers. The inductance-capacitance pulse circuit is separate from the main power circuit except during commutation. Consequently, efficiency and reliability are increased and weight and size are decreased since the components do not carry load power.

Operation of the inverter is best illustrated by the circuit in Figure 7-15. The main control SCR's, Q1/Q4 and Q3/Q2 conduct the load current on alternate half-cycles. SCR's Q5/Q8 and Q7/Q6 are the auxiliary impulse commutating SCR's.

Assume that C1 and C2 are charged positive at terminals B and D respectively, and that SCR's Q1 and Q4 are conducting. Then to commutate Q1/Q4, the auxiliary SCR's Q5/Q8 are fired. The discharge pulse through the auxiliary SCR's and their associated C and L builds up to exceed the load current through the conducting SCR's. This stops the current flowing through the conducting SCR's, and the excess current flows through

the feedback diodes, D1 and D2. The forward drop of the feedback diodes appears as reverse voltage across the conducting SCR's and turns them off. Capacitors C1 and C2 are then charged in the reverse direction, i. e. : positive at A and C, respectively. At no-load condition, when the impulse returns to zero after completion of a half-cycle, SCR's Q3/Q2 are gated on while auxiliary SCR's Q5/Q8 cease to conduct. The capacitors are now ready to commutate Q3/Q2 at the end of the conducting half-cycle, upon firing the auxiliary SCR's Q7/Q6.

While commutation with limited inverse voltage (one volt forward drop of the feedback diode) avoids the ill effects of a high-peak recovery current, a new difficulty arises at the end of the commutating pulse. Forward voltage is reapplied to the main SCR at a steep rate. Such a high rate of reapplied forward voltage can cause an SCR to gate on, resulting in a short circuit of the DC supply. Two methods can be used to correct the new problem. An RC snubber circuit may be connected in parallel with the main SCR or alternatively, an inductor may be inserted in series with the main SCR's. In this design, the RC snubber circuits have been used.

7.2.2.2.3 Screen Circuit Control — High voltage electrical system configured for the EFTR system is based upon using a single power conditioner for each ion-thruster. For this reason, separate screen circuit interrupters are not necessary.

Engine arc protection will be provided in the main power conditioners, by current limiting in the primary circuit depending upon input current and controlling the gating of the SCR's. Upon detecting 125 percent current overload, the SCR control circuit will switch from pulse-width modulating as a function of output voltage and switch to modulating on input current. Current will be limited for 2 seconds, and if the overload condition persists, the system will inhibit the thruster conditions to return to normal. After 0.2 seconds, the SCR is switched on again, re-establishing screen voltage and hopefully restoring full thruster operation. If the arc restrikes and the cycle repeats three times within ten seconds, the SCR gating is permanently

disconnected. This thruster is considered disabled and one of the six spare thrusters is placed into operation.

7.2.2.2.4 Commutation Circuit Design — To achieve adequate commutation, the impulse current must exceed load current for an interval which is longer than the turn-off time of the controlled rectifiers.

Assuming a turn-off time of 15 microseconds, and allowing 5 microseconds margin, the commutating circuit was designed to resonate at 16.7 kHz, $T=60$ microseconds. Load current was assumed to be a maximum of 90 amperes occurring with an input voltage of 90 volts dc. It was acknowledged that the source was to be a constant 120 volts dc, but allowing for non-optimum conditions, the converter was designed to operate to an input minimum of 90 volts. The commutating impulse resulting is as shown in Figure 7-18.

7.2.2.2.5 Input Filter Design — An input filter functions as an energy storage device, which stiffens source characteristics, and reduces ripple and switching spikes on the common input bus.

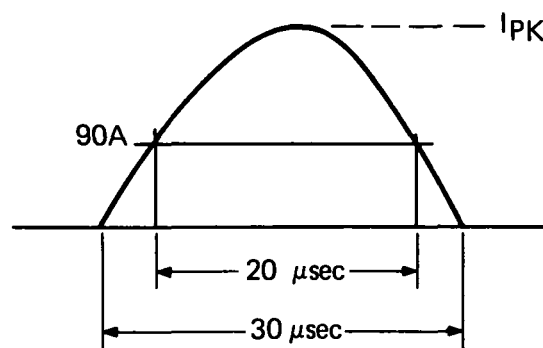


Figure 7-18. Commutating Pulse

I_{peak} was calculated to be 180 amperes

The expression for current, inductance, capacitance, and resistance is (Reference 18):

$$I_{\text{pk}} = \frac{2 E - R/2L}{(4 LC - R^2 C^2)^{1/2}}$$

Solution resulted in a commutating capacitor of 18.6 microfarads and a commutating inductor of 4.9 micronenry.

Effective current in the impulse circuit was calculated to be 13.7 amperes; consequently the auxiliary SCR was selected to be a GE Type-C35, with 35 amperes rms capability.

The switching characteristics of an impulse inverter requires an energy pulse for commutation. This energy may be dissipated in the inverter or reflected back to the power source. Should the source and transmission line impedance be small compared with the inverter, the source could receive energy as well as being a generator. Consequently, an input filter with an energy storage capacitor is required at the inverter input terminals.

A capacitor has been sized to be approximately 625 microfarads in this application, with an inductor of 0.125 millihenry.

7.2.2.2.6 Output Filter Design — The output filter is used to lower the ripple factor after the transformer output has been rectified. The filter acts as a storage device supplying power during periods when the transformer output is below the level of the output bus.

The problem was to design an LC filter which would reduce the 3100 volt, 4 kHz, rectangular wave to smooth dc with percent ripple.

Analysis has shown that for the 3100 volt system, an inductor should be at least 32 millihenry with a capacitor of at least 0.46 microfarads.

7.2.2.3 Redundancy Considerations

The electrical design for the externally fueled thermionic reactor system is based upon a single thruster being driven by one power conditioner. Thirty-seven thrusters and conditioners are on-board, which six are spares. Although this provides some power conditioning redundancy, the use of 37 ion engine-PC modules provides for ion engine isolation.

7.2.2.4 Main Converter Mechanical Design

7.2.2.4.1 Geometry — As with the power conditioners for the flashlight reactor, the components will be mounted using the baseplate as part of the radiator. Figure 7-19 shows the components configured in a minimum area design of approximately two square feet. Additional area may be required for thermal dissipation.

7.2.2.4.2 Component Size — The following components have been selected for use in the main power conditioner for the externally fueled reactor system. Weights are given in Table 7-9:

a. Input Filter

Inductor: 2.25 x 1.6 x 4.12 inches
 16 turns #6 gauge wire
 AL-19 Silectron Core
 Arnold Engineering Company

Capacitors: 6, each 1.3 x 0.75 x 2.5 inches H
 GEKSR Tantalum Foil
 100 μ f d. 100 V

b. Main SCR's, 4: 3.25 x 1.4 inches diameter
 GE type C185
 600 V, 235 Arms

c. Transformer: 8KLDe, 2kHz
 7.35 x 4 x 7 inches H

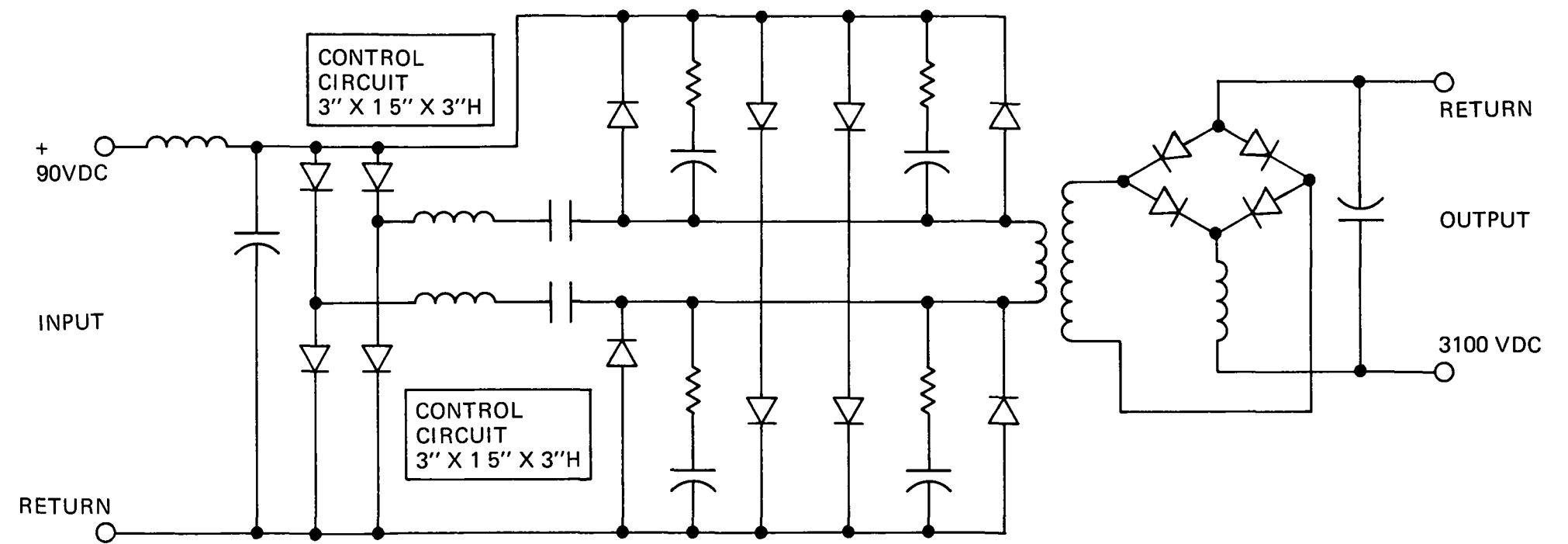


Figure 7-19. Component Geometry,
Externally Fueled Reactor
Main Power Conditioner

- d. Feedback Diodes, 4: 1.5 x 0.75 inches diameter
GE type IN248
14 ampere
- e. RC Snubber
- Capacitor, 4: 0.75 x 0.25 inches diameter
 GE type 151EC, 61F19BA223
 Lectrofilm-B Tubular
 0.02 f, 180 V
- Resistor, 4: 1.4 x 0.5 inches diameter

 20 ohm, 10 watt
- f. Commutating Circuit
- Inductor, 2: 0.6 x 1 inch diameter
 Magnetics Inc.
 125 Permeability
 Powdered Permalloy
 10 turns, #13 gauge, bifiler
- Capacitor, 2: 2.7 x 1.6 x 4.5 inches H
 GE Type 160EC SCR Commutating Capacitor
 200 PKV, 20 μ fd.
- g. Auxiliary SCR's, 4: 1.3 x 0.5 inches diameter
GE Type C35
35 Ampere, rms
- h. Output Filter
- Inductor: 1.5 x 2.3 inches diameter.
 Magnetics Inc. 55086
 Powder Permalloy
 333 turns, #16 gauge wire
 32 mh

8. SPACECRAFT DESIGN DEFINITION

8. SPACECRAFT DESIGN DEFINITION

This section of the report describes the reference designs for the externally fueled reactor spacecraft and the flashlight reactor spacecraft shown in layout in Figures 1-1 and 1-5, respectively. Each reference design has a net propulsion power of 240 kWe with a reactor output power of 274 kWe for the externally fueled reactor and a reactor output power of 318 kWe for the flashlight reactor. As an introduction to the description of each reference design, a computer code optimization of a 300 kWe reactor output design is presented. These 300 kWe designs were the starting points for each reference design.

8.1 EXTERNALLY FUELED POWERPLANT/SPACECRAFT

A 300 kWe externally fueled reactor powered spacecraft was designed and optimized with a computer code analysis. The design is based on the following assumptions regarding configuration and conditions:

- a. A reactor coolant outlet temperature of 1350° F
- b. A single heat rejection loop between reactor and main radiator
- c. A radiator arrangement with the main radiator directly behind the shield and the power conditioning radiator at the rear of the spacecraft
- d. Aluminum as the electric cable material.

The characteristics of the 300 kWe system are tabulated in Table 8-1. The total system weight listed on the first line of the table is the total spacecraft weight less the propellant subsystem weight. The total system weight is divided by the net propulsion power to obtain the system specific weight which is the parameter minimized by the optimization procedure in the computer code.

The current and voltage conditions of the reactor and the distribution of the reactor power are detailed under the heading Electric System Conditions. The subsystems and their weight characteristics are listed, followed by the usage of the spacecraft

surface area and a set of pertinent vehicle and component dimensions. Performance and dimensional characteristics of each of the active heat rejection loops are tabulated, followed by similar listing of conditions in the electrical cabling and power conditioning modules.

The characteristics of the 300 kWe design along with a similar set of characteristics for a 274 kWe reactor output design were used as the basis of the reference design for the externally fueled reactor powerplant and spacecraft. Tables 8-2 and 8-3 summarize the weight and electric power distribution results obtained for the reference design. The total spacecraft launch weight is 31,495 pounds with an in-orbit weight of 30,420 pounds. The booster adapter and launch fairing, totaling a payload penalty of 1075 pounds, is jettisoned during the launch trajectory.

Three major subsystems comprise the mission spacecraft:

- a. A propulsion subsystem weighing 13210 pounds.
- b. A propellant subsystem weighing 14975 pounds.
- c. A payload section weighing 2235 pounds.

The last two named subsystems are essentially defined by the customer and are relatively constant in weight. Only the propellant tankage and related support structure will vary with spacecraft design. The propulsion subsystem, however, can vary significantly with system and component configuration and operating conditions. It is this propulsion subsystem which requires the majority of the design effort.

The propulsion subsystem is made up of a number of smaller subsystem, some of which - those associated with the generation of power - are designated as the power plant group, with others, which relate to the conversion of the power to propulsion, are designated as the thruster group. The weights of these individual subsystems and subsystem groups are detailed in Table 8-2.

TABLE 8-1. CHARACTERISTICS OF A 300 kWe EXTERNALLY FUELED REACTOR POWER-PLANT/SPACECRAFT

Total system weight*, lbs.		16386.
Net propulsion power, kWe		262.71
System specific weight, lbs/kWe		62.37
<u>Electric System Conditions</u>		
Reactor output voltage, volts		121.02
Reactor output current, amps		2479
Reactor output power, kWe		300
Low Voltage cable losses, kWe	6.831	
Hotel PC power input, kWe	4.8458	
Hotel PC power output, kWe	4.1189	
Payload power, kWe	2.0	
Thruster PC power, kWe	18.78	
Main PC power input, kWe		267.543
Main PC power output, kWe		244.13
High Voltage cable loss, kWe	0.2	
Net propulsion power, kWe		262.71
<u>Subsystem Weights, lbs.</u>		
<u>Reactor-Radiator</u>		6079
Reactor	3922	
Main Radiator	1671	
Piping	486	
<u>Shield</u>		894
Shield	835	
Radiator	36	
Piping	23	
<u>Auxiliary Cooling</u>		111
Radiator	37	
Piping	74	
<u>Power Conditioning</u>		2462
Main PC modules	1479	
Hotel PC modules	33	
Radiator	950	
<u>Cables</u>		203
Low voltage cable	202	
High voltage cable	1	
<u>Payload</u>		2200
Radiator	71	
System Controls	71	
Payload Equipment	2058	
<u>Thruster</u>		1618
Thrusters	1233	
PC Modules	298	
Radiator	87	
<u>Structure</u>		2818
Spacecraft structure	1955	
Shroud penalty	863	
<u>Spacecraft Surface Areas, ft²</u>		
Main Radiator		691
P. C. Radiator		548
Auxiliary Radiator		16
Shield Radiator		1
Low Voltage Cable		80
High Voltage Cable		1
Payload Radiator		41
Thruster PC Radiator		50
Gaps between radiators		15
<u>System Dimensional Characteristics</u>		
Vehicle length, ft.		66.01
Vehicle diameter, ft.		9.2
Shield half angle, degrees		5.89
Reactor diameter, ft.		2.75
Reactor length, ft.		1.68
Shield thickness, ft.		1.31
<u>Reactor-Radiator Loop Conditions</u>		
Pipe diameter, inches		3.28
Coolant flow rate, lbs/hr		95523
Coolant temperature rise, °F		305
Coolant heat rejection, BTU/hr		6.18 x 10 ⁶
Loop pressure drop, psi		4.293
Loop pumping power, kWe		3.411
Maximum loop temperature, °F		1350
<u>Shield Loop Conditions</u>		
Pipe diameter, inches		1.0
Coolant flow rate, lbs/hr		222
Coolant temperature rise, °F		100
Coolant heat rejection, BTU/hr		4718
Loop pressure drop, psi		1.97
Loop pumping power, kWe		.0034
Maximum loop temperature, °F		950
<u>Auxiliary Loop Conditions</u>		
Pipe diameter, inches		0.6
Coolant flow rate, lbs./hr		249
Coolant temperature rise, °F		100
Coolant heat rejection, BTU/hr		5359
Loop pressure drop, psi		2.21
Loop pumping power, kWe		.0041
Maximum loop temperature, °F		800
<u>Power Conditioning Subsystem</u>		
P. C. module efficiency		0.9125
Maximum operating temperature, °F		200
Total heat rejection, BTU/hr		82387
Radiator fin thickness, inches		0.123
<u>Cable Conditions</u>		
LV Cable length, ft.		46.19
LV Cable cross section area, ft ²		.0257
Maximum temperature, °F		700
Total heat rejection, BTU/hr		22028
Reactor lead cross section area, ft ²		.0067

*This is the spacecraft weight less the propellant weight

TABLE 8-2. WEIGHT SUMMARY 240 kWe (NET) THERMIONIC SPACECRAFT
(EXTERNALLY FUELED REACTOR)

Component	Weight-Pounds				
Propulsion System					13,210
Power Plant Subsystem				9045	
Reactor Subsystem			4380		
Reactor (Dry)		4150			
Actuator		230			
Primary Heat Rejection			2550		
Ducts		250			
EM Pumps (2)		100			
Accumulators		140			
Main Radiator		1335			
Coolant		650			
Insulation		75			
Shield			950		
Neutron		765			
Permanent Gamma		185			
Electric and Controls			155		
Hotel Load		105			
Power Conditioning	45				
Radiator	20				
Distribution Cables	40				
Power Plant, Control		50			
Auxiliary Coolant Loop			100		
Ducts		35			
EM Pumps (2)		20			
Accumulators		10			
Radiators		10			
Coolant		25			
Structure			860		
Reactor Support		40			
Neutron Shield (external)		70			
Power Conditioning Radiator		360			
Area Blocked by LV Cables	65				
Mating/Stiffening Rings	85				
Longerons	210				
Transition Ring		55			
Main Radiator		335			
Mating/Stiffening Rings	170				
Longerons	165				
Miscellaneous			50		
Thruster Subsystem				4165	
Ion Engine Subsystems			1235		
Ion Engine Units		585			
TVC Unit		550			
Miscellaneous		100			
Power Conditioning Electronics			1660		
HV Power Supply		1390			
Special Ion Engine PC		270			
Power Conditioning Radiators			830		
HV Power Supply		745			
Special Ion Engine PC		85			
High Voltage Power Cables			15		
3100 Volt Cables		10			
Insulation		5			
Low Voltage Power Cables			385		
Main Bus		195			
Payload and Thruster Bus		30			
Electrical Insulation		80			
Thermal Insulation		80			
Structure			40		
Special PC Bay		40			
Propellant System					14,975
Propellant				14,500	
Tanks and Distribution				460	
Structure				15	
Net Spacecraft					2235
Guidance and Control				50	
Communications				60	
Science				2065	
Radiator				25	
Structure				35	
Gross spacecraft in Earth Orbit					30,420
Launch Vehicle Adapter					250
Launch Shroud Payload Weight Penalty					825
Launch Vehicle Payload Requirement					31,495

TABLE 8-3. ELECTRIC POWER SUMMARY 240 kWe (NET)
THERMIONIC SPACECRAFT (EXTERNALLY FUELED REACTOR)

Component	Power	kWe	
Reactor Output			274
Low Voltage cable loss		5.87	
Hotel load section		4.031	
Cable losses	.055		
PC losses	.5246		
Reactor pump input	2.745		
Auxiliary pump input	.0064		
Reactor controls input	.20		
Cesium heater input	.50		
Payload and Thruster section		19.1	
Cable losses	0.1		
Special Ion Engine PC input	17.0		
Payload input	1.0		
Spacecraft control input	0.5		
Powerplant control	0.5		
High Voltage PC Input		245	
PC losses	22.5		
Cable losses	0.5		
Thruster Engine Input	223		
Net Power to Thruster*			240
*The net power is the sum of the ion engine grid power input, after power conditioning, and the other special ion engine power.			

The externally fueled reactor reference design has a reactor output power of 274 kWe.

This power is distributed as follows:

- a. 5.87 kWe is dissipated as I^2R losses in the low voltage cable
- b. 4.031 kWe is used by power plant hotel requirements
- c. 19.1 kWe is utilized for the payload and thruster power conditioners
- d. 245 kWe is converted into 223 kWe of 3100 volt power for the ion engines high voltage supply.

The total net power of 240 kWe is the sum of the ion engine input and the thruster PC input power. Details of the powerplant hotel load and the payload plus thruster PC section load are given in Table 8-3.

A layout drawing of the reference externally fueled reactor spacecraft is given in Figure 1-1. The vehicle is a long cylinder with the forward one-third section conical in configuration. The overall length is 62.7 feet with the conical section 29.3 feet long and the diameter is 9.2 feet. The conical section has a shield half angle of 6.6 degrees.

The reactor end of the vehicle, is designated the forward end since the spacecraft is propelled in that direction on a line coincident with the longitudinal axis of the vehicle by the ion engine thrusters at the rear end. The reactor is so located to provide maximum separation from the payload in the rear section of the vehicle and to assure minimum volume and weight for the shadow shield. The shield is formed in two sections; a solid block of neutron shielding directly behind the reactor, followed by a tank of mercury propellant which functions as the gamma shield.

The main heat rejection radiator, which dissipates the waste thermal energy generated by the reactor, forms the conical section of the spacecraft behind the shield with an additional bay extending down the cylindrical section. A single piping loop transports the NaK reactor coolant around the shield to the main radiator feed line network. The coolant activation analysis discussed in Section 5 indicates that use of a single primary coolant loop in the externally fueled reactor powered spacecraft does not violate the integrated gamma dose limit of 10^7 rads.

A very short section of auxiliary radiator separates the main radiator from the power conditioning radiator, which occupies most of the cylindrical section of the vehicle. The PC radiator is actually eight-sided in cross section, rather than cylindrical, and separated axially into two halves by two narrow strips along which the low voltage cables are strung. The low voltage cables attach to the reactor leads at the rear of

the reactor, then run longitudinally along the surface of the shield and main radiator to the PC radiator distribution area. At 5 axial locations on the PC radiator, low voltage cables are strung circumferentially to 38 individual power conditioning modules spotted uniformly on the flat panel sides of the PC radiator.

The rear 4.8 feet of the spacecraft contain the payload and thruster subsystems. Communication antennas which extend radially for operation are shown in the stowed position behind the thrusters for launch.

Detailed descriptions of the spacecraft subsystems are presented in the following paragraphs. The descriptions will follow the subsystem definitions presented in Table 8-2 rather than the arbitrary definitions utilized in Table 8-1 for the computer code results.

The propulsion system, as defined implicitly in Table 8-2, is the major system of interest in this report. It consists of two subsystem groups, the powerplant subsystem group and the thruster subsystem group. To simplify the numerical designations of the paragraph headings and subheadings in this report section, the two subsystem groups mentioned above will be given equal importance in numerical designation with the spacecraft propellant system and payload system.

8.1.1 POWERPLANT SUBSYSTEM GROUP

The Powerplant Subsystem Group consists of the reactor subsystem, the shield, the primary and auxiliary heat rejection subsystems, the electrical and control subsystem and powerplant structure.

Figure 8-1 is a schematic representation of the externally-fueled thermionic reactor.

IN-CORE THERMIONIC FUEL ELEMENT EXTERNALLY-FUELED CORE-LENGTH CELL

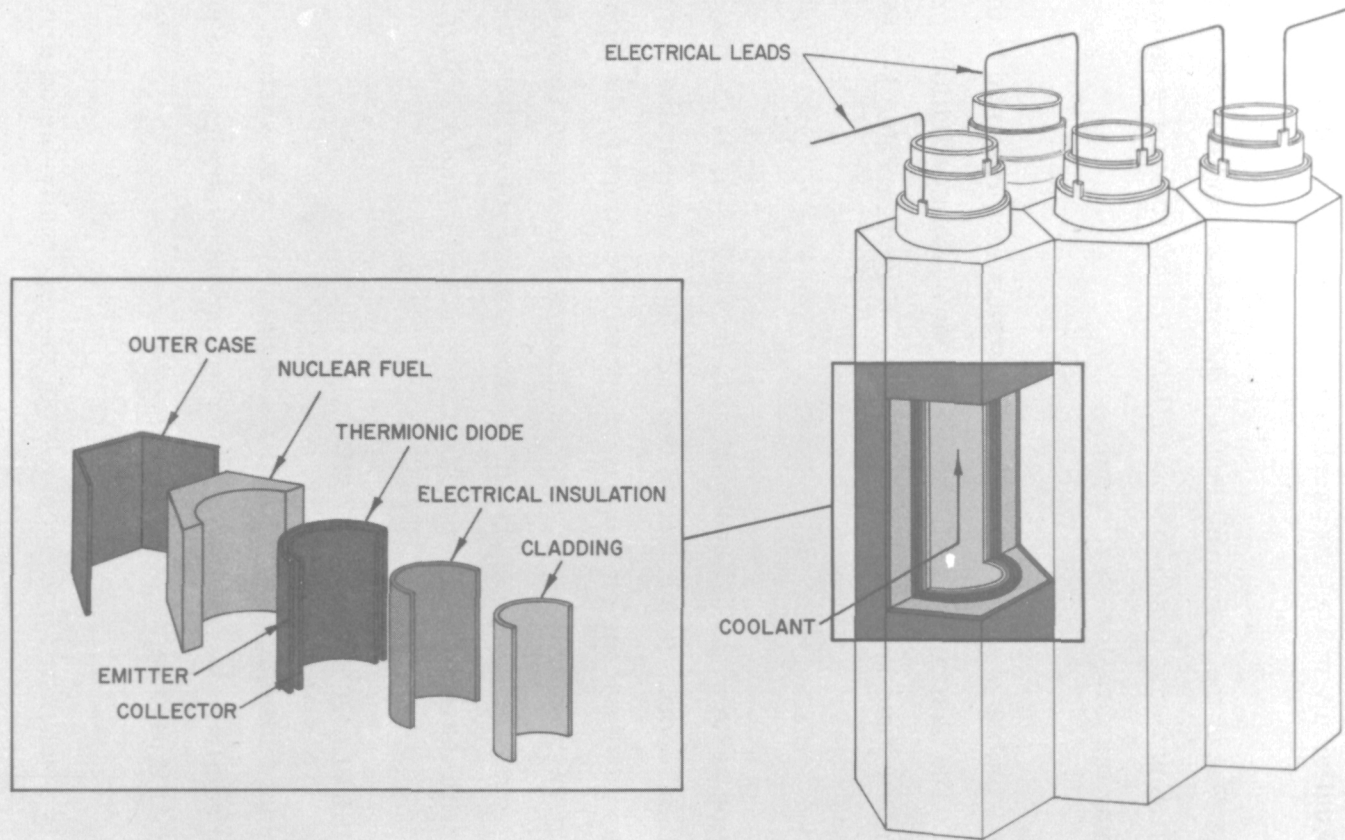


Figure 8-1. Externally Fueled Reactor Schematic

The 274 kWe externally-fueled reactor is 2.75 feet in diameter and 1.68 feet long. In the dry condition, it weighs 4150 pounds and holds 75 pounds of NaK when filled for operation. Twelve SNAP-8 type control actuators are mounted on the front face of the reactor to drive the control drums in the radial reflector. The control actuators are modified with the output drive eccentric to the motor shafts. This allows grouping the actuators closer to the axial centerline of the reactor thus reducing the radial diameter of the shadow shield. The actuators are radiatively cooled and unprotected from the reactor nuclear radiation. The weight of the twelve actuators is 230 pounds.

8.1.1.1 Shield Subsystem

From the viewpoint of weight addition to the power plant subsystem group, the shield subsystem consists of a canned block of lithium hydride and, plugs of tungsten metal which shield the holes across the outer circumference of the propellant tank caused by the passage of the reactor loop piping. The lithium hydride block performs most of the required neutron shielding with additional neutron attenuation occurring in the conically shaped mercury propellant tank placed directly behind the neutron shield. The primary reason for this mercury tank location is that it permits the mercury propellant to act as the primary gamma shield for the radiation sensitive components of the spacecraft. (See Section 6 for the details of this shield concept.)

The neutron shield component is an internally supported can filled with lithium hydride. The can is 16 inches thick and has an average diameter of 41.8 inches. It weighs 765 pounds of which 575 pounds is lithium hydride.

The total heating rate in the shield subsystem is estimated to be 1.27 kW, with almost all of this heat being deposited in the frontal region of the neutron shield. Cooling is achieved by a serpentine coil of pipe carrying the auxiliary cooling system coolant (see Paragraph 8.1.1.5).

Using the Data and computational methods of Section 6, the integrated gamma dose in the power conditioning module closest to the reactor is estimated at 1.0×10^7 rads. The corresponding total neutron dose is 1.0×10^{12} nvt. Further shield analysis is required, as these data were estimated from the shield analysis performed by ORNL for the Flashlight Reactor.

8.1.1.2 Primary Heat Rejection Subsystem

The primary heat rejection subsystem is composed of the main radiator and the piping network which pumps and transports the reactor coolant to the radiator. The radiator consists of four approximately-equal length bays, three of which form the conical surface of the spacecraft while the fourth occupies the forward section of the cylindrical spacecraft area. Each of the bays is divided into three panels, each of which cover a 120° section of the bay.

Figure 8-2 illustrates a typical offset radiator tube-fin unit of the radiator. As shown, the unit is 1.635 inches wide and has a coolant tube diameter of 0.18 inches and a thickness of 0.03 inches for the composite copper-stainless steel fin. The primary meteoroid armor protection is 0.089 inches thick and 0.021 inches of bumpered armor protection surround each coolant channel.

The weight of the twelve radiator panels, which total 661 square feet in area, and the associated headers is 1335 pounds when dry. The header description is included in the discussion of the feed line network portion of the loop piping.

The main heat rejection piping is made up of the reactor header configuration, the radiator feed line network and the intermediate piping. The coolant inlet plenum is at the forward end of the reactor and the exit plenum at the rear end. Header arrangements distribute and collect the coolant to each plenum. The inlet header is a circular torus of rectangular cross section, located at the rear and outside the outer diameter of the reactor, see Figure 8-3. Eight ducts, trapezoidal in configuration, carry the coolant from the header in a forward direction outside the diameter of the reactor to the inlet plenum. This torus-trapezoidal duct arrangement comprises the inlet header component.

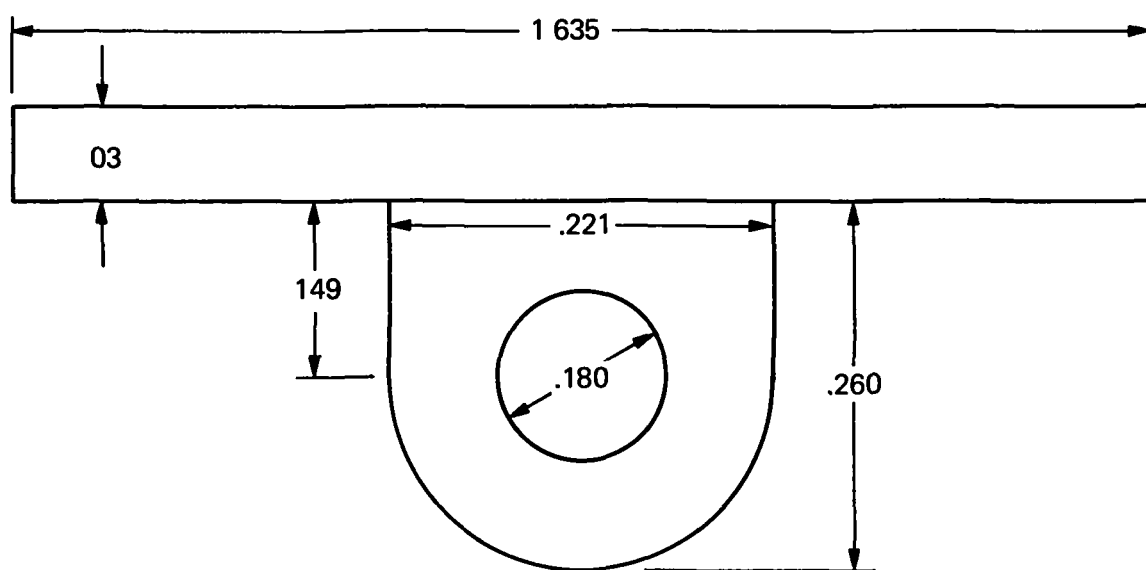


Figure 8-2. Cross Section of Main Radiator Tube-Fin Arrangement

The coolant outlet header consists of a second toroidal duct connected to the outlet plenum by eight spoke-like pipes of two inches in diameter. The outlet header toroid is smaller in overall than the inlet header toroid and is located between the reactor and shield. Both inlet and outlet header arrangements are constructed of 0.10 inch thick stainless steel and weigh a total of 95 pounds.

Two rectangular shaped ducts, 2 by 5 inches in cross section, transport the reactor coolant across the shield surface in a curving path. The rectangular configuration is utilized to minimize the depth of the channel made in the shield and to lessen the radiation dosage penetrating the resultant shield voids. These ducts connect to the feed line network which distributes the coolant to the twelve radiator panels. Figure 8-4 shows the details of this network. Five rings of headers distribute the coolant to the twelve radiator panels. Each header ring is separated into three sections corresponding to the three panels per radiator bay. The second and fourth ring of headers

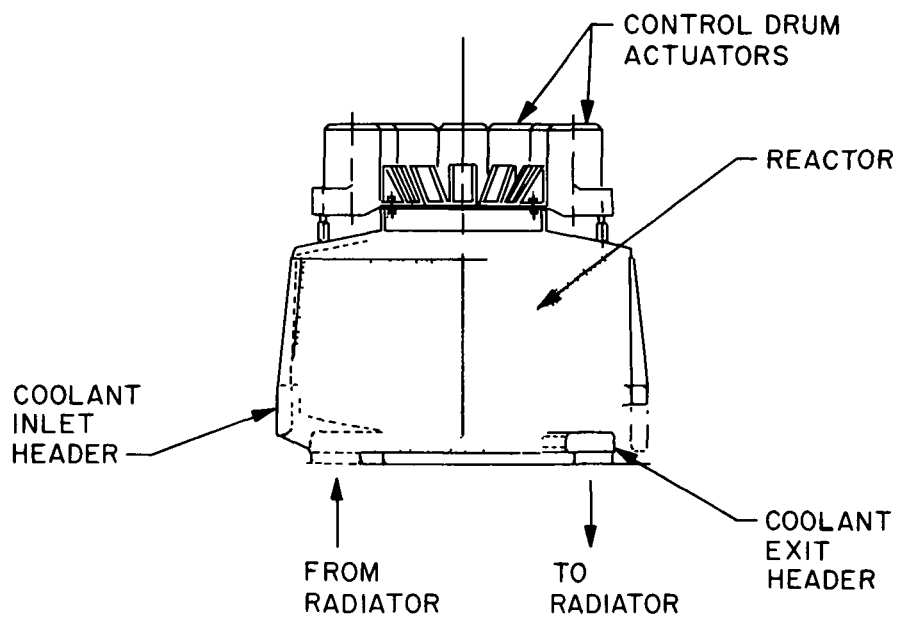


Figure 8-3. Coolant Header Arrangement For Externally-Fueled Reactor

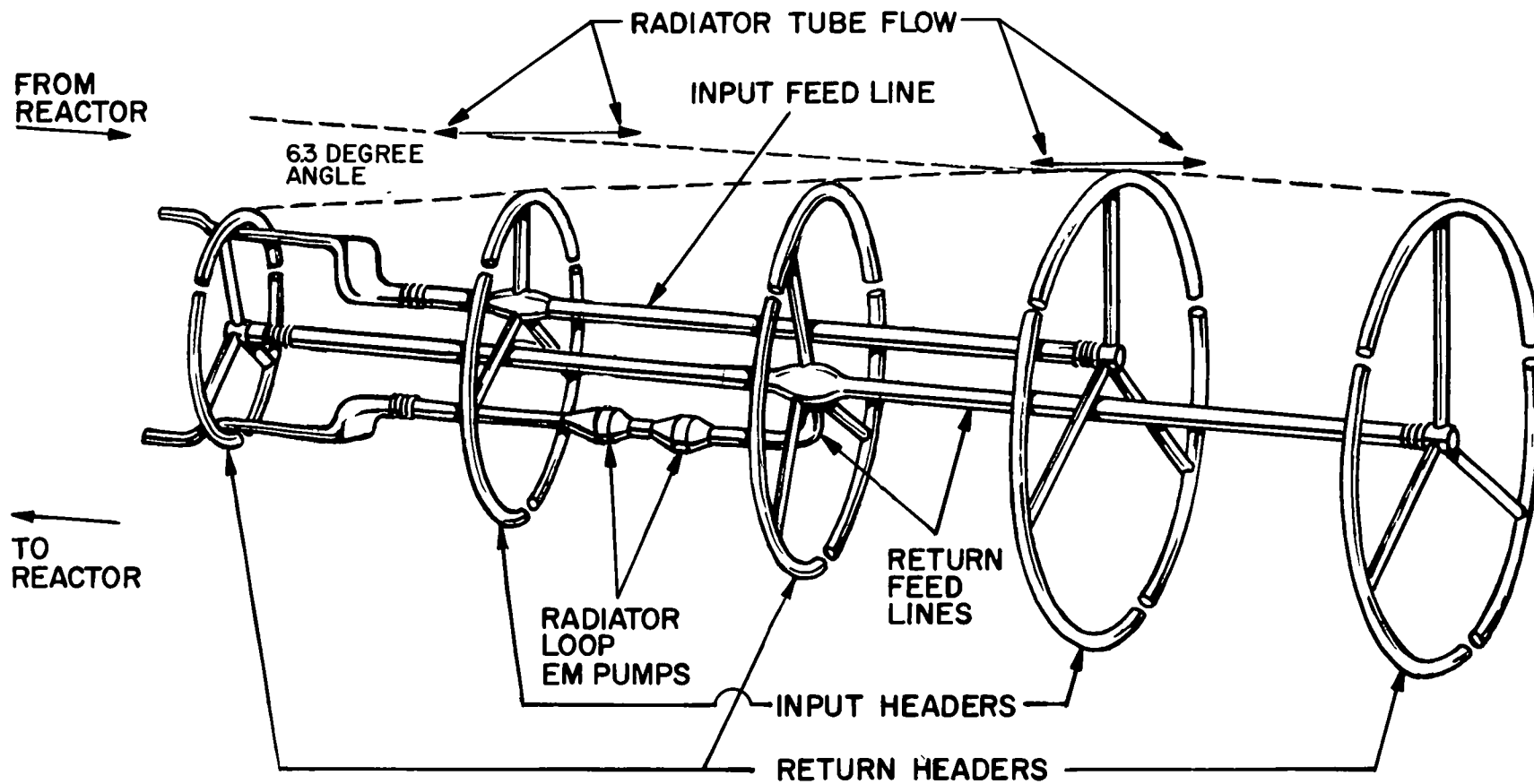


Figure 8-4. Main Radiator Feed Line Network

dispense the incoming coolant with the second header ring feeding the first two bays and the fourth ring feeding the last two bays. The middle header ring collects the coolant from the two central bays while the two end header rings collect the coolant from the respective end bays. The weights of these headers are included in the radiator weight.

The radiator feed line network consists of the axially directed input and return feed lines plus the radial, spoke-like feeders running to each header. These latter header feeders are 1.2 inches in diameter, while the input feed line has a 2.8 inch diameter and the return feed line is 1.43 inches in diameter. The piping to and from the heat exchanger up to the junction with the feed lines is the equivalent of 3.63 inches in diameter.

Two S-shaped duct segments of 13 by 0.8 inch flat rectangular cross section are located in the radiator loop piping, as shown on Figure 8-4. These duct segments bend to accommodate the relative expansion of the piping located between the reactor and the radiator, and the radiator itself. Additional bellows in the input and return feed lines take up expansion motion between the individual bays of the main radiator.

The total weight of the radiator feed line network plus the connecting piping to the reactor is 198 pounds when 0.06 inch thick stainless steel duct material is used. The total ducting weight for the heat rejection system is 295 pounds.

As shown in Figure 8-4, two EM pumps are installed in the main heat rejection pipe loop. Only one of the pumps is in operation at any one time with the second pump being in standby condition. Each pump is a dc conduction pump, similar in concept and configuration to the one shown in Figure 8-5. The coolant duct is divided into ten parallel channels which are arranged in circular fashion as shown on the figure. The parallel coolant ducts are flattened into a very thin rectangular configuration and each

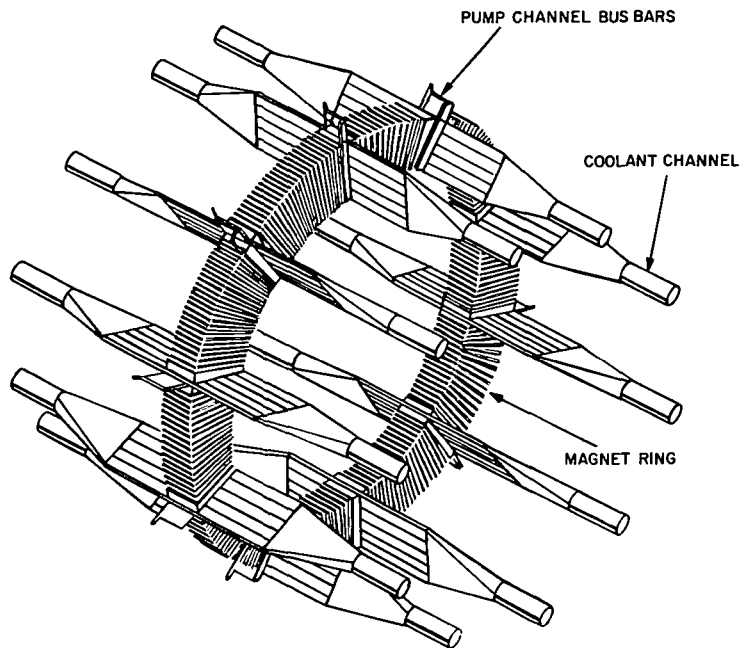


Figure 8-5. Schematic Diagram of a DC Powered EM Pump

of these duct sections traverse the magnetic field of a magnet ring. A coil of heavy wire wrapped around a magnet ring and carrying a DC current produces the magnetic field. This same current is passed through the wide dimension of each flattened section of coolant duct and in so doing passes through the coolant itself. The interaction of the magnetic and electrical fields produces a pumping force on the coolant in the same way similar interactions produce a torque on the rotor of a dc motor. Each duct section thus becomes an individual pump using a common magnetic field and the same electrical current.

The EM pumps for the reactor loop use ten parallel duct segments, with each segment in the pumping region being 0.125 by 3.83 inches in cross section and 1.2 inches long in the direction of coolant flow. The 1.2 inch thick iron magnet ring has inner and outer diameters of 3.35 and 7.15 inches, respectively. Copper leads approximately

0.033 square inches in area from the energizing coil for the magnet. The total weight of each EM pump including transition ducts and insulation is 50 pounds.

The electrical power requirements for the pump is 2.8 kW supplied at approximately 10 volts and 280 amperes.

The pressure level and coolant expansion in the heat rejection loops are accommodated by three accumulator components. Two of the accumulators are dynamic or working units operating continuously on the coolant flow. The third unit is essentially a static storage tank which accommodates most of the coolant volume expansion. The working accumulators are cylindrical in shape, 12 inches in diameter and 14.4 inches long, and contain two cylindrical metallic bellows, each capped on one end and joined together at their open ends. Coolant is contained inside the bellows volume while a pressurizing gas fills the space between the accumulator shell and the metal bellows. A pressure is imposed on the fluid by the movement of the bellows reacting to the pressure of the enclosed gas. The bellows weight, as a fraction of the total accumulator weight, increases with size, so two units are utilized, rather than one larger unit. The weight of each dynamic accumulator is 43 pounds.

The static accumulator is a spherical tank, approximately 20 inches in diameter, having a shutoff valve in the coolant input line. With a 0.06 inch wall thickness, the tank and valve assembly weights 53 pounds. The use of the static accumulator reduces the total accumulator weight, relative to providing for coolant volume changes in one or two working accumulators.

The total inventory of NaK coolant contained in the heat rejection system is 650 pounds; 75 pounds in the reactor, 195 pounds in the main radiator panels and 490 pounds in the reactor headers, the radiator feed line network and connecting ducts, the EM pump and the accumulators.

Thermal insulation protects the shield from the hot heat rejection ducts traversing its surface, and the rear section of the vehicle from the main radiator. The latter protection includes a radiation barrier across the entire cross section of the vehicle at the back end of the main radiator, a fibrous mineral type of insulation under the auxiliary radiator and thermal conduction barriers at the front and rear mating rings of the main radiator. The combined weight of all the insulation is 76 pounds.

8.1.1.3 Electrical Subsystem

The electrical subsystem includes that portion of the spacecraft electrical network which processes and supplies the hotel power required to operate the powerplant. It also includes the electronic components which monitor and automatically control the actuator drives of the reactor, and the pumps of the various heat rejection loops in the powerplant. Figure 8-6 presents schematically the hotel power distribution circuit and some of its operating conditions. The power conditioning weight, based on the analysis shown in Section 7 for the auxiliary PC units, is calculated to be 45 pounds for the calculated hotel power requirements. The corresponding portion of the PC radiator, described later in Paragraph 8.1.2.5, is 20 pounds. The weight of cabling to the PC units, pumps, and other components, is another 20 pounds while the electronic powerplant control modules are estimated to weigh 50 pounds.

8.1.1.4 Auxiliary Coolant Loop

The auxiliary loop provides cooling for the neutron shield and the electrical and magnetic components of the main heat rejection loop EM pump. Figure 8-7 is a schematic representation of the auxiliary loop which includes a radiator, pumps, accumulators, cooling coils for the neutron shield and all connecting piping. The auxiliary loop pump pressurizes the cooled fluid exiting the radiator and forces it, in sequence, through cooling passages in the main EM pump, the cooling channels in the lithium hydride shield, and the auxiliary radiator. The pump is a DC powered single duct unit. The weight

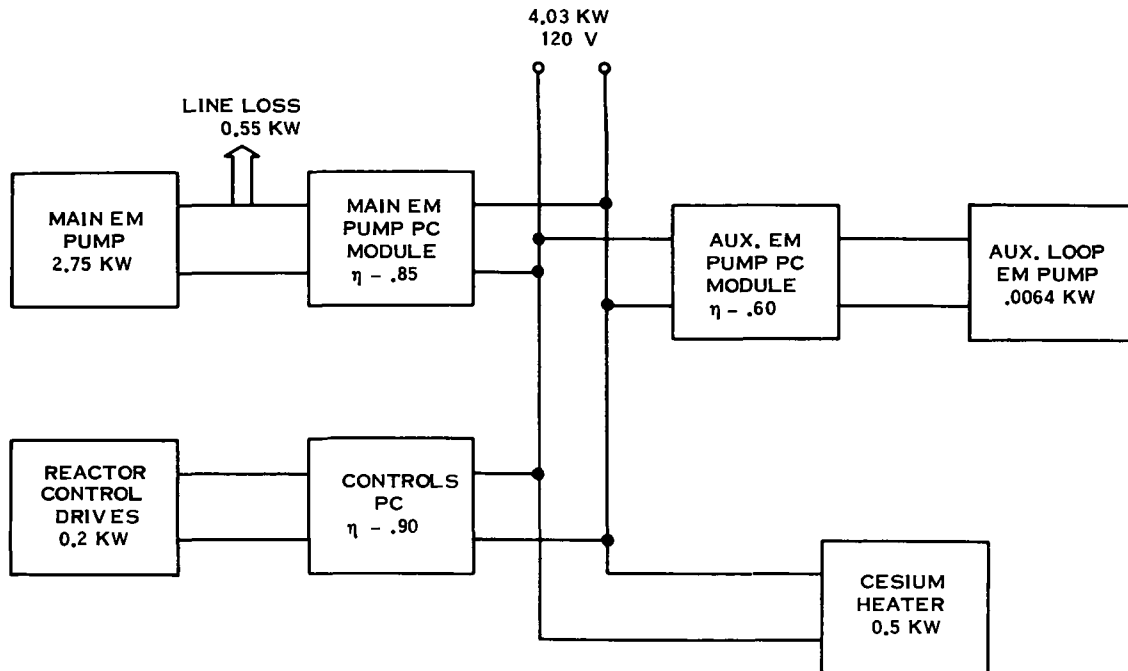


Figure 8-6. Hotel Power Distribution System for Externally Fueled Reactor Spacecraft

of both pumps, the operating and the redundant pump, is 20 pounds. The auxiliary radiator encircles the spacecraft in belt-like fashion between the main radiator and the PC radiator. It consists of a single coolant tube attached to a 2 inch wide copper-stainless steel fin and weighs 10 pounds. Accumulators of the same metal bellows type described previously but considerably smaller in size, weigh another 10 pounds. The largest weight item in the loop is the connecting piping because of some 75 feet of overall length. The piping, which is 1 inch in diameter, weighs 35 pounds and the total loop coolant inventory is another 25 pounds.

8.1.1.5 Powerplant Support Structure

The powerplant support structure includes all the spacecraft structure required except that needed for the propellant tanks, the payload and the thrusters. It includes:

- a. Reactor support
- b. Shield support

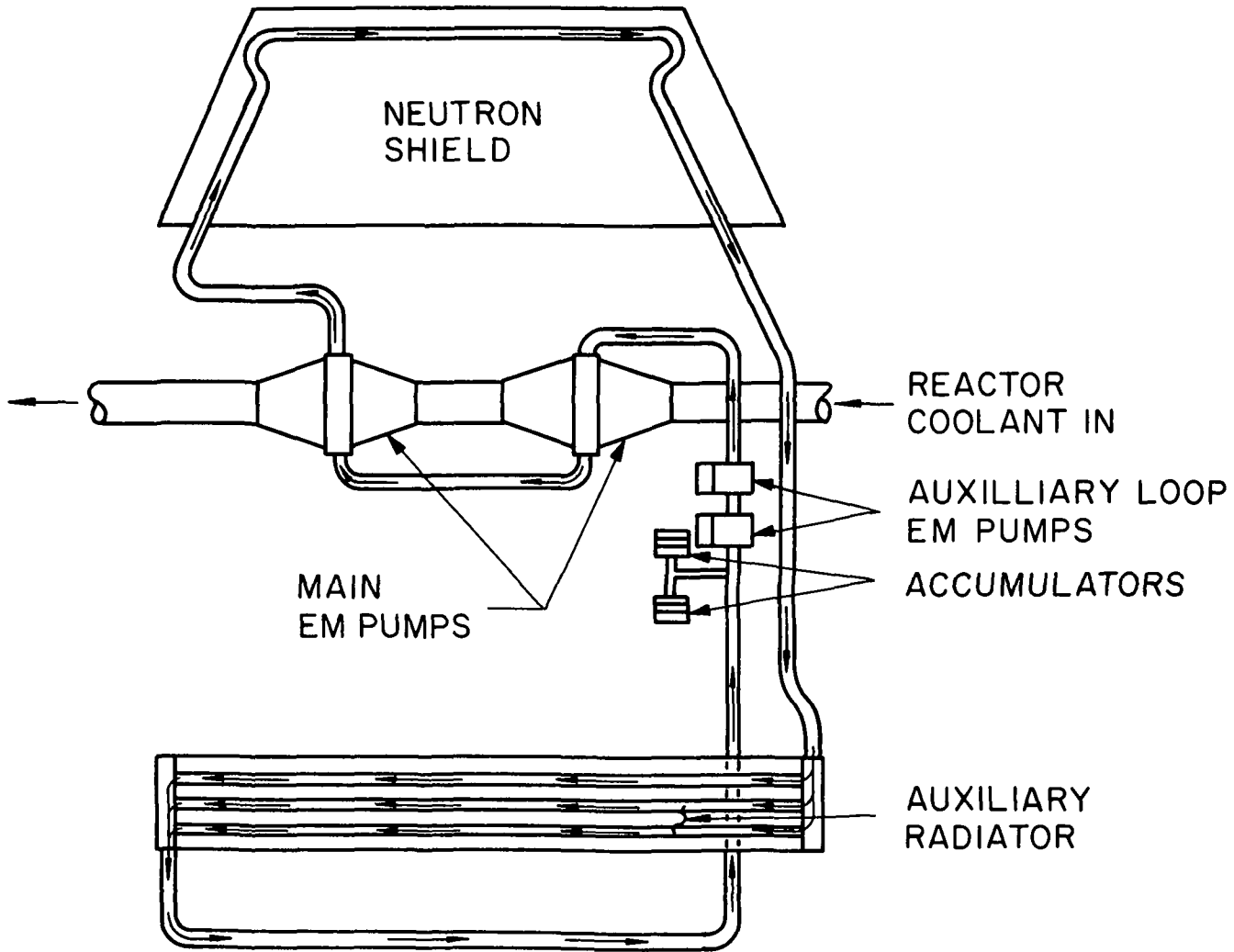


Figure 8-7. Schematic Representation of Auxiliary Loop

- c. Main radiator stiffeners and mating attachments
- d. PC radiators stiffeners and mating attachments.

The reactor support structure is a sheet metal frustum, imbedded in the neutron shield, and attached at its base to the rear edge of the lithium hydride can. The smaller diameter of the frustum is attached to the front plate of the lithium hydride can opposite the reactor. Attachment rings on both the upper and lower bases of the frustum provide the necessary connecting fixtures. The support frustum is constructed of 0.06 thick stainless steel, lightened by 50 percent by hole punchouts. The total weight of the frustum and L-shaped attachment rings is 40 pounds.

Shield support is provided by a lateral surface can wall thickness of 0.08 inch stainless steel, coupled with four circumferential Z-shaped stiffeners. The combined weight of the can wall and stiffeners is 67 pounds.

Structural additions to the main radiator section of the spacecraft include mating attachment rings, circumferential stiffeners and longerons. Mating rings are needed for the four main radiator bays which weigh a total of 140 pounds. The rings are J-shaped and made from 0.08 inch thick sheet. A Z-shaped frame or stiffening ring is required in each of the two rearward radiator bays. Constructed of 0.06 inch thick stainless steel, the stiffeners weigh a total of 30 pounds. Four L-shaped longerons in each bay provide buckling support for the radiator. Constructed of 0.125 inch thick stainless steel, they weigh a total of 165 pounds for the entire radiator.

The power conditioning radiator also has structural additions in the form of mating rings, stiffeners and longerons. In addition, a portion of the radiator surface is blocked by the low-voltage cables. This blocked surface does not dissipate heat, but it must be present to provide structural rigidity to the radiator. Consequently, the weight of this blocked surface, 65 pounds, is attributed to powerplant structure.

The two mating rings of the PC radiator, each formed from 0.08 inch thick aluminum, weigh a total of 35 pounds. Z-frames, or stiffeners, located at four axial locations

and constructed of 0.094 inch thick aluminum weigh a total of 50 pounds. Twenty-four longerons, T-shaped and constructed of 0.156 inch thick aluminum, run the length of each PC radiator panel. The weight of these longerons is 210 pounds. The total weight of all structural components in the PC radiator location is 360 pounds.

8.1.2 THRUSTER SUBSYSTEM GROUP

The thruster subsystem group includes the subsystems which transfer and convert the electrical power generated by the reactor to propulsive power. These subsystems are the low and high voltage cable networks, the high voltage supply PC units with corresponding radiator panels, and the thruster ion engines.

8.1.2.1 Ion Engine Subsystem

The ion engine subsystem, including the individual thrusters and vector control hardware, has been designated by JPL. A summary description of these components is given in Paragraph 3.2.2 and illustrated in Figure 3-6. The thirty-seven engine units weigh 585 pounds, the vector control assembly 550 pounds, and miscellaneous hardware another 100 pounds.

8.1.2.2 Low Voltage Cables

The low voltage cable assembly consists of the reactor leads and low voltage bus bars which transport the reactor electric power output to the high voltage supply PC units and to the special payload and thruster PC modules. (The hotel load low voltage distribution system is included in the powerplant subsystem weight group.) The initial, high temperature copper reactor leads exit the reactor through the walls of the coolant outlet plenum.

Both bus bars extend down the outer surface of the shield and main radiator components into the power conditioning radiator section. The bus bars extend axially along

the PC radiator with 4 pairs of leads turning 90 degrees at separate axial locations, to extend circumferentially to individual PC modules.

The high temperature copper reactor leads located near the reactor weigh less than three pounds including ceramic bead insulators. The aluminum bus bars are rectangular in cross section, 0.165 inches by 0.28 inches, with a mean length of 44 feet. The total weight of these bus bars is 195 pounds with an additional weight of 28 pounds in ceramic insulation. Multifoil insulation of A1-Ni composition is placed between the bus bars and the high temperature surfaces, the main radiator and neutron shield, which the aluminum bus bar traverses. The weight of this insulation is 80 pounds.

Two pair of aluminum bus bars extend into the payload and thruster bays carrying power to the respective PC units. The weight of this additional length of cable, plus insulation, is less than 6 pounds.

8.1.2.3 High Voltage Cables

The high voltage cables are the 3100 volt lines from the main power conditioning modules to the ion engines. A pair of leads, one positive and one negative, extend from each module to each ion engine. The total weight of these leads, averaging 10 feet in length, is 15 pounds which includes the ceramic insulation.

8.1.2.4 Power Conditioning Modules

The power conditioning subsystem includes 37 high voltage supply units (one per ion engine) plus the special thruster PC modules. The high voltage supply modules, which weigh a total of 1390 pounds, are based on the concepts and component definitions described in Paragraph 7.2.2 for these units. A similar analysis, reported in Paragraph 7.2.2, defines and computes the component weights comprising the special thruster PC modules. The total weight of these latter modules is 270 pounds.

8.1.2.5 Power Conditioning Radiators

The radiator surface corresponding to the 37 high voltage supply PC modules is 470 square feet. (The rest of the radiator is chargeable to the hotel load PC units in the powerplant subsystem group.) The weight of this radiator surface area, based on a 0.115 inch thickness for the aluminum panels, is 745 pounds.

The special thruster PC radiator, which dissipates 1.9 kW, weighs 85 pounds.

8.1.2.6 Thruster Structure

The payload and thruster bays require mating rings, stiffeners and longeron stringers for support structure. The mating rings weigh 23 pounds, the stiffeners weigh 3 pounds and the longeron weigh 50 pounds. Of this total, approximately 40 pounds is chargeable to the thruster bay.

8.1.3 PROPELLANT SYSTEM

The propellant system consists of the mercury propellant and the corresponding tanks, feed lines and structural attachments. Of the total 14,500 pounds of mercury specified in the design guidelines, approximately 4250 pounds are located in a tank behind the neutron shield to act as protection for the spacecraft from the reactor gamma radiation. The tank is a conical cylinder constructed of 0.10 inch thick stainless plate at the top and bottom and 0.08 inch thick plate for the lateral surface. The total weight of this tank with radial steel stiffening bars on the rear face and on internal expulsion bladder for the propellant is 160 pounds.

A cylindrical tank, located in the thruster bay, contains the remaining 10,250 pounds of propellant. The weight of this tank with mercury feed lines to the ion engines is 300 pounds. Attachment brackets for both propellant tanks total 15 pounds.

8.1.4 SPACECRAFT PAYLOAD COMPONENTS

The delineation of the payload science package, communications equipment, spacecraft guidance and control, etc., has been provided by JPL and summarized in Paragraph 3.2.3. The weight of conduction fin radiator corresponding to the combined payload heat rejection requirements is 25 pounds. The weight of structural stiffeners, and longerons attributable to the payload bay is an additional 25 pounds.

8.1.5 LAUNCH COMPONENTS

Two special components are required for the spacecraft during the launch phase of the mission; an adapter cone attaches the spacecraft to the launch booster, and a flight fairing or shroud protects the spacecraft from aerodynamic pressure loads and heating during the launch trajectory. The adapter cone, shown on the layout drawing, Figure 2-1, surrounding the ion engines and stowed antennas, weighs 250 pounds. The launch shroud, which is 66 feet long, weighs 3500 pounds. Since the shroud is jettisoned after peak aerodynamic pressure and heating conditions occur but before booster cutoff, only a fraction of the shroud weight is chargeable as payload weight reduction. This fractional shroud weight or payload penalty is 825 pounds for the externally fueled reactor spacecraft system, 24 percent.

8.2 FLASHLIGHT POWERPLANT/SPACECRAFT

The reference flashlight powerplant and spacecraft design is extrapolated from the results obtained with a thermionic computer code optimization for a 300 kWe reactor output system. Important conditions assigned for the computer analysis and for the reference design are:

- a. A reactor outlet temperature of 1350 °F
- b. A two loop, in-series, heat rejection system
- c. A relative radiator arrangement having the power conditioning radiator behind the shield and the main radiator at the rear of the spacecraft.
- d. Aluminum as the low voltage cable composition.

Table 8-4 lists the more important characteristics of the 300 kWe system as determined by the computer code analysis. These characteristics, along with similar results for a 316 kWe reactor output which delivers 240 kWe net power to the thruster subsystem, form the basis of the reference flashlight powerplant spacecraft design.

A weight summary and an electric power summary for the reference flashlight reactor spacecraft are given in Tables 8-5, and 8-6, respectively. The weight of the launched vehicle is 37,605 pounds of which 1280 pounds in the form of the launch fairing and booster adapter is jettisoned during launch to provide a 36,325 pound spacecraft in earth orbit. This spacecraft is comprised of three systems as follows:

- a. Propulsion system weighing 19330 pounds
- b. Propellant system weighing 14760 pounds
- c. Payload section weighing 2235 pounds

The propulsion system is made up of two main subsystems; a nuclear powerplant of 12170 pounds and a thruster subsystem of 7160 pounds. Further breakdown of system weights are detailed in Table 8-5.

As shown in Table 8-6, a reactor output power of 318 kWe is required to supply a net power of 240 kWe to the thruster subsystem. Cable losses of 20.5 kWe and power conditioning losses of 35.32 kWe occur in the low voltage end of the electrical circuit, with the remaining 262.18 kWe appearing as high voltage power from the PC components. Most of this high voltage power is at 3100 volts, and provides 223 kWe to the thruster ion engines. The remaining high voltage power, which is at 250 volts, is divided almost equally between the payload and thruster PC requirements, and the powerplant hotel load requirements. Details of the high voltages circuit losses and power usage are given in Table 8-6. The net propulsion power is the sum of the thruster engine input and the thruster PC input.

TABLE 8-4. CHARACTERISTICS OF A 300 kWe FLASHLITE REACTOR POWERPLANT/SPACECRAFT SYSTEM

Total system weight*, lbs.		21194
Net propulsion power, kWe		231.55
System specific weight, lbs/kWe		91.53
<u>Electric System conditions</u>		
Reactor output voltage, volts		14.42
Reactor output current, amps		20806
Reactor output power, kWe		300
Low voltage cable losses, kWe	18.23	
Main PC power input, kWe		281.7
Main PC power output, kWe		248.52
Hotel PC power input, kWe	14.6	
Hotel PC power output, kWe	12.4	
Payload power, kWe	2	
High voltage cable loss, kWe	0.4	
Net propulsion power, kWe		231.55
<u>Subsystem Weights, lbs.</u>		
<u>Reactor</u>		
Reactor	2997	3840
Heat Exchanger	510	
Piping	333	
<u>Main Heat Rejection</u>		
Main Radiator	2384	3435
Piping	1051	
<u>Shield</u>		
Shield	1587	1650
Radiator	36	
Piping	27	
<u>Auxiliary Cooling</u>		
Radiator	42	99
Piping	57	
<u>Power Conditioning</u>		
Main PC modules	3021	3930
Hotel PC modules	99	
Radiator	810	
<u>Cesium Radiator</u>		
		8
<u>Cables</u>		
Low voltage cable	1586	1610
High voltage cable	24	
<u>Payload</u>		
Radiator	41	2200
System Controls	62	
Payload equipment	2097	
<u>Thruster</u>		
Thrusters	1233	2030
P. C. modules	264	
Radiator	73	
Thruster isolation units	460	
<u>Structure</u>		
Spacecraft structure	1411	2392
Shroud penalty	981	
<u>Spacecraft Surface Areas, ft²</u>		
Main Radiator	907	1082
P. C. Radiator	575	
Auxiliary Radiator	5.2	
Shield Radiator	1.0	
Low Voltage Cable	192	
High Voltage Cable	5	
Cesium Radiator	4	
Payload Radiator	29	
Thruster PC Radiator	52	
Gaps between radiators	32	
<u>System Dimensional Characteristics</u>		
Vehicle length, ft.		77.94
Vehicle diameter, ft.		9.2
Shield half angle, degrees		7.75
Reactor diameter, ft.		2.37
Shield thickness, ft.		2.13
Heat exchanger length, ft.		3.55
Heat exchanger bay width, ft.		1.59
<u>Reactor Loop Conditions</u>		
Pipe diameter, inches		4.23
Coolant flow rate, lbs/hr.		1.526 x 10 ⁵
Coolant temperature rise, °F	252	
Coolant heat rejection, BTU/hr		8.11 x 10 ⁶
Loop pressure drop, psi		5.6
Loop pumping power, kWe		7.1
Heat exchanger effectiveness		0.938
Maximum loop temperature, °F		1350
<u>Radiator Loop Conditions</u>		
Pipe diameter, inches		1
Coolant flow rate, lbs/hr		190
Coolant temperature rise, °F		100
Coolant heat rejection, BTU/hr.		4041
Loop pressure drop, psi		1.97
Loop pumping power, kWe		0.003
Maximum loop temperature, °F		950
<u>Shield Loop Conditions</u>		
Pipe diameter, inches		
Coolant flow rate, lbs/hr.		
Coolant temperature rise, °F		
Coolant heat rejection, BTU/hr.		
Loop pressure drop, psi		
Loop pumping power, kWe		
Maximum loop temperature, °F		
<u>Auxiliary Loop Conditions</u>		
Pipe diameter, inches		0.6
Coolant flow rate, lbs./hr.		775
Coolant temperature rise, °F		100
Coolant heat rejection, BTU/hr.		16700
Loop pressure drop, psi		3.31
Loop pumping power, kWe		0.019
Maximum loop temperature, °F		800
<u>Power Conditioning Subsystem</u>		
P. C. module efficiency		.882
Maximum operating temperature, °F	200	
Total heat, BTU/hr.		1.21 x 10 ⁵
Radiator fin thickness, inches		0.10
<u>Cable Conditions</u>		
LV cable length, ft.		23.5
LV cable cross section area, ft ²		0.363
Maximum temperature, °F		700
Total heat rejection, BTU/hr		64604
Reactor lead cross section area, ft ²		0.144

TABLE 8-5. WEIGHT SUMMARY 240 kWe (NET) THERMIONIC SPACECRAFT
(FLASHLIGHT REACTOR)

Component	Weight - Pounds				
Propulsion System					19,330
Power Plant Subsystem Group				12,170	
Reactor Subsystem			3300		
Reactor (Dry)		3060			
Actuators		230			
CS Radiator		10			
Primary Heat Rejection			4840		
Reactor Loop		645			
Ducts	140				
EM Pumps (2)	100				
Accumulators	60				
Coolant	280				
Insulation	65				
Radiator Loop		4195			
Heat Exchanger (Dry)	180				
Ducts	440				
EM Pumps (2)	90				
Accumulators	100				
Main Radiator	2190				
Coolant	985				
Insulation	210				
Shield			1875		
Neutron		1610			
Permanent Gamma		265			
Electric and Controls			340		
Hotel Load		290			
Power Conditioning	185				
Radiator	60				
Distribution Cables	45				
Power Plant Control		50			
Auxiliary Coolant Loop			110		
Ducts		35			
EM Pumps (2)		20			
Accumulators		10			
Radiator		20			
Coolant		25			
Structure			1655		
Reactor Support		60			
Neutron Shield (External)		50			
Power Conditioning Radiator		405			
Area Blocked by LV Cables	225				
Main Coolant Duct	25				
Mating/Stiffening Rings	35				
Longerons	120				
Transition Ring		65			
Main Radiator		1075			
Mating/Stiffening Rings	425				
Longerons	650				
Miscellaneous			50		
Thruster Subsystem Group				7160	
Ion Engine Subsystem			1235		
Ion Engine Units		585			
TVC Unit		550			
Miscellaneous		100			
Power Conditioning Electronics			3220		
HV Power Supply		2640			
Special Ion Engine PC		270			
Thruster Isolation		310			
Power Conditioning Radiators			890		
HV Power Supply		770			
Special Ion Engine Units		70			
Thruster Isolation		50			
High Voltage Power Cables			70		
3100 Volt Cables		25			
250 Volt Cables		35			
Insulation		10			
Low Voltage Power Cables			1680		
Main Bus		1620			
Insulation		60			
Structure			65		
Special P. C. Bay		65			
Propellant System					14,760
Propellant				14,500	
Tanks and Distribution				245	
Structure				15	
Net Spacecraft					2235
Guidance and Control				50	
Communications				60	
Science				2065	
Radiator				25	
Structure				35	
GROSS SPACECRAFT IN EARTH ORBIT					36,325
LAUNCH VEHICLE ADAPTER					250
LAUNCH SHROUD PAYLOAD WEIGHT					
PENALTY (84.3 FT. LONG, 4400 POUNDS SHROUD)					1030
LAUNCH VEHICLE PAYLOAD REQUIREMENT					37,605

TABLE 8-6. ELECTRIC POWER SUMMARY 240 kWe (NET)
THERMIONIC SPACECRAFT (FLASHLITE REACTOR)

	POWER - kWe					
Reactor Output						318
Losses and Distribution						
Low voltage cable loss					20.5	
Main P. C. input					297.5	
P. C. loss				35.32		
Main P. C. output				262.18		
3100 volt output			224.53			
Cable losses		0.28				
Thruster interrupter		1.25				
Thruster engine input		223				
250 volt output			37.65			
Payload and ion engine section		19.3				
Cable losses	0.3					
Thruster P. C. input	17.0					
Payload input	1.0					
Spacecraft control input	0.5					
Powerplant control input	0.5					
Hotel load section		18.35				
Cable losses	0.19					
P. C. losses	2.71					
Reactor pump input	8.06					
Radiator pump input	6.5					
Shield pump input	0.16					
Auxiliary pump input	0.03					
Reactor controls input	0.2					
Cesium heater input	0.5					
Net Power to Ion Engines*						240

*The net power to the thrusters is the sum of the ion engine grid power input (223 kWe), after power conditioning, and the special ion engine power requirements (17 kWe).

Figure 1-9 in Subsection 1-3 is a layout drawing of the reference flashlight reactor spacecraft. The spacecraft is a long, narrow vehicle, 84.15 feet long and 9.2 feet in diameter, made up of a conical front end section, having a 7.4 degree half angle, attached to a cylindrical rear section. The reactor is located at the apex of front section cone to provide maximum separation distance from the payload, which is at the rear of the cylindrical section, and to assure minimum volume for the shadow shield.

The neutron shield is located as close as possible to the reactor, again to provide minimum shield volume and weight, with a portion of the mercury propellant located in a tank behind the neutron shield to act as gamma shielding.

The power conditioning modules and power conditioning radiator section are located directly behind the shield and propellant tank to minimize the length and, hence, the power losses in the low voltage cable. This is required due to the low voltage, 14 to 16 volts, characteristics of the flashlight reactor (see Paragraph 3.3). Individual PC modules are distributed uniformly on the surface of the PC radiator, one module per pair of reactor fuel elements and low voltage cables. The cables are strung along the outer surface of the shield PC radiator surface so that they can radiate their I^2R power losses directly to space.

The PC radiator occupies most of the conical surface of the spacecraft plus 9.7 feet of the cylindrical section. A very short section auxiliary radiator surface acts as a thermal buffer between the low temperature PC radiator and the high temperature main radiator which covers most of the cylindrical section surface. The reactor waste heat is transported to the main radiator in two stages. The first loop pipes the reactor coolant, NaK, outside the shield to a heat exchanger placed between the neutron shield and the gamma shield (forward propellant tank). A second NaK loop carries the heat along the outer surface of the PC radiator to the main radiator. (See Section 5 for justification of two loops in series in the flashlight reactor system.)

The payload section, thruster power conditioning section, and ion thruster engines are located in sequence at the rear of the vehicle. A single disc communication antenna is shown in the launch position behind the thruster engines on Figure 1-9. After launch, it would be extended radially beyond the vehicle diameter and forward of the thruster engines.

Descriptions of the powerplant and spacecraft subsystems will be given in the following sections. The subsystem definitions agree with the format used in weight summary Table 8-5, rather than the computer code definitions used in Table 8-4.

8.2.1 POWERPLANT SUBSYSTEM GROUP

The propulsion system is made up of the power plant subsystem and the thruster subsystem. The power plant subsystem, in turn, comprises all the subsystems which generate the propulsion power. The following paragraphs describe the subsystems in the powerplant subsystem.

8.2.1.1 Reactor Subsystem

The 318 kWe reactor is 2.37 feet in diameter, 2.96 feet long and weighs 3060 pounds in the dry condition. Twelve S8DR control actuators (SNAP-8 Ground Prototype), modified for eccentric output drive, are mounted on the front end of the reactor. These actuators are radiatively cooled and weigh a total of 230 pounds. They drive radial reflector segments in an axial direction to effect reactor control by varying neutron leakage.

Fuel element extensions, electrical leads, cesium vapor feed tubes and reactor coolant piping all emerge from the back end of the reactor into the bay between the reactor and shield. The weights of the cesium vapor feed lines and the cesium reservoir are included in the reactor weight while the coolant header weights are included in the reactor loop subsystem and the reactor lead weights are included in the low voltage cable weight. A cesium heat pipe radiator removes excess heat from the cesium reservoir and dissipates it by radiation. This radiator, which weighs approximately 10 pounds and has approximately four square feet of surface area, encloses a portion of the equipment bay which measure 15 inches in axial length.

8.2.1.2 Shield Subsystem

The shield subsystem consists of a block of lithium hydride acting as a neutron shield. A tank of mercury propellant is the main gamma shield but its weight is charged to its primary function as engine propellant.

The neutron shield is an internally supported tank filled with lithium hydride. Its configuration is a frustum of a cone, 26.4 inches thick with base diameters of 44.5 and 51.5 inches and its weight is 1610 pounds.

The total heating rate in the shield subsystem is approximately 1.8 kW with great majority of this heat being deposited in the front one-foot thickness of the neutron shield. This heat is removed by the auxiliary cooling loop (see Paragraph 8.2.1.6).

The reactor loop piping races a helical path just below the lateral surface of the neutron shield. The resultant holes in the shield barrier are covered with plugs of canned lithium hydride on the front end and rear faces of the neutron shield. Similar plugs of tungsten, 3.5 inches thick and weighing 265 pounds; cover the voids through the mercury tank caused by the passage of the radiator loop piping.

8.2.1.3 Reactor Loop Subsystem

The reactor loop subsystem is shown semi-schematically on Figure 8-8. The loop consists of two coolant headers and coolant feed pipes at the rear face of the reactor, two EM pumps and three accumulators in the heat exchanger bay and the piping between the reactor and heat exchanger. The heat exchanger itself is arbitrarily assigned to the radiator loop subsystem.

As shown on Figure 8-8, the headers are crescent shape tori which have an average width of 3.5 inches, a depth of 2 inches and an approximate diameter of 30 inches. Constructed of 0.10 inch thick stainless steel plate, each header weighs 30 pounds.

Six equally spaced 2 inch diameter pipes, weighing 9 pounds, distribute the coolant to the reactor from each header. A single duct, having a cross section area equivalent to a 4.3 inch round pipe, connects each header with the heat exchanger group. The total length of this ducting is 12.5 feet long and with a wall thickness of 0.06 inches, weighs 34 pounds.

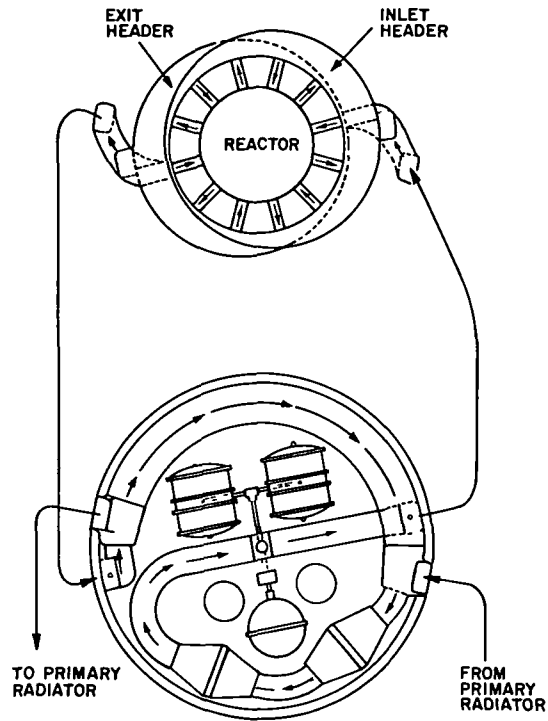


Figure 8-8. Schematic of Reactor Loop

Two EM pumps in series, one operating and one redundant, pump the reactor coolant. These pumps are similar in design and concept as those described in Paragraph 8.1.1.3 for the externally fueled power plant. The electrical power requirements for each of the pumps in the flashlight reactor loop is 8.06 kW supplied at 10 volts and 800 amperes.

The accumulator group, two dynamic and one static accumulator, are similar in concept and design to those discussed in Paragraph 8.1.1.3. The weight of each dynamic accumulator is 19 pounds while the static accumulator weighs 22 pounds.

The total coolant weight in the reactor loop is 280 pounds; the reactor holds 133 pounds, the tube side of the heat exchanger contains 27 pounds and the remaining 120 pounds is distributed in the piping, headers and EM pump ducts.

Multifoil insulation is used around sections of the reactor piping to protect adjacent equipment from the high temperatures of the coolant. The insulation is placed on the rear face of the neutron shield and the front face of the propellant tank for thermal protection from the heat exchanger, pumps, etc. Additional insulation surrounds the loop piping and headers to protect the shield, cesium system and electrical leads. The total weight of insulation in the reactor loop region is 65 pounds.

8.2.1.4 Radiator Loop Subsystem

The radiator loop transfers the reactor waste heat from the reactor loop and transports it to the main radiator for dissipation to space. The loop consists of the following components:

- a. Heat exchanger
- b. Main radiator
- c. Piping with EM pumps and accumulators
- d. Protective thermal insulation.

The heat exchanger is a tube and shell, counter-cross flow, unit with the hot reactor NaK-78 coolant flowing inside the tubes and the cooler radiator NaK-78 coolant in combination flow, across and counter to the tube flow. The characteristics of the heat exchanger are as follows:

Heat transfer rate	2520 kW
Heat exchanger length	56.5 inches
Heat exchanger diameter	4.6 inches

Tube diameter	0.2 inches
Number of tubes	433
Shell thickness	0.10 inches
Tube wall thickness	0.02 inches
Tube side pressure drop	1.67 ps ₁
Cold side pressure drop	4.37 ps ₁

The weight of the dry heat exchanger is 180 pounds.

The main radiator has a total area of 945 square feet divided into four axial bays with three panels per bay. Each panel covers one-third of a cylindrical lateral surface (120° of arc) and is 9.8 feet wide and feet in axial length. Sixty-five coolant tubes, which run the length of each panel are joined by solid fin sections of copper-stainless construction. Figure 8-9 is a cross section of a coolant channel-fin section of a panel with dimensions. The copper-stainless steel fins are 0.03 inches thick with the armor tubes spaced on 1 752 inch centers. The coolant channels are 0.18 inches in diameter with 0.095 inches of primary armor protection and 0.0244 inches of bumpered armor protection. The total weight of all the panels plus their headers, which will be described in the next paragraph, is 2190 pounds.

The network of feed lines and headers which distribute the radiator loop coolant to the radiator panels is shown on Figure 8-10. Five rings of headers distribute the coolant to the twelve radiator panels. Each header ring is separated into three sections corresponding to the three panels per radiator bay. The second and fourth ring of headers dispense the incoming coolant with the second header ring feeding the first two bays and the fourth ring feeding the last two bays. The middle header ring collects the coolant from the two central bays while the two end header rings collect the coolant from the respective end bays. The three middle header rings, which service two bays are 1.67 inches in diameter, and the two end rings are 1.18 inches in diameter. As noted above, the weights of these headers are included in the radiator weight.

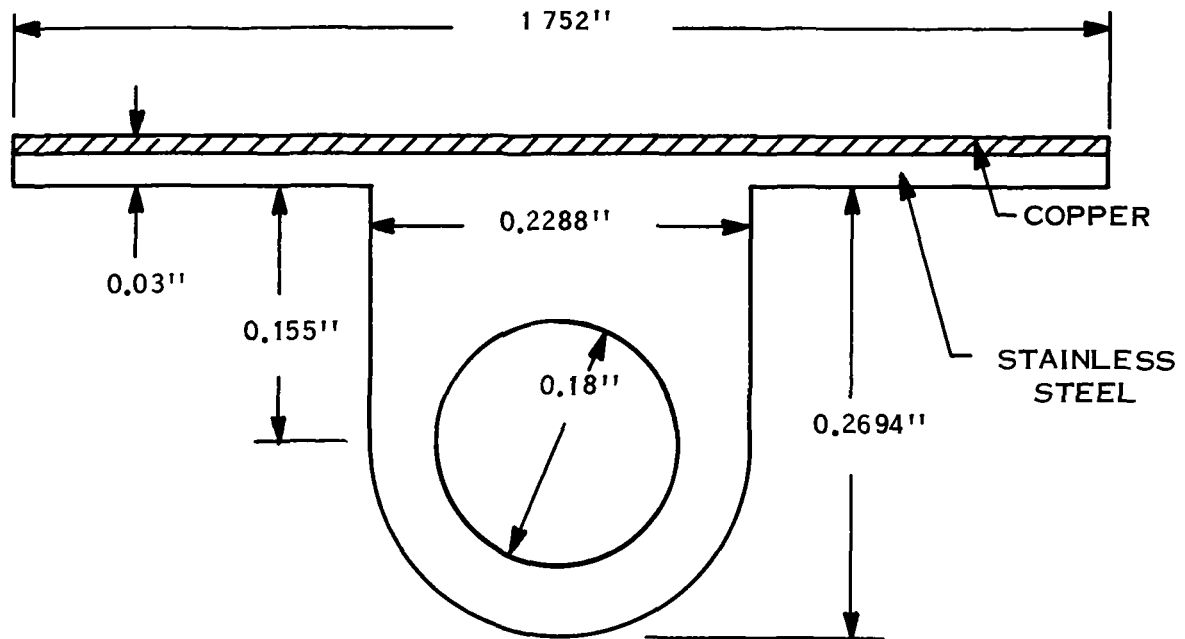


Figure 8-9. Cross Section of Main Radiator Coolant Channel - Fin Section

The radiator feed line network consists of the axially directed input and return feed lines plus the radial, spoke-like feeders running to each header. These latter header feeders are 1.75 inches in diameter, while the input feed line has a 2.9 inch diameter and the return feed line is 2.04 inches in diameter. The piping to and from the heat exchanger up to the junction with the feed lines is 4.0 inches in diameter.

Two S-shaped duct segments of flat rectangular cross section are located in the radiator loop piping, as shown on Figure 8-10. These duct segments bend to accommodate the relative expansions of the piping between the heat exchanger and the radiator and the radiator itself. Additional bellows in the input and return feed lines take up expansion motion between the individual bays of the radiator.

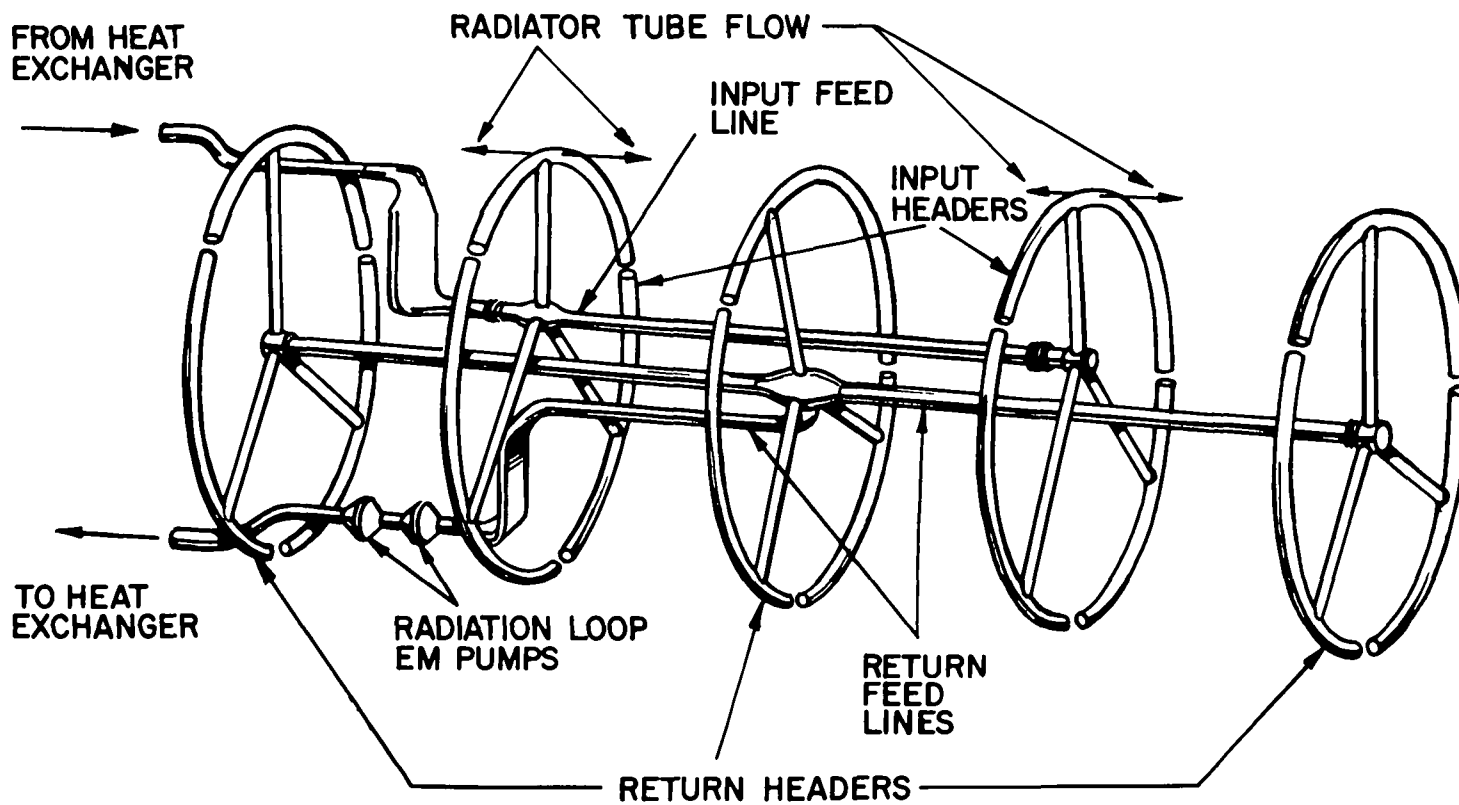


Figure 8-10. Schematic of Main Radiator Loop

The total weight of the radiator loop piping including the radiator feed lines and expansion bellows is 440 pounds.

Two EM pumps in series, similar to those previously discussed, pump the radiator loop coolant. The weight of each pump is 45 pounds.

Two dynamic and one static accumulator regulate the coolant expansion-pressure level conditions in the radiator loop. The dynamic accumulators are the same size and weight as those in the reactor loop. The static accumulator is approximately 1 foot in diameter and weighs 60 pounds for a total accumulator weight of 100 pounds.

The coolant inventory in the radiator loop consists of 263 pounds in the radiator, 112 pounds in the shell side of the heat exchanger and 608 pounds in all the piping.

Insulation surrounds radiator loop piping and separates the main radiator section of the vehicle from the auxiliary radiator and payload sections. The total weight of this insulation is 210 pounds.

8.2.1.5 Electric and Controls Subsystem

The power plant electric system consists of the hotel PC units and their radiators, plus the cabling to the pumps and equipment using the power. Special PC modules convert a 250 volt input power to the voltages required for the EM pumps and the reactor controls. The cesium heater requires no additional power conditioning. Figure 8-11 shows the power distribution, voltages and PC unit efficiencies in the hotel load circuit. The PC units have a specific weigh of 12 lb/kW so the total PC weight is 185 pounds. The weight of the corresponding 0.10 inch thick radiator panels, which total 35 square feet in area, is 60 pounds. The total weight of cabling, including 10 mils of insulation, between the hotel PC modules and the user equipment is 45 pounds. Power plant control equipment is assumed to weigh 50 pounds.

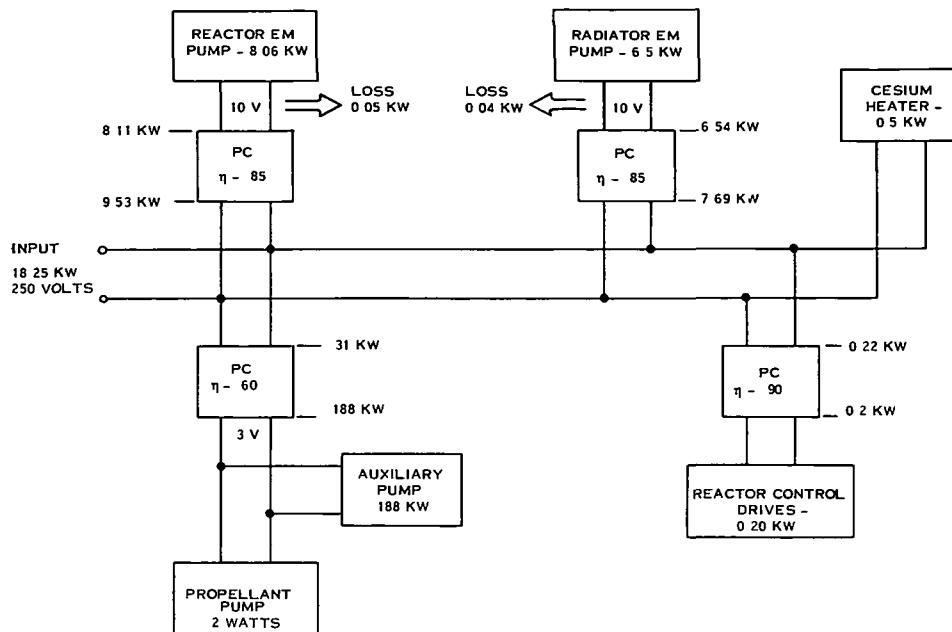


Figure 8-11. Hotel Load Power Distribution

8.2.1.6 Auxiliary Cooling Loop

The auxiliary cooling loop provides a thermal heat rejection mechanism for those system components which have temperature limitations lower than the temperatures in the main heat rejection system and higher than the electronic components in the spacecraft. These intermediate components are the electrical and magnetic sections of the EM pumps and the neutron shield. Figure 8-12 is a schematic layout of the auxiliary cooling loop. Self cooling EM pumps force the NaK-78 coolant through cooling passages in the reactor EM pump electrical section, then through cooling passages in the frontal regions of the neutron shield. The NaK is then at it's hottest temperature and is passed through the auxiliary radiator. The cooled flow is then circulated through

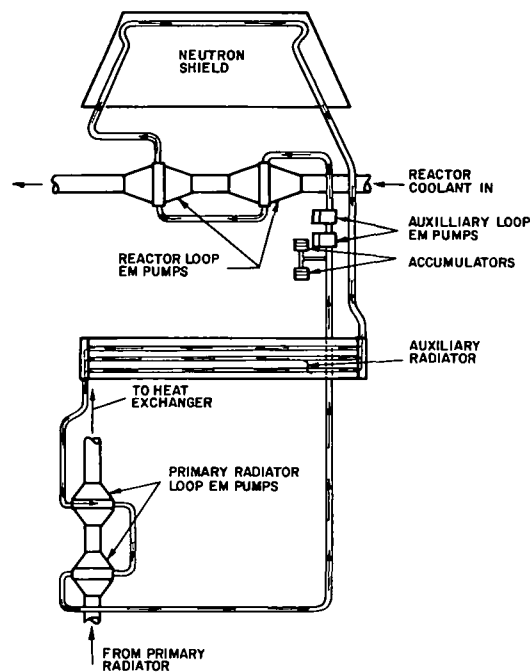


Figure 8-12. Schematic of Auxiliary Cooling Loop

the cooling passages of the radiator loop EM pump and returned to the auxiliary pump to complete the circuit. Accumulators control the expansion and pressure level of the coolant as in the other heat rejection loops.

The auxiliary radiator is a narrow fin band, containing a single cooling channel, located between the low temperature PC radiator and the high temperature main radiator. The radiating surface is ten square feet in area and only 4.5 inches wide. Its weight is approximately 20 pounds.

The total length of the 1.0 inch diameter piping is 71 feet and its dry weight is 33 pounds. The coolant weight is 20.5 pounds in the piping and 4.5 pounds in the radiator and pumps for a total weight of 25 pounds. Two accumulators approximately 6 inches in diameter and 6 inches long weigh 5 pounds apiece. EM pumps are estimated to weigh 10 pounds apiece. The total weight of the auxiliary loop is 110 pounds.

8.2.1.7 Power Plant Support Structure

The power plant support structure includes all the spacecraft structure required except that needed for the propellant tanks and the payload and thruster bay sections. It includes:

- a. Reactor and shield support
- b. PC Radiator stiffeners and mating rings
- c. Main Radiator stiffeners and mating rings.

The reactor support is a sheet metal section of a cone buried inside the lithium hydride neutron shield and an attachment ring on the front face of the shield. The sheet metal cone is formed from 0.06 inches thick SS sheet and is reduced in weight by the use of lightening holes. The total weight of this support cone and the attachment ring is 56 pounds.

Sixty mil thick, L-shaped stiffening rings at the outer rim edges of the conical shield are required to achieve required rigidity in the neutron shield can. In addition, approximately 0.08 inches of stainless steel meteoroid protection is required on the neutron shield surface areas which are not covered by the low voltage cable. The combined weight of the stiffening rings and added skin thickness of meteoroid protection is slightly less than 50 pounds.

The conical section of the power conditioning radiator is actually a six-sided prism, while the cylindrical section is actually twelve-sided. A transition section, approximately 5 feet in axial length connects the six and twelve-sided sections. The PC radiator is split in half axially by the main radiator heat rejection piping running down opposite sides of the PC radiator surface. Therefore, a U-shaped support channel joins the two halves of the radiator. The thin 0.10 skin of the PC panels does not have sufficient strength to provide launch support for the heavy weights of the reactor,

shield and propellant tank in the front end of the vehicle. Consequently, longerons and circumferential stiffening rings are added to supply the required strength.

Two U-shaped rings, 0.04 inch thick and weighing 8 pounds, provide mating connections for the twelve-sided cylindrical section of the PC radiator. A similar ring, weighing 4 pounds, allows the conical section of the radiator to be joined with the transition ring. Z-shaped stiffening rings, one in the cylindrical section and two in the conical section, weight a total of 15 pounds.

The U-shaped beams which connect the two halves of the PC radiator around the main radiator loop coolant pipes are constructed of 0.02 inch thick aluminum, and weigh a total of 25 pounds. T-shaped longerons, 14 in the cylindrical section and 8 in the conical section, provide the axial compressive strength capability. These members of 0.060 inch thick aluminum, weigh a total of 120 pounds.

A portion of the PC radiator panels can not radiate heat since they are covered by the low voltage cable. This fraction of the radiator still must be present to provide structural continuity so the weight of the blocked area is attributed to power plant structure. That weight of blocked area is 225 pounds.

A transition ring bridges the surface area occupied by the auxiliary radiator to connect, structurally, the main radiator to the power conditioning radiator. This transition ring, shaped like two U-channels placed back-to-back and joined by a connecting web, is formed from titanium plus Min-K* insulation and weighs 65 pounds. It also provides the significant function of a thermal barrier.

Stiffening rings to resist launch bending loads and mating rings are added to each bay of the main radiator. The mating rings at each end of each bay total 299 pounds. The Z-shaped stiffening rings are placed close together in the rear radiator bay and relatively far apart in the forward radiator bay, as the buckling loads decrease with

*T. M. Johns Manville Co.

increasing separation from the base of the spacecraft. The total weight of the fourteen stiffening rings is 126 pounds. Additionally, 650 pounds of longerons are required, added as increased tube wall thickness for extra, although unnecessary meteoroid protection (See Section 5). The total structural weight is 1075 pounds in the main radiator bays. The total weight of all the powerplant structural components is 1655 pounds.

8.2.2 THRUSTER SUBSYSTEM GROUP

The thruster subsystem includes the ion engine subsystem, the low and high voltage power cables, the high voltage and special ion engine power conditioning subsystems and the related power conditioning radiators. These individual subsystems will be described in the following paragraphs.

8.2.2.1 Ion Engine Subsystem

The ion engines and TVC unit which comprise the Ion Engine Subsystem are identical to the components described for the externally fueled reactor spacecraft in Paragraph 8.1.2.1.

8.2.2.2 Low Voltage Cables

A low voltage cable assembly is a two component arrangement in series; a copper cable extending from the reactor fuel element extension to the front rim of the neutron shield, and an aluminum bus bar extending from the junction with the copper cable to a power conditioning module. A low voltage cable assembly is attached to each of the 216 reactor fuel elements. Two fuel elements, two LV cable assemblies and a power conditioning module make up a common low voltage electrical circuit.

The copper reactor leads are 0.327 inches in diameter and have an average length of 18 inches. Ceramic bead insulation prevents electrical short circuiting and allows bundling of the leads for bracing and support. The leads are attached mechanically and brazed to the aluminum bus bars.

Each aluminum bus bar is rectangular with cross section dimensions of 0.39 inches by 0.667 inches. The lengths of the bus bars vary from eight feet to 35 feet with an average length of 23.6 feet. The cross section dimensions and performance evaluations are based on the average length.

The bus bars run axially along the conical surface of the shield, bend in a S-shaped curve at the juncture of the propellant tank and power conditioning radiator, proceed axially along the surface of PC radiator, then bend 90° in the plane of the radiator panel to attach to the PC module provided for each TFE pair. The busses are grouped in six bundles, one for each of the six sides of the conical section of the radiator. A thin layer of ceramic on the surfaces of the bus bars provides the required electrical isolation. Ceramic coated metal braces attach and support the bus bars to the various spacecraft components. In the shield and propellant tank areas, thermal insulation protects the bus bars from higher temperatures existing in those components.

The weight of all the copper reactor leads is 105 pounds while the total weight of the aluminum bus bars is 1515 pounds. The ceramic surface coating weighs an additional 60 pounds.

8.2.2.3 High Voltage Cables

The high voltage cable subsystem consists of the 3100 volt lines between the main power conditioning modules and the ion engines, and the 250 volt lines between the main PC modules and the special payload and thruster PC modules as shown on Figure 8-13.

The 3100 volt cabling consists of four separate wires, forming two complete circuits. The extra circuit provides greatly increased reliability with negligible penalty. Each aluminum wire strand is approximately 0.2 inches in diameter, 130 feet long and weighs 6.2 pounds. The cable starts at the rear end of one side panel of the PC radiator, runs forward the entire length of that panel, then returns down the length

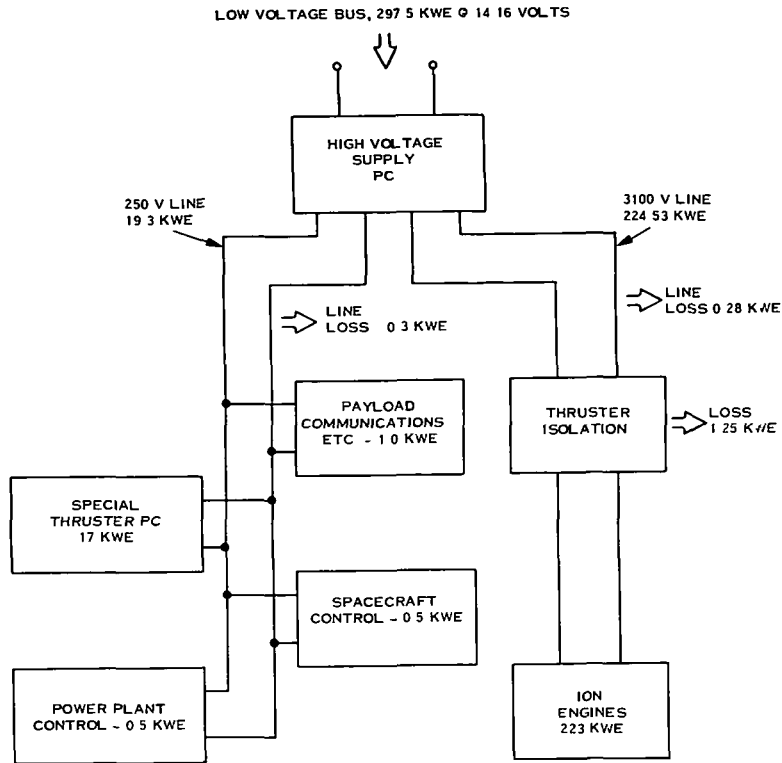


Figure 8-13. High Voltage Power Distribution

of an adjacent panel. This procedure occurs across the six side panels of the PC radiator. The cable then traverses the axial length of main radiator and payload sections to reach the ion engines. The wire strands are clamped in ceramic troughs which support and electrically insulate the feed and return strands from each other and from the spacecraft. Thermal insulation between the ceramic troughs and the main radiator surface keep cable temperatures at acceptable levels.

The 250 volt line to the payload and thruster PC modules is of similar 4 strand construction, follows the same path and is supported in the same ceramic trough as the 3100 volt line. Each wire strand is 0.3 inches in diameter and weighs 9 pounds for a total weight of 35 pounds. The total insulation weight on both the 3100- and 250-volt cables is estimated at 10 pounds.

8.2.2.4 Power Conditioning Modules

One hundred and eight power conditioning modules, constituting the high voltage power supply, are distributed on the inner surface of the PC radiator panels. The circuit concepts and component definitions follow the designs formulated in Section 7. On the basis of 8.9 lb/kW of input power, the high voltage supply PC modules weigh 2640 pounds.

The weights of the special ion engine thrusters at 270 pounds were supplied by JPL. The thruster isolation weights are estimated at 310 pounds.

8.2.2.5 Power Conditioning Radiators

The power conditioning radiator as shown on the layout drawing, rejects the heat generated in the high voltage supply and the hotel load power conditioners. The radiator weight corresponding to the hotel load PC waste heat generation has been included in the power plant electric subsystem reported in Paragraph 8.2.1.5. The remaining radiator area, 558 square feet, is attributable to the high voltage supply PC. The weight of this latter portion is 770 pounds based on 0.10 inch thick aluminum radiator panels.

The radiator heat loads from the special ion engine PC modules and the thruster isolation units are 1.7 and 1.25 kW, respectively. The corresponding radiator areas and weights are 36 square feet and 70 pounds for the PC modules, and 26 square feet and 50 pounds for the isolation units.

8.2.2.6 Thruster System Structure

Two mating rings, a circumferential stiffening ring and thirty seven longerons are required in the payload-thruster bay for spacecraft assembly and launch support. The total weight of these structural members is 100 pounds of which 65 pounds is chargeable to the thruster section.

8.2.3 PROPELLANT SYSTEM

The propellant system is made up of mercury propellant with associated tankage and support structure. The propellant weight is 14,500 pounds as in the externally fueled reactor spacecraft. Of this weight 10,800 pounds is contained in a conical tank behind the heat exchanger bay acting as a gamma shield. The tank is 9 inches thick and has a mean diameter of 56 inches. Eighty mil thick plate is used for the conical areas of the tank for meteoroid protection while the front and rear faces of the tank are 0.10 inches thick. The total weight of the tank including radial stiffeners is 210 pounds.

A cylindrical tank located in the thruster bay region holds the remaining 3700 pounds of propellant. The weight of this tank is 35 pounds and the weight of mounting brackets for both tanks is 15 pounds.

8.2.4 SPACECRAFT COMPONENTS

The guidance mechanisms, communication equipment, science payload, etc., for the flashlight reactor spacecraft, is the same as those specified for the externally fueled reactor spacecraft.

8.2.5 LAUNCH COMPONENTS

The launch adapter joining the flashlight reactor spacecraft to the booster is the same 250 pound unit designated for the externally fueled reactor spacecraft. The launch fairing for the 84 foot long flashlight reactor spacecraft weighs 4400 pounds of which 1030 pounds is the payload penalty.

8.3 WEIGHT REDUCTION CONCEPTS

This section presents recommendations for reducing the weight of the two reference designs defined in this study. Also, the key items in the program plan for the Phase II effort of this study is presented.

8.3.1 PHASE I RESULTS

It is expected that the weight of the reference designs will be reduced by consideration of the following factors:

- a. Modifications to the flashlight reactor should be made to:
 1. Increase voltage output, by placing multiple TFE's in series, to a level where location of the main radiator directly behind the shield becomes feasible.
 2. Change radiation spectrum of reactor to reduce coolant activation such that only a single primary heat rejection loop is required.
- b. An increase in the externally fueled reactor exit coolant temperature from 1350° to 1500°F results in a decrease in propulsion system specific weight of two lb/kWe, based on propulsion system power. The weight saving is realized primarily from a reduction in main radiator weight. Specific weight of the flashlight reactor is minimized near reactor exit coolant temperature of 1350°F.
- c. A calculation of shield requirements for the externally fueled reactor similar to those made for the flashlight reactor (Subsection 6.2) should be made. In this study it was assumed that the fluxes and dose rates for the two reactor/shield combinations are identical, and no credit was taken for the heavy metal reflectors in the externally fueled reactor.
- d. Shield half angle should be factored in the forward propellant tank relationship, in the computer weight optimization, to determine propellant weight. It may be advantageous to increase vehicle length and decrease forward propellant tank volume in order to maintain full thickness of the gamma shield for a longer time.
- e. Modifications to the low voltage cable should be considered to:
 1. Allow cable temperature to approach sink temperature by means of insulation, thereby decreasing I^2R power losses.
 2. Allow cable cross-sectional area, as well as cable length, to vary in the optimization process.
- f. Investigation should be made of a power conditioning thermal radiation cooling concept, in which each power conditioning module is dispersed uniformly over the individual radiator panel assigned to the module. This would eliminate the fin efficiency consideration of the power conditioning radiator, and reduce its weight.

- g. Investigation of the feasibility of raising the power conditioning temperature from 200^o to 300^oF should be made for both reactor concepts. This increase in temperature results in a decrease in propulsion system specific weight of approximately 5 lb/kWe.
- h. The feasibility of decreasing power conditioning unit to radiator ΔT , from 25^oF to 15^oF for example, by more efficient thermal contact, should be determined.
- 1. The effect of spacecraft diameter on overall weight should be considered in the event that a modified version of the Titan III C/7 is developed or a new launch vehicle is considered.

In addition to the preceding recommendations, the identified key items in the program plan for Phase II is presented in the next paragraph. These explore new design approaches, some of which may result in minimizing spacecraft weight and maximizing attainment of the mission objectives.

8.3.2 PHASE II PROGRAM PLAN

Phase II of this study is currently directed toward the evaluation of the following work elements, in the order of priority indicated by this listing.

The following items should be investigated in order after the two parallel reference designs described for Phase I are complete:

- a. Estimate system weight versus output power over the range of 70 to 500 kWe gross unconditioned power.
- b. Examine the system design modifications required if the GE "flashlight" reactor design is replaced by a GGA "dry flashlight" reactor design, if data are provided by the AEC.
- c. Determine the feasibility of placing a 70 kWe thermionic electric propulsion spacecraft aboard the Titan IIIF/Centaur launch vehicle.
- d. Determine effect on system weight of varying NaK outlet temperatures in the range 1200^o to 1500^oF.

- e. Examine the use of Li versus NaK-78 coolant. Treat startup considerations and payload shielding effects in detail.
- f. Compare conventional versus vapor fin radiators on a weight basis.
- g. Examine the system effect of an unbonded trilayer in the GE reactor.
- h. Document the computer program evolved to estimate the effects of major parameter variation, e. g. , integrated dose, system pressure drop, and radiator temperature, on system weight.
- i. Determine the effect of reactor output voltage on power conditioning, weight, temperature and efficiency.
- j. Use of beryllium in the finned radiator for meteoroid protection.
- k. Effect of extended life.
- l. Determine the effect of changing the non-puncture probability to 0.99 on the 300 kWe GE and GGA designs.
- m. Determine the effect on overall system weight of using a dynamic system for power conditioning the 300 kWe reactor system.
- n. Determine the effect on auxiliary radiator system weight of using heat pipes to transmit heat to the radiator surface. Use the auxiliary radiator designed for cooling the GE static power conditioner.

9. WEIGHT TRADEOFF COMPUTER CODE

9. WEIGHT TRADEOFF COMPUTER CODE

A computer code was written for this study which calculates the size, weight and performance of an unmanned spacecraft utilizing a thermionic reactor powered electric propulsion system. The code is designed to evaluate the relative importance of various system conditions, arrangements and component characteristics on the overall spacecraft performance.

This section of the report contains a general description of the calculational sequence employed in the code, a detailed description of the major component models and a discussion of the results achieved with the code.

9.1 CODE DESCRIPTION

Figure 9-1 presents a condensed flow chart of the major analytical steps of the system design and optimization code. Input requirements are used by the code to determine the performance and physical characteristics of the system components and their interconnections. These are then employed to calculate resultant system conditions, such as, overall system weight and power output, and then specific parameters are varied to maximize system performance. The procedure is repeated for alternate input requirements until the effects of significant system parameters on the system performance have been investigated.

The design sequence of the code, as shown on Figure 9-1, starts at the reactor component of the spacecraft and proceeds toward the thruster subsystem. The solid lines on Figure 9-1 designate the primary sequence, with the possible iterations characterized by dashed lines. The iterations are necessary because temporary assumptions must be made for the values of a few parameters in order to proceed with the calculation. Later, the values of these parameters are calculated and compared with the previously assumed value. If the discrepancy between the assumed and calculated values exceeds the tolerance designated then the calculation sequence is repeated

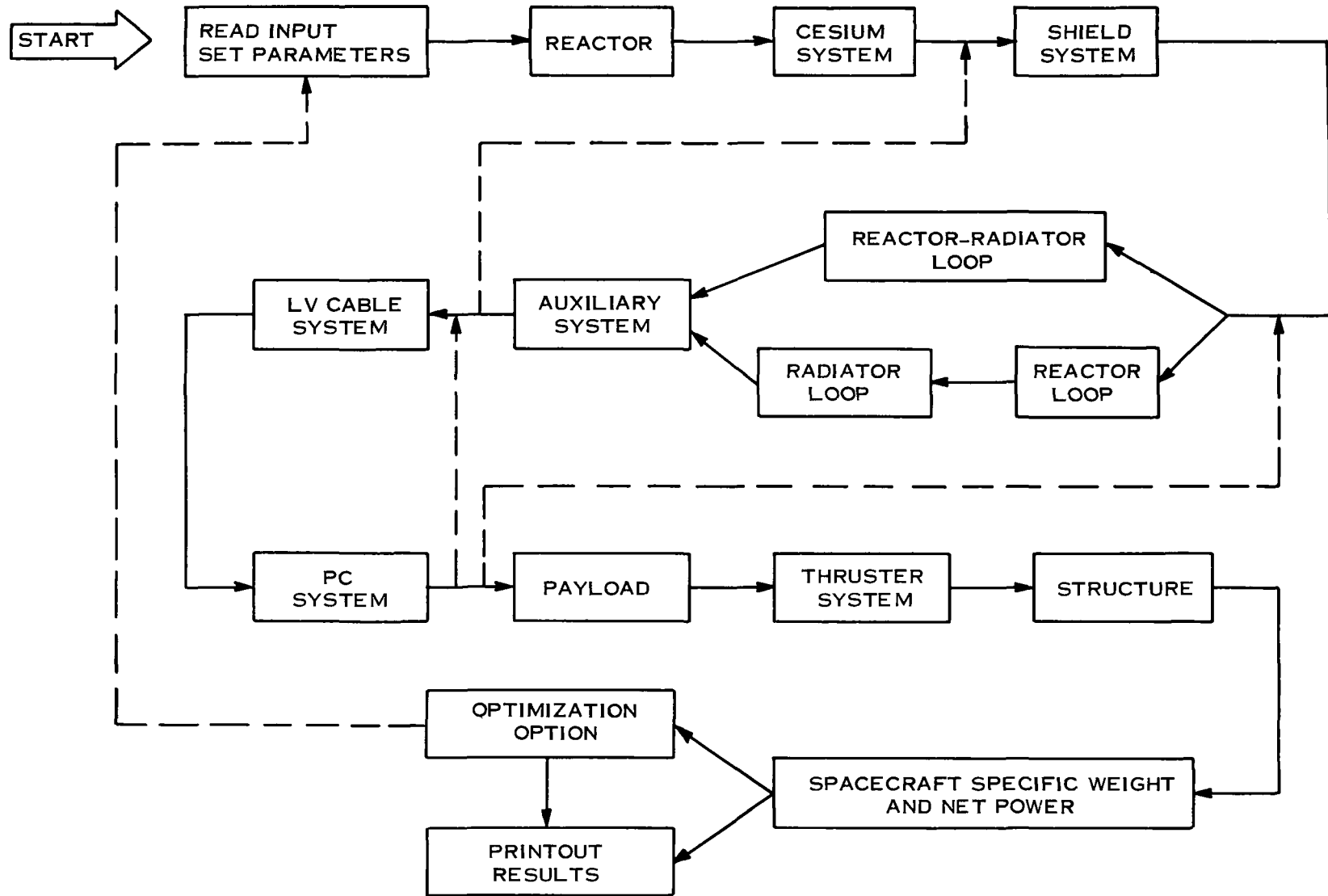


Figure 9-1. Simplified Logic Diagram for Computer Program

with a corrected value of the parameter until the tolerance is satisfied. Some of the parameters which may necessitate an iterative calculation are:

- a. Separation distance between shield and PC modules
- b. Length of the low voltage cable
- c. Length of the main radiator feed lines.

The first named parameter is calculated after the computation of the auxiliary system characteristics, and may require the regression of the design sequence back to the shield model. The actual lengths of the low voltage cable and the main radiator feed lines can be computed after the delineation of the power conditioning system and radiator. Operation of the code with the flashlite reactor type showed that, for example, it was more efficient to converge on cable length before iterating on radiator feed line length.

The remaining iteration path shown on Figure 9-1 is utilized if it is desired to exercise the optimization option and minimize system specific weight. An optimization procedure monitors the calculated specific weight and varies the optimization parameters accordingly.

The major input parameters which are kept constant for any one system calculation or optimization are:

- a. Gross reactor output power
- b. Mission and reactor operating times
- c. Integrated radiation dose limits
- d. Maximum vehicle diameter
- e. Propellant weight
- f. Payload weight
- g. Thruster weight

- h. Payload power requirements
- i. Control systems power requirements
- j. Cesium reservoir power requirement
- k. Average sink temperature
- l. Maximum reactor temperature
- m. Maximum power conditioning temperature
- n. Maximum shield temperature
- o. Maximum coolant temperature in each subsystem
- p. Number of loops in parallel for any actively cooled system
- q. Maximum PC radiator (passive) temperature
- r. Number of redundant pumps per subsystem
- s. Coolant velocities and number of passes in the heat exchanger
- t. Iteration tolerance limits.

A number of program options exist which are also designated at input time and which are kept constant for the calculation. They include:

- a. Reactor type-externally fueled, pancake or flashlight.
- b. Relative radiator location - main radiator forward or PC radiator forward.
- c. Main heat rejection loop configuration - one or two loops in series.
- d. Shield cooling mode - active or passive
- e. Materials selection for each subsystem including coolant composition, containment material, radiator material and cable material.

The shield concept used in the program assumes the presence of a neutron shield only, with the gamma shielding being achieved by a special mercury propellant tank just aft of the neutron shield. Provision has been made for future inclusion of a more common

neutron and gamma shield combination, utilizing tungsten or depleted uranium, if required. Provision has also been made for a future option of actively or passively cooled PC system. At present, only the passively cooled configuration is available.

At the beginning of the computer analysis, system parameters that may be varied during the optimization procedure must be given initial values (see Figure 9-2). Thereafter, they are varied by the program automatically. The optimization parameters are those variables which must be designated, or assumed in system or component design procedures in order to compute, in closed form, the operating characteristics of the system. They include:

- a. Shield half angle
- b. Heat exchanger effectiveness*
- c. Main radiator area ratio
- d. Cross sectional area of the low voltage cable
- e. Cross sectional area of the reactor electrical lead
- f. Heat rejection surface area of low voltage cable
- g. PC radiator fin thickness
- h. Reactor loop pipe diameter
- i. Main radiator loop pipe diameter*
- j. Shield loop pipe diameter**
- k. Auxiliary cooling loop pipe diameter
- l. PC loop pipe diameter**
- m. Reactor coolant temperature rise
- n. Ratio, main radiator flow rate-to-reactor flow-rate

* Applies only to a dual loop configuration

** Applies only if pertinent subsystem is actively cooled

- o. Shield coolant temperature rise*
- p. Auxiliary loop coolant temperature rise
- q. PC loop coolant temperature rise*

Any of these optimization parameters may be held constant for a given system calculation by an appropriate input designation.

The design calculation, which can be followed on Figure 9-2, is initiated by determining the characteristics of the reactor type selected for the given input conditions. Length, diameter, weight, coolant weight and size of equipment bay are the dimensional characteristics computed. Performance conditions determined include the output voltage and current, the coolant flow rate and pressure drop, and the optimum cesium temperature. The code then enters the cesium model where the thermal, nuclear and electrical inputs to the cesium reservoir are computed and the cesium radiator size and weight is determined.

The design sequence is focused next on the shield system. The thickness, diameter, volume and weight of the basic neutron shield are calculated along with the total integrated heating rate. If the passive cooling mode is selected, the required heat rejection area is determined. If the active cooling mode is to be used, the dimensions and conditions in the shield cooling passages, coolant loop and shield radiator are computed. A shield layer is added to the rear face of the shield to make up for the voids introduced into the shield by the cooling passages.

The next step is the design of the main heat rejection system, which is affected, in a major way, by the relative radiator location and the loop configuration selected. If the PC radiator is forward, then a preliminary estimate of its size is made to allow the calculation of the radiator feed line length. If the main radiator is forward, then the radiator feed line length can be calculated directly.

*Applies only if pertinent subsystem is actively cooled

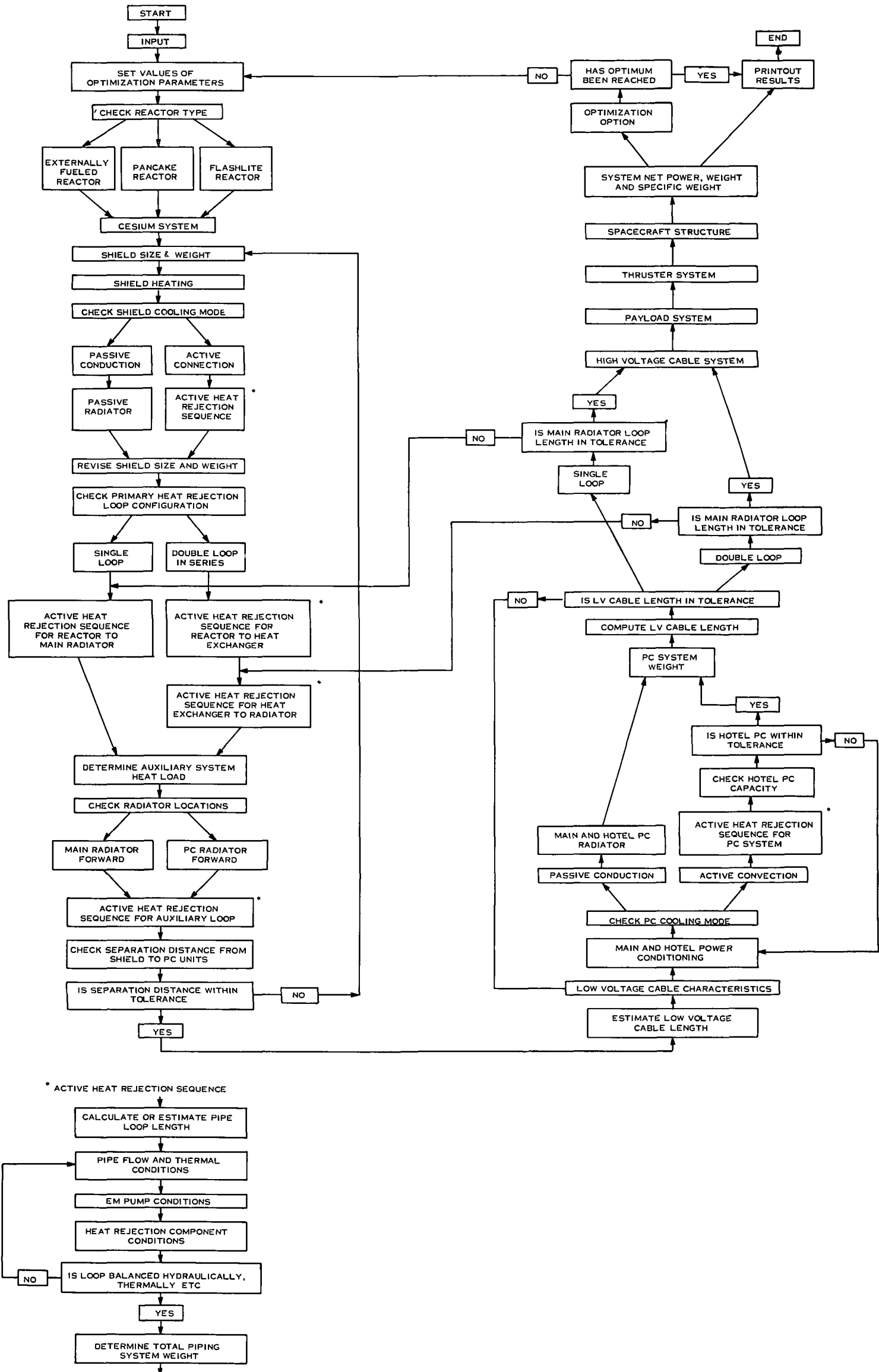


Figure 9-2. Calculation Sequence of Computer Program

As shown on Figure 9-2, the design of a single loop configuration is accomplished by applying the active heat rejection design sequence to a reactor-piping-main radiator loop. If a double loop configuration is employed, then the active heat rejection sequence is applied twice; first to the reactor-piping-heat exchanger loop and then to the heat exchanger-piping-main radiator loop. This design sequence is diagrammed at the bottom of Figure 9-2.

With the completion of the main heat rejection system design, all the auxiliary cooling loads are defined, and the auxiliary cooling loop can be calculated. The length of the auxiliary loop piping is computed as a function of the relative radiator location and the active heat rejection sequence is used for this system delineation.

As noted earlier in this section, the completion of the auxiliary cooling loop allows calculation of the separation distance between the shield and the power conditioning modules. (This is only necessary when the main radiator is located directly behind the shield. If the PC radiator is forward then the separation distance is an invariant distance of about 3 feet.) If the actual separation distance differs from the "built-in" code guess of 25 feet by more than a selected tolerance, then the computed separation distance is assumed, and the calculation sequence returned to the shield model (and the succeeding models) for recalculation.

The average length of the low voltage cable depends on the area of the passive power conditioning radiator whose size is influenced by the low voltage cable electrical losses, which in turn, are a function of the cable length. So an initial guess is made of the cable length, based on an estimated PC radiator size. The cable thermal conditions and electrical losses are determined in the cable model along with the power input to the power conditioning equipment. The PC model then computes the efficiency, weight, electrical output and thermal heat rejection of the main and hotel PC modules. Only the passive conduction cooling mode is available for the PC equipment, although provisions for future inclusion of an actively cooled sequence have been made, as

indicated on Figure 9-2. A PC radiator model computes the fin efficiency, overall area and weight of the PC radiator. Then the length of an average low voltage cable to the midpoint of the PC radiator is computed and compared with the previously estimated length. The calculation sequence is returned to the low voltage cable model, as shown on Figure 9-2, if the length difference exceeds the designated tolerance.

After cable length convergence has been achieved, the acceptability of the main radiator loop piping length is tested. If iteration is required, the calculation sequence is returned to the appropriate location depending on the loop configuration.

A high voltage cable model computes the length, weight, heat rejection area and electrical losses of the cable carrying the output of the power conditioning modules to the thrusters. The weight of the payload has been fixed at one metric ton, but the fraction of that weight contributed by the payload radiator and the spacecraft system control units are computed in the payload model, along with the area of the payload radiator. Similarly, the weights of the thruster units are fixed, but the weight of the thruster power conditioning, plus the size and weight of the corresponding thruster PC radiator are determined in the thruster model as a function of the input electric power.

The total weight of the spacecraft structure required to support the power plant, and to integrate the vehicle with the booster has been determined by separate analysis (See Subsection 5.2). A structure model in the computer code determines, as a function of relative radiator location, the additional weight of longerons, support rings and metal skin that must be added to the main heat rejection radiator and all the PC radiators in order to meet the overall structure requirements. In addition, the fixed weight of the booster adapter, and the loss in payload weight caused by the need of a flight fairing around the spacecraft at launch, are added to the "structure" weight of the vehicle.

The final calculations determine the total weight of the spacecraft less the propellant and its tankage, the net power to the thruster system and the ratio of the two; the weight per unit net power. The last value, the system specific weight, is the parameter that is minimized when the optimization option is utilized.

9.1.1 REACTOR MODELS

Reactor models were generated for use with the spacecraft weight optimization code for the externally fueled diode reactor and the flashlight reactor. No model was generated for the pancake reactor.

The key independent (input) parameters were the maximum coolant outlet temperature, T_{Cmax} , °F, and the reactor coolant temperature rise, ΔT , °F. Initially, all models were based on the 300 kWe gross EOM reactor characteristics reported in Subsection 3.3. As the spacecraft optimization proceeded, it was found that about 318 kWe gross would be required from the flashlight reactor, in order to provide the necessary 240 kWe conditioned power to the thruster units. Similarly, and because of the lower electric losses discussed in Section 8, only 274 kWe gross were required for the externally fueled reactor, to provide the 240 kWe to the thruster units. Fairchild/Hiller provided a new set of data, also presented in Subsection 3.3, to define the reactor at this lower power level. Conversations with General Electric Company personnel at the Nuclear Thermionic Power Operation (NTPO) indicated that the additional power could be provided by increasing the emitter temperature 10° to 15°K. Since the data provided for the flashlight reactor was based on an emitter temperature of 1950°F, less than the maximum allowable of 2073°K for this study, this solution was accepted. Therefore, only one reactor model was developed for the flashlight reactor, based on the data of Table 3-5.

The key dependent (output) variables provided by the reactor models are:

- a. Number of parallel loops

- b. Coolant pressure loss in the reactor
- c. Reactor diameter
- d. Reactor length
- e. Reactor weight
- f. Reactor voltage and current
- g. Thermal power to coolant
- h. Coolant flow rate in reactor
- i. Coolant weight in reactor
- j. Optimum cesium temperature.

9.1.1.1 Externally Fueled Diode Reactor Model

The externally fueled diode reactor model employed a simple table lookup and interpolation routine which operated directly on the data presented on Tables 3-1 and 3-2. As a function of the input values of maximum coolant temperature and temperature rise, the following parameters are calculated:

- a. Reactor voltage
- b. Thermal power to coolant
- c. Reactor diameter
- d. Reactor weight
- e. Coolant flow rate
- f. Coolant pressure drop in core

The electric current is calculated from the gross electric power, and the calculated voltage. The coolant weight in the reactor is constant at 75 pounds. Other constants include the reactor length at 20 inches, the optimum cesium reservoir temperature

at 630°K, and the maximum emitter temperature at 2073°K. A constant length of 2 inches was also added to the reactor length to allow for attachment to the spacecraft.

All calculations were made for a single loop system, with NaK-78 coolant.

9.1.1.2 Flashlight Reactor Model

The flashlight reactor model employs a set of equations generated from the data of Table 3-5. These equations and their limitations are presented below.

Coolant pressure loss in the reactor is seen to be a function of the maximum coolant temperature, T_{Cmax} and the coolant temperature rise. This parameter is expressed by the relation

$$\Delta p \text{ (psia)} = 3.7 + 0.128 \times 10^{-4} (T_{Cmax} \text{ (}^\circ\text{F)} - 1350)^2 + 0.8 \left(\frac{\Delta T \text{ (}^\circ\text{F)} - 180}{180} \right)$$

and is valid over the range

$$1100^\circ\text{F} \leq T_{Cmax} \leq 1600^\circ\text{F}$$

$$180^\circ\text{F} \leq \Delta T \leq 360^\circ\text{F}$$

The reactor diameter is found to be a function of only the coolant pressure loss and temperature rise. This parameter is given by the relation

$$D_R \text{ (inches)} = 28.8 - 0.8 \left(\frac{\Delta T \text{ (}^\circ\text{F)} - 180}{180} \right) - 0.4 \left(\frac{\Delta p \text{ (psia)} - 3.7}{2.3} \right)$$

which is valid over the range

$$180^{\circ}\text{F} \leq \Delta T \leq 360^{\circ}\text{F}$$

$$3.7 \text{ psia} \leq \Delta p \leq 6.0 \text{ psia}$$

The reactor weight is found to be a function of the same two variables, and is given by the relation

$$\begin{aligned} W_R \text{ (pounds)} = & 2960 + 80 \left(\frac{\Delta T (^{\circ}\text{F}) - 180}{180} \right) \\ & + 40 \left(\frac{\Delta p \text{ (psia)} - 3.7}{2.3} \right) \end{aligned}$$

which is valid over the same range as for the reactor diameter.

The reactor terminal voltage is found to be a function of T_{Cmax} and ΔT only, and is given by the relation

$$\begin{aligned} V \text{ (volts)} = & 15.70 - 0.533 \times 10^{-4} (T_{Cmax} (^{\circ}\text{F}) - 1350)^2 \\ & - 3.2 \left(\frac{\Delta T (^{\circ}\text{F}) - 180}{180} \right) \end{aligned}$$

which is valid over the range

$$1100^{\circ}\text{F} \leq T_{Cmax} \leq 1600^{\circ}\text{F}$$

$$180^{\circ}\text{F} \leq \Delta T \leq 360^{\circ}\text{F}$$

The thermal power to the coolant is found to be a function of T_{Cmax} and ΔT only, and is given by the relation

$$\begin{aligned} Q_{th} \text{ (kWt)} = & 2170 + 0.8 \times 10^{-2} (T_{Cmax} (^{\circ}\text{F}) - 1350)^2 \\ & + 510 \left(\frac{\Delta T - 180}{180} \right) \end{aligned}$$

which is valid over the same range as specified for the reactor terminal voltage.

The coolant flow rate is given by the relation

$$W(\text{lbs/sec}) = \left[0.02495 Q_{\text{th}} (\text{kWt}) \right] \left[180/\Delta T (^{\circ}\text{F}) \right]$$

which is valid over the range

$$180^{\circ}\text{F} \leq \Delta T \leq 360^{\circ}\text{F}$$

The electric current for each of the 108 TFE pairs is readily calculated from the gross electric power and the voltage computed above. The coolant weight in the reactor, required in part to calculate accumulator weights, is constant at 133 pounds of NaK-78. The optimum cesium temperature is constant at 640°F.

The area of the cesium reservoir facing the shield, required to assess thermal radiation heat transfer into the shield, is constant at 2.2 square feet. The length of the equipment bay to accommodate the coolant flow headers, the electric leads, and the cesium reservoir is constant at 16 inches, including a 4 inch allowance for the headers.

All calculations were run for a two loop system, using NaK-78 in both loops.

9.1.2 SHIELD MODEL

The shield model is based on the shield analysis described in Section 6. A neutron shield thickness of 62.5 centimeters and a mercury tank thickness of 25 centimeters is required to achieve the desired dose limits at a receiver location 3 feet from the rear face of the mercury tank. During the Phase I investigations, the reactor power levels are varied between 10 and 20 percent around the 300 kWe value, but the corresponding slight changes in shield thickness are neglected.

The required shield thickness will change primarily with the variation in receiver point separation distance from the shield rear face. An equation describing the spatial

variation of neutron flux along the axial normal to a theoretical disc radiation source is used to estimate the corresponding thickness of the neutron shield. The equation, which assumes a cosine distribution for the angular variation of emanating neutrons is as follows:

$$\frac{\phi(Z)}{\phi(0)} = 1 - \frac{1}{(1 + a^2/Z^2)^{1/2}}$$

where $\phi(Z)/\phi(0)$ = the ratio of the neutron flux at any axial location Z to the flux at the disc center.

a = the radius of the disc source.

Using the data of Section 6, the neutron flux within the shield, at any distance \pm from the shield front face is:

$$\log_{10} \phi(t) = 11 - .0804 t \text{ neutron/cm}^2\text{-sec.}$$

and the flux at the rear face of a neutron shield having a thickness of 24 inches is 8.75×10^5 n/cm²-sec. The neutron flux required at the rear face of a neutron shield to produce the desired flux level at any separation distance Z is described by the following ratio:

$$\frac{\phi(t)}{8.75 \times 10^5} = \frac{\phi(\text{nom})}{\phi(Z)}$$

where $\phi(\text{nom})$ is the neutron flux at the nominal receiver point location of 3 feet from the mercury tank rear face used in the analysis of Section 6. Substituting the pertinent equations above for $\phi(\text{nom})$ and $\phi(t)$ and solving, the required thickness of neutron shield in feet is

$$t = 2.445 + 0.408 \log_{10} \phi(Z)$$

9.1.2.1 Shield Heating

The internal heat generation rates in the shield, both by gammas and neutrons, are presented in Section 6. Gamma heating which provides approximately two-thirds of the total heat, decreases exponentially through the shield as described by the following equation;

$$q_{\gamma}(t) = q_{\gamma}(0) (.0667)^{.02t}$$

where $q_{\gamma}(t)$ = shield gamma heating rate in watts/cm³ at t

t = axial distance from shield front face, in centimeters.

The total gamma heating, q_{γ} , is determined by performing the following integration;

$$q_{\gamma} = \int_0^V q_{\gamma}(t) dV = \int_0^t q_{\gamma}(t) \left(\frac{dV}{dt} \right) dt$$

where V is the shield volume. Designating r_1 as the radius of the shield front face and θ as the shield half angle, $\frac{dV}{dt}$ becomes

$$\frac{dV}{dt} = \pi (r_1^2 + 2 r_1 t \tan \theta + t^2 \tan^2 \theta)$$

Making the following definitions;

$$S_1 = \pi r_1^2$$

$$S_2 = 2 \pi r_1 \tan \theta$$

$$S_3 = \pi \tan^2 \theta$$

$$S_7 = \frac{q_{\gamma}(t)}{q_{\gamma}(0)} = S_4 S_5 t$$

$$S_6 = S_5 \ln S_4$$

substituting in the integral equation and solving, the total gamma heating rate is

$$q_{\gamma} = \frac{q_{\gamma}(0)}{S_6} \left\{ S_1 (S_1 - 1) + S_2 \left[S_7 \left(t - \frac{1}{S_6} \right) + \frac{1}{S_6} \right] \right. \\ \left. + S_3 \left[S_7 \left(t - \frac{1}{S_6} \right)^2 + \frac{(S_7 - 2)}{S_6^2} \right] \right\}$$

The parameters S_1 , S_2 , S_3 and S_7 vary with shield dimensions while S_4 , S_5 and S_6 are only functions of the exponential decrease in gamma heating. For the data of Section 6,

$$S_4 = 0.0667$$

$$S_5 = 0.02$$

$$S_6 = -0.0541$$

$$q_{\gamma}(0) = 0.006 \text{ watts/cm}^3$$

The neutron heating rate decreases sharply with shield thickness, so that only the heat generated in the first ten centimeters is significant. The total neutron heating, q_n , is computed by summing the products of neutron heating rate and shield volume for two centimeter thick segments of shield as follows:

$$q_n = \sum_{i=1}^{i=5} q_n(i) V(i)$$

where $q_n(i)$ and $V(i)$ are the neutron heating rates and volumes, respectively, of the individual "slices" of neutron shield.

The total nuclear shield heating is the sum of q_{γ} and q_n .

9.1.2.2 Shield Cooling

For an actively cooled shield, a cooling passage of radius "a" is assumed to cool a surrounding annular section of shield having an outer radius of "b". The cooling passages are in parallel array in the front one-foot thick section of the neutron shield. An "averaged" volumetric heating rate is used by assuming that the total shield heating is uniformly distributed in the front one-foot thick section of the shield.

The temperature drop from radius "b" to radius "a" is given by

$$T_b - T_a = \frac{q a^2}{2k} \left[\left(\frac{b}{a}\right)^2 \ln \left(\frac{b}{a}\right) - \frac{1}{2} \left(\frac{b}{a}\right)^2 - 1 \right]$$

where q = averaged shield volumetric heating rate
 k = neutron shield thermal conductivity

In the above equation, everything except the ratio b/a is known. The maximum allowable shield material temperature, T_b , and the maximum shield coolant temperature, T_a , are program input values. The diameter of the shield cooling passage is designated for any one calculation and the thermal conductivity of lithium hydride is 3 Btu/hr-ft-F for the shield temperatures of interest. The above equation is solved for the ratio b/a by iteration.

To determine the approximate number of rows of cooling passages, the passages are assumed to be in triangular array. Then the number of rows, N , is determined from the equation

$$\frac{(N-1)(2b)}{0.866} + 2b = \text{CLSD}$$

where "b" is still the outer radius of shield area assigned to one cooling passage and CLSD is the cooled thickness of shield.

Solving for N,

$$N = .144 + \frac{10.4 \text{ (CLSD)}}{2a \text{ (b/a)}}$$

where CLSD is in feet and "a" is in inches. The total length of cooling passages in the shield is estimated by

$$L = \frac{576}{\pi} \frac{V_1}{a^2 \left(\frac{b}{a}\right)^2}$$

where V_1 is the volume of the cooled section of shield in ft^3 .

9.1.2.3 Revised Shield Thickness and Weight

Shield material is added to the rear face of the neutron shield to makeup for the voids introduced by the cooling passages. The additional thickness is equal to the diameter of a cooling passage multiplied by the number of passage rows which align axially.

The number of aligned rows is given by

$$N_a = \frac{N}{(b/a)}$$

so that the additional shield thickness required t_a , in feet is

$$t_a = \frac{aN_a}{6}$$

The total volume of shield material is that corresponding to the total shield thickness, $t + t_a$, less the volume of the cooling passages, as follows;

$$V_{SD} = \pi (t + t_a) \left[r_1^2 + r_1 (t + t_a) \tan \theta + \frac{(t+t_a)^2}{3} \tan^2 \theta \right] - \frac{V_1}{(b/a)^2}$$

The effective density of the neutron shield material is .038 lbs/in³. Therefore, the shield weight is given by the relation:

$$Wt_{SD} = .038 (1728) V_{SD}$$

9.1.3 HEAT EXCHANGER MODEL

The heat exchanger model is utilized in a double loop series coolant configuration where the heat exchanger transfers heat from the reactor cooling loop to the primary radiator loop. The model assumes identical heat transfer fluid on the hot and cold sides of the heat exchanger. (NaK-78 is this Phase I study) the option of using either a counterflow or a crossflow type heat exchanger is available.

To determine heat exchanger characteristics, the following parameters must be supplied to the model:

- a. Heat to be rejected, Q_{rej}
- b. Maximum and differential hot side temperature, T_{HI} and ΔT_H
- c. Hot and cold side flow rates, \dot{W}_H and \dot{W}_C
- d. Hot and cold side flow velocities, V_T and V_C
- e. Heat exchanger effectiveness, ϵ
- f. Tube inside diameter and wall thickness, d and Δt
- g. Number of passes on the cold side, NP

9.1.3.1 Crossflow Heat Exchanger

It is assumed that in the crossflow heat exchanger, the hot fluid will pass through the tubes and the cold fluid will be pumped through the shell section. Since the same fluid is used on the hot and cold sides, temperature drop on the cold side is calculated from:

$$\Delta T_c = \Delta T_h \times \frac{\dot{W}_H}{\dot{W}_C} .$$

and cold side inlet temperature is given by

$$T_{CI} = T_{HI} - \frac{T_c}{\epsilon}, \text{ when } \dot{W}_H > \dot{W}_C$$

$$\text{if } \dot{W}_H < \dot{W}_C \quad T_{CI} = T_{HI} - \frac{T_H}{\epsilon}, \text{ when } \dot{W}_H < \dot{W}_C$$

In subsequent calculations, thermodynamic properties of the heat transfer fluid in each side is determined as a function of the mean temperature of the fluid in that side.

Total hot side flow area is

$$A_H = \frac{\dot{W}_H}{(\rho_F) (V_T)}$$

where ρ_F represents fluid density. Therefore, the number of tubes required on the hot side can be determined from

$$NT = \frac{A_H}{\left(\frac{\pi}{4}\right) d^2}$$

Heat transfer through the coolant boundary layer in the tubes can be represented by the empirical relationship.

$$Nu = 0.625 (Pr \quad Re)^{0.4}$$

where Nu, Pr, and Re refer to the Nusselt, Prandtl, and Reynolds' numbers, respectively. Expansion of this equation results in an expression for hot side film coefficient,

$$h_H \text{ (Btu/hr } ^\circ\text{F)} = 0.625 \left(\frac{k_F}{D}\right)^{0.6} (\rho_F C_P V_T)^{0.4}$$

in which k_F is thermal conductivity and C_P is specific heat of the fluid. Similarly, shell side heat transfer coefficient has been empirically determined to be:

$$h_c = \frac{k_F}{d + \Delta t} \left\{ 4.03 + 0.228 \left[\frac{(d + \Delta t) V_C \rho_F \times C_p}{k_F} \right] \right\}^{0.67}$$

Overall heat transfer coefficient is consequently given by

$$U = \left[\frac{1}{h_T} + \frac{\Delta t}{K} + \frac{1}{h_C} \right]^{-1}$$

where K is thermal conductivity of the tube material.

Therefore, the required heat transfer area on the hot side is calculated from

$$A_{HT}(\text{ft}^2) = \frac{Q_{rej}}{(U) (\Delta T_m)}$$

where ΔT_m is the logarithmic mean temperature difference between the hot and cold side fluids. Tube length can then be calculated by

$$L_t (\text{ft}) = \frac{A_{HT}}{(\pi d) (NT)}$$

and by application of the Fanning equation, total pressure drop on the hot side is obtained:

$$\Delta_{P_H} (\text{LB/ft})^2 = \frac{0.092 \mu^{0.2} \rho_F^{0.8} V_H^{1.8} L_T}{g d^{1.2}}$$

where μ is fluid viscosity, and g is the sea level gravitational constant. Since a square heat exchanger has been assumed, the number of tubes in a row is given by

$$NTR = (NT)^{1/2}$$

and total cross-sectional area is, thereby,

$$A_X (\text{ft}^2) = \frac{L_T \times (d + \Delta t) \times NTR}{NP} + AC$$

in which cold side flow area is

$$A_C \text{ (ft}^2\text{)} = \frac{\dot{W}_c}{\rho_F \times V_C}$$

Pressure drop on the cold side is represented by

$$\Delta P_C \text{ (LB/ft}^2\text{)} = \frac{\rho_F^F V_C^2 \text{ (NTR)}}{2g}$$

where the friction factor, f , is estimated by:

$$f = \left[0.23 + \frac{0.11}{(XT-1)^{1.05}} \right] \left[\frac{(d + \Delta t) \dot{W}_c}{\mu A_c} \right]^{-0.15}$$

and XT is the ratio of tube pitch to outside diameter for the case of triangular tube spacing.

The width of the heat exchanger is calculated by

$$W(\text{ft}) = (\text{NTR} + 1) \left[\frac{A_c \times \text{NP}}{L_t} + (d + \Delta t) \right]$$

Then, the weight of the fluid is

$$W_{FC}(\text{LB}) = \rho_F \left[L_T \times w^2 - \frac{(\text{NT}) (\text{LT}) \pi (d + \Delta t)^2}{4} \right]$$

on the hot side. The weight of the tubes is given by

$$W_T(\text{LB}) = \rho (\text{NT}) (\text{LT}) \frac{\pi}{4} (\Delta t^2 + d \Delta t)$$

and the weight of the shell is

$$W_S(\text{LB}) = 5.2083 (4 L_T w + 2w^2),$$

which assumes a 0.125 inch thick shell of 500 lb/ft³ density.

To allow for support structure, the overall size of the heat exchanger is increased. The width of the heat exchanger is increased by 3.6 inches, and an assumed 15 percent allowance for hardware weight of the heat exchanger results in a total weight of

$$W_{TOT}(LB) = 1.15 (W_T + W_S) + W_{FC} + W_{FN}$$

9.1.3.2 Counterflow Heat Exchanger

Counterflow heat exchanger characteristics are determined by the crossflow heat exchanger model as described in Paragraph 9.2.3.1, except that the shell side flow parameters are replaced by those of tube flow. Therefore, only the differences in calculational procedure between the crossflow and counterflow type heat exchangers will be presented in this section.

The cold side coefficient is calculated from the relation

$$h_c(B+n/hr^\circ F) = 0.625 (K_F/d)^{0.6} (\rho_F C_p V_c)^{0.4}$$

which is the same relationship as derived for the hot side film coefficient in the crossflow heat exchanger. In addition, cold side pressure drop is expressed by

$$p_c(LB/ft^2) = \frac{(0.092)^{0.2} \rho_F^{0.8} V_c^{1.8} \times L_T}{g d^{1.2}}$$

Next, the weights associated with the cold side must be determined for the counterflow heat exchanger. Weight of fluid on the cold side is

$$W_{FC}(LB) = \rho_F \times L_T \times NT \times \frac{\pi}{4} d^2$$

where L_T , tube length, and NT , number of tubes correspond to the values calculated for the hot side. The width of the heat exchanger is calculated by

$$W(ft) = \left(\frac{4}{\pi} A_E\right)^{1/2}$$

where A_E , the area of the ends of the heat exchanger is given by

$$A_E \text{ (ft}^2\text{)} = A_c + \frac{\pi}{4} NT (d + .02)^2$$

Hardware weight of the cold side of the heat exchanger can thus be determined:

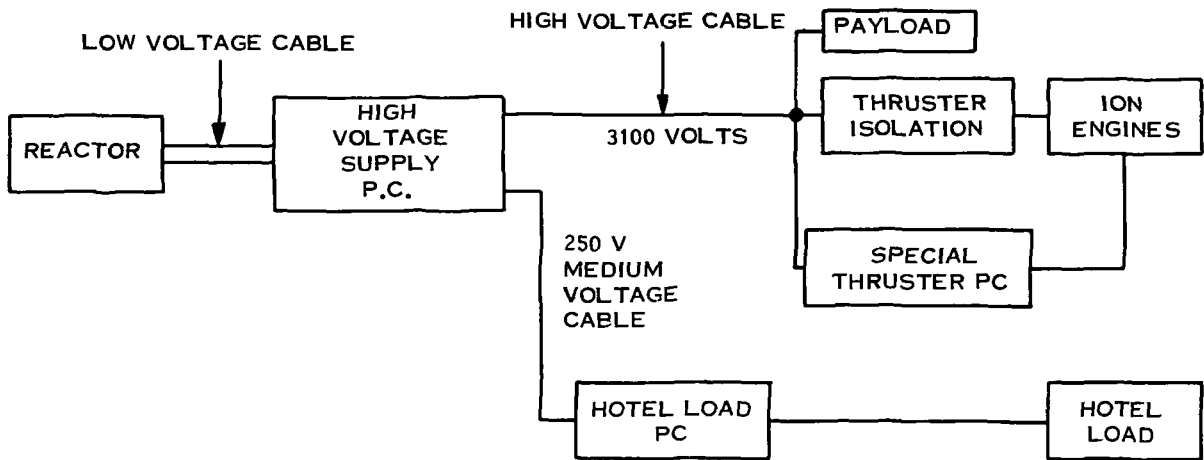
$$W_s \text{ (LB)} = 5.2083 (2 A_E + \pi w L_T)$$

The remainder of the calculations including total weight of the heat exchanger are accomplished as outlined in Paragraph 9.2.3.1 for the crossflow heat exchanger.

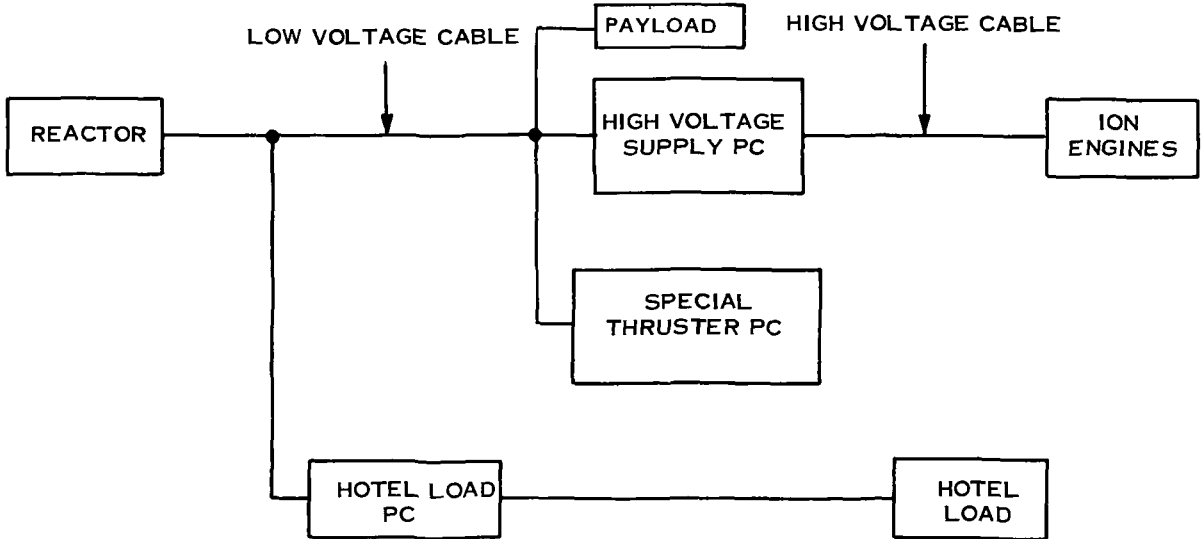
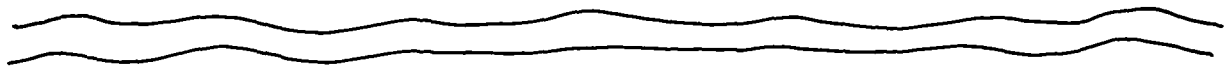
9.1.4 POWER CONDITIONING MODELS

There are essentially two power conditioning models in the computer code for each of the high and low voltage reactor types. This duplication is a basic part of the study resulting from the different voltage outputs characterized by the reactor types. Figure 9-3 shows in schematic form the assumed circuitry and relative placement of the individual PC modules for each of the reactor type systems. These assumed circuits differ slightly from those analyzed in Section 7 but the differences have negligible effect on the net power delivered to the thrusters. The following symbol definitions are used in the PC model:

PPE(X)	=	Pumping power of loop (X), kWe
PWR	=	Reactor power, kWe
PWYPL	=	Payload Power, kWe
Qei PC	=	Input power, high voltage supply PC, kWe
Qei HPC	=	Input power, hotel load PC, kWe
Qei HVC	=	Input power, high voltage cable, kWe
Qei PL	=	Input power, payload, kWe
Qei TR	=	Input power, ion engines, kWe
Qei STC	=	Input power, special thruster PC, kWe
Qeo PC	=	Output power, high voltage supply PC, kWe
Qeo HPC	=	Output power, hotel load PC, kWe



FLASHLIGHT REACTOR SPACECRAFT



EXTERNALLY-FUELED REACTOR SPACECRAFT

Figure 9-3. Electric Circuits Used in Computer Code

Q _{eo} HV	=	Output power, high voltage cable, kWe
Q _{LVPC}	=	Heat input, low voltage cable to PC, BTU/hr
Q _{TSPR}	=	Heat rejection, special thruster PC radiator, BTU/hr.
q (5)	=	Heat rejection, PC radiator, BTU/hr
q con	=	Power to reactor controls, kWe
q cs	=	Electrical power to cesium reservoir, kWe
fl	=	fractional loss in low voltage cable
fl HVC	=	fractional loss on high voltage cable
η _{pc}	=	P. C. efficiency
η _{pc} HP	=	Hotel PC efficiency
v _r	=	Output voltage of the reactor
W _{tPC}	=	Weight of high voltage supply PC, lbs
W _{tHPC}	=	Weight of hotel P. C. , lbs
W _{tSPC}	=	Weight of special thruster P. C. , lbs

9.1.4.1 Flashlight Reactor PC Model

The power input to the high voltage supply PC is:

$$Q_{ei\ PC} = PWR (1 - fl)$$

and the corresponding power output is:

$$Q_{eo\ PC} = Q_{ei\ PC} \times \eta_{PC}$$

where $\eta_{PC} = 0.882$ for the voltage level of the flashlight reactor. The hotel load is the sum of the power needed for power plant pumping, reactor controls and cesium reservoir, as follows:

$$Q_{eo\ HP} = q\ con + q\ cs + \sum PPE (X)$$

The corresponding input power to the hotel load PC unit is:

$$Q_{ei\ HP} = Q_{eo\ HP} / \eta_{PC\ HP}$$

where $\eta_{PC\ HP} = .85$

On the high voltage supply output, the input and output power to the high voltage cable are:

$$Q_{eiHVC} = Q_{eoPC} - Q_{eiHP}$$

$$Q_{eoHVC} = Q_{eiHVC} (1 - f_{L,HVC})$$

The payload power is:

$$Q_{ei PL} = 1.0 + P_{WYPL}$$

where the spacecraft and power plant controls systems are assumed to require 1.0 kw.

The input power to the ion engines is:

$$Q_{ei TR} = \frac{Q_{eo HV} - Q_{ei PL} - 1.25}{1 + \frac{17}{223}}$$

and the input power to the special thruster PC units is:

$$Q_{ei STC} = \frac{17}{223} Q_{ei TR}$$

The power to the thruster isolation unit is a constant 1.25 kW.

The heat rejection for the main PC radiator is the sum of the heat generated in the high voltage supply PC, the hotel load PC and the heat leakage from the low voltage cable as follows:

$$q(5) = 3413 \left[(1 - \eta_{PC}) Q_{ei PC} + .15 Q_{ei HPC} \right] + Q_{LVPC}$$

The heat rejection from the special thruster PC radiator is:

$$Q_{TSPR} = 3413 \left[1.25 + 0.1 Q_{ei STC} \right]$$

where the 0.1 factor follows from the assumption of 90 percent efficiency for the special thruster PC units.

The PC weights are based on the analysis of Section 7. The weights of the high voltage supply PC, the hotel load PC and the special thruster PC are as follows:

$$WtPC = 10.72 Q_{ei} PC$$

$$WtHPC = 8.0 Q_{eo} HPC$$

$$WtSPC = \frac{272}{17} Q_{ei} SPC$$

9.1.4.2 Externally Fueled PC Model

The hotel load is the same as in the flashlight PC model, as follows:

$$Q_{eo} HP = q_{con} + q_{cs} + \sum PPE (X)$$

and the input to the hotel load PC is

$$Q_{ei} HP = \frac{Q_{eo} HP}{0.85}$$

where 0.85 is the efficiency of the hotel load PC unit. The payload power is also the same as before, namely,

$$Q_{ei} PL = 1.0 + PWYPL$$

The efficiency of the high voltage supply PC is given by the following relation which is based on the results presented in section 7.

$$\eta_{PC} = .7918 + 1.416 \times 10^{-3} \nu r - 3.46 \times 10^{-6} (\nu r)^2$$

Then the input power to the high voltage supply PC is

$$Q_{ei} PC = \left[PWR(1 - fL) - Q_{ei} HP - Q_{ei} PL \right] \left[1 - \frac{17}{223} \eta_{PC} \right]$$

where the second bracket term accounts for the power drawn by the special thruster PC devices. The output power from the high voltage supply PC is:

$$Q_{eo} PC = \eta_{PC} Q_{ei} PC = Q_{ei} HV$$

which is the same as the input to the high voltage cable. The output power from the high voltage cable, which is the same as the input to the thruster engine, is:

$$Q_{ei\ TR} = Q_{eo\ HVC} = Q_{ei\ HVC} (1 - f_{L\ HVC})$$

The input to the special thruster power conditioning is:

$$Q_{ei\ STC} = \frac{17}{223} Q_{eo\ HV}$$

The heat rejection from the main PC radiator and the special thruster PC radiator are as follows:

$$q(5) = 3413 \left[(1 - P_{PC}) Q_{ei\ PC} + .15 Q_{ei\ HPC} \right] + Q_{LVPC}$$

$$Q_{TSPR} = 3413 \left[0.1 Q_{ei\ STC} \right]$$

The weight of the high voltage supply PC is based on the analysis of Section 7 which showed that the weight varied with input voltage, as follows:

$$W_{tPC} = Q_{ei\ PC} \left[5.813 - 3.21 \times 10^{-3} \nu_r + 6.98 \times 10^{-6} \nu_r^2 \right]$$

The weights of the hotel load PC and the special thruster PC are the same as in the flashlite model, thusly,

$$W_{tHPC} = 8 Q_{eo\ HP}$$

$$W_{tSTC} = \frac{272}{17} Q_{ei\ STC}$$

9.1.5 MAIN RADIATOR MODEL

The main radiator model was developed with the use of the Spartan III radiator design computer code. Individual radiator designs were computed with the code for the following conditions:

1. Radiator inlet temperature range of 1050° to 1600°F
2. Coolant temperature drop varying from 180° to 360°F

3. An average heat rejection rate of 2125 kW
4. NaK-78 coolant composition
5. Copper-stainless steel radiator material
6. Sink temperature of 300°R (Average sink temperature for Jupiter mission)
7. Mission time of 20,000 hours
8. Radiator reliability of 0.95 using Volkoff's correction for a Jupiter mission
9. Pumping power weight penalty of 200 lb/kW
10. Surface emissivity of 0.9.

The radiator panel geometry was assumed to be the offset fin/tube design shown in Figure 9-4. This configuration is most compatible with a cylindrical radiator since the tube receives meteoroid "bumper" protection from the conducting fins. Using the geometry and the conditions listed above, minimum weight radiator cases were obtained by optimizing on the fin length, fin thickness and inside tube diameter, assuming a minimum allowable fin thickness of 0.03 inches and a minimum allowable tube diameter of 0.10 inches.

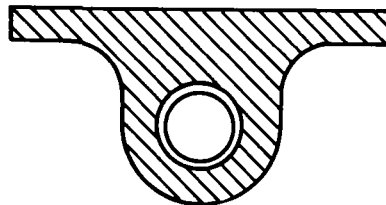


Figure 9-4. Offset Fin and Tube Configuration used in Main Radiator Design

The Spartan III results were plotted and correlated in equation form for use in the radiator model. Figures 9-5 and 9-6 present the weights and areas, respectively, for weight optimized radiators as a function of radiator inlet temperature and lines of constant coolant temperature drop. Each of the curves of constant coolant temperature drop was fitted with an exponential equation as follows:

$$W_{180} = \text{EXP} [10.314 - .001455 T_B - 1.2976 \times 10^{-6} T_B^2 + 5.8968 \times 10^{-10} T_B^3]$$

$$W_{270} = \text{EXP} [12.883 - .006959 T_B + 2.885 \times 10^{-6} T_B^2 - 5.1329 \times 10^{-10} T_B^3]$$

$$W_{360} = \text{EXP} [14.185 - .009552 T_B + 4.91 \times 10^{-6} T_B^2 - 1.08 \times 10^{-9} T_B^3]$$

$$A_{180} = \text{EXP} [8.67 + .001565 T_B - 3.968 \times 10^{-6} T_B^2 + 1.2233 \times 10^{-9} T_B^3]$$

$$A_{270} = \text{EXP} [6.5188 + .006817 T_B - 7.777 \times 10^{-6} T_B^2 + 2.102 \times 10^{-9} T_B^3]$$

$$A_{360} = \text{EXP} [7.2935 + .005459 T_B - 6.685 \times 10^{-6} T_B^2 + 1.7837 \times 10^{-9} T_B^3]$$

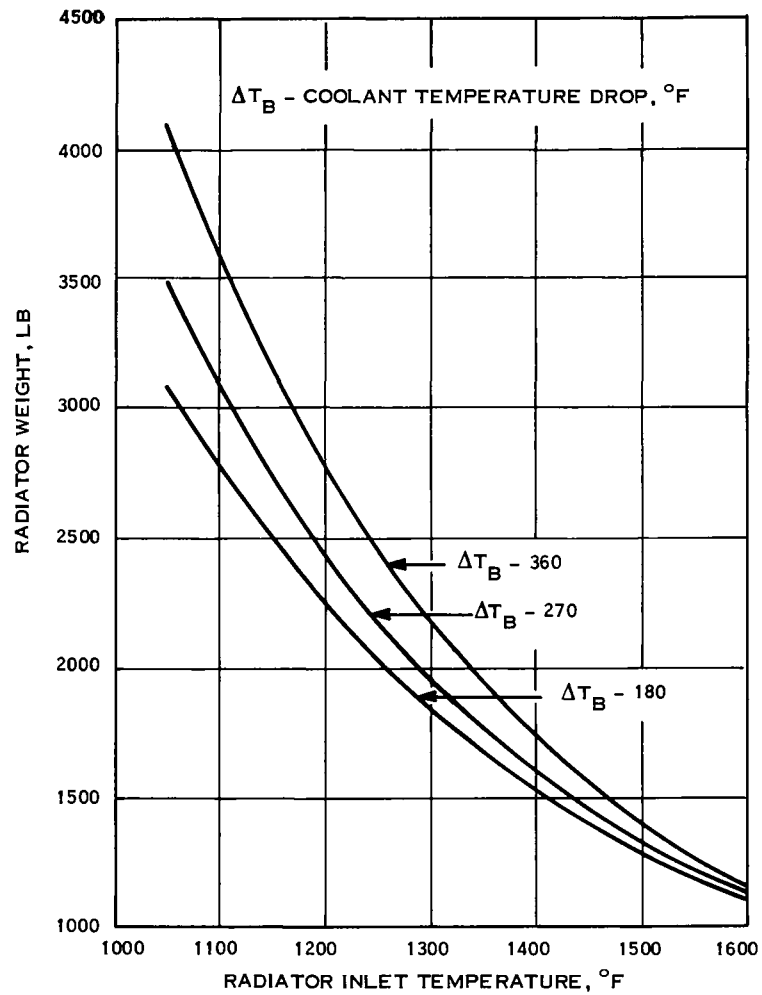


Figure 9-5. Main Radiator Weight

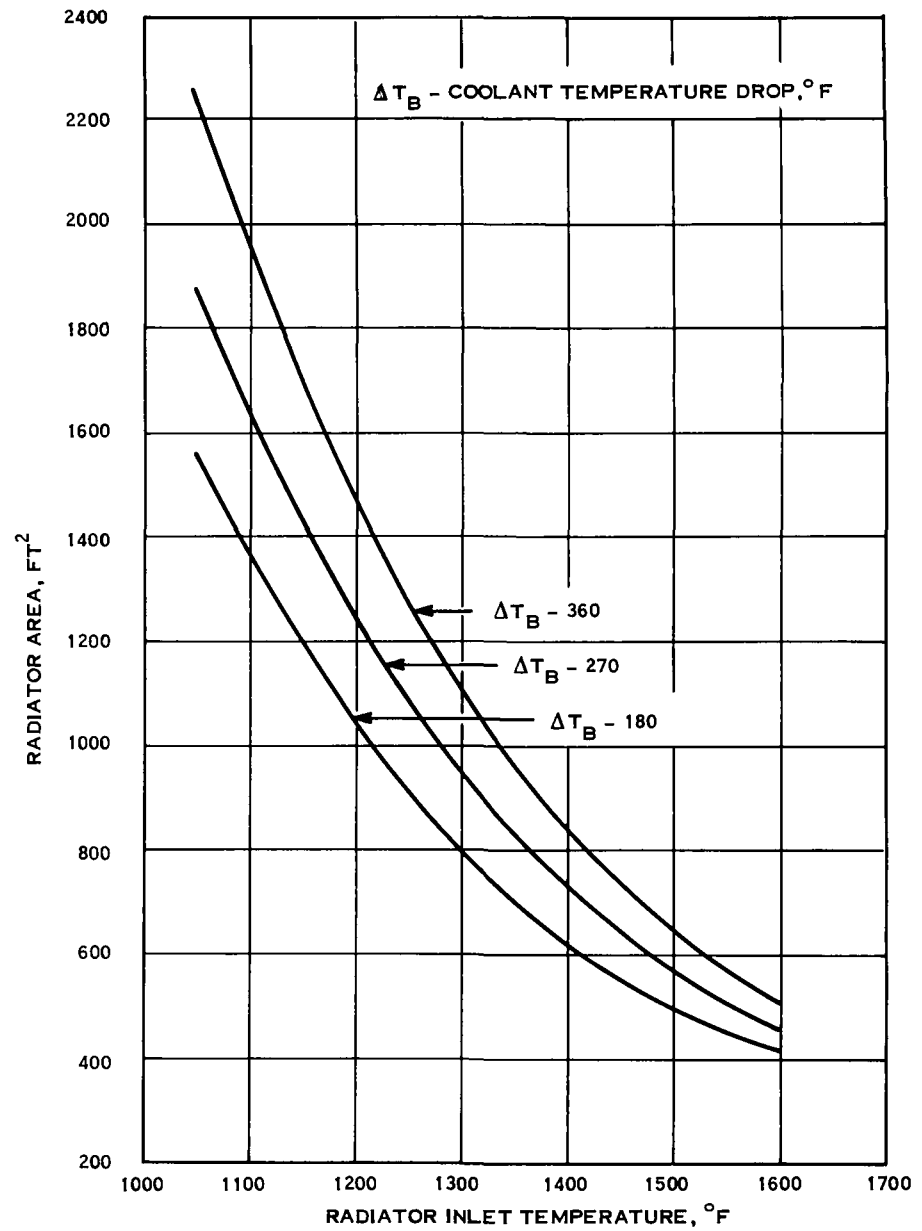


Figure 9-6. Main Radiator Area

where W_X and A_X designate weight and area, respectively, for a coolant temperature drop of X , T_B is the radiator coolant inlet temperature, and the term in brackets is the exponential factor applied to e , the base value for the natural system of logarithms. These equations form the basis for the radiator weight and area calculation in the radiator model.

For ΔT_B (coolant temperature drop) values intermediate to the 180°, 270° and 360°F curves, linear interpolation is used to estimate the desired weight and area. For ΔT_B ' values less than 180°F, the values corresponding to 180°F are assumed. For ΔT_B ' values greater than 360°F, linear extrapolation is used assuming the same variation as exists between the 270° and 360°F ΔT_B values.

The Spartan III radiator code was also used to generate area limited radiator designs for the conditions of interest. An area-limited design is one in which the radiator is limited to some area less than the area calculated for the optimum weight design, for the same set of operating conditions. This area reduction can be attained by increasing the thickness of the radiator fin, thereby increasing its efficiency, and/or decreasing the fin length between radiator tubes. Both of these changes increase the weight of the radiator. Figure 9-7 shows the increase in weight for a given decrease in area for lines of constant ΔT_B . Both the weight and area ratios are applied to the values corresponding to the optimum weight design. The data shown on Figure 9-7 corresponds to a radiator inlet temperature of 1350°F. At both higher and lower radiator inlet temperatures, the calculated radiator weight ratios were lower than those shown on Figure 9-7 and were scattered which precluded correlation. So the data for 1350°F was used for all radiator inlet temperatures which means that the weights computed in the radiator model for area limited designs may be a few percent overweight.

As shown in Figure 9-7, the weight ratio increases more steeply as the area ratio is decreased. Theoretically, the curves approach an asymptotic value which corresponds

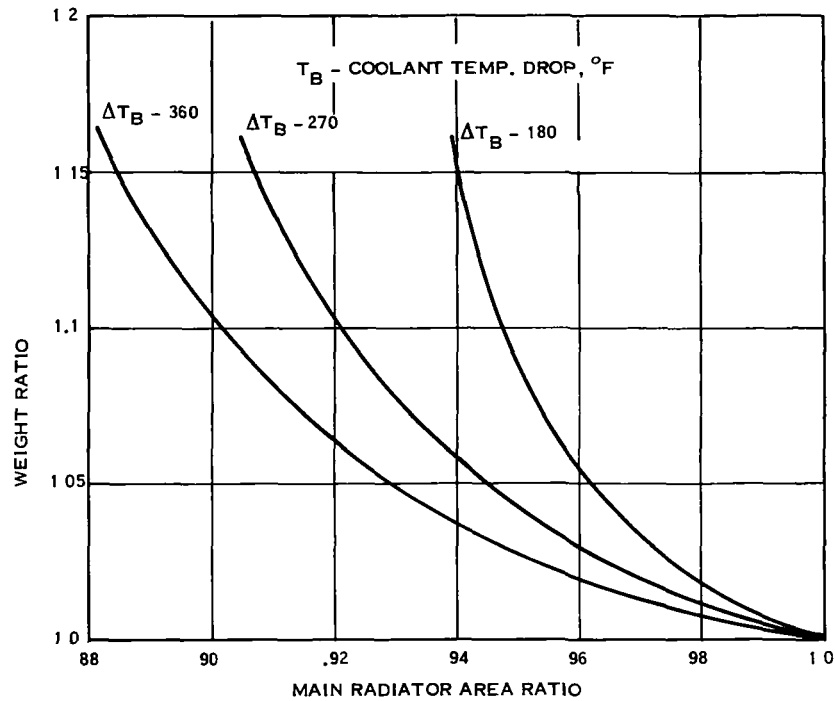


Figure 9-7. Weight Ratio of Area Limited Radiators

to the area needed when the radiator is made up only of tubes and no fins. Consequently, a practical limit on the minimum value of the area ratio exists for each value of ΔT_B . In order to factor in this restriction, and also be able to interpolate horizontally between the curves of Figure X-3, a two step procedure was formulated. For the desired value, of ΔT_B and area ratio, a pseudo-area ratio is calculated which, when applied to the 360°F ΔT_B curve, calculates the same weight ratio as the given set of ΔT_B and area ratio. The first step determines the pseudo area ratio and the second step computes the weight ratio. The equation for the pseudo area ratio, PA, is:

$$PA = A_R - [.93 (1-A_R)] \times \left[2 - \frac{\Delta T_B}{180} \right]^{1.15 + 14.25 (.98 - A_R)}$$

where A_R is the area ratio desired. The equation for the weight ratio, W_R , is an exponential relation as follows:

$$W_R = \text{EXP} [11.51 - 23.153 PA + 11.643 PA^2]$$

when PA is greater than 0.88. If PA is less than 0.88, then W_R is arbitrarily set at 10 to force the weight optimization of the spacecraft in the direction of higher area ratio values. The final weight and area of a radiator for a given radiator inlet temperature, coolant temperature drop and area ratio are:

$$W_T = W_{\Delta T_B} \times W_R \times \frac{q}{2125}$$

$$A = A_{\Delta T_B} \times A_R \times \frac{q}{2125}$$

where q is the desired heat rejection in kW_t .

The pressure drop in the main radiator is also calculated in the radiator model.

Figure 9-8 presents the pressure drops in weight optimized radiators as a function of radiator inlet temperature and coolant temperature drop. The change in pressure drop, expressed as a ratio, when the radiator is area limited is shown on Figure 9-9. The light lines on the latter figure represent various combinations of radiator inlet temperature and coolant temperature drop, while the heavy line is the average relation assumed in the model. An equation describing the $\Delta T_B = 360^\circ\text{F}$ line in Figure 9-8 is:

$$\Delta P_{360} = \text{EXP} \left[1.635 - .00171 T_B + 1.058 \times 10^{-6} T_B^2 + 4.233 \times 10^{-11} T_B^3 \right]$$

An equation for the pressure drop of any value of ΔT_B is:

$$\Delta P_{\Delta T_B} = \Delta P_{360} + (3.47 - 1.42 \times 10^{-3} T_B) \left(2 - \frac{\Delta T_B}{180} \right)^Y$$

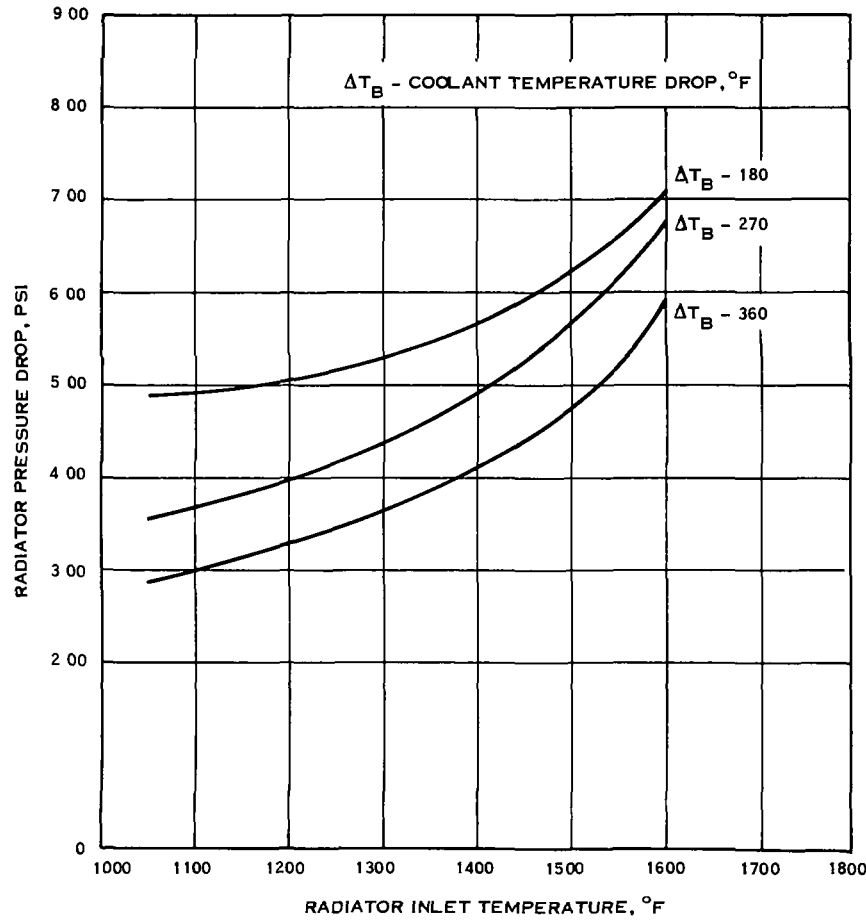


Figure 9-8. Main Radiator Pressure Drop

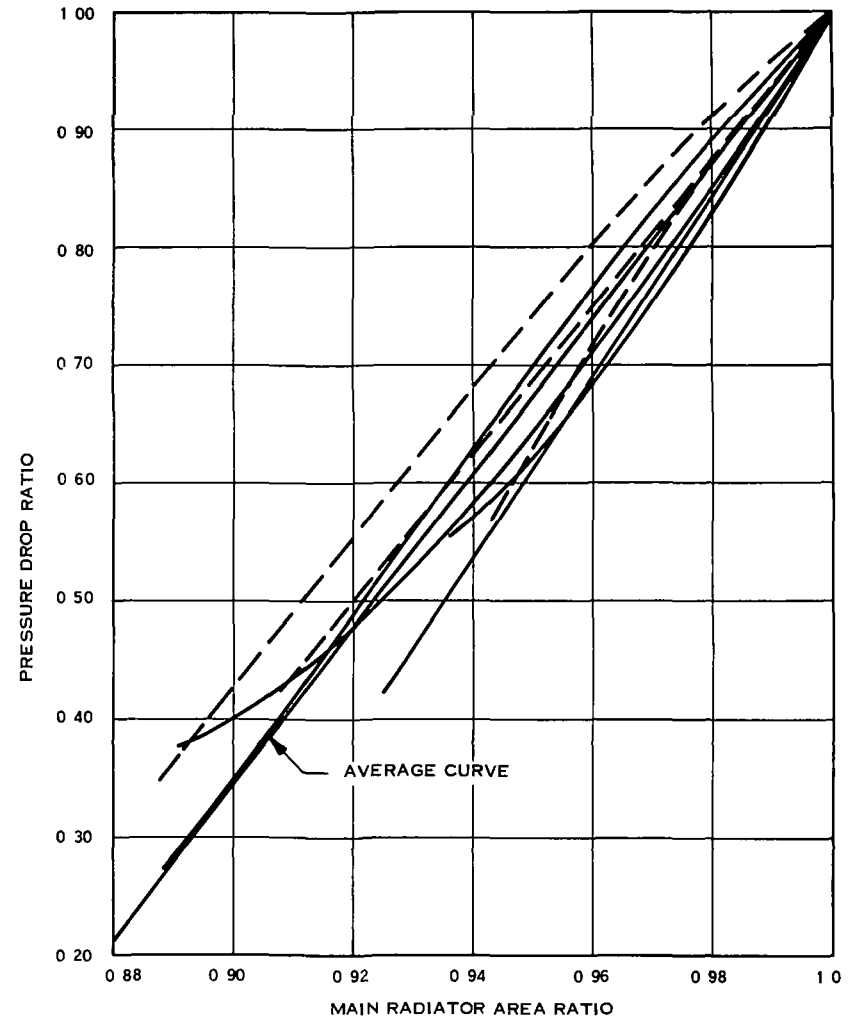


Figure 9-9. Pressure Drop Ratio in Area Limited Radiator

where the exponent Y is:

$$Y = 2.954 - 7.93 \times 10^{-4} T_B - 4.63 \times 10^{-7} T_B^2$$

The straight line relation for the average pressure drop ratio, P_R , of Figure 9-9 is described by the equation:

$$P_R = 6.6 (A_R - .88) + .21$$

Thus, the radiator pressure drop for a given set of conditions is determined by:

$$\Delta P = \left(\Delta P_{\Delta T_B} \right) \left(P_R \right)$$

The weight of the coolant inventory in the radiator as a function of radiator inlet temperature and coolant temperature drop is plotted in Figure 9-10. Since most of the coolant weight is in the header sections, the effect of area limitation on the coolant weight was ignored. The coolant weight is described by the following equations:

$$(\text{Coolant Wt})_{360} = 1062.2 - 1.048 T_B + 2.93 \times 10^{-4} T_B^2$$

$$(\text{Coolant Wt})_{\Delta T_B} = (\text{Coolant Wt})_{360} + (131.9 - .221 T_B + 1.254 \times 10^{-4} T_B^2)$$

$$\left(2 - \frac{\Delta T_B}{180} \right)^Z$$

where the exponent Z is:

$$Z = .91 + 2.47 \times 10^{-3} T_B - 1.3 \times 10^{-6} T_B^2$$

and T_B and ΔT_B are the radiator inlet temperature and the coolant temperature drop, respectively, as before.

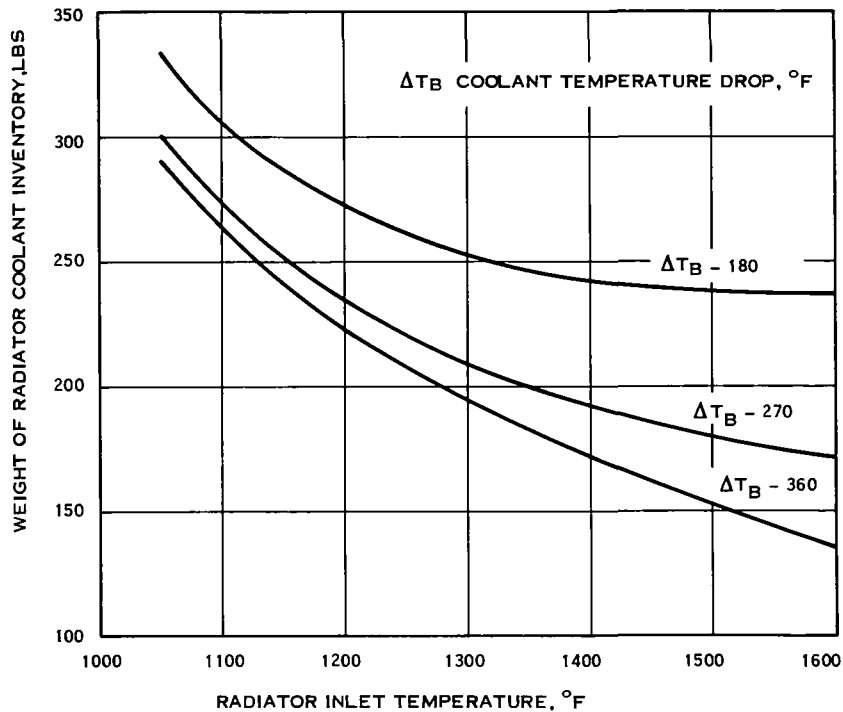


Figure 9-10. Weight of Coolant in Radiator

9.1.6 COOLANT LOOP MODELS

There are two coolant loop subroutines included in the program; PPNGI is used for the reactor loop and the main radiator loop while PPNG3 is used for the secondary cooling systems such as the shield and auxiliary loops. Most of the calculational procedure is identical for both subroutines but there are important differences, which will be described.

9.1.6.1 Main Loop Piping Model

The following parameters have known values at the time of entrance to PPNGI, the main loop piping model:

1. Coolant composition
2. Coolant temperature

3. Pipe ID
4. Total pipe length between heat source and heat sink
5. Coolant flow rate
6. Quantity of heat to be rejected by the loop

The piping model performs the following:

1. Estimates the pressure drop in the heat source and heat sink and calculates the piping pressure drop for a single circuit, if there are multiple loops in parallel.
2. Computes required pumping power and corresponding coolant temperature changes.
3. Calls the heat sink model (either the heat exchanger or main radiator) to obtain the calculated pressure drop for the conditions given.
4. Iterates until a pressure drop balance is obtained.
5. Computes weight of piping and auxiliary components for the set of balanced conditions.

The coolant mass velocity in the pipe is

$$G = \frac{\dot{W}}{\frac{\pi}{4} d^2}$$

for the given flow rate, \dot{W} and pipe diameter, d . The coolant Reynold's number is

$$R_e = \frac{dG}{\mu(Z, T)}$$

where μ , the coolant viscosity, is given as a function of coolant composition, Z , and temperature, T , in Appendix B. The pipe friction factor is

$$f = \frac{16}{Re}$$

for Reynold's number less than 2100 (laminar flow), and

$$f = .0575 \text{ Re}^{-0.2}$$

for Reynolds number greater than 2100. The pressure drop in the piping, in psf, is

$$\Delta P_P = 4.793 \times 10^{-9} \frac{G^2 f (L + \Delta L)}{dp(z, T)}$$

where

L = total pipe length

ΔL = length added to account for pressure drops in bends and fittings (see Appendix B).

$\rho(z, T)$ = density of coolant z at temperature T .

The total pressure drop in the pipe loop is

$$\Delta P_T = \Delta P_P + \Delta P_1 + \Delta P_2$$

where ΔP_1 is the known pressure drop in the pipe loop heat source and ΔP_2 is the estimated pressure drop in the pipe loop heat sink. If the piping loop being calculated is the reactor loop, then ΔP_1 is the pressure drop in the reactor and ΔP_2 is the pressure drop in the main radiator for a single loop configuration or the pressure drop in the hot side of the heat exchanger for a dual loop configuration. If the piping loop being calculated is the main radiator loop then ΔP_1 is the pressure drop in the cold side of the heat exchanger and ΔP_2 is the pressure drop in the main radiator. Estimates of ΔP_2 for the first pass through the piping model are given in Appendix B. If subsequent iterations are required to achieve a pressure drop balance, then the value of ΔP_2 is taken to be the calculated heat sink pressure drop in the previous iteration.

An EM pump model, see Paragraph 9.2.14, designates the pump weight and efficiency, maximum allowable pump temperature and fraction of electrical power removed by an auxiliary coolant, if present. The required electrical pumping power, in Btu/hr is

$$PPE = \frac{\dot{W}\Delta P_T}{778 \eta_P \rho(z, T)}$$

where η_P is the pump efficiency. If the temperature of the coolant being pumped is higher than the maximum allowable pump temperature then the heat added to the coolant at the pump is

$$\Delta q = PPE (1-CF)$$

where CF is the cooling fraction deposited in the auxiliary coolant. The total heat to be rejected in the heat sink, then is

$$q_T = q + \Delta q$$

and the required temperature drop in the heat sink is

$$\Delta T_T = \Delta T \left(\frac{q_T}{q} \right)$$

where q and ΔT are the known values of heat rejection and temperature change supplied by the pipe loop heat source.

At this point, the piping model calls the appropriate heat sink and retrieves the calculated heat sink pressure drop, $\Delta P_2'$ and uses it to determine the actual loop pressure drop as follows.

$$\Delta P_T' = \Delta P_P + \Delta P_1 + \Delta P_2'$$

It then compares the actual loop pressure drop, $\Delta P_T'$, with the estimated loop pressure drop ΔP_T , and if they do not agree within the desired tolerance, then

$\Delta P_T'$ becomes the estimated value and the calculation is returned to the EM pump model, and subsequent calculations, for iteration until the desired convergence is achieved.

The weight of coolant in the piping and the combined weight of the piping and coolant is determined directly, as follows;

$$WT_{COOL} = \left(\frac{\pi}{4}\right)d^2 L \rho (Z, T)$$

$$WT_{PIPE} = WT_{COOL} + \left(\frac{\pi}{4}\right) (d_o^2 - d^2) L \rho (y)$$

where d_o , the outer diameter of the pipe, is calculated by a pipe thickness function (see Appendix B) and $\rho (y)$ is the density of pipe material y .

An accumulator weight is estimated by determining the volumetric expansion of the total loop coolant inventory, assuming an internal volume for the accumulator 30% greater charging than the coolant expansion, assuming a configuration for the accumulator and assuming a 20% weight adder for the internal bellows. The total loop coolant weight is the sum of the piping coolant determined above, plus the coolant weights in the heat source and heat sink components. These latter coolant weights are determined in the respective models. The coolant volumetric expansion is

$$\Delta V = \text{Total Coolant Weight} \left[\frac{1}{\rho (Z, T)} - \frac{1}{\rho (Z, T_{amb})} \right]$$

where $\rho (Z, T_{amb})$ is the coolant density at an ambient temperature at time of charging the loop (assumed to be 100°F for NaK). The accumulator is assumed to be a right circular cylinder with diameter equal to length with additional hemispherical end caps. The volume of such a tank is equal to $\frac{5\pi}{12} D^3$ where D is the diameter of the tank.

Therefore D is

$$D = \left[\frac{12}{5\pi} \times 1.3 \Delta V \right]^{1/3}$$

The surface area of the tank is $2\pi D^2$ so the volume of tank wall material is $2\pi D^2 (tk)$ where tk is the tank wall thickness (assumed as 0.10 inches). Making the appropriate substitutions, and assuming a 20 percent weight added for the internal bellows, the net weight of the accumulator in pounds is

$$WT_{ACC} = \Delta V \rho (Z, T) + .0626 \rho (y) \Delta V^{2/3}$$

The weight of support brackets for the pipe loop is assumed to be 10 percent of the sum of the piping, accumulator and EM pump weights. The total piping loop weight is the sum of piping, pump, accumulator and bracket weights, multiplied by the number of loops in parallel.

9.1.6.2 Secondary Loop Piping Model

The secondary loop piping model, PPNG3, used for the shield loop and the auxiliary cooling circuit, differs slightly from PPNG1, the main loop model. The first difference is in the input parameters. In PPNG1, the coolant flow rate is known and constant and heat additions at the pump are accommodated by varying the temperature difference around the loop. The constant flow rate is required and specified by the reactor model and to a lesser extent, by the heat exchanger model. However, in the secondary loops, which have no special flow rate requirements, it is easier to specify a reasonable temperature drop around the loop and calculate the corresponding flow rate. Therefore, in PPNG3, heat additions to the loop at the pump are accommodated by changing the loop flow rate.

A second difference between PPNG1 and PPNG3 is in the nature of main loop and secondary loop conditions. In a main coolant loop, the pumping power is very small compared to the total heat transferred by the loop. In a secondary loop, however, the pumping power heat addition to the loop can be a significant portion of the total loop heat rejection so that convergence of a balanced system is more difficult. At the start of the calculation in PPNG3, the initial estimate of the coolant flow rate is

based on an assumption that the pumping power heat addition is 10 percent of the heat sources heat load. Thus,

$$W = \frac{1.1 q}{C_p (Z, T) \Delta T}$$

where q = heat source heat load

C_p = specific heat of coolant z at temperature T ,

ΔT = specified loop temperature drop.

The piping flow conditions and pressure drop, the total loop pressure drop, the pumping power, and the heat addition to the coolant at the pump are all computed in the manner described for PPNG1. Then a comparison is made of the calculated heat rejection, $q + \Delta q$ at the pump, with the assumed heat rejection of $1.1 q$. If the calculated and assumed values do not agree within the desired tolerance, then a re-estimate of the heat rejection is made and the calculations repeated until solution is achieved. It was found necessary to anticipate the changes in pumping power with heat rejection to obtain convergence. Satisfactory convergence is attained when the difference between calculated and assumed values is increased by 10 percent, and this new difference is added to the original estimate of heat rejection as follows:

$$q_{\text{new}} = q_{\text{old}} + 1.1 (q' - q_{\text{old}})$$

where q_{new} = new estimate of heat rejection

q_{old} = old estimate of heat rejection

q' = calculated value of heat rejection.

The remainder of PPNG3 is similar to PPNG1 with two exceptions. As above, it was found necessary to anticipate the effect of heat rejection changes on system conditions. The pressure drop in the secondary radiator model is proportional to the 2.8 power of heat rejection. So with every change in estimated heat rejection above, the portion of pressure drop in the radiator due to frictional loss in the radiator tubes is changed proportionally. With this procedure, satisfactory convergence of assumed and calculated loop pressure drops is readily achieved.

The final difference between PPNG1 and PPNG3 is that limits are placed on the maximum pressure drop allowed in the secondary loop piping and in the secondary loop radiator. Occasionally, user input or values selected by the optimization technique results in unrealistic values of pressure loss in the secondary loop components. If the computed piping pressure loss exceeds 30 psi then the single circuit is assumed to be split into two parallel circuits, and the pressure drop is decreased by a factor of 4. The radiator pressure loss is arbitrarily limited to 10 psi. Subsequent examination of overall system results may dictate different limits than those assumed.

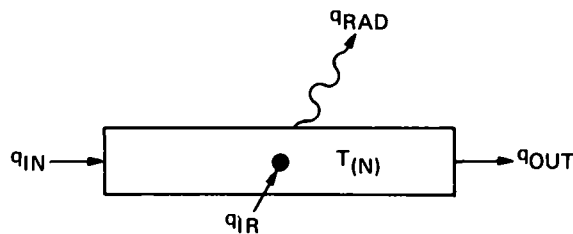
9.1.7 LOW VOLTAGE CABLE

The low-voltage cable model computes the electrical and thermal operating conditions, the weight and the physical dimensions of the cable component transporting the electrical energy from the reactor output leads to the power conditioning modules. The cable is assumed to be a flat ribbon configuration of known dimensions and composition carrying a known quantity of current. Thermal boundary assumptions include:

- a. Radiation heat transfer from one side of the ribbon to a known sink temperature
- b. A known temperature at the reactor end of the reactor electric lead
- c. A known power conditioning temperature at the cool end of the low voltage cable
- d. A maximum allowable cable temperature at the junction of the reactor lead and low voltage cable
- e. A minimum allowable low voltage cable temperature equal to the power conditioning module temperature.

For calculational purposes, the low voltage cable is assumed to be divided into 8 axial nodes; the first node is 2 percent of the total cable length while each of the remaining 7 nodes are 14 percent of the total length. The model computes an energy balance on each of the nodes in turn, and continuously repeats the calculations until an overall energy balance is achieved and all the thermal boundary conditions are met.

Schematically the thermal energy relations of a typical node, N, are as follows;



where

- q_{IR} = internal heat generation due to $I^2 R$ losses
- q_{OUT} = heat conducted from node N to node (N + 1)
- q_{IN} = heat conducted to node N from node (N - 1)
- q_{RAD} = heat radiated from node N surface
- $T(N)$ = mean temperature of node N.

The internal heat generation, in Btu/hr., is given by the equation;

$$q_{IR} = 3.413 I^2 R$$

where I is the total current in amperes and R, the resistance in ohms, is expressed as

$$R = \frac{4\Delta X(N)L r(y, T(N))}{A_X}$$

where

- $\Delta X(N)$ = fraction of total cable length associated with node N
- L = one way length of cable between reactor lead and power conditioning
- A_X = Sum of cross section areas of all cables
- $r(y, T(N))$ = resistivity of cable material y at temperature T(N)

The multiplier 4 accounts for fact the L is one-half the actual electric circuit length and A_X is twice the actual area carrying the circuit current I.

The heat conduction term, q_{OUT} , is computed by the equation,

$$q_{OUT} = \frac{k\left(y, \frac{T(N) + T(N+1)}{2}\right) A_X (T(N) - T(N+1))}{L \left[\frac{\Delta X(N) + \Delta X(N+1)}{2} \right]}$$

where $k(y, f(t))$ = the thermal conductivity of cable material y at the average temperature between nodes $T(N)$ and $T(N+1)$ and the denominator is the conduction path length between the centroids of the two nodes. The conduction term, q_{IN} is the q_{OUT} term computed for the previous node $N-1$ as follows;

$$q_{(IN)}(N) = q_{OUT}(N-1)$$

The radiation term is computed by difference as follows;

$$q_{RAD} = q_{IR} + q_{IN} - q_{OUT}$$

from which the new estimate of temperature $T(N)$ is computed from the equation;

$$T(N) = \left[T_S^4 + \frac{q_{RAD}}{.1713 \times 10^{-8} A_S \Delta X(N) E(y, T(N))} \right]$$

where

T_S = sink temperature

A_S = total radiating surface area of cable

$E(y, T(N))$ = emissivity of surface of cable material y , at temperature $T(N)$.

The equations above are used for all the nodes with slight modifications required for the first and last nodes. For example, the temperature of interest in the first node is at the front end, rather than at the node centroid. Consequently, the conduction path to the second node is the complete length of the first node plus half the second node length. Also, the heat conducted into the first node is that conducted out of the reactor lead as described in the cesium system model. The heat conducted out

of the last node traverses only the last half of the node length. This is accomplished in the calculation by assuming a fictitious 9th node of zero length at the power conditioning end of the cables.

The calculational procedure in the model is initiated by computing a starting temperature profile in the cable based on a constant temperature drop from node center to node center. Then a new temperature is calculated for each of the nodes, starting at node 1, using the equations described above. The procedure is repeated until the difference, at each node, between successive temperature calculations is less than some designated tolerance.

In order to achieve a stable temperature solution with the above procedure it was found necessary to apply large damping factors to the calculated temperatures. That is, the assumed new temperature for node N is determined by

$$T(N) = f \left[T(N)_{\text{old}} \right] + (1 - f) \left[T(N)_{\text{new}} \right]$$

where

$T(N)_{\text{old}}$ = temperature from previous iteration

$T(N)_{\text{new}}$ = new temperature just calculated

f = damping factor

A value of 0.85 is used as the damping factor for all the nodes except node 1 which requires a 0.95 factor because of the external influence of the reactor lead. A very large factor of 0.99 is needed when, occasionally, a negative value of q_{RAD} is calculated from the nodal energy balance. It was also found necessary to apply a 0.99 factor on the last node when the high conductivity material copper is the cable material.

After a stable, converged temperature profile has been calculated for the cable, the cable weight, electrical power loss and boundary heat flows are calculated. The cable

weight and power loss computed are the combined values for the low voltage cable and the reactor lead. The weight is

$$WT_{LVC} = A_X L_{LVC} \rho(y) + A_{XRL} L_{RL} \rho(y)$$

where each term is the product of the cross sectional area, length and density of material for the low voltage cable and reactor lead respectively.

The electrical power loss in the low voltage cable is calculated and summed during the nodal temperature computation. The power loss in the reactor lead is determined by the same equation using reactor lead conditions and dimensions. The fractional loss in electrical power due to the combined losses in the reactor lead and low voltage cable is

$$FL = \frac{Q_{LVC} + Q_{RL}}{3413 \text{ PWR}}$$

where

Q_{LVC} and Q_{RL} are the electrical losses, in Btu/hr, in the voltage cable and reaction lead and PWR is the gross electric power output, in kW, from the reactor.

An option has been included in the low voltage cable subroutine which will continue the temperature profile calculations with varying cable surface area until the maximum cable temperature at the juncture of the reactor lead and low voltage cable agrees with a desired value. The option is exercised by inputting a negative value for the initial cable surface area estimate. The calculation proceeds as described above until a stable temperature profile is achieved. The maximum cable temperature, T_1 , is compared with the desired maximum cable temperature, $T_{MX}^{(7)}$. If the difference between $T(1)$ and $T_{MX}^{(7)}$ is greater than 10°F, then the cable area is changed by the following relation;

$$A_S = A_S \left(\frac{T(1)}{T_{MX}^{(7)}} \right)^5$$

If the difference in temperature is less than 10°F but greater than the desired agreement of 2°F, then the surface area is changed as follows;

$$A_S = A_S \frac{T(1)^4 - T_S^4}{T_{MX}(7)^4 - T_S^4}$$

9.1.8 POWER CONDITIONING RADIATOR MODEL

The passive power conditioning radiator is assumed to be a thin metal sheet, in conical or cylindrical configuration, having individual PC modules distributed in discrete blocks on its inside surface. The heat generated in the PC modules is conducted into the metal sheet, which acts as a fin, and radiated to space from the outside surface of the cone or cylinder. The PC radiator model determines the area of the metal sheet required to dissipate the heat of one PC module and from that value constructs the size and weight of the whole radiator.

The modular PC radiator panel is assumed to be disk shaped as shown in Figure 9-11. The shaded circle in the center of the panel is the area occupied by the PC module on the back side of the panel.

Pertinent dimensions are:

- r_o = radius of panel, feet
- r_i = radius of PC module area, feet
- δ = thickness of metal sheet panel, inches

Input parameters to the PC radiator model are:

- $T_{MX}(PR)$ = maximum radiator panel temperature, °R
- T_S = sink temperature, °R
- $q(5)$ = total radiator heat load, Btu/hr
- N_{PC} = number of PC modules (includes hotel PC modules)

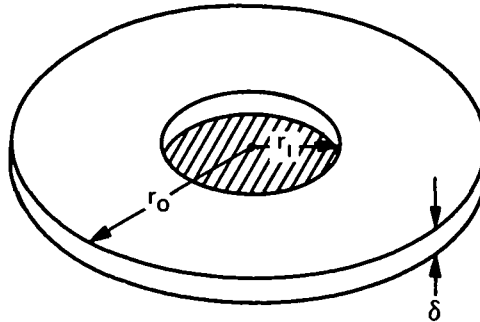


Figure 9-11. Sketch of PC Radiator Panel Model

A_{PC} = Area of PC module, ft^2 , (shaded area in sketch). In addition, the panel sheet thickness, δ , is known and the sheet material is assumed to be aluminum.

The determination of the panel area for the given set of conditions is an iterative process. A value for the ratio, r_i/r_o , is assumed which allows calculation of the fin efficiency of a panel and the total radiator area required by the input thermal conditions. The radiator area associated with the given N_{PC} , A_{PC} , and the assumed r_i/r_o ratio is also determined. Different values for the r_i/r_o ratio are tested until the calculated thermal area and geometric areas are identical.

The initial guess for the r_i/r_o ratio is computed with the following equation, which includes an assumed fin surface effectiveness value of 0.95:

$$\frac{r_i}{r_o} = \left[\frac{0.95 N_{PC} A_{PC} (0.1713 \times 10^{-8}) \epsilon(y) (T_{MX}(PR)^4 - T_S^4)}{q(5)} \right]^{1/2}$$

where $\epsilon(y)$ is the emissivity of the panel radiator surface of composition y . The radius r_i is

$$r_i = \left[\frac{A_{PC}}{\pi} \right]^{1/2}$$

and

$$r_o = \frac{r_i}{\left(\frac{r_i}{r_o} \right)}$$

The fin efficiency, η_f , for heat rejection from one side of the annular section of panel between radii r_o and r_i is computed by the relation;

$$\eta_f = \eta_{fo} + \phi \left(\frac{r_i}{r_o} \right)$$

where

$$\eta_{fo} = \frac{\tan^h m (r_o - r_i)}{m (r_o - r_i)}$$

$$m = \frac{k_r}{k\delta}$$

$$h_r = \text{equivalent heat transfer coefficient on radiating surface, Btu/hr-ft}^2 \text{ } ^\circ\text{R}$$

$$k = \text{conductivity of fin (panel) material}$$

$$\phi \left(\frac{r_i}{r_o} \right) = \text{correction factor for a disk configuration.}$$

The equivalent surface heat transfer coefficient is:

$$h_r = \frac{.1713 \times 10^{-8} \epsilon (y) \left(T_{\text{eff}}^4 - T_s^4 \right)}{T_{\text{eff}} - T_s}$$

where the effective fin temperature, T_{eff} , is assumed to be 20°F lower than the maximum panel temperature T_{mx} (PR). The disk correction factor $\phi\left(\frac{r_i}{r_o}\right)$ is based on data in Jakob* Reference 13 which can be expressed by the equation

$$\phi\left(\frac{r_i}{r_o}\right) = 0.75 \left(\eta_{fo} - \eta_{fo}^2 \right) \left(\frac{r_i}{r_o} - 1 \right)$$

The surface effectiveness, η_o , is computed with the equation,

$$\eta_o = 1 - (1 - \eta_f) \left[1 - \left(\frac{r_i}{r_o} \right)^2 \right]$$

and the total radiator area required from thermal considerations is

$$A_{\text{PR THERMAL}} = \frac{q(5)}{0.1713 \times 10^{-8} \eta_o \epsilon (y) \left(T_{\text{mx}}(\text{PR})^4 - T_s^4 \right)}$$

The total radiator area associated with designated dimensional conditions is

$$A_{\text{PR GEOMETRIC}} = \frac{N_{\text{PC}} A_{\text{PC}}}{\left(\frac{r_i}{r_o} \right)^2}$$

If an externally fueled or a pancake reactor system is being analyzed, then the converged value of A_{PR} is increased to account for the 6 extra PC modules that are on non-operating, standby condition. The final radiator is

$$A_{\text{PR}} = A_{\text{PR}} \left(\frac{N_{\text{PC}} + 6}{N_{\text{PC}}} \right) \text{ ft}^2$$

*See Figure 11-15, Page 238, in Volume I of Reference 13

The weight of the radiator is

$$\text{Wt (PR)} = A_{\text{PR}} \left(\frac{\delta}{12} \right) \rho (y) \text{ lbs.}$$

where $\rho(y)$ is the density in lb/ft³ of the radiator material y.

9.1.9 AUXILIARY RADIATOR MODEL

The auxiliary radiator model is based on test results obtained with a section of a liquid metal radiator designed and tested by General Electric's Advanced Nuclear System Operation in 1966. The radiator section was of the offset tube and fin configuration with NaK coolant flowing in stainless steel tubes which were surrounded by aluminum armor and attached to aluminum fin panels. The test section was approximately 6.5 feet long and 24 square feet in area. It was tested with coolant inlet temperatures ranging from 300°F to 700°F, with coolant temperature drops of 25 to 200°F and heat rejection rates of 1 to 10 kW. In addition to overall thermal performance, data were obtained on fin efficiency as a function of temperature level and coolant pressure drops.

The measured fin efficiencies are correlated by the equation;

$$\eta_f = .983 + 8.5 \times 10^{-5} T - 2.565 \times 10^{-7} T^2$$

where T is the maximum coolant inlet temperature. The required auxiliary radiator area in the model is computed as follows:

$$A_{\text{AR}} = \frac{0.8 q(4)}{0.88 \eta_f \left(.1713 \times 10^{-8} \right) \left[T_{\text{mx}}(4)^4 - T_s^4 \right]}$$

where the 0.8 factor in the numerator assumes the radiator area will be limited to 80 percent of its minimum weight volume. The 0.88 factor in the denominator is the emissivity of the radiating surface and

$q(4)$ = total auxiliary loop heat load, Btu/hr

$T_{\text{mx}}(4)$ = designated maximum coolant temperature.

The weight of the radiator, with an assumed 1.1 multiplier to the fin and tube weights to correspond to the 80 percent area limit, is given by

$$WT_{AR} = 0.96 A_{AR} + 22.4$$

The corresponding weight in pounds of NaK coolant in the radiation tubes and headers is:

$$\text{Coolant Wt} = 0.0184 A_{AR} + 8.5$$

The coolant pressure drop in psf is described by the equation

$$\Delta P_{AR} = 5.27 \left[\frac{\dot{W}}{9725} \right]^{1.8} + 284$$

where \dot{W} is the auxiliary loop coolant flow rate, in lbs/hr., calculated in the secondary loop piping model. If the conditions of a particular problem result in a pressure drop greater than 10 psi, then additional radiator tubes are assumed in the radiator configuration to limit the ΔP to 10 psi. The resultant modification to the radiator and radiator coolant weights is as follows:

$$(W_{T_{AR}})' = 0.2 W_{T_{AR}} \left[\frac{1440}{\Delta P_{AR}} \right]^{0.555}$$

$$(\text{Coolant Wt})' = 0.2 (\text{Coolant Wt.}) \left[\frac{1440}{\Delta P_{AR}} \right]^{0.555}$$

The basic model described above is for an aluminum-stainless steel composition radiator. Multiplying factors for the radiator weight are used if beryllium-stainless steel or copper-stainless steel composition is desired, or made necessary by designated auxiliary loop temperature conditions. The multipliers are 0.675 for beryllium-stainless steel and 1.55 for copper-stainless steel.

9.1.10 PAYLOAD MODEL

The payload, undefined in detail is assumed to be a weight and power requirement which can be designated as input. For the present study, the payload weight is one metric ton (2200 pounds) has a defined power requirement of 1 kilowatt. The payload

model adds the power re-required for system controls, computes the area required to dissipate the thermal energy of the payload and calculates the portion of payload weight attributable to system guidance and controls.

Power required for system guidance and control is assumed to be one kilowatt so the total payload model power is

$$q_{PL} = 1 + P_{PL}$$

where P_{PL} is the designated payload power. All but 200 watts of this power is converted to thermal energy which must be dissipated (a total of 200 watts is beamed by the communications equipment). In Btu/hr. this thermal energy is

$$q_{t_{PL}} = 3413 (q_{PL} - 0.2)$$

The payload radiator is assumed to be similar to the power conditioning radiator, so the required area is determined by proportionality;

$$A_{PL} = \frac{q_{t_{PL}}}{q(5)} A_{PR}$$

where

- A_{PL} = area of payload radiator
- A_{PR} = area of PC radiator
- $q(5)$ = heat rejection of PC radiator.

The minimum axial length of the payload section of the vehicle is 10 inches so the minimum payload radiator area corresponds to this dimension. If the calculated payload area is less than the minimum area it is set equal to the minimum value. The weight of the payload radiator is also determined by proportion, as follows:

$$W_{T(\text{pay rad.})} = W_{tpr} \left(\frac{A_{pl}}{A_{pr}} \right)$$

The weight of the system controls is 50 pounds plus the portion of the payload radiator which cools the controls. Thus the total system controls weight is

$$W_{T_{\text{controls}}} = 50 + \left(\frac{.55}{q_{\text{PL}} - 0.2} \right) W_T \text{ (payload radiator)}$$

9.1.11 THRUSTER SYSTEM MODEL

The total weight of the thrusters is a fixed value for this study. The thruster system model determines the weights of the thruster power conditioning and the thruster radiator and combines them with the thruster weight to determine a total thruster system weight.

The input power to the thruster PC for the externally fueled and pancake reactor systems is calculated by ratio from the output of the main PC units. For every 223 kW supplied by the main PC to the thrusters, 17 kW is required by the thruster PC units.

Therefore;

$$(q_{\text{IN}})_{\text{TPC}} = \frac{17}{223} (q_{\text{OUT}})_{\text{PC}}$$

and

$$q_{\text{thruster}} = (q_{\text{OUT}})_{\text{PC}} + (q_{\text{IN}})_{\text{TPC}}$$

where

$$(q_{\text{IN}})_{\text{TPC}} = \text{input power to thruster PC}$$

$$(q_{\text{OUT}})_{\text{PC}} = \text{output power from main PC}$$

$$q_{\text{thruster}} = \text{total power to thruster system}$$

The electrical circuit for the flashlite reactor differs in a way that requires calculation of the total power to the thruster system and then the computation of the thruster PC input, as follows:

$$q_{\text{thruster}} = (q_{\text{OUT}})_{\text{PC}} - q_{\text{PL}}$$

$$(q_{\text{IN}})_{\text{TPC}} = \frac{17}{240} q_{\text{thruster}}$$

The specific weight of the thruster PC is 16 lbs/kw so the weight of thruster PC is

$$W_{\text{T}_{\text{TPC}}} = 16 (q_{\text{IN}})_{\text{TPC}}$$

The flashlite reactor system requires an interrupter that weighs 310 pounds and consumes 1.25 kW of power. These values must be applied to the conditions computed by the above equations.

The efficiency of the thruster PC is 90 percent, so the heat to be rejected by the thruster PC radiator is

$$(q_{\text{T}})_{\text{TR}} = 3413 (0.10) (q_{\text{IN}})_{\text{TPC}}$$

The area required is determined by ratio with the main power conditioning radiator. Thus, for the externally fueled reactor,

$$A_{\text{TR}} = \frac{37}{31} \frac{(q_{\text{t}})_{\text{TR}}}{q(5)} A_{\text{PR}}$$

where the ratio 37/31 accounts for the six redundant thrusters. The weight of the thruster radiator is determined similarly;

$$W_{\text{T}_{\text{TR}}} = \frac{37}{31} \frac{(q_{\text{t}})_{\text{TR}}}{q(5)} W_{\text{T}_{\text{PR}}}$$

The total weight of the thruster system, $W_{T(9)}$, is

$$W_{T(9)} = W_{T_{TPC}} + W_{T_{TR}} + W_{T_{thrusters}}$$

9.1.12 STRUCTURE MODEL

The structure model estimates the weight of members that must be added to the power plant - spacecraft combination for structural, aerothermal or booster integration purposes. These members include:

1. Spacecraft - booster adapter
2. Structure for payload bay
3. Structure for thruster bay
4. Additional structure for power conditioning radiator
5. Additional structure for main radiator
6. Payload penalty due to shroud or fairing weight.

The weight of the spacecraft-booster adapter is 260 pounds. The total structure weight required in the payload bay and thruster bay sections includes 115 pounds of metal skin and 4 pounds of stiffening rings for each axial foot of bay length. Since the thruster PC radiator and the payload radiator will supply part of this weight, the additional weight needed, designated as structure, is

$$\left(\Delta W_{T_{ST}}\right)_1 = 119 \left[2.35 + L_{TR} + L_{PL} \right] - W_{T_{TR}} - W_{T_{(PAY. RAD.)}}$$

where the thruster section is 2.35 feet long and,

L_{TR} = Axial length of thruster PC radiator, feet

L_{PL} = Axial length of payload radiator, feet

WT_{TR} = Weight of thruster PC radiator, lbs

$WT_{(Pay-rad)}$ = Weight of payload radiator, lbs.

The additional structure required in the PC radiator and main radiator sections depends on the relative location of the two radiators. If the PC radiator is placed directly behind the shield, then the combined structural weight addition for the PC and main radiator sections is

$$\left(\Delta WT_{ST}\right)_2 = 8.32 L_{PR} + 14 L_{MAR}$$

where

L_{PR} = Axial length of PC radiator

L_{MAR} = Axial length of main and auxiliary radiator

If the main radiator is located behind the shield, then

$$\left(\Delta WT_{ST}\right)_2 = 53.3 L_{PR} + 4 L_{MAR}$$

The payload penalty for launching the thermionic spacecraft with a flight fairing is given as a function orbit altitude and flight fairing length in Figure 9-12. The orbit altitude of interest is 700 nautical miles and an equation describing the 700 nautical mile curve on Figure 9-12 is:

$$\text{Payload Penalty} = 169 + 10.51$$

where V_L is the length of the spacecraft. This payload penalty is designated as the shroud weight and is included in the total structure weight, WT_{ST} , as follows:

$$WT_{ST} = 260 + \left(\Delta WT_{ST}\right)_1 + \left(\Delta WT_{ST}\right)_2 + \text{SHROUD WT}$$

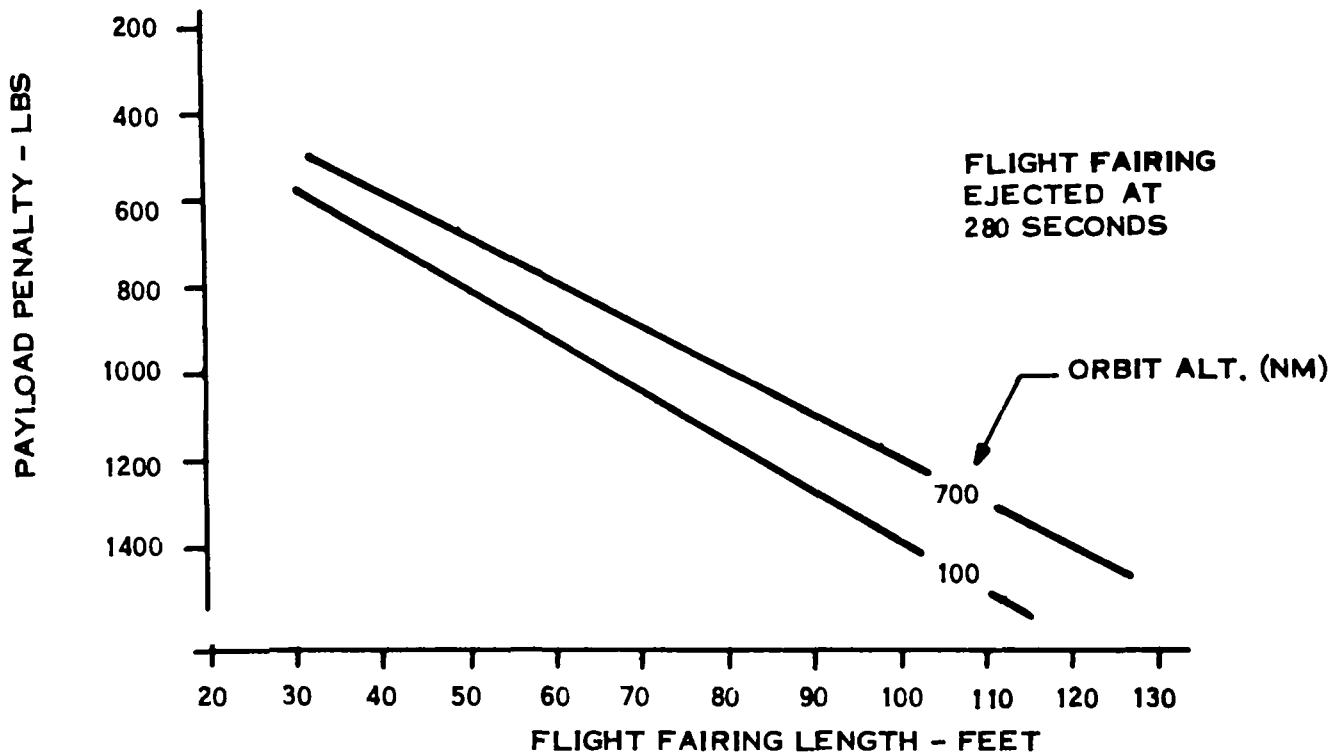


Figure 9-12. Flight Fairing Weight and Payload Penalty (Titan III C/7)

9.1.13 CESIUM SYSTEM MODEL

The cesium reservoir-radiator systems for the externally fueled or pancake reactors do not effect the conditions or dimensions of other components in the respective power plants. However, for the flashlight reactor, the cesium reservoir and radiator is located between the reactor and shield where it influences and is effected by the shield and power cables. Figure 9-13 is a schematic sketch showing the relative placement of the components in the equipment bay between the shield and reactor and some pertinent dimension designations. The reactor coolant pipes and headers have been omitted in order to show the cesium system more clearly.

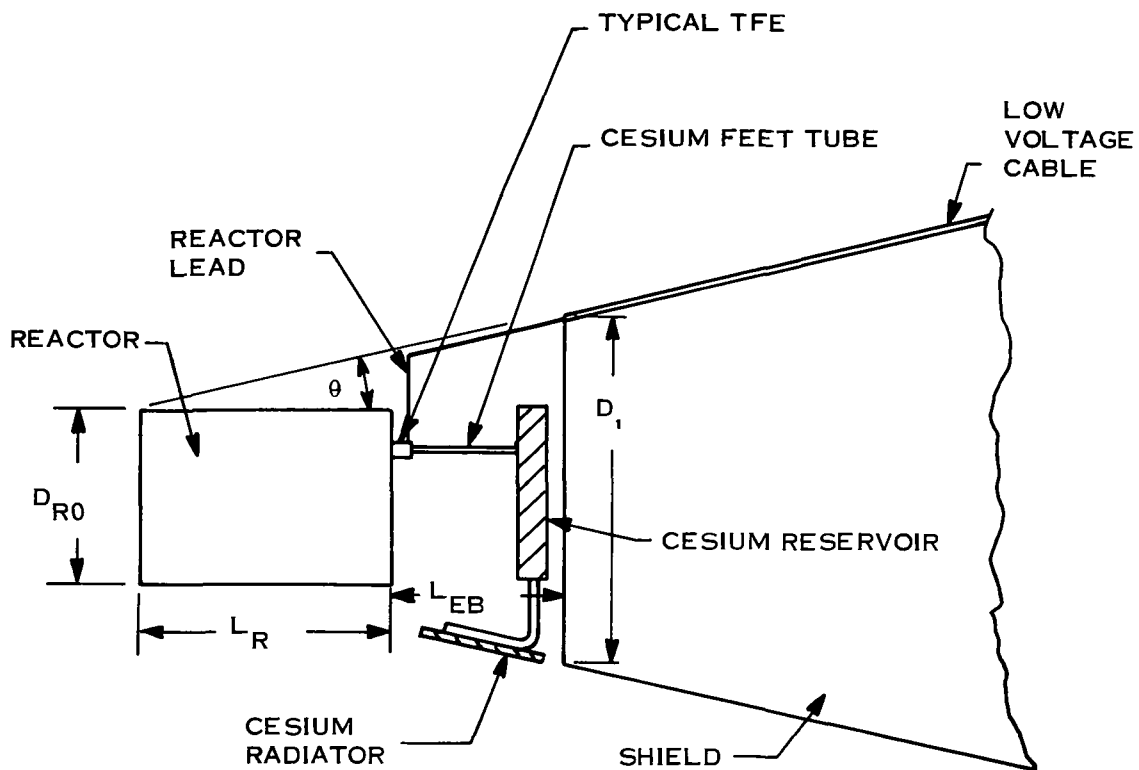


Figure 9-13. Schematic of Cesium System in Equipment Bay Between Flashlight Reactor and Shield

The cesium system model determines the thermal influences on the cesium reservoir and the size of the radiator needed to dissipate the resultant heat load. The length and thermal conditions of the reactor leads which traverse the equipment bay region are also determined.

The initial calculation in the cesium model is the determination of the reactor lead and its mean temperature. In the externally fueled, and pancake reactors, the reactor lead length is approximately one half the difference between the shield front face diameter, D_1 , and the equivalent reactor diameter, DR_0 . In the flashlight reactor, the reactor lead length is

$$L_{RLD} = DR_0 - \frac{(DR_0 - 0.5)}{1.414} + \frac{L_{EB} - 0.5}{\cos \theta}$$

The parameters in the preceding equation are identified on Figure 9-13. The mean temperature of the reactor lead, based on a parabolic temperature distribution is

$$T_{RLD} = \frac{2 T_{MXR} + T_{MAX}}{3}$$

where

T_{MXR} = maximum coolant temperature at reactor

T_{MAX} = temperature of low voltage cable at reactor lead - low voltage cable interface.

The sources of heat to the cesium system are:

1. Heat radiation from the shield front face
2. Heat radiation from the reactor leads
3. Heat conduction down the cesium feed tube
4. Nuclear radiation
5. Electrical heating units.

The electrical heating units would probably be utilized only at startup but for cesium radiator sizing purposes, they were assumed to be operating.

The heat radiated from the shield to the cesium reservoir is computed by the following equation:

$$q_{S-C} = 0.1713 \times 10^{-8} F_{C-S} A_C \left(T_{SD}^4 - T_{CS}^4 \right)$$

where

F_{C-S} = radiation interchange factor

A_C = Area of back side of cesium reservoir opposite the shield, ft²

T_{SD} = Maximum allowable shield temperature, °R

T_{CS} = Designated optimum cesium temperature, °R

A similar equation calculates the heat radiated from the reactor leads to the cesium system, with an appropriate radiation interchange factor, reactor lead area and mean temperature. Heat conducted to the cesium reservoir through the cesium vapor feed tubes is computed by

$$q_{R-C} = \frac{k A_{R-C} (T_{MXR} - T_{CS})}{L_{EB}}$$

where

k = thermal conductivity of feed tube

A_{R-C} = total cross sectional area of feed tubes.

The rate of nuclear heating is a function of the reactor characteristics and the cesium reservoir size, while the rate of electrical heating is arbitrary. The total cesium radiator heat rejection is the sum of the individual heating rates and the radiator size needed is

$$A_{CR} = \frac{q_{tCR}}{.1713 \times 10^{-8} \epsilon_{CR} (T_{CS}^4 - T_S^4)}$$

where q_{tCR} is the total heat lead and ϵ_{CR} is the emissivity of the cesium radiator surface. The radiator specific weight, SW_{CR} , is an input value so the cesium radiator weight is

$$WT_{CR} = SW_{CR} A_{CR}$$

The weight of the cesium reservoir and feed tubes is included in the reactor weight, so the additional cesium system weight includes only the cesium radiator.

9.1.14 EM PUMP MODEL

The weights of space type EM pumps as a function of coolant composition, flow rate and pressure rise was taken from a report by Verkamp and Rhudy (Reference 14).

Figure 9-14 is a correlation of data from that report separated into dc and ac pumps. The equation for the dc pump weight data is;

$$W_{T_{PUMP}} = 17.25 \left[\frac{\dot{W} \Delta P r(z, T)}{\rho(z, T)} \right]^{.648}$$

where

\dot{W} = coolant flow rate in lbs/hr

ΔP = coolant pressure rise in psf

$r(z, T)$ = coolant resistivity in ohm-feet for coolant density Z and temperature T

$\rho(z, T)$ = coolant density in lbs/ft³ for coolant composition Z and temperature T.

The efficiency of the dc pump is assumed to be constant at 15 percent. The maximum allowable operating temperature for the pump electrical components is an input value, while the pump input power that must be removed by an auxiliary cooling circuit is set at a constant 40 percent.

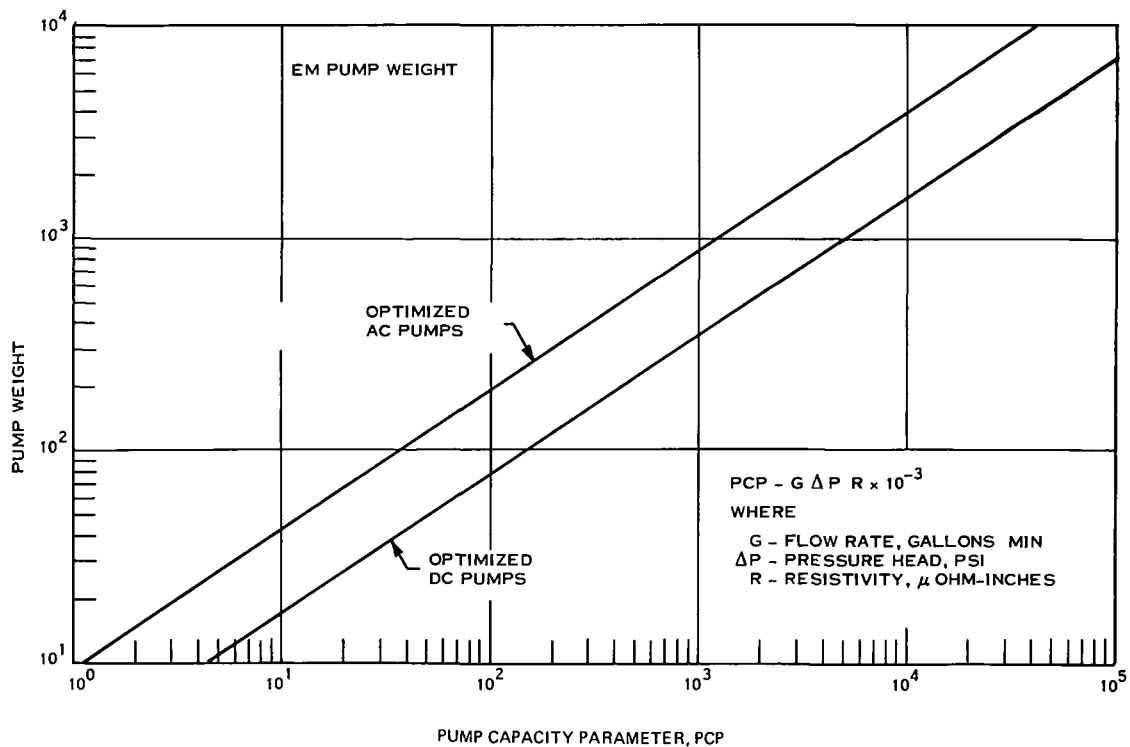


Figure 9-14. EM Pump Weight

9.2 CODE UTILIZATION

The computer code was used to investigate various spacecraft designs utilizing the flashlight and the externally fueled types of reactors. At customer direction, the investigation of the pancake type of reactor system was deleted from the study. The purpose of the investigations was to determine the influence of such parameters as cable material composition, reactor outlet temperature and reactor power level on the spacecraft weight and performance, and to get a first approximation of the best combination of power plant characteristics from the standpoint of minimum weight per net propulsion power. To obtain the latter data, a general purpose optimization technique was integrated with the design code while the former data was obtained by repeated application of the design code - optimization technique combination with appropriate input.

The values of the input parameters which were kept constant for all the code investigations and which applied to both the flashlight and externally fueled reactor systems are as follows:

- a. Maximum vehicle diameter of 9.2 feet
- b. Payload weight of 2200 pounds
- c. Thruster weight of 1233 pounds
- d. Payload power requirements of 1 kWe
- e. Reactor controls power requirement of 0.2 kWe
- f. Cesium reservoir power requirement of 0.5 kWe
- g. Average sink temperature of 300^oR
- h. Maximum power conditioning temperature of 200^oF
- i. Maximum PC radiator temperature of 175^oF
- j. Maximum shield temperature of 1000^oF

- k. Maximum shield coolant temperature of 950°F
- l. Maximum auxiliary coolant temperature of 800°F
- m. No parallel loops in any actively cooled circuit
- n. One operating and one redundant pump in each loop
- o. Iteration tolerance limits of 1 percent for length, pressure drops and flow rates, 5 percent for the radiation dose separation distance and 0.01 percent for cable temperature convergence

Program options which were kept constant and applied to both types of reactor systems are:

- a. Active shield cooling mode
- b. NaK-78 coolant composition in all loops
- c. Stainless steel containment material for all loops
- d. Copper-stainless steel material for all actively-cooled radiators.
- e. Aluminum material for all PC radiators.

Parameters such as mission time, reactor operating time, neutron and gamma dose limits and propellant weight were given input values, per the program guidelines. However, the present code models are normalized to these values.

9.2.1 FLASHLIGHT REACTOR SYSTEM INVESTIGATIONS

The flashlight type of reactor system was assumed to have two loops in series for the main heat rejection systems, as required by the coolant activation analysis in the baseline concept power plant (see Section 5). The heat exchanger was assumed to be a 2 pass configuration with the weight optimum flow rates of 7 ft/sec in the tubes and 12 ft/sec on the shell side (see Paragraph 9.2.3). The output voltage of the flashlight reactor is relatively low. Therefore, the only relative radiator location considered

for that type of reactor placed the power conditioning radiator directly behind the shield minimizing the lengths, and hence, the power losses, in the low voltage cables.

The first investigation performed was the comparison of cable material composition on overall system characteristics. Copper has low electrical resistance, good temperature capability in vacuum (assumed to be a maximum of 1200°F), but is heavy in weight. Aluminum also has fairly low electrical resistance and is relatively light weight but its temperature capability is only about 700°F. Sodium metal in a stainless steel tube is very light in weight and can probably be operated up to 1500°F but when molten, it has a higher electrical resistance than the other two materials.

The results of the cable investigation are conducted for a nominal reactor design power level of 300 kWe, shown on Table 9-1. The order of preference for the cable materials is aluminum, NaSS clad and copper. The total weights of the spacecraft-powerplant systems are within 120 pounds of one another even though the weights of individual components vary significantly. The heavier weight of the copper cable is offset by a lighter shield since the copper system optimized at a smaller shield angle and a longer vehicle length than the other systems. The main difference between the systems is in the electrical losses, and the resultant net propulsion power. The aluminum cable system ends up with about 10 kWe and 4.6 kWe more net power than the copper and NaSS clad systems, respectively, because of lower I^2R losses in the low voltage end of the electrical system. Table 9-1 shows a 6.4 percent loss in the aluminum cable, compared with 10.2 percent in the copper cable and 7.9 percent in the NaSS clad cable. The higher copper losses are due to the much smaller cross section area of the copper cable, forced in this direction by its heavy weight, while the NaSS clad cable losses are higher because of the greater electrical resistance of that material when molten. The lower temperature capability of aluminum with its corresponding requirement of large surface area which, in turn, lengthens the spacecraft is less important than its low electrical resistivity characteristics.

TABLE 9-1. FLASHLIGHT REACTOR SYSTEM - COMPARISON OF LOW VOLTAGE CABLE COMPOSITIONS

	Copper Cable	Aluminum Cable	NaSS Clad Cable
Reactor output power, kWe	300	300	300
Net propulsion power, kWe	217.7	227.8	223.2
System specific weight, lbs/kWe (net)	98.06	93.37	95.83
Subsystem Weights, lbs.			
Reactor	3690	3668	3712
Main Radiator	3425	3399	3272
Shield	1200	1754	1657
Auxiliary Cooling	107	104	102
Power Conditioning	3851	3931	3952
Cesium	9	8	10
Low Voltage Cable	2342	1684	2110
Payload	2200	2200	2200
Thruster	2005	2049	2013
Structure	2517	2478	2362
Total System Weight, lbs.	21343	21272	21390
Vehicle length, feet	81.23	80.68	73.44
Shield half angle, degrees	4.86	7.32	8.03
Low Voltage Cable Characteristics			
Electrical losses, percent	10.17	6.38	7.85
Length, feet	21.89	23.41	18.18
Cross section area, ft ²	.17	.387	.955
Heat rejection area, ft ²	33.3	156.0	31.2
Maximum temperature, °F	1125	700	1110

Copper cable was eliminated from further consideration, but both aluminum and NaSS clad cables were investigated at varying reactor output power levels with results as shown in Figure 9-15. Both the aluminum and NaSS clad cable systems demonstrate relatively constant system specific weights as the reactor power level increases. This occurs because the new power, and the total system weight increase similarly.

At all power levels, the aluminum cable system has a specific weight advantage of at least 2 lb/kWe, which combined with its much easier fabrication advantages, indicates aluminum is the best cable material for the flashlight reactor system.

A net propulsion power level of 240 kWe is required for the reference power plant designs. The data of Figure 9-15 indicated a reactor output power of 316 kWe would be required. This reactor power level was assumed for the runs investigating the effect of maximum reactor coolant temperature. Figure 9-16 is a graph of the results obtained. Minimum specific weight is attained in the range 1300°F - 1450°F, while maximum net power is achieved at 1350°F, the temperature of maximum reactor

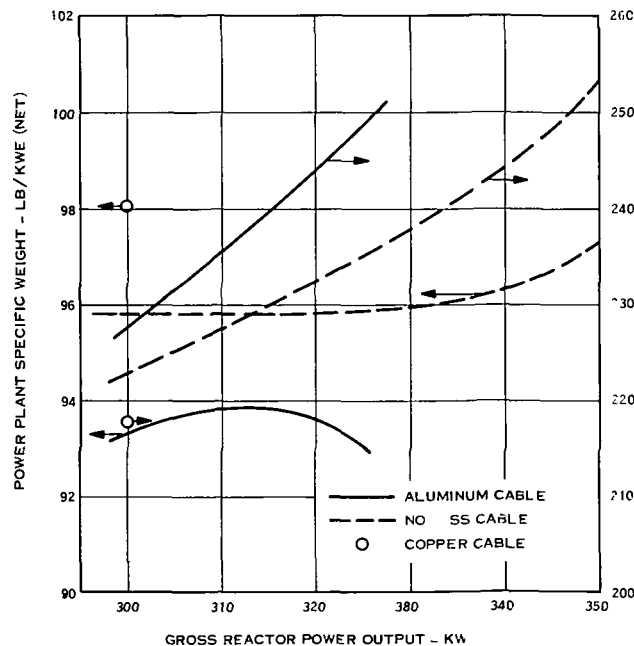


Figure 9-15. Flashlight Reactor

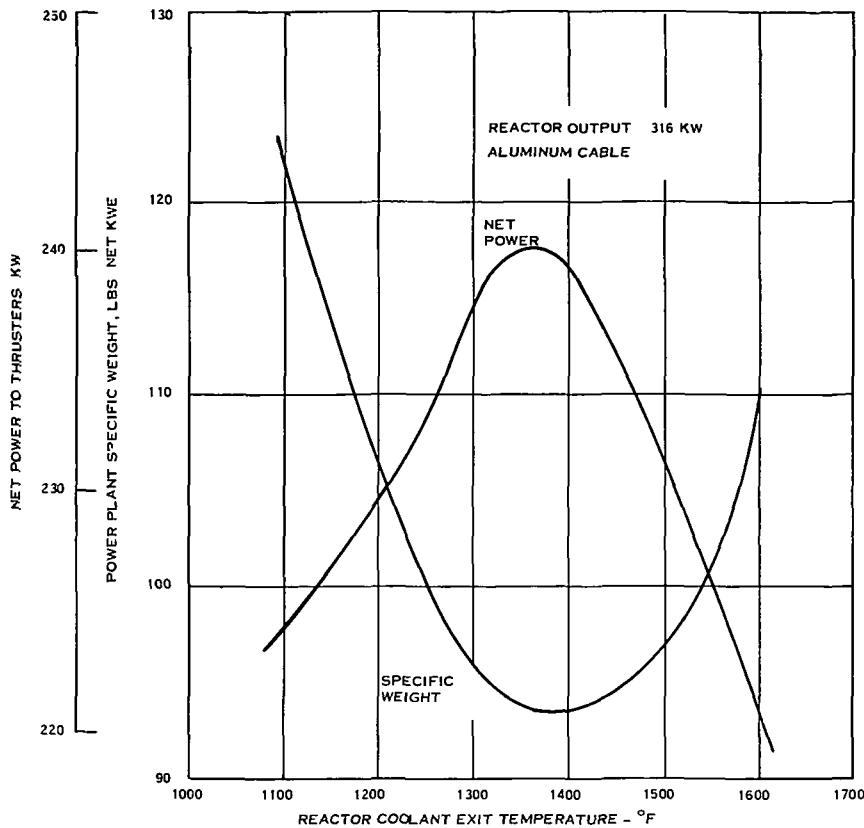


Figure 9-16. Flashlight Reactor System - Effect of Reactor Coolant Outlet Temperature

efficiency. Table 9-2 shows system details at the 1350^o and 1450^oF temperature levels. The system total weight decreases little with increasing reacting temperature. The main radiator system decreases about 500 pounds because of the smaller heat rejection area needed, but more than half of this weight advantage is offset by increased cable weight. A change in I-V characteristics in the reactor, plus additional heat leakage into the cable from the reactor, increase the cable losses at the higher temperature. Additional pumping power is also needed due to the lower reactor efficiency. The result is that the loss in net power is greater than the net savings in weight.

The cable composition and the reactor temperature investigations were performed using an optimization method of steepest ascent. This technique computes the partial

TABLE 9-2. FLASHLIGHT REACTOR SYSTEM - COMPARISON OF RESULTS FOR VARYING REACTOR COOLANT OUTLET TEMPERATURE

	Reactor-Outlet Temp. = 1350°F	Reactor-Outlet Temp. = 1450°F
Reactor Output Power, kWe	316	316
Net Propulsion Power, kWe	239.4	235.7
System specific weight, lbs/kWe (net)	93.89	94.63
Subsystem Weights, lbs.		
Total System Weight, lbs.	22568	22401
Cable Conditions		
Length, ft.	26.88	28.18
Cross section area, ft ²	.521	.579
Heat rejection area, ft ²	176	202
Input voltage, volts	14.158	13.608
Current, amps	22319	23220
Electric Power Schedule		
Reactor output, kWe	316	316
Low Voltage Cable loss, kWe	16.5	18.7
Main PC input, kWe	299.5	297.3
output, kWe	264.15	262.2
Hotel PC input, kWe	21.5	23.25
output, kWe	18.24	19.78
	242.65	238.95
Payload power, kWe	2.0	2.0
	240.65	236.95
Interrupter, kWe	1.25	1.25
Net Power, kWe	239.4	235.7

derivatives of the specific weight with respect to each of the optimization parameter. It then computes a resultant vector, which should be the shortest path to the optimum solution. All of the optimization parameters are varied simultaneously along this path of steepest ascent to the optimum result. The initial determinations of the sensitivity of the 316 kWe system design to variations in each of the optimization parameters about its optimum value indicated that with lower specific weight existed. Consequently a single variable method of optimization was used, in which each of the parameters to be optimized was varied, in turn, while the others were kept constant. Figure 9-17 shows the difference in net power output obtained with the two optimization methods. The total weights of the systems associated with the two methods did not vary by more than 100 to 200 pounds although weights of certain individual components varied more than that. All of the subsequent optimizations were made with the single-variable method.

The results of parameter variations on system specific weight are shown on Figure 9-18 for the re-optimized 316 kW powerplant. The parameters, identified by number,

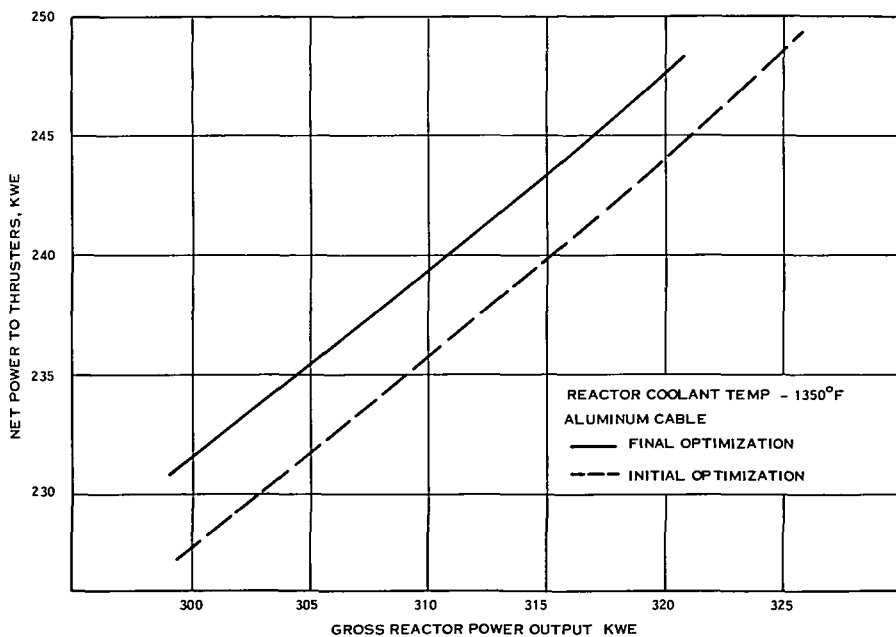


Figure 9-17. Flashlight Reactor System - Change in Output Power Level

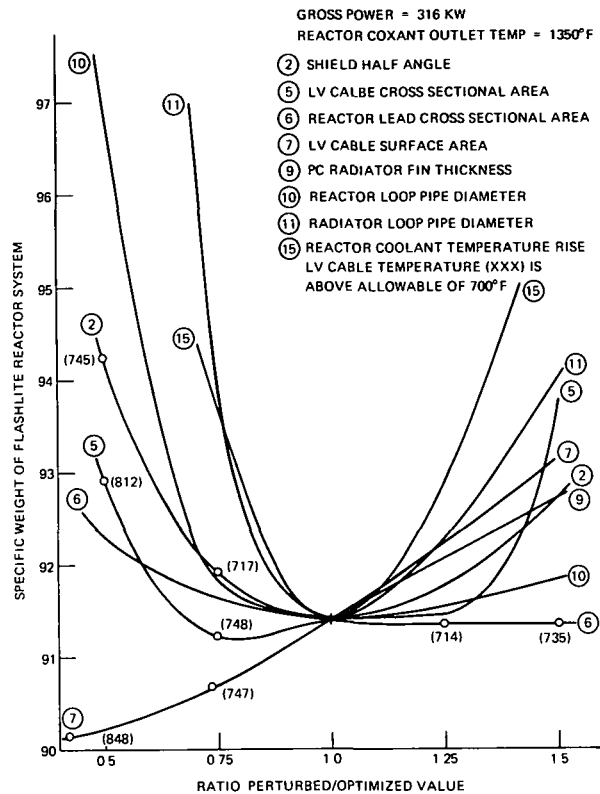


Figure 9-18. Flashlight Reactor System - Parameter Variation Effect

are varied ± 50 percent about their optimum value. As shown, the only points having a lower specific weight than the optimum value are those which have a maximum temperature greater than 700°F in the low voltage cable. During the optimization calculation, the cable temperature was not allowed to exceed this temperature. The data of Figure 9-18 shows that decreasing the cable surface area by 25 percent would lower the powerplant specific weight by 0.8 pounds per kWe and raise the maximum cable temperature to 747°F while a 50 percent area reduction would lower the specific weight by 1.25 pounds per kWe and result in a 848°F maximum cable temperature.

Figure 9-19 presents the results of variations of particular parameters which could not be varied by ± 50 percent because their normal range of interest is less than that. The main radiator area ratio is terminated at 0.9 on the lower side because below that value the radiator weight increases exponentially, but at an unknown rate. (See the main radiator model, Paragraph 9.2.5).

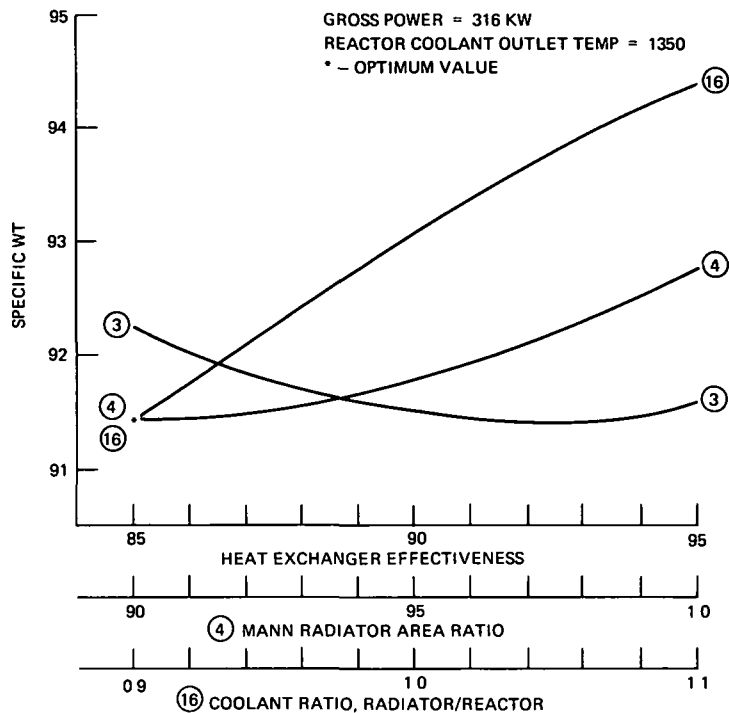


Figure 9-19. Flashlight Reactor - Parameter Variation Effect

The specific weight shown on Figure 9-19 for a coolant flow ratio of 0.9 is an approximation only. The use of this value increases the radiator loop temperature rise to a value that is outside the limits of the main radiator area ratio correction. Therefore, a base value of 1.0 instead of 0.9 was used for the main radiator area ratio in order to estimate the effect of an 0.9 coolant flow ratio.

The effect of increasing the power conditioning temperature above its nominal value of 200°F is illustrated on Figure 9-20. A decrease of 6.4 pounds per kWe and an increase in 2 kWe net power follows a 100°F increase in PC temperature level to 300°F. The PC radiator, which is assumed to be at a temperature 25°F below the PC temperature, has its area and weight cut in half at the higher temperature. The area change also decreases the length of the low voltage cable, thereby lowering both its weight and electrical losses. The system weight decreases while the net power increases thus resulting in a significant drop in specific weight.

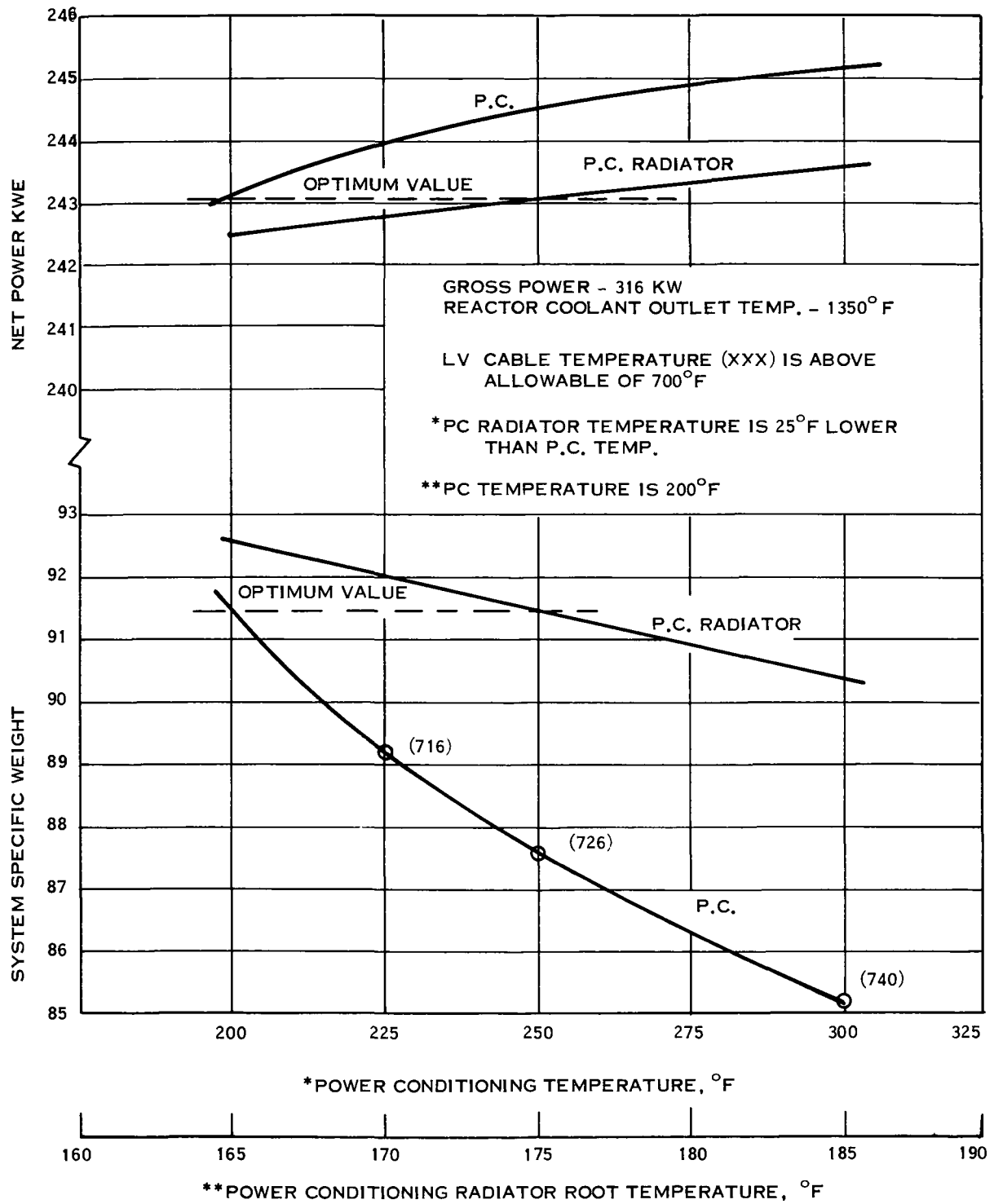


Figure 9-20. Flashlight Reactor - Influence of Power Conditioning Temperature and P. C. Radiator Temperature

The calculated temperature drop from the PC module to the PC radiator is 25°F (See Subsection 8.1). Figure 9-20 shows the changes in system conditions if this value were varied by ± 10°F. A decrease in the ΔT to 15°F would lower the power-plant specific weight by 1 pound per kWe (net).

9.2.2 EXTERNALLY FUELED REACTOR SYSTEM

A conclusion of the coolant activation analysis (see Section 5) was that the externally fueled reactor coolant could be piped directly to the main radiator without significantly increasing the radiation dosage to the spacecraft components. Thus, a single loop was assumed for all the computer code investigations of this type reactor system.

The externally fueled reactor can be designed to produce output voltage in the 50 to 150 volt range. The cable lengths can be fairly long for this voltage range before significant electrical losses accrue. For that reason, the main radiator was assumed to be placed directly behind the shield with the main power conditioning located in the rear section of the vehicle. In this way, the length and weight of the main heat rejection piping was minimized with but a small penalty in cable weight.

The initial information received from the externally fueled reactor contractor was based on a BOL output power level of 360 kWe. The data covered a range of reactor outlet coolant temperatures 1100°F to 1600°F, a coolant temperature rise range of 50 to 600°F, and an output voltage range of approximately 60 to 120 volts. These data were used for some preliminary screening runs with the computer code using the steepest ascent optimization method. The results indicated the following:

- a. The higher the output voltage the lower the system specific weight
- b. The optimum coolant temperature rise in the reactor is about 350°F
- c. The optimum reactor coolant exit temperature is in the range 1350° to 1500°F
- d. Aluminum cable and sodium-stainless steel clad cable systems are essentially equal in system specific weight

- e. Approximately 276 kWe of reactor output is needed to produce the required 240 kWe at the thrusters.

On the basis of these preliminary conclusions, the reactor contractor furnished additional reactor information for the following sets of conditions:

- a. Output voltage range of 110 to 150 volts
- b. Constant reactor coolant exit temperature of 1350° F
- c. Reactor coolant temperature rise range of 250° to 450° F
- d. Reactor physical sizes based on 332 kWe BOL which supplies the desired 20 percent diode redundancy for 276 kWe design power at EOM.

These later data were used for all the externally fueled reactor systems investigations except those determining the effect of reactor coolant exit temperature. All the optimization runs on the externally fueled reactor system were made using variable optimization method.

The variations in spacecraft specific weight, and net propulsion power, as a function of reactor output voltage is shown in Figure 9-21. Net power increases with voltage level but the minimum specific weight is attained with 120 volts at the reactor bus. The pertinent details for the system designs are listed in Table 9-3. The increase in net power with reactor voltage is due primarily to the lower cable losses and the higher power conditioning efficiency accompanying the higher voltages. The total system weight reaches a minimum at 120 volts because of conflicting component weight trends; the reactor and shield system weights increase with higher voltage while the power conditioning system and structure weights are decreasing. The predominant weight change with voltage is in the reactor-main radiator loop. The listing of the reactor and main radiator component weights show the reactor weight growing at an increasing rate with higher voltage, the radiator weight reaching a minimum around 130 to 140 volts, which is the voltage range for maximum efficiency, and the loop piping

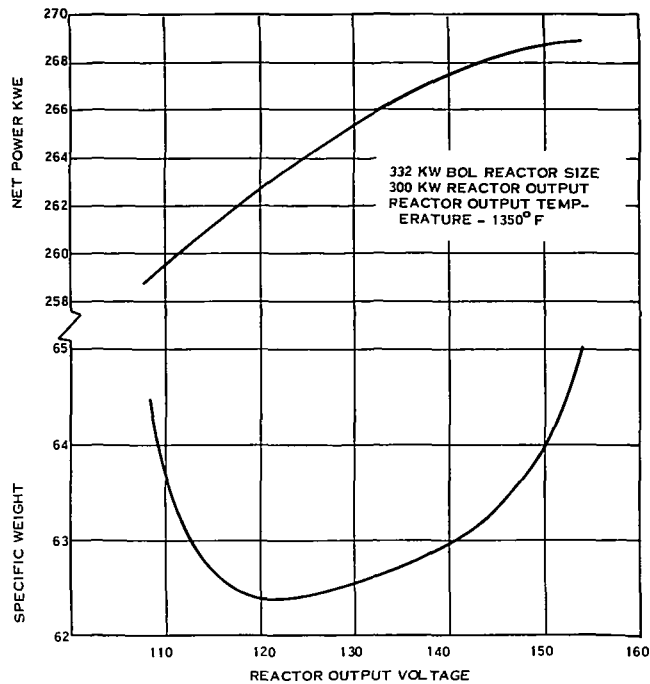


Figure 9-21. Externally Fueled Reactor - Effect of Reactor Output Voltage

weight being relatively constant at 500 pounds. So the weight trend on the reactor loop is traceable to the reactor itself. Power conditioning module weights decrease with increasing voltage, and this fact dominates the trend for the PC system weights. PC radiator fin thickness did not optimize in a uniform trend, which caused the total PC system weight at 132 volts to be higher than the corresponding weight at 121 volts. Structural weights reach a minimum because the vehicle length minimizes at a voltage corresponding to maximum reactor efficiency and minimum main radiator area.

The effect of reactor output power level on spacecraft weight and net power is shown on Figure 9-22 for reactor output voltages of 121 and 153 volts. The results show a constant advantage for 121 volts and a trend to higher specific weights as the reactor output is lowered from the nominal value of 300 kWe. The ratio of net power to reactor power is essentially constant over the range investigated, but the total system

TABLE 9-3. EXTERNALLY FUELED REACTOR SYSTEM - EFFECT OF REACTOR OUTPUT VOLTAGE

System Conditions	Voltage				
	108.9	121.0	132.7	144.1	152.9
Reactor Output Power, kWe	300	300	300	300	300
Net Power, kWe	259.2	262.7	266.3	267.9	268.2
System specific weight, lbs/kWe	64.16	62.37	62.63	63.25	64.73
Subsystem Weights, lbs.					
Reactor-Main Radiator	5939	6079	6383	6872	7512
Shield	862	894	902	991	1096
Auxiliary	112	111	116	116	113
Power Conditioning	2732	2462	2599	2375	2115
Cables	239	203	255	218	167
Payload	2200	2200	2200	2200	2200
Thrusters	1629	1618	1643	1629	1605
Structure	2912	2818	2579	2539	2558
Total Weight, lbs.	16629	16386	16677	16941	17366
Component Weights, lbs.					
Reactor	3663	3922	4304	4806	5406
Main Radiator	1761	1671	1558	1578	1653
Cable Electrical Losses %	2.18	1.87	1.33	1.27	1.28
P. C. Efficiency %	90.5	91.25	91.88	92.4	92.74

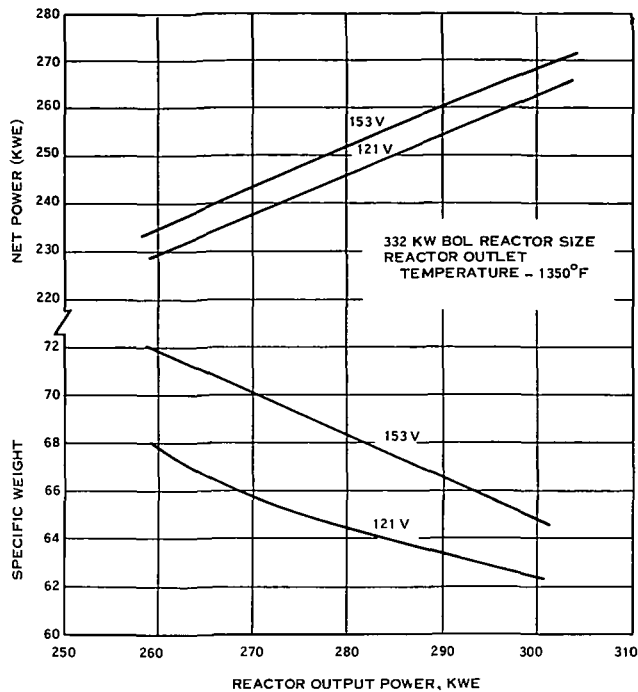


Figure 9-22. Externally Fueled Reactor - Influence of Reactor Output Power

weight does not decrease proportionally with the reactor output power. The reactor and payload weights are constant for the power range, and the weights of the shield system, cables and thruster system do not decrease in proportion with the power. Only the main radiator, power conditioning units and structural weights follow the trend of output power.

The trend in specific weight with power output would be flatter if the size of the reactor were adjusted for the output power. As mentioned previously, the reactor size (a diode redundancy of 20 percent is constant and based on a reactor EOL output power of 276 kWe, so the effective redundancy is greater than 20 percent at power levels below 276 kWe, and less than 20 percent at power levels above 276 kWe.

The data of Figure 9-22 show that a reactor output of 274 kWe is required to obtain the desired 240 kWe to the thruster system.

The sensitivity of the spacecraft specific weight to changes in system conditions about their optimum values is shown on Figure 9-23. As in the flashlite reactor investigations, each parameter is varied by ± 50 percent about its optimum value while all other conditions are kept constant. The data show the relative insensitivity of the system specific weight over the range investigated to most of the parameters. Only a decrease in the main heat rejection loop pipe diameter, or an increase in the reactor coolant temperature rise, show significant changes in the overall system specific weight.

The advantage of higher power conditioning temperatures in the externally fueled reactor systems is shown on Figure 9-24. A decrease of about 5 lb/kWe in specific weight accompanies a rise in PC temperature from 200° to 300° F. A savings of almost 1 lb/kWe would be realized if the ΔT between the PC modules and the PC radiator were decreased from 25° to 15° F.

The influence of reactor coolant outlet temperature on system characteristics was investigated. The initial reactor data based on a 360 kWe BOL reactor size had to be used since the later data was applicable for 1350° F coolant exit temperature only. The results of the analyses which assumed a 274 kWe reactor output are presented on Figure 9-25. Contrary to the preliminary results, which indicated an approximate equality in specific weights for 1350° and 1500° F reactor coolant exit temperature cases, these later optimizations show a 2 lb/kWe advantage for the 1500° F condition. A slight increase in reactor weight is more than offset by decreases in radiator weight and structure weight when the coolant temperature is raised from 1350° to 1500° F. The higher radiator temperature lowers its area and weight and the structure weight lessens because the lower radiator area results in a shorter vehicle length. In addition to the lower system weight, the net output power rises at the higher temperature. Shorter cable lengths generate lower electrical losses, and a higher coolant temperature rise in the reactor results in a lower required pumping power. The two effects combine to provide a slightly higher net power at the higher temperature.

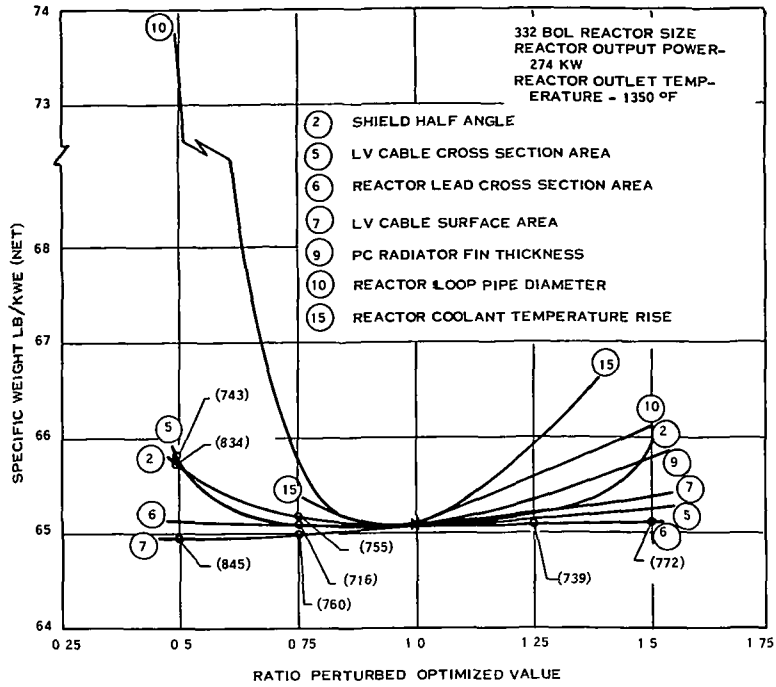


Figure 9-23. Externally Fueled Reactor - Variation of System Parameters

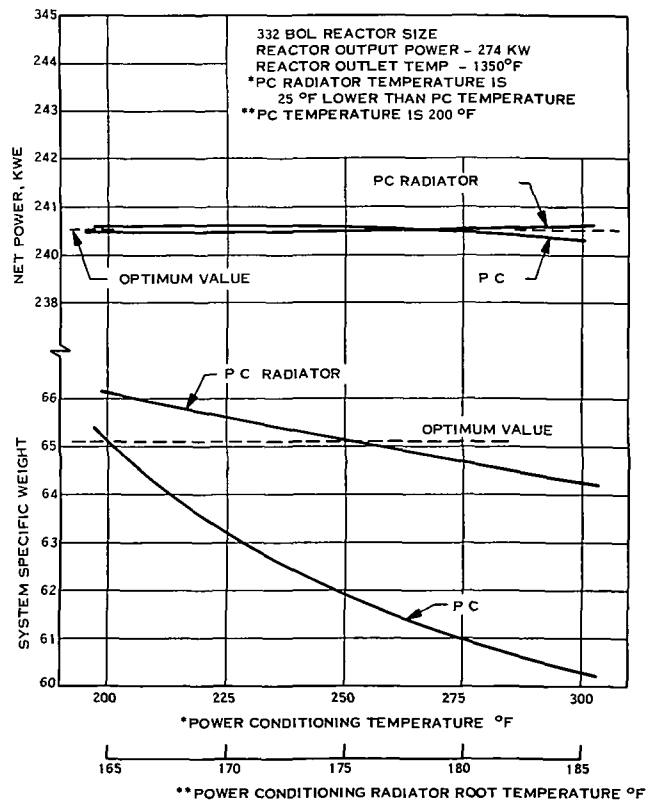


Figure 9-24. Externally Fueled Reactor - Influence of Power Conditioning Temperature and PC Radiator Temperature

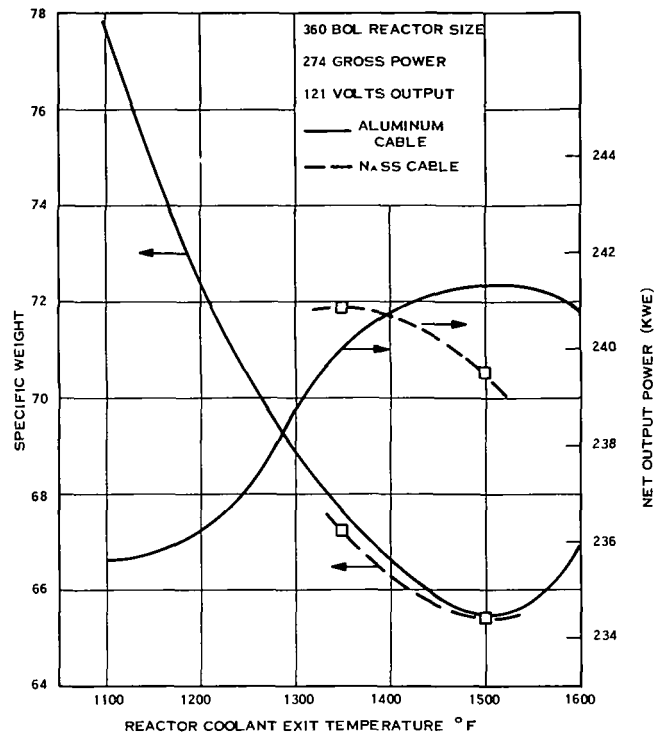


Figure 9-25. Externally Fueled Reactor - Effect of Reactor Outlet Coolant Temperature

There is some doubt about the applicability of a copper-stainless steel radiator operating above 1400°F because of possible vacuum sublimation of the copper. A columbium alloy radiator may be required at the higher temperature but the effect on system specific weight could not be evaluated since the appropriate radiator model is not presently available. Using the results of some general investigations of material composition on radiator specific weight, it is estimated that the use of a columbium radiator would only lower the spacecraft specific weight, if any change were experienced at all.

Figure 9-25 also shows the results of using sodium-stainless steel cables at 1350° and 1500°F . The difference in specific weight between the aluminum and sodium-stainless steel systems is negligible so aluminum is the obvious selection.

10. MISSION OPERATIONS

10. MISSION OPERATIONS

An integral part of the design study of a thermionic reactor spacecraft is the operations analysis of pre-launch and post-launch activities and a nuclear safety evaluation of the reactor system. This section provides a plan for insuring that the integration of all engineering operations results in accomplishment of the mission. Also, a basis for conducting power system acceptance testing as well as a reactor safety analysis are presented.

10.1 OPERATIONS ANALYSIS

The purpose of this section is to describe the established mission profile including pre-launch flow plans and post-launch operations. Plans for the integration of the power system fabrication, test, installation, and operation with associated spacecraft, payload and launch facility functions have been developed so that these individual operations can be combined in an orderly and logical fashion to meet all mission requirements.

10.1.1 DEFINITION OF MAJOR EVENTS

Figure 10-1 presents in simplified form, the mission profile for a typical thermionic reactor powered spacecraft on a Jupiter Mission. The profile is broken into three segments: factory and test operations, launch site operations, and flight operations. The various spacecraft subsystems are first assembled at their respective sites and subjected to acceptance tests. Following these tests, the subsystems are joined together for operational checkout. The NASA Plumbrook Space Power Facility could accommodate the complete spacecraft assembly and could permit short term powered operation of flight units. Such testing must be incorporated in a schedule that permits the reactor fission products to decay sufficiently prior to their use during the relatively hazardous pre-launch countdown and launch ascent operations, and to permit safe shipment to the launch site. However, it is possible that Back Emission Testing (BET) could be used to eliminate nuclear testing.

Once at the ETR launch site, the thermionic spacecraft is installed on the already assembled Titan IIIC/7 launch vehicle. Launch vehicle and spacecraft tests are performed, spacecraft systems (e. g. , coolant loops and propellant storage) are serviced, and the flight fairing is installed. The booster is then fueled, final checkout of all systems is completed, and the terminal phase of the countdown takes place.

The first three stages of the Titan IIIC/7 place the spacecraft in a low Earth orbit and the transtage is later fired to transfer the spacecraft to a 750 nautical mile orbit. At this point, communication with the spacecraft is established and the on-board systems are activated and checked out. Once acceptable performance levels have been verified and the orbit established, the reactor startup can be initiated and the radiator thermal shroud separated while the system coolant is still in no danger of freezing. (The coolant probably could be circulated during the period from launch to reactor startup, and auxiliary power must be provided for this purpose.) Following the achievement of criticality, the reactor is automatically controlled to a low power level (approximately 10 percent), and all auxiliary equipment is switched to reactor-produced power. The control system then brings the reactor to full power and the thrusters are activated, causing the spacecraft to spiral outward and ultimately assume a heliocentric orbit in its trajectory to Jupiter. During the transit time, the spacecraft is tracked and its thrust vector is controlled (by ground station commands) to maintain the desired trajectory. Commands transmitted to the spacecraft shut off the thrusters and reduce reactor power during mid-mission coast, and bring the reactor back up to full power so that retro-thrust can be applied during the latter phase of the transit.

At the appropriate point following encounter with the Jovian gravitational field and attainment of the required orbit, the science payload is deployed, the reactor power is reduced to a low level, and the thrusters are shut off. If a satellite lander capsule is included as a part of the science payload, it would be separated from the spacecraft

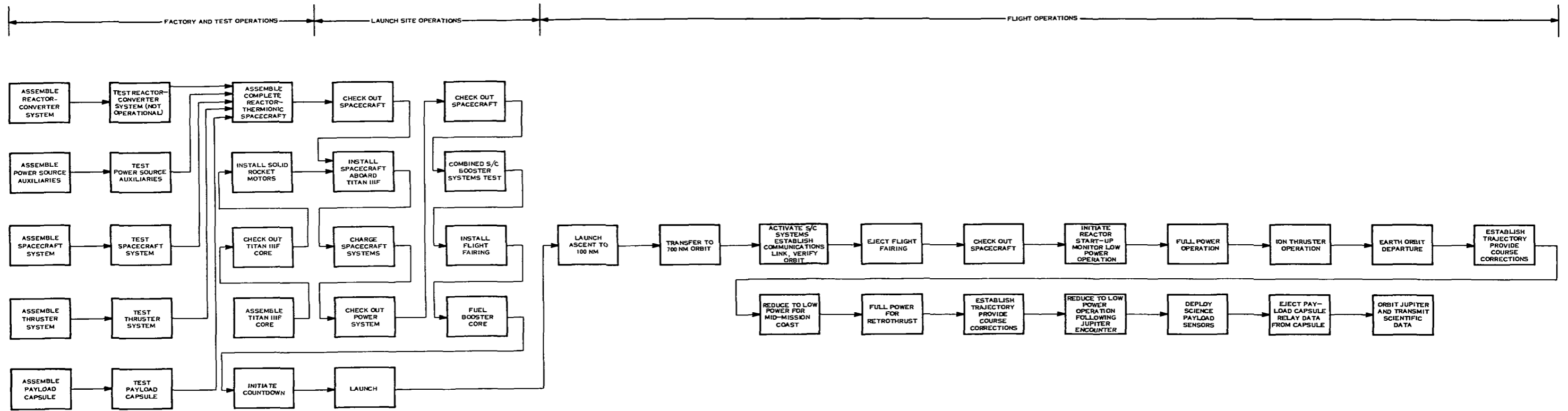


Figure 10-1. Typical Mission
Reactor-Thermionic Jupiter

when the appropriate relative orbital positions of the spacecraft and the Jupiter satellite (e.g., Callisto) is attained. The spacecraft then acts as a relay station for signals transmitted from the lander, while simultaneously transmitting data from on-board sensors as it continues to orbit the planet.

10.1.2 POWER PLANT STARTUP

Prior to reactor startup, power is required by several spacecraft systems, notably the reactor coolant loop and the reactor startup controls and instrumentation. The total power and energy requirements must be defined and a suitable auxiliary power system selected and characterized. Reactor startup cannot be initiated until the orbit altitude (750 nautical miles) prescribed by safety requirements has been attained and confirmed. Meanwhile, some of the following spacecraft functions that are dependent on electrical power must occur:

- a. Circulation of reactor coolant
- b. Heat addition to reactor coolant
- c. Communications, including the transmitting of data and acceptance of commands by the spacecraft.
- d. Instrumentation and control associated with reactor startup
- e. Instrumentation required for monitoring and housekeeping
- f. Operation of attitude control system.

Because of the potential hazards that occur during and prior to launch, the reactor probably will not be operated until the spacecraft has acquired a proper orbit. Reactor startup must therefore be remote and automatic when the spacecraft has reached the minimum safe orbit, and it has been determined that all systems are functioning properly, the reactor can be started and taken to full power operation. The spacecraft auxiliary power load can be taken over by the reactor power system and the short-lived auxiliary power sources can be deactivated, and if practical, jettisoned

to improve subsequent performance in the electric propulsion phase. Thruster operation will be initiated in accordance with ground commands. The procedures and equipment required to effect startup and the subsequent generation of power must be determined.

Procedures involved in reactor startup begin prior to launch; the step-by-step procedures required include the assembly of the reactor to the spacecraft and carry through to the production of thrust by the ion engines. Factors to be considered are the charging of the reactor coolant systems, the maintenance of sufficiently high coolant temperatures through launch ascent and during orbital flight prior to reactor startups, the detailed procedures of the startup and the controls and instrumentation required to effect it, the timing of flight fairing ejection, power requirements of the startup process, and the auxiliary equipment (both vehicle-mounted and ground support) required. In addition to detailed startup procedures, a startup system will thus be defined and consideration will be given to equipment redundancy and contingency planning in the event of component failures.

Specific areas of investigation include:

- a. Means of preventing coolant freeze-up prior to startup of the reactor
- b. Suitable means of shipping the thermionic spacecraft from the assembly and test site to the launch site
- c. Mission contingency plans.

10.1.2.1 Primary Coolant During Startup

A critical aspect of spacecraft heat rejection system design is the behavior of the radiator under startup conditions. Fundamental to the problem of startup is the necessity for the radiator to respond to increasing power loads. This requirement demands that the radiator coolant be in a fluid condition when startup is initiated.

An investigation of radiator panel temperatures was conducted for a typical fin-tube geometry in a 750 nautical mile sun oriented, ecliptic orbit to estimate if the coolant in the thermionic spacecraft radiator system would freeze during the launch and orbit stabilization period. Since the launch time, trajectory and other specifics are unknown at this time, the object was to select a typical situation and assess the severity of the radiator startup problem. The assumptions used in this investigation include:

- a. Conduction fin offset-tube geometry, stainless steel armor, stainless steel/copper fins (See Figure 10-2)
- b. Incident heat flux varies with position as in a 750 nautical mile ecliptic orbit
- c. NaK (78 wt % K) radiator coolant - freezing temperature of 12°F
- d. Radiator emissivity and solar absorptivity of 0.9.
- e. NaK is pumped into loop just prior to startup, therefore, its latent heat of fusion does not contribute to radiator heat capacity.
- f. The radiator is cylindrical and is slowly rotating.

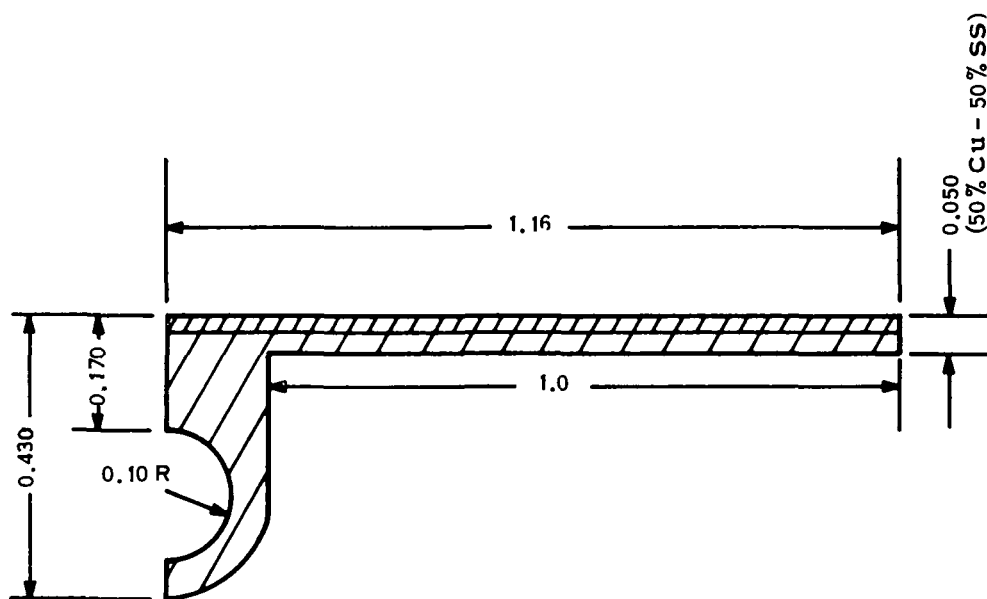


Figure 10-2. Model for Thermionic Spacecraft Radiator Startup Study

The results obtained from the analysis are shown in Figures 10-3 and 10-4. Examination of Figure 10-3 shows that for a wide range of radiator temperatures at the beginning of the sun portion of the orbit, the temperature of the radiator will reach approximately 120° to 140°F by the time it starts the shade portion. However, this situation results in a radiator temperature of -15°F by the time the vehicle again receives solar flux. In order for the radiator to remain above 12°F during the entire orbit, it must begin the swing behind the earth at about 310°F. The assumption that the NaK is not in the radiator is not required. Its effect is to reduce the temperatures during heatup by about 10°F, and increase the temperatures during cooldown by the same amount, relative to the data of Figures 10-3 and 10-4.

Whether or not the radiator will require pre-heating, insulation or an auxiliary power supply will depend on the startup power profile of the remainder of the system. A distinct possibility is present for system startup during the sun portion of the orbit, or during an orbit where a greater part of the time is spent in the solar flux.

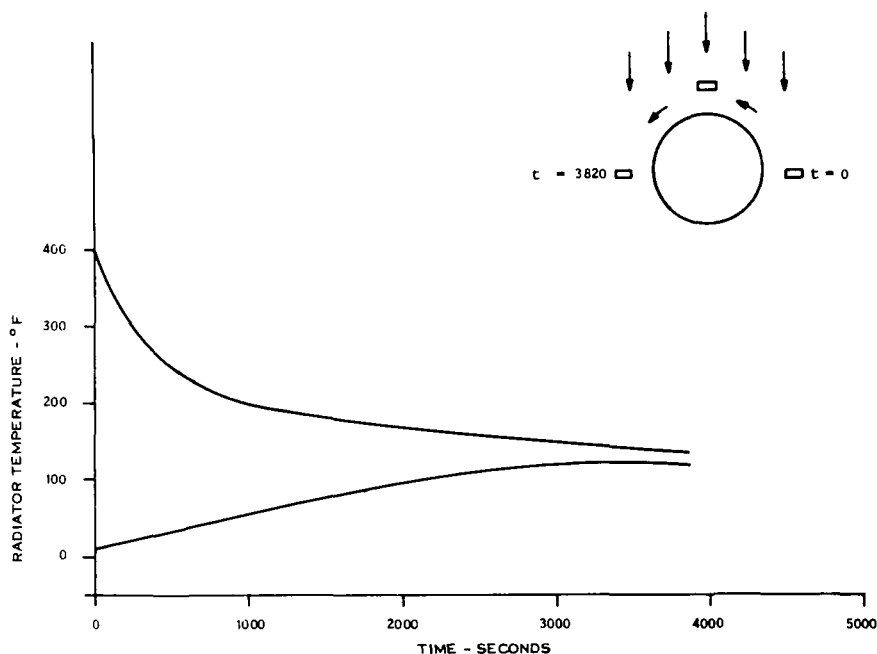


Figure 10-3. Radiator Temperature on Sun Side

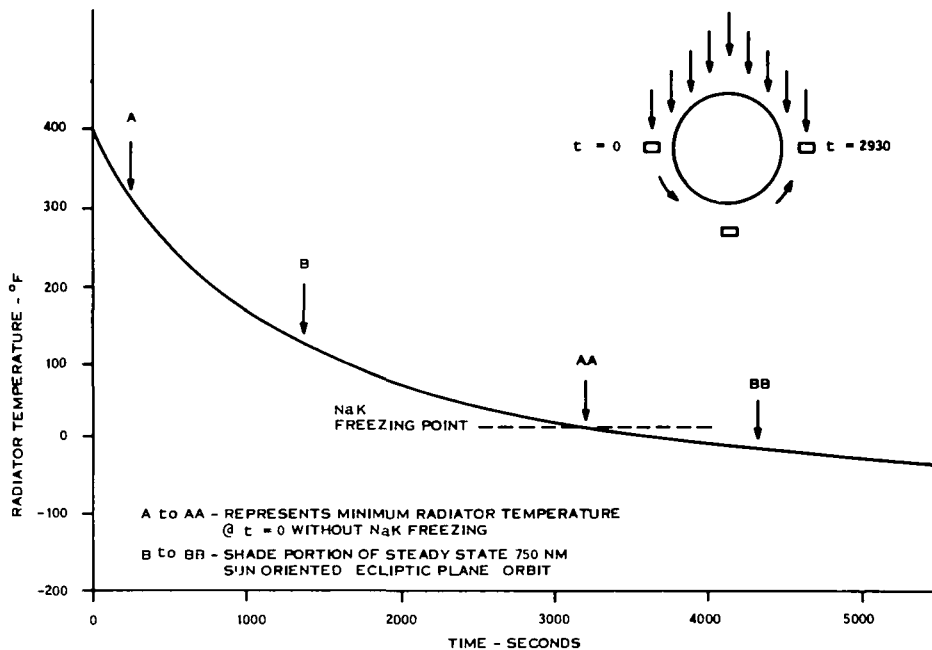


Figure 10-4. Radiator Temperature on Shade Side

Alternately, an orbit with a beta angle other than 90 degrees may be selected. The radiator average temperature as a function of beta angle (angle between the sun ray and the orbit plane) for an isothermal cylindrical shape at an altitude of 750 nautical mile is shown on Figures 10-5 and 10-6. The cylinder considered was oriented with its roll axis parallel to the earth's surface, and perpendicular to the earth's surface. The ends of the cylinder were assumed to be blocked from seeing the external sink. The external conditions used were nominal, in terms of solar, albedo, earth and day of year.

The curves labeled orbit average in Figures 10-5 and 10-6 show the temperature for the whole body averaged over the orbit. Maximum instantaneous is the highest temperature during the orbit and minimum instantaneous is the lowest. For the case with the roll axis parallel to the earth's surface, the minimum temperature is -144°F

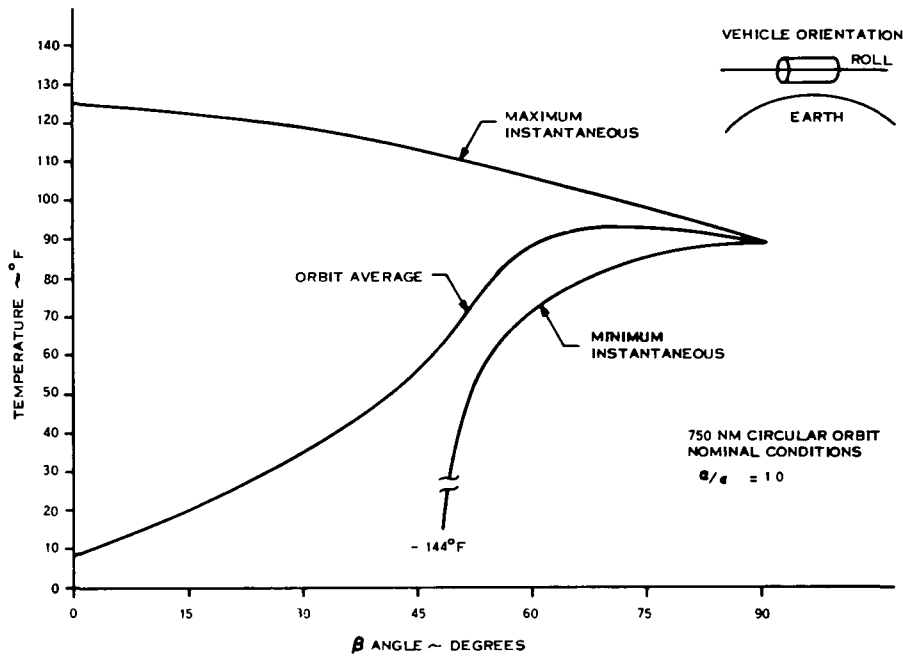


Figure 10-5. Radiator Average Temperature vs Beta Angle

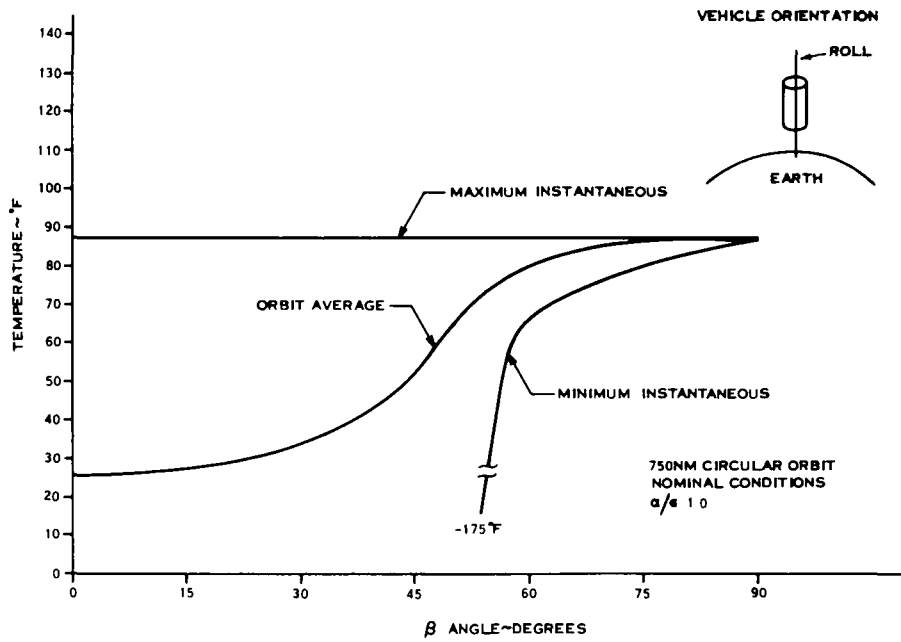


Figure 10-6. Radiator Average Temperature vs Beta Angle

and for the perpendicular case the minimum temperature is -175°F , when the beta angle is approximately less than 60° . The amount of shade time during which the sink is this minimum value can be found by referring to the curve in Figure 10-7 which gives the amount of shade time as a function of beta.

Consequently, proper selection of the earth departure orbit will eliminate the need for special startup heating or insulation for NaK-78 cooled power plants.

10.2 NUCLEAR SAFETY EVALUATION

10.2.1 PURPOSE AND SCOPE

An essential task in performing a design study for a thermionic reactor spacecraft is to provide a nuclear safety evaluation. The objective of this safety evaluation is to establish safety design criteria and performance objectives concurrent with reactor system development to assure a reactor configuration capable of safe mission operation. To obtain flight approval for the thermionic reactor powered spacecraft, the safety analysis must show that hazards and accident consequences

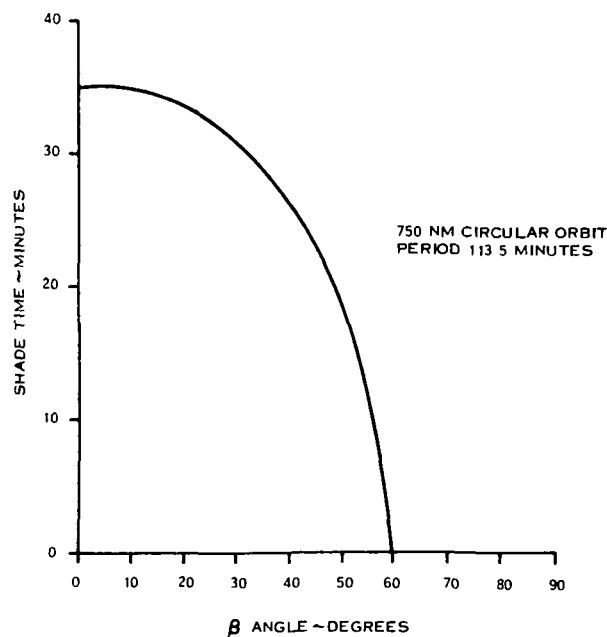


Figure 10-7. Shade Time vs Beta Angle

for each operational phase shall not involve an unacceptable risk to operational personnel and the general public.

The major areas which must be considered in reactor safety analysis are:

- a. Identification of potential modes of failure in the ground handling, prelaunch, and flight phases of the mission which can affect the safety of the thermionic reactor system.
- b. Assessment of factors affecting the probability of the identified failures.
- c. Description of the environments to which the reactor system is subjected following the identified failures.
- d. Evaluation of the effect of failure environment on the reactor system and determination of the probability for inadvertent criticality, as well as amount, condition, and location, of any fission product release.
- e. Analysis of the potential radiological consequences of an inadvertent criticality or fission product release.

The safety analyses should be made concurrent with reactor system development.

In some areas, analytical methods cannot predict failure modes or consequences with confidence. In these cases, a safety test program is conducted. Safety tests should verify the design capability to preclude radiological exposure to personnel and present data required to evaluate the potential hazard in the event that a failure occurs.

The safety of a thermionic reactor system for a Jupiter orbiter mission can be enhanced if the following approaches are employed:

- a. Through restrictions on prelaunch integrated power, there should be a low fission product hazard from conceivable accidents during checkout or launch operations.
- b. By delaying reactor startup until after the spacecraft has achieved a long lifetime earth orbit, i. e. , about 500 years or greater, fission products will have decayed to non-hazardous levels by the time re-entry occurs.

- c. By achieving a reactor design which would be incapable of (1) compaction into a critical configuration, or (2) inadvertent criticality induced through the control loop, the consequences of a pre-launch accident or post launch abort should not result in a radiological hazard to the general public.

This section provides the basis for the safety evaluation to be performed for a thermionic reactor spacecraft. Power system acceptance test requirements are presented, and a preliminary fault tree is developed to implement the application of probabilistic philosophy to the spacecraft reactor system. The information required for probabilistic definition of mission abort modes should be developed during the early phase of reactor system development. Possible hazardous operations and potential accidents are delineated for each operational phase of the mission.

10.2.2 ACCEPTANCE TESTING

Power system acceptance test requirements and mission safety requirements tend to be mutually exclusive. To reduce the possibility of undesirable radioactive fission product release in the event of a launch pad explosion or launch ascent abort, it is necessary to launch a reactor that has not been operated. This procedure is undesirable from the standpoint of acceptance testing since it affords no opportunity to verify the performance of the assembled thermionic reactor flight power plant prior to its commitment to the mission.

A number of approaches that satisfy both requirements to varying degrees are possible. Some possibilities are presented in Table 10-1, ranging from an approach that entails no direct testing of the reactor to one that involves a test of the completely assembled power system followed by a waiting period to permit fission product decay to acceptably low levels. The acceptability of each of the approaches and the selection of one as the best to employ obviously hinges on operational and design characteristics of the spacecraft power system support facility complex.

TABLE 10-1. REACTOR-THERMIONIC POWER SYSTEM PRELAUNCH TESTING

Test Approach	Comments
<p>1. Build two reactor-thermionic diode power systems simultaneously. Test one system extensively by operation in appropriate facility; install other system in spacecraft for flight use without pre-launch operation.</p>	<p>Safety hazard is minimized but the assurance of acceptable performance from the thermionic reactor power system may also be minimized.</p>
<p>2. Simulate operational conditions within the reactor through the use of heaters or BET thereby obtaining test data that can be used directly or extrapolated to represent actual operating data.</p>	<p>Reactor and diode design must lend itself to use of heaters or BET. Simulated operation must reproduce actual conditions sufficiently well to produce meaningful test data. This approach might permit testing just prior to launch.</p>
<p>3. Fabricate reactor-thermionic diode system and operate the unit in an appropriate facility. After suitable time period for the decay of fission products within the reactor then proceed with assembly of reactor into the power system and spacecraft.</p>	<p>Safety hazard presented by remaining fission products must be analyzed. Length of time required to reduce fission products to acceptable level must be established. Post-operational assembly problems must be investigated.</p>
<p>4. Fabricate and assemble the entire power plant/spacecraft assembly and operate this entity in NASA Plum Brook facility. Provide suitable time period for decay of fission products within the reactor, then transport the spacecraft to the launch site for installation on the booster and subsequent launch.</p>	<p>Provides maximum assurance of ability to meet performance requirements, provided that fission product decay period is not too long and that suitable means of transportation from test facility to launch site are available. Safety hazard must be analyzed.</p>

10.2.3 PRELIMINARY FAULT TREE ANALYSIS

The fault tree analytical technique permits the detailed evaluation of potential system incompatibilities or failure modes, and when used in conjunction with applicable failure consequence evaluation techniques, materially enhances the overall evaluation of the safety of a complex system.

The fault tree approach:

- a. Assures an understanding of the overall system and its failure modes.
- b. Identifies those areas where improved or specific data are required to predict system safety
- c. Provides the overall failure mode probability information that permits determination of the degree of safety of a particular event in terms of its probability of occurrence.
- d. Identifies those areas where program emphasis should be placed to enhance system safety.

The thermionic reactor spacecraft mission and events leading to mission completion are illustrated in Figure 10-8. The points of departure relating to mission failure or credible accidents, shown under each normal mission event define some of the failure modes in the preliminary fault tree shown in Figure 10-9. The symbols used in this fault tree are defined below:

The Rectangle identifies an event, usually a malfunction that results from the combination of fault through the logic gates.

The Diamond describes a fault that is considered basic in a given fault tree; however, the causes of the event have not been developed, whether because the event is an insufficient consequence, or the necessary information is unavailable.

The Circle describes a basic fault event that requires no further development. This category includes component failures whose frequency and mode of failure are derived through testing.

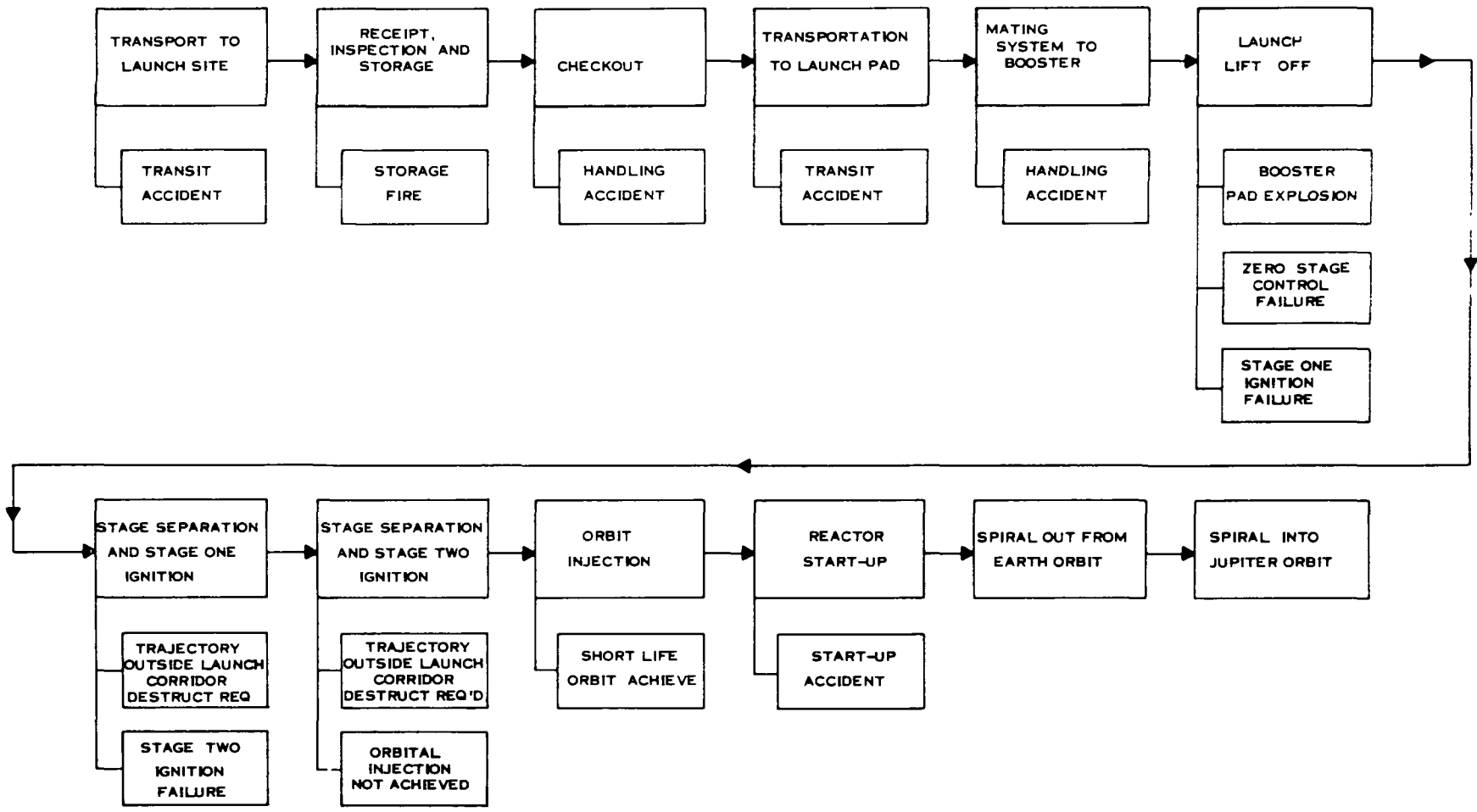


Figure 10-8. Proposal Mission Profile and Accident Groups for Unmanned Nuclear Powered Spacecraft for Planetary Exploration

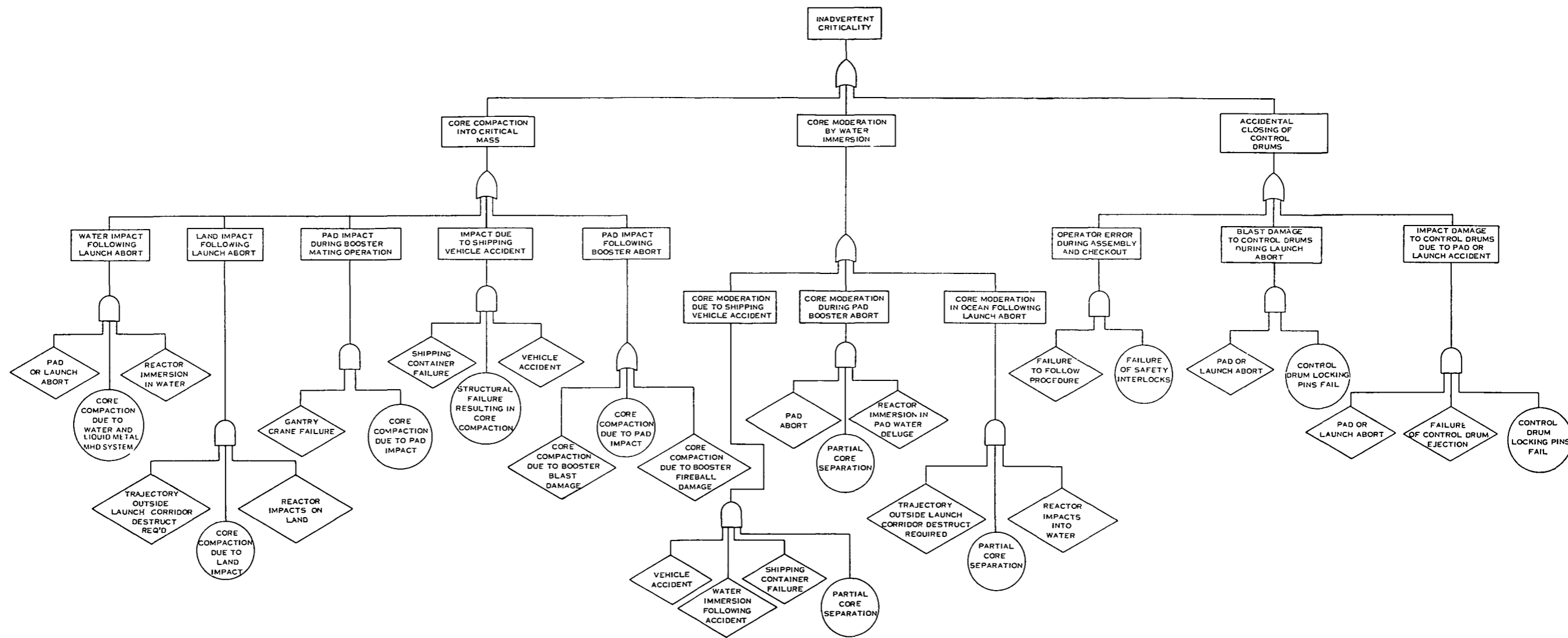


Figure 10-9. Iterations Necessary to Define Optimum Mission/Power Plant Combinations

The And Gate describes the logical operations whereby the coexistence of all input events are required to produce the output event.

The Or Gate defines the situation whereby the output event will exist if any or all of the input events are present.

Application of fault tree analysis to a thermionic reactor spacecraft system leads to the selection of the most undesired event as "Inadvertent Criticality." All the possible events that can lead up to this undesired event are defined and are used in the construction of the fault tree. Fault tree implementation requires that probability data be established for all identified events. The level of detail of this preliminary fault tree must be amplified to assure a complete safety evaluation. The identification of all contributing events and their probabilities will aid in identifying the direction and scope of the safety program, through the ability of the fault tree to focus on those areas where major effort may be required to assure that the safety requirements are achieved.

10.2.4 POSSIBLE HAZARDOUS OPERATIONS AND POTENTIAL NUCLEAR ACCIDENTS

To assess the nuclear safety problems associated with the utilization of a thermionic reactor system, a clear understanding of those types of accidents which may result in the release or generation of radioactive material is necessary. The mission phases where potential nuclear accidents may occur are:

- a. Transport of reactor to launch site
- b. Launch site handling and prelaunch checkout of reactor
- c. Mating of reactor to launch vehicle
- d. Launch
- e. Earth orbit injection.

The potential nuclear accidents are identified, and the possible engineering safeguards which could preclude these accidents or reduce their consequences are discussed for the above listed mission phase.

10.2.4.1 Transportation of Power Plant to Launch Site

Transport accidents which can result in water immersion, core compaction, or control device movement may lead to a criticality. Engineering safeguards should substantially reduce the probability of an accidental criticality during transit to launch site. This includes removal of the reflector control drums in addition to enclosing the reactor in a shipping container designed to absorb the loads associated with a transportation accident and to prevent reactor water immersion.

10.2.4.2 Launch Site Handling and Prelaunch Checkout of Power Plant

Launch site handling may involve moving the power plant from the storage building to launch pad. Since the launch site is a controlled area, strict traffic control can be enforced during the transfer. Proper approved procedures and availability of instrumentation should reduce the probability of accidents occurring during reactor assembly, prelaunch reactor checkout, and launch site handling operations. Safety interlocks must be used after reactor assembly to prevent inadvertent closure of the control drums. The reactor startup command system must be fail safe and must not be accidentally activated.

10.2.4.3 Mating of Spacecraft to Launch Vehicle

Upon completion of reactor assembly, the reactor will be mated to the launch vehicle. This mating operation is near the top of the launch vehicle. In the event that the reactor were to fall, core compaction and subsequent criticality may occur at pad impact. If the design objective of accomplishing a reactor design that is incapable of compaction into a critical configuration is met, this hazard would not exist. Aside from core compaction on pad impact, there is a remote possibility of a

criticality resulting from control drum closure. At this time in the prelaunch sequence and up to a few hours before launch, the reactor control drums should be secured in the open position by use of locking pins and/or nonreflecting void filler blocks (used on SNAP-10A).

10.2.4.4 Launch

The launch phase is perhaps the most hazardous phase from the standpoint of nuclear safety. An on-pad explosion and fireball, or an abort during boost, may subject the reactor system to the type of environment conducive to accidental criticality. Core compaction may occur from: blast or fragment damage; pad, land, or water impact; fireball damage; or liquid metal explosive reaction with pad deluge water or with the ocean where impact may occur. Core moderation may occur by reactor immersion in pad water deluge or falling into water. In fast thermionic reactors, hydrogen may have a limited worth and accidents involving water flooding of an unreflected assembly may not result in a criticality. However, partial core disassembly when reactor is immersed in water may lead to a criticality.

Another consideration in minimizing the nuclear hazard from a launch abort is to specify both prelaunch reactor operation, if any, and post operation storage times so that the fission product inventory will be at an acceptably low level at the time of launch. Then, a launch accident which leads to the destruction of the reactor should not disperse fission products in hazardous concentrations. The ideal mission plan would be to start up the reactor for the first time after the spacecraft has been inserted into a long-lived orbit so that even those pre-launch and launch accidents which do not result in criticality will not result in any fission product release.

10.2.4.5 Orbital Injection

Should a mishap occur during the final booster orbital injection phase of the mission which would destroy the spacecraft or send it into an improper trajectory, it is conceivable that the reactor system may re-enter and impact on the surface of the earth. It may be required that the launch azimuth be selected such that failure of the launch vehicle up to orbital injection will result in reactor impact into the open ocean or on an unpopulated land area. Upon ocean impact, core compaction or partial core separation can lead to a nuclear excursion. Again, reactor design can reduce this risk. Some degree of ocean contamination would occur if the reactor went critical, but natural diffusion and ocean currents should reduce activity to acceptable levels within a short time and a small distance from the impact point.

If the spacecraft achieved a short-lived orbit, the reactor may burn up to some extent and impact onto a populated area. Since the reactor startup should not occur until the spacecraft has definitely achieved a long-lived orbit, fission products will not be released on re-entry burnup or land impact.

After the spacecraft is inserted into the desired longlived orbit, reactor operation will be initiated. A startup accident at this point should not have hazardous consequences, since the released fission products will have decayed to acceptable levels before they return to the earth's surface.

Once the reactor is removed from the earth's gravitational field into a heliocentric orbit, an earth re-entry hazard should not exist. Based on safety considerations, achieving solar orbit is by far the preferred method of reactor disposal.

11. CONCLUSIONS

11. CONCLUSIONS

1. High voltage electric power is the most effective means of reducing the propulsion system weight.
2. Heavy metal reflectors in the thermionic reactor raise the average neutron energy, minimizing coolant activation, and therefore permit the use of a single loop heat rejection system.
3. The conical (or conical - cylindrical) radiator, launched in the upright (apex: top) position on the launch vehicle requires 5 lbs./kWe of support structure. The structural penalty for the inverted (apex: down) launch configuration is 1.5 to 2.0 times as great.
4. The triform, flat plate and cruciform radiator geometries require at least twice the structural penalty requirement of the conical radiator.
5. Spacecraft of the type evolving in this study will have lowest natural frequencies of the order of one cycle per second. Redesign of the autopilot for the Titan IIC/7 launch vehicle will be required to permit launching. This approach was utilized in the MOL program, and it is the best technique to maximize IMEO.
6. A spacecraft flight fairing length of about 80 to 90 feet will be required on the Titan IIC/7 launch vehicle (10 foot diameter). If this shroud is jettisoned in Earth orbit, the payload weight penalty will be 100 percent of the shroud weight. If the flight fairing is jettisoned at Stage II burnout, the payload weight penalty will be only 24 percent of the shroud weight.
7. No special thermal insulation will be required to permit power plant startup in the 750 nautical mile earth departure orbit, when NaK-78 is employed as the primary radiator fluid.
8. The system power level must be maintained below 77 percent of full power during initial spiral out from Earth orbit to limit electronic component temperatures to the maximum allowable of 200°F. Alternately, it may be acceptable to operate the electronics equipment above 200°F (about 230°F) for the 50 to 70 days required to spiral out to escape velocity from Earth orbit.
9. A two-loop primary heat rejection system will be required for the as designed flashlight reactor/spacecraft, but a single loop system is acceptable for the as designed externally fueled reactor/spacecraft.

10. The weight penalty of a two-loop primary heat rejection system, compared to a one loop system, is approximately 550 pounds.
11. Comparison of aluminum, copper, and sodium metal in stainless steel tubing for low voltage cable material has resulted in the selection of copper-aluminum for both spacecraft concepts.
12. The flashlight reactor generates 318 kWe in order to supply 240 kWe to the ion engine. The propulsion system specific weight, α , is 71.1 pounds/kWe. The resultant spacecraft is approximately 84 feet long. The spacecraft powered by the externally fueled reactor, requires a gross reactor output of 274 kWe to supply 240 kWe to the ion engines. The resultant spacecraft is approximately 62.7 feet long. Propulsion system specific weight, α , is 50.4 pounds/kWe.
13. No electrical system redundancy is required. The failure of any one of the 108 main converter units in the flashlight reactor/spacecraft will result in a power loss of less than one percent. Both reactors are designed to provide a ten percent power margin at beginning of mission.
14. All thermionic reactor main power conditioning units will require filtering of the reactor input power. For the flashlight reactor with 108 main converter units, the filter units represent a weight penalty of about 1.5 pounds/kWe. For the externally fueled reactor with 37 main power conditioning units, the filter units represent a weight penalty of 0.75 pounds/kWe.
15. The flashlight reactor electric system requires that all the thruster units operate in parallel from a single high voltage bus. Therefore, electric isolation be provided for each thruster, to prevent the dumping of all thruster beam power into a single thruster unit in the event of thruster arcing. The weight penalty for the thruster isolation system for all 37 thruster units is about 1.0 pounds/kWe.
16. The total defined payload and communications subsystems weight of these subsystems, including data handling components, is approximately 262 pounds. Since 2200 pounds has been allocated for the payload, an additional 1940 pounds is available for payload equipment.

12. RECOMMENDATIONS

12. RECOMMENDATIONS

1. The propulsion system weight penalty associated with low voltage thermionic reactors has been identified at about 20 lbs/kWe. Evaluation of the externally fueled diode reactor should be continued.
2. The neutron energy spectrum of the flashlight reactor should be raised to reduce coolant activation, permitting a single primary heat rejection loop.
3. Increased weight savings of 2 lbs/kWe can be realized if the externally fueled reactor coolant exit temperature is increased from 1350°F to 1500°F. The compatibility of the higher coolant exit temperatures with stainless steel technology, and the need for refractory metal containment, must be evaluated.
4. Copper-aluminum should be utilized for low voltage cable materials. The copper is required only at the higher temperature, near the reactor.
5. Shield analysis for the externally fueled reactor should be completed to the same degree accomplished for the flashlight reactor.
6. Investigation should be made of a power conditioning thermal radiation cooling concept in which each power conditioning module is dispersed uniformly over the individual radiator panel assigned to the module.
7. The feasibility of raising power conditioning temperature from 200°F to 300°F should be investigated, including the effect on radiator weight and low voltage cable length.
8. The feasibility of decreasing power conditioning unit to radiator ΔT , from 25°F to 15°F for example, by more efficient thermal contact should be determined.
9. During initial spiral out from Earth orbit, the system power level must be maintained below 77 percent of full power in order to limit electronic component temperatures to the maximum allowable of 200°F. Alternately, it may be acceptable to operate the electronics equipment at about 230°F for this 50 to 70 day period. The effort of these alternates on power conditioning performance and mission time should be evaluated.
10. Filtering should be provided for all thermionic reactor main power conditioning units.
11. The conical (or conical-cylindrical) radiator configuration, integrated with the spacecraft and launched in the upright (apex:up) position on the launch vehicle, should be employed to minimize spacecraft weight in Earth orbit.

12. As soon as data are available for all power plant components, a relative reliability should be completed.

13. REFERENCES

13. REFERENCES

1. Terrill, W. , Notestein, J. , "Radiator Design and Development for Space Nuclear Powerplants," Vol. II, 64SD224B, General Electric Missile and Space Division, Valley Forge, Pa. , February 1964.
2. Miscellaneous Data for Shielding Calculations; compiled by John Moteff, General Electric Company; APEX-176; December 1, 1954.
3. A design Study for a Thermionic Reactor System for a Nuclear Electric Propelled Unmanned Spacecraft, Quarterly Progress Report No. 1, GESP-7011, May 1969.
4. Bruhn, "Analysis and Design of Flight Vehicle Structure", Tristate Offset Company.
5. Masek, T. , "Thrust Subsystem Design for Thermionic - Electric Spacecraft Study", JPL Memo, February 20, 1969.
6. "Thermionic Reactor Power Plant Design Study", General Electric NTPO, Report No. GESR-2115, July, 1968, Vol. I and II.
7. Sawyer, C.D. , "Performance Data for 300 ekW Reactors", (letter), June 13, 1969, and personal communications.
8. P. D. Corey, "Analytical Optimization of Magnetics for Static Power Conversion". Supplement to IEEE Transactions on Aerospace", Vol. AS-3, No. 2, June 1965, pp 86-92.
9. Macie, T. W. , "Startup/Shutdown of a Power Conditioner". JPL Memo, February 18, 1969.
10. "Development and Test of an ION Engine System Employing Modular Power Conditioning", Project Final Report. Hughes Aircraft Company. JPL Contract No. 95144/August 1966, NASA Report No. CR-80515.
11. E. V. Pawlik, T. Macie, J. Ferrara, "Electric Propulsion System Performance Evaluation", AIAA Paper #69-236. Presented at AIAA 7th Electric Propulsion Conference, Williamsburg, Va. , March 3-5, 1969.
12. V. Truscello, R. E. Louchs, "Power System Design for a Jupiter Solar Electric Propulsion Spacecraft", Jet Propulsion Laboratory, October 15, 1968. NASA Technical Report 32-1347.

13. Jacob, M. "Heat Transfer", 1949 Edition.
14. Verkamp, J. and Rhudy, R. , "Electromagnetic Pumps in Space Power Systems", RSD, General Electric Co. , Sept. 1965.
15. Personal communication, J. Weber, Martin Marietta Company.
16. 300-ekW Thermionic Reactor Design Study, Fairchild Hiller, FHR-3428-2, 1968.
17. SCR Inverter Commutated by an Auxiliary Impulse, IEEE Vol. 83, No. 75, Nov. 1964.
18. Kerchner and Corcoran, "Alternating Currents", Wiley, 1955.
19. Gietzen, A. "Low Voltage Power Conditioning for the Thermionic Reactor Project", July 16, 1969.

APPENDIX A
STRESS ANALYSES DATA

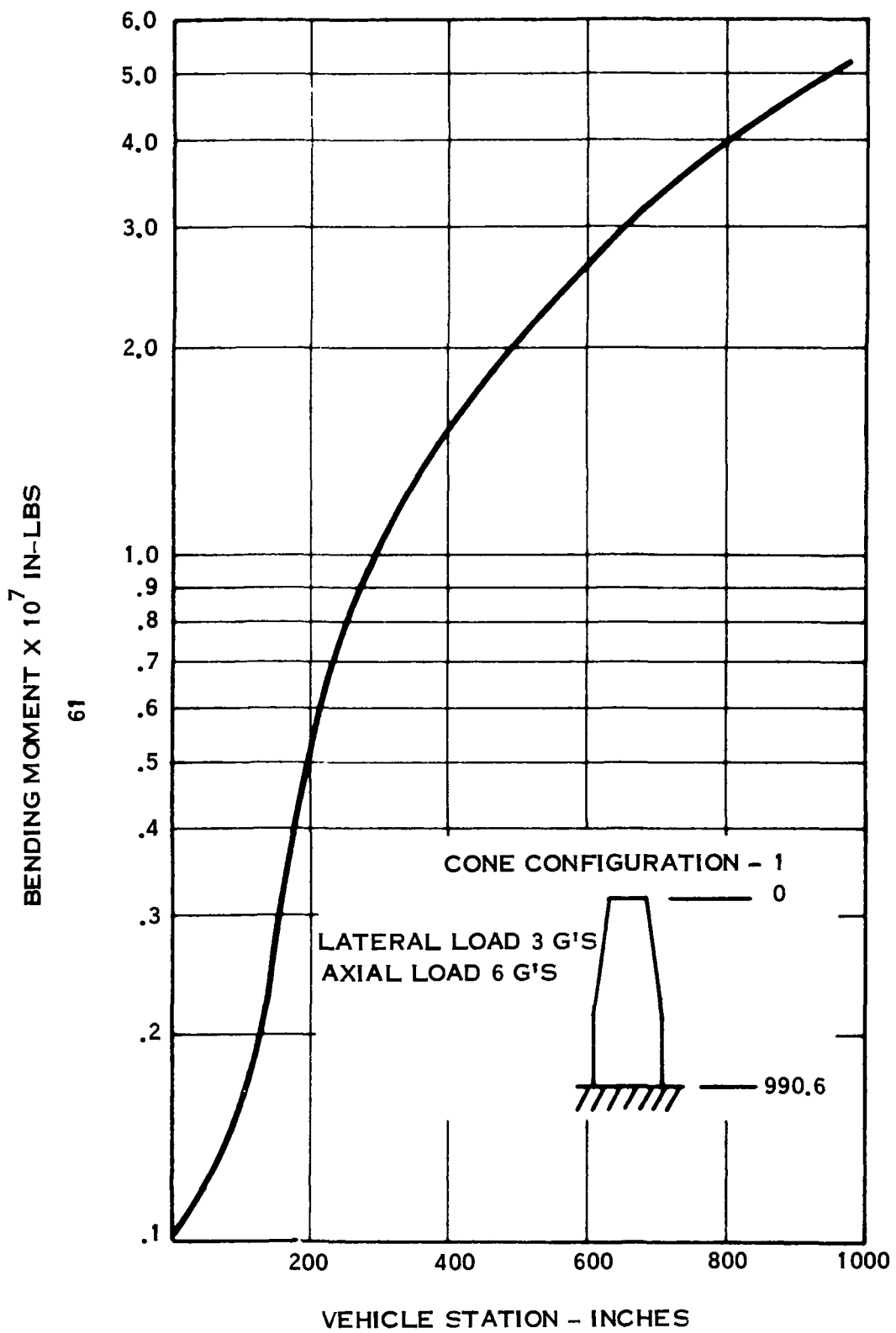
APPENDIX A. STRESS ANALYSES DATA

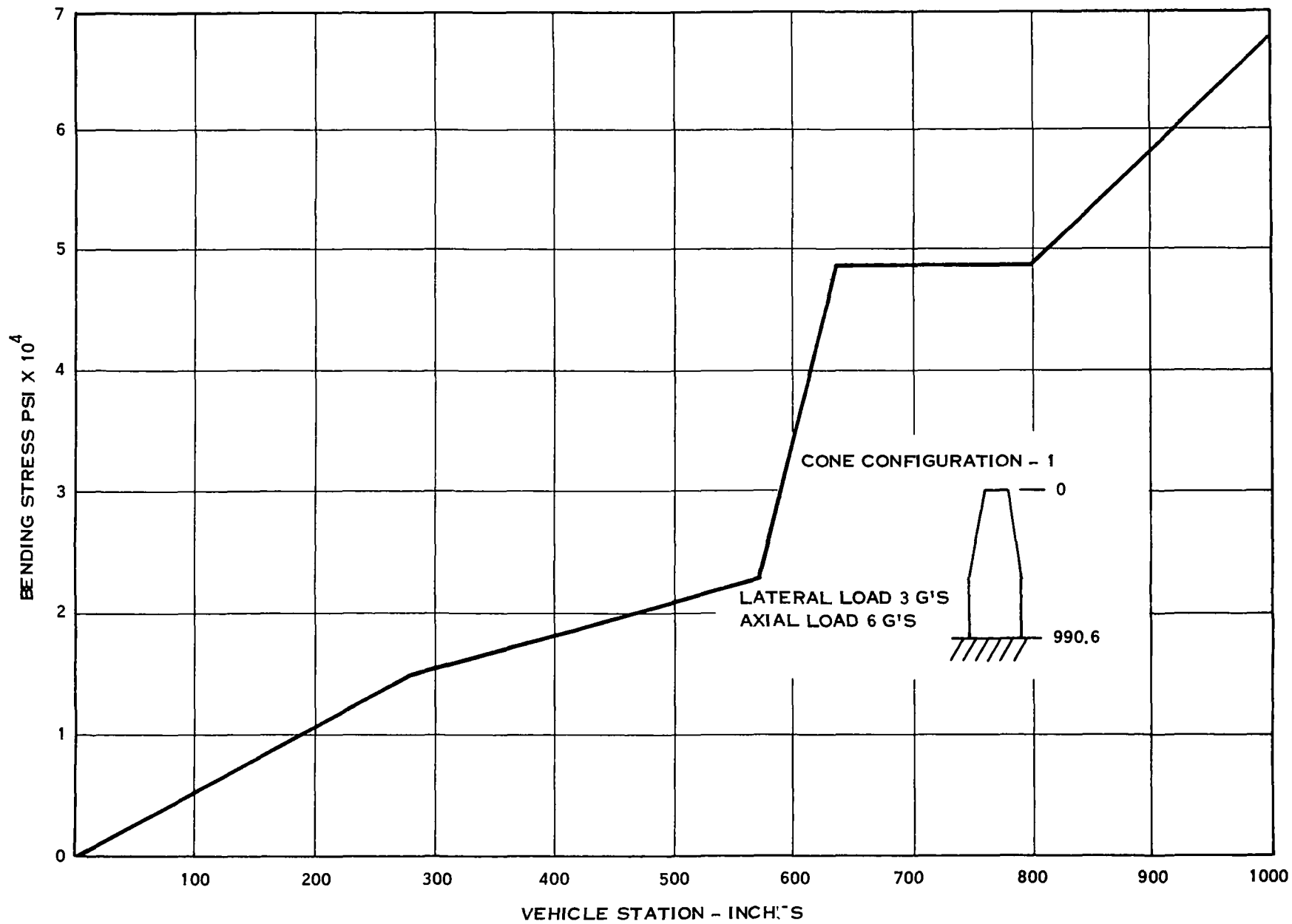
This appendix presents selected results from the computerized stress analysis. Data are presented for the following configurations:

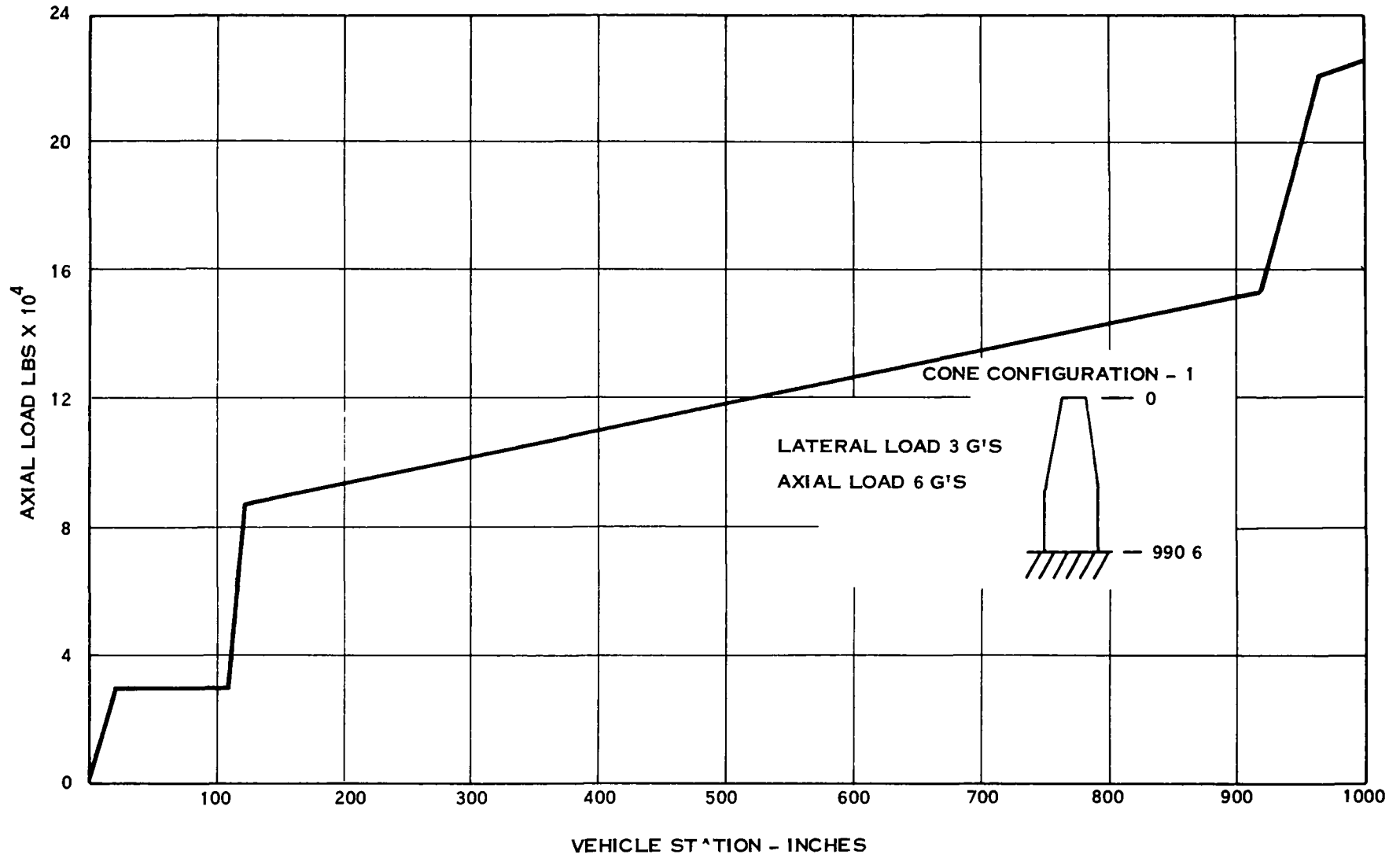
- a. Upright Conical - Unsupported
- b. Upright Conical - Two Supports
- c. Inverted Conical - Two Supports
- d. Upright Triform - Unsupported

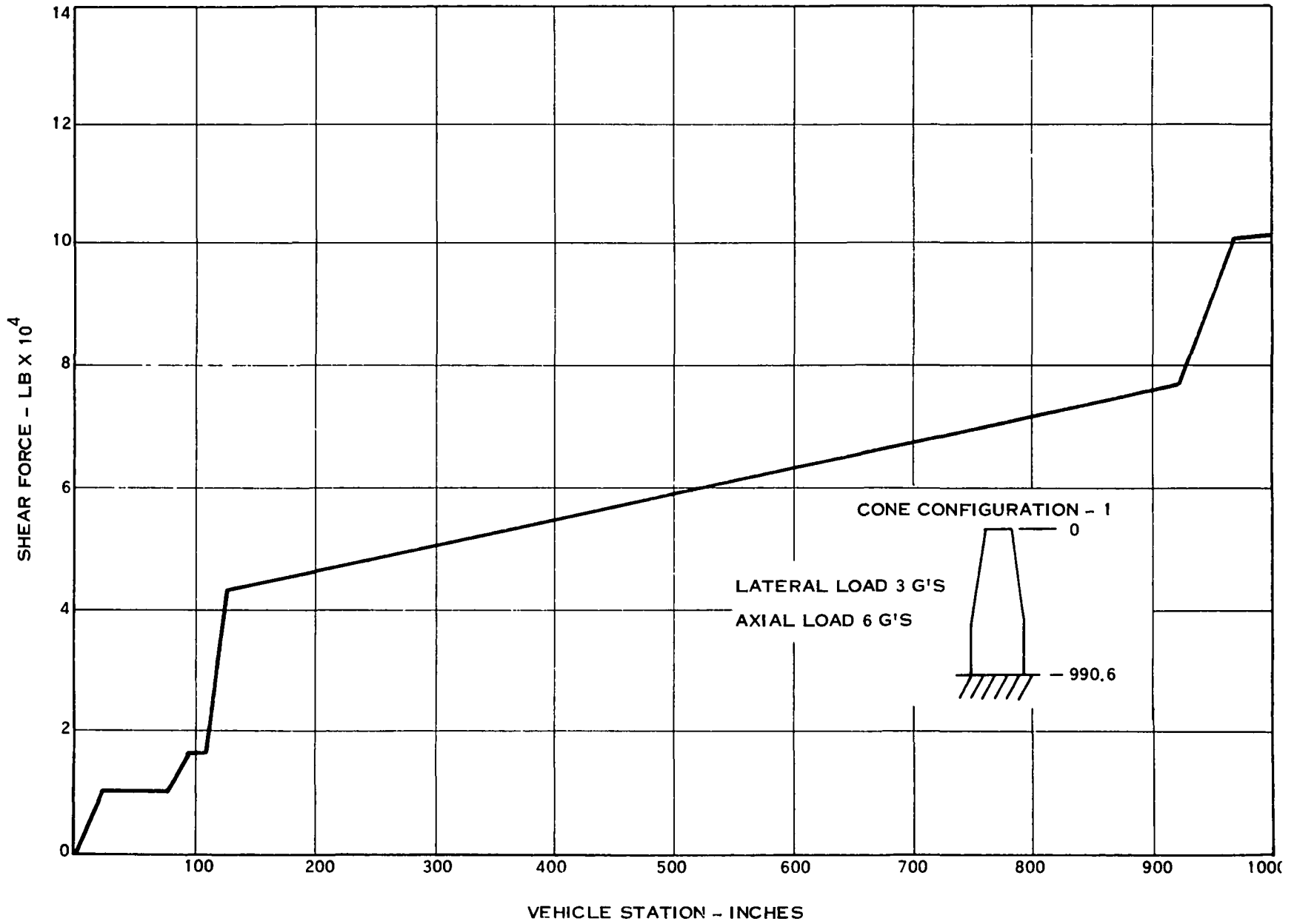
The data presented for each configuration are:

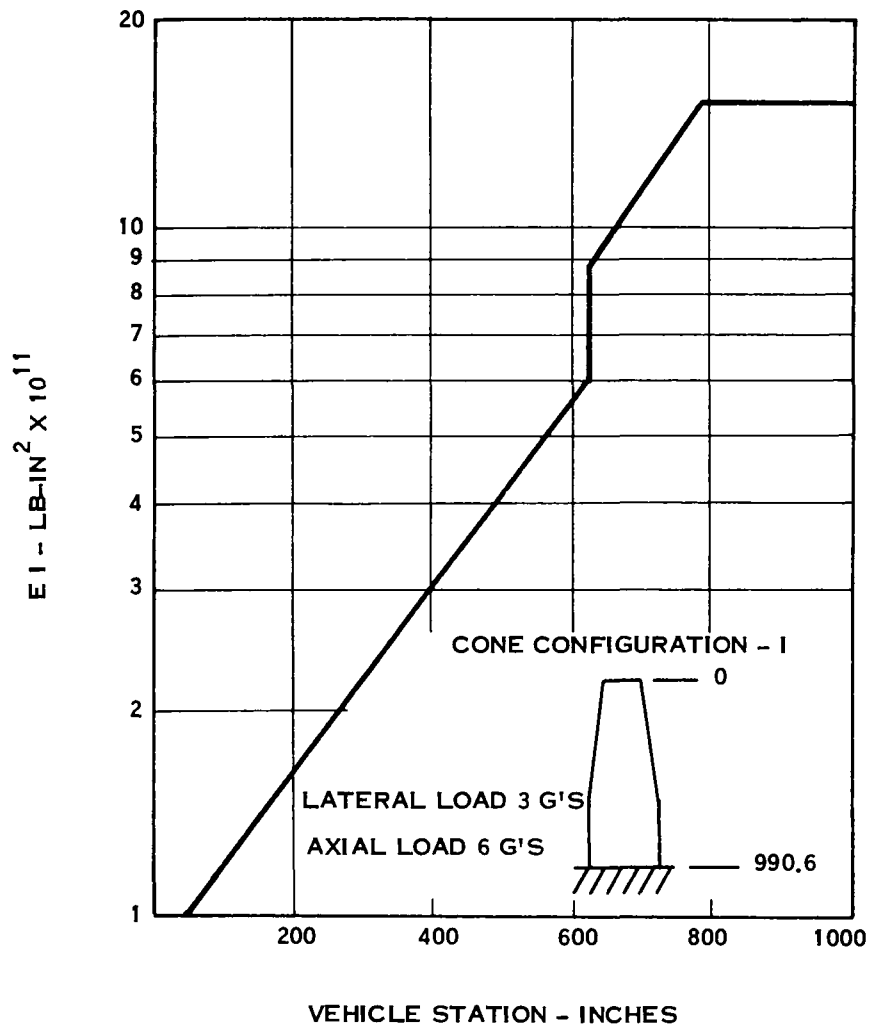
- a. Bending Moment Distribution
- b. Bending Stress Distribution
- c. Axial Load Distribution
- d. Shear Force Distribution
- e. EI Distribution
- f. Deflection Distribution

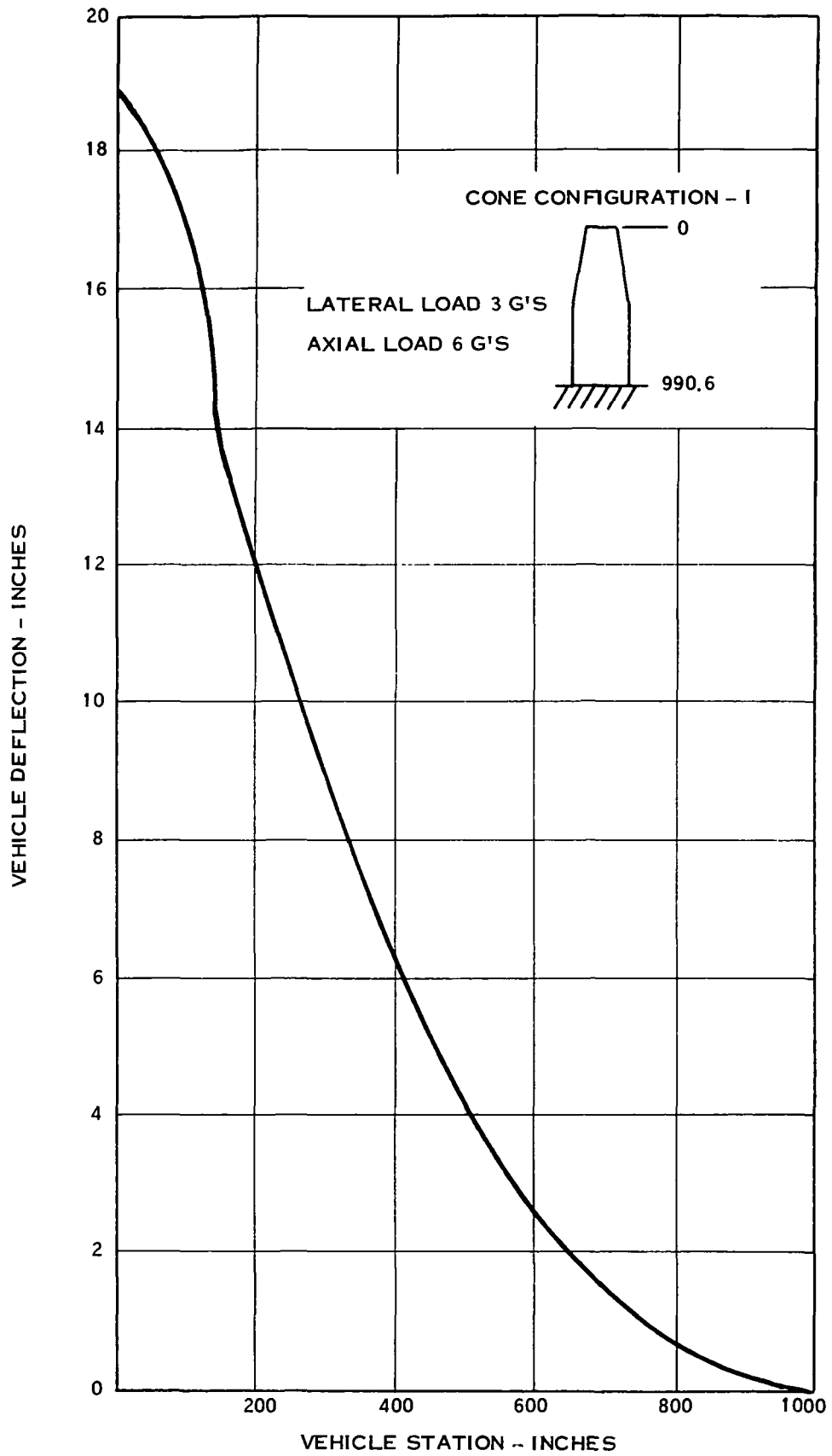


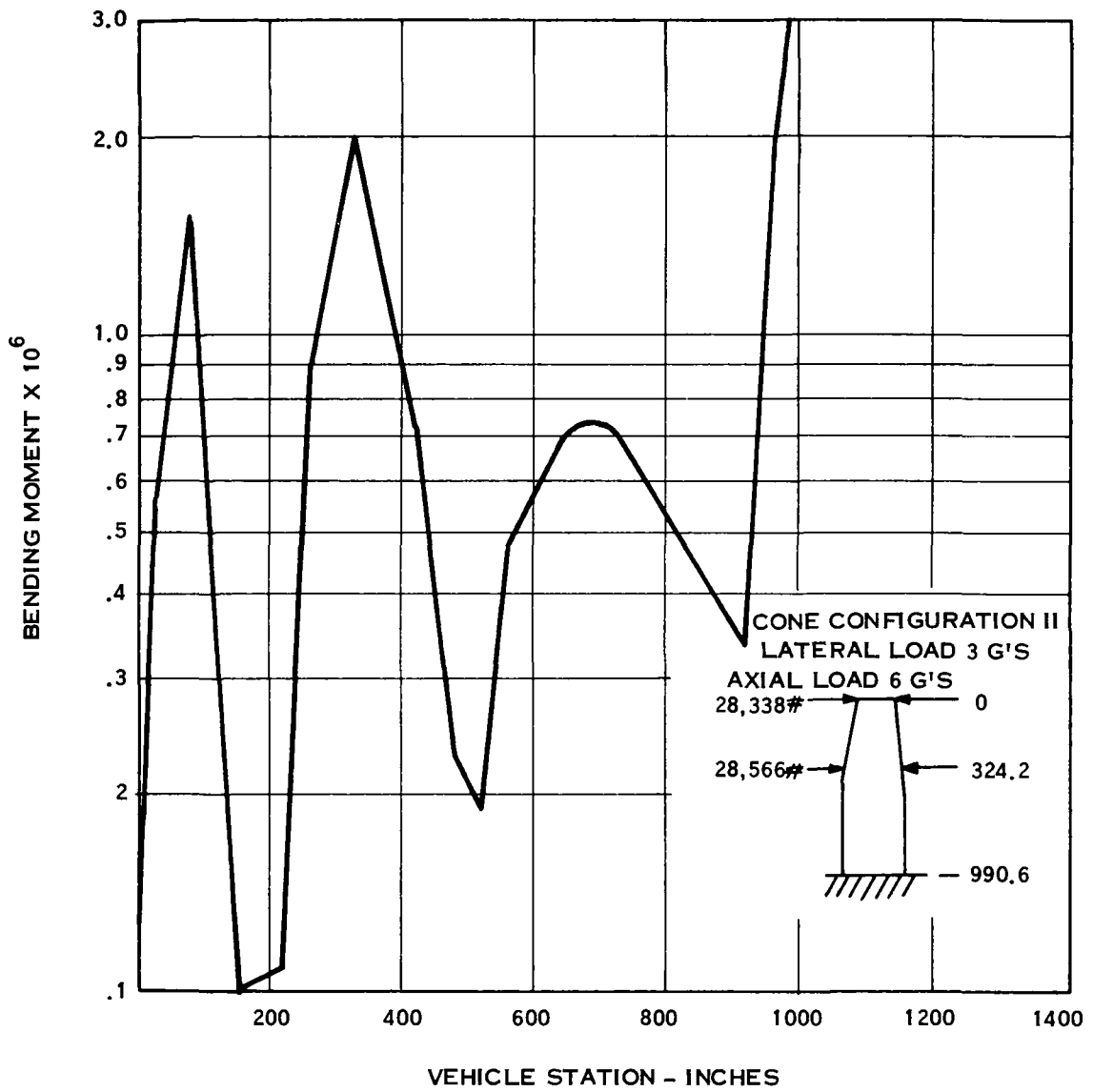


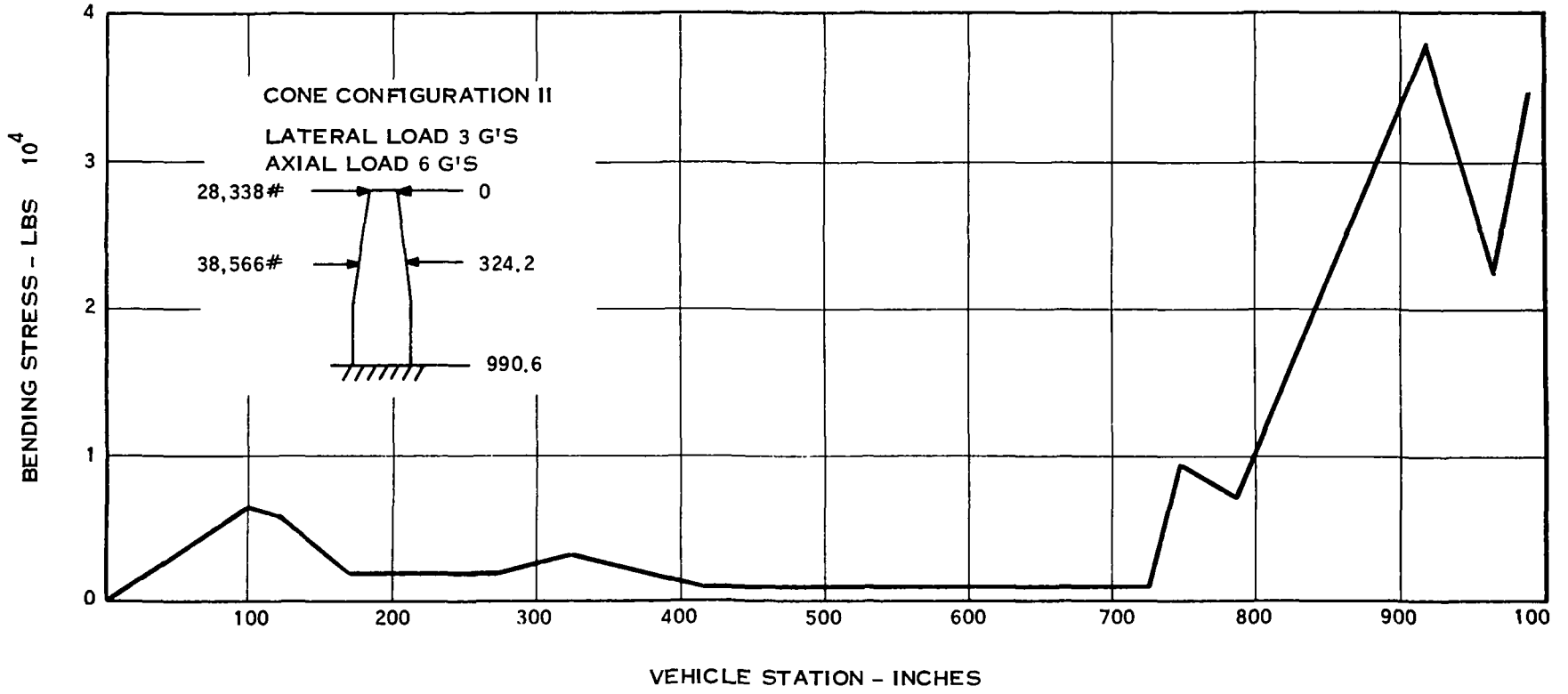


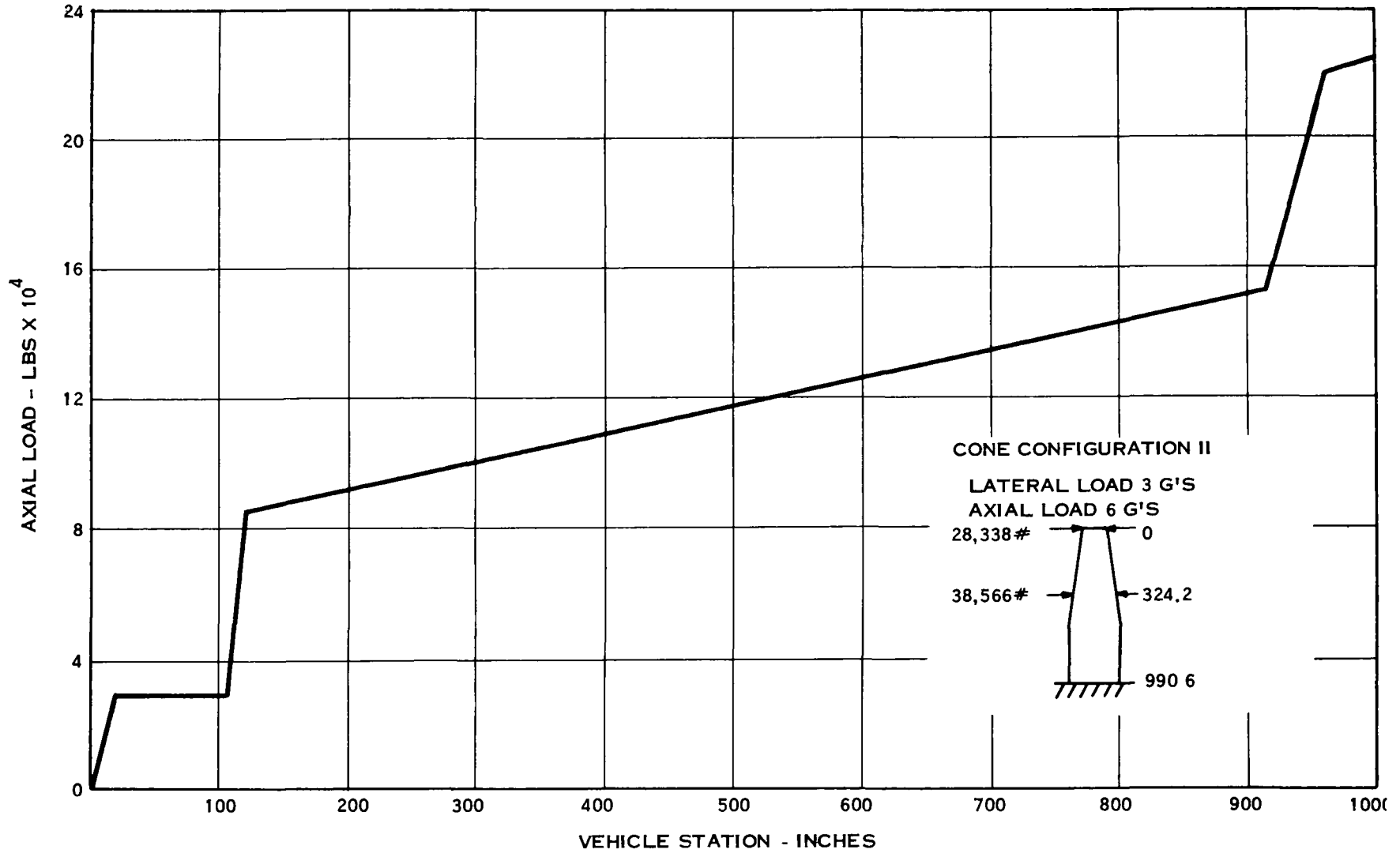


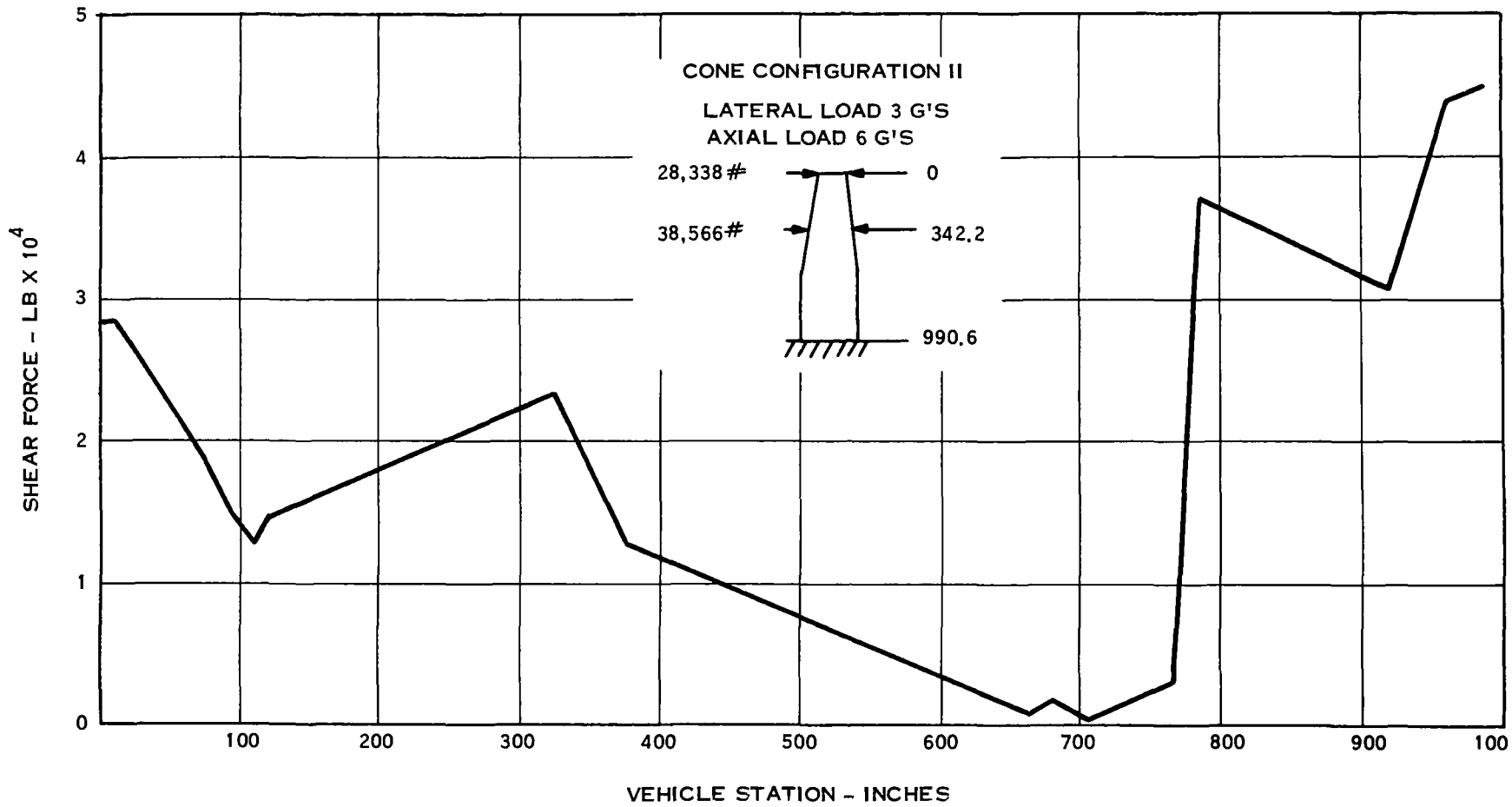


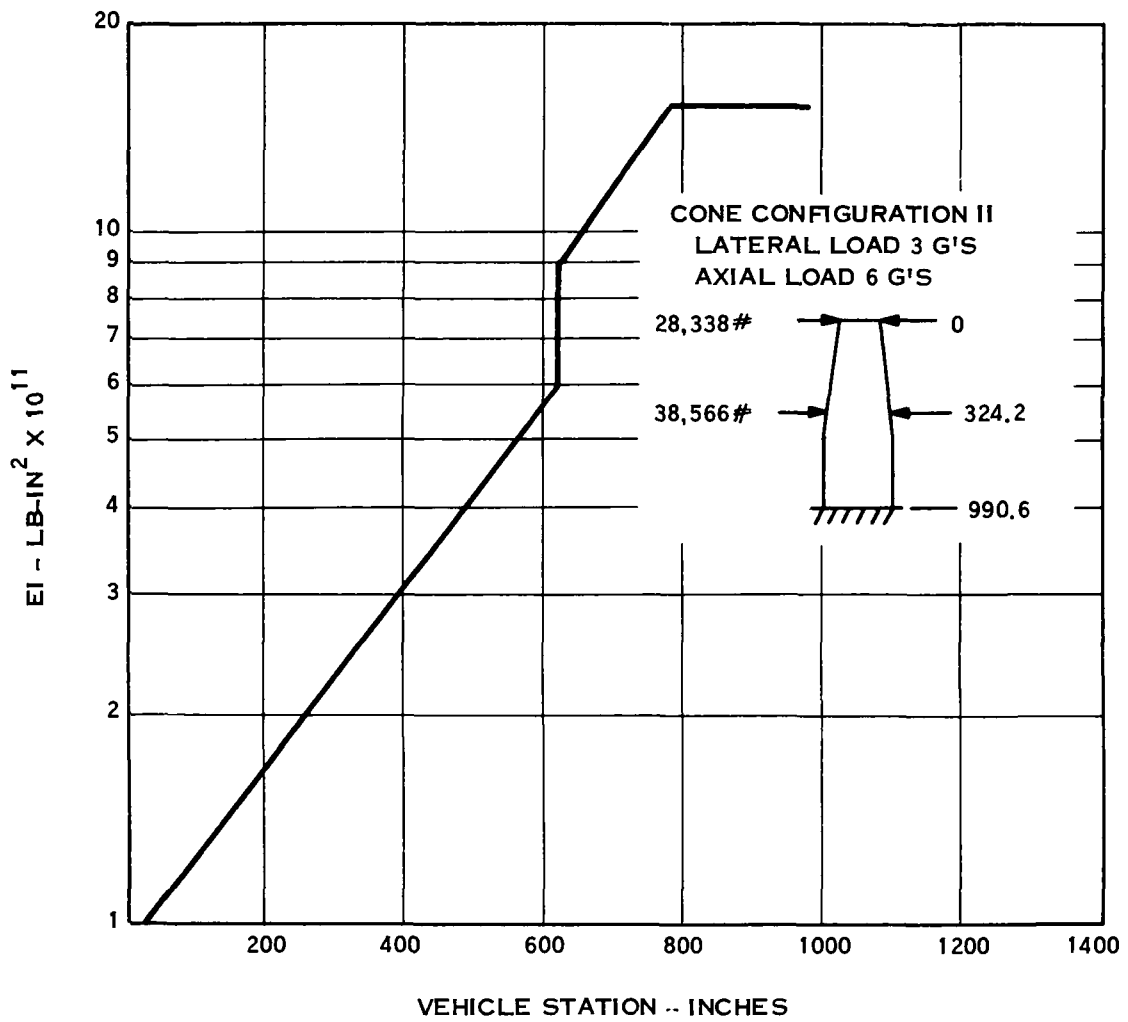


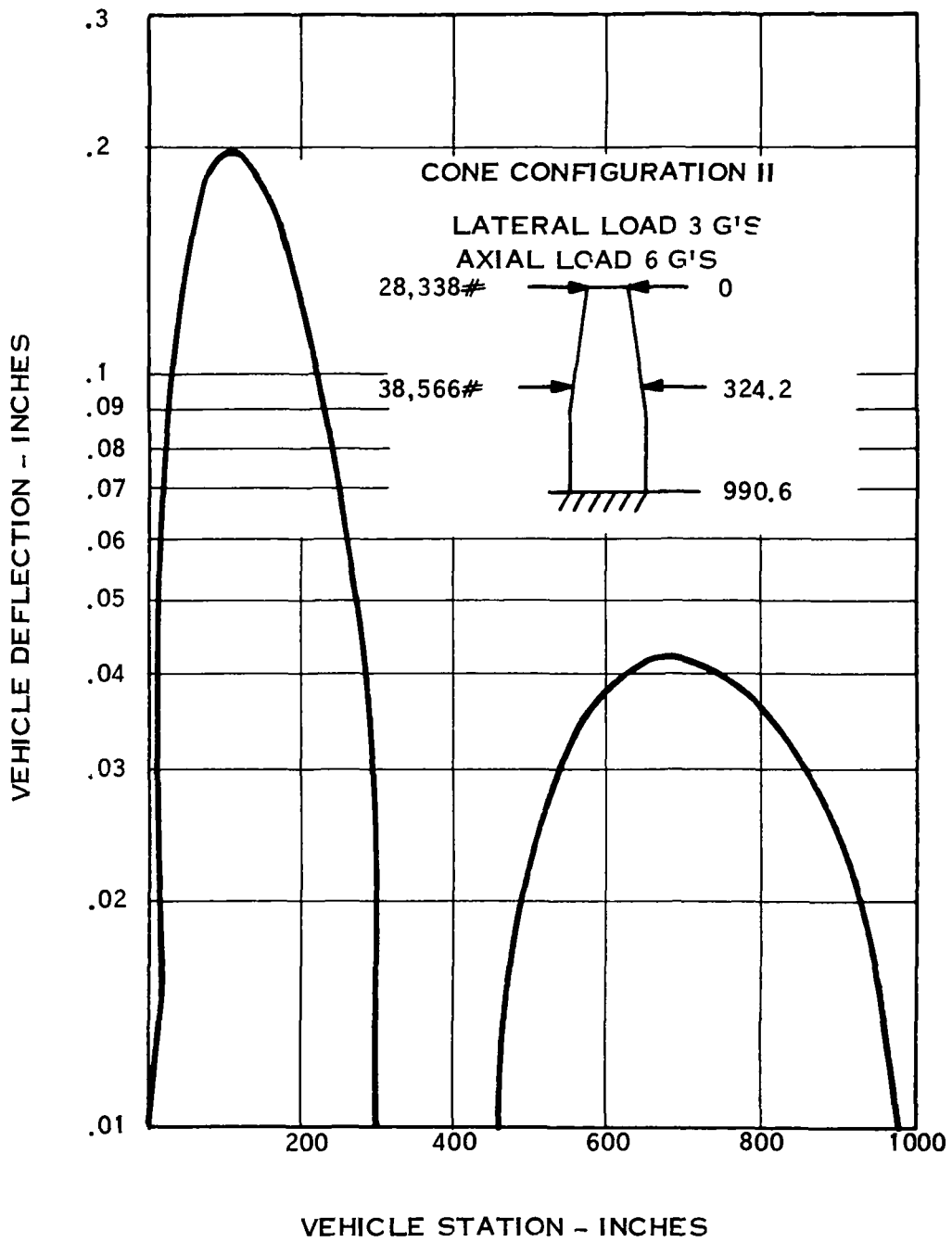


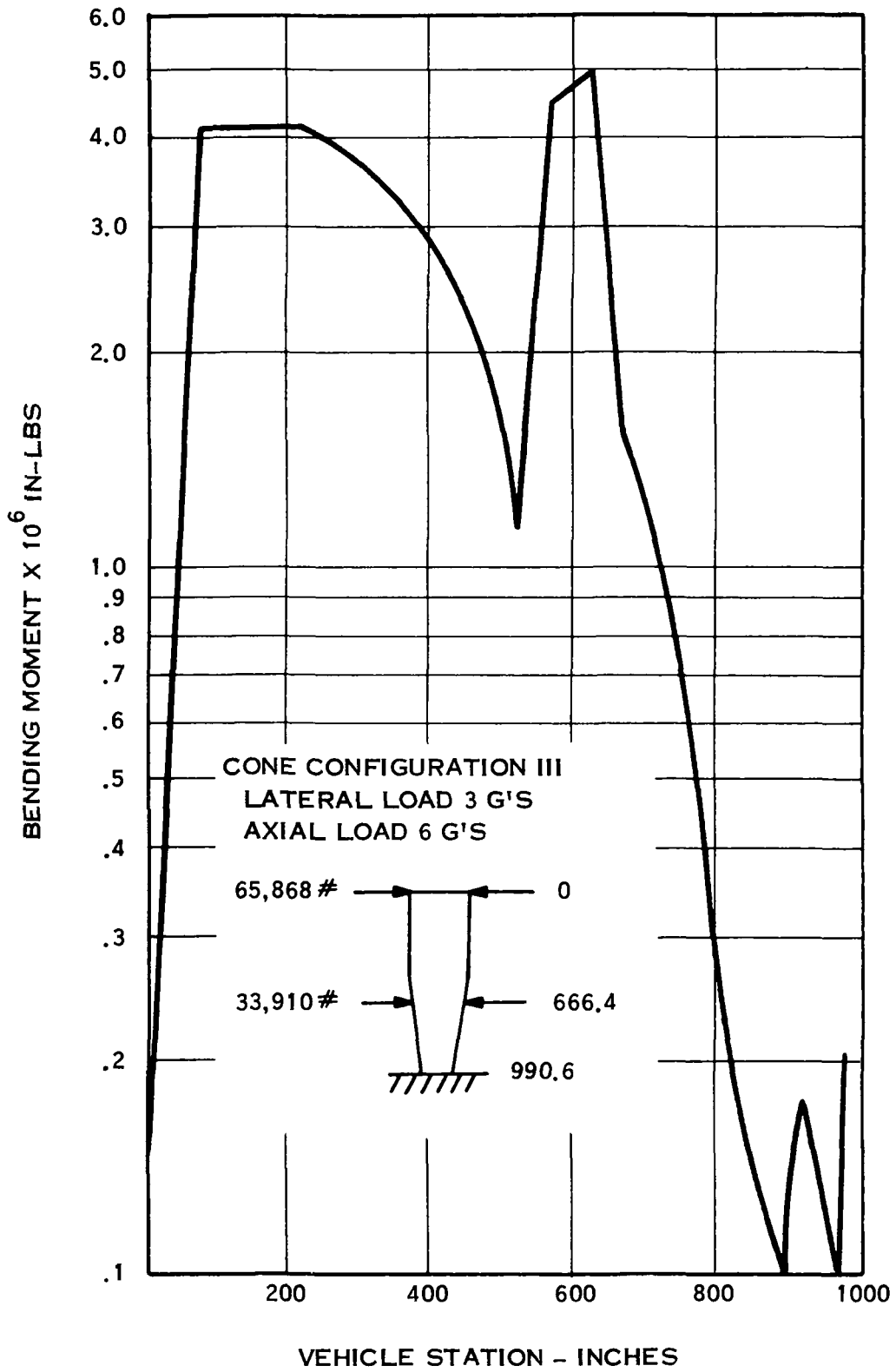


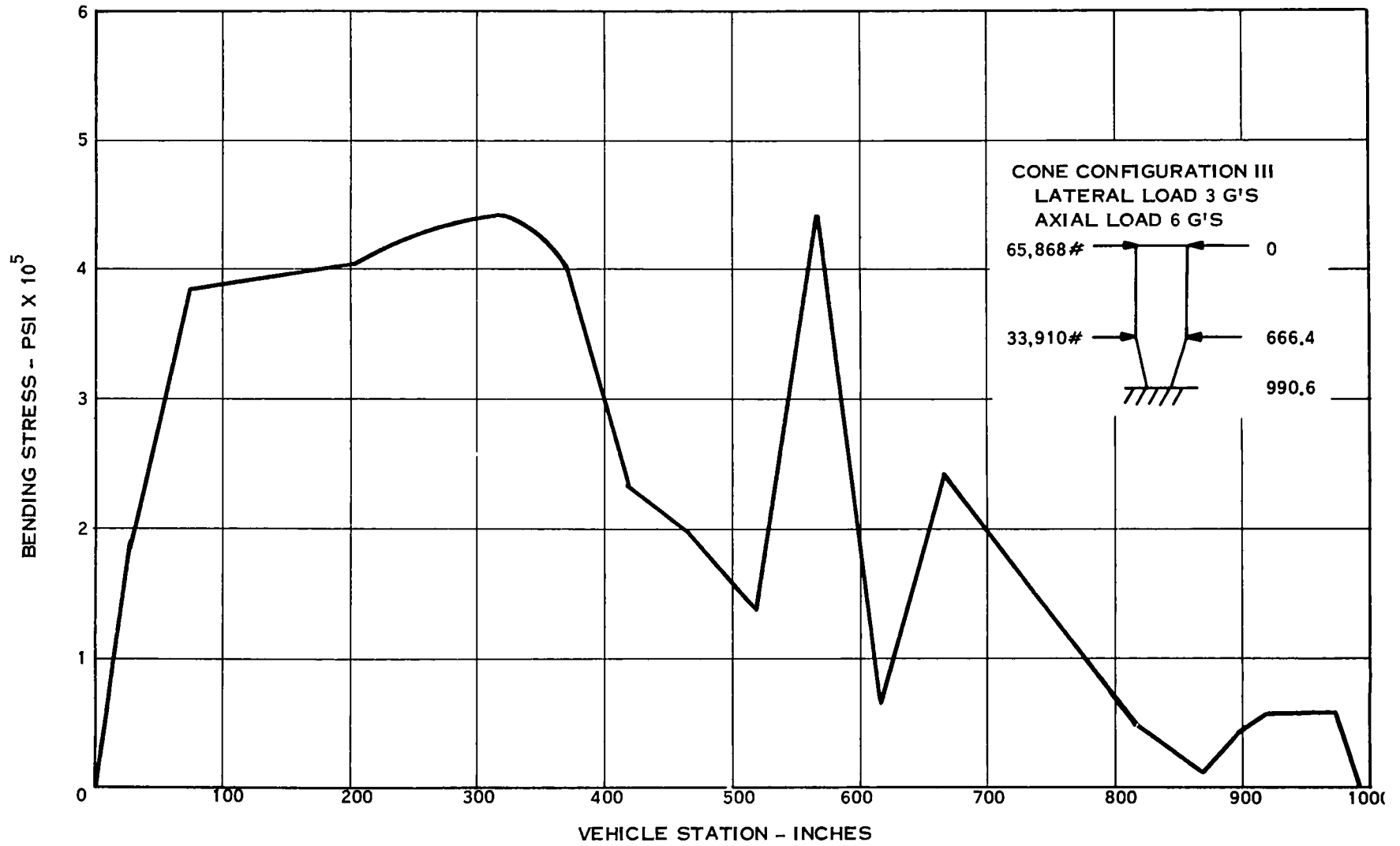


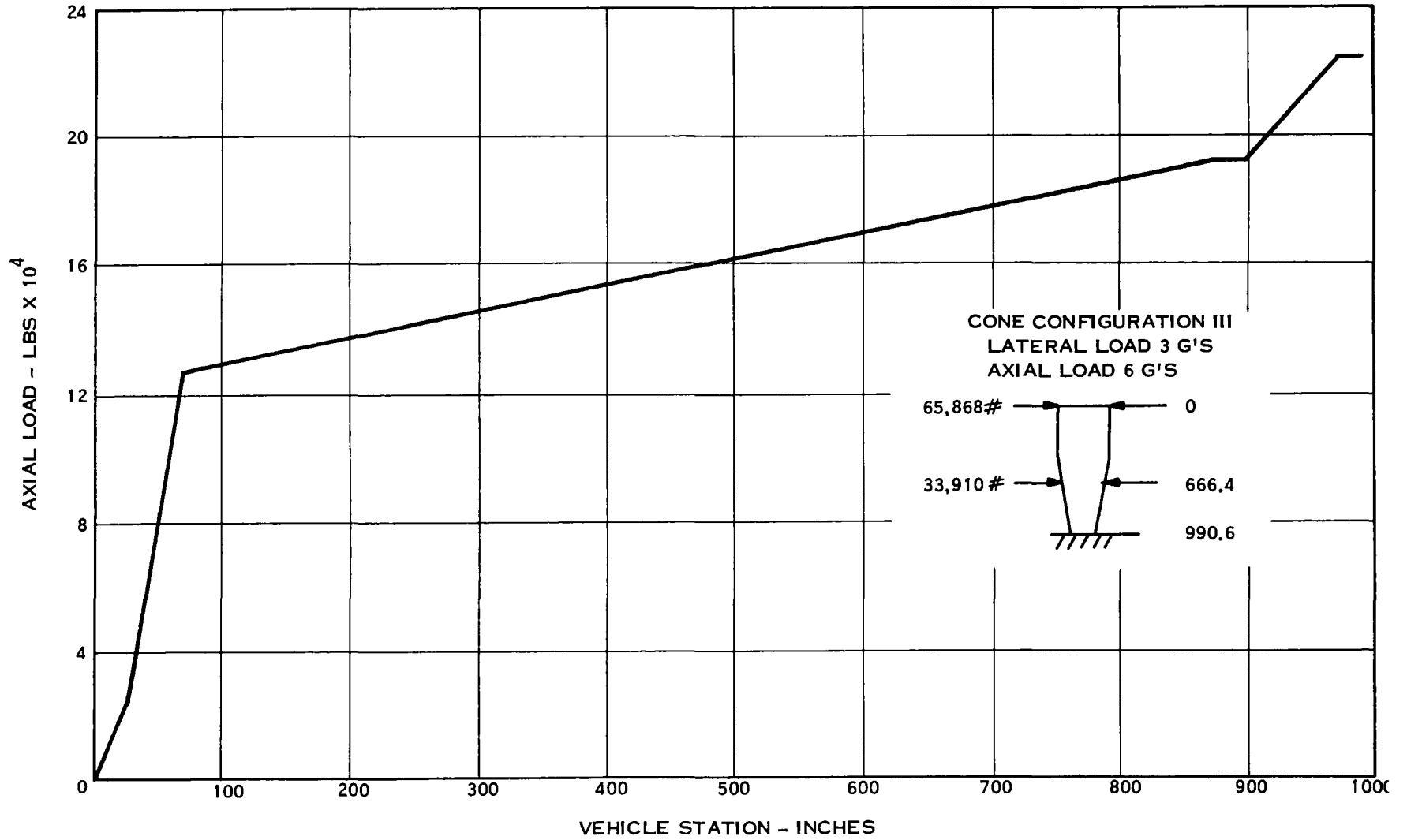


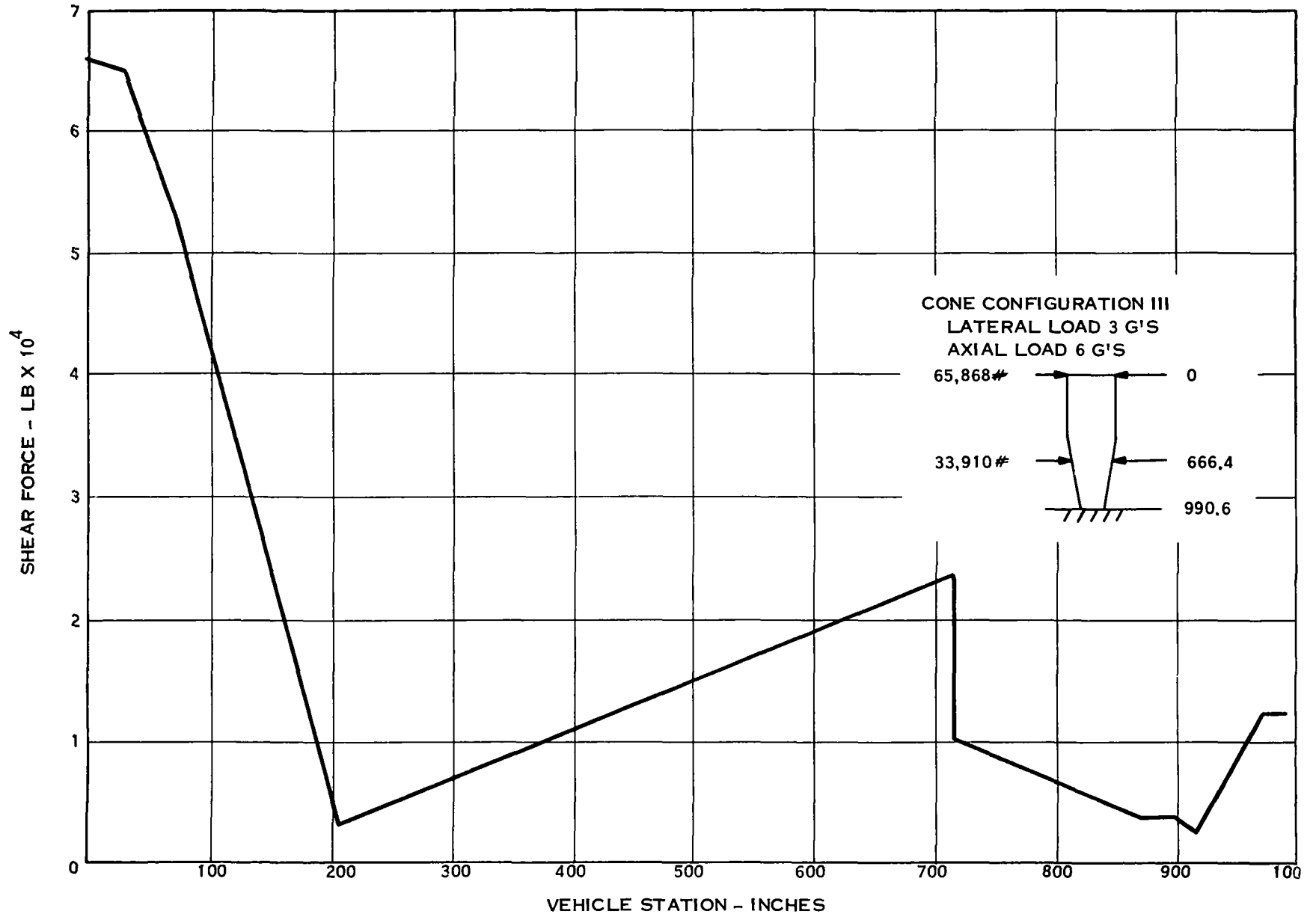


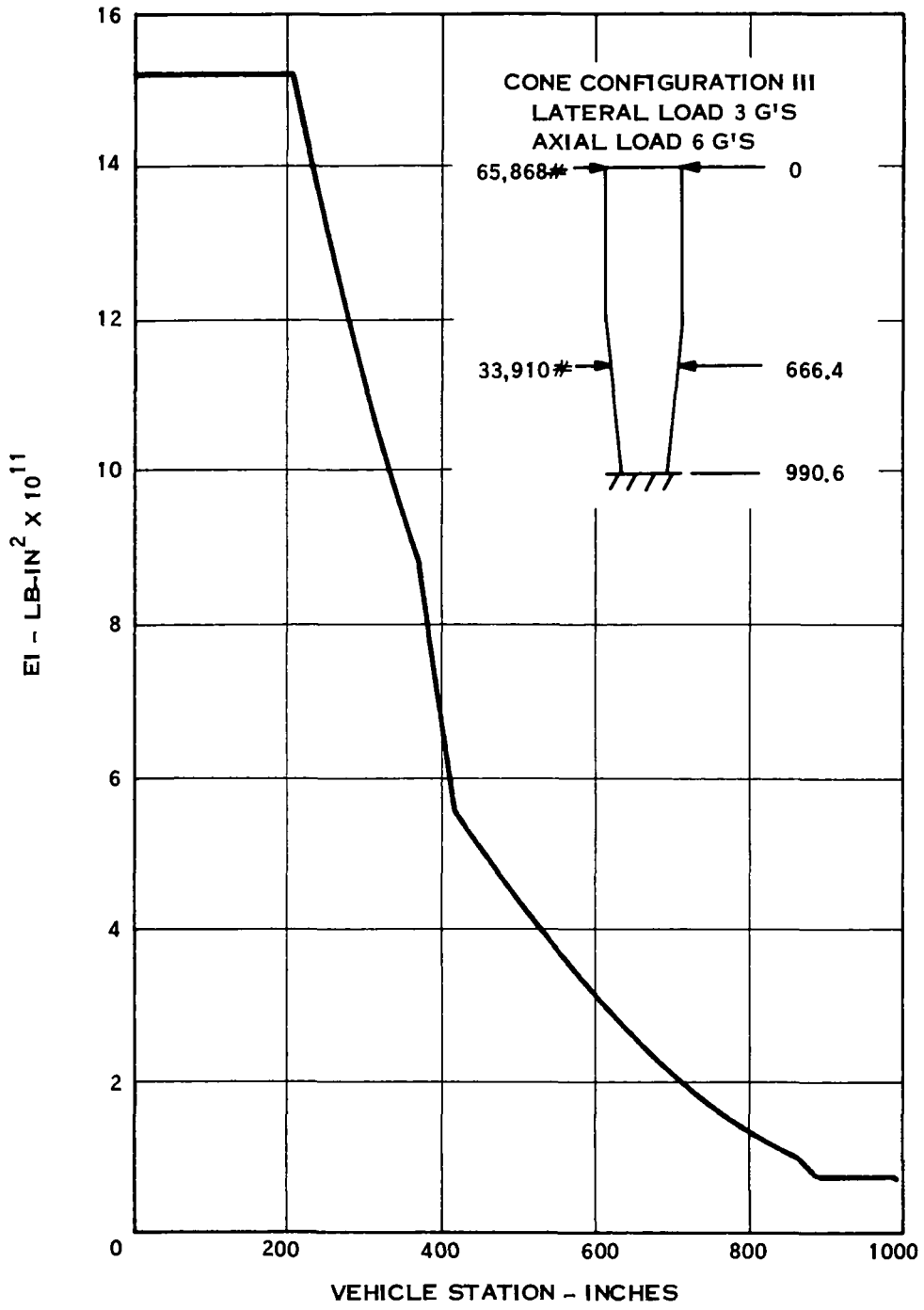


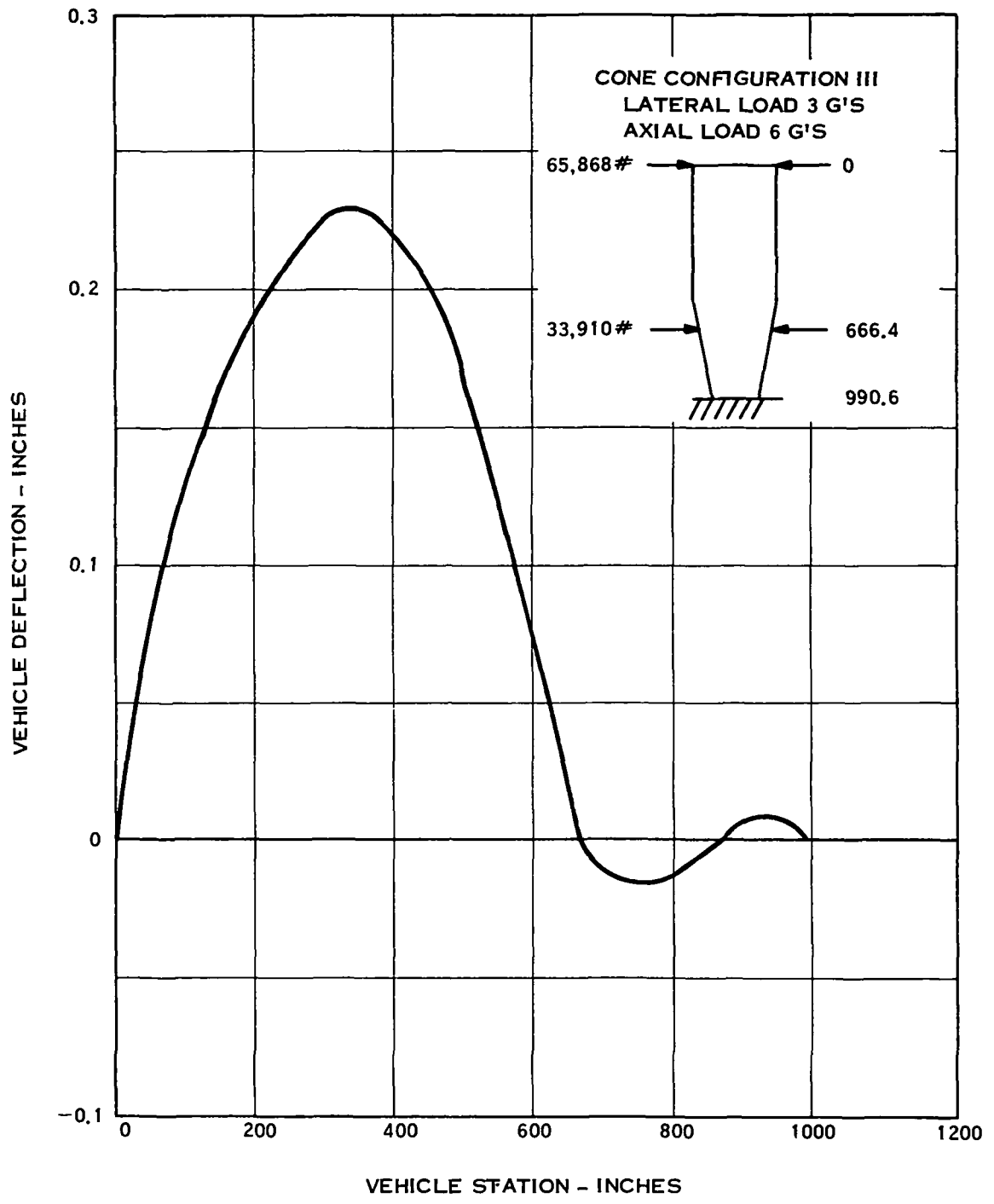


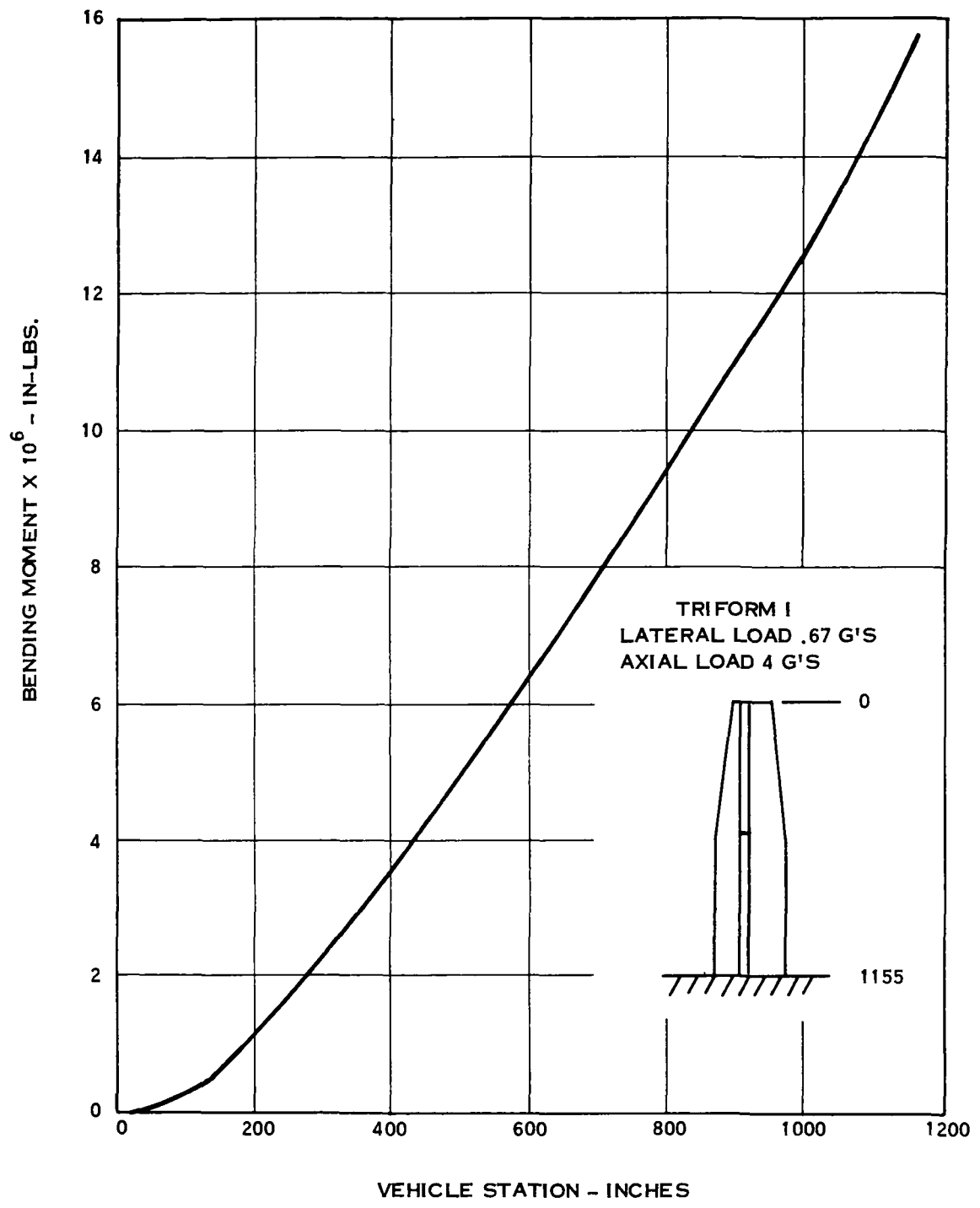


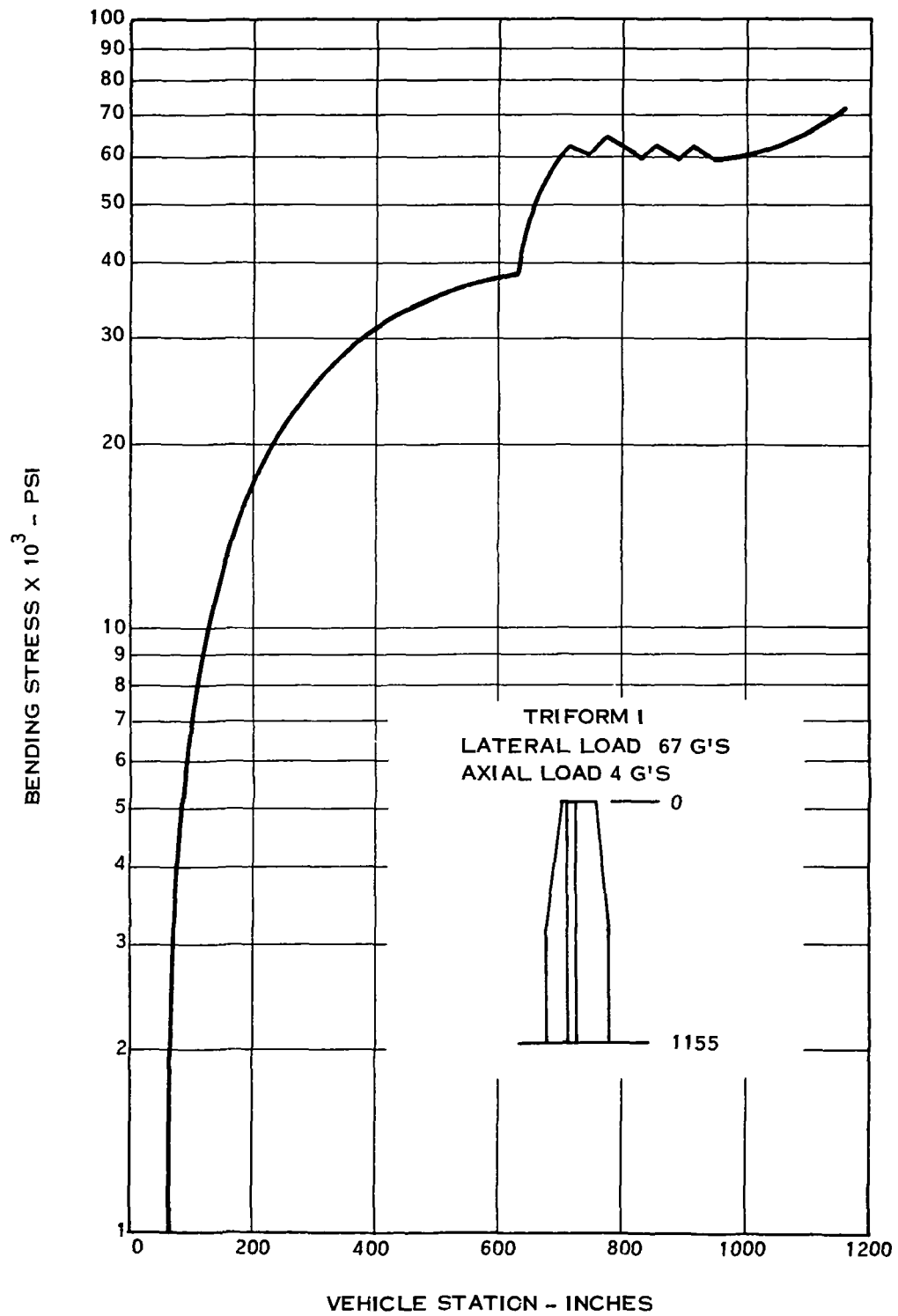


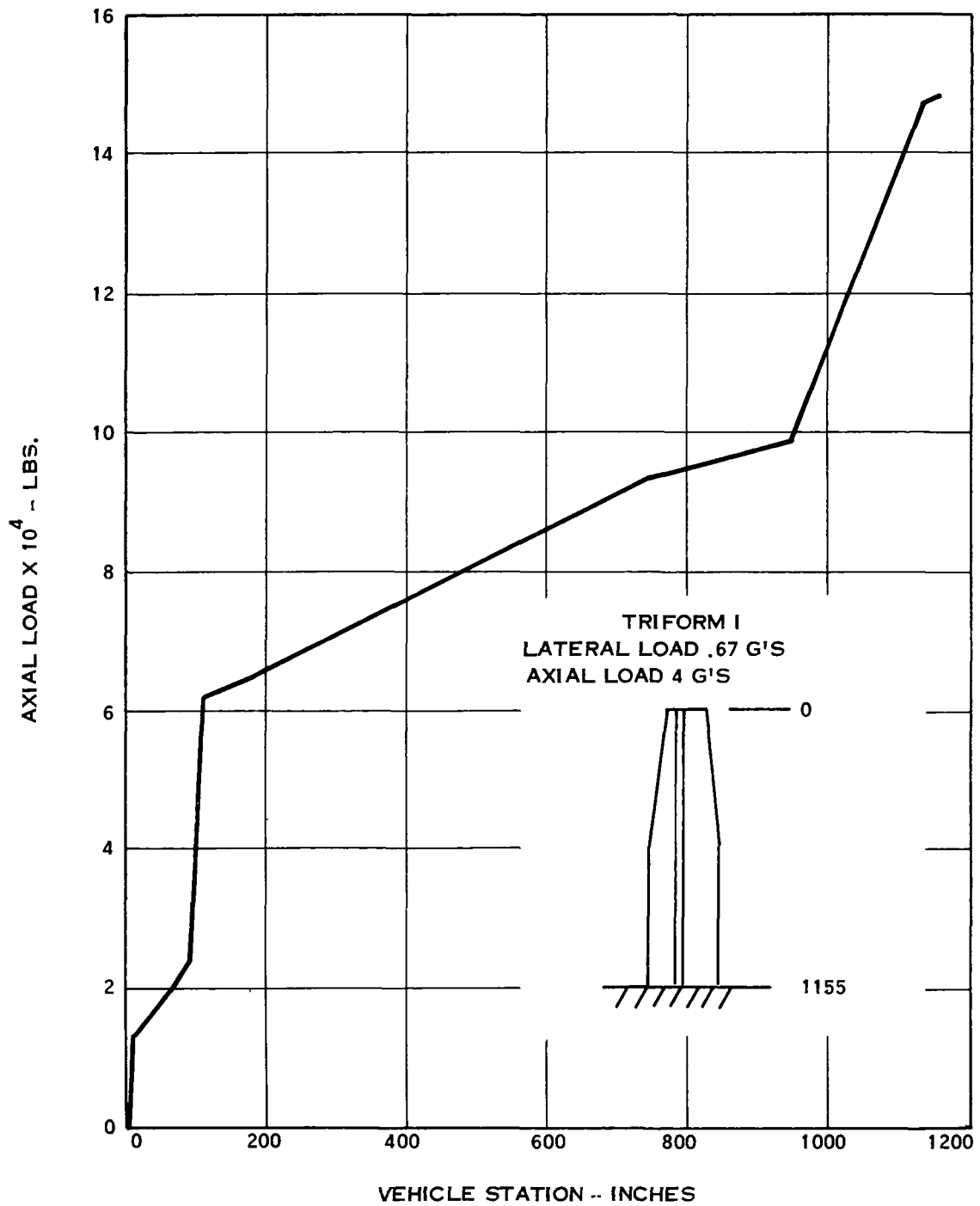


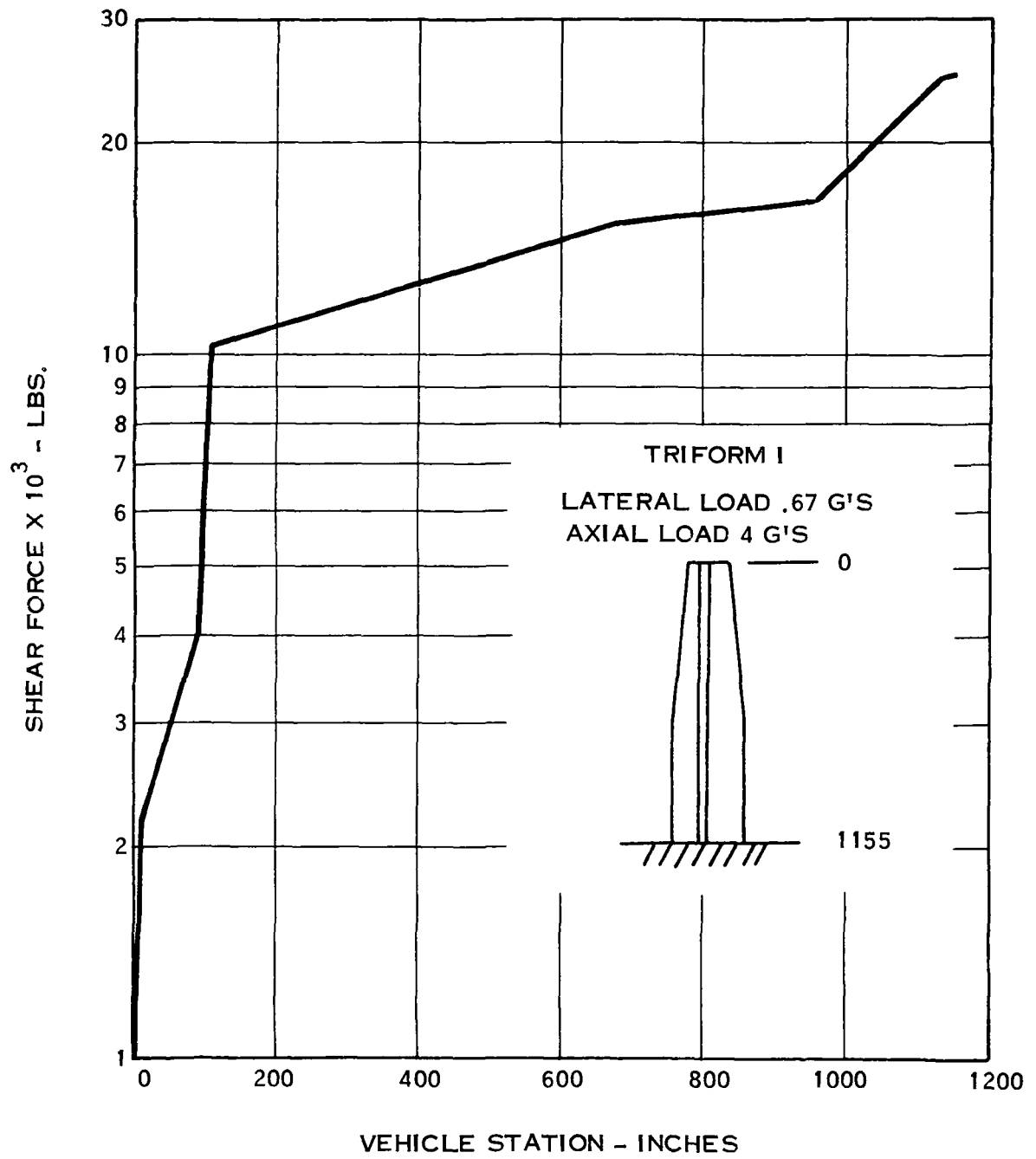


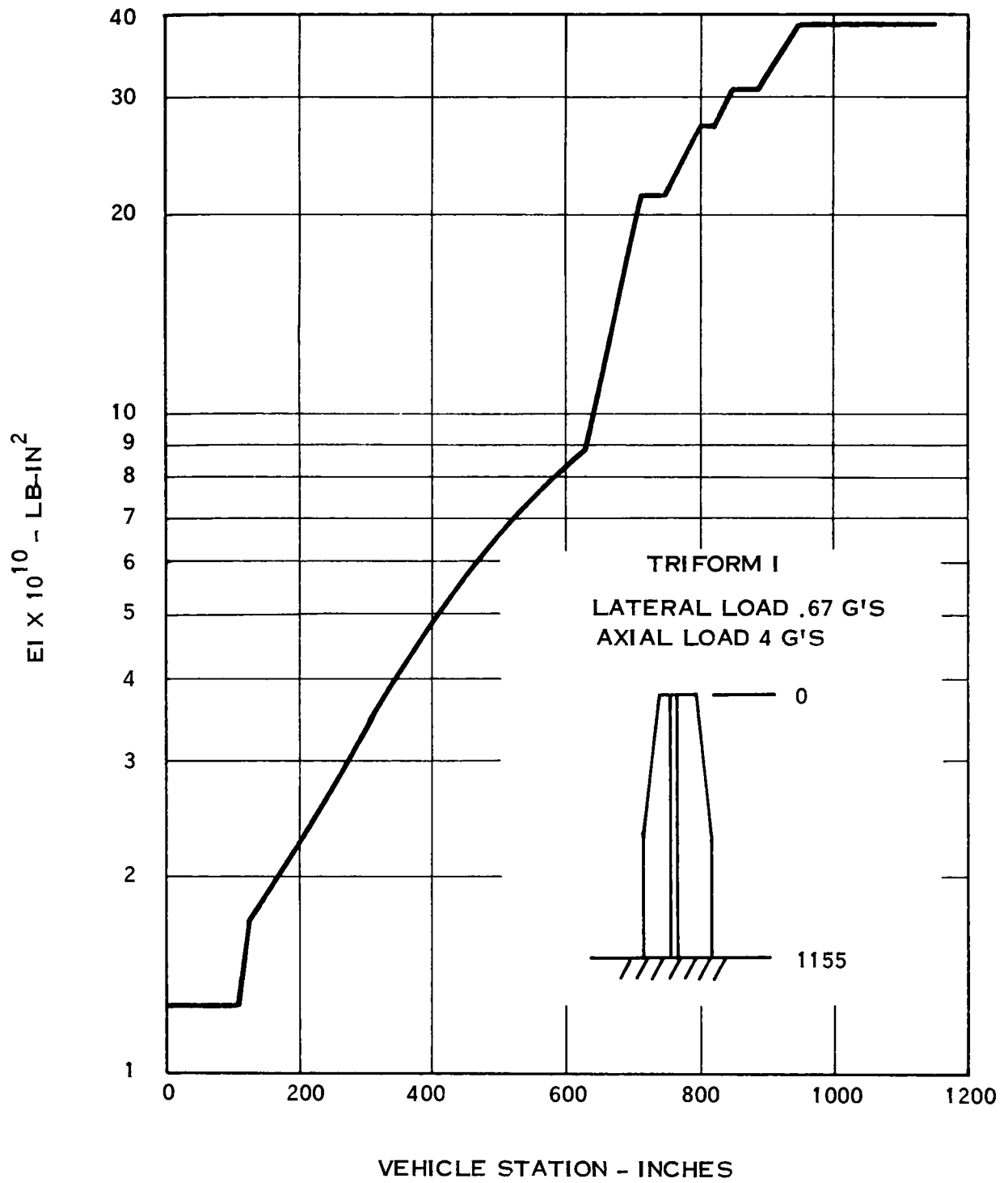


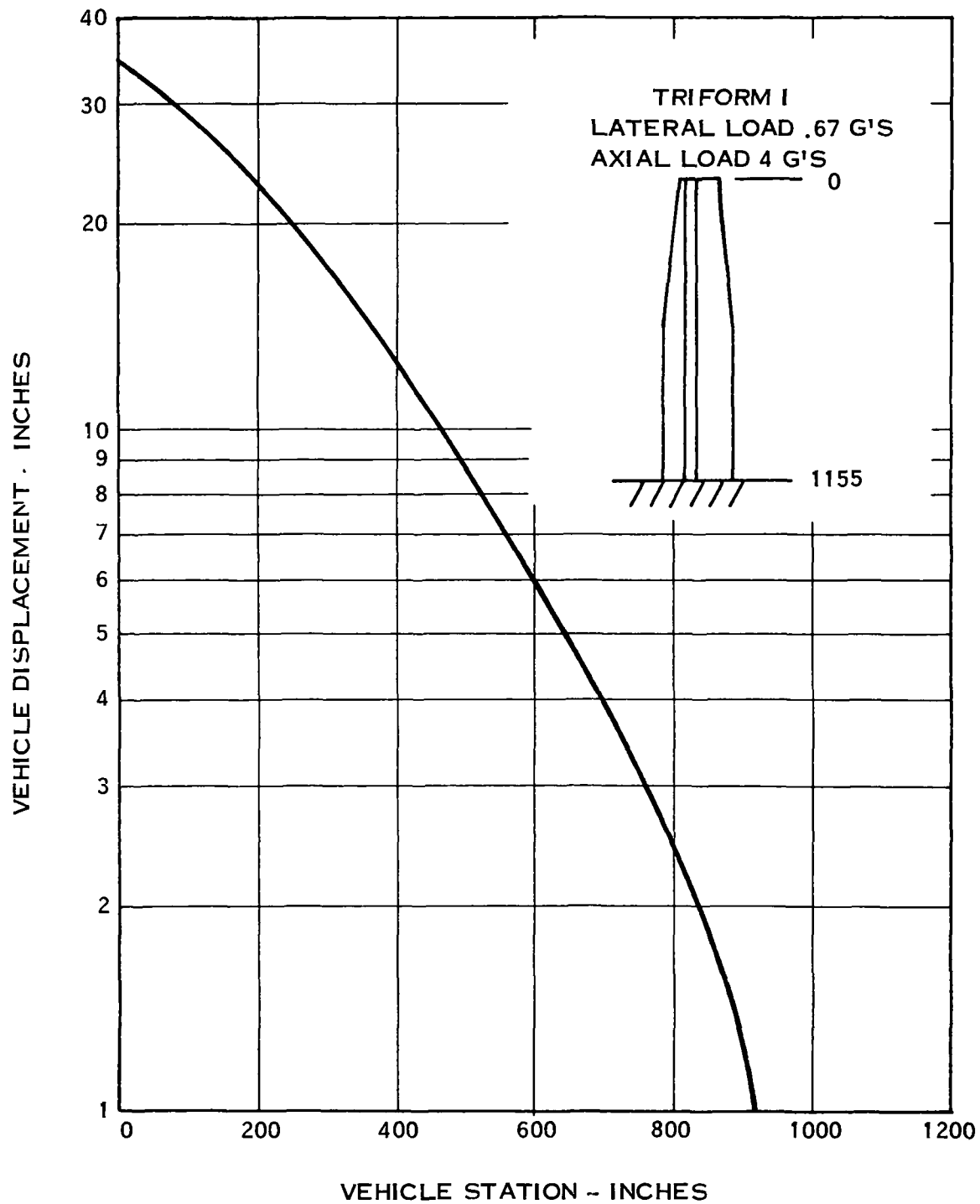












APPENDIX B

APPENDIX B

This appendix contains data and relations utilized in the computer code described in Section 9.

1. NaK-78 PROPERTIES

Physical and thermal properties of NaK-78 were expressed as a function of temperature in equation form for use in the computer code. All the coolant property relations were correlated in units of degrees Rankine. The resultant equations are as follows:

Thermal Conductivity

$$k = 12.54 + .00236 T, \text{ Btu/hr-ft-}^{\circ}\text{R where } T \text{ is the temperature in degrees Rankine.}$$

Specific Heat

$$C_p = .2392 - .00002T, \text{ Btu/lb-}^{\circ}\text{R}$$

Viscosity

$$\log_{10}\mu = 4\left(\frac{-44.5}{T}\right) - 1.362 \log_{10} T, \text{ lb/ft-hr.}$$

Density

$$\rho = 58.3 - 0082 T, \text{ lbs/ft}^3$$

Electrical Resistivity

$$r = 4.6 \times 10^{-7} + 1.2 \times 10^{-9} T, \text{ ohm-ft}$$

2. LITHIUM PROPERTIES

Lithium coolant properties were correlated in the same manner as the NaK-78 properties. The resultant lithium property equations are as follows:

Thermal Conductivity

$$k = 22, \text{ Btu/hr-ft-}^{\circ}\text{R}$$

Specific Heat

$$C_P = \frac{1}{4184} \left[4425 - .5084 \left(\frac{T}{1.8} - 273 \right) + 2.237 \times 10^{-4} \left(\frac{T}{1.8} - 273 \right)^2 \right], \text{ Btu/lb} - ^\circ\text{R}$$

Viscosity

$$\log_{10} \mu = 4.8026 - \frac{280.8}{T} - 1.615 \log_{10} \left(\frac{T}{1.8} \right), \text{ lb/ft-hr}$$

Density

$$\rho = 7.74 + 0.331 \left(3173 - \frac{T}{1.8} \right)^{0.5} + 0.00258 \left(3173 - \frac{T}{1.8} \right), \text{ lb/ft}^3$$

Electrical Resistivity

$$r = 5.65 \times 10^{-7} + 4.25 \times 10^{-10} T, \text{ ohm-ft}$$

3. COPPER CABLE PROPERTIES

The material property data required for the analysis of the low and high voltage electrical cables include the electrical resistivity, thermal conductivity, density and thermal emissivity. The first three pertain to the base cable material while the last value corresponds to a special surface coating having a high thermal emissivity. The electrical resistivity and thermal conductivity were correlated as a function of temperature in degrees Rankine while the density and emissivity were assigned constant values.

Electrical Resistivity

$$r = 5.66 \times 10^{-8} + 1.174 \times 10^{-10} (T-528), \text{ ohm-ft}$$

Thermal Conductivity

$$k = 236 - 0.02145 T, \text{ Btu/hr-ft-}^\circ\text{R}$$

Density

$$\rho = 558, \text{ lbs/ft}^3$$

Emissivity

$$\Sigma = 0.88$$

4. ALUMINUM CABLE PROPERTIES

Aluminum cable material properties were correlated in the same manner as the copper properties. A high purity aluminum was assumed for the cable application.

Electrical Resistivity

$$r = 9.25 \times 10^{-8} + 2.15 \times 10^{-10} (T-528), \text{ ohm-ft}$$

Thermal Conductivity

$$k = 140.5 - 0.000793 T, \text{ Btu/hr-ft-}^{\circ}\text{R}$$

Density

$$\rho = 169, \text{ lbs/ft}^3$$

Emissivity

$$\Sigma = 0.85$$

5. SODIUM-STAINLESS STEEL CLAD CABLE PROPERTIES

The sodium-stainless steel clad cable is a thin-walled stainless steel tube, having a wall thickness of 0.02 inches, filled with sodium metal. At operating temperatures most of the sodium will be molten except for the end connected to the power conditioning module. The sodium will transmit most of the electrical current but the clad tube is also an electrical conductor so the tube electrical properties must be factored into the cable analysis.

Electrical Resistivity

The electrical resistivity of the NaSS clad cable depends on the resistivity properties of the sodium and the stainless steel plus the relative cross sectional area of sodium compared to the stainless steel tube. The tube wall thickness is assumed to be 0.02 inches independent of the tube diameter. If R_2 is the outer radius of the clad tube and R_1 is the inner radius, then the relative cross sectional area of the sodium core to the tube cross sectional area is;

$$\frac{A_1}{A_2} = \frac{R_1^2}{R_2^2 - R_1^2}$$

The total cross sectional area A_X of all the cables is a known quantity for any one calculation so the outer radius, R_2 , can be determined from

$$R_2 = \left[\frac{A_X}{\pi (\text{NTFE})} \right]^{0.5} \text{ ft}$$

where NTFE is the number of individual tubes comprising the cable bundle. Since the tube wall thickness is given as 0.02 inches, the inner radius is

$$R_1 = R_2 - \frac{0.02}{12} \text{ , ft.}$$

The cross sectional area ratio can then be computed directly.

It can be shown from Ohm's Law and the definition of electrical resistance, that the mean resistivity, \bar{r} , of a NaSS cable is;

$$\bar{r} = \frac{r_1 r_2 \left(\frac{A_1}{A_2} + 1 \right)}{r_1 + r_2 \left(\frac{A_1}{A_2} \right)}$$

where

r_1 = resistivity of the sodium core

r_2 = resistivity of the stainless steel tube

$\frac{A_1}{A_2}$ = cross sectional area ratio as previously defined

The resistivity of sodium is discontinuous at the melting point with molten sodium having twice the electrical resistance of solid sodium at the melting temperature. If this discontinuity is duplicated in the computer program it can interfere with the operation of the optimization method and produce inaccurate results. Consequently, the sodium resistivity is assumed to vary linearly between 50°C and 150°C, which brackets the 98°C melting point. For temperatures above 150°C (762°R), sodium resistivity is described by the equation;

$$r_1 = \frac{618.44 - 25.338 T_c^{0.5} + 0.3164 T_c - 0.001128 T_c^{1.5}}{3.048 \times 10^7}$$

Where

$$T_c = 2573 - \frac{T}{1.8}$$

T = sodium temperature in degrees Rankine.

For temperatures below 150°C (762°R), the sodium resistivity is;

$$r_1 = 1.73 \times 10^{-7} + 7.05 \times 10^{-10} (T-582)$$

The resistivity of the stainless steel tube, is;

$$r_2 = 1 \times 10^{-6} + 1.875 \times 10^{-9} T$$

Thermal Conductivity

The mean thermal conductivity, \bar{k} , of the NaSS cable is computed from the equation;

$$\bar{k} = \frac{k_1 \left(\frac{A1}{A2} \right) + k_2}{\left(\frac{A1}{A2} \right) + 1}, \text{ Btu/hr-ft-}^{\circ}\text{R}$$

where

k_1 = thermal conductivity of sodium

k_2 = thermal conductivity of SS tube

$\frac{A1}{A2}$ = cross sectional area ratio previously defined

The sodium thermal conductivity as a function of temperature in degrees Rankine is;

$$k_1 = 60 - 0.015 T, \text{ Btu/hr-ft-}^{\circ}\text{R}$$

The stainless steel thermal conductivity is;

$$k_2 = 4.7 + 0.005 T, \text{ Btu/hr-ft-}^{\circ}\text{R}$$

Density

The density of the NaSS cable is assumed to be independent of temperature but dependent on the cross sectional area ratio of the sodium and SS tube. The density relation is;

$$\rho = \frac{53 \left(\frac{A1}{A2} \right) + 485}{\left(\frac{A1}{A2} \right) + 1}$$

Emissivity

$$\epsilon = 0.88$$

6. STAINLESS STEEL CONTAINMENT MATERIAL

Relations for the thermal conductivity, density and pipe wall thickness of the power plant piping and containment material are included in the computer code.

Thermal Conductivity

$$k = 4.85 + .00457 T \quad , \text{ Btu/hr-ft } ^\circ\text{R}$$

where T is the temperature degrees Rankine.

Density

$$\rho = 485 \quad , \text{ lb/ft}^3$$

Pipe Wall Thickness

The containment wall thickness is set by the minimum thickness that can be fabricated or welded in the assembly of the system. The minimum thickness for pipe or tubing is assumed to be a function of the pipe diameter. The relation used in the computer code is as follows:

$$\text{TK} = 0.206 D^2 + 0.059$$

where

TK = wall thickness in inches

D = pipe diameter in feet

7. POWER CONDITIONING RADIATOR MATERIAL

The passive power conditioning radiator panels are assumed to be constructed of aluminum alloy in the computer code.

Thermal Conductivity

$$k = 76.6 + 0.08 T - 5 \times 10^{-5} T^2, \text{ Btu/hr-ft}^{\circ}\text{R}$$

where T is the temperature in degrees Rankine.

Density

$$\rho = 169, \text{ lbs/ft}^3$$

Emissivity

$$\epsilon = 0.85$$

GENERAL  ELECTRIC
MISSILE AND SPACE DIVISION